

# Numerical simulations of fire-induced smoke propagation from an apartment into a corridor based on the Oudewater experiments

Pim van Rede

Student number: 01911428

Supervisor: Prof. dr. ir. Bart Merci

Counsellors: dhr. Ruud van Liempd (IFV), dhr. Lieuwe De Witte (IFV), Dr. Andrea Lucherini

Master's dissertation submitted in order to obtain the academic degree of  
Postgraduaat Fire Safety Engineering

Academic year 2021-2022

# NUMERICAL SIMULATIONS OF FIRE- INDUCED SMOKE PROPAGATION FROM AN APARTMENT INTO A CORRIDOR BASED ON THE OUDEWATER EXPERIMENTS

Master's dissertation submitted in order to obtain the academic degree  
of Postgraduate Fire Safety Engineering

Student: ir. Pim van Rede  
Supervisor: Prof. dr. ir. Bart Merci  
Counselors: dr. Andrea Lucherini, ing. Ruud van Liempd, ing. Lieuwe de Witte  
Date: May 23<sup>rd</sup> 2022

[Intentionally left blank]

The author gives permission to make this master dissertation available for consultation and to copy parts of this master dissertation for personal use. In all cases of other use, the copyright terms have to be respected, in particular with regard to the obligation to state explicitly the source when quoting results from this master dissertation.

This master's dissertation is part of an exam. Any comments formulated by the assessment committee during the oral presentation of the master's dissertation are not included in this text.

## ACKNOWLEDGEMENTS

---

What started in the late summer of 2019 with the drive for more fundamental knowledge behind fire engineering methodologies used in the industry, ended in the spring of 2022 with the finalization of this work. This thesis is written within the framework of the postgraduate studies in fire safety engineering, as taught at Ghent University. The subject, numerical simulations of under-ventilated fires, is one of personal and professional interest and is of significant relevance given the current trends in the building industry.

The last couple of years spend on the postgraduate were as turbulent (no pun intended) as they were educational. The Covid-pandemic and the birth of our first child introduced a new dynamic in the life of my wife and me. Nevertheless, I can honestly say that the last 3 years were some of the most educational years I've experienced. This can wholly be attributed to the high quality of teaching in the fire safety engineering track at Ghent University.

First and foremost, this thesis would not have been possible without the support and insight of Bart Merci and Andrea Lucherini. Their constructive feedback and technical know-how prompted me to finish this thesis to its current shape. Moreover, Ruud van Liempd and Lieuwe de Witte from the Dutch Institute for Personal Safety (NIPV) provided insightful discussions and gave me the possibility to use their experimental data. A well-deserved thank you is in order!

Furthermore I'd like to thank my colleagues for giving me the possibility to take the postgraduate studies. Proof-readers Nick and Tom, thank you as well. Your feedback was very welcome.

Last, but certainly not least, I'd like to thank my wife Irene for her support and bearing with me as I indulged in countless hours of modelling, post-processing and writing this thesis. Could not have done it without you!

Pim van Rede,  
May 23<sup>rd</sup> 2022

## ABSTRACT

---

### **Numerical simulations of fire-induced smoke propagation from an apartment into a corridor based on the Oudewater experiments.**

Student: ir. Pim van Rede  
Supervisor: Prof. dr. ir. Bart Merci  
Counselors: dr. Andrea Lucherini, ing. Ruud van Liempd, ing. Lieuwe de Witte

Date: May 23<sup>rd</sup> 2022

This thesis studies the abilities of the CFD-tool (Computational Fluid Dynamics) Fire Dynamics Simulator (FDS) relating to the numerical simulations of under-ventilated fires. It uses an experimental data-set obtained in the 'Oudewater experiments' as a benchmark. The experimental campaign consisted of several full scale fire experiments, which were carried out by the Dutch Institute for Personal Safety (NIPV) in a vacated apartment building.

Out of the available experimental data, three scenarios were chosen to be used as a benchmark for numerical simulations. Each scenario chosen differentiated from the others in terms of available ventilation. Available experimental data includes the mass loss rate of the sofa used as the seat of fire and gas concentrations, temperatures and pressures in both the apartment in which the sofa was placed and the adjacent corridor.

The numerical simulations show divergent results. In the case with the highest level of ventilation, FDS predicts the quantities of interest to an acceptable level of accuracy. In the cases with limited ventilation, results are less satisfying, with the primary reason being flame extinction and the involved chemistry not being modelled and predicted accurately. Alterations to the numerical setup showed better results. The alterations however, are not substantiated.

The thesis concludes that using the current version of FDS to predict phenomena related to under-ventilated fires without a benchmark (experimental data) should be done with caution.

Keywords:

Under-ventilated fire, numerical simulations, FDS, CFD, extinction model, combustion model, Oudewater experiments.

## SAMENVATTING

---

### **Numerieke simulaties van de verspreiding van door brand veroorzaakte rook vanuit een appartement naar een gang op basis van de Oudewater experimenten**

Student: ir. Pim van Rede  
Promotor: Prof. dr. ir. Bart Merci  
Begeleiders: dr. Andrea Lucherini, ing. Ruud van Liempd, ing. Lieuwe de Witte

Datum: 23 mei 2022

Deze thesis bestudeert de mogelijkheden van de CFD-tool Fire Dynamics Simulator (FDS) met betrekking tot de numerieke simulaties van ondergeventileerde branden. Daartoe wordt gebruik gemaakt van een experimentele dataset verkregen in de 'Oudewater experimenten'. De experimentele campagne bestond uit een aantal grootschalige brandexperimenten, die werden uitgevoerd door het Nederlandse Instituut Persoonlijke Veiligheid (NIPV) in een leegstaand appartementencomplex.

Uit de beschikbare experimentele gegevens zijn drie scenario's gekozen die als basis voor de numerieke simulaties zijn gebruikt. Elk gekozen scenario verschilt van de anderen in termen van beschikbare ventilatie. De beschikbare experimentele gegevens omvatten het massaverlies van de sofa die als brandhaard werd gebruikt en de gasconcentraties, temperatuur, zichtlengten en relatieve drukken in zowel het appartement waarin de sofa was geplaatst als de aangrenzende gang.

De numerieke simulaties laten uiteenlopende resultaten zien. In het geval met het hoogste ventilatieniveau voorspelt FDS de onderzochte grootheden met een aanvaardbare nauwkeurigheid. In de gevallen met beperkte ventilatie zijn de resultaten minder accuraat, met als voornaamste reden dat vlamuitdoving en de betrokken chemie niet accuraat worden gemodelleerd en voorspeld. Wijzigingen in de numerieke opzet laten betere resultaten zien. Die wijzigingen zijn echter niet onderbouwd.

De thesis concludeert dat het gebruik van de huidige versie van FDS om verschijnselen in verband met ondergeventileerde branden te voorspellen zonder experimentele gegevens met voorzichtigheid moet gebeuren.

# NUMERICAL SIMULATIONS OF FIRE-INDUCED SMOKE PROPAGATION FROM AN APARTMENT INTO A CORRIDOR BASED ON THE OUDEWATER EXPERIMENTS

---

ir. Pim van Rede

Supervisor: Prof. dr. ir. Bart Merci,

Counselors: dr. Andrea Lucherini, ing. Ruud van Liempd, ing. Lieuwe de Witte

**This thesis studies the abilities of the CFD-tool Fire Dynamics Simulator (FDS) relating to the numerical simulations of underventilated fires. It uses an experimental data-set obtained in the ‘Oudewater experiments’ as a benchmark.**

## *i. Introduction*

In the summer of 2019, the NIPV (Dutch Institute for Personal Safety) carried out several full-scale fire experiments in a vacated apartment building located in Oudewater, the Netherlands. The experimental campaign sought to give insight in the extent and effects of smoke propagation in the event of a fire in a dwelling. During the experiments, several boundary conditions were changed, among which the amount of available ventilation. As such a significant amount of experiments showed signs of underventilation [1].

Over the past decades, the ability of Computational Fluid Dynamics (CFD) to simulate fire phenomena has seen exponential growth as a result of increasing computational resources and efforts to improve the underlying physics. However, its application still has several imperfections, one of which being the inability to accurately predict phenomena related to underventilated combustion, which is an active field of research. This poses a problem given the fact that, as a results of trends in the building industry, more underventilated fires are expected.

In this work, the data-set from the experimental campaign is used to study the ability of Fire Dynamics Simulator (FDS) to numerically predict the fire-related phenomena measured and observed during the experiments. Should an overall acceptable correlation between the numerical and experimental data be found, the numerical results can be extended to include scenarios not studied experimentally.

## *ii. Complexities related to underventilated combustion*

In a Large Eddy Simulations (LES), as is the methodology used in FDS to numerically simulate flow phenomena, eddies with a length-scale larger than 1 grid cell are numerically resolved using the LES-formulation of the Navier-Stokes equations. Phenomena occurring at a smaller length-scale are typically modelled using subgrid-scale (SGS) models [2].

Phenomena associated to combustion occur at SGS. Therefore, combustion is modelled rather than resolved directly. The main issues in modelling phenomena related to underventilated combustion lie in the complexity of the involved chemistry and its associated kinetics. The combustion model needs to account for a wide spectrum of phenomena to be able to accurately predict (amongst others) flame extinction due to dilution of oxygen and generation of product of incomplete combustion such as CO and HCN. Currently in FDS, extinction is de-coupled from the combustion model and is accounted for through the critical flame temperature-concept. Furthermore, in its default settings, FDS does not allow for transient chemistry to be modelled, which in underventilated fires is of significant importance.

A limited amount of studies exist that deal with the numerical simulations of large-scale underventilated fires. The studies that were examined show that the numerical prediction of fires that are diluted from oxygen indeed is complex and not straightforward.

## *iii. Experimental data*

Through analysis of the available experimental data, three experiments are selected to be used as a benchmark in one of three case studies. The selected experiments differentiate in terms of available ventilation: one experiment had the balcony door open while in the other two experiments that door was closed. Furthermore, in all experiments, the door between the corridor between the apartment and the corridor was opened after 300 seconds. In one experiment, that door was closed 30 seconds later.

All experiments used a two-seater sofa as the fire object. During the experiments, several quantities were measured, among which mass loss of the sofa, temperatures, gas concentrations, relative pressure and visibility. One measurement tree was placed in the apartment and two were located in the corridor. Thermocouples were fitted with a protective hood, which is expected to have affected the overall heat exposure of the thermocouple. The representativeness of those measurements is questionable.

The mass loss rate and heat release rate (HRR) derived from the experimental data are shown in Figure 1. Effects of oxygen starvation are clearly observable in most notably scenario 16, in which the mass loss rate drops moments after the door between the apartment and corridor is dropped. The effective heat of combustion,  $\Delta H_{c,eff}$ , was derived from thermocouple measurements in the apartment. A value of 16 MJ/kg was found and consequently used in deriving the HRR.

Prior to the experiments, the airtightness of the apartment was measured to determine both the leakage area and leak pressure exponent of the enclosure.

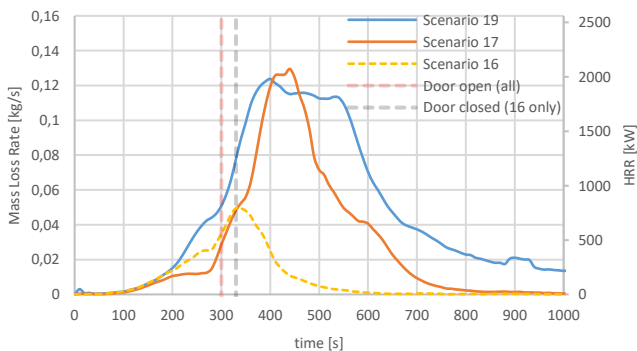


Figure 1: mass loss rate and heat release rate derived from experimental data for the used experiments. Data is time-averaged over 30 seconds.



Figure 2: Modelled geometry

iv. Numerical setup

The modelled domain consists of the apartment and corridor. The balcony door is modelled as a permanent opening in the specific case study, while the door between the apartment and corridor is modelled to (de)activate at the appropriate time. The modelled geometry is shown in Figure 2. B1, B5 and B6 represent the measurement trees which were discussed earlier. In one such tree, several thermocouples, gas samplers and pressure gauges were placed. In FDS, these were modelled either as thermocouples or as gas phase devices (in all cases except for the thermocouples).

| Description | Resolution  | Number of cells | Number of processors |
|-------------|---|-----------------|----------------------|
| Moderate    | 10*10*10 cm                                       | 380.000         | 10                   |
| Fine        | 5*5*5 cm  | 2,6 million     | 32                   |
| Extra fine  | 2,5*2,5*2,5 cm in apartment, 5*5*5 cm in corridor | 9 million       | 96                   |

Table 1: grid resolutions used in the grid sensitivity study

The resolution of the numerical grid is chosen based on a sensitivity study. The studied resolutions shown in Table 1.

In most case studies, the sensitivity to the used grid was limited and a 'fine' resolution would suffice. In the case of the case study with the door opened and left open, some differences were observable between the 'fine' and 'extra fine' resolution. In this specific instance, the default extinction model of FDS, which relies on local temperatures and is therefore sensitive to the used cell size, predicts a somewhat higher HRR in the case of the 'extra fine' resolution. Running the models on such a fine resolution would result in excessive computational cost and was therefore not opted for.

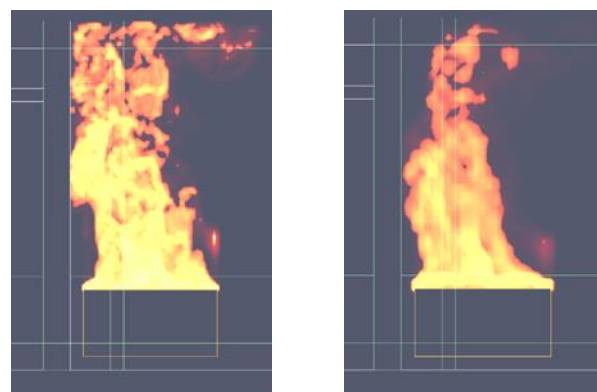


Figure 3: HRRPUV for the 'extra fine' and 'fine' resolution. Notice differences in flame geometry near the ceiling.

The chemical composition of the fuel was taken to be polyurethane foam ( $CH_{1.8}O_{0.3}N_{0.05}$ ). Species yields are initially estimated from the species yields under well ventilated burning conditions with empirical correlations [3] [4] and an estimated equivalence ratio based on the measured  $O_2$  concentration in the apartment during the

experiments. The parameters relating to the default extinction model are either calculated based on the imposed reaction (the critical flame temperature, CFT) or taken as default values (lower oxygen limit, LOL). Based on a literature review, an auto-ignition temperature of 400°C is prescribed, with the need for modelling ignition being bypassed through an auto-ignition exclusion zone above the fire seat.

Leakages are implemented by using both the localized leakage (for the door between the apartment and corridor) and bulk leakage (rest of the enclosure) models. Given the uncertainties associated with the measurements of the airtightness, a parametric study was conducted to find the appropriate settings.

#### v. Numerical results

A series of numerical simulations using FDS show that most quantities of interest are approximated correctly in the case study with the balcony door open. The O<sub>2</sub> concentrations show a relative error of approximately 5% in the initial period of the fire, prior to the extinction model predicting extinction. Afterwards, errors of up to 25% are observed but similar minimum values and trends are predicted. CO concentrations in the apartment are initially over-estimated as a result of the static nature of the used combustion model. Given the uncertainties in the experimental results with regards to the thermocouple measurements, a lag between the numerical and experimental data is observed. Trends however, do show similarities. The drop in visibility in the corridor is predicted to an adequate extent.

A similar setup was used in the case study with the balcony door closed and the door between the apartment and the corridor opened (case study 2). It showed ill-matched results as a result of the chemistry being transient to a significant extent given the severe hypoxic environment in the apartment, with O<sub>2</sub> concentrations to as low as 2 %vol measured. This is not taken into account by FDS' simple one step combustion model.

After adjusting the extinction parameters and setting up a two-step combustion scheme, better correlation between numerical and experimental data was obtained. The used parameters and model however are questionable and rudimentary in their essence. In this setup, the O<sub>2</sub> concentrations show a similar trend as seen in the case study with the balcony open. Until the moment extinction is modelled, relative errors are approximately 5% while afterwards, the errors go up to 60%. After 600 seconds or so, simulations predict lower O<sub>2</sub> concentrations than measured experimentally, indicating either more (flaming) combustion is predicted by FDS, or less oxygen is used for combustion (smoldering combustion). Given the fact that around that time CO<sub>2</sub> and CO are

respectively over- and under-predicted by FDS the latter seems the most likely. Furthermore, in the case of case study 2, the artificially lowered extinction parameters can result in more combustion being modelled than occurred in reality. The results for CO show the same trends as measured experimentally.

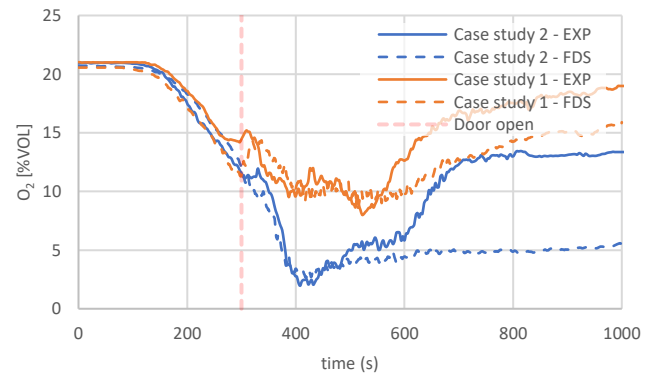


Figure 4: O<sub>2</sub> concentrations for case study 1 and case study 2 (the latter with artificially lowered extinction parameters)

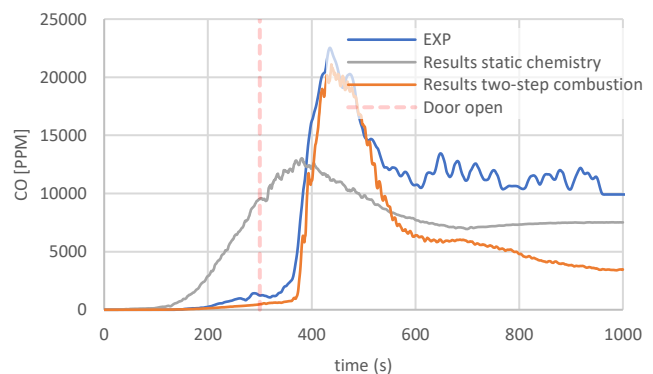


Figure 5: Experimental and numerical data for case study 2, showing results for single- and two-step combustion, with the latter having the extinction parameters lowered.

The same setup for extinction and combustion used in case study 2 did not result in appropriate results in case study 3. While the O<sub>2</sub> concentrations show appropriate correlation, CO and CO<sub>2</sub> concentrations do not, which shows the imposed two-step combustion scheme is not fit-for-purpose (the purpose given here is modelling the generation of CO). Given the fact that the O<sub>2</sub> concentration in the initial period is predicted at least to an approximative extend, is an indication that the (final) moment at which extinction sets in is predicted accurately. This is underlined by the fact that the final drop in relative pressure in the apartment is predicted to an acceptable extent, given the imposed uncertainties (e.g. sensitivity of the used equipment).

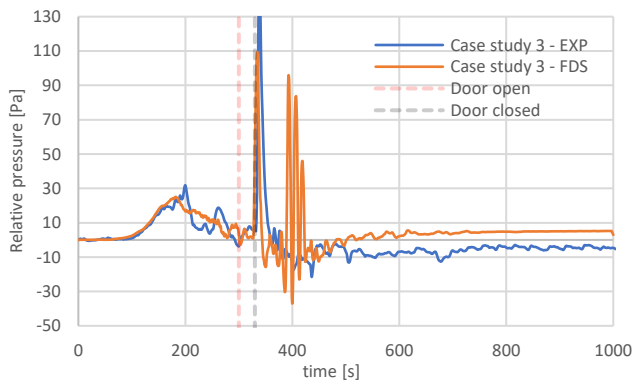


Figure 6: Relative pressure in the apartment for case study 3. Note that the sensitivity and resolution of the used equipment is respectively 25 Pa and 10 Pa.

The initial (steep) drop in pressure that is predicted by FDS just prior to opening of the door, which coincides with the moment extinction is modelled. The experimental data however, shows an initial drop earlier, around 200 seconds and once more around 260 seconds. The mass loss rate was time-averaged and peaks and troughs are averaged away. Around 200 seconds, the unfiltered data shows a more spurious behavior, which explains the sudden drop in pressure. The final peak, just after the door towards the corridor is closed again, is predicted accurately by FDS. The oscillatory behavior afterwards is a result of the bulk leakage model. From 500 seconds onwards, FDS shows an overpressure, while the experimental data shows an underpressure. This indicates that the predicted HRR is higher than what would be the case in reality, which is a result of the exclusion zone of the auto-ignition temperature. In this zone, some (flaming) combustion is observed from 500 seconds onwards that, based on the mass loss rate of the sofa, is not expected to have occurred in reality.

Concluding, the predictions made by FDS only showed appropriate results in the case study with the balcony door open. For the case studies with a limited amount of ventilation, the extinction parameters needed to be artificially altered to obtain appropriate results with regards to  $O_2$  concentrations. The results for CO were promising in case study 2. In case study 3 however, the used two-step combustion model showed to be unfit-for-purpose.

#### vi. Sensitivity study

The numerical results show to be sensitive to several parametric changes. The chemical composition of the fuel and its associated species yields affect the gas concentrations in the apartment. Furthermore, the results are found to be significantly sensitive to changes to parameters associated with the extinction model. Using the alternative extinction model included in FDS, which is meant for simulations using a coarse grid, also results in significant different results. Compared with the default extinction model without forced setting, those results are

more conservative in the case study with the balcony door open and more approximative (in its default, unforced settings) in the case with the balcony door closed and door towards the corridor left open.

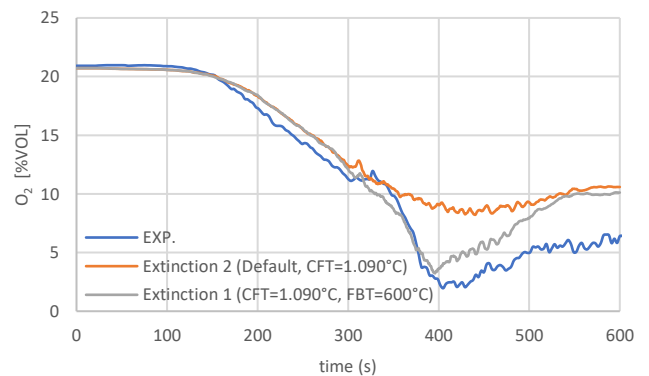


Figure 7: Results for different extinction models

#### vii. Results from an engineering point-of-view

Both the experimental and numerical data was used to set up execute a tenability study. The experimental data showed the visibility dropping prior to opening of the door as a result of the leaking gases through the door. This was not accurately predicted by FDS, given the fact that limitations in the leakage models affect the buoyancy of the leaking gases. When setting a tenability-criterion of 10 meters however, no significant differences were observed as the final drop in visibility is predicted accurately by FDS.

Given the uncertainties in the thermocouple measurements, a lag is observed when assessing thermal exposure within the Fractional Effective Dose (FED) methodology [5]. Given the similar trends however, it is concluded that the results obtained from FDS might be more representative than the experimental data.

The toxicological effects of the fire effluents are assessed by means of the FED methodology. While it showed generally acceptable results for the case study with the balcony door open (well ventilated), it performed poor for the case study with the door closed 30 seconds after being opened as the CO concentration is underestimated by FDS. Using the FED-methodology for toxicological effects to assess tenable times in underventilated conditions therefore is ill-advised. Using visibility as a proxy for toxic effects is advised, albeit the concept currently used in fire engineering is crude and conservative.

#### viii. Conclusion

Concluding, using FDS in its current build to perform blind simulations (not using experiments as a reference) of underventilated fires should be done with caution. If used, a thorough sensitivity study on the extinction parameters and its grid dependence is in place. Furthermore, using the alternative extinction model might lead to more

conservative results without altering the default parameters. A tenability framework based on toxicological effects should only be used when over-conservatism is acceptable, given the static nature of species yields in FDS. Estimating tenable times based on visibility (which also holds conservatism) and/or heat exposure is more reliable.

### *References*

- [1] J. Elbus, T. Geertsema, V. Jansen, M. Leene, R. Van Liempd, M. Polman, L. De Witte and L. Wolfs, "Rookverspreiding in woongebouwen. Hoofdrapport van de praktijkexperimenten in een woongebouw met inpanidige gangen," Brandweeracademie, Arnhem, 2020.
- [2] NIST, Fire Dynamics Simulator Technical Reference Guide, Maryland: NIST, 2020.
- [3] M. M. Khan, A. Tewarson and M. Chaos, SFPE Handbook of fire protection engineering, chapter 36: combustion characteristics of materials and generation of fire products, London: Springer, 2016.
- [4] L. Staffansson, "Selecting Design Fires," 2010.
- [5] SFPE, Guide to Human Behavior in Fire, Gaithersburg, Maryland , USA: Springer, 2019.

# INDEX

---

|           |  |           |
|-----------|--|-----------|
| <b>1.</b> | <b>Introduction .....</b>  | <b>1</b>  |
| 1.1       | General.....   | 1         |
| 1.2       | Technical relevance and research gaps .....  | 1         |
| 1.3       | Research objectives .....  | 1         |
| 1.4       | Structure of the thesis .....  | 2         |
| <b>2.</b> | <b>Literature review.....</b>  | <b>3</b>  |
| 2.1       | General.....   | 3         |
| 2.2       | PRISME-project.....  | 3         |
| 2.3       | VIPA3-project .....  | 4         |
| 2.4       | Fire Dynamics and Forensic Analysis of Limited Ventilation Compartment Fires .....   | 4         |
| 2.5       | Different concepts for personal safety in a multi-story residential complex in relation to internal smoke propagation..... | 5         |
| 2.6       | Literature review: conclusion.....   | 6         |
| <b>3.</b> | <b>The Oudewater experiments .....</b>   | <b>7</b>  |
| 3.1       | General.....   | 7         |
| 3.2       | Technical buildup .....  | 7         |
| 3.3       | Goal of the Oudewater Experiments .....  | 7         |
| 3.4       | Experimental methodology.....  | 7         |
| 3.5       | Measurements.....  | 10        |
| 3.6       | Relevant scenarios.....  | 12        |
| 3.7       | Analysis of experimental results.....  | 12        |
| 3.8       | Chosen scenarios.....  | 16        |
| <b>4.</b> | <b>Theoretical framework.....</b>  | <b>17</b> |
| 4.1       | Introduction.....  | 17        |
| 4.2       | Fire Dynamics Simulator (FDS) .....  | 17        |
| 4.3       | Heat Release Rate and heat of combustion .....   | 18        |
| 4.4       | One step combustion model .....  | 19        |
| 4.5       | Species generation in under-ventilated fires .....   | 19        |
| 4.6       | Two-step simple combustion model in FDS.....   | 21        |
| 4.7       | Flame extinction .....   | 21        |
| 4.8       | Fire growth .....  | 24        |
| 4.9       | Modelling leakage .....  | 24        |
| 4.10      | Soot deposition.....   | 25        |
| <b>5.</b> | <b>Numerical Setup .....</b>   | <b>26</b> |
| 5.1       | Modelled geometry.....   | 26        |
| 5.2       | Devices.....   | 26        |
| 5.3       | Thermophysical characteristics of the enclosure .....  | 27        |
| 5.4       | Leakages.....  | 27        |
| 5.5       | Initial fire characteristics .....   | 28        |
| 5.6       | Post-processing of results .....   | 30        |
| 5.7       | Numerical grid .....   | 31        |
| 5.8       | Grid sensitivity study .....   | 31        |
| <b>6.</b> | <b>Results case study 1: Balcony door open.....</b>  | <b>36</b> |
| 6.1       | Description of experimental setup.....   | 36        |
| 6.2       | Results in the apartment .....   | 36        |
| 6.3       | Results in the corridor .....  | 39        |
| 6.4       | Sensitivity study.....   | 43        |

|            |   |           |
|------------|---|-----------|
| 6.5        | Case study 1: conclusion .....  | 50        |
| <b>7.</b>  | <b>Results case study 2: door to corridor open.....</b>                         | <b>52</b> |
| 7.1        | Description of experimental setup .....   | 52        |
| 7.2        | A-priori parametric study: fire-induced pressure in apartment .....             | 52        |
| 7.3        | Initial results in the apartment .....  | 54        |
| 7.4        | Multiple fast reactions and (mis)using the extinction model.....                | 56        |
| 7.5        | Numerical setup for final simulation results.....                               | 58        |
| 7.6        | Results in the apartment .....  | 58        |
| 7.7        | Results in the corridor .....   | 62        |
| 7.8        | Sensitivity study.....  | 64        |
| 7.9        | Case study 2: conclusion .....  | 68        |
| <b>8.</b>  | <b>Results Case study 3: Door opened and closed.....</b>                        | <b>70</b> |
| 8.1        | Description of experimental and numerical setup .....                           | 70        |
| 8.2        | A-priori parametric study: fire-induced pressure in apartment and corridor..... | 70        |
| 8.3        | Results in the apartment .....  | 72        |
| 8.4        | Results in the corridor .....   | 75        |
| 8.5        | Case study 3: conclusion .....  | 77        |
| <b>9.</b>  | <b>Implications for practical fire engineering.....</b>                         | <b>78</b> |
| 9.1        | Introduction.....   | 78        |
| 9.2        | Visibility in smoke .....   | 78        |
| 9.3        | Heat exposure .....   | 79        |
| 9.4        | Toxicological effects .....   | 80        |
| 9.5        | Tenability: conclusion .....  | 82        |
| <b>10.</b> | <b>Discussion .....</b>   | <b>83</b> |
| 10.1       | General.....  | 83        |
| 10.2       | Extinction model .....  | 83        |
| 10.3       | Combustion model with regards to underventilation .....                         | 84        |
| 10.4       | Leakage model.....  | 84        |
| 10.5       | Suggested further research.....   | 85        |
| <b>11.</b> | <b>Conclusion.....</b>  | <b>86</b> |
| 11.1       | Sub-questions .....   | 86        |
| 11.2       | Main research question .....  | 87        |
| <b>12.</b> | <b>References .....</b>   | <b>88</b> |

## Appendices

1. Used experimental equipment
2. Selection of experimental results
3. Expanded theoretical framework
4. Expanded grid sensitivity study
5. Selection of results
6. Expanded parametric studies (fire-induced pressure and extinction)
7. Input files for final simulations

# 1. INTRODUCTION

---

## 1.1 General

This document is the culmination of the Postgraduate Studies in Fire Safety Engineering, as given at Ghent University and deals with numerical simulations of fire-induced smoke propagation. The overall scope of the thesis is to study the possibilities of accurately simulating smoke propagation using Fire Dynamics Simulator. As a basis, the Oudewater experiments are used, as carried out in 2019 by the Dutch Institute of Safety (in Dutch: 'Instituut Fysieke Veiligheid', abbreviated IFV. Now NIPV).

## 1.2 Technical relevance and research gaps

Over the past decades, the ability of CFD to simulate fire phenomena has seen exponential growth as a result of increasing computational resources and efforts to improve the underlying physics. However, its application still has several imperfections that can be attributed to the complex nature of combustion and fire driven flows. One of these limitations is the (in)ability to accurately predict phenomena attributed to under-ventilation (e.g. extinction and re-ignition of diffusion flames due to oxygen dilution, generation of products of under-ventilated combustion) [1]. In future engineering studies, this could lead to problems as the number of under-ventilated fires is expected to grow due to amongst others the tendency to build more airtight buildings and use more robust glazing in conjunction with significantly faster fire development in contemporary furniture [2].

As of today, Fire Dynamics Simulator as developed by NIST is the most widely used CFD-solver to simulate fire driven flows [3]. Its validation and verification guide is extensive [4] [5] and the CFD-solver is explicitly developed for simulating low-mach buoyancy-driven flows as is typical for fire driven flows. This thesis studies the capabilities of FDS to accurately simulate under-ventilated fires based on data set incorporating several full-scale experiments. Furthermore, should the numerical results prove useful, they can be used to expand the experimental results.

## 1.3 Research objectives

The overall goal of this thesis is to study the fire induced smoke propagation through numerical simulations using Fire Dynamics Simulator. The experiments of the Oudewater experiments, which all are to some extent under-ventilated, are used as a basis.

### 1.3.1 Main research-question

The overall research question is formulated as follows:

*To what extent can the CFD-tool FDS be used to realistically simulate a fire driven flow as studied in the Oudewater Experiments, knowing the fire is prone to growing under-ventilated?*

### 1.3.2 Sub-questions

To answer the research question, several sub-questions are formulated:

1. What studies were carried out relating to the numerical simulation of under-ventilated fires and what were the conclusions?
2. What scenarios were studied during the Oudewater experiments and what scenarios will be used in this thesis?
3. What are the general technical characteristics of FDS and what are its limitations when dealing with under-ventilated fires?
4. To what extent can specific scenarios from the Oudewater Experiments be simulated using FDS, given the available data?

The sub-questions are answered through a literature review and a series of CFD-simulations using FDS.

#### 1.4 Structure of the thesis

In this chapter of the thesis, the subject and research questions are introduced and formulated, as well as the technical relevance of the subject. Chapter two gives a short literature review in which several projects which aim to simulate under-ventilated fires are described. Chapter 3 outlines the Oudewater experiments and summarizes some experimental results which are then used to select the experiments to be simulated in FDS. In total, three scenarios are chosen.

Chapter 4 gives the technical and theoretical framework in which this thesis is written. It describes relevant information relating to fire dynamics and how this is handled in FDS. In chapter 5, the chosen numerical setup is described; an explanation is given on how the theoretical framework is used to model among others fire, device and enclosure characteristics. In chapter 6, 7 and 8, the numerical results are presented and compared with the experimental findings. Chapter 9 studies the results are studied from an engineering perspective; a comparison is made between experimental and numerical data within a tenability framework.

Chapter 10 discusses the results and its implications for the fire-engineering community. Moreover, it gives recommendations for further research. In chapter 11, a conclusion is given in which sub-questions and the main research question is discussed.

## 2. LITERATURE REVIEW

---

### 2.1 General

This chapter deals with the analysis of earlier work carried out on the numerical simulation and modelling of under-ventilated fires.

### 2.2 PRISME-project

The Fire Propagation in Elementary Multi-room Scenarios (French: 'propagation d'un incendie pour des scénarios multi-locaux élémentaires', or PRISME) deals with several fire and smoke propagation phenomena through both experiments and modelling/simulations. Over the course of the project, several experiments were carried out in the DIVA facility, consisting of several confined and mechanically ventilated compartments. Calorimetry ('free burn') experiments were carried out in the SATURNE facility during which the fires' Heat Release Rate (HRR) (among others) was measured using oxygen consumption calorimetry. The PRISME-campaign consisted of 4 'sub-campaigns', all with a specific goal. The PRISME 'Source' experiments aimed to gain insight in fundamental combustion phenomena through the free and confined burning of Hydrogenated Tetra-Propylene ( $C_{12}H_{26}$ ). The PRISME 'Leak' and PRISME 'Door' experiments dealt with leakage of smoke respectively small leaks and open doorways. The PRISME 'Integral' experiments dealt with a different fire sources (electric cables and cabinets) and the effect of fire dampers and sprinklers [6].

The scenarios carried out in the DIVA facility all dealt with different boundary conditions (e.g. variations in ventilation flow-rates, the location of the air inlet and the number of connected rooms through open doors). The fires' HRR ranged from 200 kW to approximately 1 MW. Fire extinction was either due to fuel burnout or oxygen dilution. Given the fact that these experiments were well documented, they are suitable for the validation of numerical models dealing with fire and smoke phenomena. Two of the studies are discussed here.

Wahlqvist and Van Hees carried out numerical simulations using Fire Dynamics Simulator (a pre-release of v6 was used) to verify the correctness of the HVAC-system which was introduced at that time [7]. Given the goal, limited attention is given to the fire behavior under different oxygen levels. Their paper deals with the pressure evolution in the fire room, given a certain heat release rate and ventilation setup. While the fires studied in their paper were under-ventilated to a certain extent, only limited attention is given to this phenomenon. They state that the ghosting flames seen in the simulation are a result of the suppression model used in FDS. It seems no auto-ignition temperature was set for the modelled reaction. This indeed causes unburned fuel to combust should sufficient oxygen become available near vents, independently from the local gas-phase temperature.

Bonte, Noterman and Merci carried out simulations using both CFD-model ISIS (Incendie Simulé pour la Sécurité, uses a RANS-approach) and zone model CFAST (Consolidated Fire And Smoke Transport) [8]. While the primary goal of this study was to validate models for the prediction of fire-induced pressure and the effects on the burning rate of the fuel, some details are given on the observed oxygen levels and the calculated burning rate. To account for extinction as a result of oxygen dilution the empiric Peatross-Beyler correlation was used in ISIS. CFAST uses a correlation based on the oxygen entrained in the fire plume and includes the lower oxygen limit through a damping function. They concluded that ISIS was in fact capable of predicting fire-induced pressures and the decrease in oxygen accurately. In CFAST, the leakages in the enclosure and the lower oxygen limit of the fuel were chosen to fit the measurements in fire-induced pressure best. Given the inability of CFAST to model reverse flow over the ventilation system, oxygen concentrations were not modelled accurately.

Compared to the data-set used in this thesis, the measured oxygen concentrations in the PRISME-campaign are relatively high. In PRISME, no values below 10 %vol were measured, while in the campaign used in this thesis, concentrations below 5 %vol are registered. Furthermore, FDS uses a

different, more fundamental, methodology to model extinction than the Peatross-Beyler correlation. Therefore, results are not directly comparable.

### 2.3 VIPA3-project

The VIPA-project was funded by the Belgian government (the department 'Welzijn, Volksgezondheid en Gezin' or 'wellbeing, public health and family'). Its main goal is to formulate new legislation relating to the fire safety of elderly homes within a fire engineering framework. The project consisted of several experimental and numerical studies (VIPA1, VIPA2 and VIPA3). Results are written down in [9], [10] and [11].

During the VIPA1 and VIPA2 studies, experiments were carried out to study the effectiveness of certain fire safety measures and combinations thereof. The experimental setup was composed of a sofa located in the communal area of a care home. The communal area was connected to corridors and bedrooms. The heat release rate of the used sofa was measured under a calorimetry hood. Experiments were carried out using different fire safety measures, among which:

- No specific fire safety measures.
- Implementing fire and smoke doors between the different areas in the enclosure.
- Implementing a smoke and heat control system in the communal area.
- Implementing active fire control in the form of sprinklers.

During the experiments, measurements were made so quantitative evaluation and comparison between the different experiments was possible. Among others temperatures, gas concentrations and pressures were measured during the experiments.

The VIPA3-project consisted wholly of numerical studies in which a CFD-model (Fire Dynamics Simulator) was both validated and used to expand the experimental results from the VIPA1 and VIPA2 studies. After adjusting the heat release rate to account for the effects of re-radiation from the hot gases in the enclosure, an adequate correlation was found between the experimental and numerical data. Results for pressures in the enclosure however, appeared sensitive to the airtightness of the enclosure and the exact heat release rate of the fire. Limited attention is given to whether the extinction model played a role in the results. For simulations ran for the scenario with no safety measures included, some influence of the extinction model is expected.

Given the overall well-enough correlation between the experimental and numerical results, the numerical setup was used to carry out additional simulations in which the effects of several stochastic parameters were studied. Deviating from the VIPA2 study, the fire was modelled to be located in a bedroom rather than in the communal area. Given the significant lower volume of the bedroom, the heat release rate of the fire is shown to be dictated by the extinction model of FDS. The default settings for the extinction model were used and a single step combustion scheme for propane was used.

The validation in this study is limited to adequately ventilated fires. No value judgement is made on the impact of underventilation on the additional simulations.

### 2.4 Fire Dynamics and Forensic Analysis of Limited Ventilation Compartment Fires

This study is composed of two parts. In the first part [12], an experimental campaign is documented. The experimental campaign focusses on under-ventilated fire scenarios. Experiments were carried out in a four room, apartment style enclosure with fire sources such as sofas and cabinets. The experiments used different ventilation scenarios, ranging from no ventilation to an open entrance door. During the experiments, several quantities were measured, among which temperatures, radiant heat flux', pressures, velocities and gas concentrations. The second part of the report deals with numerical simulations [13] based on the experimental campaign.

The study used FDS version 5 to predict the phenomena related to fire driven flows. Version 5 of FDS used the Constant Smagorinsky subscale-model, included a combustion model which (in theory) could predict the formation of CO and used an extinction model based on the concept of a critical flame temperature. The combustion model for CO-production used a two-step reaction scheme with the first reaction being an infinitely fast reaction from fuel to CO and other products. The second reaction scheme involved oxidation of CO into CO<sub>2</sub> using a finite rate reaction scheme. The reaction scheme was based on a three parameter mixture-fraction model which was dropped in FDS 6. The extinction model in FDS 6 remained identical but the default subgrid-scale model for turbulence was changed to Deardorff's model.

The study used both free burn calorimetry data and mass loss measurements to specify the fires' heat release rate in FDS. Using the calorimetry data resulted in deviations explainable through re-radiation from the hot smoke layer in the apartment, which intensifies the pyrolysis rate.

Generally speaking, appropriateness of the correlation between numerical and experimental results varies per scenario. Simulations with some form of ventilation in place (e.g. door or window open) show to better correlate with the experiments compared to the simulations using a closed compartment. CO concentrations in the enclosure were not predicted appropriately as FDS underpredicted the concentration in all the numerical simulations. Furthermore, in the case of the experiments using a fuel package which was placed at a lower height in the room, the extinction model did not show to have significant influence on the outcome of the simulations as the O<sub>2</sub> concentrations were shown to still be above, or just somewhat under the imposed lower oxygen limit of the fuel. In the scenario in which a cabinet was placed at a higher elevation in the room, vitiated combustion (the fire plume entraining a mixture of air and combustion products) is expected as the cabinets are located in the smoke layer. In these instances, the O<sub>2</sub> concentrations and temperatures deviate quite significantly from the measured values, indicating that the extinction model does not predict flame extinction accurately. In the FDS simulations, some combustion might be taking place away from the fire seat that in reality was not occurring.

## **2.5 Different concepts for personal safety in a multi-story residential complex in relation to internal smoke propagation**

In his Master's thesis [14], Scholman carried out a validation study using the data from the Oudewater experiments and the zone models CFAST by NIST and B-RISK by Branz before using the model which gave the best results to study the effectiveness of some technical measures to limit smoke propagation.

The main upside of zone modelling is the fact that these models are computationally cheap, which enables a great number of scenarios to be calculated in a limited amount of time. This makes parametric modelling and probabilistic studies accessible. Furthermore, the physics behind zone models are transparent, which makes the calculation methods more comprehensive in contrast to for example CFD-based methodologies.

The main downside of using (multi-)zone models lies in the fact that they use an assumption of homogeneity in various volumes of the enclosure. Typical models (CFAST, B-RISK) use an upper-layer zone, which is formed by the hot smoke, and a lower-layer zone, which is composed of 'clean' air. Within these volumes, quantities of interest (e.g. temperature, gas concentrations) are assumed to be uniform. In cases that are spatially dependent to a significant degree, as would appear is the case in the Oudewater experiments, that assumption is problematic. Furthermore, while the models typically do solve for the conservation laws of mass and energy, the conservation of momentum is not solved. This means that turbulence only is implicitly taken into account in the (semi-)empiric plume models used in the model. As these models are based on experimental data, they have a limited range of applicability.

Both CFAST and B-RISK calculate the heat release rate in under-ventilated conditions based on the mass of air entrained in the fire plume. They include the lower oxygen limit of the fuel through a damping

function which estimates the amount of fuel that can be burned given the amount oxygen available. The main difference however, is that B-RISK imposes a temperature dependency on the under-ventilated combustion scheme: at higher temperatures, combustion can occur at lower O<sub>2</sub>-concentrations. Furthermore, where CFAST only allows for manual input of the species-yields, B-RISK can estimate them using empirical correlations (see paragraph 4.4) based on an equivalence ratio [15] [16].

The thesis does not state which of the experiments was used as a reference in the validation study. Furthermore, it uses data from the thermocouples located at a height of 2,2 meters as a reference in both the apartment and the corridor, which is questionable given the homogeneous nature of the models used and the fact that a temperature gradient is expected on the vertical direction. Using an averaged value over several thermocouples might be more appropriate, depending on the expected depth of the smoke layer.

Nevertheless, the experimental and numerical results for temperature in the apartment and corridor show an appropriate correlation. The O<sub>2</sub>-concentration shows a more ill-fitted correlation, with both CFAST and B-RISK under-estimating oxygen consumption. CFAST however, does show the same minimum with regards to O<sub>2</sub> concentration. No information is given on gas concentrations other than O<sub>2</sub>.

## **2.6 Literature review: conclusion**

Only limited number of studies exist which deal with the numerical simulations of large-scale under-ventilated fires. The studies described here show that significant difficulties exist when dealing with the simulation or modelling of under-ventilated fires. These difficulties can most notably be attributed to the inherent complexity of flame extinction due to oxygen dilution and the inability to accurately predict the flame chemistry.

## 3. THE OUDEWATER EXPERIMENTS

### 3.1 General

In the summer of 2019, the Dutch Institute for Safety ('Instituut Fysieke Veiligheid' or 'IFV', now: 'Nederlands Instituut Publieke Veiligheid' or 'NIPV') carried out fire experiments in a vacant apartment building located in the village of Oudewater in the province of Utrecht. The vacated apartment-building 'Schuylenburcht' was primarily used as a care-home and consisted of multiple apartments and several supporting functions. In total, it consisted of four floors. In most cases, apartments were located around a central corridor, which is typical for Dutch carehomes build in the 1970's. An image is shown below.

In this chapter, the experimental setup and a selection of relevant results are discussed. For a more detailed description of the experiments and its results the reader is directed to the report which is available on the website of the NIPV [17].



Figure 1: Schuylenburcht-complex in Oudewater, copied from [17]

### 3.2 Technical buildup

The building consisted of a concrete structure with masonry facades. All the apartments had a window over the full height and width of the façade and had access to a small balcony. The apartments were ventilated using natural ventilation through the façade and vertical standpipes in the kitchen and bathroom. Drawings of the building were made available by the NIPV.

### 3.3 Goal of the Oudewater Experiments

Fire-driven smoke propagation has become more problematic over the past decades as a result of changing fuel characteristics and changing boundary conditions (e.g. airtight building envelopes [18]). The Oudewater experiments were carried out to gain insight in the severity of the smoke propagation and the effects thereof on fleeing occupants. Furthermore, the experiments were carried out to study the efficacy of different repressive strategies.

### 3.4 Experimental methodology

#### 3.4.1 Scenarios

During the Oudewater experiments, several scenarios were studied. All but two scenarios used the same fire source which was a sofa composed of (mostly) polyurethane foam. Scenarios differed in the level of ventilation and the present passive and active fire safety measures. Two apartments were used as fire-rooms (apartment 1.19 and apartment 1.21).

This resulted in a total of 18 scenarios:

| Scenario   | Date*      | Fire object | Fire room | Door apartment** | Measure/remarks                             |
|--|------------|-------------|-----------|------------------|---|
| 1  | 24-06-2019 | Sofa        | 1.21      | Open             | Baseline                                    |
| 2  | 25-06-2019 | Sofa        | 1.21      | Closed           | <b>Experiment failed</b>                    |
| 3  | 25-06-2019 | Sofa        | 1.19      | Open             | -   |
| 4  | 26-06-2019 | Sofa        | 1.21      | Closed           | Door control                                |
| 5  | 26-06-2019 | Sofa        | 1.19      | Open             | -   |
| 6  | 27-06-2019 | Sofa        | 1.21      | Closed           | Mobile watermist system                     |
| 7  | 27-06-2019 | Sofa        | 1.19      | Open             | Mobile watermist system                     |
| 8  | 28-06-2019 | Sofa        | 1.21      | Closed           | Mobile watermist system                     |
| 9  | 28-06-2019 | Sofa        | 1.19      | Open             | Mobile watermist system                     |
| 10   | 01-07-2019 | Sofa        | 1.21      | Closed           | Mobile watermist system, airtight enclosure |
| 11   | 01-07-2019 | Sofa        | 1.19      | Closed           | Mobile watermist system, airtight enclosure |
| 12   | 02-07-2019 | Sofa        | 1.21      | Closed           | Airtight enclosure                          |
| 13   | 02-07-2019 | Sofa        | 1.19      | Closed           | Airtight enclosure                          |
| 14   | 03-07-2019 | Wood crib   | 1.21      | Closed           | Traditional fire load                       |
| 15   | 03-07-2019 | Wood crib   | 1.19      | Open             | Traditional fire load                       |
| 16   | 04-07-2019 | Sofa        | 1.21      | Closed           | Door control                                |
| 17   | 04-07-2019 | Sofa        | 1.19      | Open             | Baseline                                    |
| 18   | 05-07-2019 | Sofa        | 1.19      | Open             | Balcony door open                           |
| 19   | 05-07-2019 | Sofa        | 1.19      | Open             | Balcony door open                           |
| * Experiments on mornings and afternoons   |            |             |           |                  |   |
| ** In all cases, the door was opened 300 seconds after the experiment started. In the 'open' scenarios it was kept open for the rest of the experiment. In the 'closed' scenario, it was closed 30 seconds after being opened. |            |             |           |                  |   |

Table 1: scenarios studied in the Oudewater experiments

### 3.4.2 Fire sources

During all but two experiments, the same sofa was used as a fire source. The sofa is depicted in Figure 2 and can be seen as good representation of a contemporary sofa sold in the Netherlands. The sofa consists predominantly of flexible polyurethane foam, with a wooden frame. No fire retardants are present in the fabric. The sofa was ignited using a small wood crib on which 1,4 ml Isopropyl alcohol was administered beforehand. The crib was placed in the righthand corner between the armrest, seating and backrest of the sofa. The location of the sofa in either fire room is shown in Figure 3.



Figure 2: sofa used in the experiments, placed on a scale. Copied from [17]

The location of the sofa was chosen strategically to prevent the façade glass breaking. During the experiment, the weight of the sofa was measured to get an indication of the mass loss. The initial weight is approximately 86 kg.

### 3.4.3 Fire rooms

During the experiments, two rooms were used as fire room: apartment 1.19 and 1.21. This allowed the team to conduct two experiments per day while minimizing problems regarding the enclosure already being heated up as a result of prior experiments or having a high moisture content as a result of extinguishment of the fire. The two fire rooms are depicted in the following image.

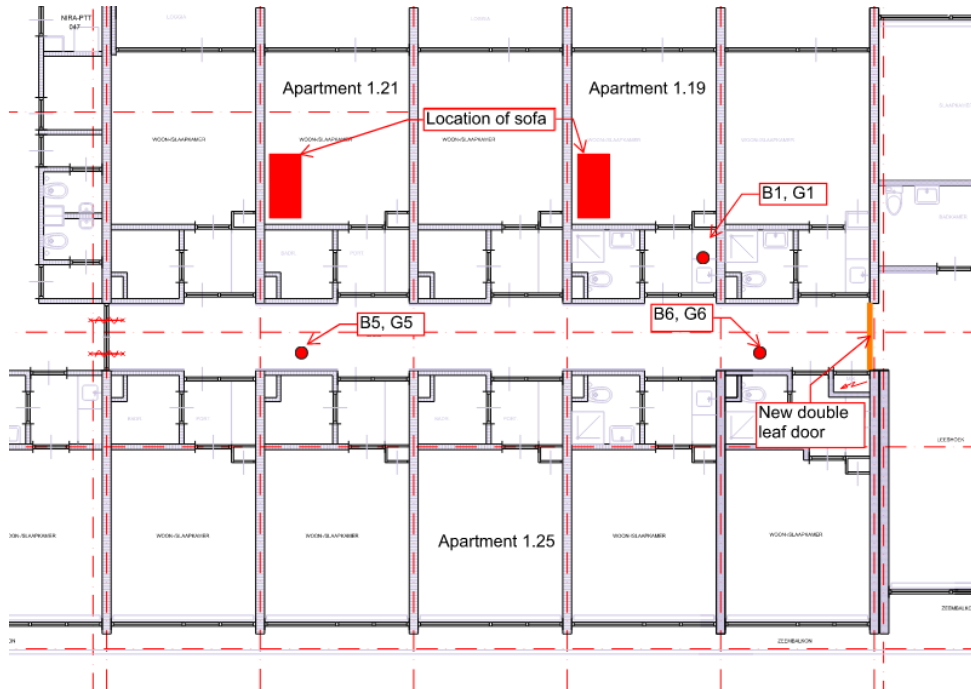


Figure 3: fire rooms, measuring trees, apartment with open door and location new door.

### 3.4.4 Simulating egress

To simulate the persons in the apartment fleeing from their apartment, during the experiments, the entrance door to the apartment was opened. This was done 5 minutes after the experiment started. In some experiments, the door was kept open while in others, the door was closed again 30 seconds after opening. This was done to check the effectiveness of door-control. In all scenarios, the door between apartment 1.25 and the corridor was left open.

### 3.4.5 Adjustments to the building

To protect the building and measuring equipment from extensive fire damage, adjustments were made to the building. This includes (but not limited to):

- The overhead wire-glass in wood-framing between the pantry and the living was removed in the fire room;
- The glass in the external façade was boarded over with a calcium-silicate fiber board (Promatect) to prevent the glass from failing;
- A new (non-combustible, non-asbestos) ceiling was installed in the corridor adjacent to the fire rooms.
- To limit the smoke buffering capacity of the corridor to a more generic situation an existing set of double fire doors was relocated, as shown in Figure 3.
- During the experiments, natural ventilation in the apartments was left open. The opening in the bathroom of the fire room was closed to limit smoke damage to the measuring equipment.
- All combustible materials other than the sofas are removed from the apartments. This also includes the kitchen and built-in wardrobe.

### 3.5 Measurements

During the experiments, several measurements were carried out to quantify several quantities during the scenario. A full overview of the used instruments is given in appendix 1. In Figure 3, the location of measurement trees B1, B5 and B6 is shown. In these trees, various equipment was present. The notions G1, G5 and G6 relate to gas measurements made in the respective trees. The location for measuring tree B5 and B6 were fixed, while B1 was moved to the used fire-room per experiment.

Measurement trees consisted of a stand with a height of approximately 2,4 meters with several joists attached. At the end of these joists, measurement equipment was mounted. While the exact location of the stand was measured during the experiments, the location of the equipment was not. A measurement tree is depicted in Figure 4.



Figure 4: example of a measurement tree

#### 3.5.1 Temperature measurements: thermocouples

In total 7 nickel-alloy K-type thermocouples with a bead diameter of 0,75 millimeter were placed in measuring trees B1, B5 and B6 each.

##### *Protective hoods*

Most thermocouples were fitted with a hood to shield them from water used to extinguish the fire by the fire department. The hoods consist of a steel cover with a rockwool inlaying. An opening of 3\*3 centimeters is present through which gases can flow and expose the thermocouple that is located inside. Figure 5 shows the protective hoods located in measuring tree B6.

The protective hood will affect the heat exposure of the thermocouples. Radiant heat fluxes are prevented from reaching the thermocouple. From a convective point-of-view, the small opening in the hood will act as a natural vent which imposes a resistance on the flow. That resistance is a function of the geometry of the vent and the roughness of its surfaces. That resistance results in a pressure drop that needs to be overcome by the conditions outside of the hood before the thermocouples are exposed. This makes the exposure of the thermocouples sensitive to the pressure buildup in the room.

Also, the protective hood introduces a mechanism in which it is expected the hood to alter the turbulent characteristics of the flow and altering the heat exchange between the thermocouple and the flow. In fact, the overall flow characteristics inside the hood are expected to be laminar to a certain extent<sup>1</sup>, which is also seen in the measurement results: almost no turbulence is observable. Furthermore, the

<sup>1</sup> Indicative calculations for the Reynolds number show values < 2.000 for the expected velocities (approximately 1-2 m/s) and temperature ranges (50-400°C).

effects of the hood depend on the angular placement of the hood with regards to the flow. Poor placement in the flow will further affect the exposure of the thermocouple. Lastly, the low thermal inertia of the rockwool will result in surface temperatures quickly following the gas phase temperature. At higher temperatures, the radiant exposure from the rockwool can result in higher temperatures, most notably in the cooling phase.



Figure 5: protective hoods

To study the effects of the protective hoods to some extent, the raw data for the plate thermocouple heat flux meters, located at a height of 0,3 (plate thermocouple 1.1.2) and 1,5 meters (plate thermocouple 1.1.1) in the apartment are compared with the thermocouple measurements (thermocouple 1.1.6 and 1.1.4) and measurements. As the thermocouple included in the plate thermocouple heat-flux meter is attached to a steel plate, some lag is expected between the gas phase temperature and the plate thermocouple.

The results for the experiment executed on the afternoon of the 4<sup>th</sup> of July are shown in the figure below. While the differences halfway over the height of the room are small, big differences are seen lower in the room, signifying the difference in radiant exposure.

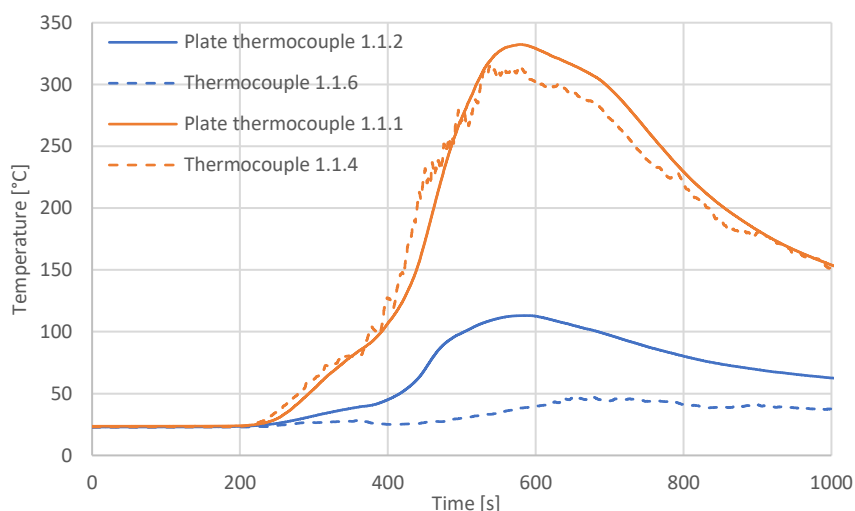


Figure 6: comparison between thermocouple measurements and raw data for the heat-flux measurements

In conclusion, the representativeness of the thermocouple measurements is questionable. It is likely a significant lag in both heating and cooling exists between the actual gas phase temperature near the measurement tree and the thermocouple measurement. The actual effects of the protective hoods is not further studied quantitatively, as this would derive the main objective of this thesis.

### 3.5.2 Gas samplers

During the experiments, gas samplers for (amongst others) O<sub>2</sub>, CO<sub>2</sub> and CO are used. During some experiments, measurements for HCN were carried out in the corridor. Given the fact that data on HCN is limited to some experiments only and information regarding to its generation in fires is limited, it is not taken into account in this thesis. Gas measurements were carried out at a height of 1,5 meters in the apartment (fire room) and at a height of 0,3 and 1,5 meters in the corridor.

Due to the nature of the gas-measurements (aspiration), a delay between the actual and measured values is expected. Given the available experimental data, the following delay time is taken into account in the results:

O<sub>2</sub>: 20 seconds.  
CO: 40 seconds.  
CO<sub>2</sub>: 15 seconds.

Note that these values might change per measurement location as the length of the tubing differed per scenario.

### 3.5.3 Pressure gauges

During the tests, pressures were measured at every measurement tree at a height of 0,2 meters. Two different gauges were used: one with a range of 0-50 Pa ('PL meter') and one with a range of -2500-2500 Pa ('PH meter'). The first having a high sensitivity (1,5 Pa) and low resolution (0,5 Pa) while the second has a lower sensitivity (25 Pa) and high resolution (10 Pa). Given the sensitivities, the lower range pressure measurements are favored over the higher range measurements. In some instances (e.g. under pressures or higher pressures) however, this is not possible.

### 3.5.4 Visibility

In the corridor, visibility is measured using photovoltaic cells at four points of which two are located at measurement tree B5 and two at measurement tree B6. In both cases, the height was 1,5 m and 0,3 m.

### 3.6 Relevant scenarios

As seen in Table 1, a variety of scenarios is available. In this thesis, a choice was made to only simulate baseline scenarios without additional measures such as the mobile watermist system or the airtight enclosure as these measures typically introduce a significant amount of complexity and uncertainty into the numerical simulations. Therefore, a choice was made to study three scenarios all with a differing expected level of ventilation:

- Balcony door open, with a choice between scenario 18 or 19.
- Door to corridor open with a choice between scenario 1, 3, 5 or 17.
- Door to corridor closed with a choice between scenario 4, 6 or 16.

### 3.7 Analysis of experimental results

In this paragraph, an analysis of the relevant scenarios as described in paragraph 3.6 is given. Only relevant experimental results are given in this part of the report. More results are included in appendix 2. For a complete overview, the reader is referred to [17]. As seen in appendix 2, similar trends are observable between the scenarios with similar boundary conditions (e.g. balcony door open), which is logical as the overall experimental conditions were similar. In this paragraph, experimental results are compared, both qualitatively and quantitatively.

While experiments typically lasted for approximately 45-50 minutes, this thesis focusses on the first 1.000 seconds (approximately 17 minutes) only as this is the most relevant timeframe for egress. Furthermore, the engineers who carried out the experiments noticed the weighing scale not working correctly during the first experiments.

### 3.7.1 Visual observations

Based on the available photographs taken of the sofas after the experiments, a similarity between different scenarios under the same ventilation conditions is noticeable. This is an indication that the overall combusted mass is comparable in scenarios with similar boundary conditions. Clear differences between scenarios with the corridor closed and scenarios with the door opened are noticeable. The combusted mass is significantly less in the scenarios with the door closed again after 30 seconds after being opened. This indicates those scenarios suffered from oxygen starvation, with the consequence being a lower reaction rate or (at some point) total extinction.



Figure 7: sofa after experiments for scenario 18 (left) and 16 (right), clear differences are observable relating to combusted mass.

In all scenarios, the main contribution to the overall combustion process is expected to be from the polyurethane foam inside the sofa. Some contribution from its wooden frame is to be expected, most notably in the scenarios with the balcony door and corridor door open.

### 3.7.2 Mass loss rate and heat release rate

As mentioned earlier, the mass loss measurements carried out in the first week of experiments failed. These include scenarios 1, 3, 4, 5 and 6. A clear indication of a faulty measurement lies in the fact that, while in those scenarios significantly lower mass loss rates were observed, temperatures and  $O_2$  concentrations were found did not show noteworthy differences compared to other scenarios. Data from the scenarios mentioned earlier is therefore not usable for deriving a heat release rate.

The mass loss rate and derived heat release rate for scenarios 16, 17 and 19 is shown in Figure 8. Note that an effective heat of combustion of 16 MJ/kg is used. This is derived in paragraph 4.3.

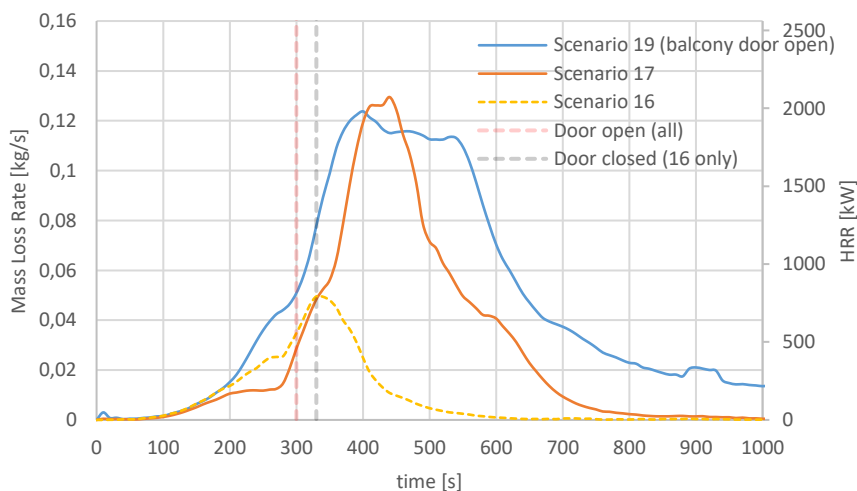


Figure 8: mass loss rate and derived heat release rate for several scenarios. The mass loss rate was time averaged over 30 seconds to limit the noisiness of the signal.

In the presented data, the effect of opening the door between the apartment and the corridor is visible through the fact that the mass loss rate rises exponentially directly after 300 seconds. At that point, extra oxygen becomes available, increasing the reaction rate. Note that the time averaging introduces some inaccuracies with regards to sudden increases or decreases in the mass loss rate.

### 3.7.3 Gas concentrations

Gas concentrations were measured at different locations and heights in the enclosure. The discussion in this paragraph is limited to oxygen and carbon monoxide measured in the apartment. Measurements done for CO<sub>2</sub> typically are a derivative of these results and are therefore not discussed.

Scenarios upon which similar boundary conditions are imposed show the overall same trends. In the experiments with the balcony door open (18 and 19), O<sub>2</sub> concentrations of approximately 10 %vol were measured, with a minimum of approximately 6-8 %vol being noticeable around 500 seconds. The initial trend with regards to the inclination of the initial drop also correlates well between scenarios. In these scenarios, significant differences exist between the measured CO concentrations. In scenario 18, values up to 20.000 ppm were measured. In scenario 19, the maximum value is approximately 7.000 ppm. This indicates that, even though the boundary conditions are similar, significant differences with regards to CO generation and the flame chemistry exist between scenarios.

Scenarios with the door to the corridor opened after 300 seconds (and left open afterwards, scenario 1, 3, 5 and 17) also show similar trends. The initial inclination of the initial drop in scenario 1 however, shows to deviate significantly from the others. This scenario was carried out in a different apartment, which might lead to some deviating boundary conditions such as leakage. The O<sub>2</sub> concentration in scenario 17 is shown to remain significantly lower after the minimum is reached. Minima of approximately 2-3 %vol were measured at a height of 1,5 meters. This indicates severe hypoxic circumstances. In these experiments, the CO concentration in the apartment shows a similar trend with the concentration remaining relatively low in the first 350-400 seconds followed by an exponential increase up to 20.000-30.000 ppm. At around this point, effects of oxygen deprivation are noticeable, which correlates well with the measured oxygen concentrations. During experiment 17, two doors to other apartments on the fire floor were accidentally not properly closed: a small slit is expected.

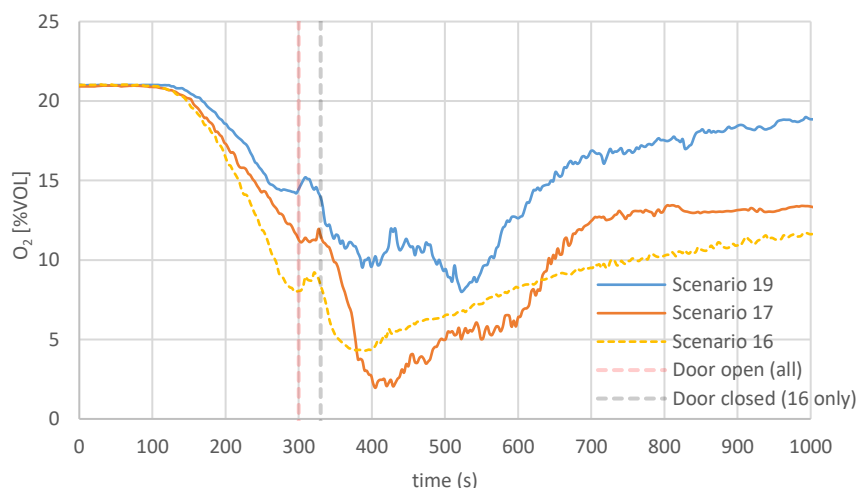


Figure 9: O<sub>2</sub> concentrations for scenario 16 (door closed), 17 (door kept open) and 19 (balcony door open).

Scenarios with the door opened after 300 seconds and closed again 30 seconds later show the same trends as observed in the scenarios described in the previous paragraph, with the exception of the O<sub>2</sub> concentrations reaching a minimum of approximately 5 %vol. That minimum is observed at an earlier time compared to the scenarios with the door kept open (350 seconds as opposed to 400 seconds). The CO concentration show to increase exponentially up to 20.000 ppm after the door is closed. This

coincides with the mass loss rate and pressure in the apartment dropping substantially, which is an indication of under-ventilated combustion taking place.

### 3.7.4 Temperatures

Scenarios using similar boundary conditions all result in comparable temperatures. Maximum temperatures lie around 400-500°C in the case of scenarios with the balcony door open and scenarios with the door to the corridor being opened. In the case of the scenarios in which the door to the corridor is opened and closed, maxima lie in the range of 250-300°C. This correlates well with the mass loss rates measured.

In all cases, significant lag exists between the peak in mass loss and the peak in temperature. This correlates with the statement made relating to the protective hoods being placed over the protective hoods.

### 3.7.5 Pressure evolution

In the case of the scenarios with the balcony door open, no significant increase or decrease of pressure is expected and observed. Only slight underpressures were measured as a result of the thermal stratification in the apartment. In the case of the scenarios with the balcony door closed, significant increase in pressure is observed prior to the door to the corridor being opened. After the door is opened, the pressure dissipates as hot gases are vented through the door. Maximum relative pressures measures are in the range of 30-50 Pa.

In the case of the scenarios with the door being closed again 30 seconds after being opened, a sharp peak in pressure is observed after the door is closed. That peak cannot be measured using the more accurate 'PL' pressure meters as it exceeds 50 Pa. The 'PH' pressure meter registered an overpressure of approximately 150 Pa prior to the pressure dropping to approximately -20 Pa, indicating the fire has grown to be under-ventilated. Note the accuracy of the of the 'PH' meter.

In several experiments, pressure measurements do not show logical results. In scenario 1 and 3, instant over-pressures are measured, which indicates either interference from an external source (e.g. wind-induced pressures) or a faulty measurement.

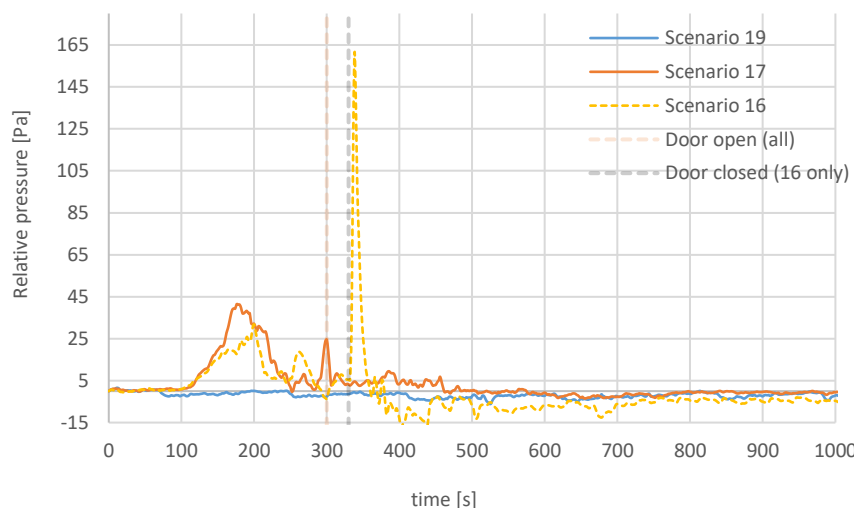


Figure 10: pressure evolution for scenario 16, 17 and 19 using the less accurate 'PH' pressure meters.

### 3.8 Chosen scenarios

Based on the observations made in paragraph 3.7, three scenarios are chosen to be used as a basis for case study CFD-simulations with FDS.

#### 3.8.1 Case study ‘balcony door open’

The scenario chosen as the variant with the balcony door open serves as an example of ‘overall well-ventilated burning’. This implies that the results of the simulation do not heavily rely on the extinction model included in FDS (described in paragraph 4.7). Both scenario 18 and 19 show the same trends in oxygen consumption, which can be seen as a proxy for the level of under-ventilation. In scenario 18 a minimum of approximately 6% is reached, while scenario 19 reaches a minimum of approximately 8%. While differences are small, it is expected that scenario 19 is less under-ventilated. The CO concentrations underline this.

Furthermore, the mass loss rate of scenario 18 shows a more hectic trend, indicating more spurious combustion as opposed to scenario 19, in which the mass loss rate curve is more fluid. The mass loss rate curve of scenario 19 will serve a better purpose for modelling the heat release rate of the fire.

Based on these observations, the choice was made to use scenario 19 as a basis for the simulations of the scenario with the balcony door open.

#### 3.8.2 Case study ‘door open after 5 minutes’

The scenario chosen as the variant with the corridor door open serves as an example of ‘overall under-ventilated burning’. In scenario 5, the mass loss measurements failed, which makes it hard to make an adequate estimate for the fires’ heat release rate. In scenario 17, some apartment doors were not closed appropriately, indicating more uncertainty.

Scenario 1 and 3 were carried out in the first week of experiments, which means the mass loss measurements might not be accurate. Using this data is therefore prone to error. The pressure-measurements in the fire room for scenarios 5 and 17 show a more logical trend as opposed to scenarios 1 and 3. As a result of the weight-loss measurements of the other scenarios either having failed or being unreliable and the pressure measurements showing a more logical trend, scenario 17 is chosen as a basis for the simulations with the door to the corridor opened after 5 minutes.

#### 3.8.3 Case study ‘door open after 5 minutes and closed again after 30 seconds’

In scenario 4, the measured mass loss rates is prone to error as the measurements were carried out in the first week. This makes estimating the fires’ heat release rate difficult. Scenario 16 shows a more straightforward mass loss rate curve. Relating to the oxygen depletion and temperature development in the apartment, only nuance differences are observed. This also translates to differences in the development of the relative pressures in the apartment.

Based on these observations, scenario 16 is chosen as a basis for the simulations with the door to the corridor opened after 5 minutes and closed again 30 seconds later.

#### 3.8.4 Overview

The following table outlines the chosen scenarios used as a basis to carry out simulations in FDS.

| Case study | Description                           | Scenario used | Date experiments | Apartment used as fire room |
|------------|---------------------------------------|---------------|------------------|-----------------------------|
| 1          | Balcony door open                     | 19            | 05-07-2019       | 1.19                        |
| 2          | Corridor door open                    | 17            | 05-07-2019       | 1.19                        |
| 3          | Corridor door closed after 30 seconds | 16            | 04-07-2019       | 1.21                        |

Table 2: overview of the used scenarios in this thesis

## 4. THEORETICAL FRAMEWORK

---

### 4.1 Introduction

This section of the thesis deals with the methodologies used to predict and simulate phenomena related to fire. This section is limited to the numerical methodology and sub-grid scale models employed by FDS. Furthermore it explores the methodology used to predict specie yields. An expanded theoretical framework is included in appendix 3 in which some of the fundamentals of CFD are discussed.

### 4.2 Fire Dynamics Simulator (FDS)

Fire Dynamics Simulator is a computational fluid dynamics model that is developed by the National Institute of Standards and Technology (NIST) [19]. The model revolves around a LES-formulation (Large Eddy Simulation) of the Navier-Stokes equations which is specifically designed to simulate low-Mach, buoyancy-driven flows. In the work presented in this thesis, version 6.7.6 of FDS is used.

#### 4.2.1 Large Eddy Simulations

Large Eddy Simulations (or LES) underlines the fact that large eddy structures are typically anisotropic as opposed to smaller eddies, which are typically of a more isotropic nature. This leads to a methodology in which eddies with a large length scale are directly resolved while the more universal smaller eddies can be accounted for using turbulence models.

The LES-methodology uses a filtering function to define a cutoff width. Eddies with a larger length-scale than a cutoff width are directly resolved while eddies with a smaller length scale are modelled using SGS-turbulence models (SGS: sub-grid scale). This directly links to the resolution of the computational mesh used in the simulations, as with a higher resolution, more eddies are expected to be directly resolved [20]. Given this numerical method, the quality of a LES is dependent on the resolution of the mesh. Checking the mesh for sensitivity therefore is a fundamental part of LES-simulations.

#### 4.2.2 Numerical characteristics of FDS

Computations are carried out using a rectilinear grid. The cutoff width used in the filtering operation under uniform cell sizes (cubical) is equal to the used cell width. This implies that eddies with a larger length scale than the cell width are directly resolved using the Navier-Stokes. Eddies with a smaller length scale are modelled using a SGS-model. By default (from version 6 onwards), FDS uses Deardorff's model for eddy viscosity to model eddies at SGS. It was chosen as a default model based on good comparisons with full-scale experiments. More SGS-turbulence models are available, with the most prominent being the Constant Smagorinsky model, which was the default value up to version 5 of FDS [21]. As the 'bulk-flow' turbulence models are ill-defined in close vicinity to an obstruction, a near-wall eddy viscosity model is used. By default, the WALE (wall-adapting local eddy-viscosity) model is used.

FDS uses four basic modes of operation: DNS (Direct Numerical Simulation), LES (Large Eddy Simulations), VLES (Very Large Eddy Simulations), SVLES (Simple Very Large Eddy Simulations). Differences between DNS and LES are discussed in appendix 3. The main difference between the VLES- and LES-mode is the imposed Courant-Friedrichs-Lewy (CFL) Constraint. The CFL-constraint is the main imposed restriction on the maximum time step. In VLES-mode, the CFL is less restrictive compared to LES-mode. In its essence, restricting the time steps results in a more stable simulation. SVLES-mode limits the maximum number of pressure iterations to 3 instead of 10. It also uses a different near-wall eddy viscosity model.

By default, thermal radiation is modelled using a grey-gas radiation model with 100 radiation angles. The emissivity and absorptivity of gases are calculated using RadCal. In LES, a specific radiative fraction is prescribed to the fires' heat release rate, with the default value being 0,35. In this thesis, the default value for the radiative fraction in FDS is used, which is 0,35. This corresponds quite well with values

found for polyurethane flames in literature [22]. This states that, depending on the equivalence ratio of the fire (see paragraph 4.5.1), a radiative fraction between 0,3 and 0,4 is expected.

FDS has a number of SGS-models included to predict fire related phenomena. These models include, but are not limited to: combustion, extinction and leakage. The used models in this thesis are discussed in the following paragraphs.

For the baseline simulations, the default numerical scheme of FDS is used in this thesis. To study the sensitivity of the results to the default settings, some settings are changed as part of a sensitivity study.

### 4.3 Heat Release Rate and heat of combustion

In FDS, the Heat Release Rate is calculated as:

$$\dot{Q} = \dot{m} * \Delta H_c * X$$

|                |                         |         |
|----------------|-------------------------|---------|
| $\dot{Q}$ =    | Heat Release Rate (HRR) | (kW)    |
| $\dot{m}$ =    | Mass Loss Rate (MLR)    | (kg/s)  |
| $\Delta H_c$ = | Heat of combustion      | (kJ/kg) |
| $X$ =          | Combustion efficiency   | (-)     |

During the experiments, weight-loss measurements were carried out. Therefore, the mass loss rate is known and is directly prescribed in FDS, bypassing the need for more complex pyrolysis modelling. The heat release rate of the fire is then calculated as the product of the mass loss rate, heat of combustion and combustion efficiency. The latter two are typically combined into the 'effective heat of combustion', which assumes the combustion efficiency remains constant over the duration of the fire. Typical values for the combustion efficiency of polyurethane foams range from 0,7-0,8 [22].

In fires suffering from oxygen starvation, the combustion efficiency is expected to become transient at some point [22]. Including transient effects in the heat of combustion is not possible using the simple one step combustion scheme included in FDS. When using multi-step combustion schemes, the effective heat of combustion can be calculated by FDS through the enthalpy of reaction of the involved species.

#### 4.3.1 Estimating the effective heat combustion

Literature indicates the effective heat of combustion differs heavily per experiment. As mentioned before, it is a function of the equivalence ratio of the fire but is also effected by the geometry of the fuel source, impurities in the fuel and temperatures in the enclosure. Methodologies to measure the effective heat of combustion, such as cone calorimetry, lead to values ranging from 16-22 MJ/kg [23]. Typical values for the effective heat of combustion of polyurethane filled sofas found in calorimetry experiments (mostly well-ventilated circumstances) range from approximately 22 MJ/kg to as low as 14 MJ/kg [24] [25] [26] [12]. Given the wide distribution found, simply selecting one value found in literature leads to uncertainties. Therefore, the effective heat of combustion is calculated using an energy balance, which is based on the 'MQH-correlation' for layer temperature [27] [28]:

$$\dot{m}\Delta H_{c,eff} = \sqrt{\left(\frac{\Delta T}{6.85}\right)^3 * A_0\sqrt{H_0}h_kA_t}$$

Where  $h_k$  is the overall heat transfer coefficient,  $A_t$  is the surface through which heat losses occur,  $\Delta T$  is the temperature difference and  $A_0\sqrt{H_0}$  is the ventilation coefficient.

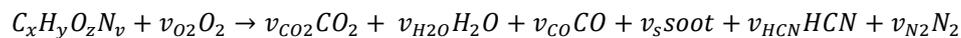
This correlation is only valid for well-ventilated fires. Furthermore, fires flush in corners or walls should be handled with care. For these fires, other entrainment coefficients are proposed in the literature [29]. However, more recent data suggests the effects of the corner position on the entrainment rate in the fire plume is limited if a small gap is present between the wall and the fire seat [30]. The original correlation is used in this thesis.

To avoid using data from under-ventilated or smoldering fires, data from 100-300 seconds is used. As the thermocouple probe is located at some distance from the seat and is located in a corner of the enclosure, its overall representativeness for the 'layer temperature' is questionable. Furthermore, the protective hoods (see paragraph 3.5.1) are expected to affect the representativeness of the measurements. As such, the normative thermocouple is used to calculate the temperature difference. Also, it is expected that the floor of the compartment has negligible effect on the overall heat transfer in this timeframe, the area is excluded from the calculations. Using this method results in an effective heat of combustion of approximately 16 MJ/kg, which fits the values found in literature quite well.

#### 4.4 One step combustion model

Directly simulating combustion in a CFD-simulation in a large scale fire application is not possible due to the fact that the area where the reaction occurs (e.g. the flame sheet) is subgrid-scale. Therefore, a combustion model is used.

As a default, FDS uses an infinitely fast, single-step combustion model. The combustion is only controlled by the mixing of the fuel with oxidizer and can therefore be seen as an approximation of reality (in literature, this type of 'Eddy Dissipation Concept' model is typically characterized as 'mixed=burned'). Due to the infinite fast reactions, the resulting flame temperatures are adiabatic. The simple combustion model assumes a chemical reaction in the general form of:



The stoichiometric constants (denoted  $v_{xx}$ ) for CO, soot and HCN are calculated based on the post flame specie yields, which are prescribed by the user. The other stoichiometric yields are then calculated based on the conservation of mass. Per its formulation, the single-step combustion model does not enable transient specie yields over time. This is problematic, as in under-ventilated fires (e.g. fires with an equivalence ratio > 1), the yields are transient to an exponential extent.

#### 4.5 Species generation in under-ventilated fires

As fires grow more under-ventilated, the combustion becomes more sooty and the fire starts to generate more products of incomplete combustion such as carbon monoxide and hydrogen cyanide. This principle is shown in the next images [31].

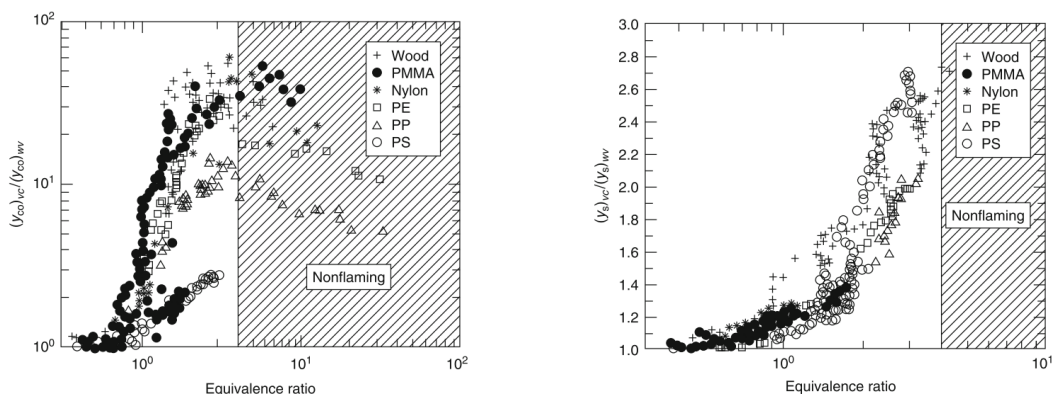


Figure 11: generation of CO and smoke as a function of the equivalence-ratio. Copied from [31]

Given the restrictions imposed by the single-step combustion scheme used by FDS (no transient yields), selecting one yield to account for the entirety of the fires' duration is problematic, given the fact that the experimental data used is composed of under-ventilated fires. Selection of specie yields of under-ventilated fires is possible through empirical correlations derived from (amongst others) Figure 11. For the relation between the well-ventilated CO yield and the under-ventilated CO yield of a material, the correlation reads:

$$\frac{(Y_{CO})_{VC}}{(Y_{CO})_{WV}} = 1 + \frac{\alpha}{\exp(2.5 * \Phi^{-\xi})}$$

In which  $\alpha$  and  $\xi$  are correlation coefficients that depend on the chemical structure of the fuel.  $\Phi$  is the equivalence ratio of the fire.

The same relation is derived for the soot yield:

$$\frac{(Y_{soot})_{VC}}{(Y_{soot})_{WV}} = 1 + \frac{\alpha}{\exp(2.5 * \Phi^{-\xi})}$$

For the hydrocarbon yield, it reads:

$$\frac{(Y_{HC})_{VC}}{(Y_{HC})_{WV}} = 1 + \frac{\alpha}{\exp(5 * \Phi^{-\xi})}$$

No data is available on the correlation coefficients for polyurethane and we therefore need to make a valid assumption. Data for nylon (CH1.8O0.17N0.17) is available and resembles the chemical composition of polyurethane closest. This yields the following correlation coefficients [31]:

|       | CO       |       | HC       |       | Soot     |       |
|-------|----------|-------|----------|-------|----------|-------|
|       | $\alpha$ | $\xi$ | $\alpha$ | $\xi$ | $\alpha$ | $\xi$ |
| Nylon | 36       | 3     | 1200     | 3,2   | 1,7      | 0,8   |

Table 3: correlation coefficients for nylon

#### 4.5.1 Estimating the equivalence ratio

The equivalence ratio of a fire gives an indication on the dilution of the oxygen supply with regards to the oxygen necessary for complete combustion. Generally, the equivalence ratio can be specified as the actual fuel-to-air ratio divided by the stoichiometric fuel-to-air ratio. This implies the available oxygen for combustion needs to be estimated. Several methods for calculating the equivalence ratio exist, two of which (the global equivalence ratio and the plume equivalence ratio) are described in detail in appendix 3 of this document.

In the framework of this thesis, the concept of the plume equivalence ratio is used to estimate the equivalence ratio of the fire. While the concept is ill-validated, it allows direct correlation of the equivalence ratio with the measured oxygen concentrations in the apartment. Furthermore, it assumes all oxygen available in the fire plume can be used for combustion. This is fundamentally incorrect, as the tendency of oxygen to be used for combustion depends on the efficiency of the chemistry and the involved kinetics, which in turn depends on quantities such as temperature.

The plume-equivalence ratio is calculated by:

$$\varphi_p = \frac{\dot{m}_f / \dot{m}_{O_2,reacting}}{\dot{m}_f / \dot{m}_{O_2,stoich}} = \frac{\dot{m}_f}{\dot{m}_{O_2,reacting}} * \Psi_O$$

|                            |   |         |
|----------------------------|---|---------|
| $\varphi_p$ =              | plume equivalence ration (PER)                          | (-)     |
| $\dot{m}_f$ =              | mass of reacting fuel                                   | (kg/s)  |
| $\dot{m}_{O_2,reacting}$ = | mass of oxygen available for reaction in the fire plume | (kg/s)  |
| $\Psi_O$ =                 | stoichiometric mass oxygen-to-fuel ratio.               | (kg/kg) |

The mass of the reacting fuel is directly taken from the mass loss measurements. The stoichiometric oxygen-to-fuel ratio is calculated from the chemistry. The available mass of oxygen in the fire plume needs calculation using empirical correlations. A correlation for the entrained mass in the fire plume is derived by Heskestad in [32]:

$$\dot{m}_{ent,L} = 0.878 * \left[ \left( \frac{T_L}{T_\infty} \right)^{5/6} \left( \frac{T_\infty}{T_L} \right) + 0.647 \right] \frac{\dot{Q}_c}{c_p T_\infty}$$

|                     |  |
|---------------------|--|
| $\dot{m}_{ent,L}$ = | entrained mass over length of the fire-plume (kg/s)        |
| $T_L$ =             | Flame temperature at the flame-tip (estimated to be 500K)  |
| $T_\infty$ =        | Temperature in the compartment, averaged from measurements |
| $\dot{Q}_c$ =       | Convective part of the heat release rate (kW)              |
| $c_p$ =             | specific heat of air (1 kJ/kg*K)                           |

More in-depth information is available in appendix 3.

#### 4.6 Two-step simple combustion model in FDS

As an alternative to the single-step simple combustion model, FDS has a two-step combustion model included. In its essence, the two-step combustion model first lets the fuel react with oxygen to produce carbon-monoxide, soot and other products. The second step involves the remaining oxygen reacting with the soot and carbon-monoxide to carbon-dioxide. Both reactions are carried out serially and are assumed to be infinitely fast.

As a default value, in the first step, two out of three carbon atoms in the fuel are converted to carbon-monoxide and soot. There is not yet a valid scientific basis for this assumption. Furthermore, one out of five nitrogen atoms are converted to HCN. Details are outlined in [21] and [33]

While this model does enable FDS to account for CO and soot generation in under-ventilated fire conditions, its validation is limited to the near-field region. Moreover, the FDS Users Guide states that this model should only be used if there is special interest in near-field radiant heat fluxes as a result of heightened CO and soot concentrations within the flame envelop.

This methodology underlines the fact that chemistry in fires (and in general) consists of multiple intermediate reactions. In reality however, a multitude of reactions are expected to occur. Furthermore, the only variable in this method is the available oxygen in the grid cell. In reality, a multitude of variables are of importance on the efficiency of the chemical kinetics (e.g. gas phase temperature). It does however, enable FDS to include transient chemistry, albeit rudimentary (if not fundamentally incorrect).

#### 4.7 Flame extinction

Handling extinction of a diffusion flame due to underventilation or introduction of a suppression agent in a CFD-model is difficult as the involved mechanisms typically occur at a sub-grid scale. Therefore, an extinction model is used. In general, flames are extinguished because the flame temperature drops below a certain value or the oxygen supply is diluted.

By default, FDS uses an extinction model that uses the concept of the critical flame temperature (abbreviated: CFT). The default model is model 2 as shown in Figure 12. For combustion to occur, there must be enough fuel and oxygen present to raise the cell temperature to the CFT of the imposed

reaction. This relation is depicted in the user guide of FDS [21] and is shown in the right-hand image in Figure 12.

The default value for the CFT is a common value for hydrocarbon fuels (1.427°C). For generic engineering studies, [34] states a value of 1.300°C can be used. This concept only takes into account thermal quenching. Kinetic and aerodynamic quenching are not taken into account. In this study, the fire is expected to be smothered as a result from oxygen dilution. Therefore, taking into account only thermal quenching is appropriate.

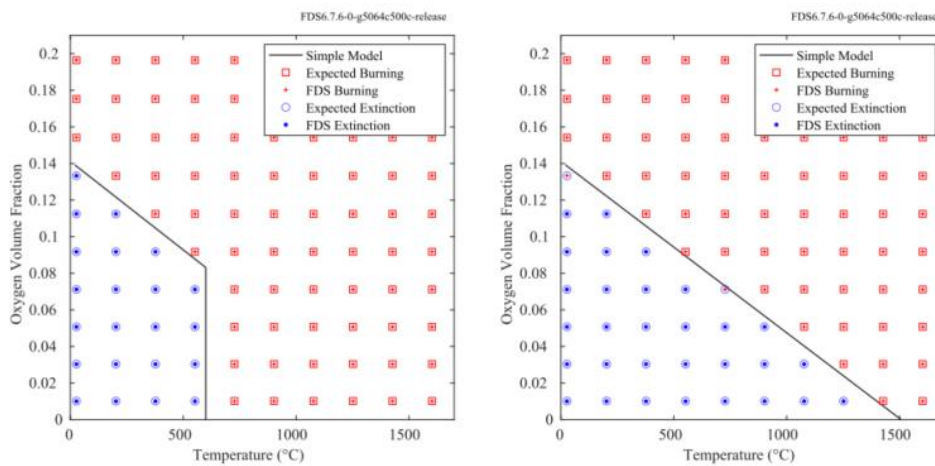


Figure 12: Extinction model 1 (left) and 2 (right) used in FDS. Copied from [19].

The temperature in a cell in LES depend on the cells dimensions. Some grid-dependency is in place. Therefore for under-ventilated fires, the importance of simulating with a high grid-resolution (at least in the near-field region) is important to model extinction accordingly.

The CFT can be calculated through the oxygen index and calorific energy output of the fuel:

$$T_{OI} = T_o + X_{OI} * \frac{\Delta H_c / r}{n * \bar{c}_p}$$

In which  $T_o$  is the ambient temperature (293°K),  $\Delta H_c / r$  is the heat of combustion per mole of oxygen consumed, which depends on the modelled reaction.  $n$  is the number of moles of products per mole of mixture fuel/air which also depends on the reaction, as does  $\bar{c}_p$  which is the specific heat of the products at constant pressure in the range of  $T_o - T_{OI}$ . In this thesis, the specific heat of the products is taken as an average over the ambient temperature and 1.000K. While the critical flame temperatures for the prescribed reactions are expected to be of a higher order, a lower value is opted for to account for the temperature dependency of the specific heat of the products. As this is arbitrary in essence, the critical flame temperature is subjected to a sensitivity study.  $X_{OI}$  is the lower oxygen limit, which is discussed in more detail in the next paragraph.

For coarse-grid simulations, FDS has another extinction model included (extinction model 1 in Figure 12). It underlines the fact that, in numerical setups using a relatively coarse grid, the temperatures near the flame sheet are not well resolved. It therefore depends less on the CFT-concept and more on the lower oxygen limit. It assumes that, should a cell temperature exceed the free burn temperature (default value is 600°C for flashed-over fires), the fuel is allowed to burn. This model is used to check sensitivity of the scenarios.

#### 4.7.1 Lower Oxygen Limit/Index

The lower oxygen limit (LOL, sometimes referred to as the lower oxygen index) is the lowest oxygen concentration in %vol at which flaming combustion is sustained at room temperature. The LOL is typically measured using bench-scale measurement techniques in which the oxygen concentration available for combustion is slowly decreased. Typical values for the LOL of polyurethane foams range from 15-22 %vol [35]. However, the test method for the oxygen index for liquids and gases, which is used in the extinction model of FDS, is not equivalent nor comparable to the test method for the oxygen index for solids. Differences exist in the test setup, but more importantly the extinction mechanisms for solids lie in both the solid phase and the gas phase where the main extinction mechanisms for liquids and gases lie more in the gas-phase. The oxygen index of solids should therefore not be used to calculate the critical flame temperature [23]. As such, the default value of 0,135 [19] is used in this thesis and is checked for sensitivity to limit uncertainty. Also, as no complex pyrolysis model is used, the solid-phase holds limited relevance for flame extinction.

#### 4.7.2 Auto-ignition of unburned fuel

Should the oxygen-source of the fire be diluted to the extent combustion is not possible within the framework of the extinction model, the unburned fuel, which is introduced in the computational domain by the pyrolysis model, is tracked. Should sufficient oxygen become available elsewhere, ignition of the fuel can still occur, given enough fuel and oxygen are available to satisfy the burn-criterion imposed by the extinction model. By default, no temperature dependency is assumed. This means the fuel will combust should sufficient fuel and oxygen be available. In under-ventilated situations, this can lead to unrealistic combustion away from the fire seat at places where oxygen becomes available, such as vents. An example from an early iteration of one of the CFD-models is given in Figure 13.

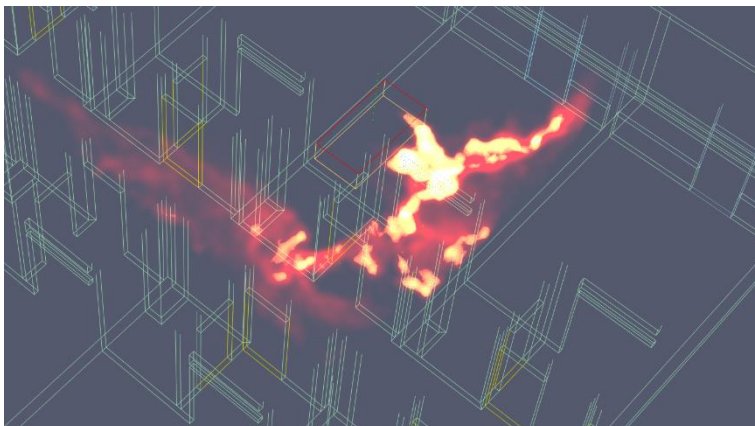


Figure 13: Combustion in the corridor without taking into account an auto-ignition temperature

In reality, whether or not a fuel will combust depends (among others) on temperature of the gas-phase in which the fuel is located. Given the fact that the fuel-source is a solid, no exact data is available on the auto-ignition temperature of pyrolyzate of polyurethane foam [23]. For most gaseous fuels, the AIT is stated to be between 150-500°C.

In experimental research regarding the ignition of polyurethane foams, Rein et al. found that, dependent on sample thickness, the average temperature which denotes the onset for flaming combustion is approximately 425 °C [36]. The experiments used a cone heater to heat the surface of the fuel. Quintiere [37] states that generic flexible foam plastics typically have an ignition temperature of approximately 390°C. Note that this is only a crude proxy for the auto-ignition temperature.

Based on these findings, an auto-ignition temperature of 400°C is used in the simulations. This is checked for sensitivity in one of the case studies. Ignition is simulated by excluding the volume above the fire seat from the auto-ignition temperature.

## 4.8 Fire growth

In the experimental results, the fire source is defined by the mass loss rates of the sofas. As the fuel is a solid, the fire area and flame location is expected to be transient over time and has influence on the development of the fire driven flows in the enclosure. In this work, the surface area of the sofa is simplified to a rectangular horizontal surface with an area of 2 m<sup>2</sup>. Accounting for transient behavior of a fire in FDS is possible using a ramp function or by assuming a radially growing fire.

By using a ramp function, the mass flow rate of the fuel is equally divided over the area of the surface of the fuel. In dynamic fire growth, flame-lengths and resulting plume temperatures are not estimated correctly. The momentum of a fire plume is very much dependent on the flame length and temperature of the plume and is essential in predicting the capabilities of the plume penetrating an already present hot smoke layer. This will result in a less 'sharp' stratification in the enclosure when compared more realistic fire growth modelling.

The fires' heat release rate and area can typically be defined using an exponential fire growth curve and a Heat Release Rate per unit area (HRRPUA in kW/m<sup>2</sup>):

$$\dot{Q} = \alpha t^n$$

$$A_{fire} = \frac{\dot{Q}}{\dot{Q}''}$$

In which  $\alpha$  is the fire growth parameter,  $t$  is the time after the start of flaming combustion in seconds and  $n$  is the fire growth exponent.  $A_{fire}$  is the area of the fire seat and  $\dot{Q}''$  is the heat release rate per unit area (HRRPUA). Most commonly, an exponent of 2 is used to model radially spreading fire. In this specific instance, fire growth is more complex as it involves both horizontal and vertical fire growth. Using a different exponent might be more appropriate.

Typically, modelling physical fire spread is a more justified approximation of reality as the flame length and consequently the momentum of the fire driven flow are simulated more realistic. Therefore, modelling physical fire spread is favored over using a ramp function in this thesis. There are however scenarios in which closely following the fires' mass loss rate curve is essential (e.g. in the case of pressure buildup in an enclosure as a result of fire). In these cases a ramp-function is used. Sensitivity of the results is checked using either methodology.

## 4.9 Modelling leakage

Leakage through cracks and joints in the modelled enclosure typically occurs at subgrid-scale and therefore needs to be modelled. In FDS, leakage can be modelled using two specific methods:

- Using bulk leakage;
- Using localized leakage.

### 4.9.1 Bulk leakage

In most cases, the exact location of leakage is not known. Therefore, leakage needs to be addressed in a generic way, using bulk-leakage. Bulk leakage uses pressure zones in the model to quantify the pressure differences in the domain. The used pressure is the same everywhere in the pressure zone and can therefore not take into account omnidirectional leakage in one pressure zone. This can result in pressure oscillations over time. Volume flows are calculated by the leakage area  $A_L$ , the pressure difference  $\Delta p$  and the ambient density  $\rho_\infty$  by:

$$\dot{V}_{leak} = A_L \text{sign}(\Delta p) \sqrt{2 \frac{|\Delta p|}{\rho_\infty}}$$

In a typical building, the leakage area tends to grow as pressure differences increase as a result of cracks and gaps opening up more. To account for this, the leakage area can be modified over the increase of pressure using the leak pressure exponent:

$$A_L = A_{L,ref} \left( \frac{\Delta p}{\Delta p_{ref}} \right)^{n-0.5}$$

By default,  $n$  is taken as 0,5 (no pressure dependency) and  $\Delta p_{ref}$  is 4 Pa. This method assumes the shape and length of cracks and gaps is relatively low and the gas leaking exchanges sufficient heat with the inner surface of the crack to assume the leaking gas is of the same temperature as the wall surface.

#### 4.9.2 Localized leakage

To account for local pressure differences instead of using one 'bulk' pressure, the localized leakage method can be used. This method can take into account omnidirectional flows in the enclosure but does necessitate the location and characteristics of the cracks to be known. Volume flows are calculated in the same way as with the bulk-leakage model, but use local pressure. When using localized leakage no pressure-dependent alterations to the leak area can be made.

Enabling leak enthalpy allows FDS to account for the heat losses from the leaking gases to the obstruction. It does so by adding the temperature difference between the temperatures of the flow and the wall to the cell adjacent to the leak. If disabled, the temperature of the outflowing gases is assumed to be equal to the temperature of the surface of the wall where the gases exit the leak. In reality, heat transfer inside leaks is more complex and expected to be much less binary in nature.

#### 4.9.3 Measured airtightness

During the Oudewater experiments, the air-tightness of the apartments was measured. The blowerdoor-tests were carried out in accordance with the Dutch standard NEN 2686 and the European standard EN-ISO 9972 with the aim of gaining insight in the airtightness of the rooms in which the experiments were to be carried out. The measurements were carried out with the natural ventilation in the apartment open and closed. Also, an indication was given regarding the leakage through the façade and internal separations. Results are shown in Table 4 [38].

| Apartment | Natural ventilation | Leakage area (cm <sup>2</sup> ) | Leakage exponent n (-) |
|-----------|---------------------|---------------------------------|------------------------|
| 1.21      | Open                | 227                             | 0,56                   |
|           | Closed              | 136                             | 0,68                   |
| 1.20      | Open                | 191                             | 0,65                   |
|           | Closed              | 125                             | 0,59                   |
| 1.19      | Open                | 164                             | 0,56                   |
|           | Closed              | 61                              | 0,68                   |

Table 4: results of the airtightness measurements

A significant amount of variation is observed between the apartments. Prior to the fire experiments, minor alterations to the enclosure of the apartments were carried out to minimize these differences. As a result of these modifications, the results of the measurements should be seen as an indication. No information is known on the leakage area in the enclosure to the hallway. In the scenarios where pressure buildup plays a significant role in the smoke propagation, the airtightness is checked for sensitivity.

#### 4.10 Soot deposition

While FDS incorporates a soot deposition model, it is not used in the work presented in this work. This implies soot concentrations in the simulations are to a certain extent over-estimated.

## 5. NUMERICAL SETUP

### 5.1 Modelled geometry

The geometry was modelled using Pyrosim. The first floor of the apartment-complex was modelled, but the numerical grid is limited to the apartment with the fire seat, corridor and apartment 1.25. By doing so, it is assumed that the gases leaking to other enclosures than the corridor vent directly to the ambient. This is justified, as the experimental results do not show significant pressure buildup in the adjacent apartments. The model is shown in the following figures. Initial temperatures in the enclosure are set at the average temperature in the apartment for each case study. During the experiments, some temperature differences existed between the apartment and the corridor. This is not further taken into account.



Figure 14: model layout with relevant information given (left) and close-up of apartment (right). Note that in the case of apartment 1.21 being used as the fire room, the geometry is altered.

### 5.2 Devices

During the experiments, data on (among others) temperatures, gas concentrations and pressures was collected using several devices located on three measuring trees. The location of the measurement trees is specified in Figure 3 and Figure 14. The experimental equipment is modelled in FDS as follows:

- Thermocouples are modelled as thermocouples with a bead diameter of 0,75 millimeter.
- Gas samplers are modelled as gas phase devices measuring the gas concentration of the specie of interest (volumetric fraction).
- Pressure gauges are modelled as gas phase devices measuring the relative pressure.
- Visibility: see 5.2.1.

Note that the exact location of the equipment was not specified during the experiments. The location of the stand was therefore used as a proxy for the location of the equipment.

#### 5.2.1 Special topic: visibility

Visibility is modelled using gas-phase devices. The visibility is calculated using the light extinction coefficient  $K$  and the intensity of monochromatic light  $I$  passing a distance  $L$  through the smoke [39]:

$$\frac{I}{I_0} = e^{-KL}$$

The light extinction coefficient  $K$  can be estimated as the product of the mass specific extinction coefficient  $K_m$  and the density of smoke particulate  $\rho Y_s$ :

$$K = K_m \rho Y_s$$

The mass specific extinction coefficient  $K_m$  is fuel dependent and is by default set at 8.700 m<sup>2</sup>/kg, which the FDS User's Guide [19] specifies as a value common for the burning of woods and plastics and was derived by Mulholland et al for a multitude of experiments [40]. The default value is not changed.

The visibility in a homogeneous smoke filled environment can then be estimated by:

$$S = C/K$$

Where  $C$  (the 'visibility factor') is a non-dimensional empirical constant which depends on the object being viewed through smoke. Values described in the original publication by Jin in 1970 range between 5-10 for lighted signs and 2-4 for a non-lighted sign [41]. During post-processing of the experiments, a value for 3 was used. This value is typically used in situations where the object viewed does not emit light but rather reflects it. Therefore, in the simulations, that value is used accordingly.

Its description directly shows the downside of using this methodology in CFD-simulations or experiments in which homogeneity of smoke is not expected. This method is therefore only a convenient way to correlate a smoke density to a 'visibility length', which in fact does not say anything about the actual visibility at all.

### 5.3 Thermophysical characteristics of the enclosure

To implement heat transfer between the enclosure and the hot gases, the enclosure was modelled with specific characteristics relating to its thermophysical behavior. The following characteristics are modelled:

| Part                     | Material               | $\rho$ (kg/m <sup>3</sup> ) | $k$ (W/mK)           | $c_p$ (kJ/kgK) | $\epsilon$ (-) |
|--------------------------|------------------------|-----------------------------|----------------------|----------------|----------------|
| Floors, walls            | Concrete               | 2.280                       | 1,8                  | 1,04           | 0,9            |
| Doors                    | Wood                   | 640                         | 0,14                 | 2,85           |                |
| Fire protective boarding | Calcium silicate       | 720                         | 0,12                 | 1,25 – 1,55*   |                |
| Façade glazing           | Double glazing         | 2.500                       | $5,68 \cdot 10^{-3}$ | 0,72           |                |
| False ceiling hallway    | Calcium silicate board | 720                         | 0,12                 | 1,25 – 1,55*   |                |
| Inner walls corridor     | Calcium silicate stone | 1.900                       | 0,75                 | 0,84           |                |

\* Temperature dependent: 1,25 kJ/kgK at ambient, 1,55 kJ/kgK at 600°C

Table 5: thermophysical characteristics

Please note that the emissivity of the surface is relevant as during the experiments soot is deposited on the materials surface. Using an emissivity of 0,9 is assumed to be an appropriate assumption. All surfaces are modelled to be backed by an air gap with a constant temperature (20°C), which given the experimental results in the other apartments is justifiable.

### 5.4 Leakages

Leakage from both the apartment and the corridor is accounted for using the bulk leakage model. As the leakage from the apartment to the corridor through the apartment door is of special interest, this leakage path is modelled using the localized leakage method. The leakage area for the door is assumed to be 10 cm<sup>2</sup>, which is arbitrary and therefore checked for sensitivity. The leakage area over the door is divided over four localized leakage paths: one below the door (75%) and three on the top and two sides of the door (in total 25%). The choice was based on expert judgement. The bulk leakage area is then calculated as the measured leakage area minus the assumed door leakage area.

The leakage pressure exponent  $n$  is set to 0,56 for both apartments in the simulations. As the leakage area is prone to uncertainty (see paragraph 4.9.3) an a-priori sensitivity study is carried out in scenarios 2 and 3 to study the effects of the airtightness on the fire-induced pressure differences in the apartment. In his thesis, M. Scholman [14] states that, based on a visual inspection, he found that the double doors in the corridor both have a leakage area of approximately 200 cm<sup>2</sup> each. As there is no further information available regarding these doors, this information is used in the model. Furthermore, the doors to the other apartments are also expected to be prone to leakage. These doors swing away from the pressurized space, whereas the door between the apartment in which the sofa is burning and the corridor swings towards the pressurized space. This affects the leakage area over those doors. Based on data given in the EN 12101-6 [42], doors swinging outwards from a pressurized space typically will have double the leakage area of a door swinging inwards. Therefore, a leakage area of 20 cm<sup>2</sup> per door is assumed. A total leakage area of 560 cm<sup>2</sup> was used in the corridor, with leaks modelled using the bulk leakage method.

## 5.5 Initial fire characteristics

### 5.5.1 Methodology

Over the course of the different case studies, choices were made with regards to the method by which different parameters for the fires' definition are modelled. Most notably, during case study 2 the method of modelling fire growth by means of a  $\alpha t^n$ -curve was dropped as it results in unrealistic pressure evolutions in the enclosure. Instead, a static fire area is modelled. Furthermore, in case study 2, the default single step combustion model of FDS was dropped in favor of the two step combustion model to (crudely) account for increased CO and soot generation as a result of underventilation. This implies that:

- No  $\alpha t^n$ -curve is used in case study 3. It is however, shown in paragraph 5.5.2 for the sake of completeness.
- No static yields for CO and soot are calculated in case study 3. The equivalence ratio and static yields are however, are shown in paragraph 5.5.3 for the sake of completion.

### 5.5.2 Heat release rate

The heat release rate of the different fires is prescribed in the model as a mass flow rate of fuel that is generated over the surface of a vent. In the case of a static fire area, one vent is used. In the case of a radially spreading fire, numerous smaller vents are used. The following graph shows the imposed heat release rate per case study. An effective heat of combustion of 16 MJ/kg was used to calculate the heat release rate from the mass loss rate.

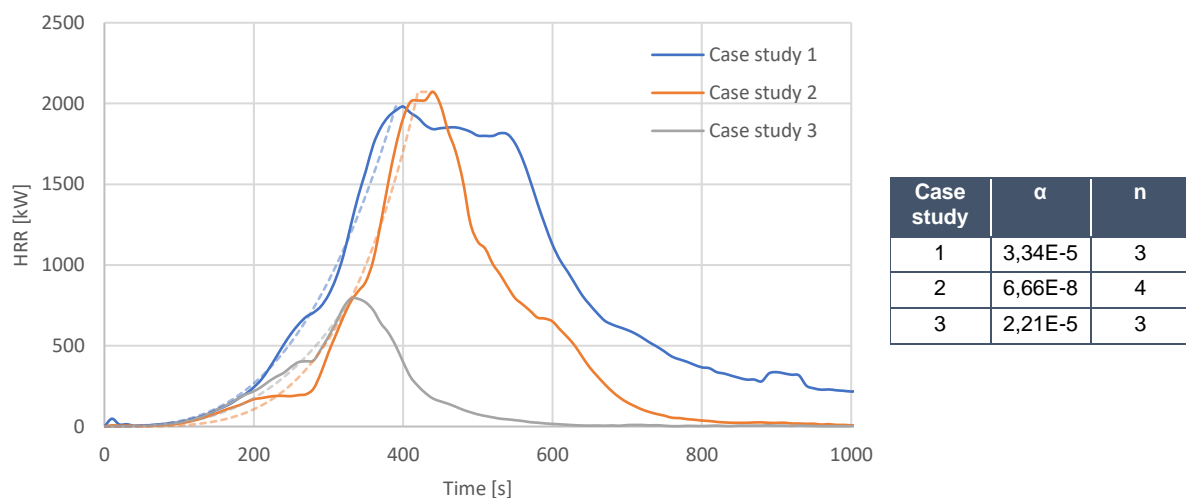


Figure 15: the imposed heat release rate per case study. Dotted lines show the best fit  $\alpha t^n$ -curve for which the parameters are shown in the table on the right.

### 5.5.3 Prescribed chemistry

Several methodologies were used to model the combustion chemistry. In case studies 1 and 2, the default single step combustion model of FDS was used. As that approach performed poorly in case study 2, it was dropped in favor of a two-step combustion model in which the transient CO and soot generation over the fires' development is (crudely) accounted for. As such, for case study 3, no static CO and soot yields are calculated using the equivalence ratio approach. Instead, well ventilated post-flame yields are imposed initially. For the sake of completion and comparing different scenarios however, the equivalence ratio of case study 3 is included in the next figure. As mentioned earlier, the used concept is ill-validated and can be used as a crude approximation at best. In all calculations, the chemical composition of polyurethane GM21 was used, with a stoichiometric oxygen-to-fuel ratio of approximately 2,2 kg/kg. Well ventilated species yields for polyurethane GM21 are taken from [43].

The choice for polyurethane GM21 is not substantiated and differences between most notably the yields between different types of foam are substantial. This is therefore checked for sensitivity.

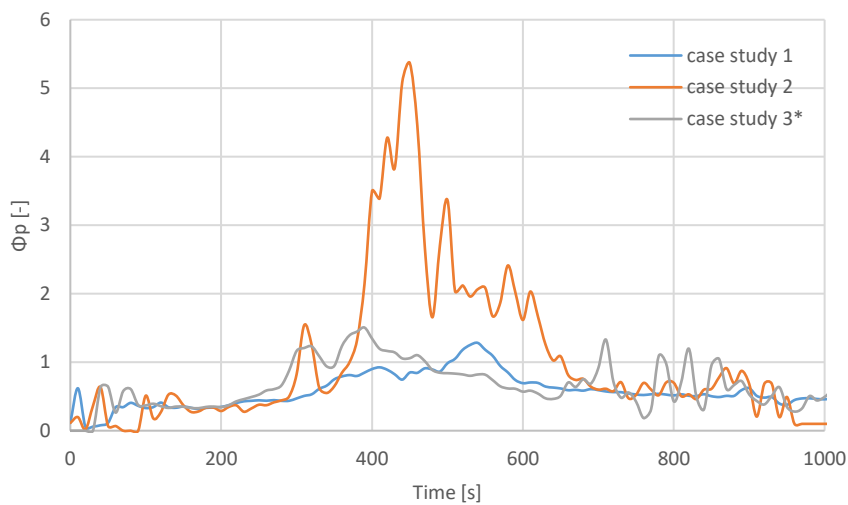


Figure 16: Calculated plume equivalence ratio for the case studies. \* the plume equivalence methodology was not used in case study 3.

Directly calculating the species yields using the maximum equivalence ratio will result in significant over-estimates for CO and soot in the early stages of the fire. Therefore, the species' yield is calculated per time-step and a 90-percentile (arbitrarily chosen) of the found values is used as a static yield in the simulations. This results in the following species post-flame yields:

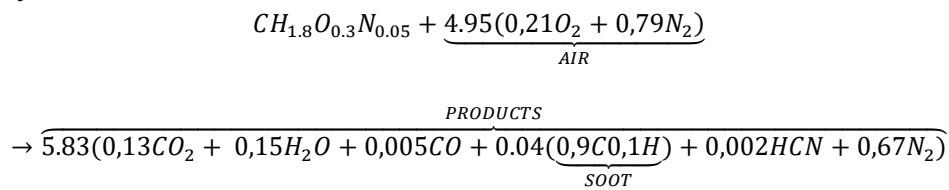
| Case study  | Description                       | CO yield [kg/kg] | Soot yield [kg/kg] | HCN yield [kg/kg]** |
|---|-----------------------------------|------------------|--------------------|---------------------|
| -   | Well ventilated polyurethane GM21 | 0,01             | 0,13               | 0,002               |
| 1   | Balcony door open                 | 0,04             | 0,14               | 0,035               |
| 2   | Door opened and left open         | 0,22             | 0,19               | 1,22                |
| 3*  | Door opened and closed            | 0,07             | 0,15               | 0,15                |
| * Not used in the simulations, only shown for comparative purposes.   |                                   |                  |                    |                     |
| ** These values are unrealistic and in one case defies the conservation of mass. As HCN is not studied in detail in this work, a value of 0,02 is assumed for under-ventilated burning. |                                   |                  |                    |                     |

Table 6: Calculated species' yields

Note that the results directly show the effects of the problematic assumption of all oxygen being readily available for combustion in the equivalence ratio concept when compared with the experimental results. Experimental results for case study 3 clearly show an exponential increase in CO in the enclosure, which is not readily expected when looking at the plume equivalence ratio for case study 3.

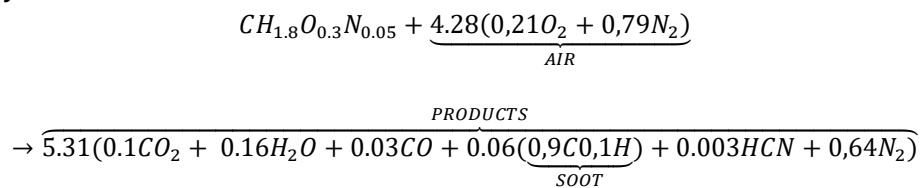
Given the chosen yields, the following chemical reactions are modelled in case studies 1 and 2. The chemistry for case study 3 is discussed in chapter 8.

#### Case study 1



In this reaction, the oxygen-to-fuel ratio is 1,72 kg/kg.

#### Case study 2



In this reaction, the oxygen-to-fuel ratio is 1,49 kg/kg.

#### 5.5.4 Extinction parameters

In this work, the default extinction model of FDS ('extinction model 2') is used primarily. Parameters associated with that model are the critical flame temperature (CFT) and lower oxygen limit (LOL. As discussed in paragraph 4.7, the default value for the lower oxygen limit is used (0,135) while the critical flame temperature is calculated from the defined reaction. The used values are shown in Table 7.

| Case study | Description  | CFT [°C] | LOL [%vol] |
|------------|--|----------|------------|
| -          | Well ventilated polyurethane GM21, $\Delta H_{c,eff}=16$ MJ/kg | 1.090    | 0.,135     |
| 1          | Balcony door open  | 1.140    | 0,135      |
| 2          | Door opened and left open                                      | 1.350    | 0,135      |
| 3          | Door opened and closed   | 654      | 0,08       |

Table 7: used extinction parameters

During case study 2, it was found that using the calculated critical flame temperature did not result in acceptable results. A parametric study was carried out to find extinction parameters that do give appropriate results. The found values for the CFT and LOL were then used in case study 3 as a form of verification. This is further elaborated on in chapter 7.

In case studies 1 and 2, the used parameters are checked for sensitivity. Furthermore, sensitivity is checked against the alternative extinction model (see paragraph 4.7).

#### 5.6 Post-processing of results

Results are time averaged during post-processing to limit the effects of the numerical model. The averaging period is chosen based on the parameters studied. However, a minimum of approximately 5 seconds is used. In the case of gas concentrations, the error between the numerical and experimental results is quantified using a relative error, which is calculated as follows:

$$Relative\ error\ [\%] = \frac{Numerical\ results - Experimental\ results}{Experimental\ result} * 100\%$$

## 5.7 Numerical grid

The numerical grid is initially chosen in such a way the enclosure can easily be modelled. The initial level of refinement is chosen in line with the non-dimensional expression  $D^*/\delta_x$ , where  $D^*$  is a characteristic fire diameter. This method gives an indication of how well the flow field involving buoyant plumes is resolved.

$$D^* = \left( \frac{\dot{Q}}{\rho_\infty c_p T_\infty \sqrt{g}} \right)^{2/5}$$

In which ratios of  $D^*/\delta_x = 4, 10$  and  $16$  represent a course, moderate and fine mesh refinement [19]. This correlation holds true in near-field locations. Elsewhere in the domain, different cell sizes can be used. However, resolving more complex flows such as vent flows and ceiling jets can also heavily depend on the used grid resolution. It is therefore necessary to check the grid for sensitivity.

In the scenario's studied, a moderate mesh refinement translates into a mesh-size of  $10*10*10$  cm (total of 380.000 cells), while a mesh size of  $5*5*5$  cm (total of 2,6 million cells) can be seen as a fine mesh refinement. A further refinement in the apartment is studied as the extinction model is prone to sensitivity to the mesh resolution: a mesh resolution of  $2,5*2,5*2,5$  cm is used in the apartment and a small part of the corridor. Elsewhere in the domain, a resolution of  $5*5*5$  cm is used. This results in an overall cell amount of approximately 9 million cells. However, as these simulations are significantly computationally heavy, the simulations were run only for a limited time, with a minimum of 450 seconds of simulated time.

### 5.7.1 Used infrastructure and MPI-processing

Simulations ran on the high performance computing infrastructure (HPC) of UGent. MPI-processing was used to speed up simulations:

- For the moderate refinement, 10 processors were used.
- For the fine refinement, 32 processors were used.
- For the extra fine refinement, 96 processors were used.

The used clock speed of the physical processors depended on the available computation clusters.

## 5.8 Grid sensitivity study

The used grid resolution is chosen based on a grid sensitivity study. While the study was carried out for all three case studies using the numerical setup described in this chapter, it goes beyond the purpose of the main text of this document to discuss all results in detail as all scenarios show the same trends. Therefore, the overall effects of the grid resolution are discussed, after which a resolution is chosen. Note that, as the 'moderate' refinement did not result in appropriate results in case study 1, it was dropped for the other case studies. A more comprehensive description of the grid sensitivity study per case study is included in appendix 4.

### 5.8.1 Heat Release Rate

The fires' heat release rate is shown to be affected to a limited extent by the grid resolution. Some differences are noticeable in case study 2, which is shown in Figure 18 and Figure 19. These differences are explainable through the sensitivity of the extinction model to the grid resolution as a result of local temperatures being predicted more accurate in a finer mesh, as explained in paragraph 4.7. In both case studies 1 and 3, the differences are shown to be negligible.

Given the level of ventilation in case study 1, the extinction model is expected to be less sensitive to the used grid resolution. In case study 3, temperatures in the near-field region are not elevated to a high enough extent to affect the extinction model.

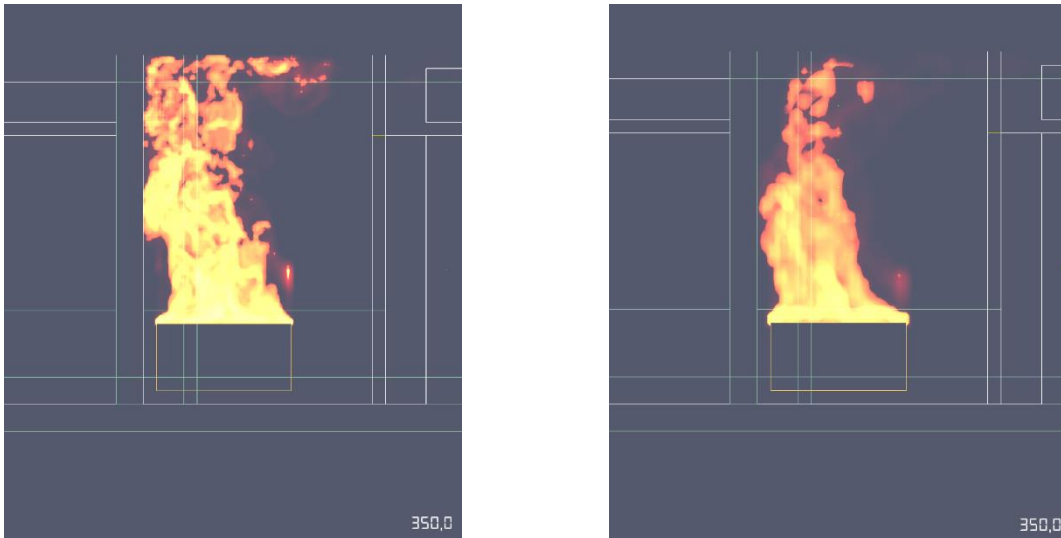


Figure 17: HRRPUV (side view) of case study 2 at 350 seconds for both a 'extra fine' (left) and 'fine' (right) grid resolution. Notice the differences near the ceiling of the apartment.

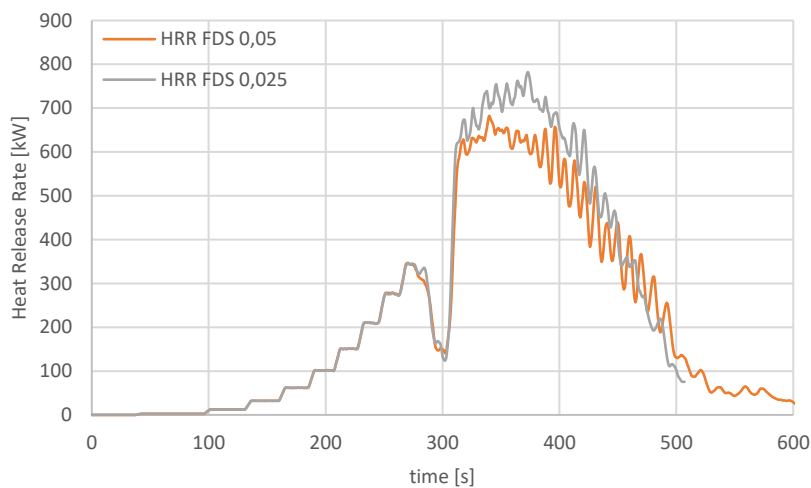


Figure 18: heat release rate of case study 2 for both a 'fine' and 'extra fine' grid resolution. Notice the higher peak in the 'extra fine' mesh.

### 5.8.2 Gas concentrations

In all case studies, the gas concentrations in apartment show limited sensitivity to the used grid resolution. In case study 1 however, the 'moderate' mesh resolution resulted in a higher oxygen concentration in the apartment in the initial phase of the fire. This can be attributed to the fact that the mass flow rate over the balcony door is over-predicted when using the moderate mesh compared to the other two grid resolutions.  $O_2$  concentrations in the apartment are shown in Figure 19. In the corridor, the results at a height of 0,3 meters show some sensitivity to the grid resolution as a result of the interface of the smoke layer being predicted more accurately in the simulations using a finer grid.

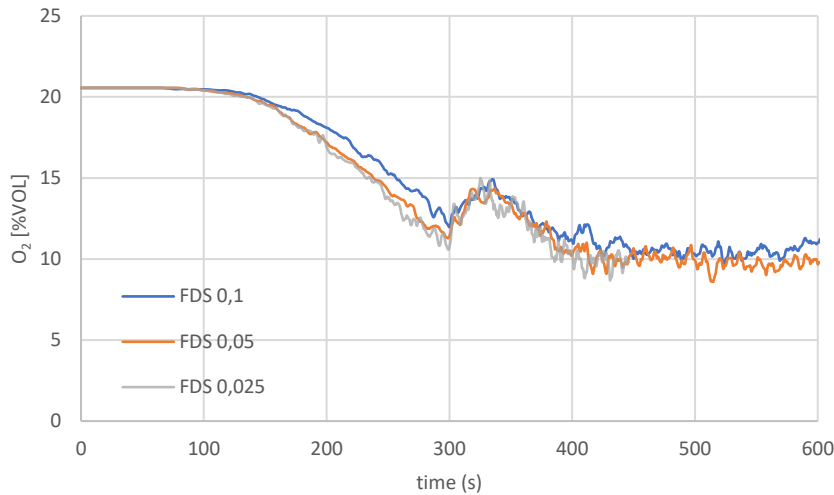


Figure 19: O<sub>2</sub> concentration in the apartment for case study 1 for a 'extra fine' (0,025), 'fine' (0,05) and 'moderate' (0,1) grid resolution.

In the case of case study 3, the CO concentrations in the apartment are somewhat affected by the resolution of the numerical grid. These differences are in the order of magnitude of 500 ppm and are a result of slight differences in combusted mass.

### 5.8.3 Pressures and mass flow rate over vents

During the initial period of the simulations, in which the fire is sufficiently ventilated, pressures do not show significant sensitivity to the used grid resolution. Afterwards, when underpressures are observed, the pressure starts to oscillate as a result of the principles behind the bulk leakage model. At that point, significant differences are observed.

As discussed in paragraph 5.8.2, the mass flow rate over the balcony door in case study 1 shows to be overestimated in the grid with a 'moderate' resolution. The difference between the fine and 'fine' and 'extra fine' resolution is negligible. The mass flow over the door between the apartment and the corridor however, is somewhat higher in the 'extra fine' mesh, compared to the other two. This is observed in all case studies. While no definitive explanation is given, the reason might lie in the complexity of the flow in the kitchen area. Resolving these to a high enough extent might necessity a grid resolution of a high order. Qualitative differences are noticeable between the structure of the eddies in the 'fine' and 'extra fine' grid resolutions. Some quantitative nuance differences exist with respect to the velocity of the flow, as shown in Figure 21.

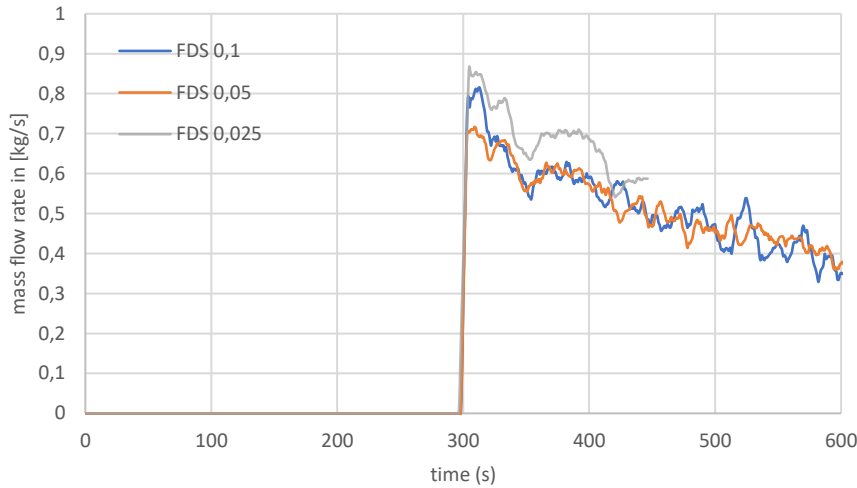


Figure 20: mass flow rate over the door to the corridor for case study 1 for a 'extra fine' (0,025), 'fine' (0,05) and 'moderate' (0,1) grid resolution.

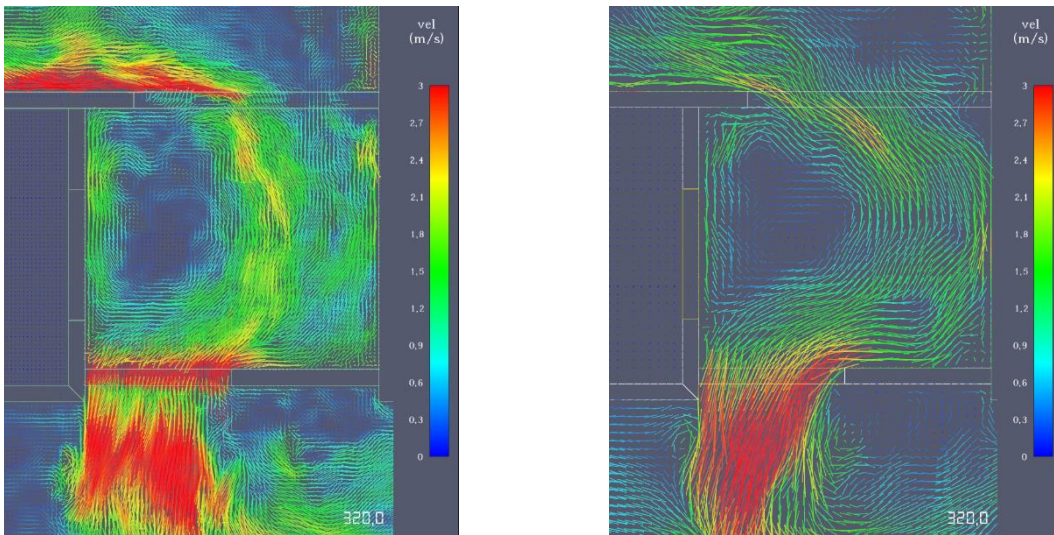


Figure 21: velocity vectors in the kitchen for case study 2 and over the door towards the corridor at a height of 1,8 meters and 320 seconds. Results for an 'extra fine' (left) and 'fine' (right) grid resolution are shown. Differences in the structure and velocity of the eddies are observable.

### 5.8.4 Temperatures

In case studies 1 and 3, the temperatures in the apartment do not show significant sensitivity to the used grid resolution. An example for case study 1 is given in the left image in Figure 22. In the corridor, differences are more pronounced.

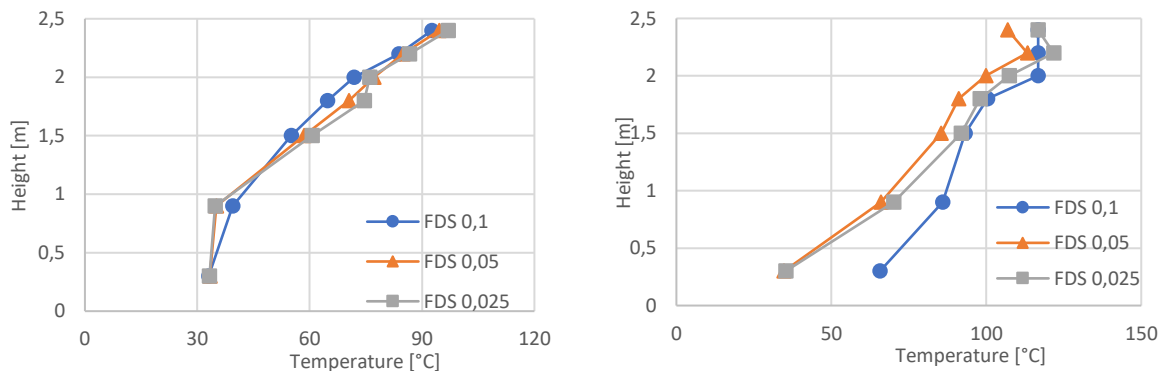


Figure 22: temperatures at measuring tree B1 at t=150 seconds (left) and at tree B5 at t=400 seconds (right) for case study 1.

As mentioned in paragraph 5.8.1, a higher heat release rate is observed in case study 2 in the simulation with a 'extra fine' grid resolution. This directly results in higher temperatures in the enclosure.

### **5.8.5 Used grid resolution**

Results for a uniform numerical grid with cell dimensions 10\*10\*10 cm (moderate) showed some deviations from the higher resolution grids with regards to mass flow rates over vents, gas concentrations and temperatures. This grid resolution is therefore not chosen.

The simulations with a numerical grid with cell dimensions 2,5\*2,5\*2,5 cm showed a somewhat higher heat release rate in case study 2 compared to a numerical grid with cell dimensions 5\*5\*5 cm as a result of the grid dependency of the extinction model. Furthermore, it showed to better resolve the flow over the door between the apartment and the corridor. However, differences relating to the gas concentrations and temperatures in the corridor are relatively small. Furthermore, models ran with that grid resolution counted approximately 9 million cells, and showed computational times of approximately 5 days (wall time) on 96 cores for 450 seconds of simulation time. This is impractical as multiple iterations of the same case study are run in the form of a sensitivity study.

As a result, the 'fine' grid resolution is chosen for all case studies. It consists of a uniform numerical grid with approximately 2,6 million cells with a 5\*5\*5 cm dimension. While the computational time varies per simulation, all models finished within 36 hours (wall time) on 32 cores.

## 6. RESULTS CASE STUDY 1: BALCONY DOOR OPEN

### 6.1 Description of experimental setup

The experiments used as the data set for this case study took place in the afternoon of July 5<sup>th</sup>. Apartment 1.19 was used as the room in which the fire seat was located. During the experiments, the balcony door was left open. Furthermore, the door to the corridor was opened after 300 seconds and left open for the remaining duration of the fire.

More numerical results are included in appendix 5 of this work.

### 6.2 Results in the apartment

The numerical results show flame extinction occurring as a result of low O<sub>2</sub> concentrations in the apartment. While the experimental data, combined with an effective heat of combustion of 16 MJ/kg suggest a peak heat release rate of approximately 2 MW, the numerical results show a peak of approximately 1,5 MW. As shown in the following figures, combustion does take place primarily above the fire seat. As the fire grows more under-ventilated, minor combustion in the smoke layer is observed. No external combustion or combustion in the proximity of the door towards the corridor is observed as the local temperatures do not exceed the prescribed auto-ignition temperature of 400°C.

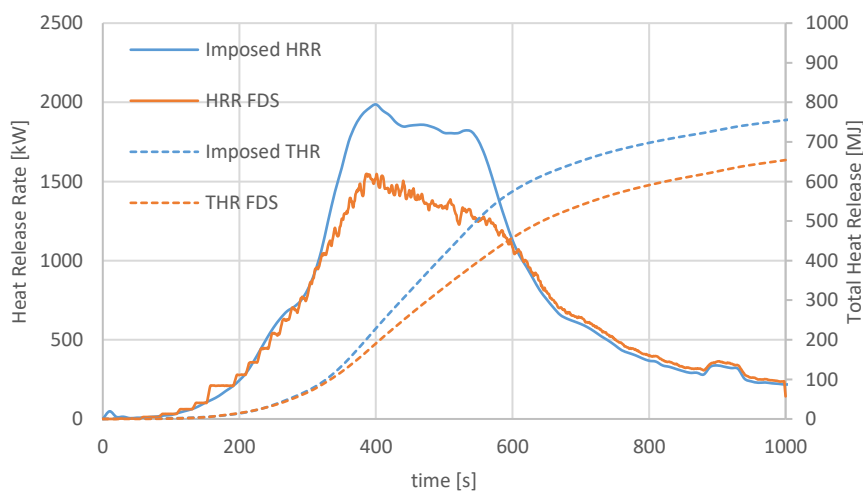


Figure 23: Heat Release Rate for case study 1

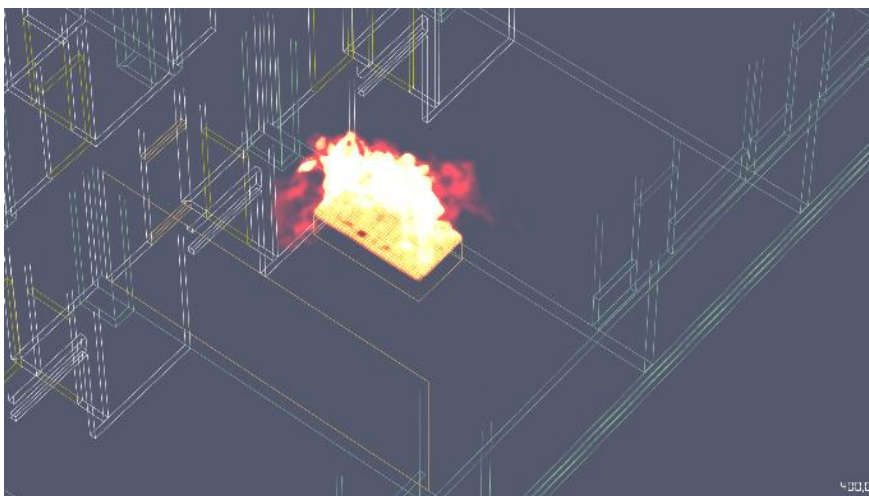


Figure 24: HRRPUV at 400 seconds. Some combustion occurs away from the fire source, underneath the ceiling. No external combustion or combustion near the door towards the corridor is observed.

The trends relating to the O<sub>2</sub> concentration are captured correctly by FDS, which indicates the overall chemistry, fluid dynamics and extinction phenomena in the apartment are modelled and predicted to an acceptable level of accuracy. Just prior to opening the door at 300 seconds, notable differences are observed that could be caused by some flame extinction occurring in reality that is not accurately predicted by FDS. After opening the door, the heat release rate predicted by FDS shows a less steep slope compared to the experimental data. This relates to the O<sub>2</sub> concentration dropping significantly faster in the experimental data. Here, FDS predicts flame extinction that in reality is not likely to have occurred.

Taking into account the initial difference in O<sub>2</sub> concentration in the apartment, the maximum relative error between the experimental and numerical results in the initial 250 seconds is approximately 3%, which is acceptable given the involved uncertainties. At a later stage, after the door is opened at 300 seconds up to the point the O<sub>2</sub> starts to increase again at approximately 500 seconds, differences become more apparent, with relative differences up to 25% being observed. The minimum O<sub>2</sub> concentrations and overall trends in the first half of the simulation however, are predicted to an acceptable level of accuracy.

From 500 seconds onwards, the oxygen level recovers more slowly in FDS. This can most likely be attributed to a more smoldering combustion in reality which uses less oxygen but produces more carbon monoxide. This also relates to the higher CO concentrations and lower CO<sub>2</sub> concentrations in this stage of the fire. Smoldering combustion is not taken into account by FDS in its default settings (it always models flaming combustion).

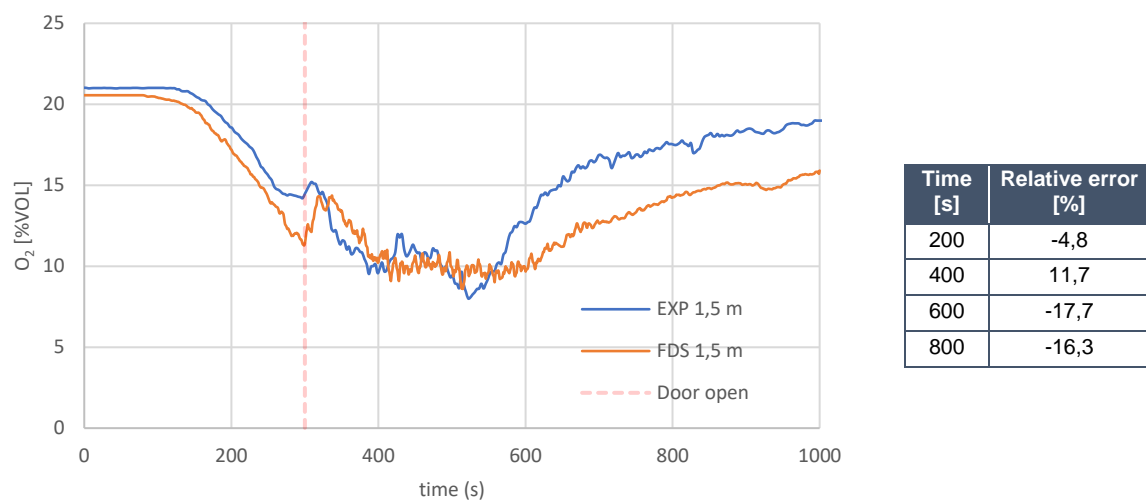
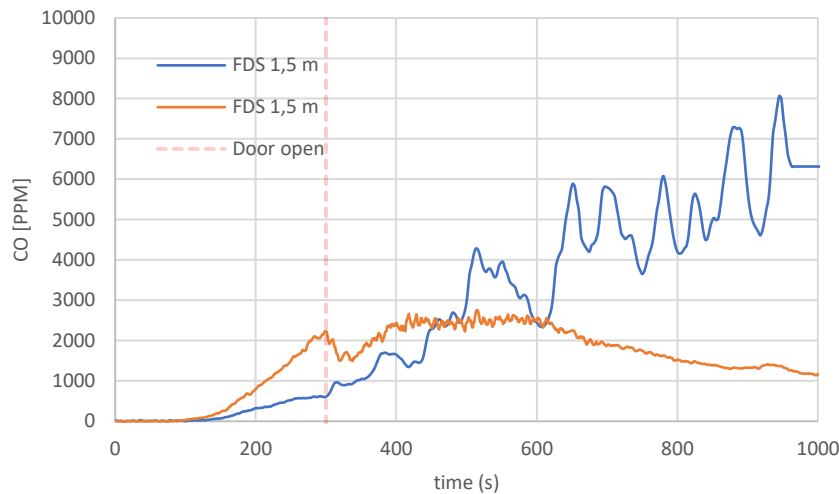


Figure 25: O<sub>2</sub> concentrations for case study 1. The relative differences take into account the initial difference between the numerical and experimental data.

Given the static nature of the combustion model, CO concentrations are over-estimated by FDS in the initial stage of the fire. After approximately 500 seconds, the experimental values for CO become significantly higher than predicted by FDS. The smoldering combustion mentioned earlier, the inability of FDS to account for transient CO generation in its simple combustion model and the wooden doorframe in the apartment showing some surface degradation after the experiments ended could account for this difference.

Given the fact that the O<sub>2</sub> concentration in the apartment is predicted to an acceptable level, and the overall CO concentrations are relatively low, the CO<sub>2</sub> concentration is predicted accurately as well.



| Time [s] | Relative error [%] |
|----------|--------------------|
| 200      | 158,4              |
| 400      | 46,5               |
| 600      | 0,24               |
| 800      | -64,5              |

Figure 26: CO concentrations for case study 1.

Numerical results for temperatures in the apartment show clear deviations from the experimental data, with the experimental lagging behind the numerical results. This is observed clearly in Figure 27, which depicts the thermocouples located at a height of 2,2 (TK1,1,1) and 2,0 (TK1,1,2) meters. As discussed in paragraph 3.5.1, the protective hoods over the thermocouples affect the overall heat exposure to a significant extent of which the observed lag between the numerical and experimental is a result. Note that, given the limitations imposed by the protective hoods, only a qualitative comparison of the results is made. Given the trends in the numerical and experimental data being similar, the moment at which flame extinction occurs is expected to be predicted to an appropriate extent. The trends with regards to temperatures are shown to be predicted relatively well by FDS. However, significant uncertainty is present in the experimental data.

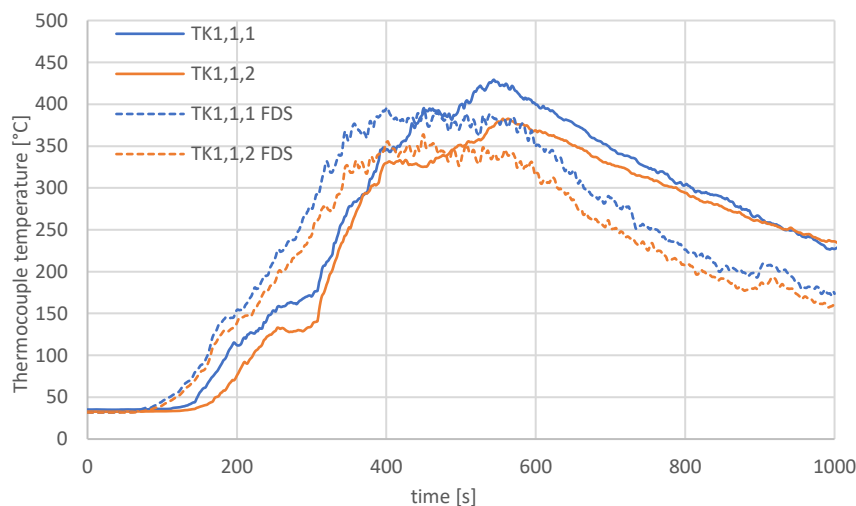


Figure 27: Temperatures in the fire room for case study 1.

As a result of the geometric configuration with regards to the location of the fire seat, a complex flow forms in the kitchen leading to a thermal gradient higher in the enclosure. This is graphically shown in Figure 29, in which the velocity vectors give an indication of the flow characteristics. The isosurface showcases the thermal gradient. The thermal gradient makes measuring the temperatures with point measurements such as thermocouples very sensitive to the exact placement of equipment. The location of the thermocouples in the FDS model is an approximation of reality as only the location of the stand was known. The thermocouples are located on joists connected to the stand and are located more to the center of the kitchen, which is shown in Figure 4 earlier in this work. This is expected to affect the

thermal exposure to a certain extent. Moreover, the angular placement of the protective hood is expected to pronounce its aerodynamic effects on the thermal exposure of the thermocouple, given the shown flow characteristics.

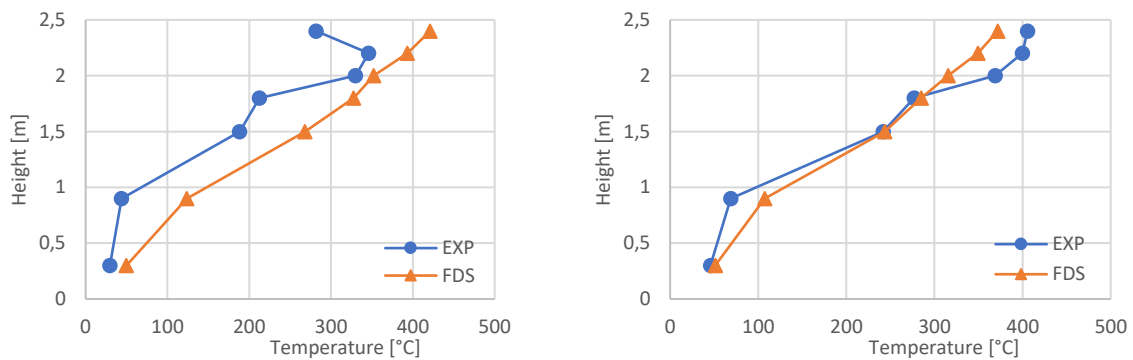


Figure 28: Temperature distributions over the height of the enclosure at t= 400 seconds (left) and t=600 seconds (right).

In a later timeframe, after the door has opened and a more or less steady state situation is achieved (between 400-600 seconds) the flow in the kitchen starts to become more uniform and the thermal gradient becomes less pronounced. At this moment an adequate comparison between the CFD-simulations and experimental results is observed, as shown in Figure 27. Given these arguments, it is likely that the temperatures predicted by FDS are a more reliable representation of the actual gas phase temperature than the actual measurements, at least in the stage prior to flame extinction.

Lastly, while the extinction model of FDS predicts the oxygen consumption in the domain to an acceptable extent in the growing and steady burning phase, an overshoot is observed around 500 seconds. At this time, the temperature in the apartment is significantly higher than the simulated temperatures. This indicates a higher heat release rate. Given the static nature of the combustion and extinction models however, it is not possible to predict this.

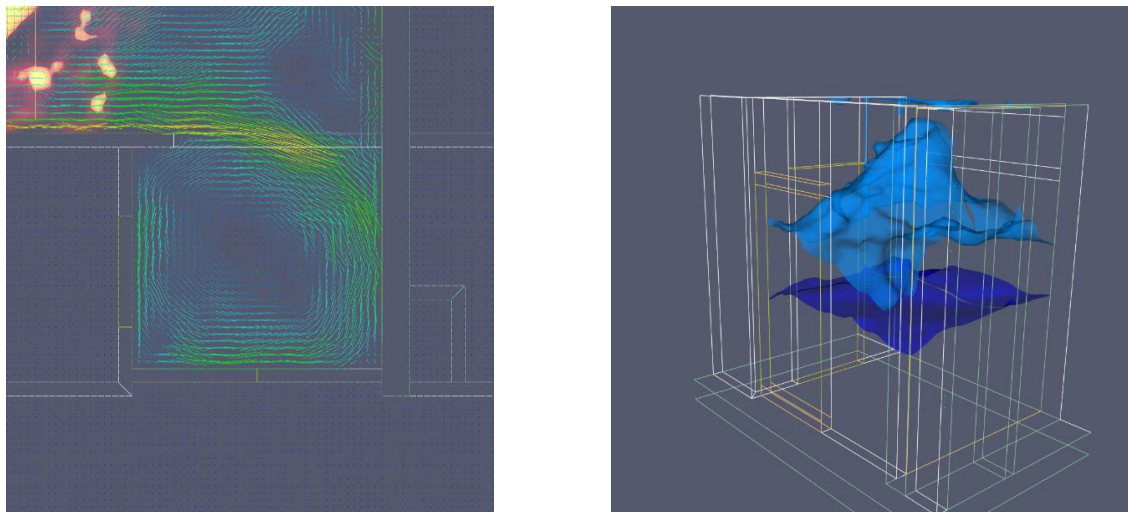


Figure 29: left: velocity vectors in the kitchen at a height of 2 meters, t= 300 (left) red=4 m/s, right: isosurface in the kitchen at t = 170 seconds (dark-blue = 50 °C, light blue = 100 °C)

### 6.3 Results in the corridor

In the initial time after the door is opened, the  $O_2$  concentration is shown to follow the trends measured experimentally reasonable well. Up to 500 seconds, relative differences in both measuring tree B5 and B6 are below 10% which is acceptable given the uncertainties at hand. In a later time-frame, differences tend to increase significantly with relative errors up to 25% being noticeable. This coincides with the observations made in the apartment. At a lower level in the corridor, differences are more pronounced.

At this height, a turbulent interface of the smoke layer and wall effects lead to more local differences. This phenomena is observed in all gas concentrations. An example for CO<sub>2</sub> is given in Figure 31. Given the location of measurement tree B6 with regards to the spill plume towards the corridor and its location near a wall, bigger deviations at a height of 0,3 meters are seen.

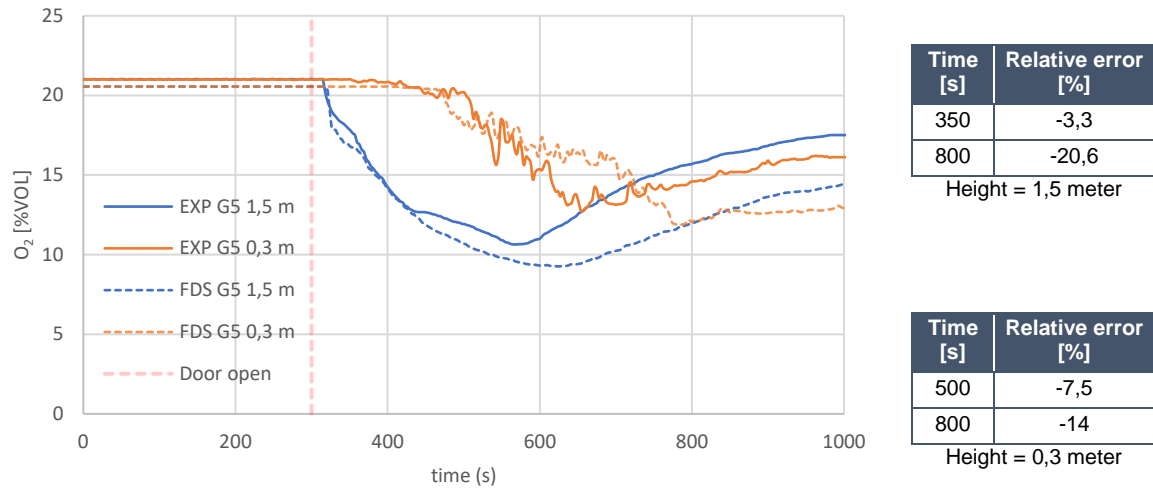


Figure 30: Oxygen concentration at measuring tree B5.

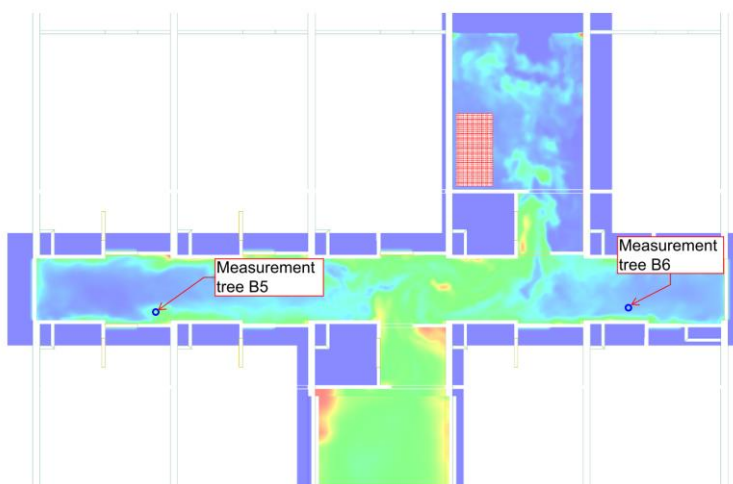


Figure 31: CO<sub>2</sub> concentrations at a height of 0,3 meters at 500 seconds. Red = 4 %vol, blue = 0 %vol

When comparing the experimental and numerical data for CO<sub>2</sub> in the corridor for all case studies, it is noticeable that the overall measured concentrations at a height of 1,5 meters are significantly higher than both the concentrations measured in the apartment and the numerical results. Differences up to 4 %vol are noticeable (concentrations in the apartment are 6 %vol maximum). This could imply combustion occurring near the door, which is not predicted by FDS given the imposed numerical settings. While measurement tree B6 shows differences in temperature (discussed further on in this paragraph), with the experimental data being higher than the numerical data, these differences are only limited in quantity. Differences are expected to be significantly higher, would combustion be occurring. This would also result in significant higher temperatures in measurement tree B5. This is not observed.

Combustion occurring away from the fire seat would also lead to differences with regards to O<sub>2</sub> and CO concentrations in the enclosure. The limited deviations in those gas concentrations do not justify combustion occurring near the door. Furthermore, combustion occurring elsewhere in the enclosure would eventually also lead to significant differences in CO<sub>2</sub> concentrations in the apartment which is not

observed. Local buildup of CO<sub>2</sub> as a result of local effects (e.g. wall effects) would at least be approximated by FDS, which does not show signs of local effects being dominant at a height of 1,5 meters as shown. Furthermore, no sharp stratification of CO<sub>2</sub> in the corridor is predicted by FDS. Finally, faulty measurements might lead to these differences. As of this moment, no clear explanation is found relating to the reason of these elevated CO<sub>2</sub> concentrations. The results for CO follow the same trends as found in the apartment, with FDS over-estimating the concentration prior to it being under-estimated as a result of the prescribed static CO yield.

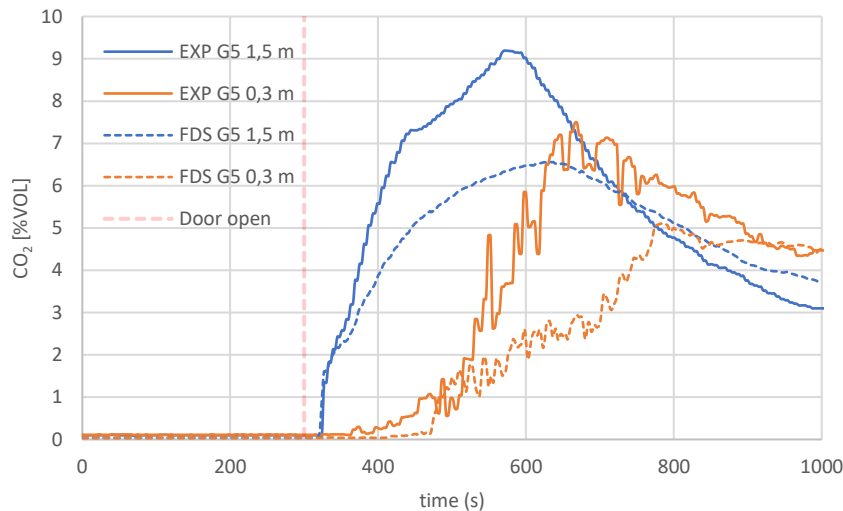


Figure 32: CO<sub>2</sub> concentrations in the corridor at measurement tree B5.

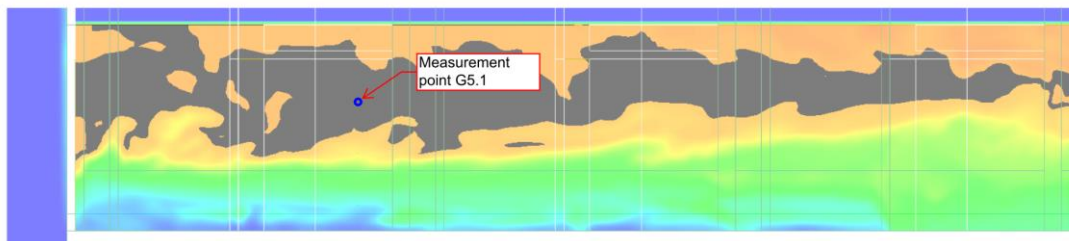


Figure 33: section of the corridor over the measuring trees showing CO<sub>2</sub> concentration at 600 seconds. Red = 8 %vol, highlighted = 6,5 %vol

Experimental and numerical data for temperatures in the corridor show significant differences. As shown in Figure 34, the experimental data shows a distortion in the stratification in the corridor, which is not observed in the numerical data. The distortion can (most likely) be attributed to the protective hoods placed over the thermocouples. Furthermore, closer to the door at measurement tree B6 temperatures in the higher part of the room are underestimated to a significant degree while the temperatures in the lower part are simulated correctly. The spill plume causes significant local effects which lead to local temperature variations in the vicinity of the door. Measuring temperatures with thermocouples near the spill plume therefore is sensitive to the exact location of the equipment.

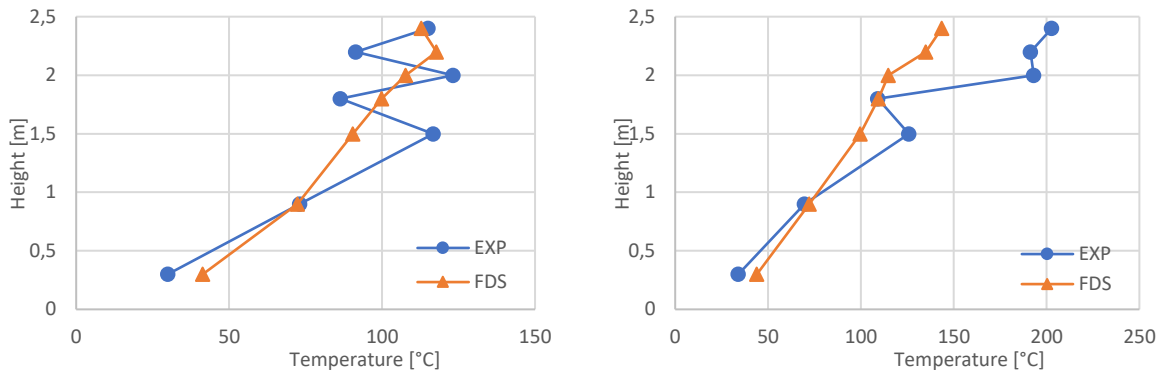


Figure 34: Temperature distributions over the height of the enclosure at t= 500 seconds for tree B5 (left) B6 (right).

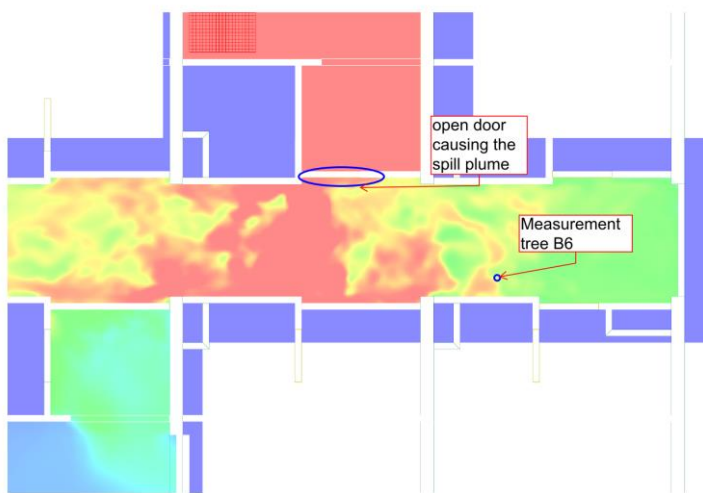


Figure 35: temperature slice in the corridor at 2 meters above the floor and t=400 seconds, red=180°C. Notice the variations in the vicinity of measurement tree B6.

The drop in visibility shows to be predicted appropriately at a height of 1,5 meters. The visibility is binary in the sense that only some seconds after the door is opened, the visibility almost immediately decreases to zero. At a lower height, some discrepancies appear as was the case with the gas concentrations. These can once more be attributed to the turbulent interface of the smoke layer and exact the placement of the light intensity meters. The visibility is predicted to an overall acceptable extent. This does not directly imply the soot generation by the fire is modelled correctly as the visibility concept is only a crude approximation of the soot concentration.

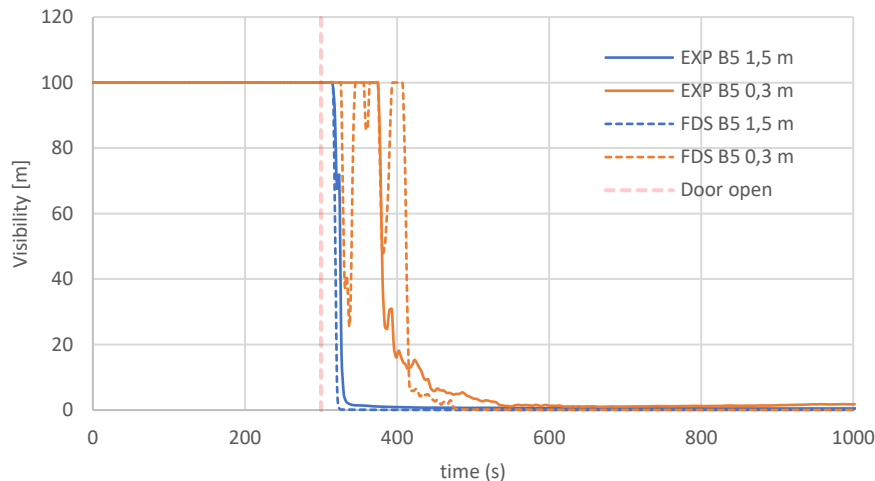


Figure 36: Visibility in the hallway at measuring tree 5

### 6.4 Sensitivity study

Several parameters used in the simulations presented in this chapter were chosen based on values found in literature, were derived from the experimental data using engineering correlations or were chosen based on expert judgement. To limit the inherent uncertainty in the simulations, the results are checked for sensitivity. The parameters changed are described in Table 8. To conserve computational time, simulations were run for 600 seconds. Results are compared both with the initial simulation results and with the experimental results. More results are included in appendix 5.

| # | Combustion model | PUR  | $\Delta H_c$ (MJ/kg) | CFT / LOL ( $^{\circ}C/-$ )               | Simulation mode | SGS turbulence model | Fire growth modelling | Extinction model |
|---|------------------|------|----------------------|---|-----------------|----------------------|-----------------------|------------------|
| 1 | 2 step           | GM21 | 16                   | 1.050/0.135                               | VLES            | Deardorff            | $\alpha^3$            | 2                |
| 2 | 1 step           | GM23 | 16                   | 1.140/0.135                               | VLES            | Deardorff            | $\alpha^3$            | 2                |
| 3 | 1 step           | GM21 | 14,4 & 17,6          | 1.140/0.135                               | VLES            | Deardorff            | $\alpha^3$            | 2                |
| 4 | 1 step           | GM21 | 16                   | 1.055/0.125<br>1.140/0.145<br>1.222/0.135 | VLES            | Deardorff            | $\alpha^3$            | 2                |
| 5 | 1 step           | GM21 | 16                   | 1.140/0.135                               | LES             | Deardorff            | $\alpha^3$            | 2                |
| 6 | 1 step           | GM21 | 16                   | 1.140/0.135                               | VLES            | Const. Smag.         | $\alpha^3$            | 2                |
| 7 | 1 step           | GM21 | 16                   | 1.140/0.135                               | VLES            | Deardorff            | Ramp                  | 2                |
| 8 | 1-step           | GM21 | 16                   | 1.140/0.135                               | VLES            | Deardorff            | $\alpha^3$            | 1                |

Table 8: sensitivity study for case study 1

#### 6.4.1 Two step simple combustion model

The two-step simple combustion model is described in paragraph. 4.6. In the simulations using the two-step simple combustion model, the well-ventilated yields for polyurethane GM21 are used and the extinction model parameters are adjusted for the altered chemistry. The two step combustion model essentially makes transient production of CO and soot possible should limited oxygen be available, which is not done when using static yields.

The numerical results show limited differences for the heat release rate and the temperatures in the enclosure. Small differences are observed for both the O<sub>2</sub> and CO<sub>2</sub> concentrations in the initial period of the fire, as the oxygen-to-fuel ratio for the initial reaction differs from the one step combustion model used in the primary simulations (1,72 kg/kg for the one step model versus and 1,79 for the two step model). Differences however, are in the order of 1 %vol. Extinction is modelled to occur at a similar time.

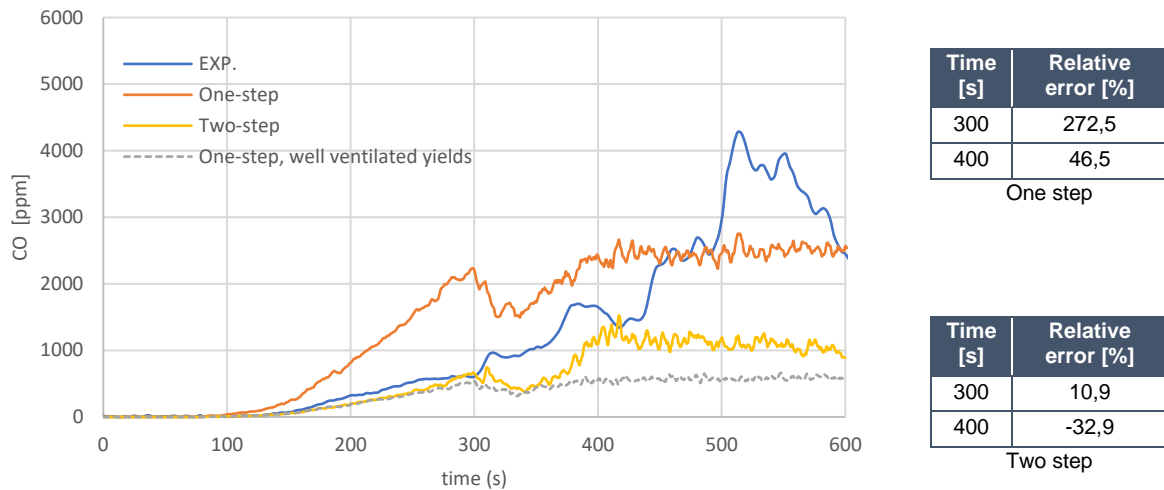


Figure 37: CO-concentrations in the apartment at a height of 1,5 m.

Figure 37 compares the experimental results for CO in the apartment with the results of the one step and two step combustion models. For comparative purposes, simulation results using the one step model with well-ventilated species yields is shown as well.

Significant differences can be observed as in the one step model the concentrations are over-estimated up to approximately 450 seconds. Relative differences of approximately 400 % are found in that timeframe, after which the CO concentration is under-estimated until the end of the simulation. Using the two step model, the CO concentration is predicted to an acceptable level of accuracy, given the limited concentrations involved, with relative differences of approximately -20% up to 10% being shown. After 300 seconds, the numerical data shows to deviate from the experimental data significantly, indicating that either the CO generation is not properly predicted by the two step model or the uncertainties in the experiments are increasing (with a clear example being the doorframe showing signs of degradation).

Overall, the two step model is shown to predict the CO concentration to a higher level of accuracy in the earlier stages of the fire. This can be attributed to the fact that in the initial period, the fire is not under-ventilated and no significant increase in CO generation is expected.

#### 6.4.2 Polyurethane GM23

In the base simulations, the fuel is composed of polyurethane GM21 with composition  $\text{CH}_{1.8}\text{O}_{0.3}\text{N}_{0.05}$ . As this is not substantiated, the sensitivity of the used fuel is studied in a sensitivity using polyurethane GM23 with chemical composition  $\text{CH}_{1.8}\text{O}_{0.35}\text{N}_{0.06}$ . Species yields for under-ventilated combustion (calculated based on the equivalence ratio) and the critical flame temperature are changed accordingly ( $1.558^\circ\text{C}$ ). The following under-ventilated post-flame species-yields are used:

- CO yield: 0,067
- Soot yield: 0,245
- HCN yield: 0,02

No significant differences are observed for the predicted heat release rate and temperatures as the critical flame temperature is changed to fit the used chemical reaction. Most notably, the gas concentrations in the enclosure are affected by the changed chemistry. As the fuel-to-oxygen ratios of the reactions for polyurethane GM21 and GM23 differ significantly (1,78 versus 1,28 kg/kg), the simulation with GM23 shows a less steep initial inclination and predicts overall higher oxygen concentrations. With the fuel-to-oxygen ratio of polyurethane GM23 being significantly lower, the overall simulated oxygen concentrations are higher for that simulation.

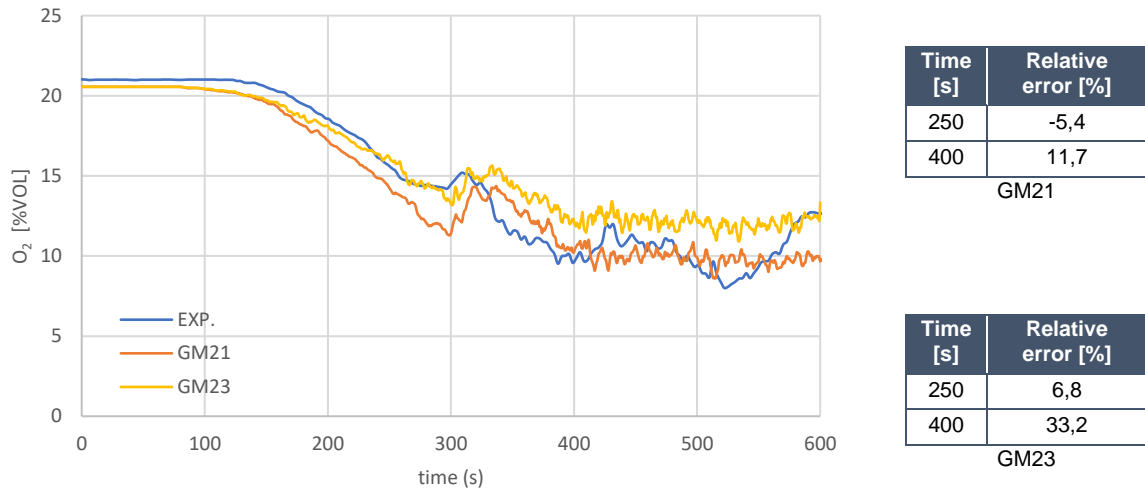


Figure 38: O<sub>2</sub> concentration in the apartment at a height of 1,5 m. Relative differences take into account initial differences in O<sub>2</sub> concentrations.

Given the higher CO yield used for polyurethane GM23, the predicted CO concentration in the enclosure is higher in that simulation. Taking into account the slope of the initial drop in O<sub>2</sub> concentration, the overall predicted O<sub>2</sub> and CO, it is concluded that the modelling the chemical composition of the sofa as polyurethane GM21 best fits the experimental data.

### 6.4.3 Effective heat of combustion

The initially chosen effective heat of combustion is based on an energy balance in which the thermocouple temperatures are used as input. The thermocouple measurements however, have uncertainties included as discussed in paragraph 3.5.1. The effective heat of combustion is prone to uncertainty and is therefore checked for sensitivity.

To study the sensitivity of the effective heat of combustion in the simulations, a sensitivity study is carried out using values of 14,4 MJ/kg and 17,6 MJ/kg (respectively 10% lower and higher than the initially chosen value of 16 MJ/kg). This results in the heat release rate in the simulations being respectively 10% higher and lower compared to the initial simulations. As the value of the critical flame temperature relies on the calorific heat generation, this is changed accordingly. Gas concentrations in the apartment therefore show no significant changes when compared with the initial simulations.

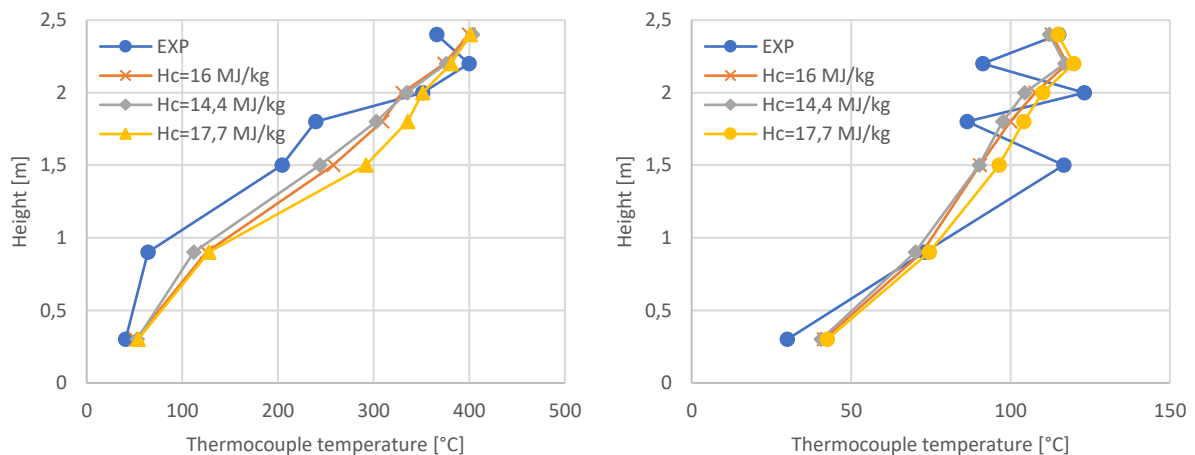


Figure 39: temperature-profile in the apartment (left) and corridor (right) at t=500 seconds

Altering the effective heat of combustion results in changes in the predicted temperatures in the enclosure. Changes however, are limited in quantity. Furthermore, changes in mass flows over vents scale accordingly and are therefore limited as well.

#### 6.4.4 Extinction parameters

In the initial simulations, a value for the critical flame temperature (CFT) of 1.140°C is used, which was calculated using the formulation given in literature and the default value for the lower oxygen level (LOL). Given the fact that the used value for the LOL is not based on data found in literature, it is subject to uncertainty. Therefore, the sensitivity of this parameter is checked along with the CFT.

This study uses a LOL of 0,125 and 0,145. The values for the CFT used are 1.056°C and 1.222°C. The values for the lower oxygen limit are changed as well in FDS. In practical fire engineering studies, the default values for the critical flame temperature are expected to be used. To check the possible level of error, a simulation is ran with the default values.

In the simulation of under-ventilated fires, the extinction model predicts whether a cell will generate combustion. Therefore, the influence of the CFT and LOL on all studied quantities is shown to be significant. Higher values for the CFT and LOL results in flame extinction being modelled in an earlier stage and vice-versa. This leads to the observation that in studied case with a CFT of 1.056°C, the predicted peak heat release rate is approximately 200 kW higher than the initial numerical data. In the case with a CFT of 1.222°C, the peak heat release rate is shown to be 200 kW lower than the initial numerical data. Changing the CFT therefore significantly alters the amount of combusted mass in the domain, which in turn results in changes in gas concentrations and temperatures.

Figure 40 shows the heat release rate for different extinction parameters. As the gas concentrations are correlated with the heat release rate through the reaction rate and oxygen-to-fuel ratio of the fire, the same trend is visible. Results for a CFT of 1.032°C show lower minimum values for the O<sub>2</sub> concentration in the apartment, while a CFT of 1.115°C show higher values. The overall absolute differences lie in a range of approximately 3-4 %vol. Based on the data presented below, the initially selected CFT gives the best approximation of the experimental data.

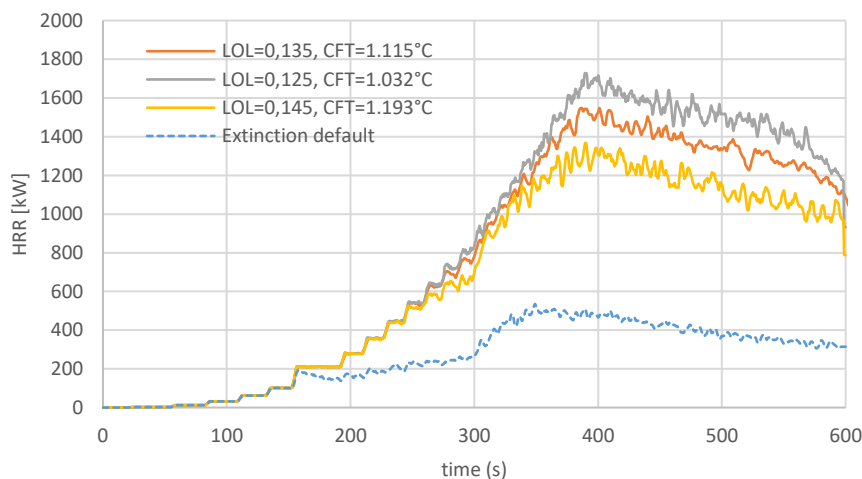


Figure 40: Heat Release Rate for different extinction model settings

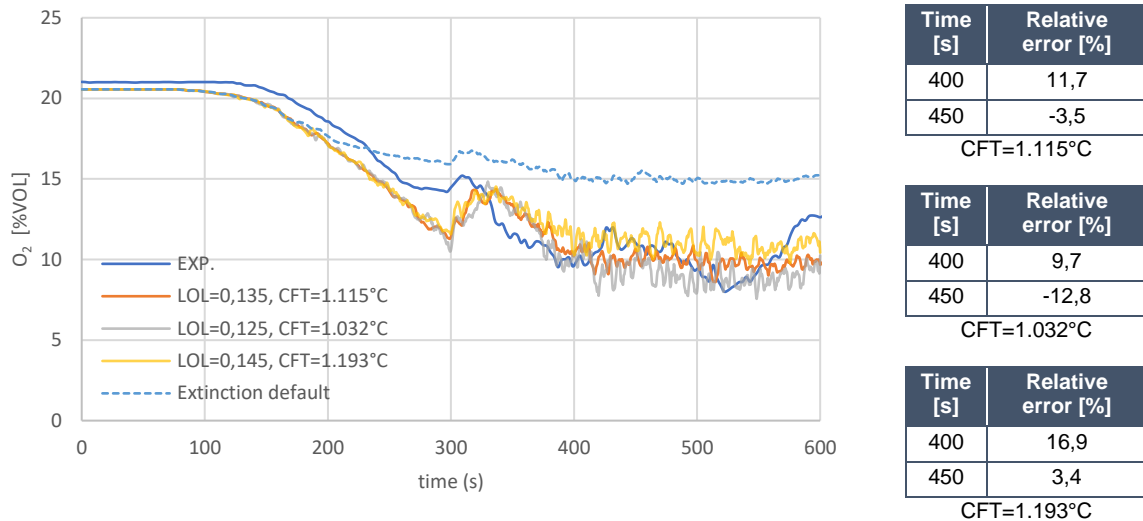


Figure 41: O<sub>2</sub> concentrations in the apartment at a height of 1,5 m. Relative differences take into account initial differences in O<sub>2</sub> concentrations.

Using the default values of FDS for the CFT and LOL results in a significantly lower heat release rate. It should however be noted that the work presented here uses a lower effective heat of combustion than would normally be used in practical engineering studies, which would affect the extinction model.

#### 6.4.5 Simulation mode: LES

By default, FDS runs in 'VLES' mode. In VLES mode, the 'Courant-Friedrichs-Lewy (CFL) Constraint' is less strict than when using LES mode. In LES-mode, the CFL-constraint limits the maximum time-step in such a way that the fluid flow cannot traverse more than one cell width per time step. To study the effects of using the more precise LES-mode, a sensitivity study is carried out. Using LES will result in longer computation times as the overall time-step is expected to be smaller than when VLES is used. No significant differences were found between the numerical data. In this case study, imposing a smaller time-step on the numerics does not result in a higher accuracy. It does however, result in a more stable simulation and significantly higher computational times as the simulations in LES mode ran twice as long on the same computational setup.

#### 6.4.6 SGS-turbulence model: Constant Smagorinsky

By default, the Deardorff subgrid-scale (SGS) model is used to model the eddy viscosity of eddies smaller than the width of a cell, in conjunction with the near-wall turbulence model 'Wall-adapting Local Eddy viscosity' (or WALE), as the Deardorff model is ill-defined in the first-of cell next to a wall. To check the sensitivity of the turbulence model, the Constant Smagorinsky turbulence model is used, which was the default model up to FDS version 5. The default value for the model constant are used (Smagorinsky: 0,2, Deardorff: 0,1). The near-wall turbulence model is kept the same.

No significant differences between the simulations using the Constant Smagorinsky and Deardorff SGS-models for eddy viscosity were found. Therefore, it can be concluded that either small eddies (with a smaller length-scale than the width of a cell) are not relevant in this case given the relatively high mesh-resolution, or that differences between the models are negligible.

#### 6.4.7 Fire growth modelling

As described in paragraph 4.8, the way the fire is modelled is expected to have significant influence on the buoyancy and thus on the momentum of the fire- and smoke plume. As modelling the fire using a radially growing fire is expected to give the most realistic results, this method was opted for in this case. However, using a radially growing fire might result in under- or overestimations of the Heat Release Rate.

Other than differences as a result of the mass loss rate of the fire being modelled more accurately with the ramp-function, no significant differences on the heat release rate are noticeable. Flame extinction is modelled to occur in the same time-frame for both simulation. This however does not directly imply that the method by which the fire is modelled does not affect the extinction model. In this specific case, the fire already is nearing its full surface by the time extinction is modelled. In more under-ventilated fires, the extinction model can be affected by the method for fire modelling.

Figure 42 shows significant differences in the thermal stratification in the apartment. This can be attributed to due to the stronger momentum in the fire/smoke plume in the case of the radially spreading fire. Differences in fire plume length are clearly visible, while the heat release rate is similar. This affects the Froude-number of the fire driven flow and subsequently the stratification in the enclosure. Differences are also clearly visible in Figure 43 in which the HRRPUV and thermal stratification are visually depicted. Given the observed differences between the experimental and numerical data, no quantitative comparison is carried out.

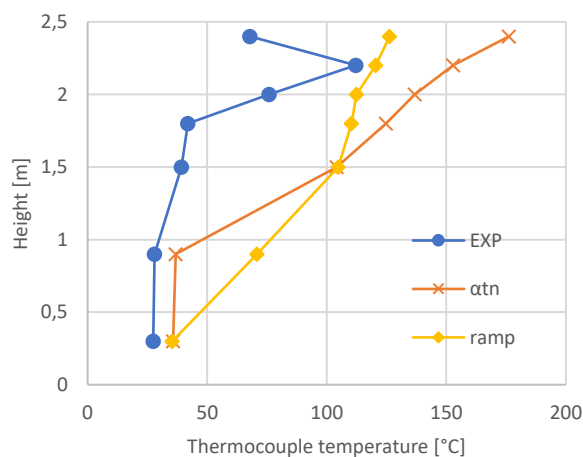


Figure 42: temperature-profile and deviation in the apartment (measuring tree B1) at t=150 seconds

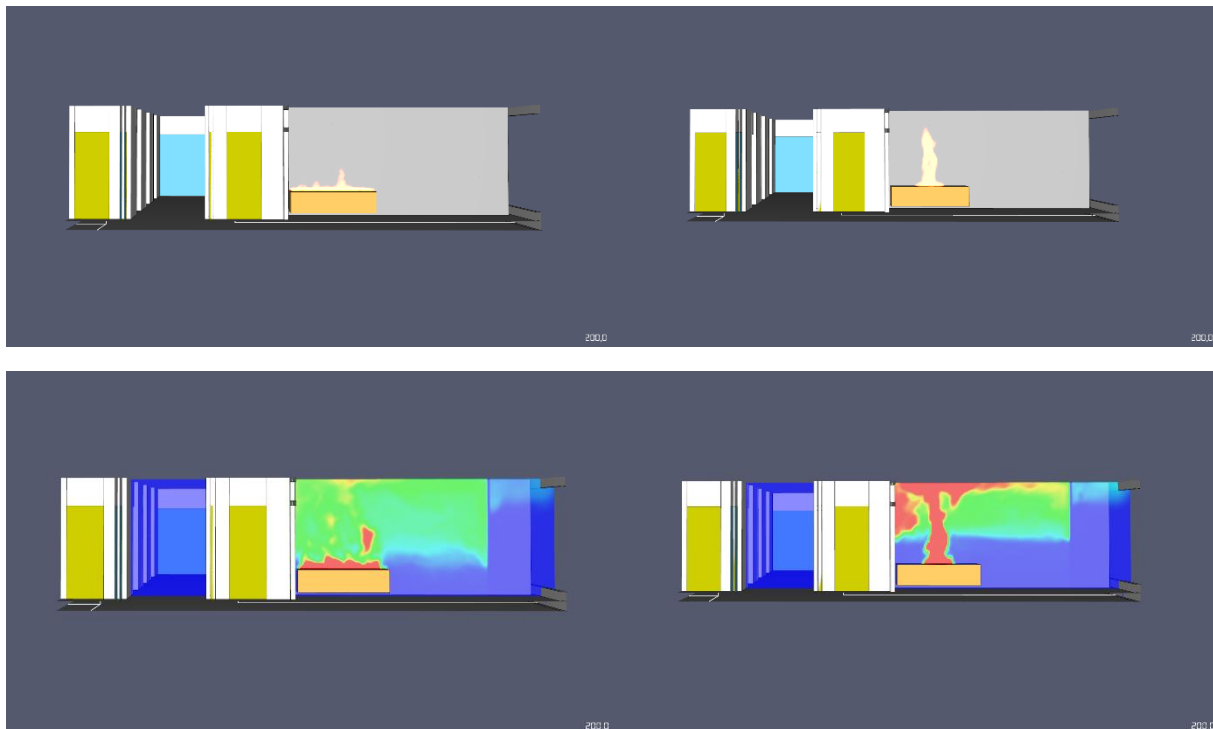


Figure 43: HRRPUV and temperature profile over the fire at t=200 seconds (left: ramp, right αtn) red = 300°C, blue = ambient.

### 6.4.8 Extinction model

By default, FDS uses 'extinction model 2', which relies heavily on the critical flame temperature. For coarse mesh resolutions, a more simple extinction model (extinction model 1) is available. Extinction model 1 relies less heavily on the critical flame temperature, but more on the Lower Oxygen Level. In this paragraph, the initial results with extinction model 2 are compared with the results of extinction model 1. The used parameters are the same for both cases, with the exception of the free burn temperature, which is only used in extinction model 1 and is set to 600°C (default).

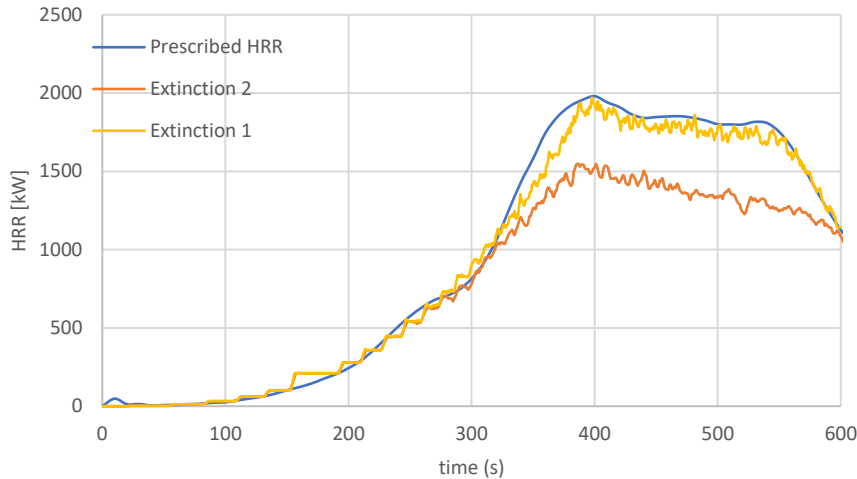
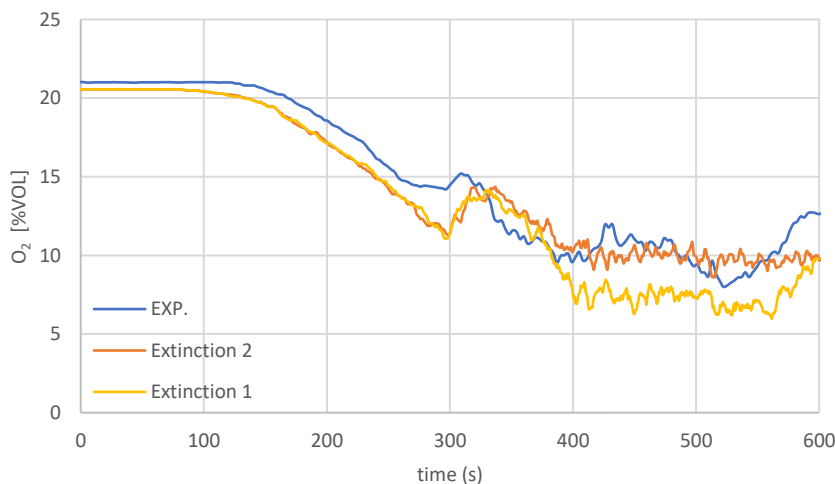


Figure 44: heat release rate for both extinction model 1 and 2.

The O<sub>2</sub> concentration in the apartment shows significant differences between models. The simulations using extinction model 1 predict a minimum concentration of 5-6 %vol while both results for extinction model 2 and the experimental data show minimum concentrations of approximately 9 %vol. The heat release rate for extinction model 1 shows that almost no flame extinction is modelled resulting in a peak heat release rate of 2 MW whereas the results for extinction model 2 show a peak of 1,5 MW. This is shown in Figure 44.



| Time [s] | Relative error [%] |
|----------|--------------------|
| 200      | -4.8               |
| 400      | 11.7               |
| 450      | -3.5               |

Extinction 2

| Time [s] | Relative error [%] |
|----------|--------------------|
| 200      | -5.0               |
| 400      | -10.4              |
| 450      | -38.9              |

Extinction 1

Figure 45: O<sub>2</sub> concentration for different extinction models at a height of 1,5 m. Relative differences take into account initial differences in O<sub>2</sub> concentrations.

Given the fact that more mass combusts using extinction model 1 and a higher heat release rate is observed, species concentrations and temperatures in the enclosure are also higher for 'extinction model 1'. Temperatures for extinction model 1 were found to be approximately 50°C higher when

compared to the results of extinction model 1. Given the uncertainty in the experimental data with regards to temperatures however, no clear conclusion can be given on what extinction model predicts flame extinction the most accurately. With regards to O<sub>2</sub> concentrations, extinction model 2 is found to match the experimental results best. From an engineering point-of-view, the results for extinction model 1 are more conservative.

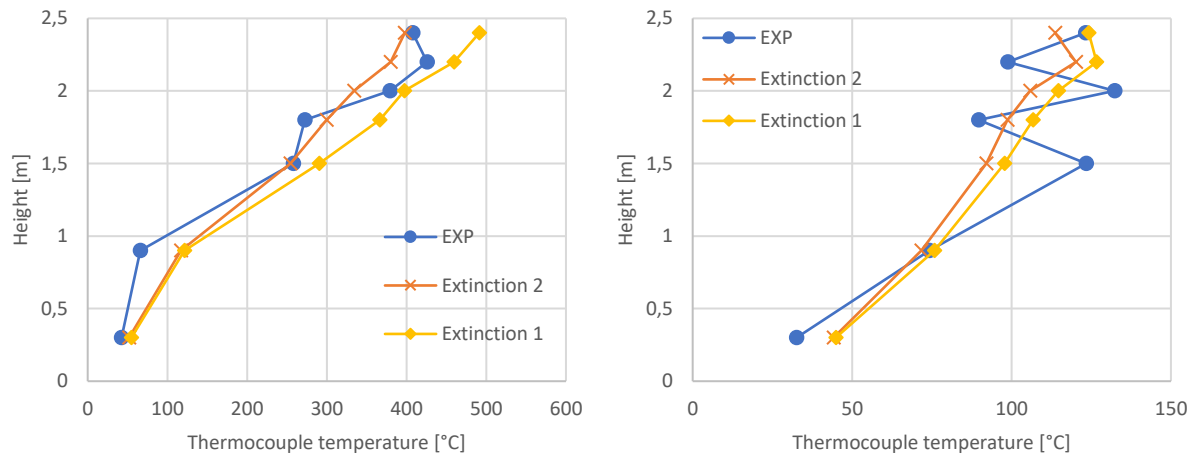


Figure 46: temperature profile between numerical and experimental data in the apartment (left) and corridor (right) at t=550 seconds.

## 6.5 Case study 1: conclusion

### 6.5.1 Overall results

Taking into account inaccuracies in the experimental data, the simulations show to adequately predict the fire related phenomena. O<sub>2</sub> concentrations in both the apartment and corridor are predicted to an acceptable level of accuracy, at least in the initial 600 seconds of the fire. After 600 seconds, FDS overestimates the oxygen consumption of the combustion process. At this point, the burning is expected to become more of a smoldering type, resulting in less oxygen used and more CO being produced. This cannot be simulated by FDS in its default settings.

Temperatures are initially over-estimated by FDS and under-estimated in a later time-frame. Explanations can be found in the presence of the protective hoods. Furthermore, local phenomena are shown to be of importance. While not studied in-depth, heat transfer to the enclosure can also play a significant part in the difference.

The production of CO is shown to be on the conservative side using a static CO yield based on an equivalence ratio. Visibility in the corridor is shown to follow the trends observed in the experiments quite well. However, at a lower height in the corridor (0,3 meters), local transient effects as a result of the location of the measurements and turbulence in the interface of the smoke layer are dominant, which results in some deviations between the simulated and experimental data.

Moreover, CO<sub>2</sub> concentrations in the corridor are significantly under-estimated by FDS, while in the apartment, it is simulated more or less accurately. Typically, this would be an indication of combustion taking place near the door between the apartment and the corridor. The results for oxygen and CO however, do not show significant differences that would suspect combustion taking place. Furthermore, temperatures near the door are somewhere around 200°C maximum, which typically results in an unreactive gas mixture [44]. Therefore, no oxidation is expected.

### 6.5.2 Sensitivity study

The sensitivity study shows that :

- The chemical composition of the fuel results in a significant different outcome compared with the primary simulation. Significant differences are observed with regards to gas-concentrations. The chemical composition of the fuel should therefore be chosen with care. Generalizing the composition can result in significant different outcomes.
- Using a multi-step combustion model can result in a better prediction when it comes to gas-concentrations in the enclosure. The used model however, has limited validity.
- A higher or lower effective heat of combustion does not result in drastic changes. Significantly higher or lower values however, can result in higher or lower temperatures in the enclosure.
- Using different parametric setting for modelling extinction greatly affects the simulation results. Generalizing the critical flame temperature and lower oxygen limit therefore might result in unrealistic outcomes. Using a different extinction model which is based on a free burn temperature results in a more conservative outcome in the framework of this case study.
- Using a more strict restraint on the maximum time-step by using a lower CFL-constraint does not result in significant differences. It might however result in a more stable simulation.
- Changing the SGS-model for turbulence from Deardorff's model to the Constant Smagorinsky model does not result in significant differences. This is an indication that either the used grid resolution is appropriate or differences between the two models are negligible.
- Modelling a horizontally growing fire results in a more realistic stratification in the enclosure when compared to modelling the fire area to be static and prescribing the heat release rate over that entire area. Other than that, differences are small.

## 7. RESULTS CASE STUDY 2: DOOR TO CORRIDOR OPEN

### 7.1 Description of experimental setup

The experiments used as the data set for this case study took place in the afternoon of July 4<sup>th</sup>. Apartment 1.19 was used as the room in which the fire seat was located. During the experiments, the balcony door was closed for the entire duration of the fire. Furthermore, the door to the corridor was opened after 300 seconds and left open for the remaining duration of the fire.

A large part of work done on case study 2 involves parametric studies to find appropriate settings for the leakage and extinction model, so that the numerical data fits the experimental data. For the sake of readability, only the most important findings are included in the main text of this thesis. A more comprehensive description is included in appendix 6 of this work.

### 7.2 A-priori parametric study: fire-induced pressure in apartment

The airtightness of the apartment was measured prior to the experiments, giving insight in the leakage area of the enclosure. After the blowerdoor measurements but before experiment of this scenario however, alterations to the enclosure were made to make the of the apartment airtightness more representative. Therefore, the airtightness of the enclosure is prone to uncertainty. To limit this uncertainty, an a-priori parametric study in which a series of CFD-simulations are ran and compared is carried out to determine the most appropriate settings.

Using a best fit  $\alpha t^n$ -curve to model fire growth will result in over- or underestimates of the Heat Release Rate, as the fires' mass loss rate shows a plateau at 200 kW between 200 and 280 seconds, as shown in Figure 8. Therefore, the heat release rate is modelled as a ramp to closely follow the experimental data. As stated earlier, the used data is time averaged to limit the noisiness of the signal.

As shown in Figure 47, the measured value of 164 cm<sup>2</sup> and a leak pressure exponent of  $n=0,56$  results in an under-estimation of the fire-induced pressure. This indicated that either the leakage area and/or leak pressure exponent are lower in reality, or that the heat release rate is higher in reality. Figure 47 shows the effects of decreasing the leakage area of the enclosure. Note that the shifted peak at approximately 285 seconds is a result of time-averaging the mass loss rate, in combination with FDS modelling flame extinction (effectively lowering the heat release rate), which based on the experimental results is not expected to happen.

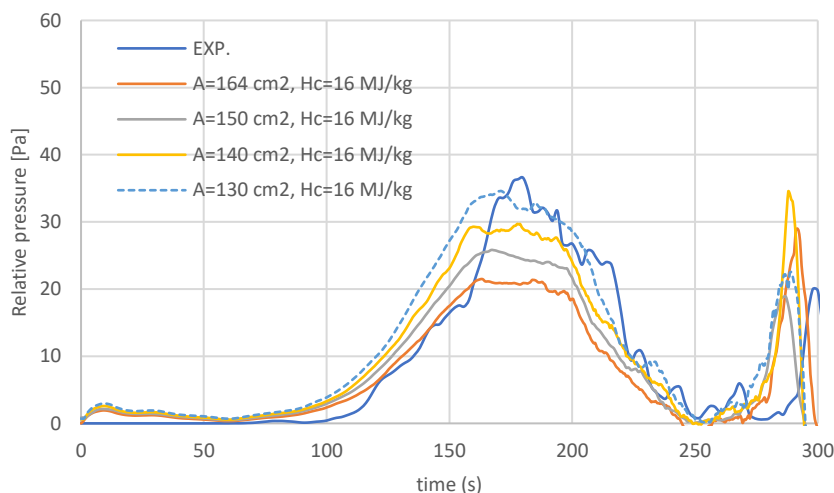


Figure 47: pressure development in the apartment

The effects of altering the leak pressure exponent and effective heat of combustion are shown in appendix 6. While altering these parameters indeed results in higher pressures, the effects are not as pronounced as lowering the leakage area. Most likely, a combination of changes in these parameters will dictate the actual measured pressure-rise in the apartment. There is currently no indication of the leak pressure exponent actually being altered as a result of the changes to the enclosure. Furthermore, prescribing a higher effective heat of combustion will likely result in over-estimates in temperatures elsewhere in the domain.

Based on these observations and for the sake of simplicity, the following simulations are run with a better airtightness of the enclosure. An airtightness of 130 cm<sup>2</sup> best approximates the measured values and is therefore selected. The leak pressure exponent is kept at 0,56, while the effective heat of combustion is kept at 16 MJ/kg.

The experimental results show the visibility at measuring tree B6 (at a height of 1,5 meters) declining before the door was opened at around 240 seconds. Aside from the pressure in the apartment, the smoke leaking from the apartment into the corridor depends on the leak area of the door and the location of the leaks. Furthermore, the method by which heat transfer from the leaking gases to the leaks surface is taken into account defines the temperature and thus the buoyancy of the leaking gases. The effects of altering the leakage area of the door, the location of the leak and the methodology by which heat transfer is included in the model are shown in Figure 48.

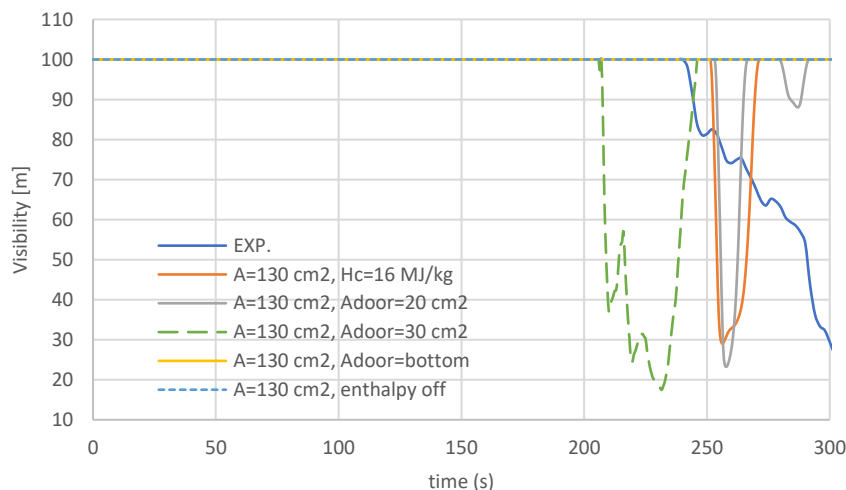


Figure 48: Visibility in the corridor at B6 at a height of 1,5 meters.

None of these results show to correlate well with the experimental data, indicating that the movement of the leaking smoke in the corridor is not accurately predicted. The main reason for this, might lie in the method by which heat transfer is taken into account. Either the leaking gases are assumed to have a temperature equal to the surface the gases are leaking from ('enthalpy off') or their temperature is defined as the temperature difference between the cell on the one side of the wall and the temperature of the other side of the wall. This approach is binary in nature and is to some extent rudimentary. Reality is expected to lie anywhere in between.

The differences between the results of the two methods is depicted in Figure 49. In the case of the simulation with the enthalpy disabled, smoke movement is stagnant and limited to the area directly in front of the apartment door in the simulations with enthalpy off. In the case of the simulations with the enthalpy turned on, heat losses are (somewhat) more realistically taken into account. This results in the escaping gases being more buoyant with entrainment of ambient air and smoke propagation as a result. The following images show the soot concentration in the area in front of the apartment door. Differences are significant.

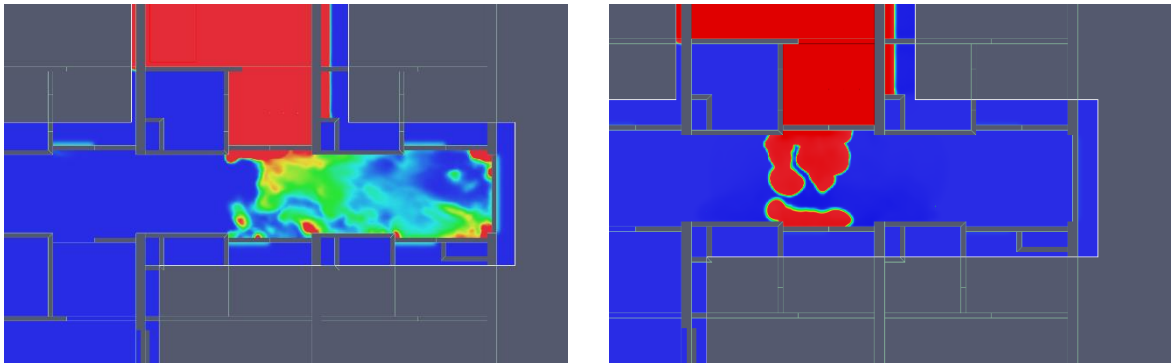


Figure 49: soot concentration at a height of 1,5 meters,  $t = 270$  seconds, enthalpy on (left) and off (right).  
Red =  $9,5 \cdot 10^{-6}$  kg/kg, blue = 0 kg/kg.

While the methodology for heat transfer from the gases to the inside of the leak implemented in FDS is to a certain extent rudimentary, it is clear to have a significant effect on the smoke movement in the corridor, prior to opening the apartment door. Therefore, enthalpy is left on for the remainder of the simulations.

A similar study is executed for the airtightness of the corridor. Fully describing the results of that study bypasses the goal of the main text of this thesis as the airtightness in that corridor is only of secondary importance in this study. A leakage area of  $1.000 \text{ cm}^2$  was found to fit the experimental data best, which is significantly higher than initially assumed. Reasons lie in the fact that, during the experiments, one door was not closed properly (a small crack was present between the frame and door leaf).

### 7.3 Initial results in the apartment

In this paragraph, the simulations are compared with the experimental results. In the simulations, the following parameters were used, based on the previous results:

- Heat release rate modelled using the ramp method, for reasons explained in the previous paragraph and (more comprehensive) appendix 6;
- Airtightness of the apartment of  $130 \text{ cm}^2$  with a leak pressure exponent of 0,56;
- One step simple chemistry with the reaction and critical flame temperature as specified in paragraph 5.5.3.

As shown in the following image, FDS models extinction to occur at around 280 seconds. After the door is opened, extra oxygen becomes available and the heat release rate is modelled to increase to approximately 650 kW. This is significantly less than the expected heat release rate. While it is expected that in reality some pyrolyzed mass is not combusting due to oxygen dilution, the differences are not justifiable.

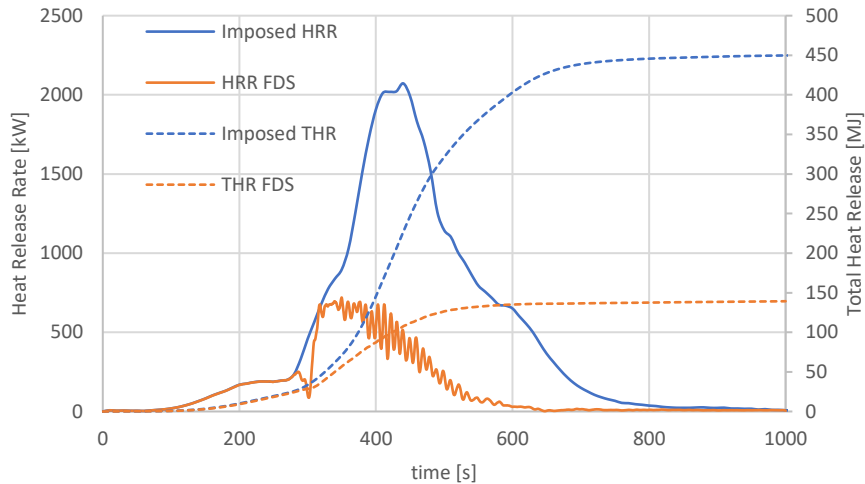


Figure 50: simulated heat release rate compared with the potential heat release rate

The minimum oxygen concentration is over-estimated as a result of extinction being modelled where in reality this is not occurring (at least not to the extent modelled). The experimental data shows values as low as 2%vol, while FDS predicts a minimum of approximately 9 %vol.

Furthermore, FDS predicts the oxygen-concentration to decrease less rapid compared to the experimental results. This is due to the modelled chemistry in which static yields are used to model CO- and soot-generation, which affects the oxygen-to-fuel ratio as well. To account for this, a combustion model which allows transient effects on the chemistry needs to be used.

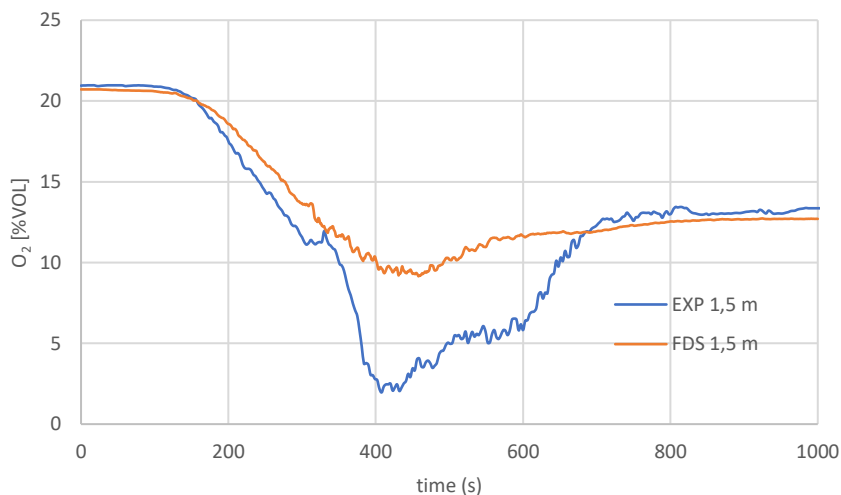


Figure 51: oxygen concentration in the apartment

The CO-concentration in the experiments remains relatively low, up until the point the fire starts to be diluted of oxygen. At around 350 seconds, CO generation increases rapidly. This showcases the transient nature of CO generation in under-ventilated fires. Using a prescribed CO-yield that remains constant over the entire duration of the fire as is done in the simulations will result in an over-estimate in the early phase of the fire, followed by a under-estimate in the later phase of the fire.

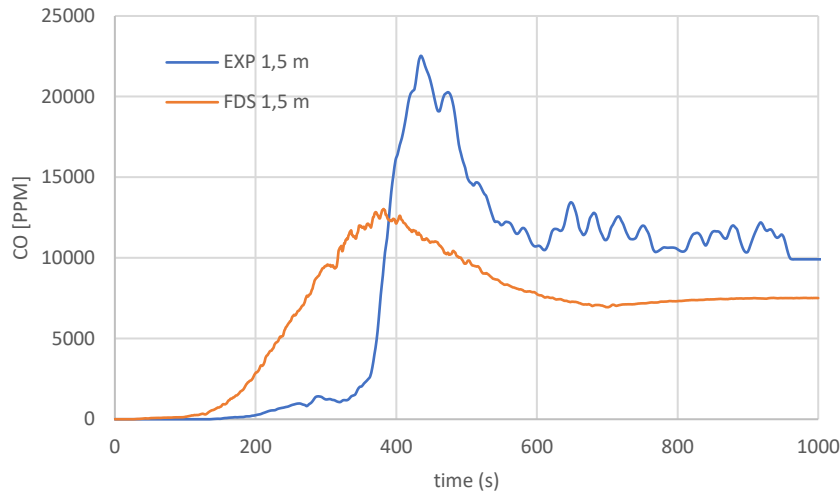


Figure 52: CO concentrations in the apartment

The simulation results do not show a good correlation with the experiments. Several explanations are possible:

- The chemistry is simplified to the extent no transient phenomena in CO and soot generation are possible. As such, the fuel-to-air ratio of the chemical reaction is static and underpredicted in the earlier stages of the fire and over predicted at the time the fire becomes severely under-ventilated.
- Extinction is modelled using the critical flame temperature concept, which uses the cell temperature to predict whether or not combustion is suppressed. The temperature and thus the extinction model are sensitive to the used grid resolution.

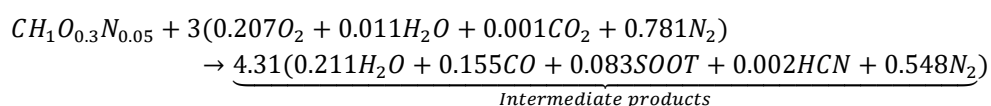
A solution might lie in (crudely) taking into account transient soot and CO generation and forcing the extinction model to allow combustion to occur up to the minimum  $O_2$  concentrations measured.

#### 7.4 Multiple fast reactions and (mis)using the extinction model

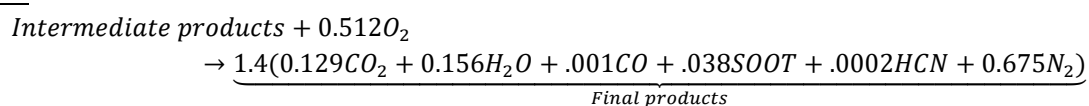
To take into account CO- and soot-generation inside the flame envelope as a result of oxygen starvation into account, a multiple step reaction scheme is employed. Several methods of setting a multiple step fast reaction scheme are possible in FDS. Most favorably, to take into account CO generation, a finite rate reaction can be used. Finite rate reaction schemes depend quite extensively on local quantities and might necessity excessive an grid resolution or a DNS methodology [21]. This is not desirable. Therefore, a simple two step combustion scheme is used in which two infinitely fast reactions are executed in series.

In the reaction scheme below, the well ventilated post-flame yields for CO and soot are used, so that FDS models CO and soot to be formed even though sufficient oxygen is available in the initial stages of the fire development. The concept of the two step combustion model is discussed in paragraph 4.6. While HCN generation is also taken into account, it is not further discussed here. The following reaction scheme is employed in the simulations, in which polyurethane GM21 reacts with air:

Step 1:



Step 2:



Step 2 is only invoked should sufficient oxygen be available. Therefore, in the simulations, should the oxygen be diluted, the reaction stops at step 1, resulting in a heightened CO and soot generation. In reality, these chemical reactions and associated kinetics are significantly more complex. Moreover, no temperature dependence is in place while in reality, higher temperatures typically lead to more efficient kinetics [44]. The model in its essence is rudimentary and bypasses some fundamental phenomena that are associated with the flames' chemistry.

By default, when using multiple step reaction schemes, FDS calculates the effective heat of combustion based on the species' enthalpy of formation/reaction. This essentially allows the effective heat of combustion to be transient over the duration of the simulation: should step 2 not be allowed to occur, the energy released by that reaction is not accounted for. Using this methodology will result in a higher initial effective heat of combustion than used in earlier simulations. The calculation of the effective heat of combustion is therefore initially overruled. A value of 16 MJ/kg is used instead in the following results. In appendix 6, the effects of the enthalpy based heat of combustion is studied in more detail.

To effectively model CO formation in the apartment as a result of oxygen dilution, extinction needs to be modelled in a way that more closely follows the oxygen concentration in the apartment. To that extent, a parametric study is carried out to study the effects of different parameters related to the extinction model. The default extinction model of FDS, extinction model 2, is used. The lower oxygen limit and critical flame temperature are changed incrementally until a reasonable fit with the experimental data is found. Note that the used values might not be realistic.

Figure 53 shows several simulation results for the oxygen concentrations at the measuring tree in the apartment compared with the experimental data. Both results for a lower oxygen limit of 0,08 and 0,07 show an overall good resemblance with the experimental data.

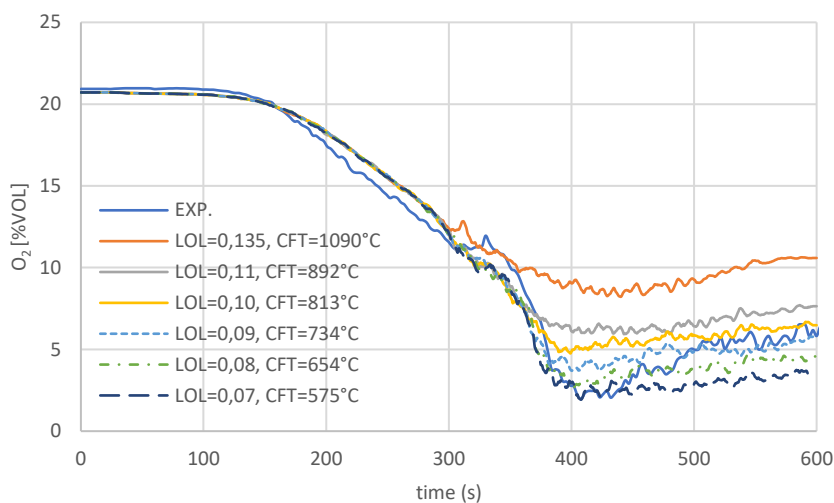


Figure 53: oxygen concentrations in the apartment for different values associated with the extinction model

As discussed in the previous paragraph, the CO concentrations are expected to increase exponentially at lower oxygen-concentrations in the apartment. This is observed in Figure 54. While some nuance differences are observable. The overall trends and maximum values for most notably the results using a lower oxygen limit of 0,08 and a critical flame temperature of 654°C show good comparison with the experimental data. At around 500 seconds, the O<sub>2</sub> concentrations are simulated to be lower when compared with the experimental values while the CO-concentrations are found to be higher in the experiments. The inverse is true for the CO<sub>2</sub> concentrations in the enclosure. This is a result of FDS modelling flaming combustion as a result of the lower flame extinction parameters, while in reality, a more smoldering combustion is expected.

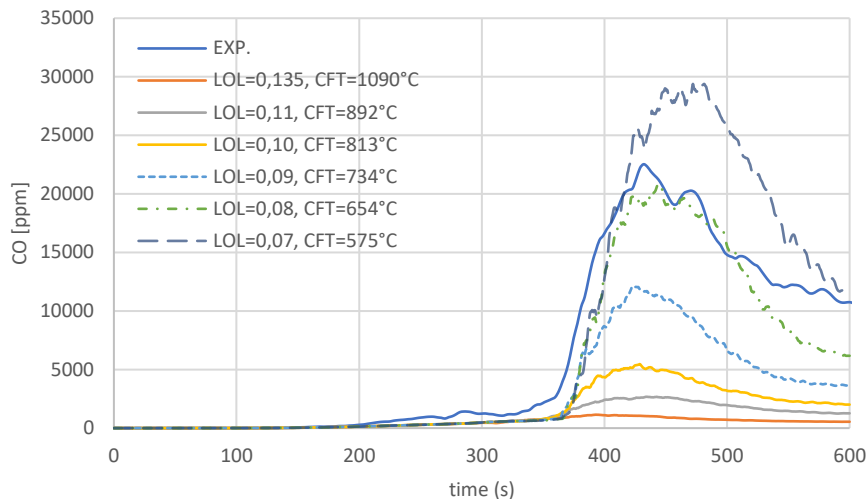


Figure 54: CO-concentrations in the apartment for different values associated with the extinction model

Given the fact that the fuel-to-air ratio is transient over the duration of the fire simulations, the critical flame temperature should also be of a dynamic nature to more accurately predict flame extinction. This however, is currently not implemented in FDS.

## 7.5 Numerical setup for final simulation results

Based on results from the previous paragraphs, the following settings were chosen to be the definitive numerical setup for the simulations for case study 2:

- Heat release rate modelled using a ramp-method.
- A leakage area of the apartment of 130 cm<sup>2</sup>, of which 20 cm<sup>2</sup> is attributed to the apartment door. A leak pressure exponent of 0,56 is used which was found experimentally prior to the experiments.
- Multiple fast reactions in series using the two-step simple combustion model at default settings to model soot-, CO- and HCN-generation at low oxygen concentrations.
- Fuel: polyurethane GM21 with a well-ventilated oxygen-to-fuel ratio of 1,8 kg/kg. Soot-, CO- and HCN-yields are taken to be 0,131, 0,01 and 0,002 g/g respectively.
- Default extinction model (model 2) using a lower oxygen limit of 0,08 and a critical flame temperature of 654°C. Note that these values were found to best fit the experimental data, the validity is questionable.
- A static effective heat of combustion of 16 MJ/kg.
- A leakage area of the corridor of 1.000 cm<sup>2</sup>. A leak pressure exponent of 0,5 is used (default).

## 7.6 Results in the apartment

The following image shows the predicted heat release rate (HRR) over time. The simulation follows the prescribed HRR (prescribed by means of a mass loss rate) up to approximately 370 seconds, after which the extinction model dictates the simulation results. The simulated maximum HRR is significantly lower than the curve based on the measured mass loss rate. FDS predicts a maximum heat release rate of 1 MW, while the mass loss rate suggests a maximum of approximately 2 MW. In total, approximately 9 kilo of pyrolyzed mass does not combust in the FDS-simulation.

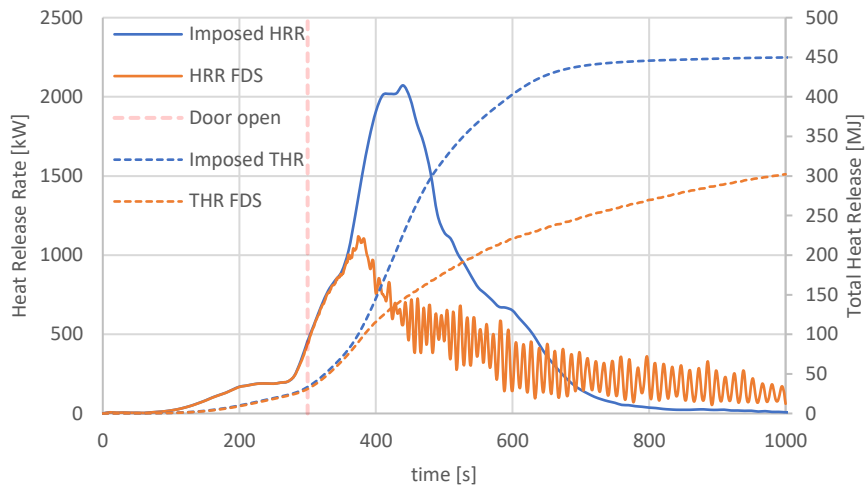
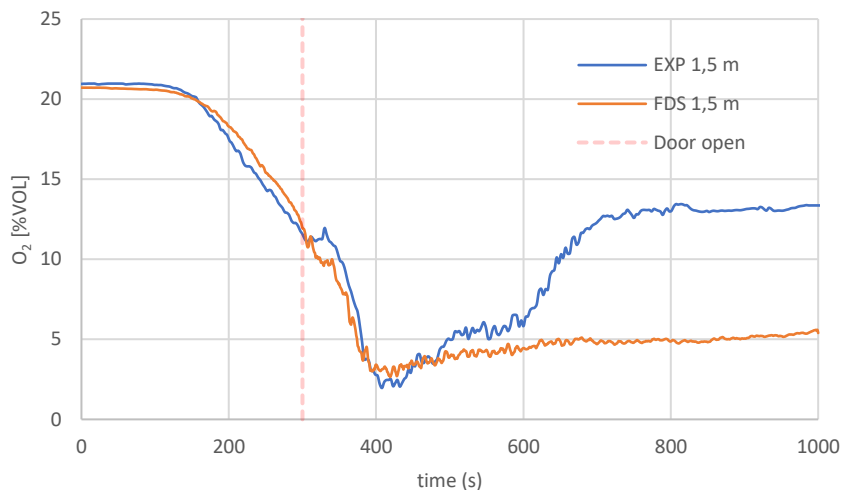


Figure 55: Heat Release Rate

As depicted Figure 56 and Figure 57 the gas concentrations in the simulations follow the measurements well up to approximately 550 seconds after which significant differences are observed. The suspected reason lies in the fact that either the lowered extinction parameters results in a higher heat release rate, the fire is starting to smolder or the exclusion zone of the auto-ignition temperature makes spurious re-ignition of pyrolyzed mass possible that might not happen in reality.

The last explanation also explains a higher heat release rate in the later time-frame (700 seconds onwards) of the simulations. Using a smaller exclusion zone or modelling a more realistic ignition might lead to more appropriate results and is studied in the sensitivity study. A smoldering combustion results in less oxygen used in the combustion process, while respectively more CO and less CO<sub>2</sub> are produced. Other than that, the wood frame of the sofa might be starting to contribute to the fire at some point during the fire, changing the fuel mixture and thus the chemistry.



| Time [s] | Relative error [%] |
|----------|--------------------|
| 200      | 4,7                |
| 400      | 29,1               |
| 600      | -24,5              |
| 800      | -60,7              |

Figure 56: O<sub>2</sub> concentration in the apartment. The relative differences take into account the initial difference between the numerical and experimental data. Note that, while the relative error around 400 seconds is high, it can be attributed to the absolute values being low. The absolute difference around 400 seconds is -0,8 %vol.

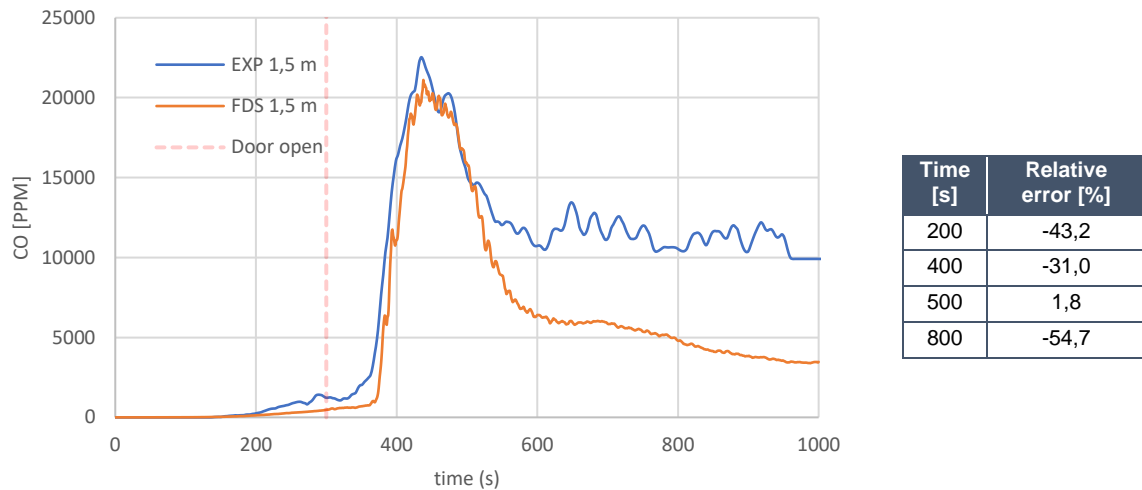


Figure 57: CO concentration in the apartment.

Qualitatively, trends in gas concentrations are predicted accurately up to approximately 550 seconds. Quantitatively,  $O_2$  concentrations are predicted accurately up to 350 seconds, the maximum relative error is approximately -5%, which is acceptable given the imposed uncertainties. In a later time-frame, after extinction is predicted to occur, the errors are in the order of 50-60 %, which is due to reasons described earlier. Trends relating to CO concentrations are shown to be captured accurately. As the experimental data shows a somewhat earlier exponential increase in CO concentrations, observed errors are in the order of 30-40%. Differences in  $O_2$  concentrations around the moment the door is opened can be attributed to the time-averaging of the mass loss rate.

The fire-induced pressure in the apartment is shown in Figure 58. The trends in relative pressure are adequately simulated, the peak at 180 seconds shows a relative error of approximately 5-10%. The peak just prior to the opening of the door is not properly predicted. That peak is explainable through the fact that the mass loss rate signal was time-averaged prior to it being used as input in FDS. While the mass loss rate does in fact start to grow prior to the door opening, in reality, the start of that growth is in a somewhat later time-frame. To check the validity of that claim, an additional simulation was run using the 'raw' mass loss rate data acquired from the experiments, of which the results are included in the following graph. It clearly shows a lower pressure peak which directly after the door is opened dissipates. After extinction (at 370 seconds), the pressure drops in the simulations, while the experimental data still shows slight overpressures. While differences are in the order of Pascals, this might be an indication some combustion is continuing in reality that is not properly simulated.

The extinction model directly affects the fire-induced pressure. Therefore, in the later stages of the fire, pressures are expected to show significant deviations from the experimental values. After approximately 450 seconds, underpressures are observed. A comparison of the simulation data with the experimental data for the equipment capable of measuring under-pressures is shown in appendix 4. It shows the predicted pressures are in the right order-of-magnitude.

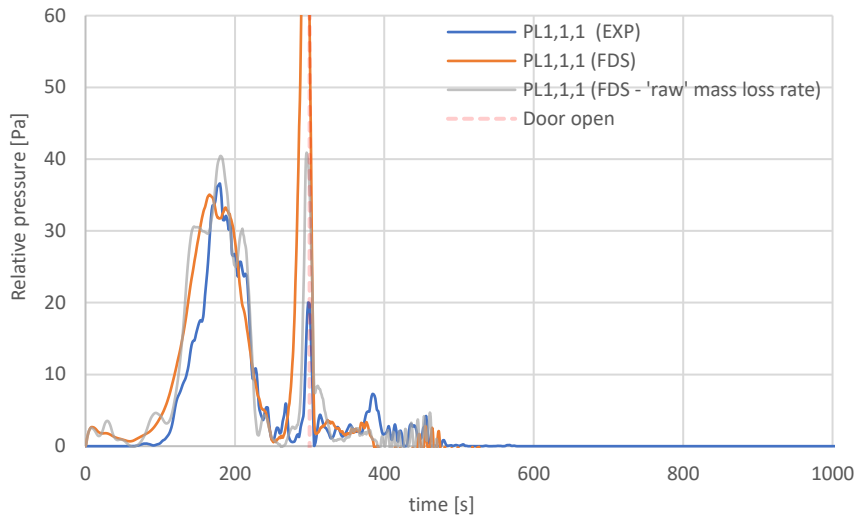


Figure 58: fire-induced pressure in the apartment

Initially, temperatures are adequately simulated, taking into account the probable lag as a result of the thermocouple hoods. After the extinction model starts to dictate the Heat Release Rate, temperatures are severely under-estimated. This is an indication of combustion occurring in reality that is not simulated adequately. The maximum temperatures however, are simulated accurately. This leads to the observation that in reality, the heat release rate is expected to remain more or less constant after extinction occurs.

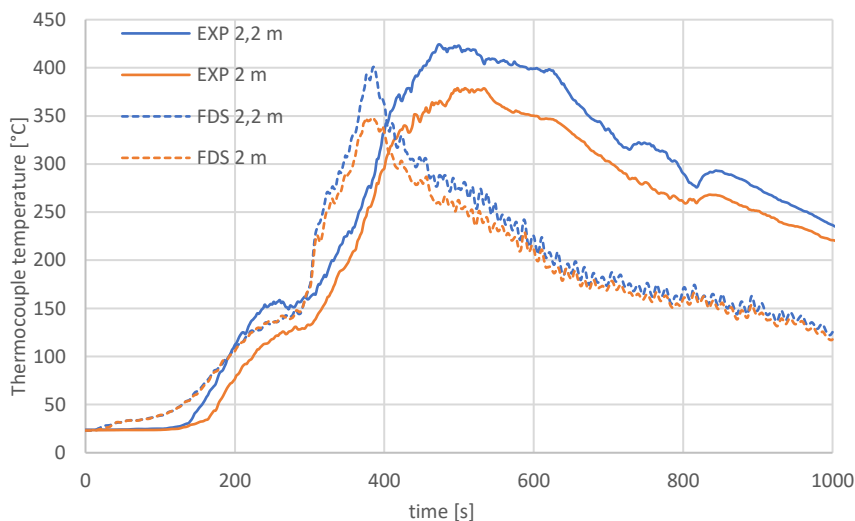


Figure 59: temperatures in the apartment, at a height of 2,2 meter and 2 meter (respectively TK1,1,1 and TK1,1,2).

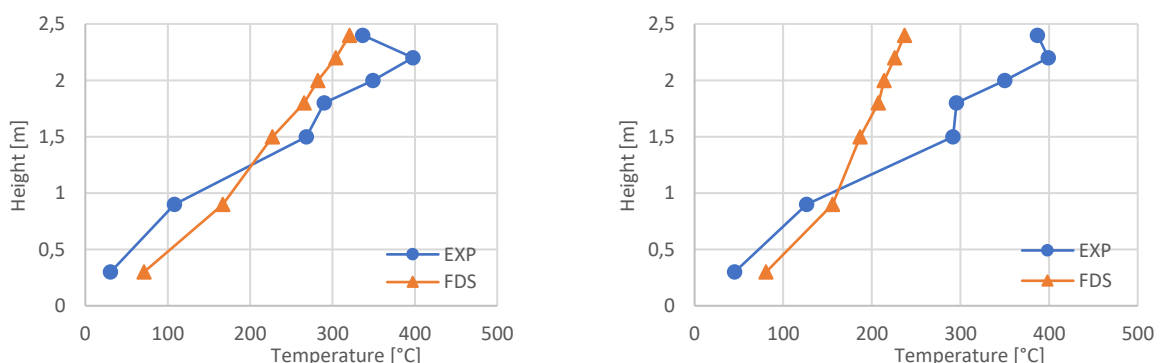


Figure 60: temperature-profiles at different times in the apartment (left: 450 seconds, right: 600 seconds)

### 7.7 Results in the corridor

The following images show the gas concentrations in the corridor, both measured and simulated. As expected, the simulations compare quite well with the experimental results in the initial phase of the fire. After flame extinction occurs, the results start to show more significant divergence, with FDS consequently under-estimating the O<sub>2</sub> concentration and under-estimating the CO concentration. Simulation results in the lower part of the room (at 0,3 meters above the floor of the corridor) show more significant deviation with the measured values. These differences can be accounted to local transient effects, as the measurements were done close to a wall, which was also seen in case study 1.

Results for CO<sub>2</sub> in the corridor show the same trends as observed in case study 1: experimental values measured in the corridor are significantly higher compared to the values in the apartment. FDS does not predict these higher values.

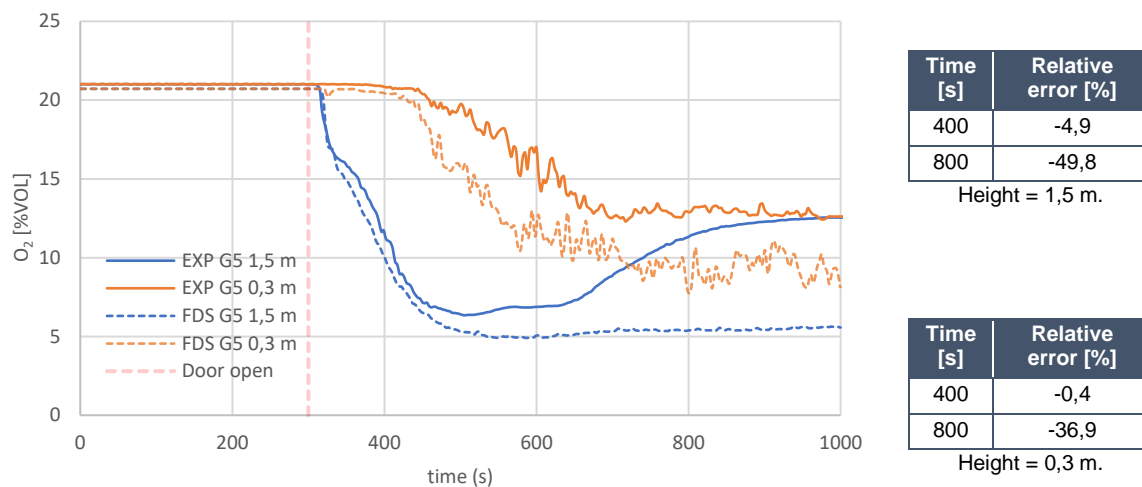


Figure 61: O<sub>2</sub> concentrations at measurement tree G5 at 1,5 meters and 0,3 meters height.

Overall, the gas concentrations are observed to be simulated to an adequate extent, with relative errors of approximately 13% being noticeable in the initial 500 seconds. Afterwards, significant deviations with errors of approximately 30-50% are observed as a result of FDS not adequately taking into account the combustion phenomena occurring after extinction is modelled.

The relative pressure in the corridor during the experiments was in the order-of-magnitude of 1-5 Pa. While FDS predicts relative pressures in the same range, the uncertainties related with these low values (with the fire not being the only possible dominant force in the pressure rise) makes comparing the numerical and experimental results prone to uncertainty. The results are shown in appendix 5.

As was seen in the apartment, temperatures are under-estimated as in reality the heat release rate is expected to be higher after extinction occurs. The initial trends are simulated adequately. It is expected that, should the heat release rate to be more or less steady after extinction, the temperatures in the corridor correlate better with the measurements. Figure 62 shows the temperature development in the corridor at measurement tree B5.

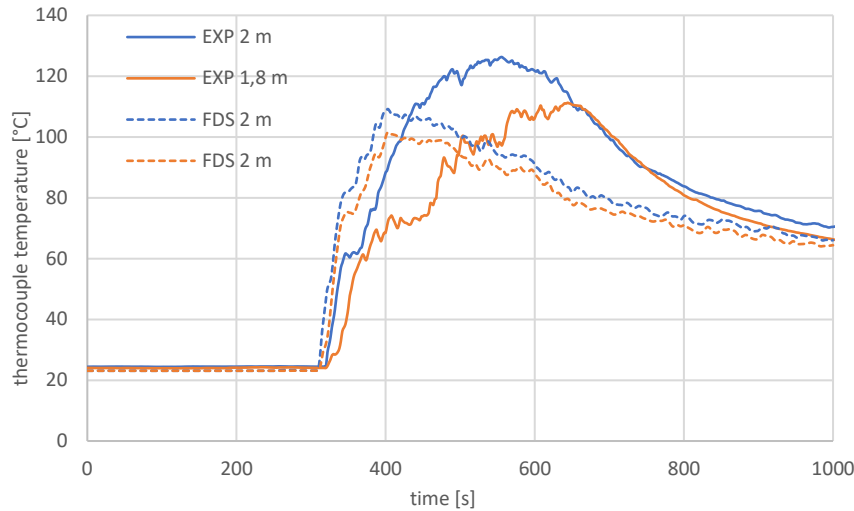


Figure 62: Results at measuring tree B5 at a height of 1,8 (TK1,5,3) and 2 meters (TK1,5,2) respectively.

Results at measuring tree B5 show quite a binary drop in visibility. After the door is opened and the smoke layer drops to the specific height, visibility is shown to drop instantaneously. At a lower height, more local transient effects are expected due to turbulence in the smoke layer, which was also observed in case study 1. The visibility in measurement tree B6 is shown to drop prior to opening the door. This was discussed earlier in paragraph 7.2. Differences are explainable through assumptions made in the modelling of the leakage from the apartment to the corridor and the associated heat losses.

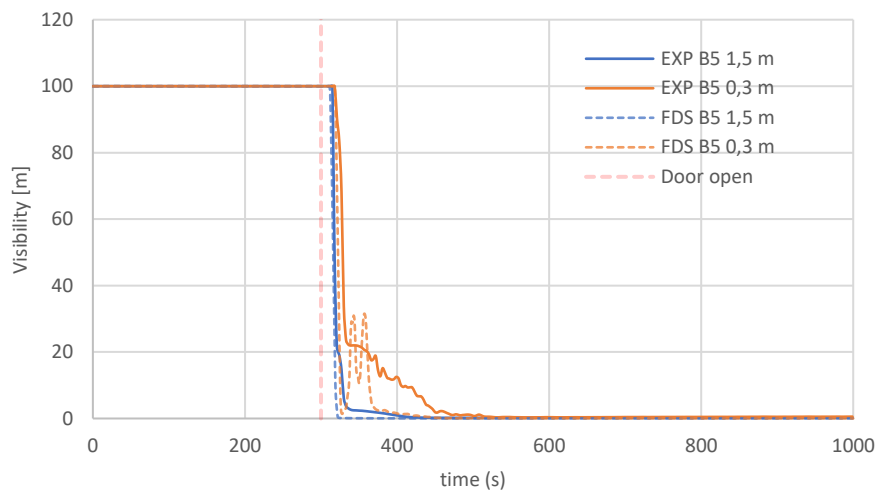


Figure 63: Visibility at measurement tree B5 at 1,5 (G5.1) and 0,3 (G5.2) meters height

## 7.8 Sensitivity study

The sensitivity of the numerical results presented in this work has been quite extensively explored in case study 1 and through the parametric studies in this case study. The work presented in this paragraph is meant to expand those results. The following parametric changes were made to study sensitivity:

| # | Auto-ignition temperature (°C) | AIT-Exclusion zone                                  | Extinction model  |
|---|--------------------------------|---|---|
| 1 | 350 & 450                      | Width and length of sofa, height of room            | 2 (settings from primary simulations)   |
| 2 | 400                            | Width and length of sofa, 40 centimeters above sofa | 2 (settings from primary simulations)   |
| 3 | 400                            | Width and length of sofa, height of room            | 1 (CFT=1.090°C, LOL=0,135, FBT=600°C)<br>1 (CFT=654°C, LOL=0,08, FBT=600°C)<br>1 (CFT=654°C, LOL=0,08, FBT=500°C)<br>1 (CFT=654°C, LOL=0,08, FBT=400°C)<br>Extinction=OFF |

Table 9: sensitivity study for case study 2

### 7.8.1 Auto-ignition temperature (AIT)

In the primary simulations, an AIT of 400°C was used, which was chosen based on information available in literature. However, as the fuel is a solid, the AIT of its pyrolysis gases is not easily measured. As such, the associated uncertainty is relatively high. To study the level of uncertainty on the results, simulations are run with a different value for the AIT. Consequently, values of 350°C and 450°C are used. Given the nature of the parameter, using a lower AIT might result in combustion away from the fire seat, while this might not be occurring when using a higher value.

Oxygen concentrations do not show significant differences between simulations. The heat release rate and temperatures in the enclosure predicted in the simulation with a lower AIT, show to be somewhat higher when compared with the primary results between 360 and 400 seconds. This is a result of FDS predicting some combustion to be taking place at some distance from the fire seat, more closely located to the measurement tree. This also results in slight differences in CO concentration in the enclosure.

Differences in temperature are not pronounced but noticeable. As shown in Figure 64, thermocouple temperatures are higher than the set AIT only in the case of the value of 350°C. Figure 65 clearly shows combustion taking place away from the fire seat, that in the other two numerical setups does not occur. The numerical results using an AIT of 450°C show to be somewhat lower than the initial results, indicating a somewhat lower heat release in the apartment.

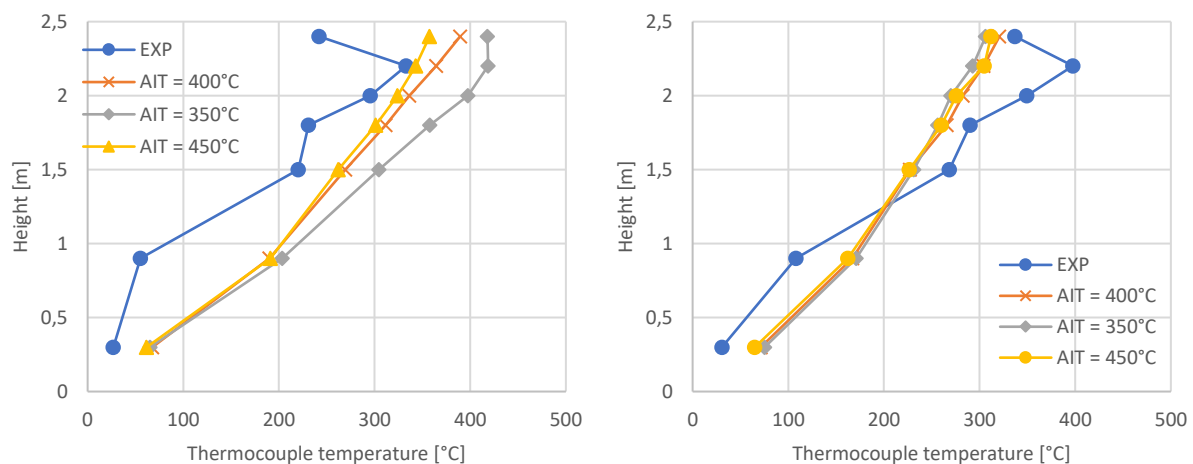


Figure 64: temperature-profile in the apartment at t=400 seconds (left) and t=450 seconds (right)

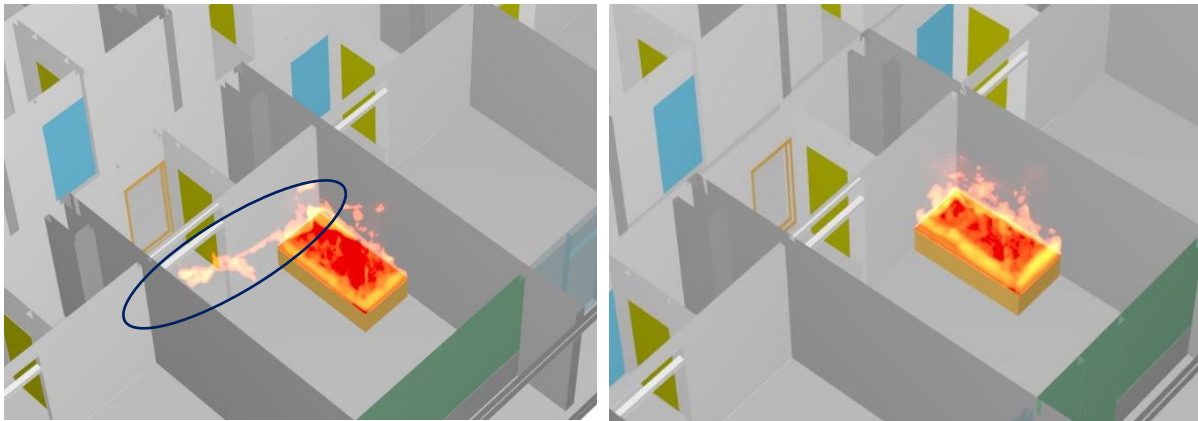


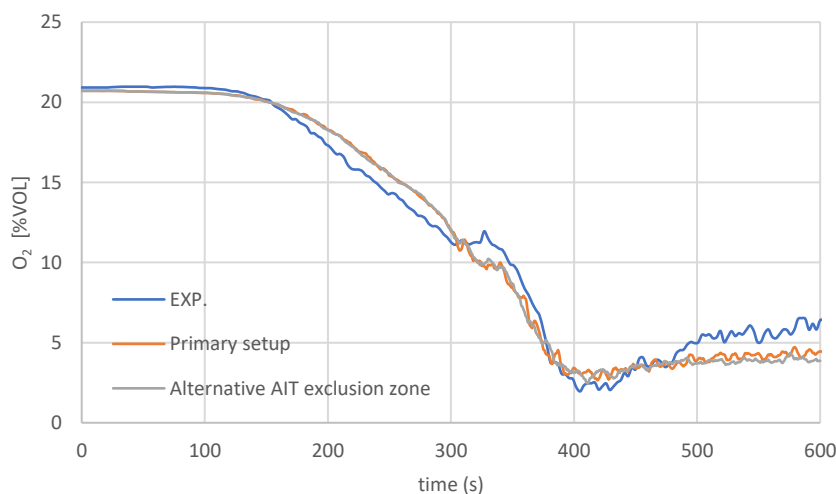
Figure 65: HRRPUV at 420 seconds for AIT=350°C (left) and 400°C (right). Notice the combustion taking place away from the fire seat.

### 7.8.2 Auto-ignition temperature exclusion zone

To prevent the need for modelling ignition, which is not straightforward when using a prescribed mass loss rate over an area and can be quite computationally expensive given the needed grid resolutions, the primary simulations use an AIT 'exclusion zone' in which the fuel is allowed to combust, regardless of the cells' temperature. The exclusion zone consists of the width and length of the sofa and spans the entire height of the room. In under-ventilated situations, this might result in spurious combustion near the fire seat which in reality might not occur, should the temperature above the fire seat locally drop below the AIT. To study the sensitivity to the size of the exclusion zone, one additional setup was studied, on top of the primary simulation:

- 2\*1\*2,6 meters (width\*length\*height), primary simulation;
- 2\*1\*0,4 meters above the sofa, alternative setup.

The oxygen concentrations in the apartment show the same trend and errors, as shown in Figure 66. Interestingly, the CO concentration and the associated errors in the apartment is somewhat higher in the simulation using the alternative setup. Given the fact that the heat release rate still more or less captures the same peak value, the same amount of mass is simulated to combust. It does so however, in a smaller volume. This results in lower O<sub>2</sub> concentrations locally and therefore less complete combustion. The results after extinction show to be sensitive to the setup for the exclusion zone. Based on this, it can be assumed that modelling an actual ignition source will have more pronounced effects.



| Time [s] | Relative error [%] |
|----------|--------------------|
| 200      | 7,5                |
| 500      | -13,7              |

Primary

| Time [s] | Relative error [%] |
|----------|--------------------|
| 200      | 6,7                |
| 500      | -21,8              |

Alternative

Figure 66: O<sub>2</sub> concentration in the apartment for different AIT exclusion zone setups

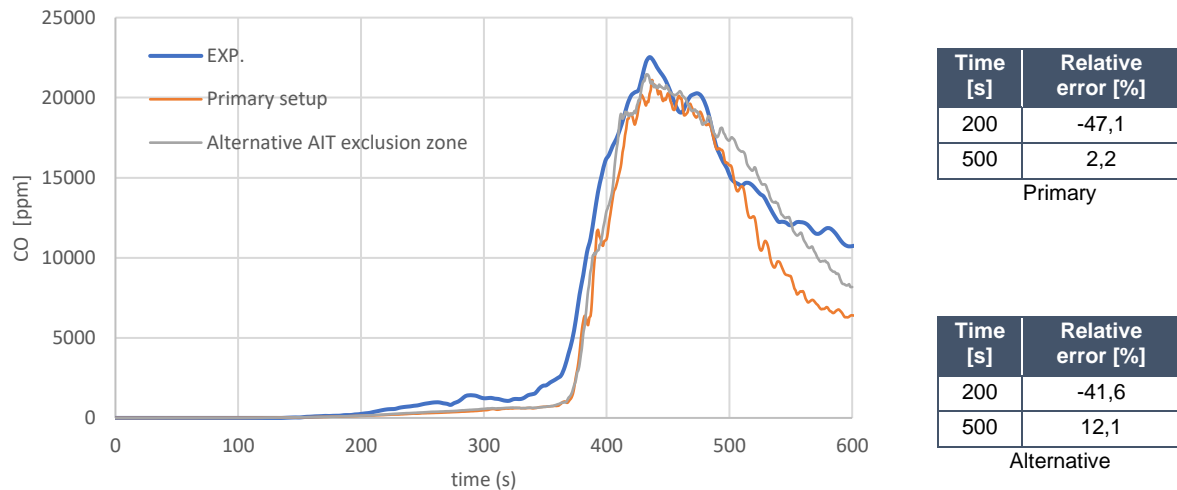


Figure 67: CO concentration in the apartment for different AIT exclusion zone setups

### 7.8.3 Extinction model

Differences between different parametric setting for the default extinction model (extinction model 2) are studied in the parametric study associated with paragraph 7.4 and case study 1. As the sensitivity study in case study 1 showed that extinction model 1 gives more conservative results, its effects are studied in more detail in this paragraph. Furthermore, the effects of not modelling extinction altogether are studied.

#### *Extinction model 1*

The theoretical framework behind Extinction model 1 is described in paragraph 4.7. The results presented in this paragraph use different settings for extinction model 1 and makes a comparison with the primary numerical results. The used settings are:

- A CFT of 1.090°C, LOL of 0,135 (settings used in primary simulations) and a Free Burn Temperature (FBT) of 600°C;
- A CFT of 654°C, LOL of 0,08 and FBT of respectively 600°C, 500°C and 400°C

Generally speaking, the differences on the fires' heat release rate and temperatures in the enclosure are small. One exception is the setup which uses a CFT and LOL of respectively 1.090°C and 0,135. In this setup, some extinction is predicted just prior to the door opening. This was also observed in the initial simulations as described in paragraph 7.3. The effects of extinction in that time-frame however, are not pronounced and do not directly translate to other quantities. After the door is opened, all setups show sustained combustion until a O<sub>2</sub> concentration of approximately 2-4 %vol is met. At that point, extinction is modelled. The setup with a CFT of 1.090°C and a LOL of 0,135 is first to show signs of extinction. It should be noted however, that extinction model 1, using a default LOL and FBT and a calculated CFT shows to perform better compared to the default extinction model. This is an indication that the used grid size of 5\*5\*5 cm might be too coarse to properly model extinction with the default model. In the grid sensitivity study, this was observed as well. This simulation also follows the CO concentration in the apartment to an acceptable extent.

Furthermore, differences in gas concentrations are pronounced. This mainly can be attributed to the fact that, when using extinction model 1, more combustion is modelled to be taking place after extinction. This effects grows more pronounced when a lower FBT is prescribed. Due to the lower O<sub>2</sub> concentrations near the flame sheet, an exponential increase in CO is modelled generated as a result of the two-step combustion model.

Overall, using a different extinction model does result in pronounced changes with regards of heat release rate when using values for the CFT and LOL that are taken and calculated from the FDS User's

Guide. However, when the initial values for the critical flame temperature and/or lower oxygen limit are already significantly low, no significant changes are observed. The gas concentrations in the enclosure however, deviate to quite an extent. This is explainable through the fact that CO generation increases exponentially at lower oxygen concentrations near the combustion zone.

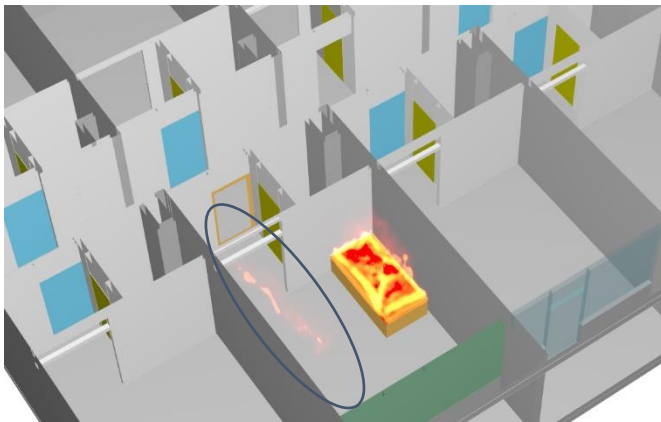


Figure 68: HRRPUV at 400 seconds for the simulation using a free burn temperature of 400°C, notice the combustion occurring away from the fire-seat.

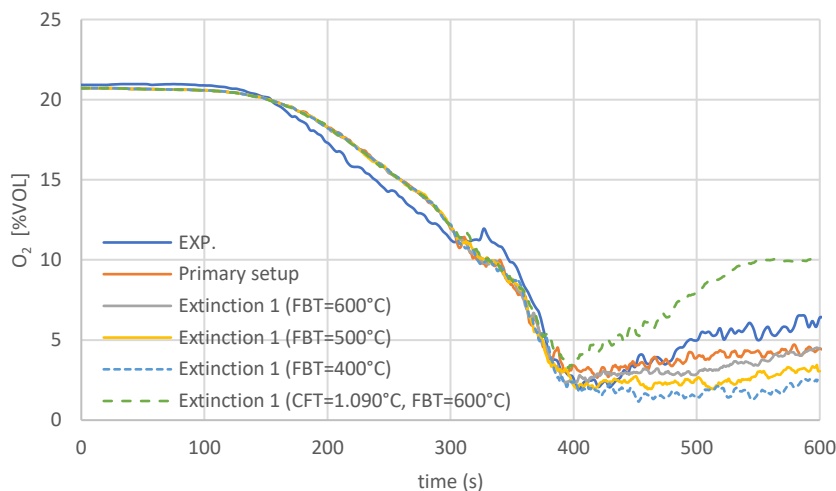


Figure 69: O<sub>2</sub> concentration using different parametric setups for extinction.

### No extinction

Not taking into account extinction allows combustion to continue as long as there is sufficient oxygen available to keep the reactions going. No temperature dependency or lower oxygen limit are taken into account. Not enabling extinction is crude but gives insight in the maximum heat release rate and temperatures in the enclosure, given the prescribed mass loss rate and available oxygen.

The results in Figure 70 show the same trends as the primary simulation results up to approximately 360 seconds. Around that time, extinction is modelled to occur in the primary simulation and the heat release rate is modelled to significantly drop. In the simulation without an extinction model, the heat release rate is allowed increase up until the point no O<sub>2</sub> is available to maintain combustion, which occurs at approximately 450 seconds. Effects are clearly visible in Figure 70. Given the imposed chemistry, there is insufficient oxygen in the enclosure to let the pyrolyzed mass fully combust. This underlines the fact that (under the imposed chemistry) in the experiment, more mass pyrolyzed than could actually combust. As expected, temperatures in the enclosure are severely over-estimated when not modelling extinction. Furthermore, at some point a significant amount of combustion is simulated to

occur away from the fire seat as a result of low oxygen concentrations around the fire seat, as shown in Figure 71.

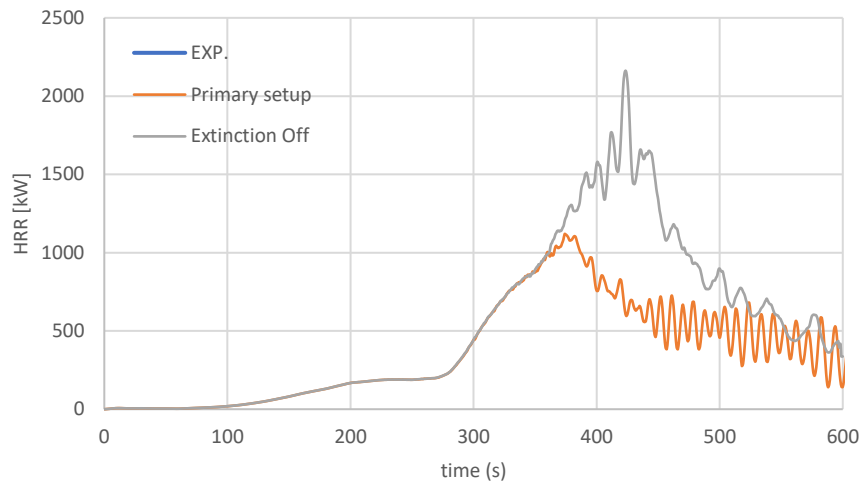


Figure 70: Heat Release Rate derived from the experiment, primary simulation and with no extinction model enabled

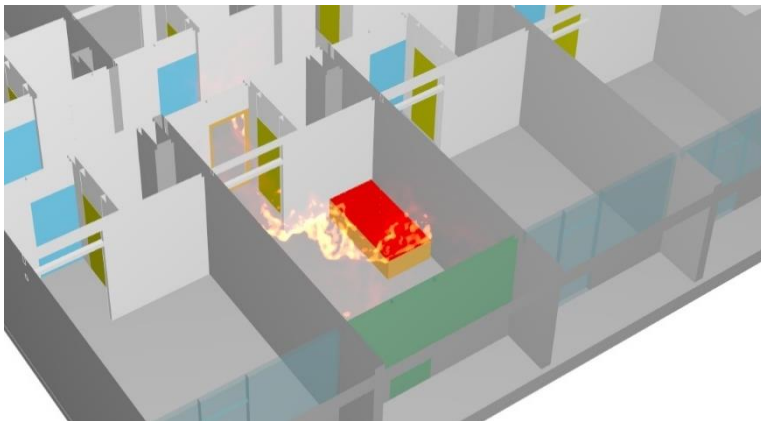


Figure 71: HRRPUV at t=420 seconds with no extinction modelled. Notice combustion taking place away from the fire seat.

## 7.9 Case study 2: conclusion

### 7.9.1 Overall results

The initial results for case study 2, using static yields for soot and CO showed a poor correlation with the experimental data. In the initial 400 seconds, the CO-concentrations are severely over-estimated, while in a later time-frame, an under-estimation is observed. This also results in a less rapid decrease in oxygen in the apartment, as no dynamic effects in the fuel-to-air ratio are taken into account. Using static species-yields to account for the transient effects that are expected in under-ventilated fire conditions might lead to results which, from a toxicology standpoint, are severely over-conservative. Moreover, as the oxygen concentration is predicted to decrease less rapid, flame extinction also is modelled at a later time. In practical fire-engineering studies, this might result in over-investments or even fire engineering problems which are impossible to solve.

The flame extinction model of FDS is shown to predict flame extinction to occur at a higher oxygen concentration than observed in the experimental results. The experimental results show a minimum oxygen concentration in the apartment of approximately 2 %vol while in the simulations a minimum value of 9 %vol is seen. This results in fundamental problems, as the results of the simulation are at some point wholly determined by the extinction model.

The simulated oxygen concentrations are more or less expected given the fact that a lower oxygen limit of 13,5 %vol was used in the simulations. Taking into account the effects of the combustion being vitiated (higher temperatures lead to faster kinetics, which is the underlying principle of the critical flame temperature concept) somewhat lower oxygen concentrations are modelled to sustain combustion.

Altering the lower oxygen limit and critical flame temperature to more closely follow the experimental data and using a two-step combustion model to account for CO and soot generation resulted in a good correlation for gas concentrations in both the apartment and corridor. In the initial period, errors ranging from 5 to 10% were found, which is acceptable given the imposed uncertainties. At a later time, the numerical results showed to diverge from the experimental results, with errors up to 60% being observed.

The validity of the used inputs however, is questionable. After 600 seconds, FDS starts to significantly deviate from the experimental results. This can be attributed to a more non-flaming combustion taking place instead of the flaming combustion modelled by FDS. Moreover, temperatures are significantly under-estimated by FDS after extinction is modelled. Finally, the values for CO<sub>2</sub> in the corridor are significantly lower in the FDS simulations compared with the experimental results, which was also observed in case study 1.

While the gas-concentrations show a good agreement with the experimental data, this might very well be a coincidence given the fact that the two-step simple combustion model is rudimentary to a significant extent. Given the nature of the model, the significant increased CO and soot generation is only observed at very low oxygen-concentrations. In reality, the formation of CO and soot is much more complex and depends on more parameters than just the available oxygen. This is further explored in case study 3.

## 7.9.2 Sensitivity study

The sensitivity study shows that :

- Altering the auto-ignition temperature does not result in significant differences other than the fact that, when using a lower value, combustion is simulated to occur at some distance from the fire seat. This results in somewhat higher temperatures. Differences however, are not very pronounced. With substantially higher or lower values, the differences are expected to be more pronounced.
- Furthermore, the exclusion zone of the auto-ignition temperature shows to have some influence on the outcome of the simulation. Carefully choosing the exclusion zone therefore is necessary.
- Using a different extinction model which is based on a free burn temperature in conjunction with the critical flame temperature and lower oxygen limit results in a more conservative outcome in the framework of this case study as combustion is modelled to be occurring at somewhat lower oxygen-concentrations. Extinction model 1 showed to perform better than extinction model 2 using the calculated and default values for respectively the CFT and LOL.

## 8. RESULTS CASE STUDY 3: DOOR OPENED AND CLOSED

### 8.1 Description of experimental and numerical setup

The experimental scenario chosen to model is scenario 16. The experiments took place in the morning of July 4<sup>th</sup>. The experiments were carried out using apartment 1.21 as the room in which the fire seat was placed. During the experiments, the door to the corridor was opened after 300 seconds. 30 seconds later, it was closed again. Given the fact that area of the sofa showing signs of degradation is restricted to approximately one half of the sofa, the area of the vent modelled from which the pyrolysis gases are introduced in the domain is modelled to be 1 m<sup>2</sup>.

The main goal of this case study is to study the validity of the numerical setup found in case study 2. Therefore, the final setup found in that case study is used as a starting-point in this chapter. Some alterations might be necessary for taking into account differences between the underlying experiments. Experiments were carried out in a different apartment, which leads to slight differences in airtightness. The model was adjusted to account for the different fire room, which is shown in the following image.

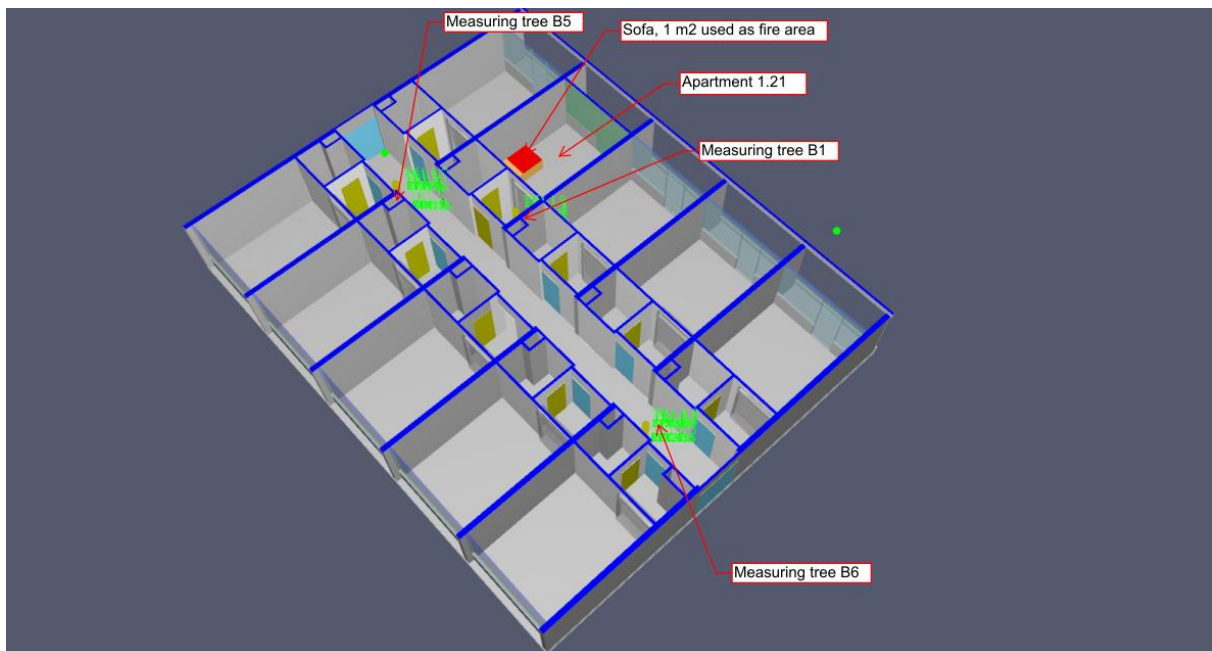


Figure 72: numerical setup for case study 3, using apartment 1.21 as the fire room

### 8.2 A-priori parametric study: fire-induced pressure in apartment and corridor

The measured airtightness of apartment 1.21 is somewhat higher than the airtightness of apartment 1.19. As was the case with case study 2, alterations to the enclosure were made to make the airtightness of both apartments more identical. The exact airtightness therefore is not known. Given the carried out adjustments to the enclosure, the airtightness of apartment 1.21 is expected to be more or less identical with apartment 1.19. Therefore, the same value as the one used for case study (leakage area of 130 cm<sup>2</sup> with a leak pressure exponent of 0,56) is used as a starting point.

The actual leakage area is assumed to lie anywhere in between the measured and assumed. Therefore, the effects of the leakage are once again studied before a setting for the final simulations is chosen. In the following images, the results for a total leakage area of 130 (assumed), 150 (not shown in plot), 200 and 227 cm<sup>2</sup> (measured) are shown. Leakage is modelled using the bulk leakage method, with the exception of the door between the apartment and the corridor, for which the same methodology as used in case study 2 was chosen. Therefore a leakage area of 20 cm<sup>2</sup> with a distribution of 75%-25% (bottom-rest) was used.

Notice that the upper-limit for the measurements using the 'PL' equipment is 50 Pa. The peak measured by the less sensitive 'PH' equipment directly after the door is closed is significantly higher. Therefore, the data captured by the 'PH' equipment is used in the following figure, which shows the pressure evolution at a height of 0,2 meters in the apartment.

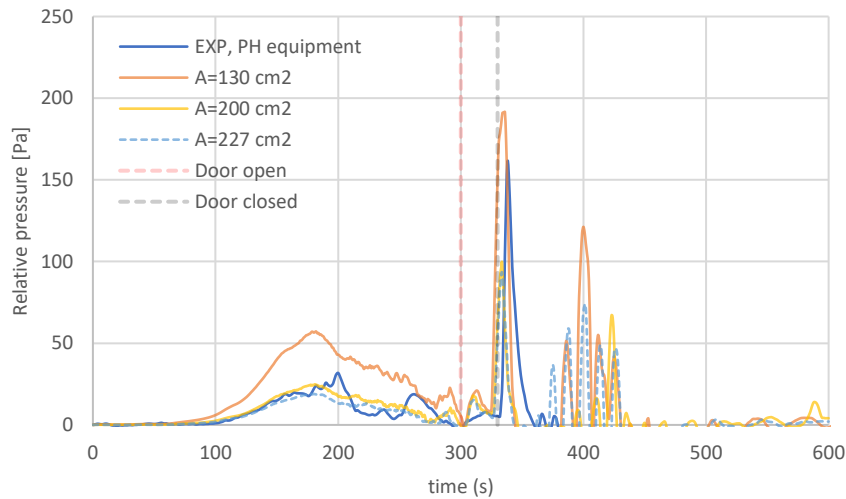


Figure 73: Pressure evolution in the apartment for different leakage areas. Red and black dotted lines indicate opening and closing of corridor door.

Using a leakage area of 130 cm<sup>2</sup> and 150 cm<sup>2</sup> clearly over-estimate the initial pressure increase in the apartment while both a leakage area of 200 and 227 cm<sup>2</sup> show an appropriate correlation. Just prior to the door being opened, both the experimental and numerical data show an underpressure being recorded, which is an indication that the fire is growing more under-ventilated. After the door being opened at 300 seconds, the pressures rises exponentially as more oxygen is made available for combustion. Around 340 seconds (10 seconds after the door is closed) flame extinction is expected to occur in both the experimental and numerical data given the sudden decrease in pressure. This is an indication that the moment at which flame extinction occurred is at least approximated accurately and coincides with the experimental data showing a drop in mass loss rate (see Figure 74). Peaks in the pressure from 400 seconds onwards are a result of oscillations due to the bulk leakage model.

If the limited accuracy and wide resolution of the used equipment and the limitations of the bulk leakage model are taken into account, the simulation results for correlate quite well with the experimental data. Based on this, a leakage area of 200 cm<sup>2</sup> is chosen to carry out the remaining simulations.

A similar study is executed for the airtightness of the corridor. Fully describing the results of that study bypasses the goal of the main text of this thesis as the airtightness in that corridor is only of secondary importance in this study. A leakage area of 1.000 cm<sup>2</sup> was found to fit the experimental data best, which is equal to the value found in case study 2.

### *Maximum pressure iterations*

In multiple mesh FDS runs the simplified form of the Poisson equation otherwise used in single mesh-runs cannot be used to calculate the global pressure solution. In these cases, the simplified Poisson solver is used per mesh in parallel. The pressure field on each mesh boundary is forced to match the adjacent one by an iterative approach. This results in a slight error in velocity at the mesh boundary. To limit the error, several iterations are run to reach the velocity tolerance which by default is half the cell width ( $\delta x/2$  or 2,5 m/s). The maximum number of iterations is set at 10 by default to limit excessive computational work. To check whether a smaller velocity tolerance (and more pressure iterations) result

in more accurate results, a simulation was run with a velocity tolerance ( $\delta x/8$  or 0,625 m/s) and a maximum of 25 pressure iterations. No significant differences are observed, as shown in appendix 6.

### 8.3 Results in the apartment

The following results were found using the numerical settings used in the final numerical setup used in case study 2 (see paragraph 7.5). The only variable changed is the airtightness of the apartment, which was set to 200 cm<sup>2</sup> based on the results of the previous paragraph.

The following image shows the simulated Heat Release Rate over time. The simulated Heat Release Rate follows the prescribed curve, up until the first point of extinction is modelled just before the door to the corridor is opened at 300 seconds. After the door is opened, extra oxygen is made available and the heat release rate peaks shortly after, with a maximum of 800 kW. After that point, extinction is modelled and the heat release rate drops. In total, approximately 2 kilo of pyrolyzed mass does not combust in the simulation. From 600 seconds onwards, FDS shows some combustion taking place, which in the experiments is not likely to be the case due to low temperatures in the enclosure. This is a result of the imposed auto-ignition temperature exclusion zone.

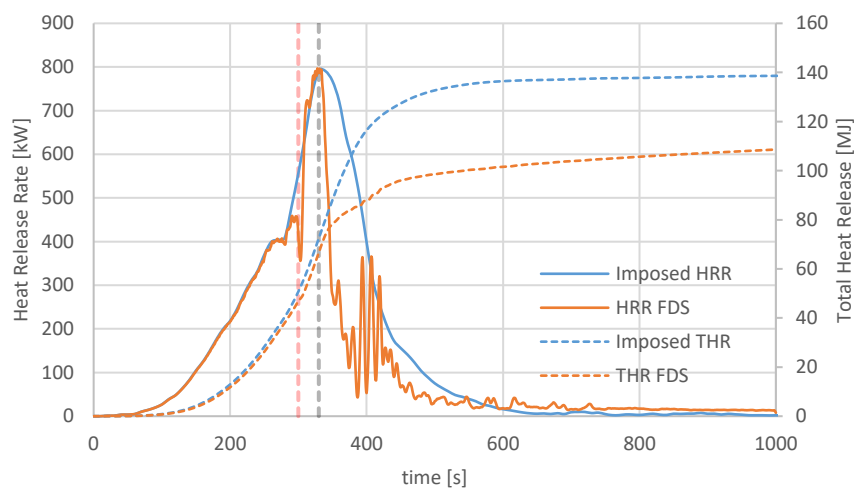
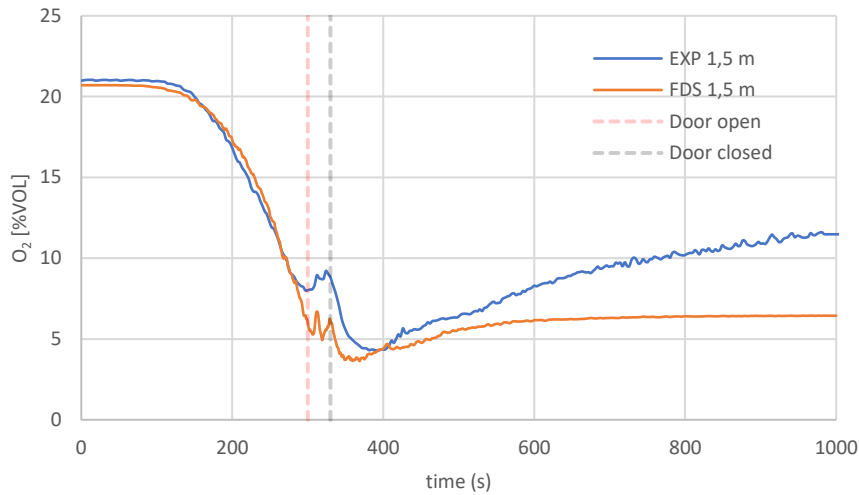


Figure 74: Heat release rate. Red and black dotted lines indicate opening and closing of corridor door.

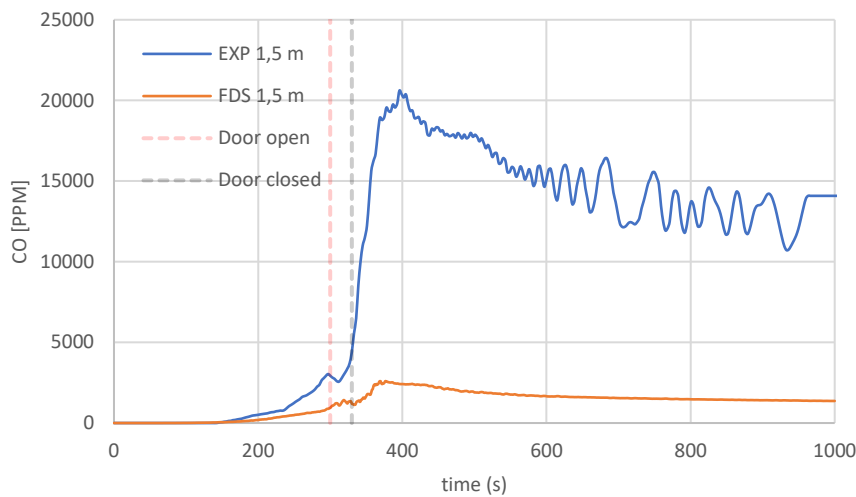
The gas concentrations in the apartment follow the experimental data well up to approximately 300 seconds. While the simulated oxygen concentration does follow the same trends as seen in the experiments, some nuance differences exist between 270-400 seconds and 600 seconds onwards. This indicates that in the period between 270-400 seconds, some effects of extinction might be happening in reality that are not modelled appropriately. The experimental mass loss rate shows a clear drop at 330 seconds, which is caused by underventilation. This coincides with the lower pressures observed in the experimental data at that point, as seen in Figure 77.

The CO concentration does not follow the experimental data after 200-300 seconds. The two-step simple combustion model does only predict a limited amount of CO being generated due to the relatively high O<sub>2</sub> concentrations in the enclosure. This illustrates that modelling CO generation by methods done is not appropriate. Due to the CO concentrations being severely under-estimated (with absolute differences up to 15.000 ppm) from approximately 300 seconds, the CO<sub>2</sub>-concentrations are over-estimated from the same point onwards.



| Time [s] | Relative error [%] |
|----------|--------------------|
| 200      | 4.1                |
| 400      | 6.7                |
| 600      | -21.5              |
| 800      | -34.2              |

Figure 75: O<sub>2</sub> concentration in the apartment. The relative differences take into account the initial difference between the numerical and experimental data.



| Time [s] | Relative error [%] |
|----------|--------------------|
| 200      | -62.1              |
| 400      | -88.1              |
| 600      | -88.7              |
| 800      | -88.9              |

Figure 76: CO concentration in the apartment.

The fire-induced pressure in the apartment is shown in Figure 77. In the initial fire growth-phase, the pressure evolution is adequately predicted. Around 280 and 330 seconds, phenomena related to extinction (drops in pressure) are observed, which coincides with observations made relating to both the O<sub>2</sub> concentration and heat release rate. At that time, the peak in relative pressure is over-estimated. This is an indication that the actual heat release rate during the experiments was lower.

The drop in pressure in the experiments at 200 seconds is not captured by FDS and can be attributed to the time-averaging of the mass loss rate. In reality, a more spurious mass loss rate is observed at that moment. Furthermore, sharp peaks in the pressure level are susceptible to uncertainties. As was the case in case study 2, the fire-induced pressure shows significant sensitivity to the heat release rate and thus to the extinction model.

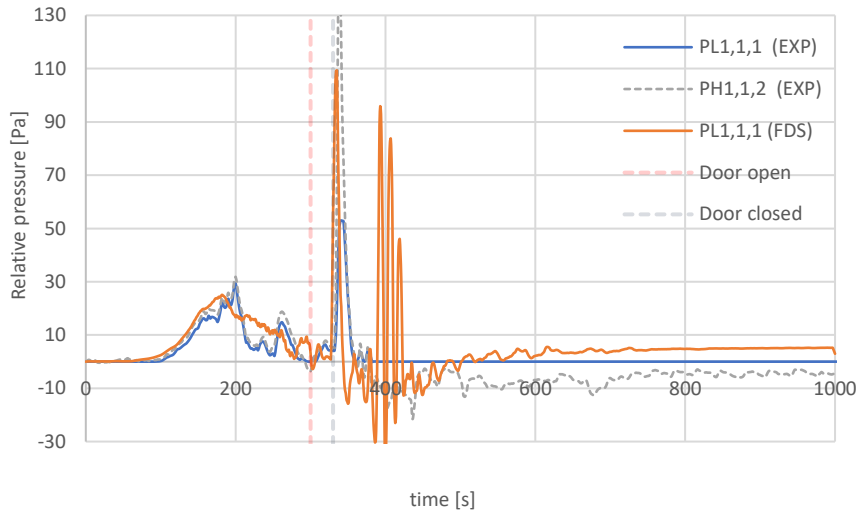


Figure 77: fire-induced pressure in the apartment showing both the experimental data for 'PL' and 'PH' equipment.

As with the other casestudies, the simulated temperatures are somewhat ahead of the experimental data. Generally speaking, the initial trends are predicted in line with observations made in case studies 1 and 2. However, after extinction, temperatures are severely underpredicted which is an indication that the actual heat release rate of the fire is in reality somewhat higher than predicted by the extinction model. The experimental uncertainties associated with thermocouple measurements quantifying differences and drawing conclusions difficult.

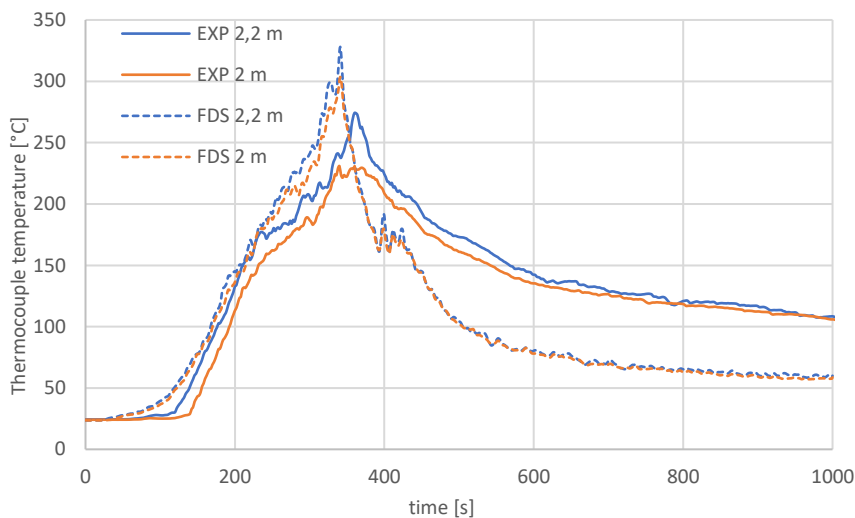


Figure 78: temperatures at different heights (TK1,1,1 = 2,2 m<sup>1</sup>, TK1,1,2 = 2m<sup>1</sup>) in the apartment

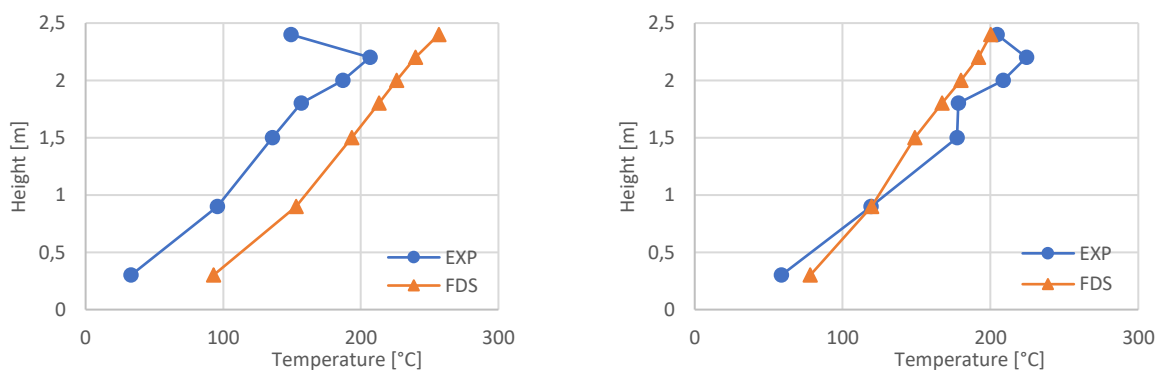


Figure 79: temperature-profiles at different times in the apartment (left: 300 seconds, right: 400 seconds)

### 8.4 Results in the corridor

The concentrations of O<sub>2</sub>, CO and CO<sub>2</sub> at a height of 1,5 meters near the corridor door show to drop or rise prior to the opening of the door in the experiments, which is not observed in the simulations. This is a result of FDS not taking into account heat transfer for the leaking gases properly as discussed in paragraph 7.2. Moreover, as the experimental transport time is not accurately known, some deviation can be expected.

For O<sub>2</sub> and CO<sub>2</sub>, respectively the minimum and maximum values at a height of 1,5 meters show good correlation. Given the fact that the CO<sub>2</sub>-concentration in the apartment is over-estimated by FDS prior to opening the door, somewhat higher concentrations in the corridor would be expected as well. This is not the case, which is in line with the observations in case studies 1 and 2 in which the CO<sub>2</sub> concentrations are significantly higher in the corridor compared to the apartment. Results for CO show significant deviations when comparing both trends and maximum values. This can be attributed to the significant lower concentrations in the apartment due to the fact that CO generation is not appropriately taken into account.

At some point (600 seconds onwards) in the experimental results, results for 0,3 and 1,5 meters more or less converge, indicating some level of homogeneity in the corridor. This is not observed in the simulations. Both the fires' heat release rate and the pressure in the apartment are shown to be over-estimated in the simulations, which in the simulations results in some leakage of gasses through the door, which is not likely to be the case in the experiments.

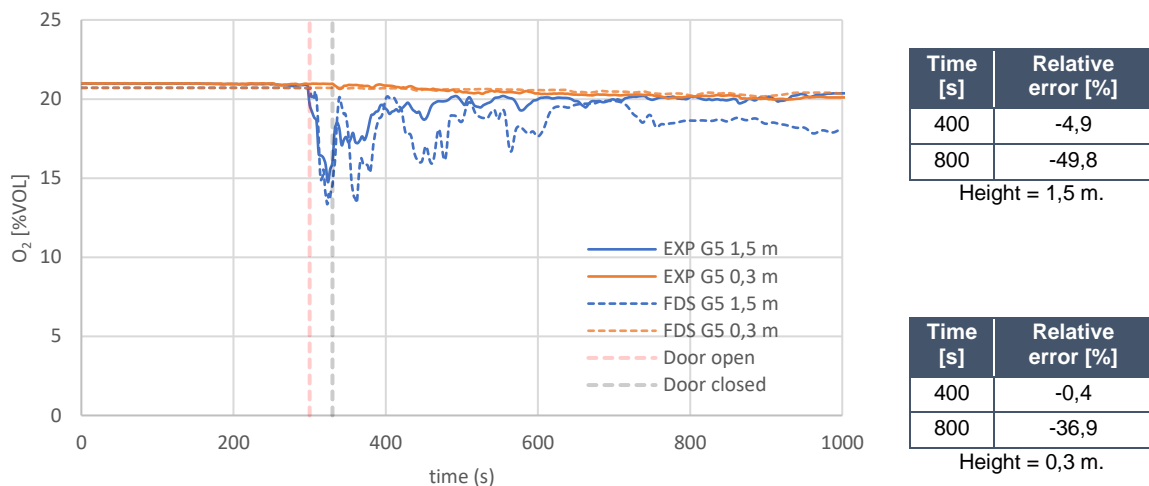


Figure 80: Oxygen concentrations at measurement tree G6 at 1,5 meters and 0,3 meters height.

Relative pressures in the corridor are in the order of single Pascals, which makes the experimental data susceptible to external influences (e.g. wind, opening and closing of doors). The experimental and numerical data however, demonstrate the same trends and show to be in the same order-of-magnitude.

As shown in Figure 81 and Figure 82, the temperatures in the corridor are shown to be predicted quite well at some distance from the door of the apartment (measuring tree B6). Differences observed closer to the door can be attributed to local phenomena, as was the case in case studies 1 and 2.

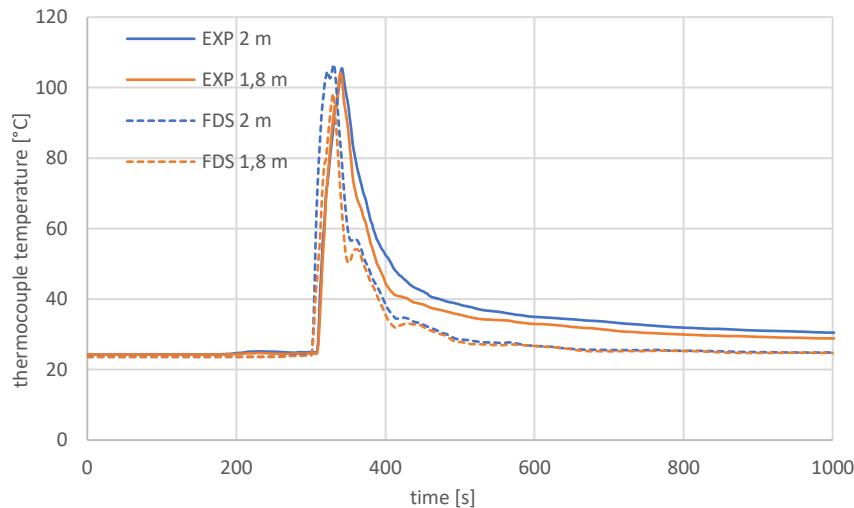


Figure 81: Results at measuring tree B5 at a height of 1,8 (TK1,5,3) and 2 meters (TK1,5,2) respectively.

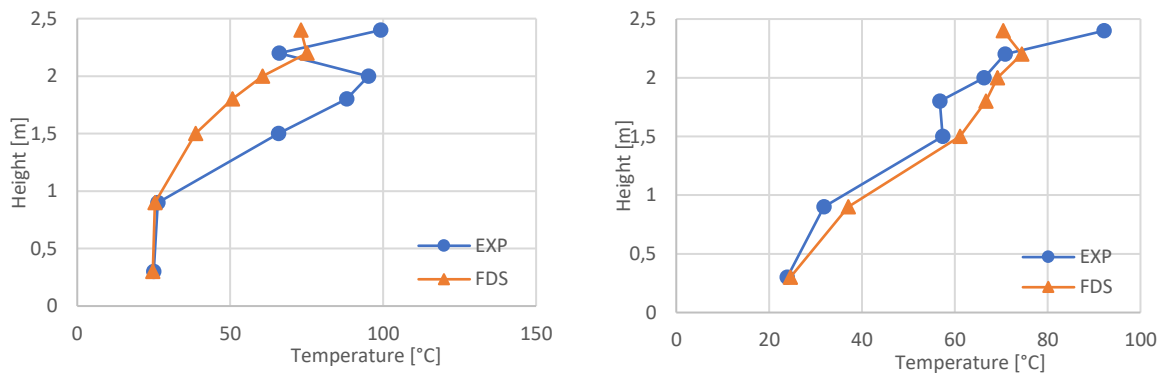


Figure 82: results at measurement tree B5 (left) and B6 (right) at t=350 seconds

The following figure shows the development of the visibility in the corridor. The experimental data for both measuring points indicate a more transient decay of visibility, while the FDS results show a somewhat more binary decay. However, the moment at which the visibility drops to approximately 0-10 meters at 1,5 meters is comparable. At a lower level, the experimental and numerical data do not correlate well. This can be attributed to the fact that this scenario relies heavily on the leakage model of FDS, and the over-prediction of pressures in the apartment by FDS, leading to more mass leaking into the corridor. This will result more mass leaking from the apartment into the corridor. Furthermore, local transient effects related to the exact location of the equipment can be of importance as seen in case studies 1 and 2.

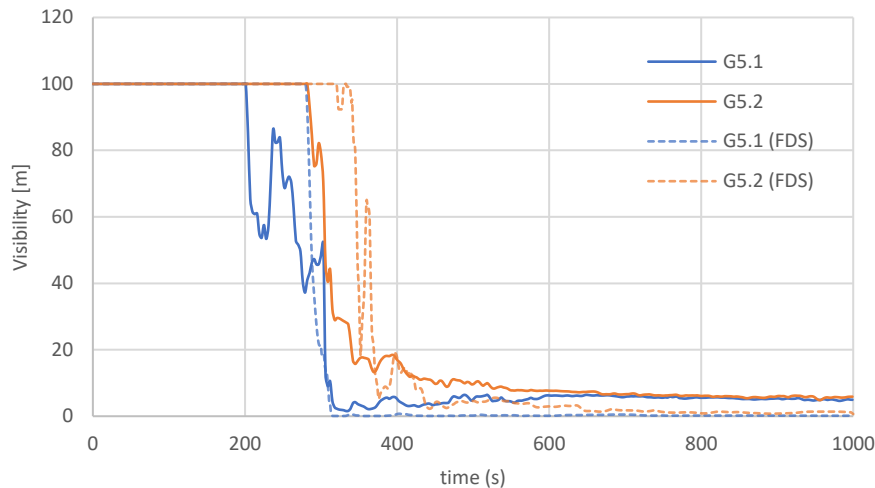


Figure 83: Visibility at measurement tree B5 at 1,5 (G5.1) and 0,3 (G5.2) meters height

## 8.5 Case study 3: conclusion

To check the validity of the setup used in case study 2, an additional case study was carried out. The used experimental data was acquired during an experiment in apartment 1.21 in which the door to the balcony was closed and the door to the corridor was opened after 300 seconds. 30 seconds later, it was closed again. The experimental data shows a significantly lowered  $O_2$  concentration in the apartment, albeit not as low as was the case in case study 2. Clear indications of the fire being under-ventilated are seen (drop in pressure, drop in mass loss rate and increase in CO production).

While the settings for the extinction model that were found to give good results in case study 2 resulted in adequate predictions relating to the  $O_2$  concentrations in the apartment, CO is significantly underestimated. As such, the formation of  $CO_2$  is over-estimated from that same point in time. This shows that simply limiting the formation of CO and  $CO_2$  based on the available  $O_2$  is a severe over-simplification of reality.

Fire-induced pressures were found to correlate well with the experimental data for the initial period in which no extinction is modelled. Afterwards, while the order-of-magnitude was found to be adequate, deviations are observable. These differences can most notably be attributed to the leakage and extinction models used by FDS. The same trend is observable for temperatures in the enclosure.

Given the complexity of the used methodology many more variables can be changed to gain slight improvements in results. In this case however, the extinction model dominates the entire simulation after extinction.

## 9. IMPLICATIONS FOR PRACTICAL FIRE ENGINEERING

### 9.1 Introduction

In practical engineering studies, whether or not an enclosure threatened by fire and smoke is tenable for its occupants is determined by means of tenability criteria. Used tenability criteria differ per case but are mostly related to visibility in smoke, heat exposure and/or toxicological effects of fire effluents on the occupants.

In this chapter, the implications for tenability studies of the results presented in earlier chapters of this thesis are studied. More results are available in appendix 6.

### 9.2 Visibility in smoke

Given the results of the comparison between the experimental and numerical results, it can be concluded that visibility in the corridor is adequately simulated at a height of 1,5 meters. Lower in the corridor, turbulent flow characteristics and local transient phenomena start to become important. Most notably in casestudies 2 and 3, the initial drop in visibility at a height of 1,5 meters just before the door is opened is not predicted accurately due to both uncertainties in the experimental data and limitations related to heat transfer in the leakage model.

The secondary and final steep drop in visibility at a height of 1,5 meters sometime after the door is opened is modelled accurately in all casestudies. Please note that the measured (experimental) visibility does not directly say anything about the smoke density in the enclosure (see paragraph 5.2.1).

Tenability limits mentioned in literature range from 5 meters [45] up to 30 meters [46], with the latter being viewed upon as 'severely conservative' and only being appropriate in very large enclosures with long possible exposure times to fire effluents. Values are typically chosen on the basis of occupants being able to 'see' the exit of the enclosure they are in and typically do not give information on the actual physiological effects of the smoke on the occupant. Furthermore, it is considered that for limits of both 5 and 10 meters the effects of toxic gases are limited for a duration of respectively 20 and 60 minutes [45].

When setting a tenability limit of 10 meters for visibility, which is considered appropriate given the geometry and expected exposure time, the following results apply for the different casestudies. Results are taken from the measuring tree located furthest away from the door of the apartment (B5 for case study 1 and 2, B6 for case study 3) at a height of 1,5 meters.

| Case study | Tenable time as per visibility > 10 meters [s] |     |
|------------|--|-----|
|            | FDS  | EXP |
| 1          | 323  | 327 |
| 2          | 321  | 328 |
| 3          | 308  | 313 |

Table 10: tenable time in the corridor based on data at 1,5 meters high from measuring tree B5 (casestudies 1 and 2) and B6 (case study 3).

While the overall experimental and numerical data show significant deviations for most notably case study 3, the implications for fire engineering studies using a deterministic tenability limit for visibility seem minor. In all cases the visibility is shown to behave more or less binary after the door is opened.

Off course reality is more complex as visibility does not say anything about physiological effects. A lower visibility will typically result in lower movement speeds of occupants and therefore longer exposure times to toxic gases and heat. These effects however, cannot be taken into account without resorting to more

complex egress models. This goes beyond the purpose of this thesis and is therefore not done. It can however, be done in a follow-up study.

### 9.3 Heat exposure

Exposure to excessive heat can result in hyperthermia, skins burns and damage to the respiratory tract. Typically, tenability limits for heat exposure are used in fire engineering studies. These can be based on a fixed temperature, fixed (radiant) heat-flux or a dosage within the framework of the fractional effective dose methodology [45].

Especially inside the apartment in which the fire is located, exposure to heat is of significant importance in the early stages of the fire. Not taking into account thermal radiation, which at lower temperatures in the early stages of the fire holds limited relevance in the far-field region<sup>2</sup>, the Fractional Effective Dose for thermal exposure is calculated as [45]:

$$FED_{heat} = \int_{t_1}^{t_2} \left( \frac{1}{5 * 10^7 * T^{-3,4}} \right) * \Delta t$$

In which  $FED_{heat}$  is the Fractional Effective Dose for heat exposure,  $T$  is the gas-phase temperature which is taken as the thermocouple temperature at a height of 2 meters and  $\Delta t$  is the time-step. This correlation is based on a tolerance time for unprotected skin to convective heat exposure. As the correlation best applies when humidity approaches RH=100%, it is a somewhat over-conservative expression for lower temperatures (and under-conservative for higher temperatures).

Incapacitation is assumed to occur if the FED is unity. To be conservative and to account for uncertainties in the fitness of the population in the building, a tenable limit of 0,3 is chosen for the  $FED_{Heat}$ .

The following graphs show an example of the evolution of the FED for thermal exposure over. In the apartment, significant differences are observable which can most likely be attributed to experimental uncertainties. In the corridor, the differences are less pronounced.

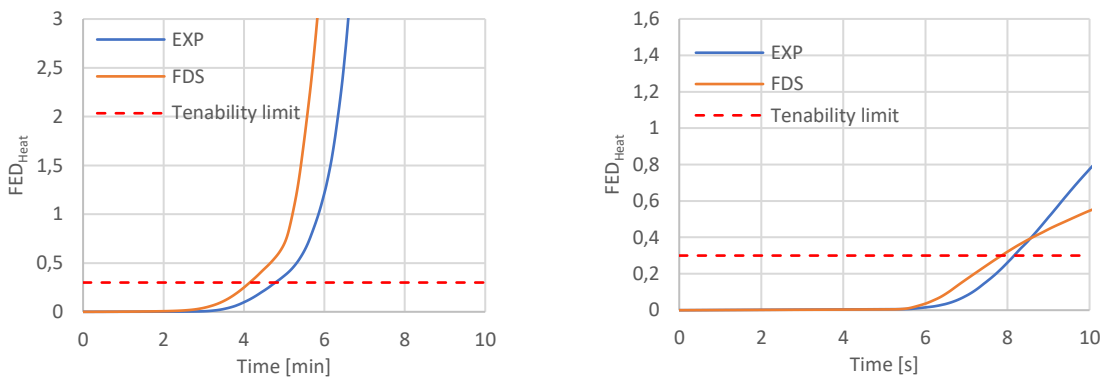


Figure 84:  $FED_{heat}$  for case study 2. Left: apartment, right: corridor, measuring tree B5.

In the corridor, results seem to correlate quite well. It must be noted however, that since the data of just one thermocouple is used, differences in stratification are not appropriately taken into account. As these differences were shown to be substantial, they can have significant effects. The following table lists the tenable times in the both the apartment and the corridor. Results for case study 3 show the importance of door control in the case of fire.

<sup>2</sup> Which is assumed here, as the temperature in the apartment is approximately 150°C when the tenability limit is reached. This leads to radiant heat exposures of approximately 1,3 kW/m<sup>2</sup>, which is not relevant in the framework of FED. Off-course, radiant heat from the fire itself cannot be neglected.

| Case study | Tenable time as per $FED_{heat} < 0,3$ [s] |             |           |             |
|------------|--|-------------|-----------|-------------|
|            | FDS  |             | EXP       |             |
|            | Apartment                                  | Corridor    | Apartment | Corridor    |
| 1          | 212  | 481         | 276       | 474         |
| 2          | 248  | 471         | 286       | 488         |
| 3          | 217  | Not reached | 236       | Not reached |

Table 11: tenable time in the enclosures based on data at 1,5 meters high from measuring tree B5 (case study 1 and ) and B6 (case study 3).

#### 9.4 Toxicological effects

Fire effluents typically contain asphyxiants and irritants that can result in loss of consciousness, confusion, impaired vision and eventually death. Most common asphyxiant gases include CO, HCN and CO<sub>2</sub>. In this thesis, simulation data for O<sub>2</sub>, CO and CO<sub>2</sub> was compared with experimental data. Differences were found to be present in most notably case study 2 and 3. In this paragraph, it is examined what these differences mean from a tenability point-of-view.

To study the effects of gases on the occupants in the enclosures, a fractional effective dose methodology for asphyxia is used [45]. Note that this methodology uses an exposure time, which for the used calculation methodology is equal to the time since the start of the experiment/simulation. The calculation assumes a 'static' occupant, which in reality is not the case as occupants start egressing after some time. This reduces the exposure duration. The fractional effective dose for incapacitation is calculated by:

$$F_{IN} = F_{ICO} * VCO_2 + F_{IO}^3$$

The fraction of an incapacitation dose of CO  $F_{ICO}$  is calculated as follows:

$$F_{ICO} = 3,317 * 10^{-5} * [ppm CO]^{1,036} * \frac{V * t}{D}$$

Where V is the breathing rate (taken to be 25 L/min for light work), D is the exposure dose (taken to be 30 %COHb for light work) and t is the exposure time in minutes. The fraction of an incapacitation dose of low-oxygen hypoxia  $F_{IO}$  is calculated as:

$$F_{IO} = \frac{(20,9 - \%O_2) * t}{(20,9 - \%O_2) * \exp [8,13 - 0,54 * (20,9 - \%O_2)]}$$

In which %O<sub>2</sub> is the volumetric percentage of O<sub>2</sub> and t is the exposure time in minutes. The multiplication factor as a result of hyperventilation from CO<sub>2</sub> intake  $VCO_2$  can be calculated using:

$$VCO_2 = \frac{\exp (0,1903\%CO_2 + 2,0004)}{7,1}$$

In which %CO<sub>2</sub> is the volumetric percentage of CO<sub>2</sub>. The following images show the evolution of the fractional effective dose over time for the three casestudies. For casestudies 1 and 2, both the results for the one-step and two-step combustion model are shown. In the case of case study 2, the initial simulation results (one-step) and the final simulation results (two-step) are used. Gas concentrations are taken at a height of 1,5 meters.

The simulations using the one-step model combustion model with species yields for under-ventilated fires show an over-estimate of the fractional effective dose for incapacitation, with differences in tenable

<sup>3</sup> CO<sub>2</sub> is toxic at higher concentrations. The calculation of the fraction of an incapacitation dose for CO<sub>2</sub> showed that it is not normative in this framework.

time up to 2 minutes being predicted. The two-step models all show an acceptable correlation up to the point of the fire becoming significantly under-ventilated, with the exception of case study 2. In that case study, the fractional effective dose shows good correlation with the experimental results. This however, is coincidental as outlined in chapter 8.

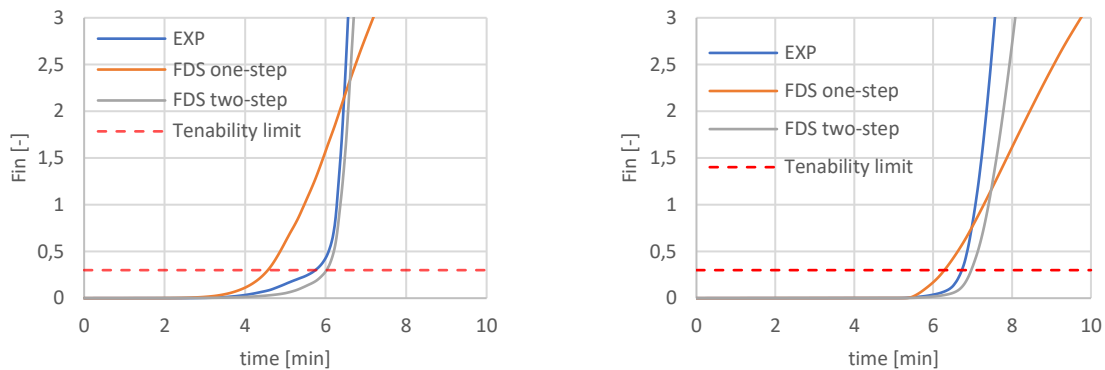


Figure 85:  $F_{in}$  for case study 2. Left: apartment, right: corridor, measuring tree B5.

Case study 3 (see appendix 6) actually shows a good correlation between the numerical and experimental results in the apartment while the actual gas-concentrations do not. This is a result of the oxygen-concentration being under-estimated in the FDS-simulation, while the CO-concentration is significantly higher in the experiments. Both the fraction of an incapacitation dose of CO and low- $O_2$  hypoxia are shown in Figure 86. Given the nature of the calculation procedure, these differences counterbalance each other. It is nothing more than coincidental.

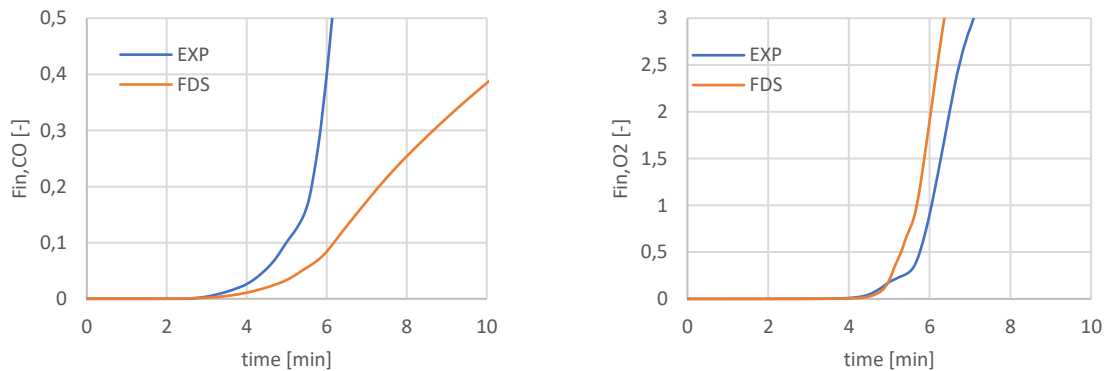


Figure 86:  $F_{iCO}$  (left) and  $F_{iO}$  (right) for case study 3 in the apartment

| Case study | Tenable time as per $F_{in} < 0,3$ [s] |          |              |             |           |          |
|------------|--|----------|--------------|-------------|-----------|----------|
|            | FDS one-step                           |          | FDS two-step |             | EXP       |          |
|            | Apartment                              | Corridor | Apartment    | Corridor    | Apartment | Corridor |
| 1          | 308                                    | 462      | 403          | 512         | 387       | 504      |
| 2          | 273                                    | 377      | 361          | 417         | 345       | 405      |
| 3          | -                                      | -        | 298          | Not reached | 288       | 645      |

Table 12: tenable time in the enclosures based on data at 1,5 meters high from measuring tree B5 (case study 1 and ) and B6 (case study 3).

While differences between the numerical results using the two-step model seem acceptable to some extent for case study 1 and 2, the good correlation is accidental at best.

## 9.5 Tenability: conclusion

From a tenability point-of-view, the numerical results show an overall good correlation for both visibility and heat exposure, taking into account lag as a result from experimental uncertainties. From a toxicology point-of-view the good correlation is accidental at best. Unless over-conservatism is acceptable in a fire engineering project, using gas concentrations and the Fractional Effective Dose methodology is not recommended when simulating under-ventilated fires.

At the moment, using a methodology in which visibility or soot density is used as a proxy for toxicology is recommendable. The soot yield should however be chosen carefully.

## 10. DISCUSSION

---

### 10.1 General

In this chapter, the simulation results presented in this thesis and their implications for practical fire engineering studies are discussed. Given the results of the performed simulations, it can be concluded that FDS is indeed capable of predicting fluid dynamics related to smoke propagation. In case studies 1 and 2, FDS showed to predict gas concentrations in the apartment and corridor quite accurate, given the boundary conditions and restrictions imposed on the model.

Most notably, deviations between the experimental and simulation results can be attributed to the subgrid-scale models used by FDS to predict fundamental phenomena related to chemical reactions and their associated kinetics. The deviations and their implications are discussed in detail in this paragraph.

### 10.2 Extinction model

The extinction model is shown to appropriately model flame extinction in moderately under-ventilated conditions as seen in case study 1 with O<sub>2</sub> concentrations to as low as 8-10 %vol. For case study 2 and 3 however, in which O<sub>2</sub> concentrations to as low as 2-5 %vol were measured, artificial alterations needed to be made to force FDS to reach the low O<sub>2</sub> concentrations measured in the experiments. Probable shortcomings in the critical flame temperature concept lie predominantly in the static and infinitely fast nature of the prescribed chemistry and the model itself. Furthermore, it relies on local phenomena (cell temperature) which in a LES methodology are typically heavily dependent on the used mesh resolution. This sensitivity was observed in the grid sensitivity study. As a results, most studies relating to the numerical simulations of flame extinction use a DNS-methodology [47] with more advanced chemistry modelling. This is impractical for large-scale fire phenomena.

More extinction models exist, but are not readily available in FDS. Models based on a critical flame Damköhler number and variable critical flame temperature were shown to give appropriate results [47] [48], but (to the knowledge of the author) is only used to simulate small-scale fires with relative simple reaction schemes (e.g. methane with the oxidizer being diluted by nitrogen). Moreover, the results presented in these papers use significantly high resolved grid resolutions, ranging from cell sizes of 25 to 6,5 millimeters. These cell-sizes are impractical in the simulation of large-scale fire phenomena, as it drastically increases computational time.

The extinction model is shown to be of significant influence when simulating under-ventilated fires. In case study 1, using the default value used by FDS (1.427 °C) resulted in a significant under-estimate of temperatures and an over-estimate of O<sub>2</sub> concentrations in the enclosure. Using the value for the critical flame temperature calculated from the imposed reaction did result in an adequate correlation with the experimental results. Further studying the sensitivity of the extinction model showed a clear dependence of the simulation results on the parameters used in the extinction model. This signifies the importance of being cautious when using the default parameters for the extinction model, especially when dealing with non-hydrocarbon fuels that have a lower overall effective heat of combustion. Given its results in the sensitivity studies for case study 1 and 2, using the alternative extinction model included in FDS, which is meant for coarse-meshed simulation, in practical engineering studies might be more appropriate. It showed more conservative results in case study 1 and more accurately approached the experimental results in case study 2 under default settings.

As a result of advances in building technology and the composition of furniture, we can expect more heavily under-ventilated fires as seen in case study 2 and 3. In these casestudies, the parameters of the extinction model needed to be artificially lowered to force FDS to give appropriate results. This is an indication that, in practical engineering studies, careful considerations must be made as to what parameters are used. A revision or reconsideration of the extinction model might be necessary to limit

the issues observed in this work. As of the current state of technology, the only method of increasing the predictive capabilities of the extinction model involves more concise combustion modelling which in turn leads to higher required spatial and temporal robustness of the used CFD-model.

### 10.3 Combustion model with regards to underventilation

The numerical results presented in this thesis use the one-step and two-step fast chemistry reaction schemes included in FDS to model combustion. For case study 1, which uses a moderately under-ventilated fire, both the one-step and two-step model showed appropriate correlation with the experimental data (with the two-step model being less conservative in the initial minutes). The chemistry in this case study is expected to be transient only by a limited amount. Casestudies 2 and 3 however, involve significant underventilation and therefore significant transient chemistry. Imposing a single reaction to model combustion will result in significant over- or under-estimates of species in the enclosure in both the growth and decay period of the fire. This in turn can lead to significant errors when performing tenability studies based on the concentrations of species. This is further explored in chapter 9. While the two-step simple combustion model showed promising results in case study 2, it performed poor in case study 3 as the only variable on which the model depends is the available oxygen.

To more appropriately model the formation of these species, a more complex reaction scheme needs to be used in which (among others) temperature dependency is taken into account. Experiments carried out by Zukoski et al. in 1991 show that CO-generation by a vitiated fire plume decreases at increasingly higher temperatures [49] [44]. Indeed, higher gas phase temperatures lead to higher flame temperatures in vitiated combustion as both convective and radiative heat losses are significantly reduced compared to well ventilated fires.

Being more concise about the kinetics in a fire plume typically results in situations in which accuracy in spatial and temporal quantities in the flow become more important. For example using the more complex finite-rate combustion model based on Arrhenius type correlations included in FDS might necessitate the use of a DNS approach [21]. This is impractical in large-scale fire simulations.

Developing and implementing a combustion model in which transient effects in the chemical kinetics are taken into account is necessary to more accurately predict species production in under-ventilated fires. Given the current state of the combustion models implemented in FDS, prediction post-flame species yields with certain precision is not possible. In practice, this should be done with severe care and while using static species-yields is crude and can result in extreme conservatism, it currently is the only method in which conservatism can be obtained.

### 10.4 Leakage model

While the leakage model does predict pressure buildup in the apartment to an acceptable level of accuracy, the fluid dynamics and heat transfer of the leaking gases are not appropriately predicted. Once the smoke exits the leak, its further propagation is dependent on its initial momentum and its thermal properties. Depending on the composition of the smoke, it can hinder egress due to limited visibility.

The composition of the leaking smoke in the case of the casestudies (both numerical and experimental) in this thesis do not result in significant effects relating to toxicology. It does however, result in limited loss of visibility prior to opening the door between the apartment and the corridor. The overall importance of accurately modelling the actual smoke propagation from a leak is limited in the framework of this thesis.

## 10.5 Suggested further research

Based on the conclusions drawn in this thesis, the author suggests the following fundamental further research:

- Development of a more accurate extinction model: in the case of under-ventilated fires, the extinction model, together with the combustion model, wholly determine the eventual outcome. The extinction model predicts the reaction rate of the fuel, the heat release rate of the fire and subsequently the generated products of incomplete combustion. It should however be stated that, to be of practical use, the to be developed extinction model should not necessitate excessive computational resources.
- Development of a more accurate combustion model: as stated in the previous suggestion, the combustion model is of significant importance in under-ventilated fires. It determines oxygen-depletion, specie generation and (in some cases) the heat generation in the combustion process. Especially in the case of under-ventilated fires, in which the generation of products of incomplete combustion are of importance on the overall chemistry and tenability, the combustion model is of significant importance.

Given the current trends in the building industry, more under-ventilated fires are to be expected. Fire engineers therefore should have access to the right tools to predict their effects.

The three casestudies presented in this thesis show an acceptable level of correlation between the numerical and experimental results, especially when looking at visibility and heat exposure. The casestudies can be used as a basis for further research in which the effectiveness of different fire safety measures are explored. It can then be used as a substantiated benchmark for the formulation of new standards and regulations.

# 11. CONCLUSION

---

## 11.1 Sub-questions

In chapter 1 of this thesis, several sub-questions were formulated with the goal of studying phenomena related to the numerical simulations of under-ventilated fires using the available experimental data in a structured manner. Each sub-question contributes to the formulation of an answer to the main research question. The sub-questions are discussed in this paragraph.

*What studies were carried out relating to the numerical simulation of under-ventilated fires and what were the conclusions?*

Only a limited number of studies exist which deal with the numerical simulations of large-scale under-ventilated fires. The studies described in this thesis show that numerically predicting phenomena related to under-ventilation is not straightforward and a significant number of complexities inherent to flame extinction and the flame chemistry exist.

*What scenarios were studied during the Oudewater experiments and what scenarios will be used in this thesis?*

The Oudewater experiments consisted of several experiments with differentiated boundary conditions. Most notably the ventilation conditions and the fire protection provisions were changed. A detailed description of the experiments is given in chapter 3 of this thesis. Based on an analysis of the experimental results, 3 experiments were chosen to be used as a basis for numerical simulations using Fire Dynamics Simulator.

*What are the general technical characteristics of FDS and what are its limitations when dealing with under-ventilated fires?*

The main limitations of FDS when dealing with under-ventilated fire phenomena lie in the fact that the associated chemistry and physics occur at a subgrid-scale (e.g. smaller than the length-scale of one mesh-cell). This means these phenomena need to be modelled, instead of being directly resolved. The associated models (combustion, extinction and to a more limited extent the leakage model) all have their specific limitation in terms of applicability and fundamental correctness. They however, show to affect the outcome of an FDS simulation to a significant extent.

*To what extent can specific scenarios from the Oudewater Experiments be simulated using FDS, given the available data?*

Chapter 5 up to chapter 9 deal with the numerical simulations and the implications of the results for fire engineering of three case studies. Case study 1 showed that, should the oxygen supply of the fire be diluted to a limited extent (e.g. to as low as 8-10 %vol), FDS and its sub-grid scale models appropriately predict the fire related quantities such as O<sub>2</sub> concentration, CO<sub>2</sub> concentration, CO concentration (to some extent), temperatures and visibility in both the apartment and corridor, given the uncertainties in the experimental data.

Case study 2 and 3 however, showed that when dealing with a severely hypoxic environment (e.g. to as low as 2-5 %vol), FDS does not give appropriate results. Reasons being most notably the extinction model predicting extinction significantly earlier than what is observed in the experiments and the combustion model not being able to take into account the dynamic nature of the flames' chemistry. The extinction model showed some sensitivity to the used grid resolution. Using a higher resolution grid (higher than 5\*5\*5 cm) however, leads to a significant increase in computational cost and is not desirable.

When the extinction model is forced to generate combustion at lower O<sub>2</sub> concentrations by imposing different parametric settings and when a two-step combustion model is employed, the overall correctness of the results in the initial period (up to and including the moment of flame extinction)

becomes better. Trends in gas concentrations, temperatures, pressure and visibility are appropriately predicted in case study 2. The validity of the used input parameters and the combustion scheme is questionable. The models were used to 'fit' the numerical results to the experimental results.

However, the setup used in case study 2 did not result in correct results for case study 3. While the O<sub>2</sub> concentrations are predicted to an adequate extent, the CO and CO<sub>2</sub> concentrations are respectively under- and over-estimated. Trends in temperatures are captured to an acceptable extent up to the moment of extinction, but are under-estimated afterwards. Pressures in the apartment in which the sofa is located are predicted to an acceptable extent, but show significant oscillatory behavior after extinction as a result of the bulk leakage model. In case study 2 and 3, visibility in the corridor showed to drop prior to the door is opened as a result of the leaking gases which was not predicted by FDS. This is caused by under-predictions in pressure in the apartment prior to the door opening and the leakage model of FDS not realistically taking heat transfer from the leaking gases to the surface of the leak into account.

For case studies 1 and 2, a sensitivity study was carried out. Out of all the studied parameters, the chemical composition of the fuel, its associated species yields and the parameters related to the extinction model showed to affect the outcome most. Moreover, the alternative extinction model (extinction model 1) included in FDS showed to either be more conservative (as seen in case study 1) or better approximative for the minimum O<sub>2</sub> concentrations (as seen in case study 2) under default and calculated values.

## 11.2 Main research question

In paragraph 1.3.1, the main research question is presented. In this paragraph, the main research question is discussed.

*To what extent can the CFD-tool FDS be used to realistically simulate a fire driven flow as studied in the Oudewater Experiments, knowing the fire is prone to growing under-ventilated?*

The results for a moderately under-ventilated fire (in which O<sub>2</sub> concentrations to as low as 8-10 %vol were observed in the apartment) as seen in case study 1 are appropriate in the sense that the studied quantities are approximated relatively well given the imposed experimental uncertainties. In the case of severe hypoxic environments (O<sub>2</sub> concentration in the apartment of 2-5 %vol), which were observed in both case studies 1 and 2, poor results were observed. After fitting the numerical model for case study 2 with the experimental data, a better correlation is observed. Using the same fitted setup in case study 3 showed that, while extinction was predicted more or less accurate, the gas concentrations (most notably CO) are not, which can be contributed to the rudimentary nature of the two step combustion model. Improvements in the extinction model and combustion model are necessary to realistically simulate effects of underventilation.

From an engineering point-of-view, the tenable times for both the final (fitted) numerical results and experimental results were in good agreement with regards to visibility and heat exposure. From a toxicological point-of-view, the results for case study 1 and 2 showed appropriate results, but only under fitted conditions (case study 2). Case study 3 performed poorly when dealing with toxicological tenability as a result of the severe under-estimate of CO concentrations.

Concluding, using FDS in its current build to perform blind simulations (not using experiments as a reference) of under-ventilated fires should be done with caution. If used, a thorough sensitivity study on the extinction parameters and its grid dependence is in place. Furthermore, using the alternative extinction model might lead to more conservative results without altering the default parameters. A tenability framework based on toxicological effects should only be used when over-conservatism is acceptable, given the static nature of species yields in FDS. Estimating tenable times based on visibility (which also holds conservatism) and/or heat exposure are more reliable.

## 12. REFERENCES

---

- [1] A. Björklund, "Risks in using CFD-codes for analytical fire-based design in buildings with a focus on FDS's handling of under-ventilated fires," Lund University, Lund, 2009.
- [2] D. Purser and J. McAllister, "Assessment of Hazards to Occupants from Smoke, Toxic Gases, and Heat," in *SFPE Handbook of Fire Protection Engineering, fifth edition*, 2015.
- [3] G. Baker, C. Wade, D. Nilsson and P. Olsson, "Results are in - International Fire Engineering Tools Survey," no. 93, 2022.
- [4] NIST, "Fire Dynamics Simulator, Technical Reference Guide Volume 2: Verification," U.S. Department of Commerce, Gaithersburg, 2021.
- [5] NIST, "Fire Dynamics Simulator TEchnical Reference Guide Volume 3: Validation," U.S. Department of Commerce, Gaithersburg, 2021.
- [6] L. Audouin, L. Rigollet, H. Prétel, W. Le Saux and M. Röwekamp, "OECD PRISME project: fires in confined and ventilated nuclear type multi-compartments - overview and main experimental results," vol. 2013, no. 62, 2013.
- [7] J. Wahlqvist and P. van Hees, "Validation of FDS for large-scale well-confined mechanically ventilated fire scenarios with emphases on predicting ventilation system behavior," vol. 2013, no. 62, 2013.
- [8] F. Bonte, N. Noterman and B. Merci, "Computer simulations to study interaction between burning rates and pressure variations in confined enclosure fires," vol. 2013, no. 62, 2013.
- [9] Het Vlaams Infrastructuurfonds voor Persoonsgebonden Aangelegenheden (VIPA), "Brandveiligheid in ouderenvoorzieningen: onderzoek naar de doelmatigheid van alternatieve brandveiligheidsmaatregelen in nieuwe zorgconcepten," Vlaanderen is zorgzaam samenleven, Brussel, 2016.
- [10] WFRGent N.V., "Innovatieve toepassing van rookbeheersing in woonzorggebouwen: brandproeven en analyse," 2021.
- [11] A. Lucherini and B. Merci, "Analyse van experimenten en numerieke simulaties van brandproeven voor de ontwikkeling van een beoordelingskader voor brandveiligheid in zorggebouwen," Welzijn, Volksgezondheid en Gezin, Leuven, 2021.
- [12] A. J. Wolfe, C. L. Mealy and D. T. Gottuk, "Fire Dynamics and Forensic Analysis of Limited Ventilation Compartment Fires Volume 1: Experimental," Highes Associates, Inc., Baltimore, 2009.
- [13] H. Boehmer, J. Floyd and D. T. Gottuk, "Fire Dynamics and Forensic Analysis of Limited Ventilation Compartment Fires. Volume 2: Modelling," Hughes Associates, Inc., Baltimore, 2009.
- [14] M. Scholman, "Different concepts for personal safety in a multi-story residential complex in relation to internal smoke propagation," Eindhoven University of Technology, Eindhoven, 2020.
- [15] NIST, "CFAST - consolidated Fire and Smoke Transport (version 7) - Volume 1: Technical reference guide," U.S. Department of Commerce, 2020.
- [16] C. Wade, G. Baker, K. Frank, R. Harrison and M. Spearpoint, "B-RISK 2016 user guide and technical manual," BRANZ, 2016.
- [17] J. Elbus, T. Geertsema, V. Jansen, M. Leene, R. Van Liempd, M. Polman, L. De Witte and L. Wolfs, "Rookverspreiding in woongebouwen. Hoofdrapport van de praktijkexperimenten in een woongebouw met inpandige gangen," Brandweeracademie, Arnhem, 2020.
- [18] S. Hostikka and R. Janardhan, "Pressure management in compartment fires," 2017.
- [19] NIST, "Fire Fynamics Simulator - User's guide Sixth edition," U.S. Department of Commerce, Gaithersburg, 2021.
- [20] H. Versteeg and W. Malalasekera, *An introduction to Computational Fluid Dynamics - the finite volume method*, Harlow, United Kingdom: Pearson, 2007.
- [21] NIST, *Fire Dynamics Simulator Technical Reference Guide*, Maryland: NIST, 2020.

- [22] A. Tewarson, "Combustion Efficiency and its radiative component," vol. 2004, no. 39, 2003.
- [23] SFPE, *SFPE Handbook of Fire Protection Engineering*, fifth edition, Springer, 2016.
- [24] V. Babrauskas, J. R. Lawson, W. Walton and W. H. Twilley, "Upholstered Furniture Heat Release Rates Measured With A Furniture Calorimeter," U.S. Department of Commerce, Washington D.C., 1982.
- [25] H.-J. Kim and D. G. Lilley, "Heat Release Rates of Burning Items in Fires," AIAA, Reno, 2000.
- [26] B. Sundstrom, "Fire Safety of Upholstered Furniture - the final report on the CBUF research programme. EUR 16477," European Commission , 1993.
- [27] B. J. McCaffrey, J. G. Quintiere and M. F. Harkleroad, "Estimating room temperatures and the likelihood of flashover using fire test data correlations," vol. 1981, 1981.
- [28] J. G. Quintiere, "NBSIR 83-2712 A simple correlation for predicting temperature in a room fire," U.S. Department of Commerce, Washinton D.C., 1983.
- [29] F. W. Mowrer and R. B. Williamson, "Estimating room temperatures from fires along walls and in corners," 1987.
- [30] K. McGrattan and D. Stroup, "Wall and Corner Effects on Fire Plumes as a Function of Offset Distance," vol. 57, 2020.
- [31] M. M. Khan, A. Tewarson and M. Chaos, *SFPE Handbook of fire protection engineering*, chapter 36: combustion characteristics of materials and generation of fire products, London: Springer, 2016.
- [32] G. Heskestad, "Chapter 13: fire plumes, flame height and air entrainment," in *SFPE Handbook of Fire Protection Engineering, 5th edition*, 2015.
- [33] J. Floyd and K. McGrattan, "Extending the mixture fraction concept to address under-ventilated fires," vol. 2008, no. 44, 2008.
- [34] A. Rangwala, "Chapter 11, diffusion flames," in *SFPE Handbook of fire protection engineering, fifth edition*, 2015.
- [35] B. Kukfisz and M. Pólka, "Analysis of oxygen index to support candle-like combustion of polyurethane," vol. 2017, no. 172, 2016.
- [36] R. Hadden, A. Alkatib, G. Rein and J. Torero, "Radiant ignition of polyurethane foam: the effect of sample size," vol. 2014, no. 50, 2012.
- [37] J. Quintiere, *Principles of fire behavior*, Delmar Publishers, 1997.
- [38] Nieman, "Lucht- en rookdoorlatendheidsonderzoek Schuylenburgt te Oudewater," 2019.
- [39] SFPE, "Chapter 33: Enclosure Smoke Filling and Fire-Generated Environmental Conditions," in *SFPE Handbook of Fire Protection Engineering, fifth edition*, 2015.
- [40] G. W. Mulholland and C. Croarkin, "Specific Extinction Coefficient of Flame Generated Smoke," vol. 2000, no. 24, 2000.
- [41] T. Jin, "Visibility through Fire Smoke," 1970.
- [42] CEN, "EN 12101-6:2005; Smoke and heat control systems - Part 6: Specification for pressure differential systems - Kits," CEN, 2005.
- [43] L. Staffansson, "Selecting Design Fires," 2010.
- [44] D. Gottuk and B. Lattimer, "Chapter 16: Effect of Combustion Conditions on Species Production," in *SFPE Handbook of Fire Protection Engineering, 5th edition*, 2016.
- [45] SFPE, *Guide to Human Behavior in Fire*, Gaithersburg, Maryland , USA: Springer, 2019.
- [46] DGMR, "F.2011.1584.00.R001 'niet-besloten ruimte in relatie tot brandveiligheid'," DGMR, Den Haag, 2015.
- [47] S. Vilfayeau, J. White, P. Sunderland, A. Marshall and A. Trouvé, "Large eddy simulation of flame extinction in a turbulent line fire exposed to air-nitrogen co-flow," no. 86, 2016.
- [48] G. Maragkos and B. Merci, "Large eddy simulations of flame extinction with infinitely fast chemistry," 2018.

- [49] E. Zukoski, J. Morehart, T. Kubota and S. Toner, "Species Production and Heat Release Rates in Two-Layered Natural Gas Fires," vol. 1991, no. 83, 1991.
- [50] B. Karlsson and J. Quintiere, *Enclosure Fire Dynamics*, CRC Press, 2000.
- [51] NIST, "Smoke Component Yields from Bench-scale Fire Tests: 4. Comparison with Room Fire Results," U.S. Department of Commerce, Gaithesburgh, 2013.
- [52] J. Hou, "Distribution curves for interior furnishings on CO<sub>2</sub>, CO, HCN, Soot and Heat of Combustion," University of Canterbury, Christchurch, 2011.
- [53] D. Drysdale, *An Introduction to Fire Dynamics*, New York: John Wiley, 2011.
- [54] P. Thomas and A. Heselden, "Fully developed fires in single compartments," Fire Research Station, Boreham, England, 1972.
- [55] D. A. Purser, "Toxic combustion product yields as a function of equivalence ratio and flame retardants in under-ventilated fires," 2016.
- [56] M. Yuan, B. Chen, C. Li, J. Zhang and S. Lu, "Analysis of the combustion efficiencies and heat release rates of pool fires in ceiling vented compartments," vol. 9, 2013.
- [57] W. M. Pitts, "The global equivalence ratio concept and the prediction of carbon monoxide formation in enclosure fires," NIST, Gaithesburg, 1994.

## APPENDIX 1: USED EQUIPMENT

### Measurements

During the experiments, several measurements were carried out. As this thesis only deals with simulating the smoke propagation from the fire room to the adjacent corridor, only the relevant measurements are discussed here. In more detail, measuring trees B1, B5 and B6 are used to check the simulation results. The trees are composed as follows:

#### Measuring tree B1, fire room, located in the kitchen

| Sensor/instrument   | Number  | Height above floor (m) | Orientation (°) |
|---------------------|---------|------------------------|-----------------|
| Thermocouple        | TK1.1.0 | 2,40                   | n.a.            |
|                     | TK1.1.1 | 2,20                   |                 |
|                     | TK1.1.2 | 2,00                   |                 |
|                     | TK1.1.3 | 1,80                   |                 |
|                     | TK1.1.4 | 1,50                   |                 |
|                     | TK1.1.5 | 0,90                   |                 |
|                     | TK1.1.6 | 0,30                   |                 |
| Radiative heat flux | SP1.1.1 | 1,50                   | 0               |
|                     | SP1.1.2 | 0,3                    | 0               |
| Pressure LOW        | P1.1.1  | 0,2                    | n.a.            |
| Pressure HIGH       | P1.1.2  | 0,2                    |                 |

Table 13: Measuring tree B1

#### Measuring tree B5, corridor, lefthand side

| Sensor/instrument   | Number  | Height above floor (m) | Orientation (°) |
|---------------------|---------|------------------------|-----------------|
| Thermocouple        | TK1.5.0 | 2,40                   | n.a.            |
|                     | TK1.5.1 | 2,20                   |                 |
|                     | TK1.5.2 | 2,00                   |                 |
|                     | TK1.5.3 | 1,80                   |                 |
|                     | TK1.5.4 | 1,50                   |                 |
|                     | TK1.5.5 | 0,90                   |                 |
|                     | TK1.5.6 | 0,30                   |                 |
| Radiative heat flux | SP1.5.1 | 1,50                   | 0               |
|                     | SB1.5.2 | 0,3                    | 0               |
| Pressure LOW        | P1.5.1  | 0,2                    | n.a.            |
| Visibility          | ZL5.1   | 1,5                    |                 |
|                     | ZL5.2   | 0,3                    |                 |

Table 14: Measuring tree B5

### Measuring tree B6, corridor, righthand side

| Sensor/instrument   | Number  | Height above floor (m) | Orientation (°) |
|---------------------|---------|------------------------|-----------------|
| Thermocouple        | TK1.6.0 | 2,40                   | n.a.            |
|                     | TK1.6.1 | 2,20                   |                 |
|                     | TK1.6.2 | 2,00                   |                 |
|                     | TK1.6.3 | 1,80                   |                 |
|                     | TK1.6.4 | 1,50                   |                 |
|                     | TK1.6.5 | 0,90                   |                 |
|                     | TK1.6.6 | 0,30                   |                 |
| Radiative heat flux | SP1.6.1 | 1,50                   | 0               |
|                     | SB1.6.2 | 0,3                    |                 |
| Pressure LOW        | P1.6.1  | 0,2                    | n.a.            |
| Visibility          | ZL6.1   | 1,5                    |                 |
|                     | ZL6.2   | 0,3                    |                 |

Table 15: Measuring tree B6

### Temperatures

Gas-phase temperatures were measured using thermocouple-trees. All thermocouples used were of the type K RVS 1.4841, with different lengths and a diameter of 0,75 mm. In the fire room, one thermocouple tree was present, with thermocouples placed over different heights. In the corridor, two measuring trees were placed, with thermocouples placed at the same height. The thermocouples have a sensitivity of 2,2°C or 0,75% of the measured value. The response-time is 0,06-1,8 seconds.

### Radiative Heat Fluxes

In the same measuring trees, radiative heat fluxes were measured using radiative heat flux gauges. In the locations where high radiative exposures were expected, plate thermocouple heat flux meters (PTHFM) were used while in other locations, water-cooled Schmidt-Boelter fluxmeters were used. The sensitivity of the PTHFM-sensor is equal to the sensitivity of the thermocouple. The sensitivity of the Schmidt-Boelter fluxmeters depends on the calibration value.

### Pressure Low and High

During the tests, pressures were measured at various locations. Two different meters were used: one meter with a range of 0-50 Pa and one with a range of -2500-2500 Pa. The first having a high sensitivity (1,5 Pa) and low resolution (0,5 Pa) while the second has a lower sensitivity (25 Pa) and high resolution (10 Pa). Where possible, data from the 'pressure low' meters is used.

### Visibility

In the corridor, visibility is measured using photovoltaic cells at four points of which two are located at measurement tree B5 and two at measurement tree B6. In both cases, the height was 1,5 m and 0,3 m. Visibility is calculated using the measured light-intensity using the following correlation:

$$Z = \frac{-Z_f L}{\ln\left(\frac{I}{I_o}\right)}$$

In which  $Z_f$  is a compensation-factor which relates to the (non)reflective nature of an object. For non-light-emitting objects, this value can be taken as 3 while for light-emitting objects this value can be taken as 8.  $L$  is the length between the light-source and the receiver in the experiment in centimeters.  $I$  is the measured light intensity and  $I_o$  is a reference intensity which is calculated as the average of the first 500 measurements made.

### Gas measurements

Gas concentrations were carried out in the fire room and in the corridor using a Testo 350 sampling device. The sampling point in the fire room was located on measuring tree B1 at a height of 1,5 meters. In the corridor, four sampling points were located: two per measurement tree at heights of 0,3 and 1,5 meters. The following gases were sampled:

- O<sub>2</sub>
- CO
- CO<sub>2</sub>
- NO<sub>x</sub>
- NO<sub>2</sub>
- SO<sub>2</sub>

Typically, experimental gas samplers have a transport time as the actual measurement equipment is located in a different location from where the gas is aspirated. The following transport times and sensitivities are mentioned in the report of the IFV [17]:

- O<sub>2</sub>: <20 seconds and a sensitivity of 0,2 %VOL;
- CO<sub>2</sub>: <10 seconds and a sensitivity of 0,3 for values under 25 %VOL or 0,5%VOL for values over 25%VOL
- CO: <40 seconds and a sensitivity of 10 ppm, 5%, 10% for measured values of respectively <25 %VOL and >50 %VOL;.

In this thesis, data for the oxygen, carbon-monoxide and -dioxide measurements is used.

## APPENDIX 2: SELECTION OF EXPERIMENTAL RESULTS

### Scenario 18 and 19: balcony door open

Graphical depiction sofa after experiment

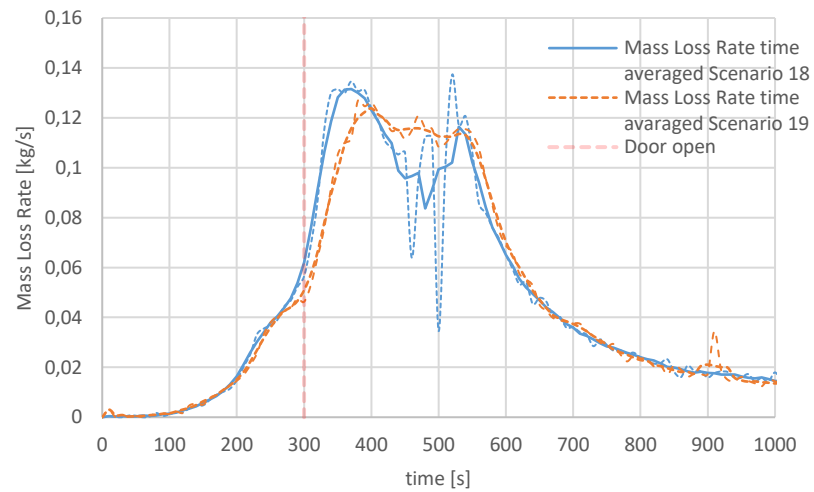
Scenario 18



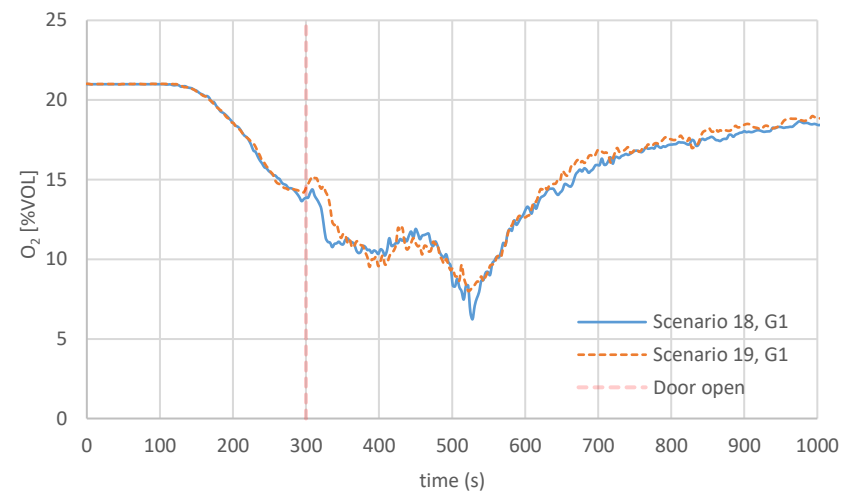
Scenario 19



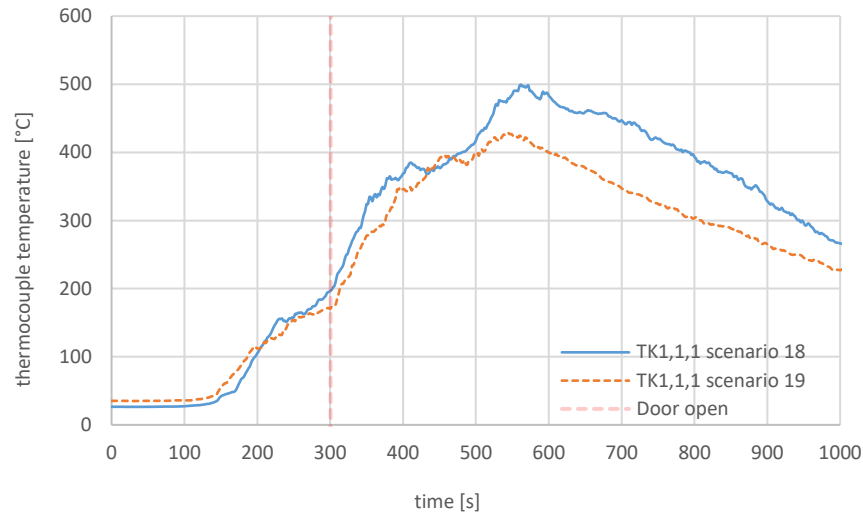
### Mass loss rate



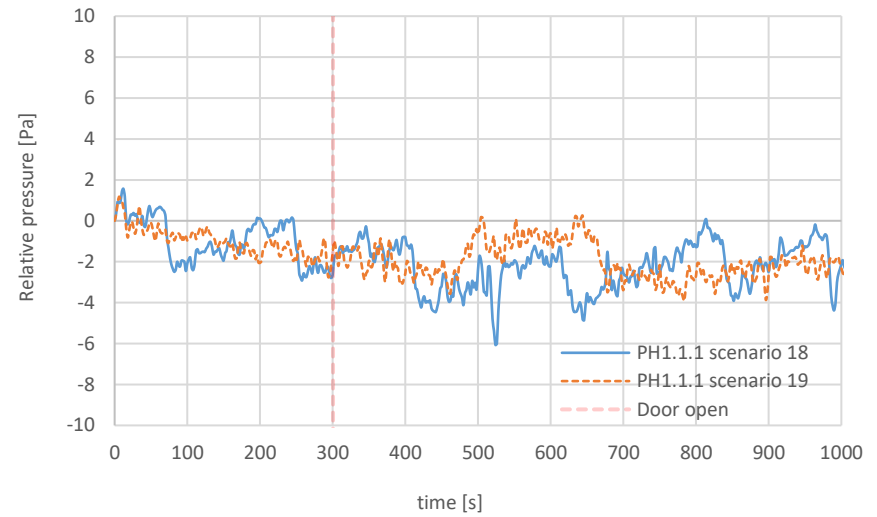
### O<sub>2</sub> concentration in the apartment (1,5 meters)



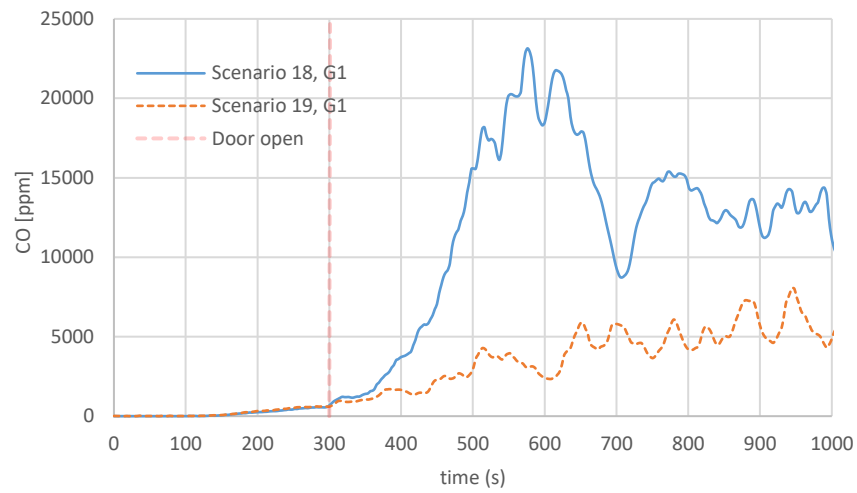
Temperature underneath ceiling in apartment (2,2 meters)



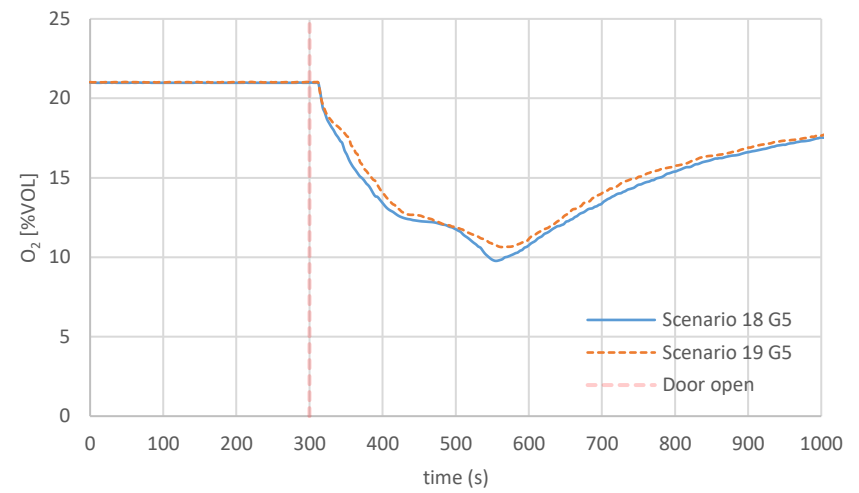
Pressure in the apartment (PH equipment) (0,2 meters)



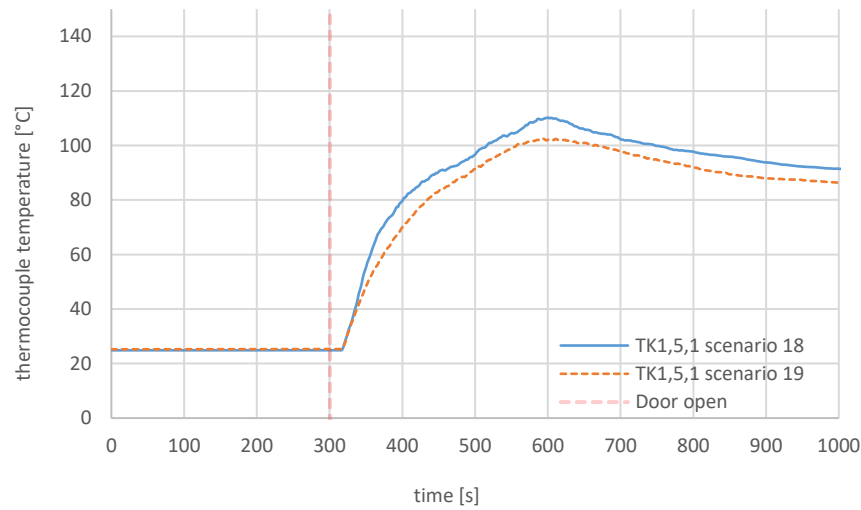
CO concentration in the apartment (1,5 meters)



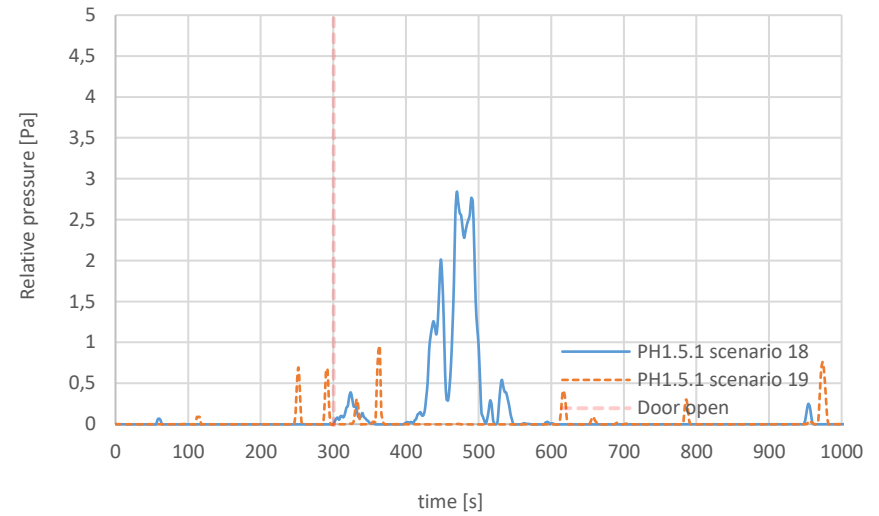
O<sub>2</sub> concentration in the corridor (1,5 meters)



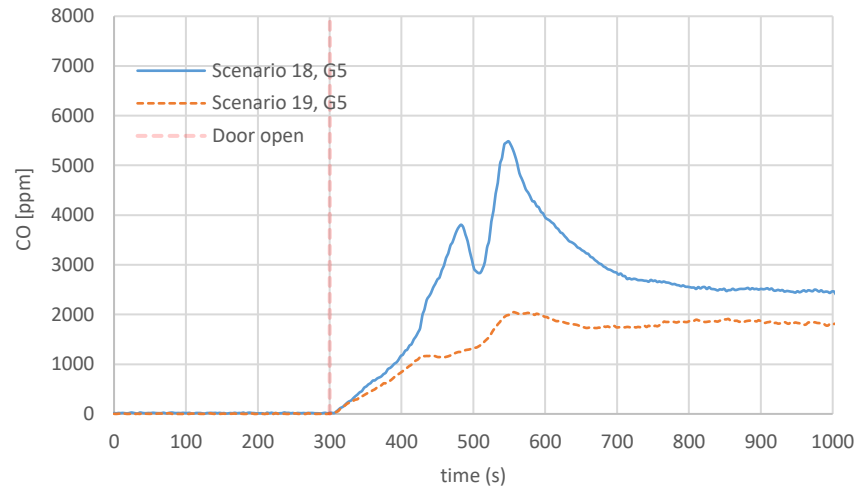
Temperature underneath ceiling in corridor (2,2 meters)



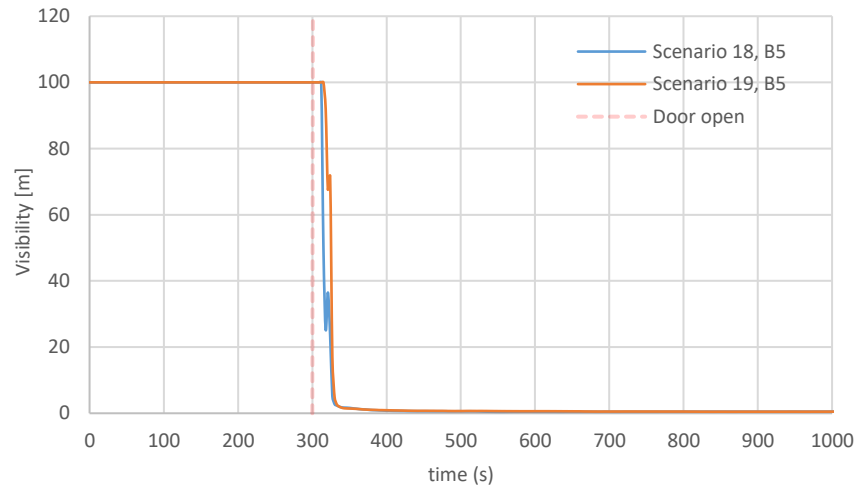
Pressure in the corridor (PL equipment) (0,2 meters)



CO concentration in corridor (1,5 meters)



Visibility in corridor (1,5 meters)



**Scenario 1, 3, 5 and 17: door corridor left open**

Graphical depiction sofa after experiment

Scenario 3



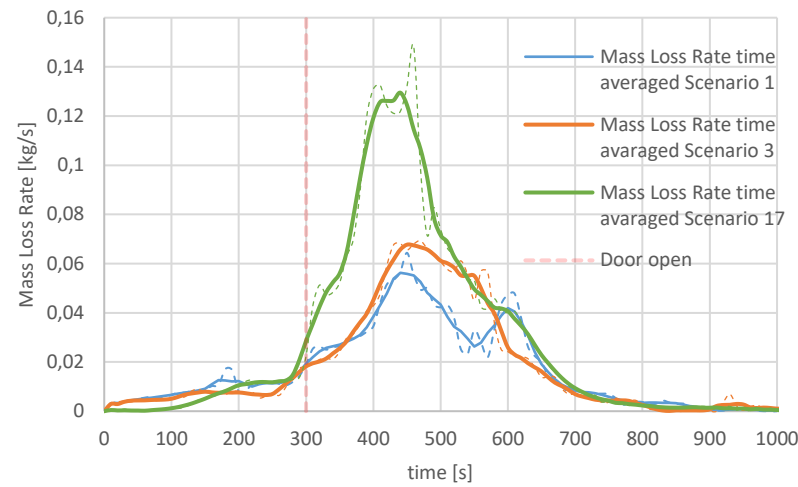
Scenario 5



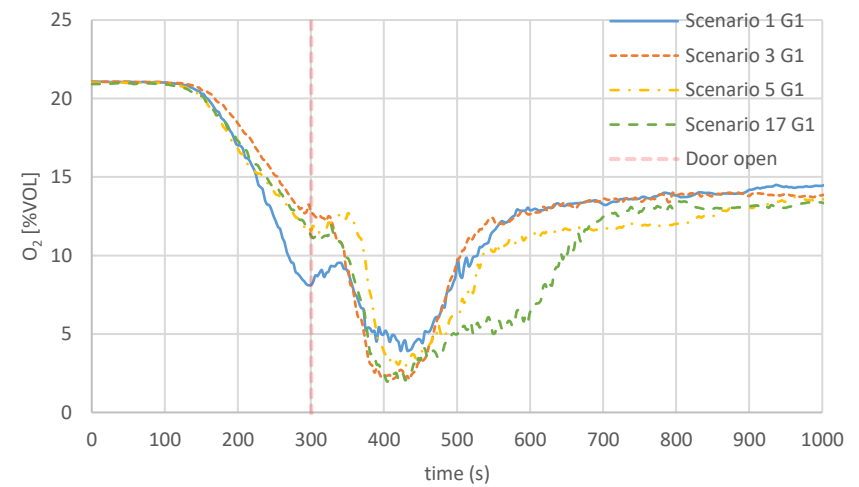
Scenario 17



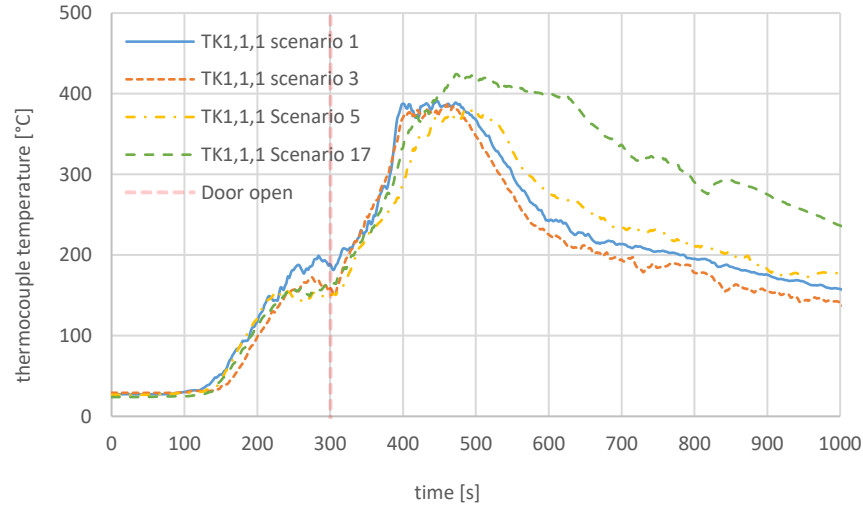
Mass loss rate



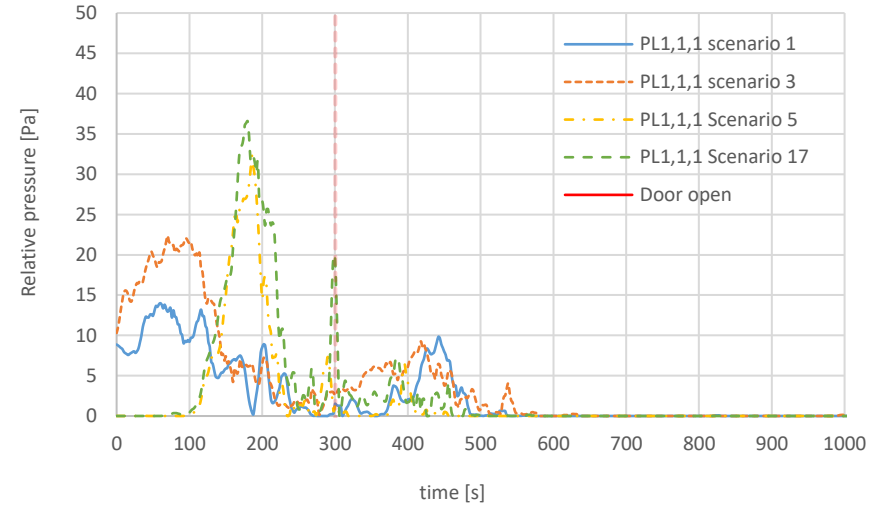
O<sub>2</sub> concentration in the apartment (1,5 meters)



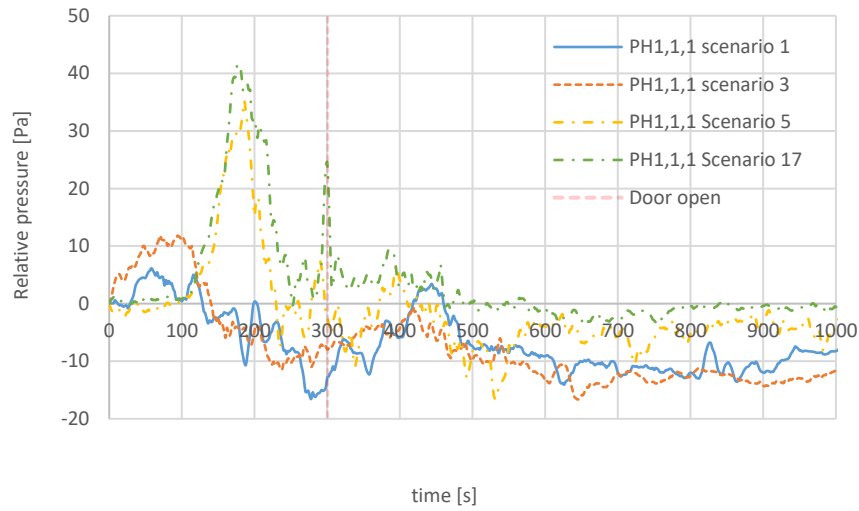
Temperature underneath ceiling in apartment (2,2 meters)



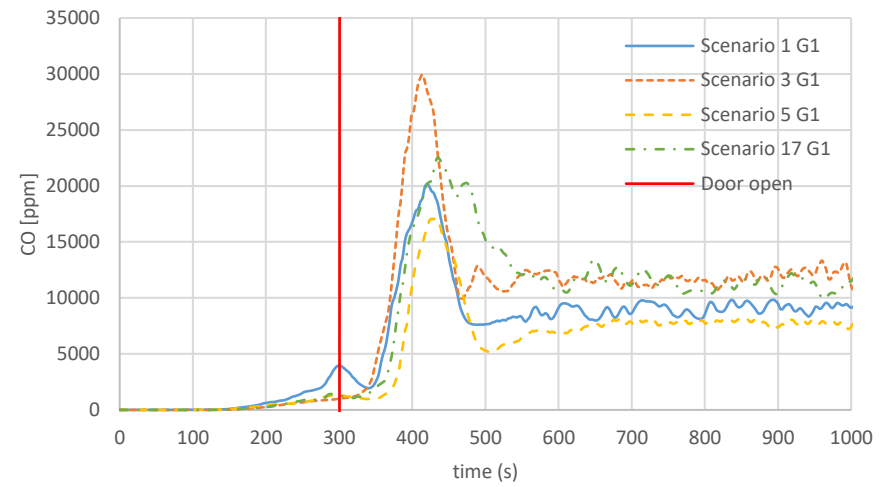
Pressure in the apartment (PL equipment) (0,2 meters)



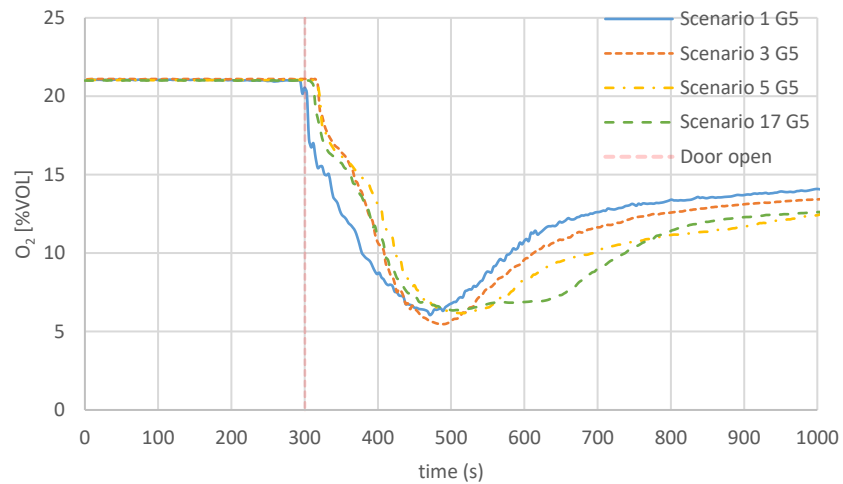
Pressure in the apartment (PH equipment) (0,2 meters)



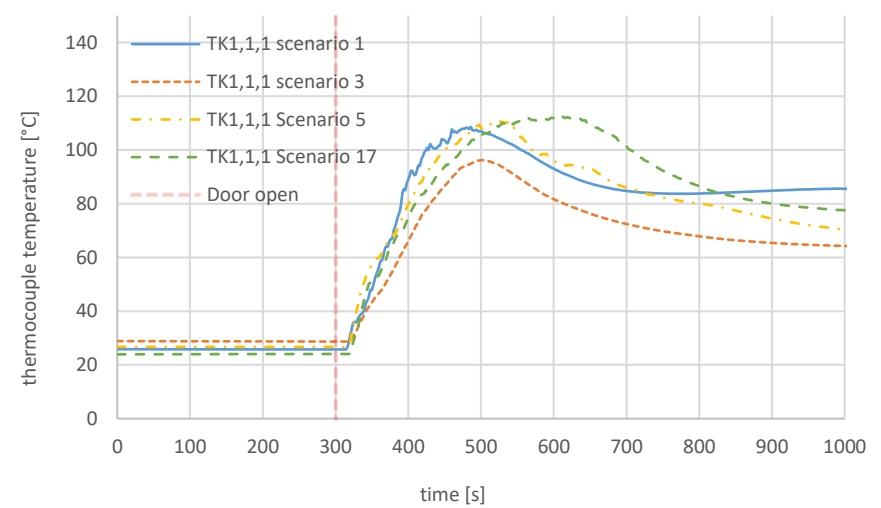
CO concentration in the apartment (1,5 meters)



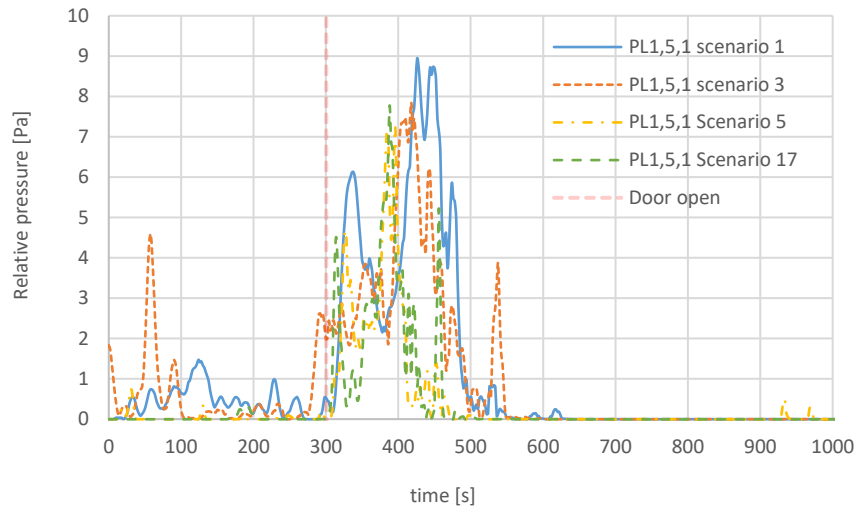
O<sub>2</sub> concentration in the corridor (1,5 meters)



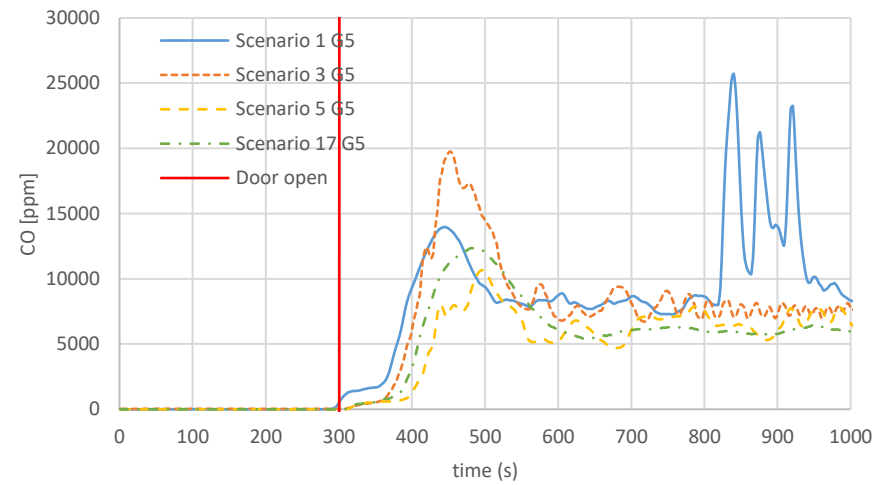
Temperature underneath ceiling in corridor (1,5 meters)



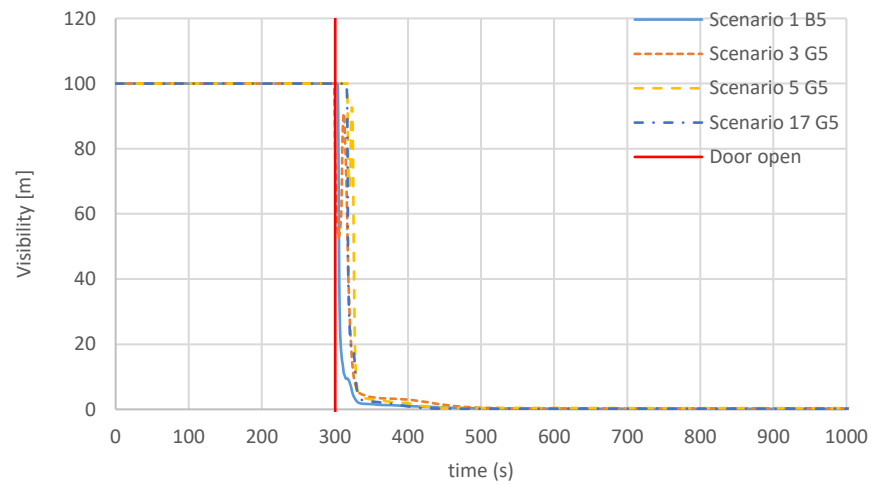
Pressure in the corridor (0,2 meters)



CO concentration in corridor (1,5 meters)



Visibility in corridor (1,5 meters)



**Scenario 4 and 16: door corridor closed**

Graphical depiction sofa after experiment

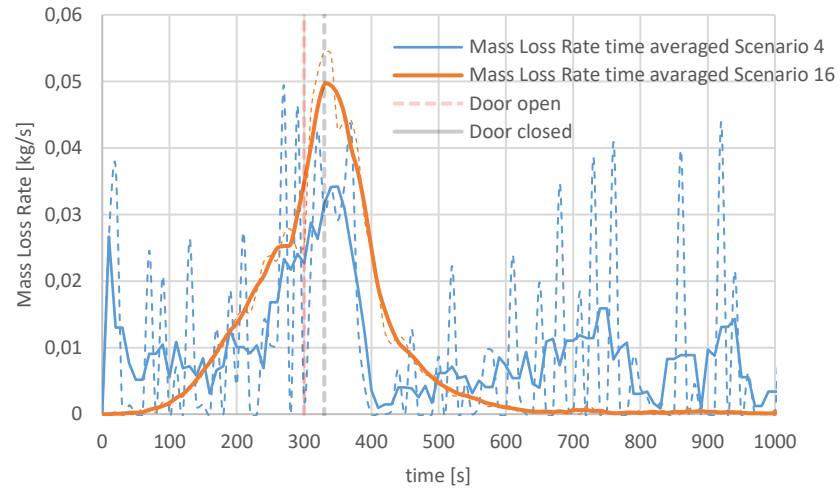
Scenario 4



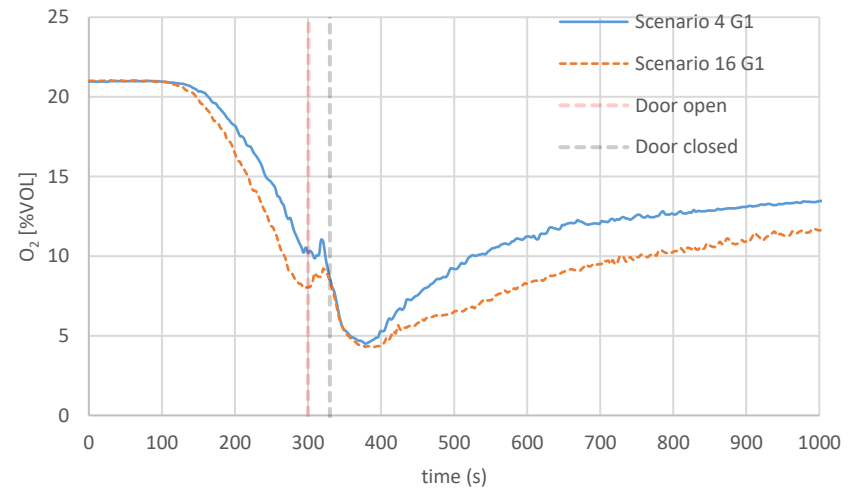
Scenario 16



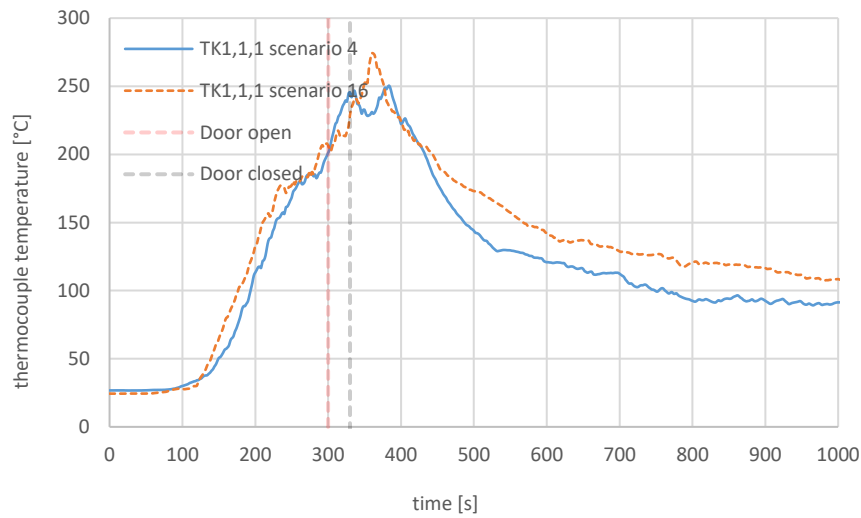
Mass loss rate, weight measurement scenario 4 failed



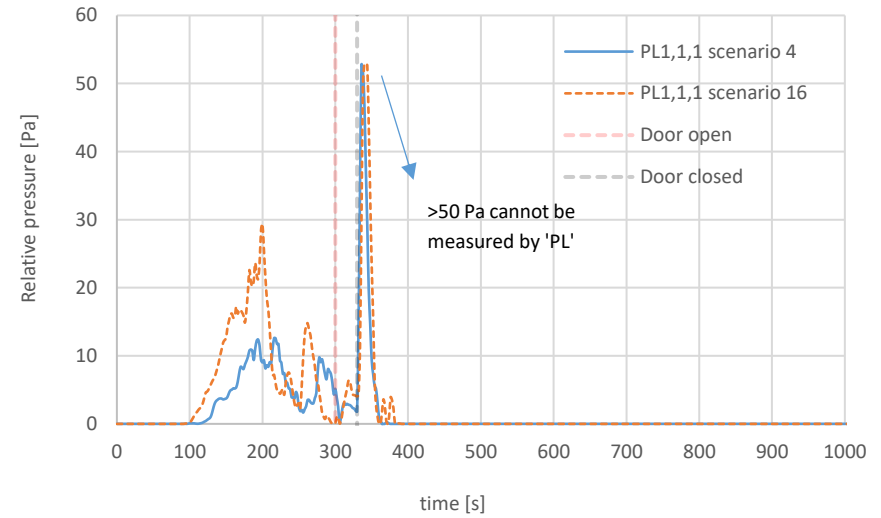
O<sub>2</sub> concentration in the apartment (1,5 meters)



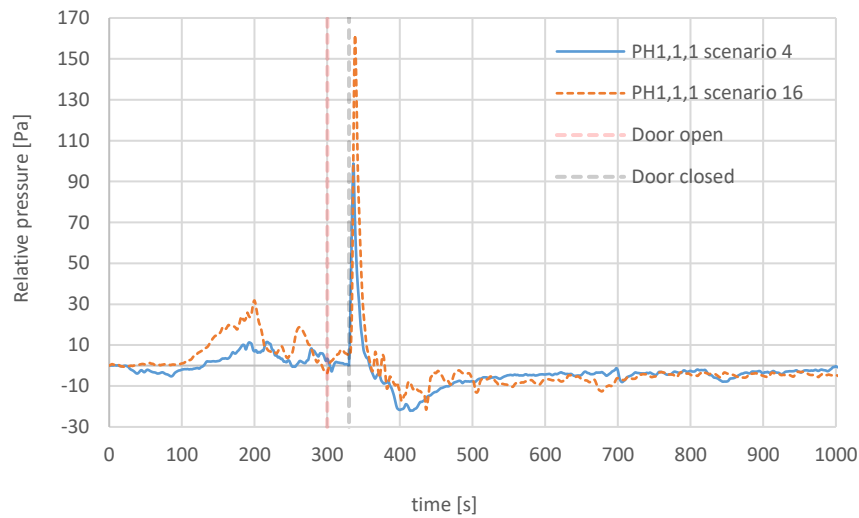
Temperature underneath ceiling in apartment (2,2 meters)



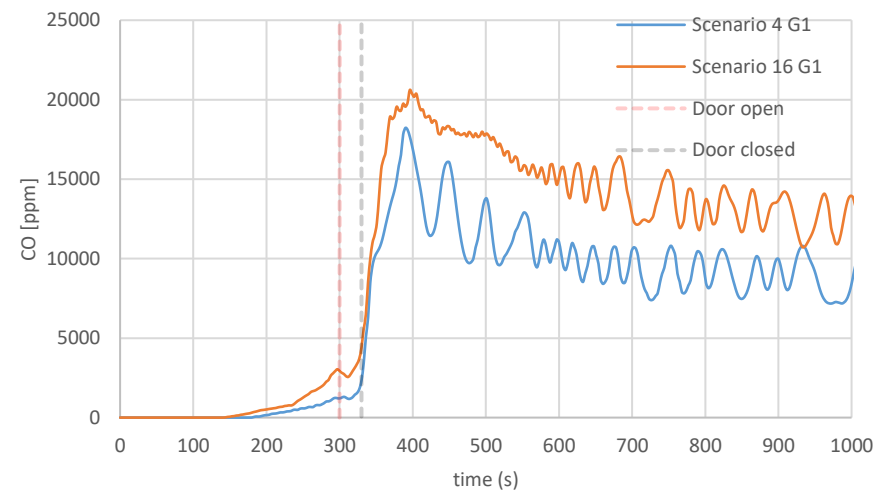
Pressure in the apartment (PL equipment) (0,2 meters)



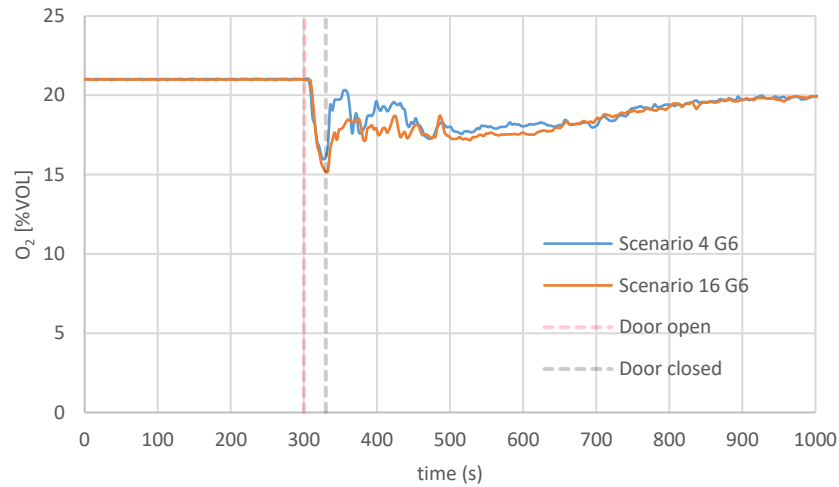
Pressure in the apartment (PH equipment) (0,2 meters)



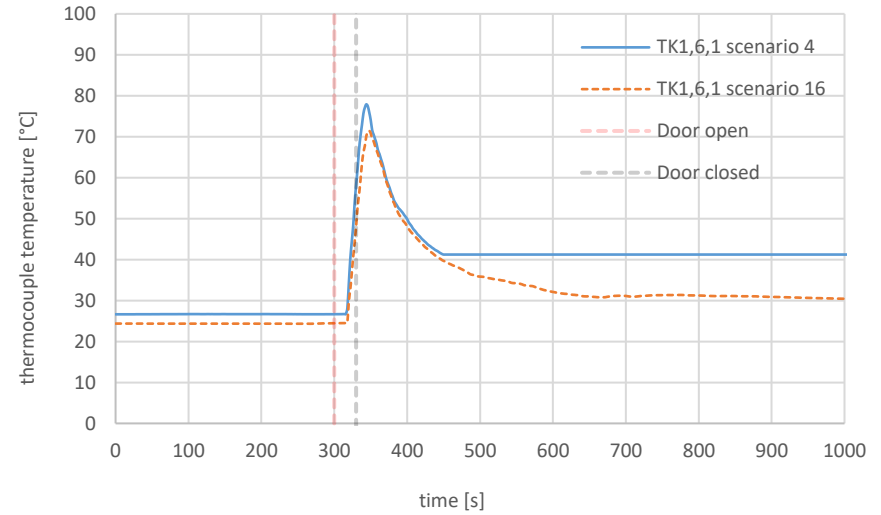
CO concentration in the apartment (1,5 meters)



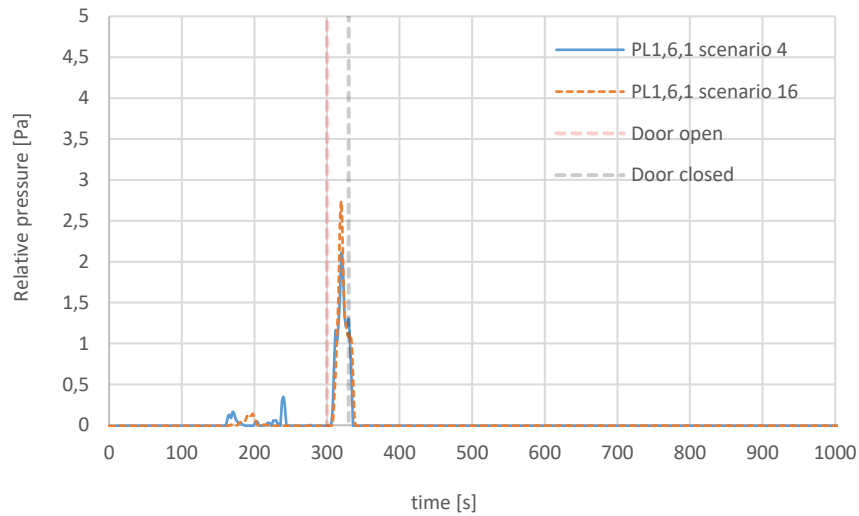
O<sub>2</sub> concentration in the corridor (1,5 meters)



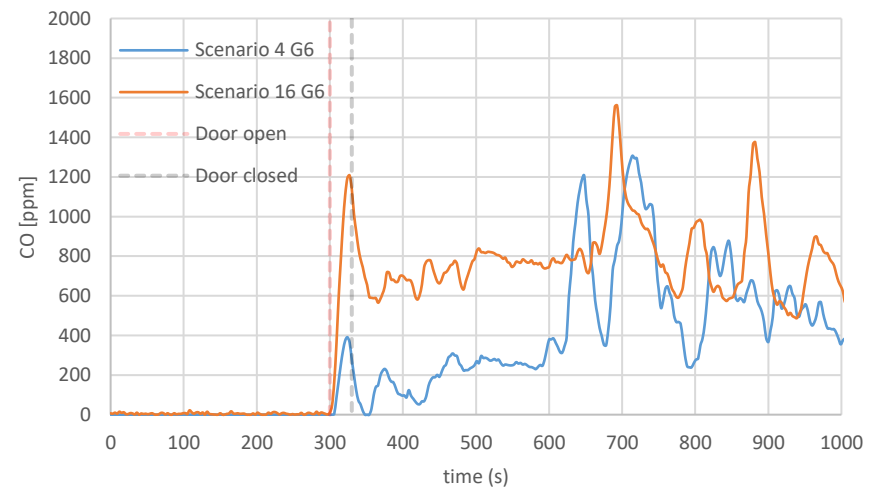
Temperature underneath ceiling in apartment (1,5 meters) measurement failed in scenario 4



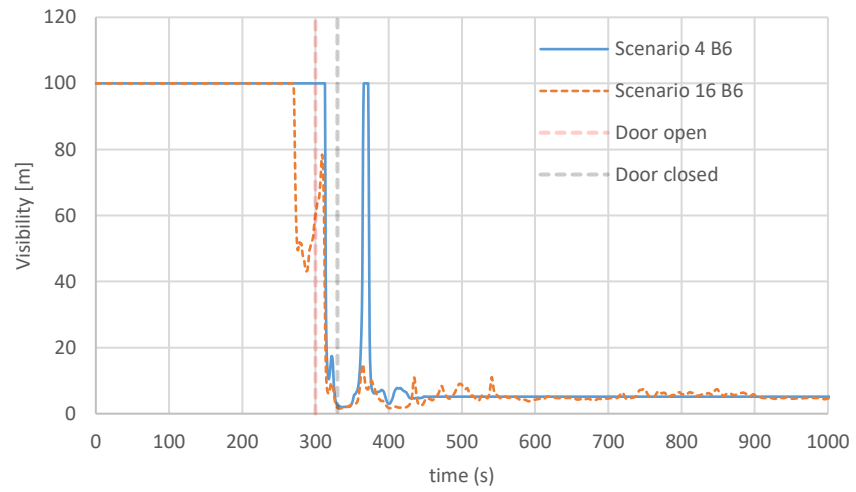
Pressure in the corridor (0,2 meters)



CO concentration in corridor (1,5 meters)



Visibility in corridor (1,5 meters)



More results are available in the report as written by the NIPV [17].

## APPENDIX 3: EXPANDED THEORETICAL FRAMEWORK

### Computational Fluid Dynamics

Computational fluid dynamics, or CFD, is the analysis of systems involving among others fluid flow and heat transfer by means of a computer based simulation. CFD-codes are structured around the governing equations of fluid dynamics. The equations solved are a form of the Navier-Stokes equations, which are a representation of the conservation laws of physics: conservation of mass, energy and momentum. These equations are solved numerically to estimate flow characteristics in a domain in space and time [20].

To do so, the domain of interest is divided into small volumes called 'cells' in which the quantities are uniform. Cells form a numerical grid for which calculations are carried out. Generally, the numerical process entails, per time-step:

1. Integrating the governing equations of the fluid flow over the entire domain;
2. Translating the resulting integral equations into a system of algebraic equations through discretization techniques;
3. Solving the algebraic equations iteratively until a convergence criteria is met.

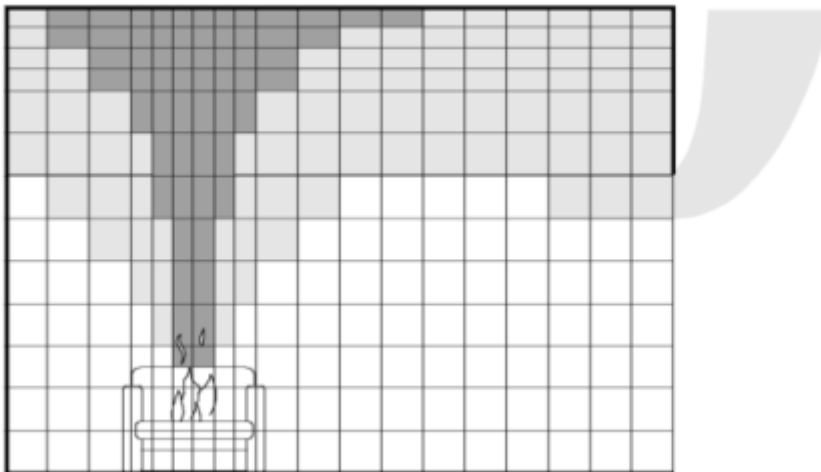


Figure 87: schematization of a 2D numerical grid in a fire CFD-simulation. Copied from [50]

Typically, turbulent flows include eddies with a wide range of length scales. For most engineering purposes, not all eddies are relevant to the overall flow dynamics of interest. Therefore, several methods are developed to solve a problem related to fluid flows.

### Reynolds Averaged Navier-Stokes

In Reynolds averaged Navier-Stokes methods (or RANS) methods, the attention is focused on the mean effects of turbulence on the flow properties. Initially, the Navier-Stokes are time-averaged (or Reynolds-averaged) after which the numerical method is executed. The time-averaging introduces multiple extra terms which need to be modelled using turbulence models. As such, eddies of all length scales are modelled using (classical) turbulence models. Well established examples are the  $k\epsilon$ - and  $k\omega$ -models.

The main advantage of RANS-modelling is its computational efficiency compared with LES and DNS. RANS is by far the most used methodology given its relatively limited computational cost and reasonable predictive capabilities for most engineering purposes.

RANS-methodologies were and still are commonly used in the simulation of fire phenomena. The main downside of using the RANS-models in fire simulations lies in the fact that the computational methodology causes information on mid- to large scale eddies to be lost. These eddies are typically

dominant in fire driven flows. Another issue is including more complex chemistry in the simulations, which relies heavily on local transient events [21].

### Large Eddy Simulations

Large Eddy Simulations (or LES) underlines the fact that large eddy structures are typically anisotropic as opposed to smaller eddies, which are typically of a more isotropic nature. This leads to a methodology in which eddies with a large length scale are directly resolved while the more universal smaller eddies can be accounted for using turbulence models.

The LES-methodology uses a filtering function to define a cutoff width. Eddies with a larger length-scale than the cutoff width are directly resolved while eddies with a smaller length scale are modelled using SGS-turbulence models (SGS: sub-grid scale). This directly links to the resolution of the computational mesh used in the simulations, as with a higher resolution, more eddies are expected to be directly resolved. With increasing mesh resolutions, LES starts to behave more like DNS [20].

Given the numerical method described earlier, the quality of the Large Eddy Simulation shows a significant dependency on the resolution of the mesh. Checking the mesh for sensitivity therefore is a fundamental part of LES-simulations.

Given the fact that the dominant eddies in fire driven flows can be resolved, rather than modelled, LES has gained ground over RANS in the simulation of fire phenomena. In practical engineering studies however, quite a bit of fire related phenomena occur at SGS (e.g. combustion, pyrolysis, etc.) These phenomena still need to be modelled using sub-grid scale models.

### Direct Numerical Simulations

In Direct Numerical Simulations (or DNS), eddies of all length and time scales are solved numerically. To do so, a significantly fine grid and small time-steps are required, leading to highly costly simulations in terms of computational resources. In general engineering practices, DNS is therefore not usable. It is most often used in the research on fundamental flow problems in simple configurations (e.g. to study the effectiveness or development of new turbulence models).

### Heat Release Rate and heat of combustion

In FDS, the Heat Release Rate is calculated as:

$$\dot{Q} = \dot{m} * \Delta H_c * X$$

|                |                         |         |
|----------------|-------------------------|---------|
| $\dot{Q}$ =    | Heat Release Rate (HRR) | (kW)    |
| $\dot{m}$ =    | Mass Loss Rate (MLR)    | (kg/s)  |
| $\Delta H_c$ = | Heat of combustion      | (kJ/kg) |
| $X$ =          | Combustion efficiency   | (-)     |

During the experiments, weight-loss measurements were carried out. Therefore, the mass loss rate is known. During the experiments, it was observed that the primary fuel contributing to the fire was composed of polyurethane. It is therefore assumed that the fuel is composed entirely of polyurethane GM21 flexible foam, as it is referenced in literature. According to [23], polyurethane GM21 has a net heat of combustion of 26.200 kJ/kg.

The correlation above indicates the MLR and the heat of combustion are directly related with the HRR through a constant, the combustion efficiency X. While for well-ventilated fires with a equivalence ratio well below 1, the combustion efficiency is more or less constant (with values for 0,7-0,8 being mentioned in literature [22]), for under-ventilated fires it is not. The relation between the effective heat of combustion and the equivalence ratio is shown below [31] for different fuels.

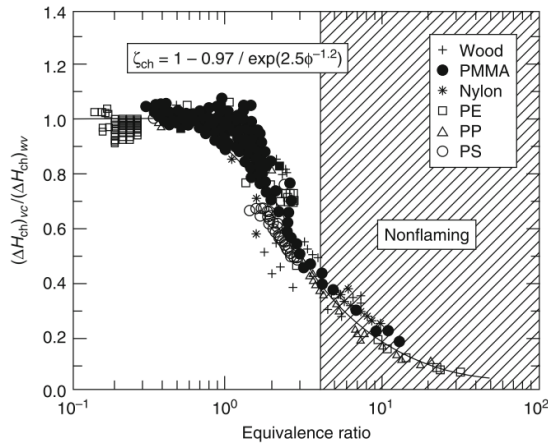


Figure 88: relation between the combustion efficiency and the fires equivalence ratio. Copied from [31]

As an alternative to the previous correlation, the HRR of a fire can also be calculated by the mass of oxygen consumed in the combustion process:

$$\dot{Q} = \dot{m}_{O_2 \text{ consumed}} * \Delta H_O$$

$\dot{m}_{O_2 \text{ consumed}} =$  Mass of O<sub>2</sub> consumed (kg/s)

$\Delta H_O =$  Heat of combustion per mass of oxygen consumed (kJ/kg)

For most fuels, the heat of combustion per mass of oxygen consumed is approximately 13.100 kJ/kg. Tabulated data [23] shows that in the combustion of polyurethane GM21 12.100 kJ/kg is released per kilogram of oxygen consumed.

### Estimating the effective heat of combustion

Several studies indicate the effective heat of combustion differs heavily per experiment. As mentioned before, it is a function of the vitiation of the fire but is also effected by the geometry of the fuel source, impurities in the fuel, the location of the fuel package in the enclosure and the initial burning object. Typical values for the effective heat of combustion of polyurethane filled sofas found in calorimetry experiments (mostly well-ventilated circumstances) range from approximately 22 MJ/kg to as low as 14 MJ/kg [24] [25] [26] [12]. This makes generalizing the effective heat of combustion in ways described earlier susceptible to error.

As no calorimetry was carried out on the burned sofas, an indication of the effective heat of combustion is obtained using a simple correlation (the 'MQH-correlation') for layer temperature [27] [28]:

$$\dot{m}\Delta H_{c,eff} = \sqrt{\left(\frac{\Delta T}{6.85}\right)^3 * A_0\sqrt{H_0}h_kA_t}$$

Where  $h_k$  is the overall heat transfer coefficient,  $A_t$  is the surface through which heat losses occur,  $\Delta T$  is the temperature difference and  $A_0\sqrt{H_0}$  is the ventilation coefficient.

This correlation is only valid for well-ventilated fires. Furthermore, fires flush in corners or walls should be handled with care. For these fires, other entrainment coefficients are proposed in the literature [29]. However, more recent data suggests the effects of the corner position on the entrainment rate in the fire plume is limited if a small gap is present between the wall and the fire seat [30]. The original correlation is used in this thesis.

To avoid using data from under-ventilated or smoldering fires, data from 100-300 seconds is used. As the thermocouple tree is located at some distance from the seat of the fire and the protective hoods are expected to affect the representativeness of the measurements, the normative thermocouple is used to calculate the temperature difference. Also, it is expected that the floor of the compartment has negligible effect on the overall heat transfer in this timeframe, the area is excluded from the calculations. Using this method results in an effective heat of combustion of approximately 16 MJ/kg, which fits the values found in literature quite well.

### Radiative fraction

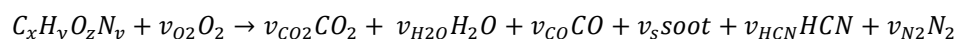
As a fire starts to grow more ventilation controlled, the soot-production is expected to increase. This results in a higher in-flame soot concentration. Higher soot concentrations in a flame will result in higher radiative heat outputs compared to well-ventilated fires. In fire engineering studies, the part of the heat release rate that is radiated away from the flame is called the radiative fraction of the heat release rate. The part of the heat that is transported away by convection in the smoke plume is called the convective fraction. The sum of both is equal to unity as per the conservation of energy.

In this thesis, the default value for the radiative fraction in FDS is used, which is 0,35. This corresponds quite well with values found for polyurethane flames in literature [22]. This states that, depending on the equivalence ratio of the fire, a radiative fraction between 0,3 and 0,4 is expected.

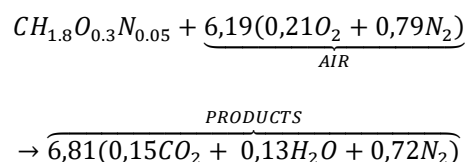
### Combustion model

Directly simulating combustion in a CFD-simulation in a large scale fire application is not possible due to the fact that the area where the reaction occurs (e.g. the flame sheet) is subgrid-scale. Therefore, a combustion model is used.

As a default, FDS uses an infinitely fast, single-step combustion model<sup>4</sup>. The combustion is only controlled by the mixing of the fuel with oxidizer and can therefore be seen as an approximation of reality (in literature, this type of 'Eddy Dissipation Concept' model is typically characterized as 'mixed=burned'). Due to the infinite fast reactions, the resulting flame temperatures are adiabatic. The simple combustion model assumes a chemical reaction in the general form of (fuels containing other molecules than C, H, O or N are possible but the user needs to model and input the reaction manually):



For complete combustion under stoichiometric conditions, the products are composed of only water vapor, carbon dioxide and nitrogen. The reaction is as follows (in which the molecular composition for air is for simplicity taken to be 21% oxygen and 79% nitrogen):

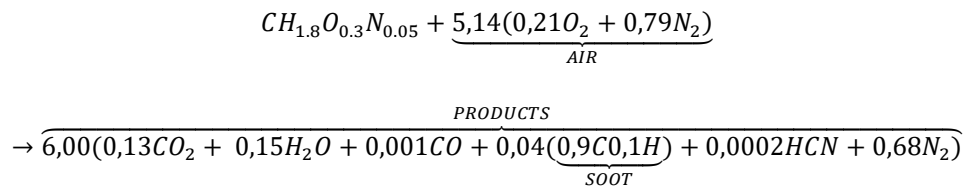


To completely burn one mole of polyurethane GM21, 6,19 moles of air are needed. The molecular weight of the fuel and air are respectively 19,8 gram/mole and 28,8 gram/mole. Therefore, to fully burn one kilogram of polyurethane GM21, 9,24 kilogram of air is needed or to be more concise 2,15 kilogram of oxygen.

In reality, combustion never occurs stoichiometric and will generate other products such as soot, CO and HCN. The user needs to input the post-flame yields of CO, HCN, soot and the hydrogen fraction in

<sup>4</sup> As an alternative, FDS also has a finite-rate combustion model included. This method of combustion modelling however requires a very fine grid resolution, which is not practical in large scale fire simulation. This method is not further elaborated on.

the soot. Species yields for various fuels can be found in literature [23] [51] [52], but are typically only available for well ventilated conditions (with an equivalence ratio well below one). Using the single step-combustion model, the combustion of for example polyurethane GM21 is modelled as follows:



In which the yields for soot, CO and HCN are taken as 0,131, 0,01 and 0,002 g/g respectively [43]. In this specific combustion reaction, 7,7 kilogram air (or 1,8 kilogram of oxygen) is needed to fully burn 1 kilogram of polyurethane GM21. Relating to paragraph 4.3, this means the effective heat of combustion is approximately 21.640 kJ/kg. At higher species yields, the fire needs less oxygen for combustion, this results in a lower effective heat of combustion. This results in a drop of the combustion efficiency as the oxygen becomes more diluted.

It is currently not possible to account for transient effects due to oxygen dilution in the combustion model. This can affect the results quite heavily. Therefore, care should be taken when species yields are chosen.

### Equivalence ratio

The equivalence ratio of a fire gives an indication on the dilution of the oxygen-supply with regards to the oxygen necessary for complete combustion. Generally, the equivalence ratio can be specified as the actual fuel to air ratio divided by the stoichiometric fuel to air ratio. This implies the available oxygen for combustion needs to be estimated. In practice several methods for calculating the equivalence ratio exist, two of which are specifically described in this thesis.

#### Global equivalence ratio

As shown in the previous paragraphs, the species generation and the combustion efficiency relies heavily on the Equivalence Ratio of the fire. The equivalence ratio is a concept that shows the level of vitiation of the fire. A low equivalence ratio ( $\ll 1$ ) means the fire is generally well-ventilated while a high value denotes a ventilation controlled fire. Several methods for calculating the equivalence ratio exist, in which the 'Global Equivalence Ratio' method is used the most. The GER is calculated as follows:

$$\varphi = \frac{\dot{m}_f / \dot{m}_{air}}{r}$$

|               |  |         |
|---------------|--|---------|
| $\varphi =$   | Global equivalence ratio (GER)                     | (-)     |
| $\dot{m}_f =$ | mass loss rate fuel                                | (kg/s)  |
| $\dot{m}_a =$ | mass of air added to the compartment through vents | (kg/s)  |
| $r =$         | stoichiometric ratio air/fuel                      | (kg/kg) |

This correlation is only applicable to static or quasi-static situations in which the burning fuel is easily reached by the air flow. The mass loss rate of the fuel was measured during the experiments. The mass of air added to the compartment through vents can be calculated using Bernoulli's law (for the scenario with the open balcony door) [53]:

$$\dot{m}_{air} = C * A\sqrt{h}$$

|                   |                                   |        |
|-------------------|-----------------------------------|--------|
| $\dot{m}_{air} =$ | Mass flux of air inwards/outwards | (kg/s) |
| $C =$             | Ventilation constant              | (-)    |

$A =$  Area of the opening (m<sup>2</sup>)  
 $h =$  height of the opening (m)

C is a constant which is determined by the discharge coefficient of the opening and the gravitational acceleration constant. A value typically used is 0,5 but more values are reported in literature [54].

### *Plume equivalence ratio*

Another concept, more related directly with the combustion chemistry, is that of the 'plume equivalence ratio' (PER), in which the ratio of the mass loss rate to the mass of the reacting oxygen in the fire plume are the most important parameters. The entrained air in the fire plume does indeed contain oxygen. Whether or not the oxygen is actually used in the combustion reaction however, depends (among others) on the flame temperature as it affects the chemical kinetics. At higher temperatures, oxygen is more likely to be used in the combustion process. This relates well with the oxygen-index methodology used in the extinction model of FDS, which is described in more detail in paragraph 4.7.

While the PER-methodology is referenced in literature [23] [55] [56] [57], the concept is not well-validated as measuring the related parameters (entrainment in the fire plume) is difficult in large-scale fire experiments. This method should therefore be used with caution.

Information is available on the volume fraction of the available oxygen in the apartment, as measurements were carried out. As the measurements were taken at some distance from the fire seat, using the data to calculate a plume equivalence ratio is to some extent questionable.

The plume-equivalence ratio is calculated by:

$$\varphi_p = \frac{\dot{m}_f / \dot{m}_{O_2,reacting}}{\dot{m}_f / \dot{m}_{O_2,stoich}} = \frac{\dot{m}_f}{\dot{m}_{O_2,reacting}} * \Psi_O$$

|                            |   |         |
|----------------------------|---|---------|
| $\varphi_p =$              | plume equivalence ration (PER)                          | (-)     |
| $\dot{m}_f =$              | mass of reacting fuel                                   | (kg/s)  |
| $\dot{m}_{O_2,reacting} =$ | mass of oxygen available for reaction in the fire plume | (kg/s)  |
| $\Psi_O =$                 | stoichiometric mass oxygen-to-fuel ratio.               | (kg/kg) |

The mass of the reacting fuel is directly taken from the mass loss measurements. The stoichiometric oxygen-to-fuel ratio is approximately 2,2 kg/kg for polyurethane GM21. The available mass of oxygen in the fire plume needs calculation using empirical correlations. A correlation for the entrained mass in the fire plume is derived by Heskestad in [32]:

$$\dot{m}_{ent,L} = 0.878 * \left[ \left( \frac{T_L}{T_\infty} \right)^{5/6} \left( \frac{T_\infty}{T_L} \right) + 0.647 \right] \frac{\dot{Q}_c}{c_p T_\infty}$$

|                     |   |
|---------------------|---|
| $\dot{m}_{ent,L} =$ | entrained mass over length of the fire-plume (kg/s)   |
| $T_L =$             | Flame temperature at the flame-tip (estimated to be 500K)   |
| $T_\infty =$        | Temperature in the compartment, averaged from measurements  |
| $\dot{Q}_c =$       | Convective part of the heat release rate (kW), taken as 0,7Q multiplied by the combustion efficiency. |
| $c_p =$             | specific heat of air (1 kJ/kg*K)  |

Please note that this correlation is only valid for axisymmetric plumes with a sufficiently high turbulence. As the sofas are placed in a corner, an axisymmetric shape is not directly expected, with the adjacent walls to some extent limiting air entrainment in the fire plume. Some studies stipulate that this has

significant effect on the air entrainment in the fire plume, while more recent studies show that the effects are limited if only a small gap is present between the fire seat and the adjacent walls [23] [30]. This correlation will therefore only give a rough indication of the entrained air. Please note that the calculated heat release rate is only used in this calculation and serves no further purpose. The combustion efficiency in the heat release rate is assumed to be 0,75 [22]. No dilution effects are taken into account.

### *Methodology used in this thesis*

While the global equivalence ratio is in its essence a more simplistic method, it requires calculation of vent flows using simple correlations with limited validity. It is however not possible to account for the extra air through the door opening in simple calculations which are carried out to calculate the GER as it is unclear what the exact composition of the incoming air through the door is. It is safe to assume that, sometime after the door has opened in the experiments, the incoming air also contains combustion products. Lastly, the correlation for mass flux of air inside the apartment is not entirely accurate as would appear from the CFD-simulations later on as mass-flows are over-estimated in the correlation.

The PER-concept relates more to the complex chemical reaction in the flame sheet, and is therefore more susceptible to error. However, as it allows a direct correlation between the experimental results and the modelled species-yields, this method is used in this thesis.

### **Pyrolysis model**

Modelling pyrolysis can be done using several methods in FDS. The simple pyrolysis model assumes a certain mass loss rate. This can be prescribed by directly imposing a Heat Release Rate to a surface. The mass loss rate then is calculated by dividing the Heat Release Rate by the effective heat of combustion. Another method is directly imposing a mass loss rate to a surface. The Heat Release Rate is then calculated by multiplying the mass loss rate with the effective heat of combustion. This methodology is commonly used in generic (commercial) fire engineering studies. The main downside of this methodology is that an assumption on the expected HRR must be made. Furthermore, more complex phenomena involving the effects of the enclosure (e.g. thermal feedback) are not accounted for. These phenomena can be very dominant in the overall mass loss rate of the fuel source.

To account for these phenomena, more complex pyrolysis models are available in FDS. In these models, the gas-phase and solid-phase reactions are coupled using either characteristics such as the 'ignition temperature' and the latent heat of vaporization or by using Arrhenius expressions. The main downside of these applications is the limited availability of material property data.

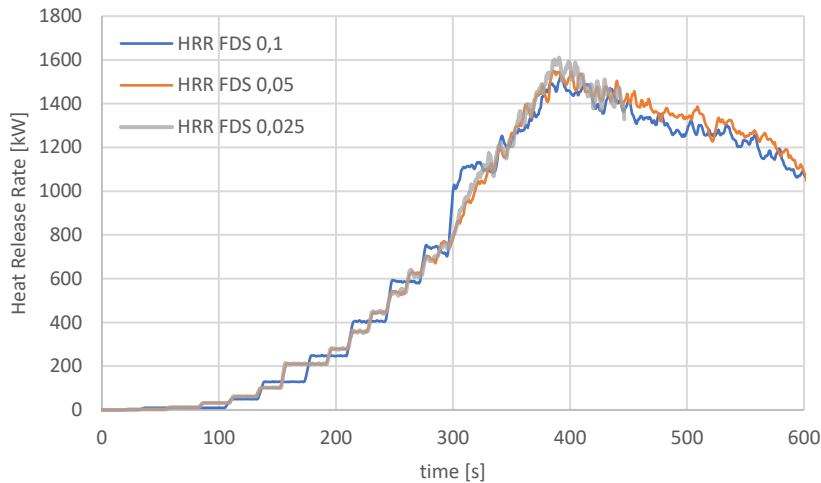
In this study, the simple pyrolysis model is used. The weight loss measured during the experiments is used to calculate the mass loss rate of the fuel packages. This way, the effects of the enclosure are taken into account by proxy.

## APPENDIX 4: EXPANDED GRID SENSITIVITY STUDY

### Case study 1: balcony door open

#### Heat Release Rate

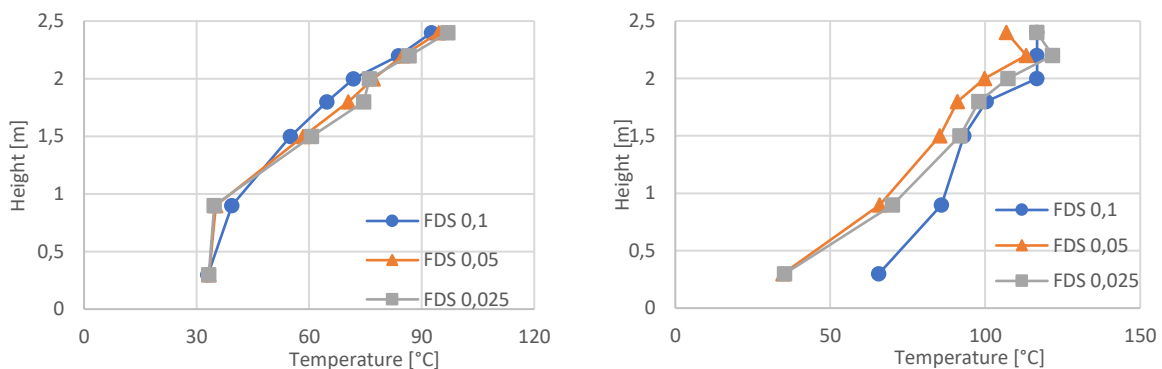
The Heat Release Rate does not show significant differences between models as seen in the following figure. This indicates the cell size has limited influence on the extinction of the fire.



Modelled HRR for fine and moderate mesh

#### Temperatures

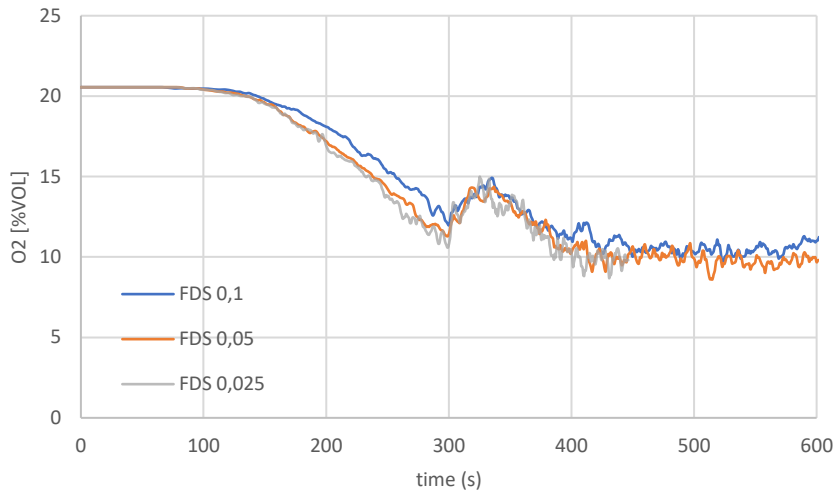
Temperatures in the fire-room do not show significant differences. Sometime after opening the door between the apartment and the corridor, significant differences occur between the moderate and fine mesh as seen in the following figures.



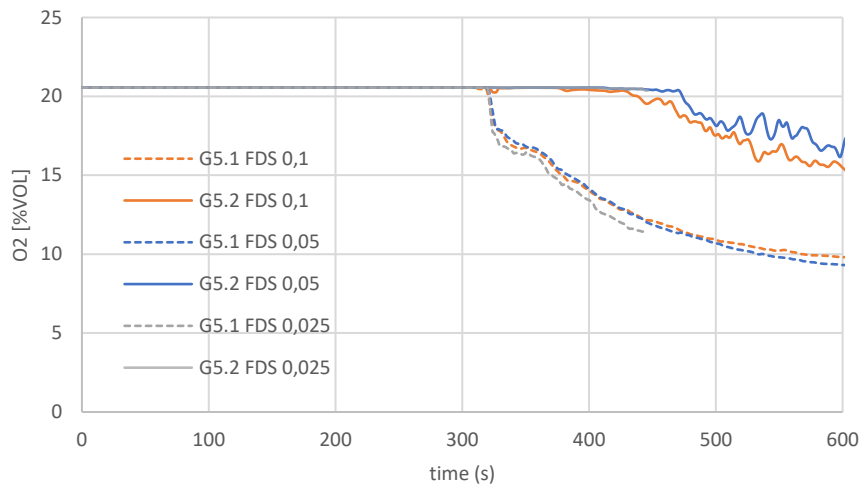
Temperatures at measuring tree B1 at t=150 seconds (left) and at tree B5 at t=400 seconds (right)

#### Oxygen concentrations

With regards to the simulated oxygen concentrations, values in the fire-room show significant differences between models. Comparing these results with the vent flows over the balcony door, it is clear that the smaller vent-flows lead to lower oxygen concentrations in the fire-room. As to oxygen concentrations in the corridor, the upper part does not show significant differences while the lower part of the corridor does. This indicates the turbulent mixing in the corridor is sensitive to the used cell-sizes.



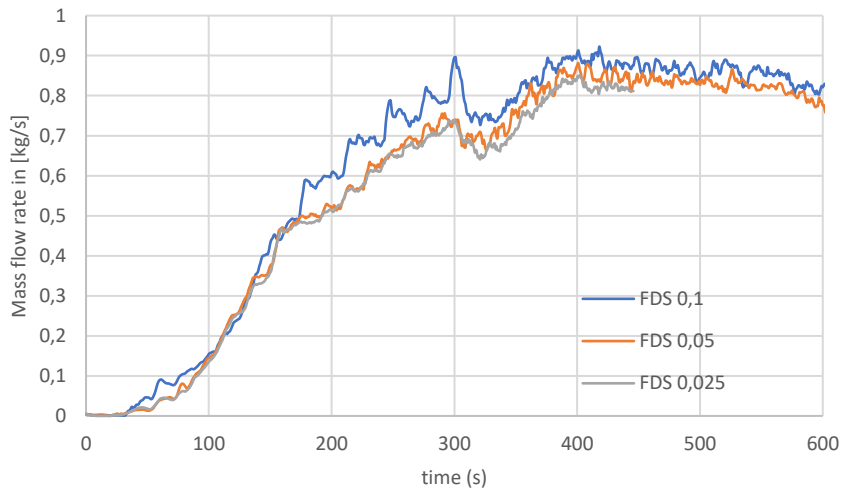
Oxygen concentrations in the fire room (measuring tree B1)



Oxygen concentrations at measuring tree B5

### Vent flows

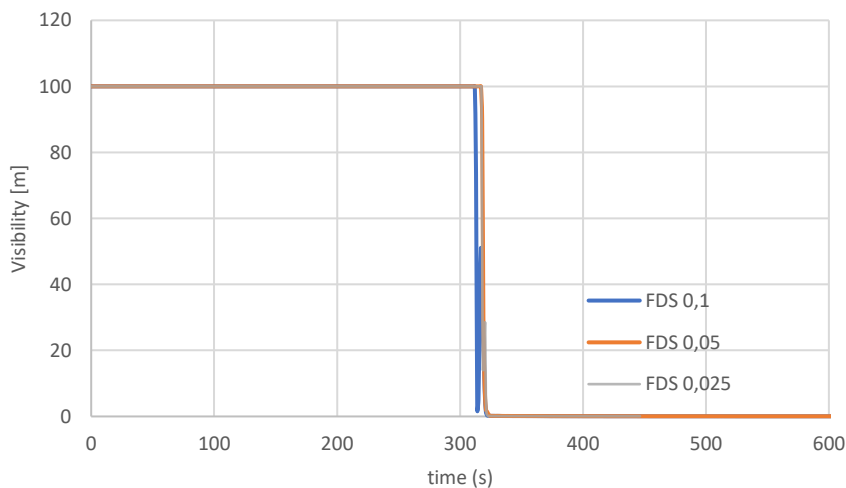
Vent-flows over the balcony-door and door between the hallway and the apartment do show differences. The following image shows the mass-flows over the balcony door.



Mass flow rate over balcony door (inwards)

### Visibility

The development of visibility in the hallway does show some, but limited differences, indicating the turbulent mixing in the hallway is to some extent sensitive to the used cell-sizes.

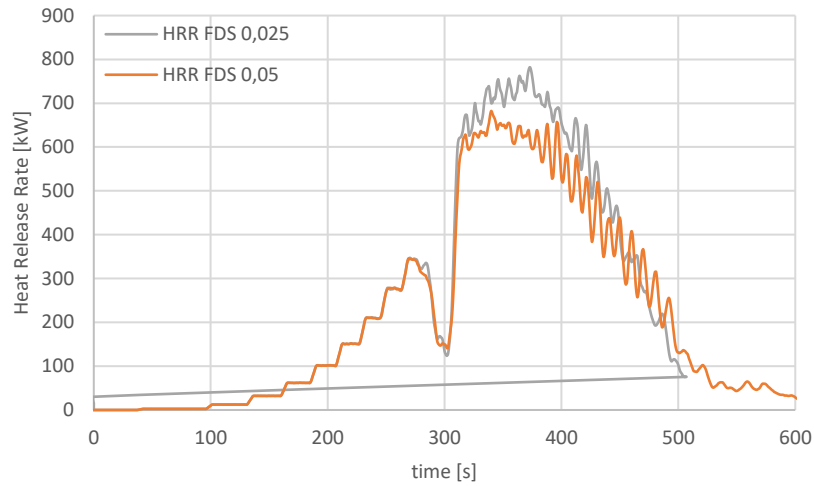


Visibility in the hallway, point G5.1

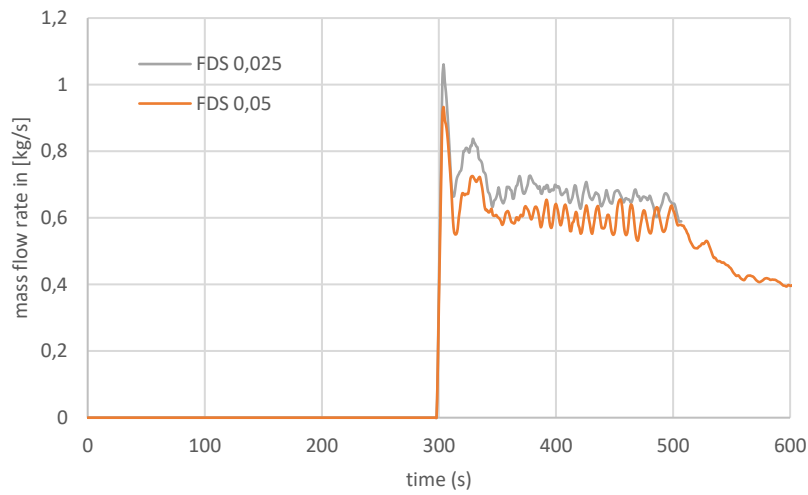
## Case study 2: door to corridor opened after 300 seconds and left open

### Heat Release Rate

The following figure shows the simulated Heat Release Rate for both the mesh resolutions. Some deviations are apparent but limited. In both simulations, the fire is quenched by the extinction model at around 280 seconds. After the door to the corridor is opened, extra oxygen is made available and a higher heat release rate is showcased from 300 seconds onwards. This is mainly due the fact that the mass flow rate over the entrance door of the apartment is somewhat higher in the finer simulations.



Comparison of the Heat Release Rate for this mesh sensitivity study



mass flow rate over the door

### *Oxygen concentrations*

The oxygen concentrations in the apartment do not show significant differences, as shown in Figure 89. The finer mesh-resolution shows a somewhat lower oxygen concentration around the moment the Heat Release Rate peaks.

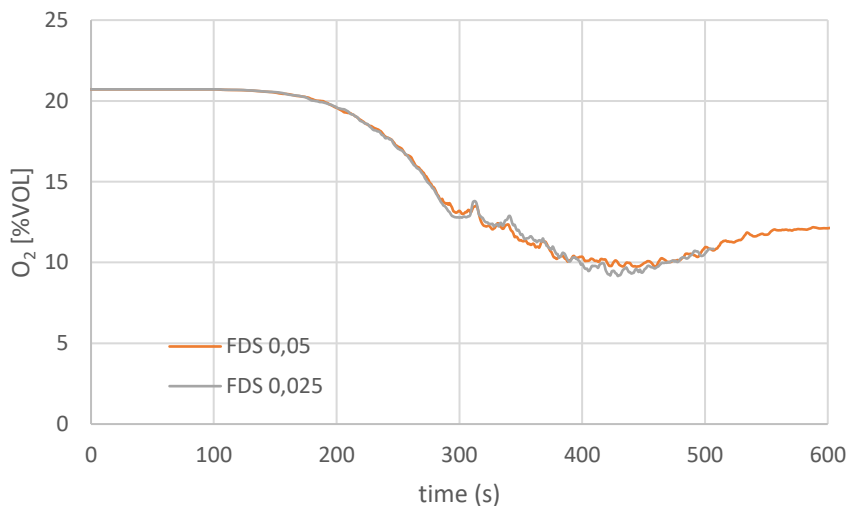


Figure 89: oxygen concentrations in the apartment

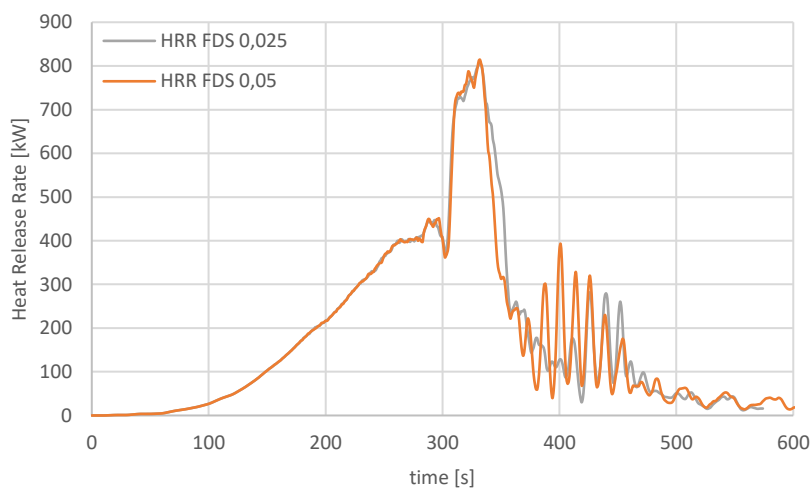
### Case study 3: door opened after 300 seconds and closed again 30 seconds later

Given the results of the mesh-sensitivity study for case study 1, the minimum mesh-size used in this case is 5\*5\*5 cm. Given the fact that the extinction model used in FDS depends on the mesh resolution, the sensitivity of the mesh is checked against a non-uniform mesh with a resolution of 2,5\*2,5\*2,5 cm in the apartment. In the corridor, the mesh resolution is kept at 5\*5\*5 cm.

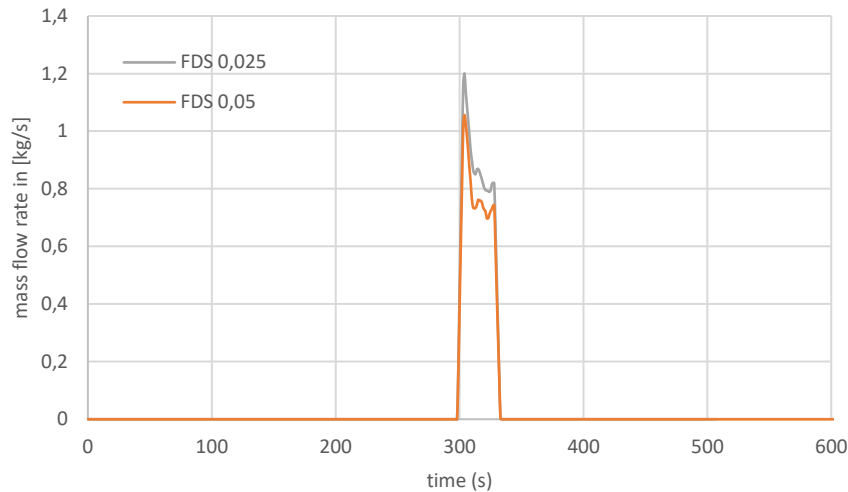
As the mesh resolution in the corridor is the same for both scenarios, no significant differences are expected. This sensitivity study focusses on the fires' heat release rate and gas-concentrations.

### Heat Release Rate

The fires' Heat Release Rate is shown in the next figure. Aside from nuance differences from 350 seconds onwards, no significant differences are observable. As was the case in case study 2, the mass flow rate over the apartment door is slightly higher in the scenario which uses a mesh of 2,5\*2,5\*2,5 cm.



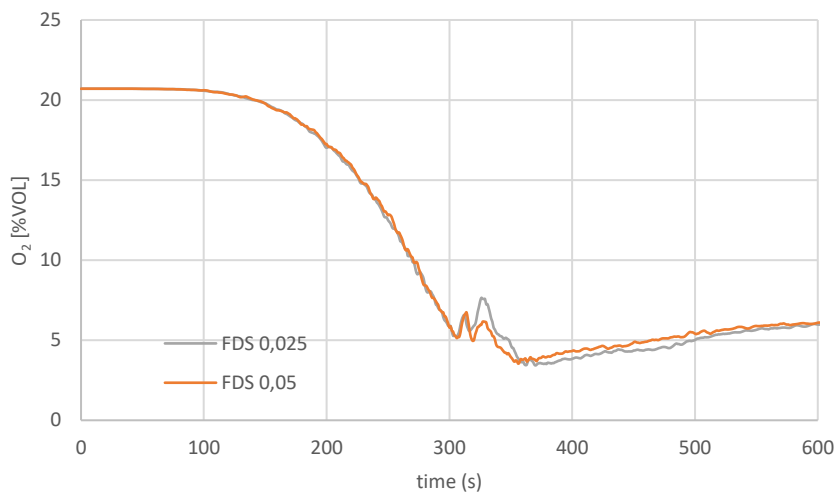
Comparison of the Heat Release Rate for this mesh sensitivity study



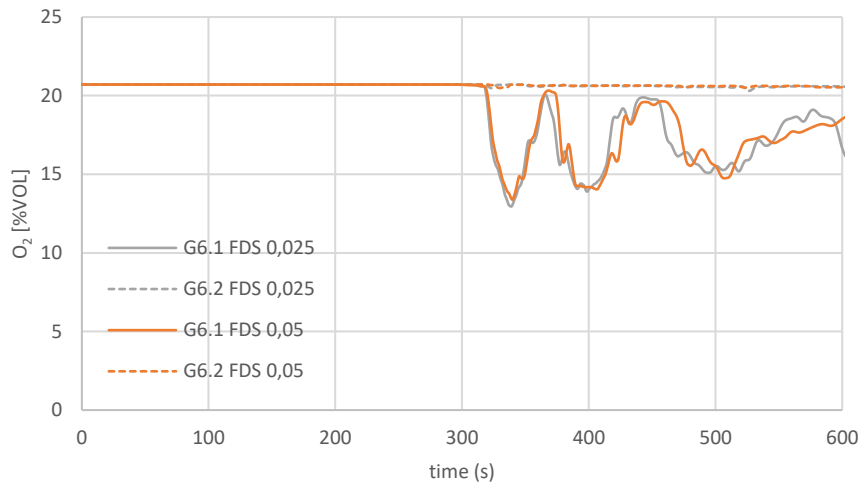
Comparison of the mass-flow rate over the apartment door for this mesh sensitivity study

### Gas concentrations

The oxygen concentration in both the apartment and the corridor (measuring tree B6) are shown in the following figures. Other than nuance differences from the moment flame extinction is modelled, no significant differences are observed. In the corridor, nuance differences are observable. These can be attributed to differences in the mass-flow rate over the apartment door and turbulence in the fire driven flow.

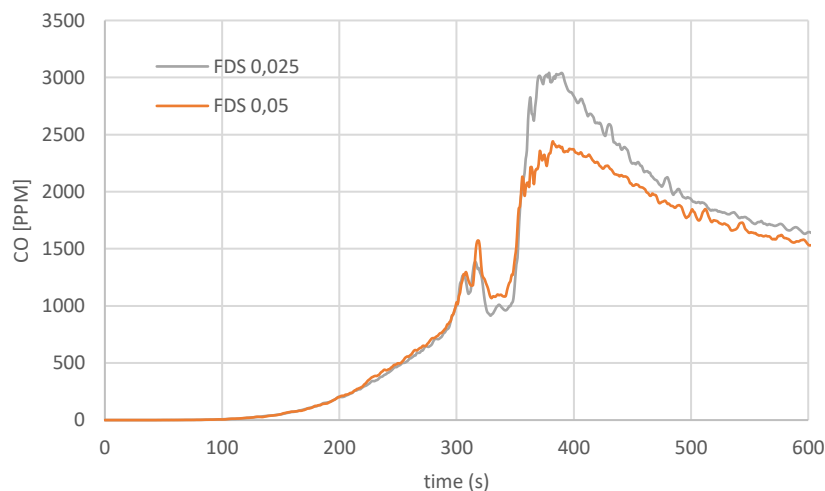


Comparison of the oxygen concentration for this mesh sensitivity study



Comparison of the oxygen concentration at measuring tree B6 for this mesh sensitivity study

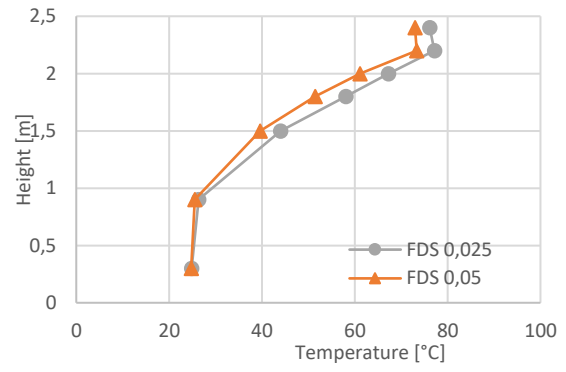
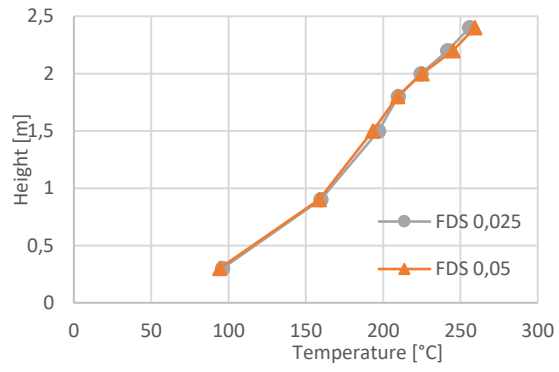
As shown in the next figure, the simulation with a mesh of 2,5\*2,5\*2,5 cm results in significantly higher CO-concentrations in the apartment. This shows the two-step combustion model is sensitive to the used mesh resolution. Due to the smaller mesh cells, oxygen depletion near the flame body is more appropriately approximated, leading to nuance differences in near-field oxygen concentrations. They are predicted to be somewhat lower, and therefore results in more CO being generated by the fire.



Comparison of the CO-concentration for this mesh sensitivity study

### *Temperatures*

Temperatures in the enclosure (both in the apartment and the corridor) do not show significant differences.

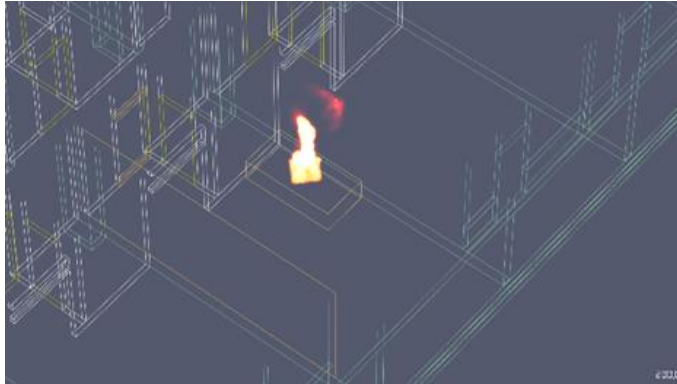


Temperature distribution over the height of the enclosure for B1 at t=300 seconds (left) and B5 at t=350 seconds (right)

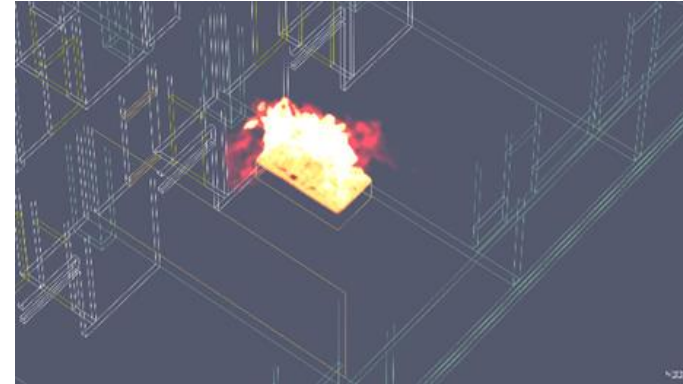
## APPENDIX 5: NUMERICAL RESULTS

### Case study 1: balcony door open and door to corridor opened after 300 seconds

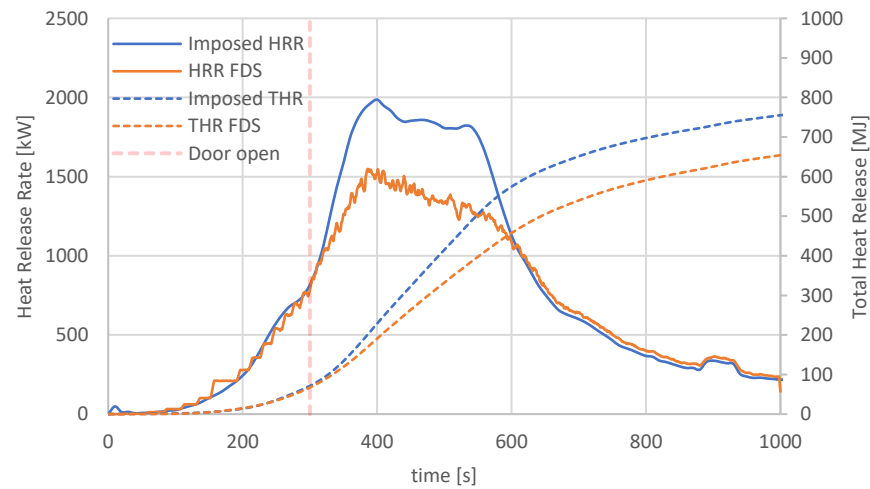
HRRPUV  
200 seconds



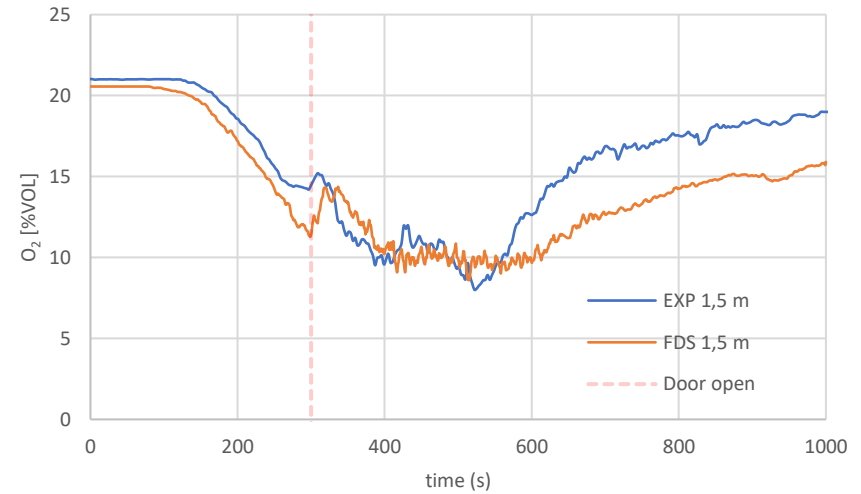
HRRPUV  
400 seconds



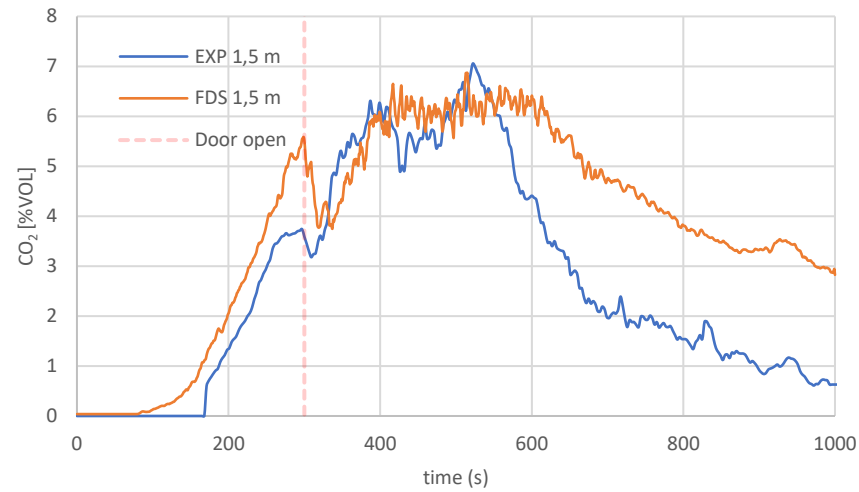
### Heat Release Rate



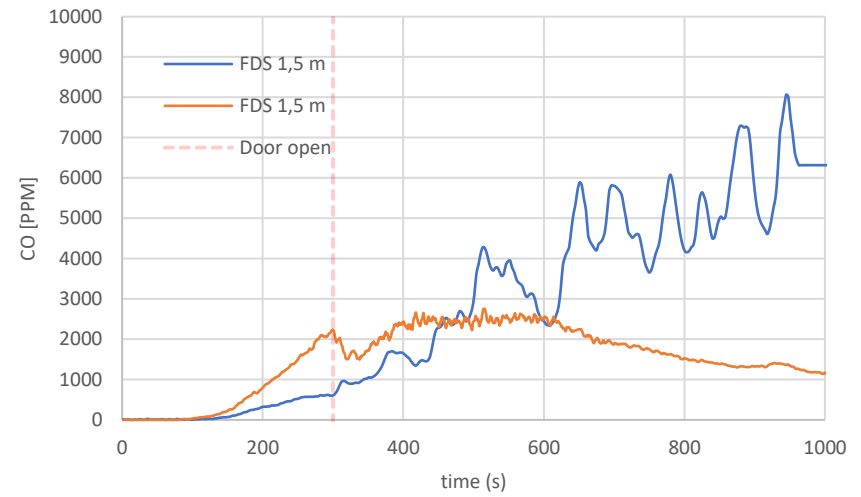
### O<sub>2</sub> concentration in the apartment (1,5 meters)



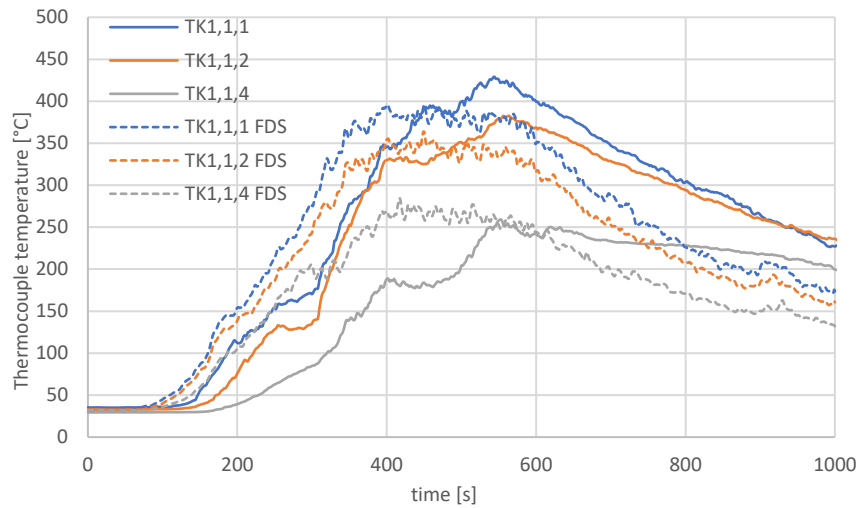
CO<sub>2</sub> concentration in the apartment



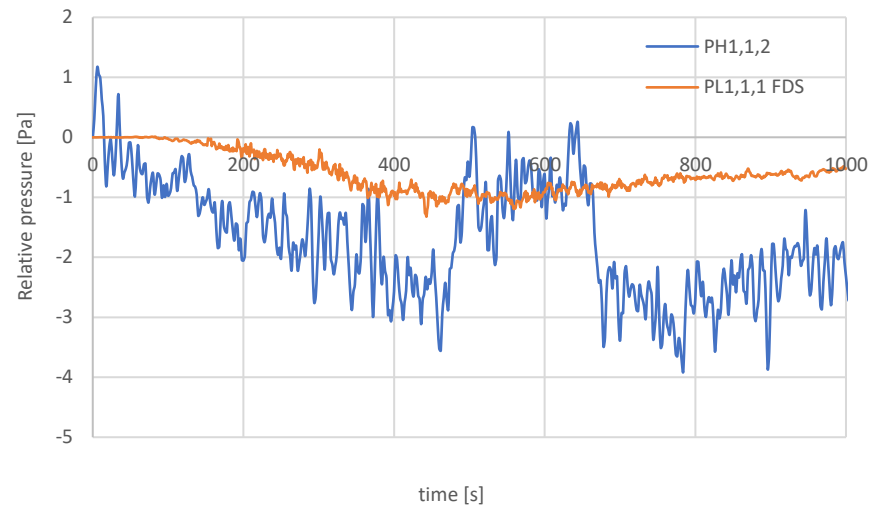
CO concentration in the apartment



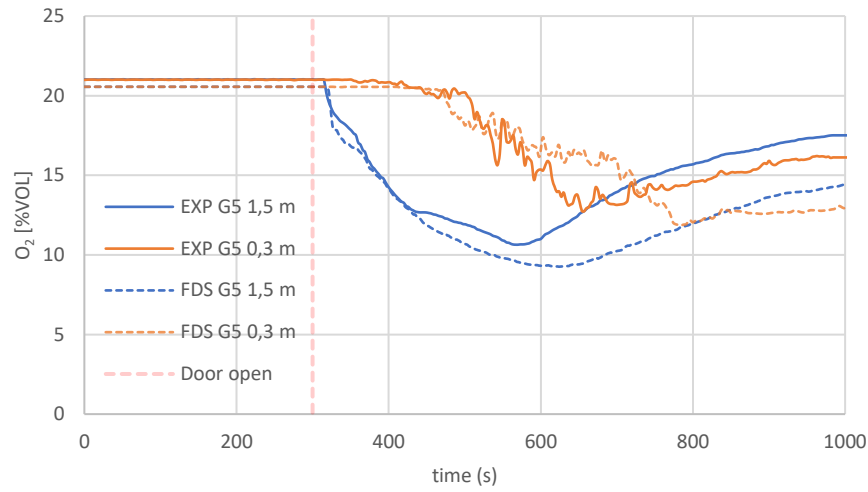
Temperatures in the apartment



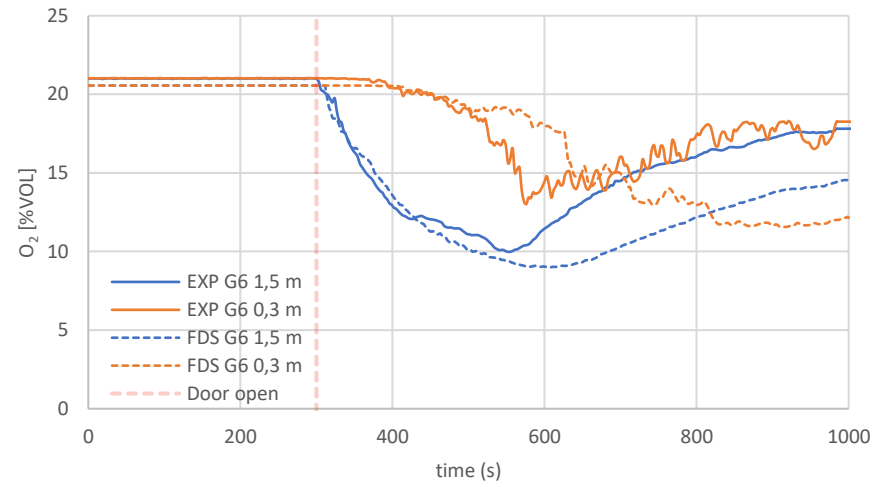
Pressure in the apartment (note: PH equipment with low sensitivity used)



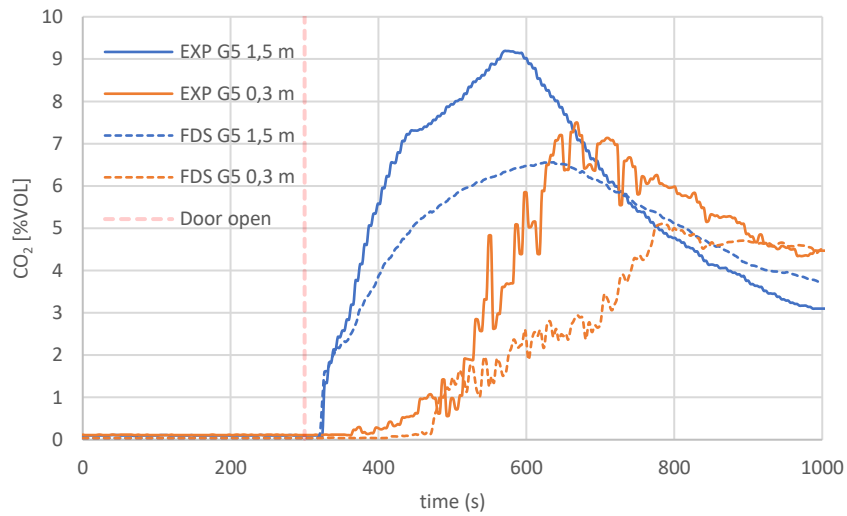
O<sub>2</sub> in corridor (G5)



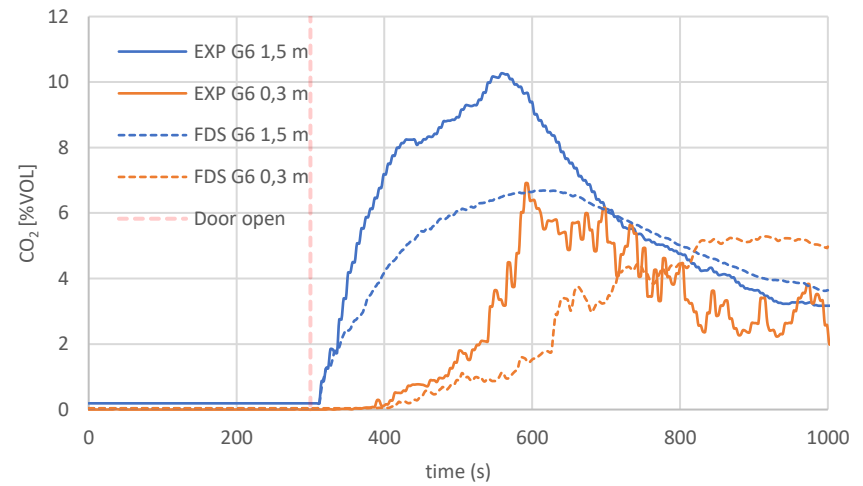
O<sub>2</sub> in corridor (G6)



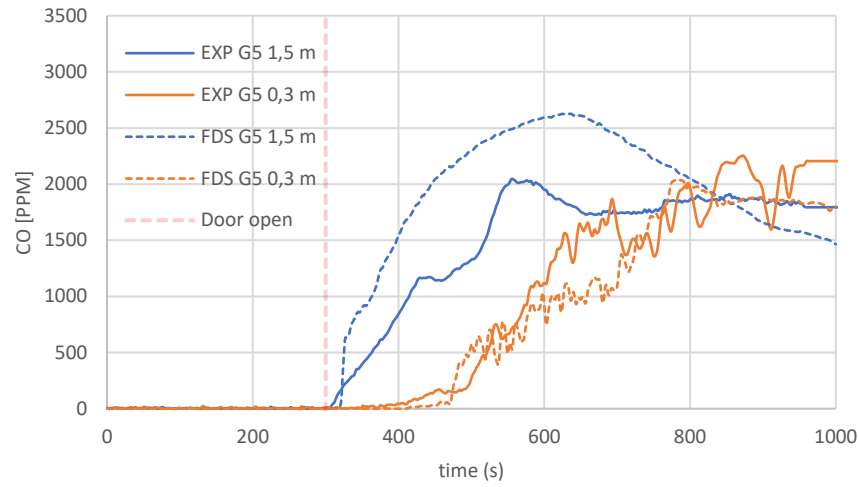
CO<sub>2</sub> in corridor (G5)



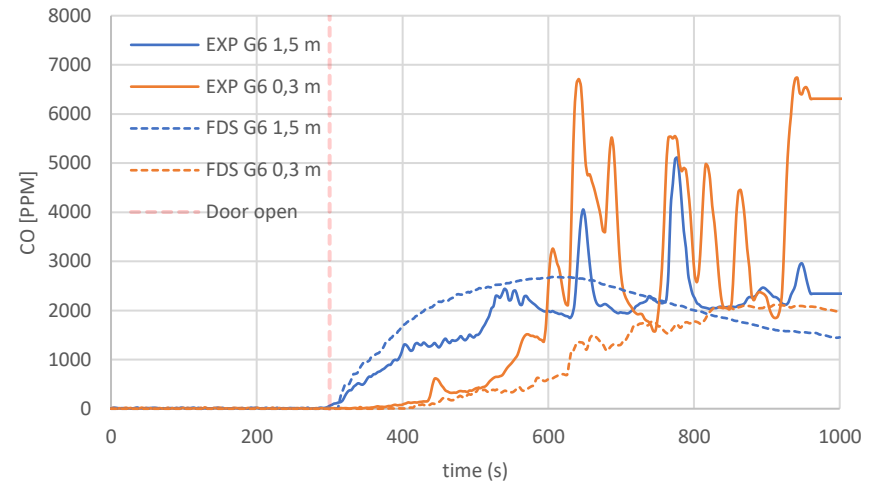
CO<sub>2</sub> in corridor (G6)



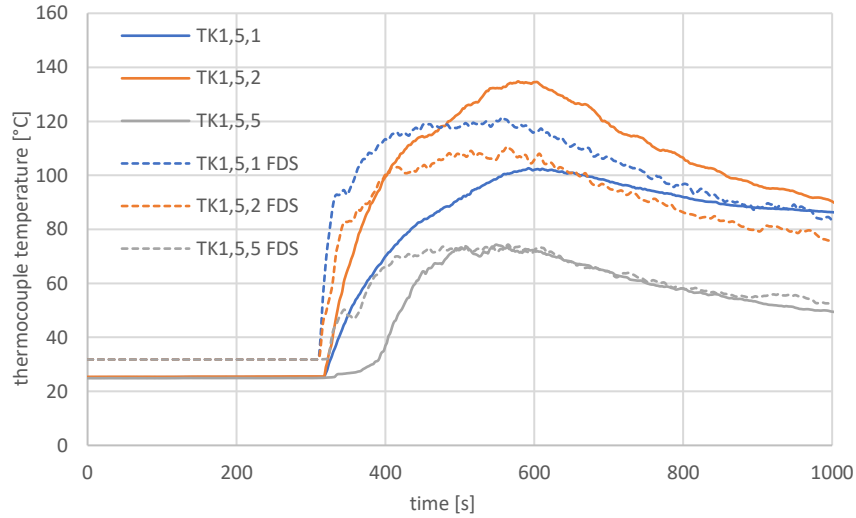
CO in corridor (G5)



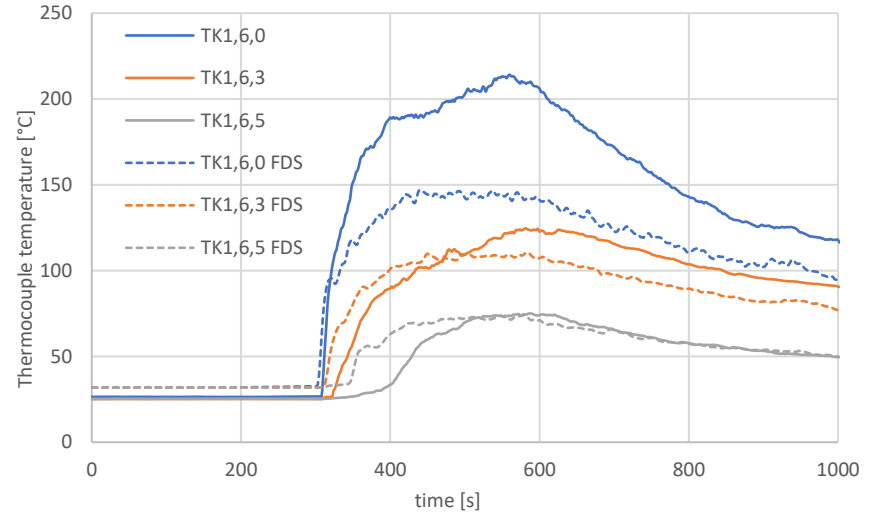
CO in corridor (G6)



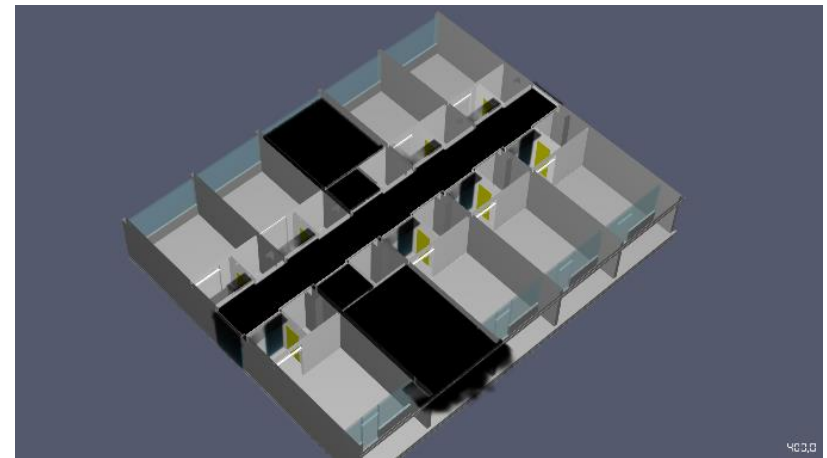
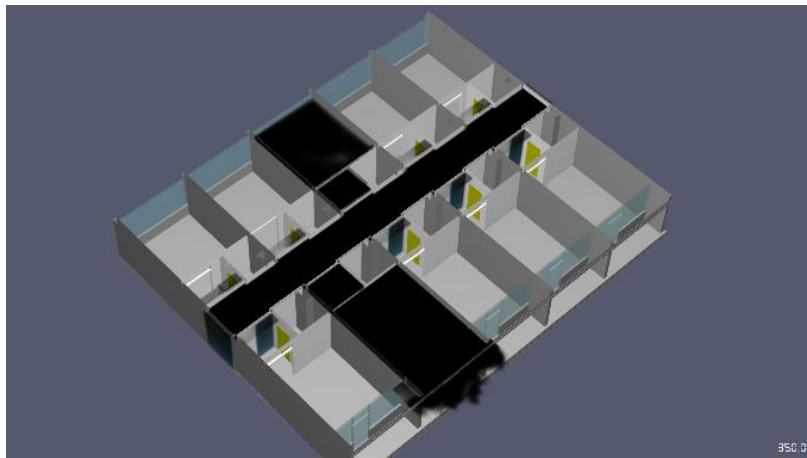
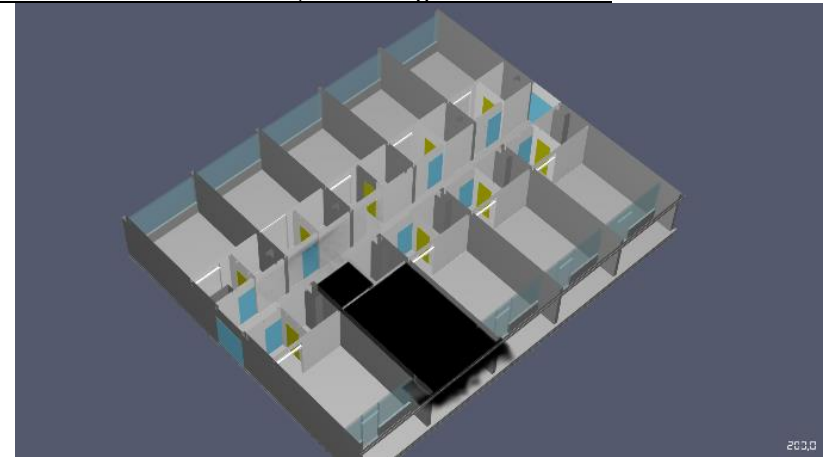
Temperatures in corridor (B5)



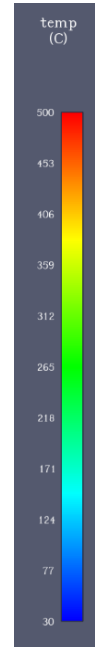
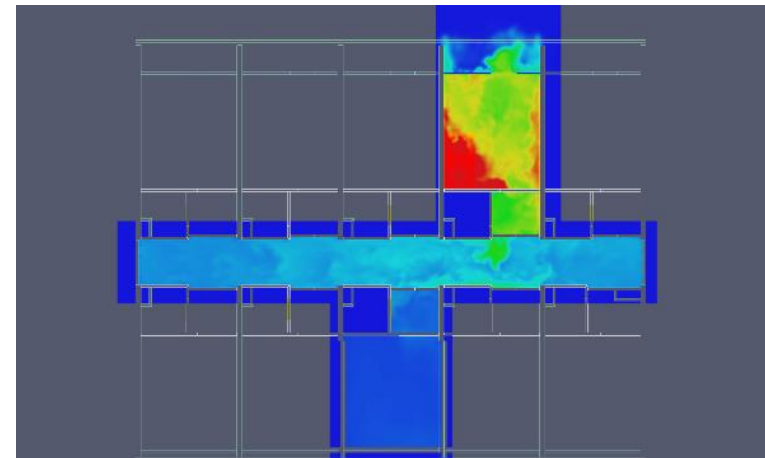
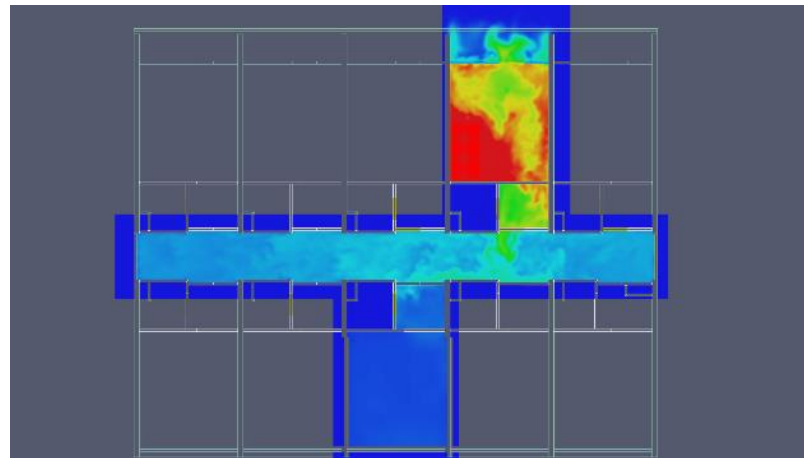
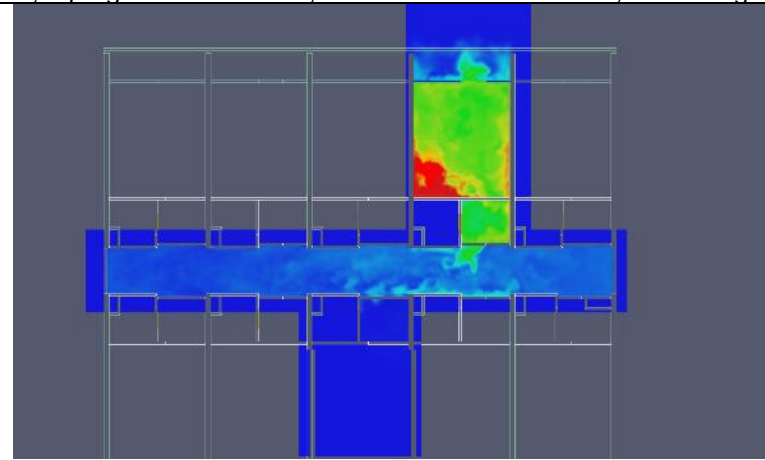
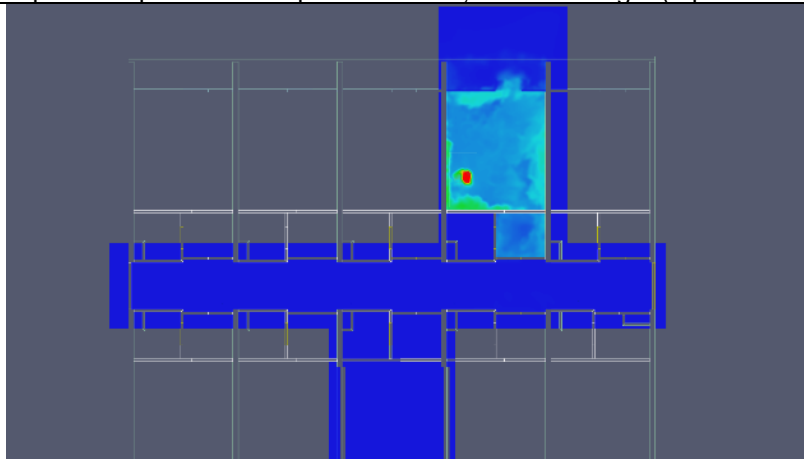
Temperatures in corridor (B6)



Graphical depiction of smoke spread (top left: 50 seconds, top right: 200 seconds, bottom left: 350 seconds, bottom right 400 seconds)



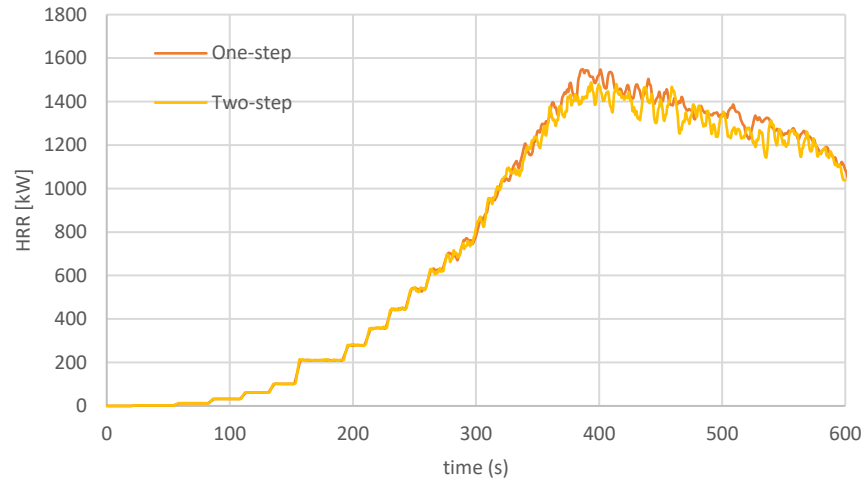
Graphical depiction of temperatures at 1,8 meters height (top left: 160 seconds, top right: 320 seconds, bottom left: 480 seconds, bottom right 600 seconds)



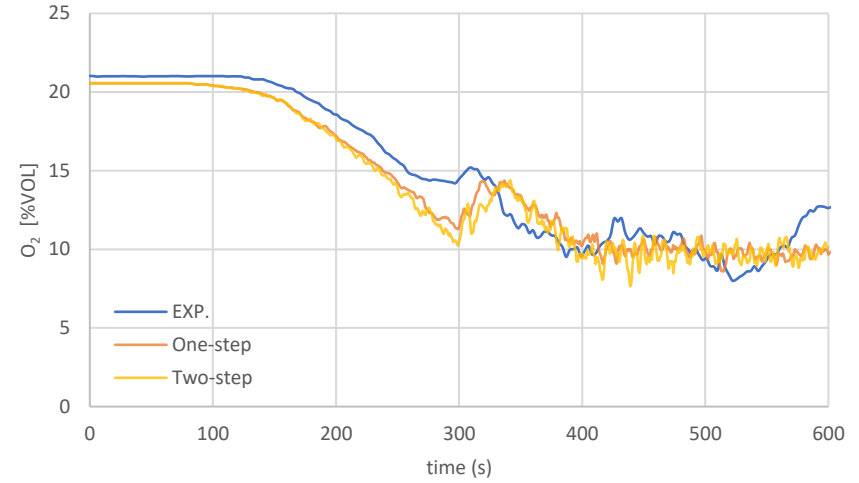
### Case study 1: sensitivity study

Two step combustion model

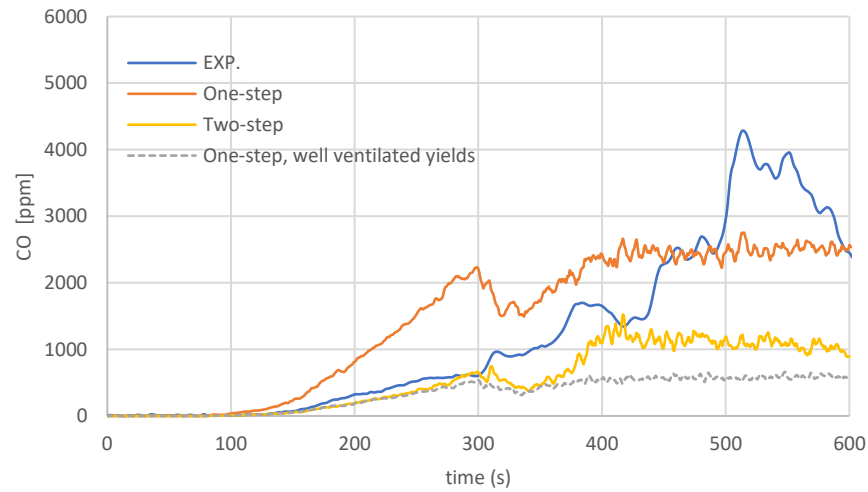
#### Heat Release Rate



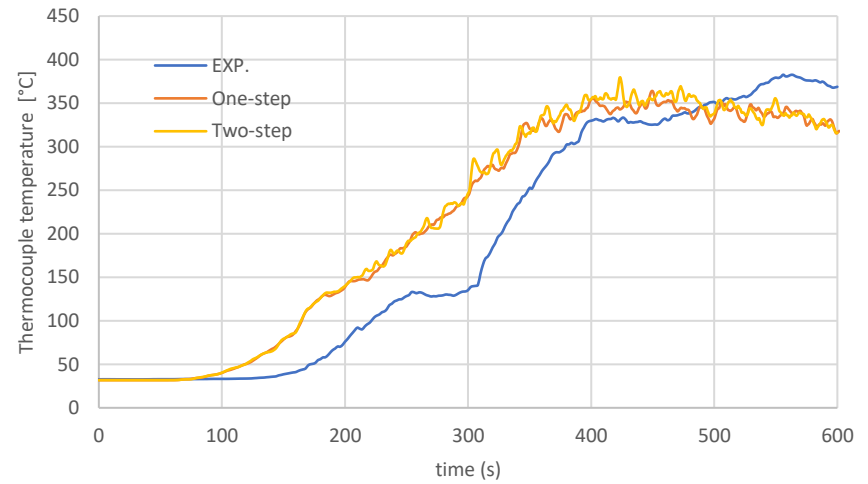
#### O<sub>2</sub> concentration in the apartment (1.5 meters)



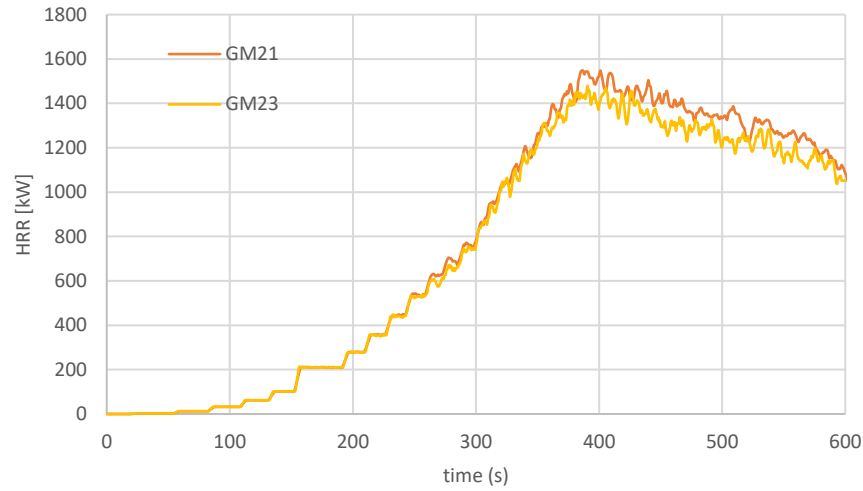
#### CO concentration in the apartment



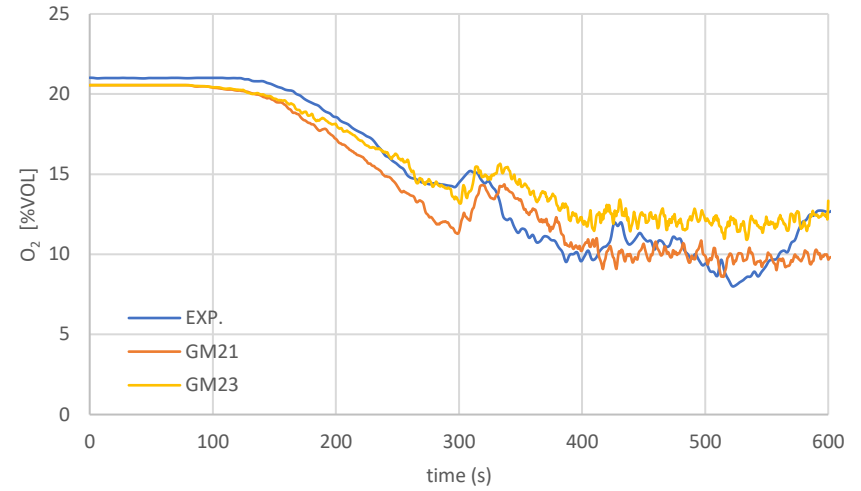
#### Temperature in the apartment (TK1.1.2)



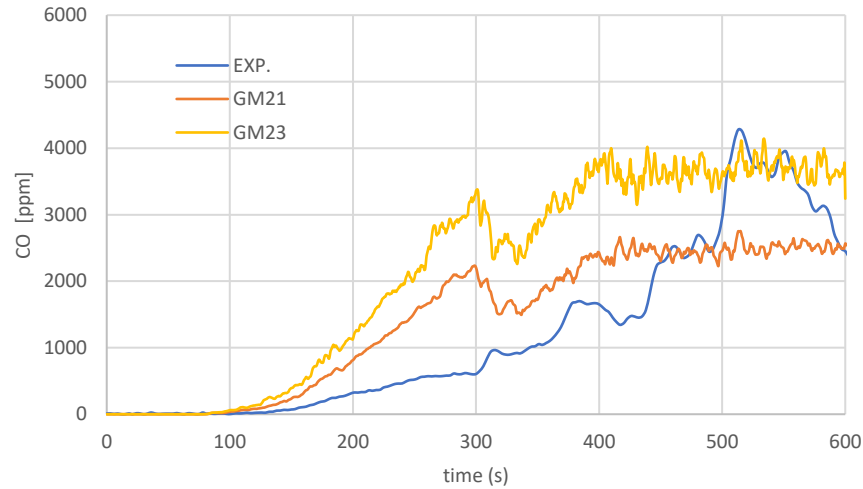
**Polyurethane GM23**  
**Heat Release Rate**



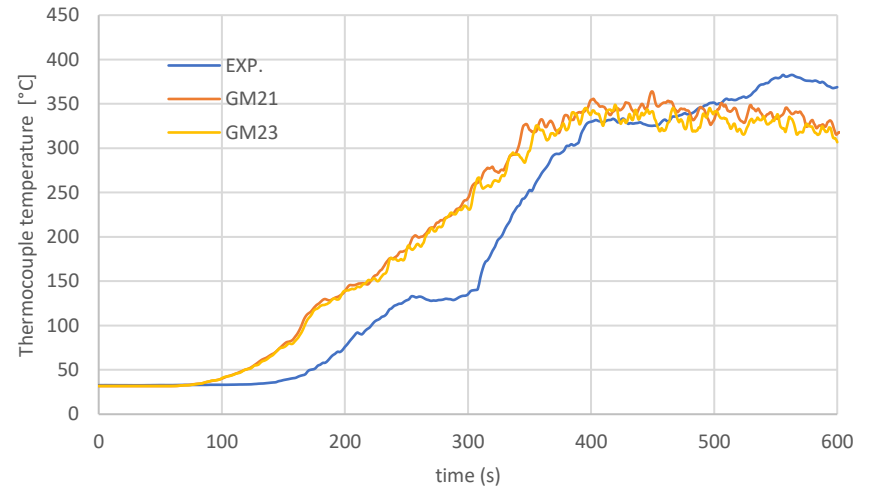
**O<sub>2</sub> concentration in the apartment (1.5 meters)**



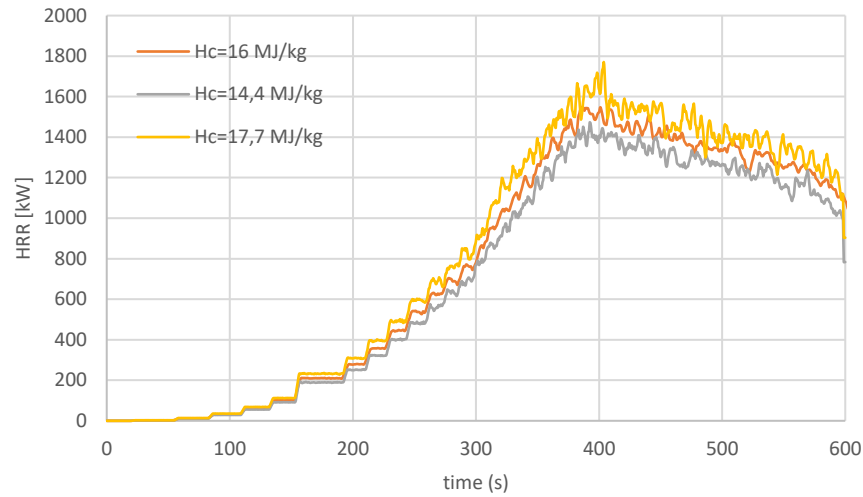
**CO concentration in the apartment**



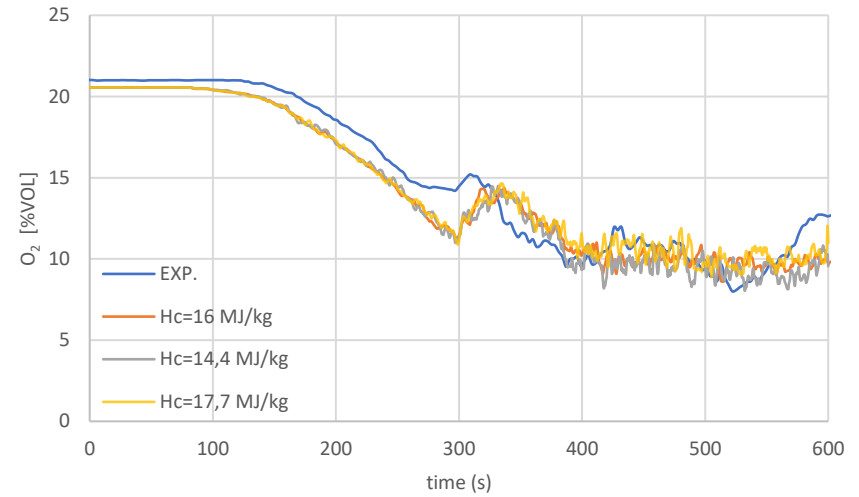
**Temperature in the apartment (TK1.1.2)**



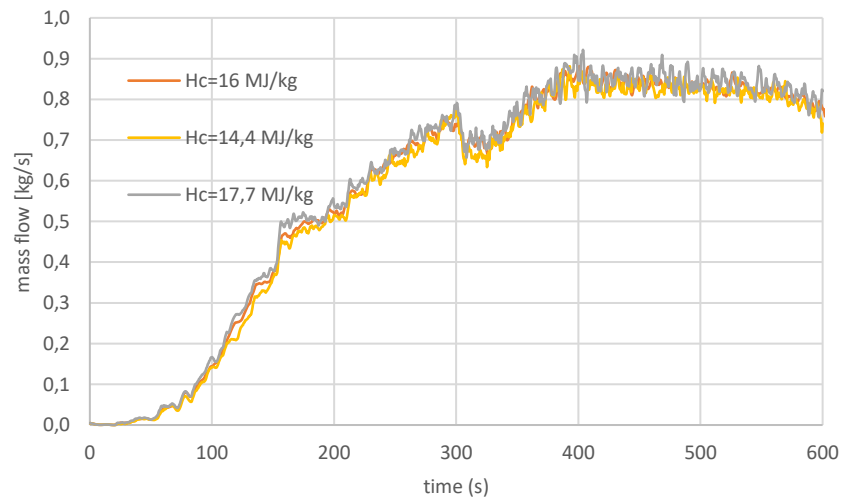
**Effective heat of combustion  
Heat Release Rate**



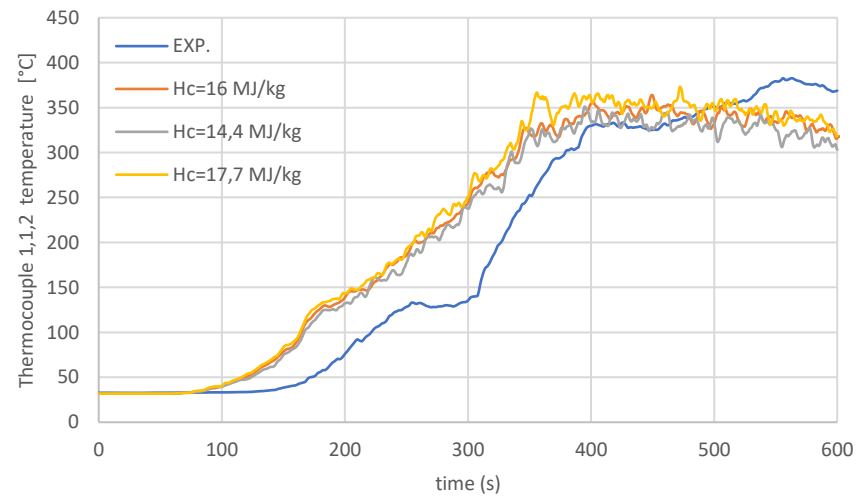
**O<sub>2</sub> concentration in the apartment (1.5 meters)**



**Mass flow over the balcony door**

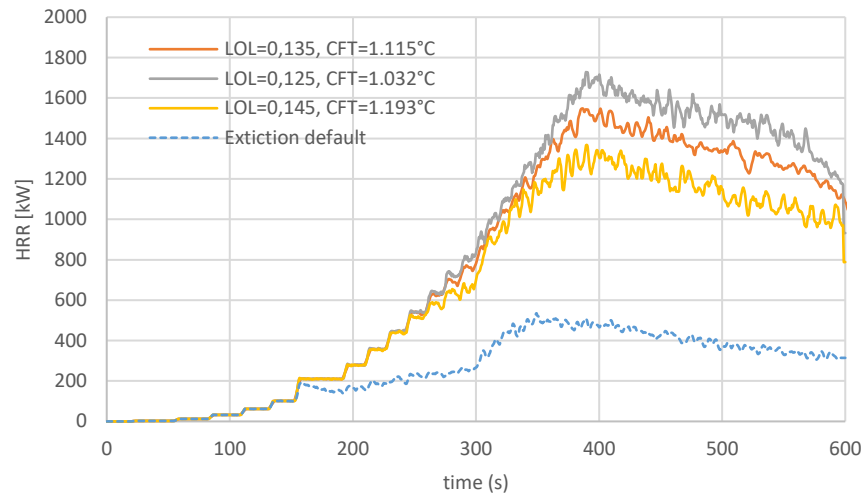


**Temperature in the apartment (TK1.1.2)**

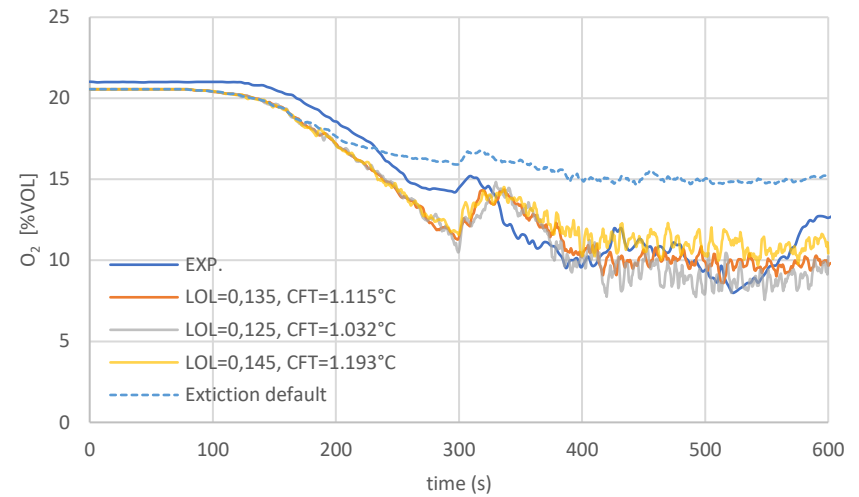


**Extinction parameters**

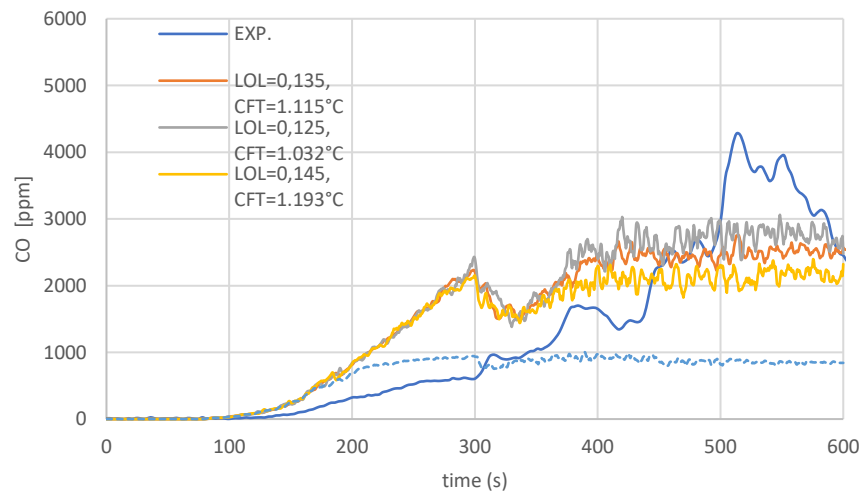
**Heat Release Rate**



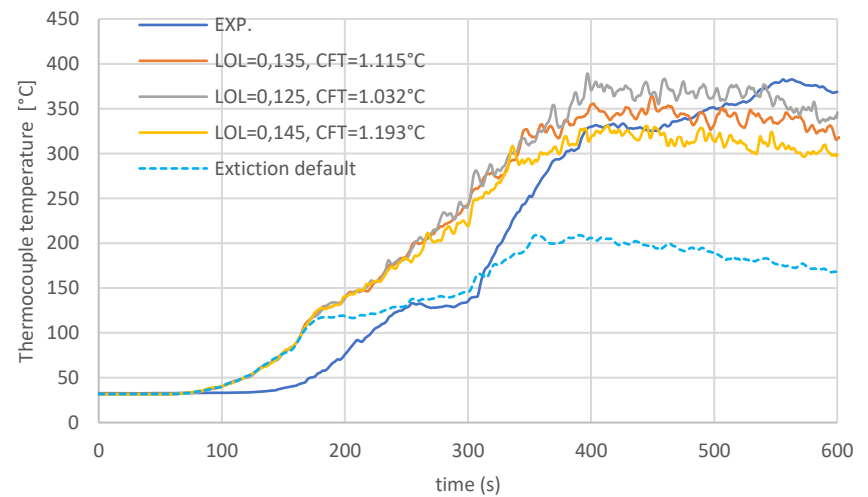
**O<sub>2</sub> concentration in the apartment (1.5 meters)**



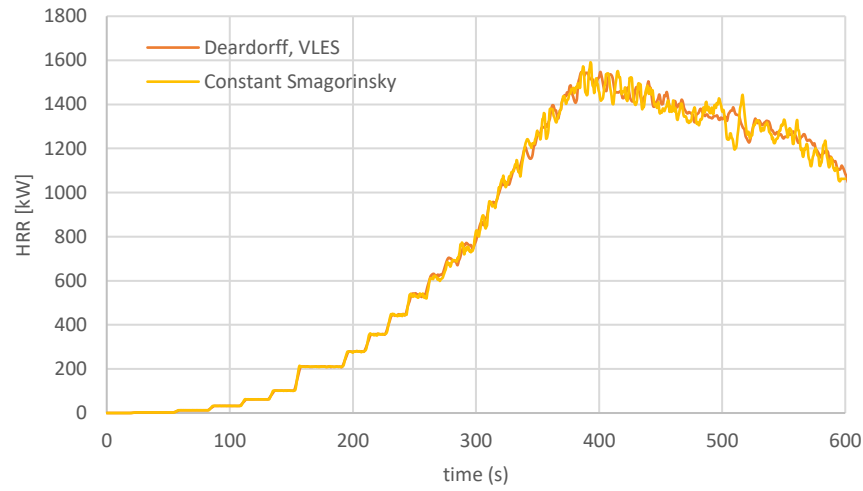
**CO concentration in the apartment**



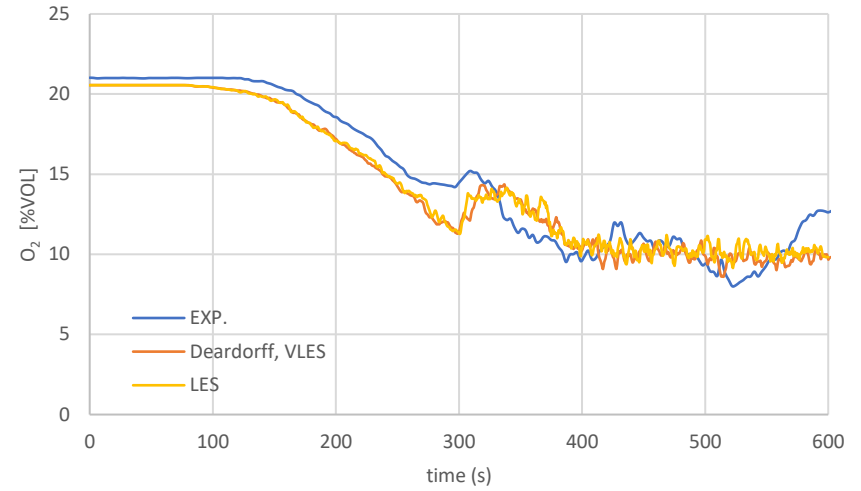
**Temperature in the apartment (TK1.1.2)**



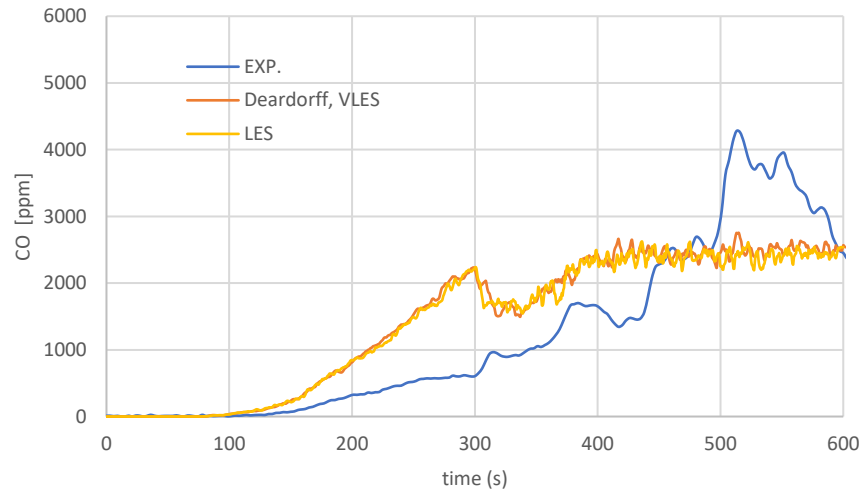
**VLES and LES**  
**Heat Release Rate**



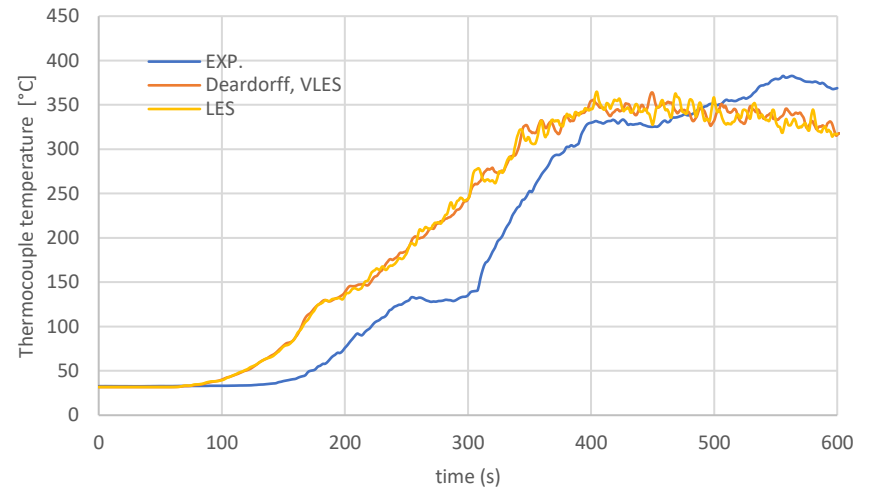
**O<sub>2</sub> concentration in the apartment (1.5 meters)**



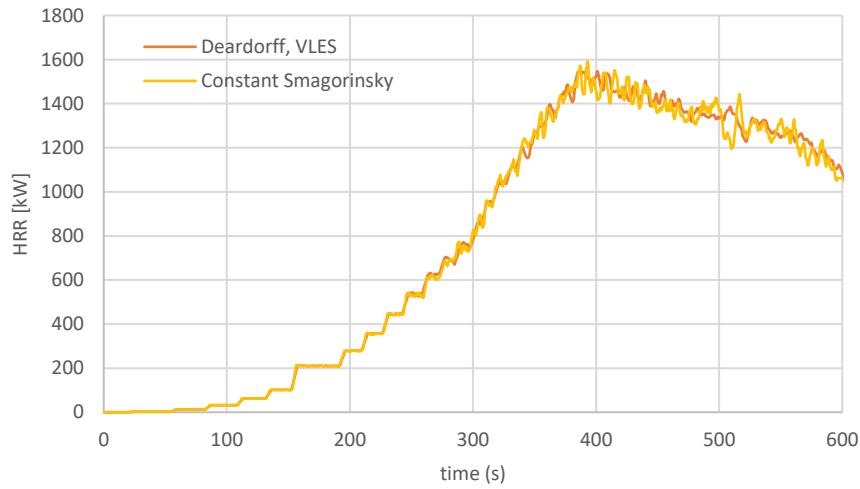
**CO concentration in the apartment**



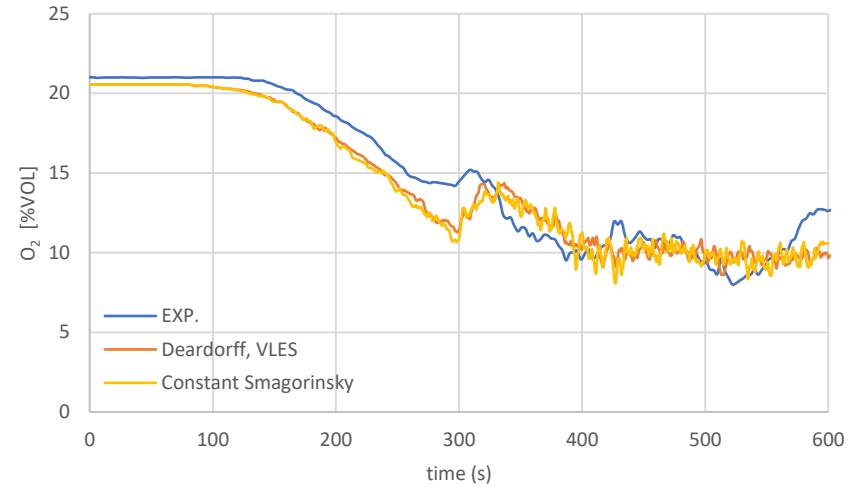
**Temperature in the apartment (TK1.1.2)**



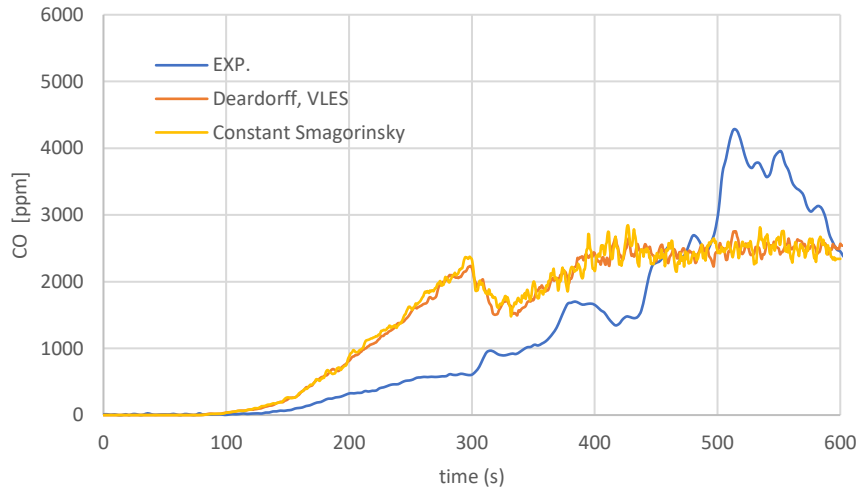
**Constant Smagorinsky and Deardorff's model for SGS turbulence**  
**Heat Release Rate**



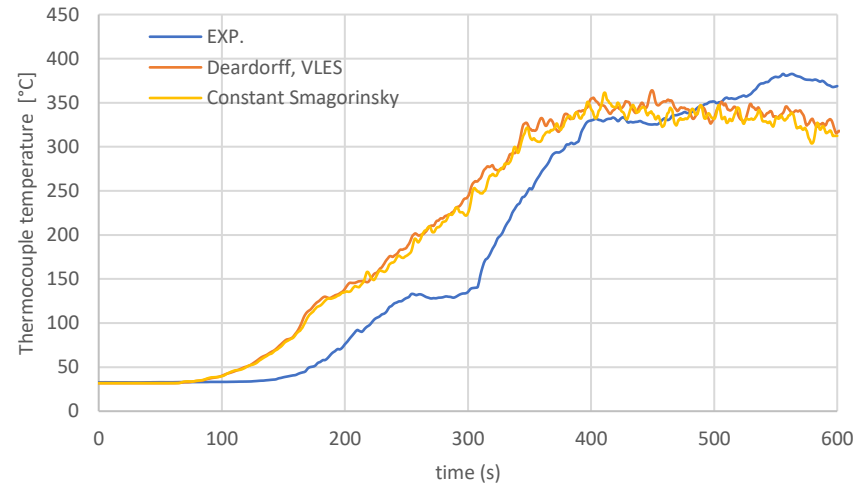
**O<sub>2</sub> concentration in the apartment (1.5 meters)**



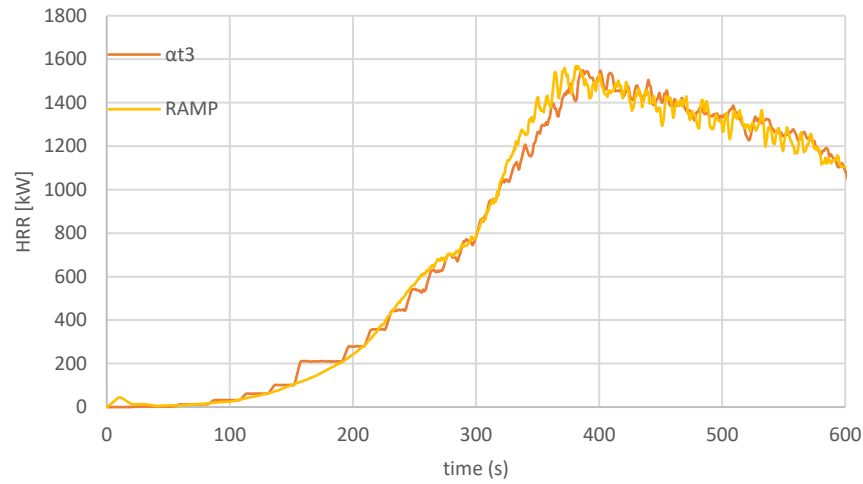
**CO concentration in the apartment**



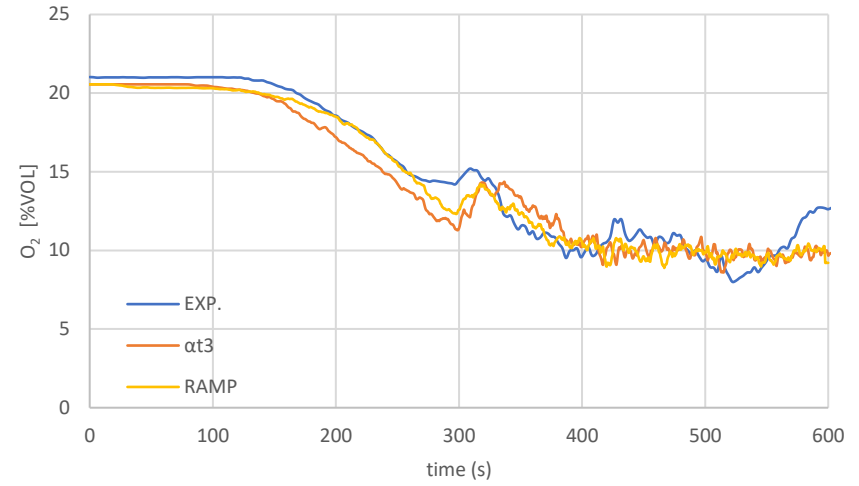
**Temperature in the apartment (TK1.1.2)**



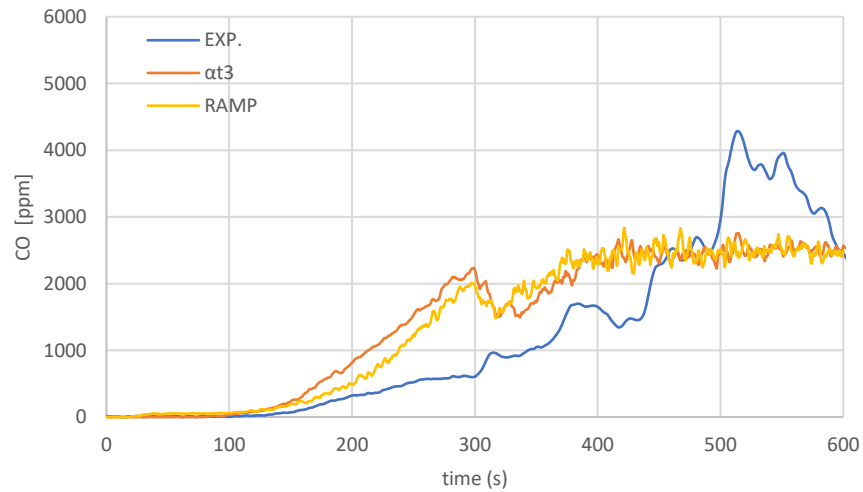
*Fire growth modelling*  
Heat Release Rate



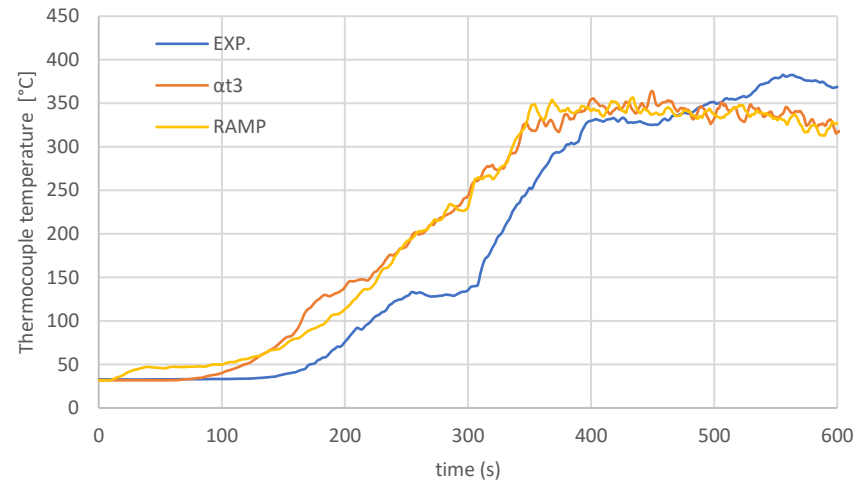
O<sub>2</sub> concentration in the apartment (1.5 meters)



CO concentration in the apartment

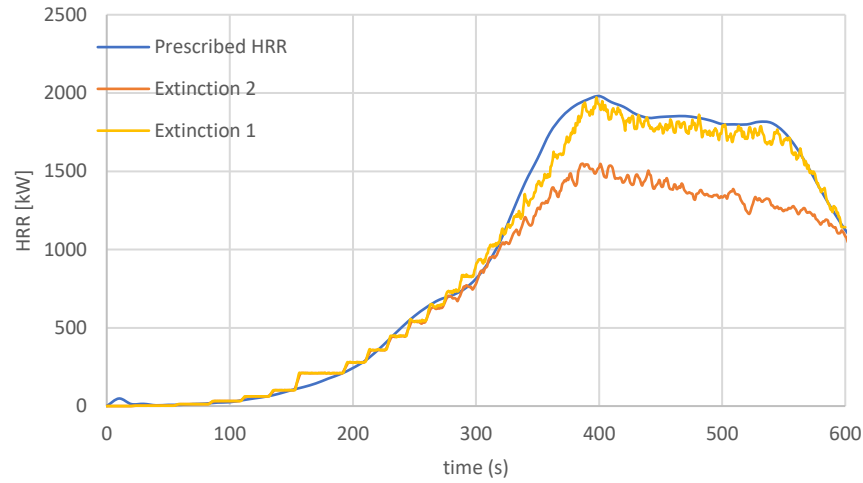


Temperature in the apartment (TK1.1.2)

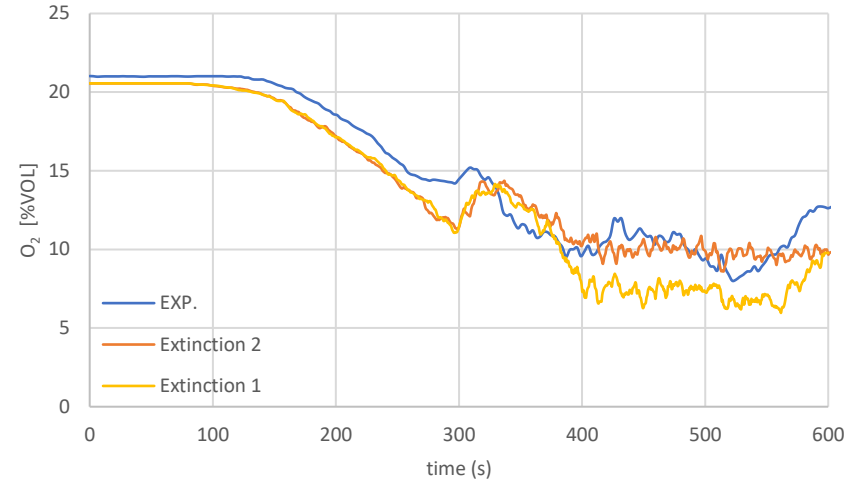


*Extinction model 1 and 2*

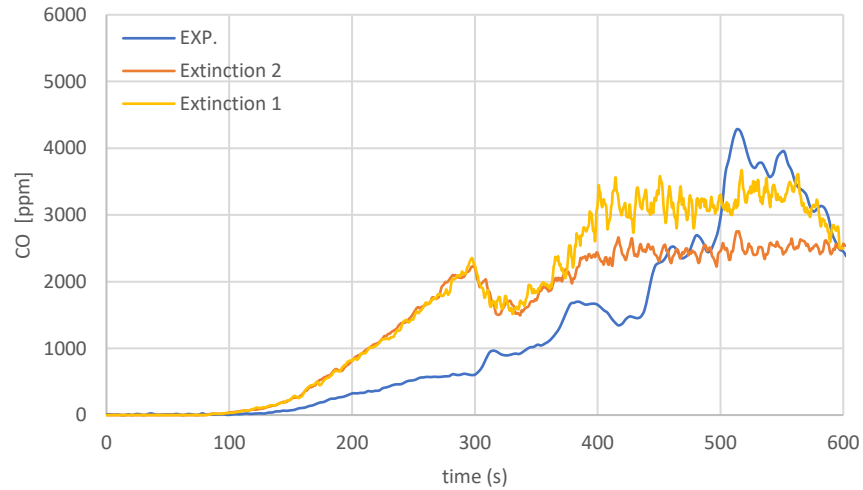
Heat Release Rate



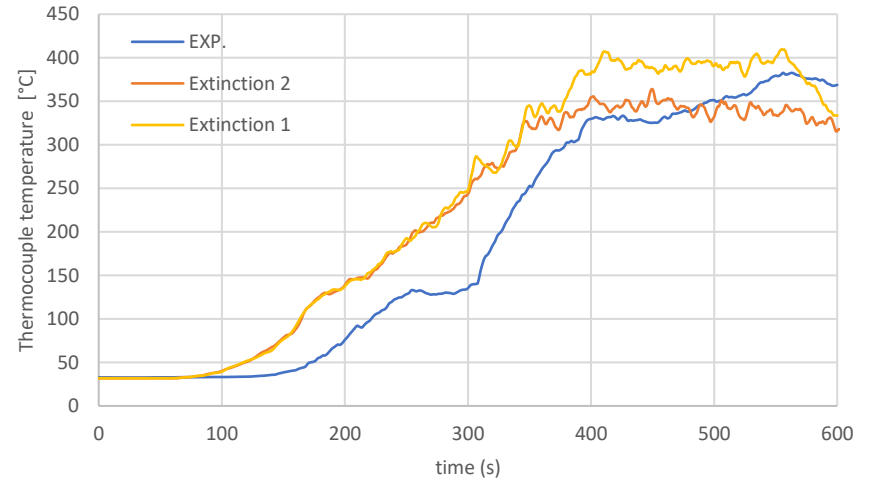
O<sub>2</sub> concentration in the apartment (1.5 meters)



CO concentration in the apartment

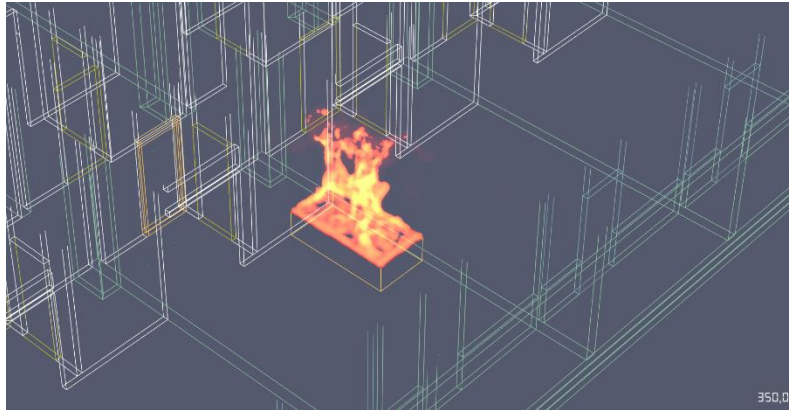


Temperature in the apartment (TK1.1.2)

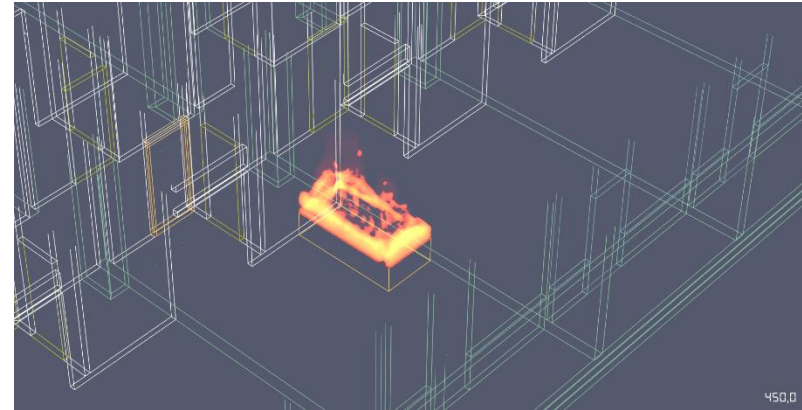


**Case study 2: door to corridor opened after 300 seconds and not closed afterwards**

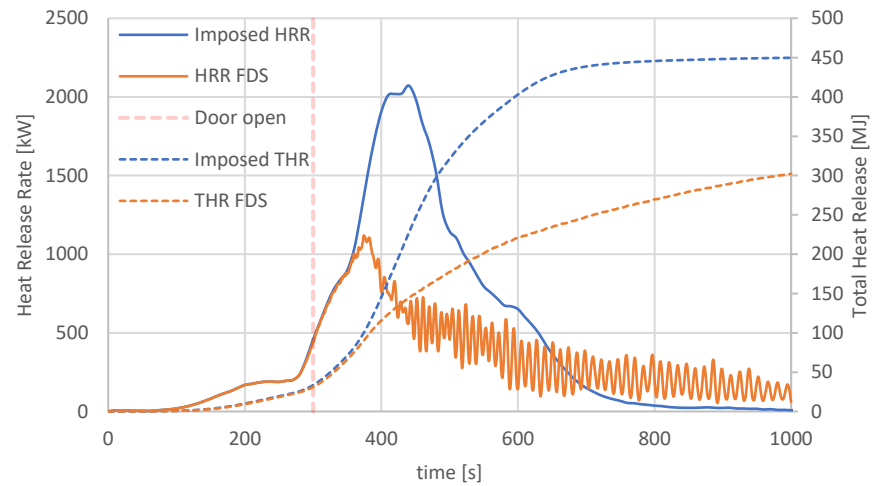
HRRPUV  
350 seconds



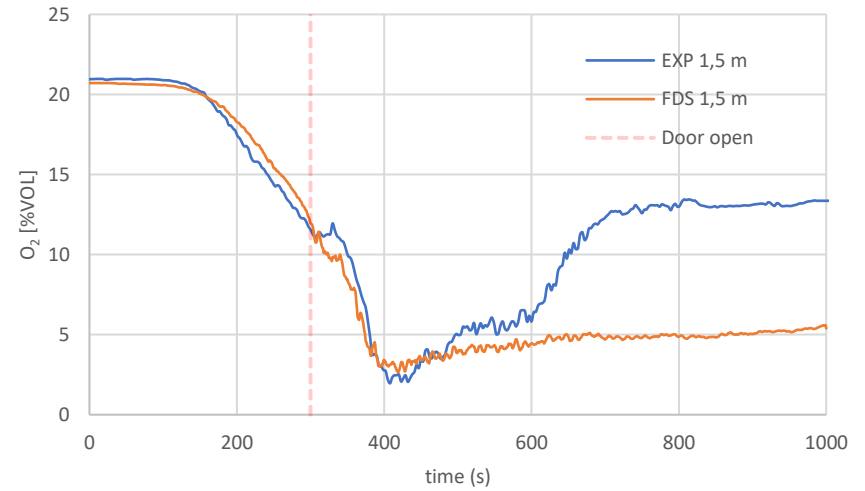
HRRPUV  
450 seconds



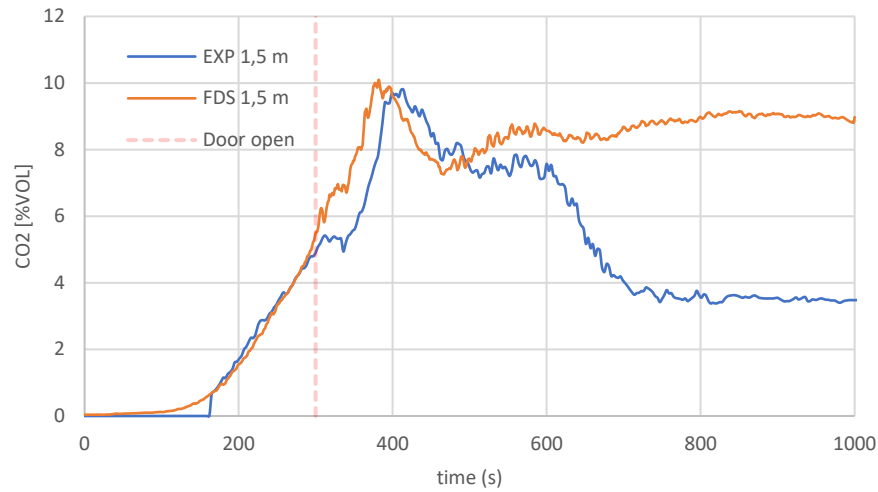
Heat Release Rate



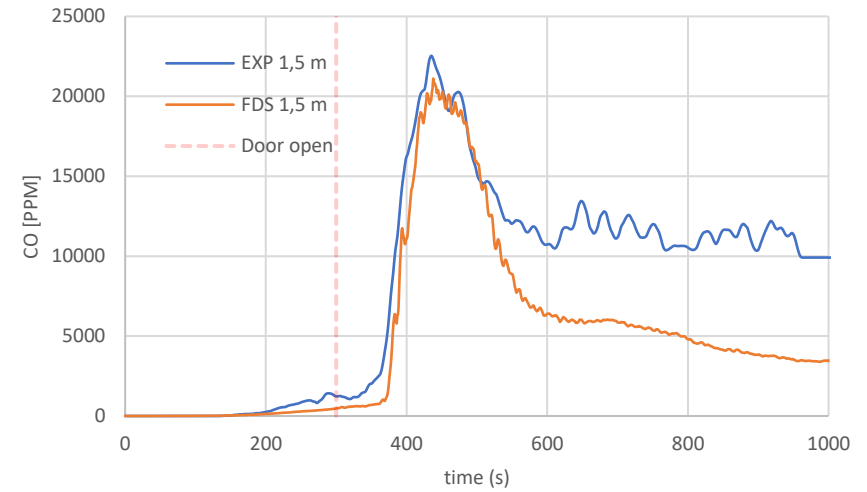
O<sub>2</sub> concentration in the apartment (1,5 meters)



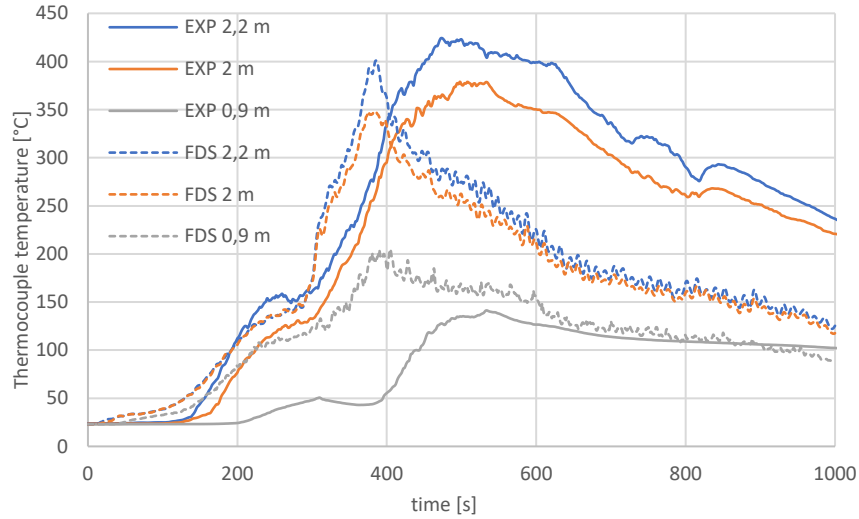
CO<sub>2</sub> concentration in the apartment



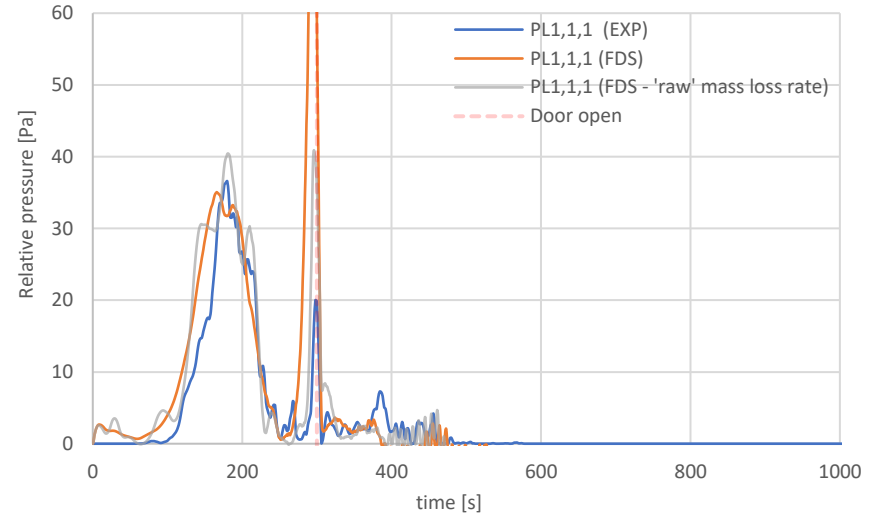
CO concentration in the apartment



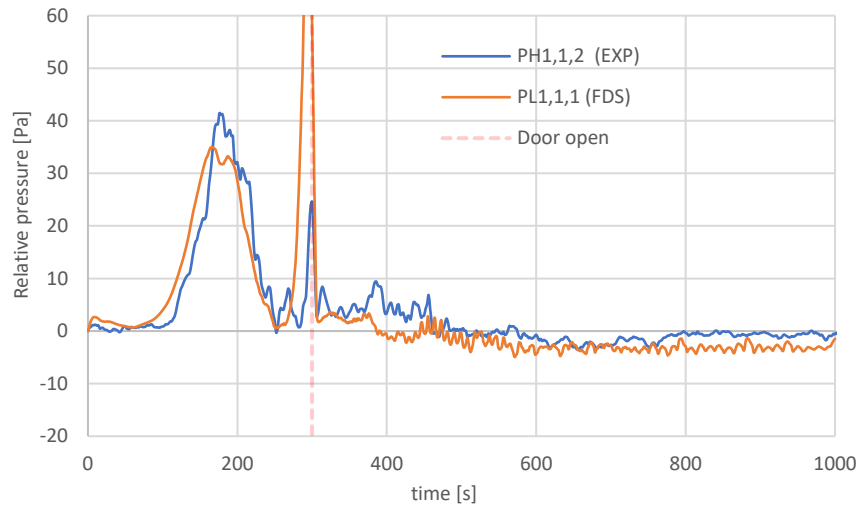
Temperatures in the apartment



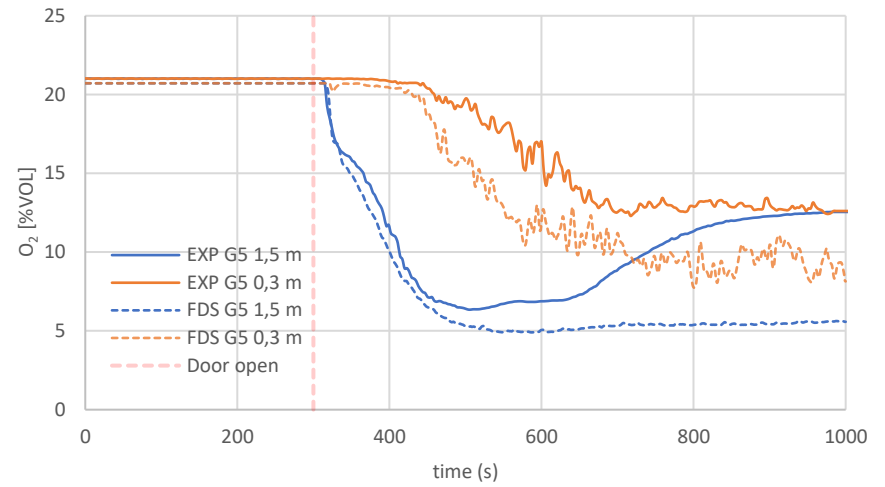
Pressure in the apartment (PL equipment)



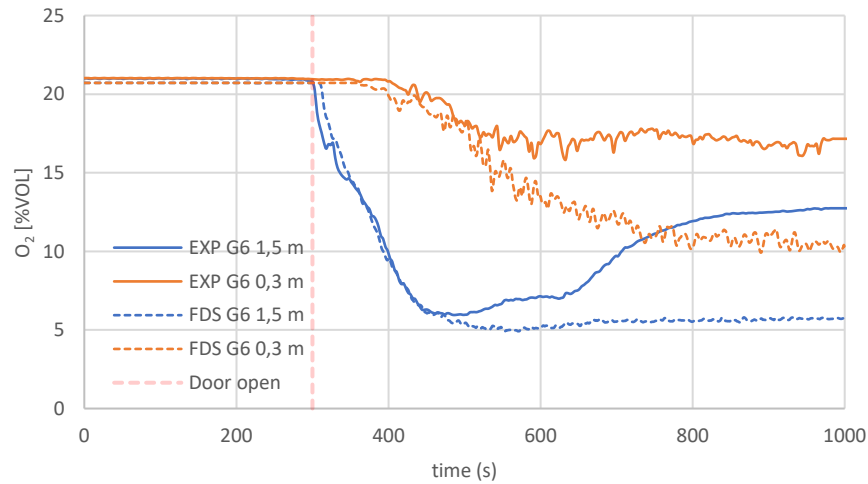
Pressure in apartment (PH equipment)



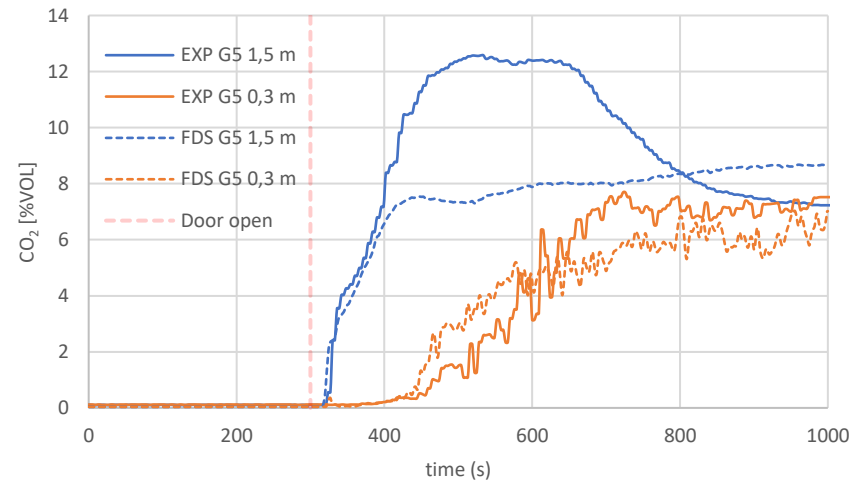
O<sub>2</sub> in corridor (G5)



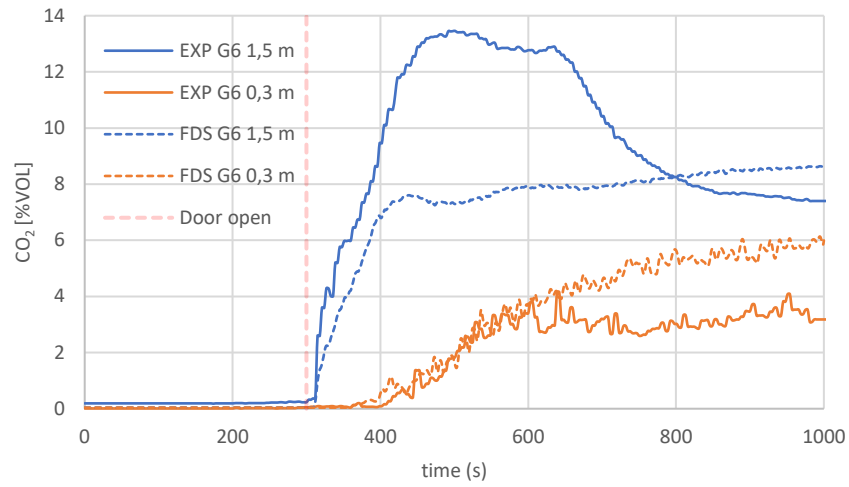
O<sub>2</sub> in corridor (G6)



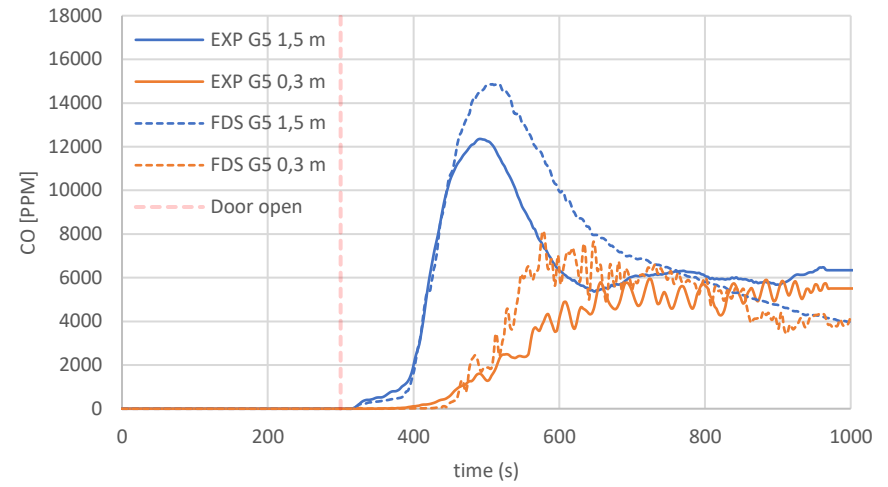
CO<sub>2</sub> in corridor (G5)



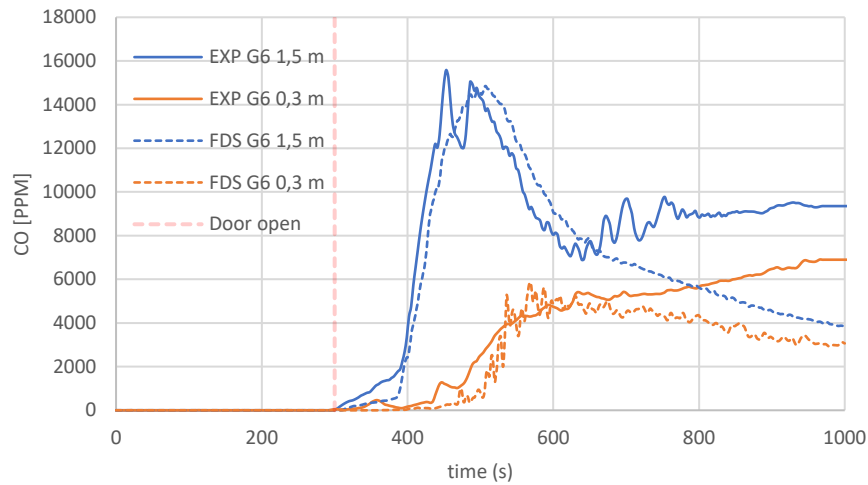
CO<sub>2</sub> in corridor (G6)



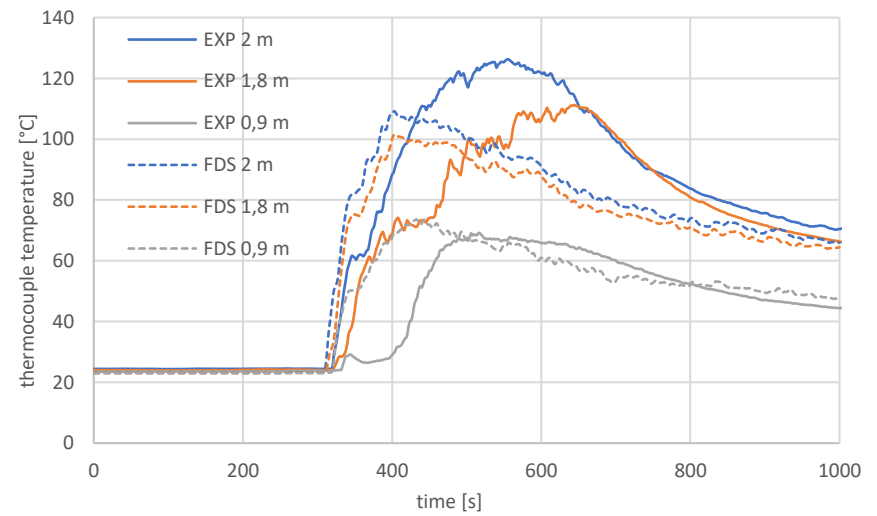
CO in corridor (G5)



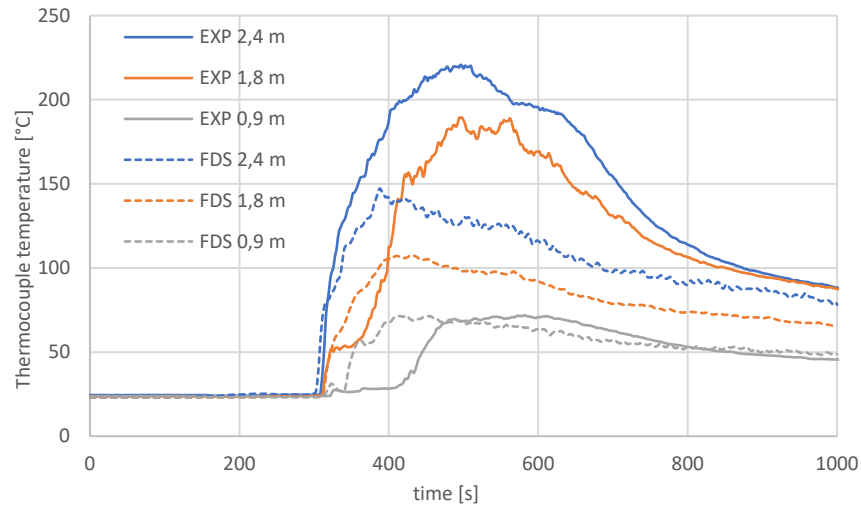
CO in corridor (G6)



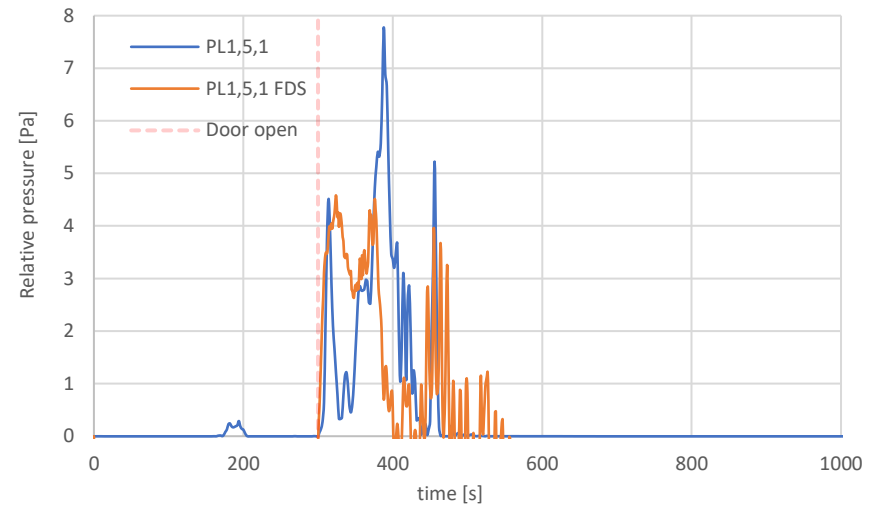
Temperatures in (B5)



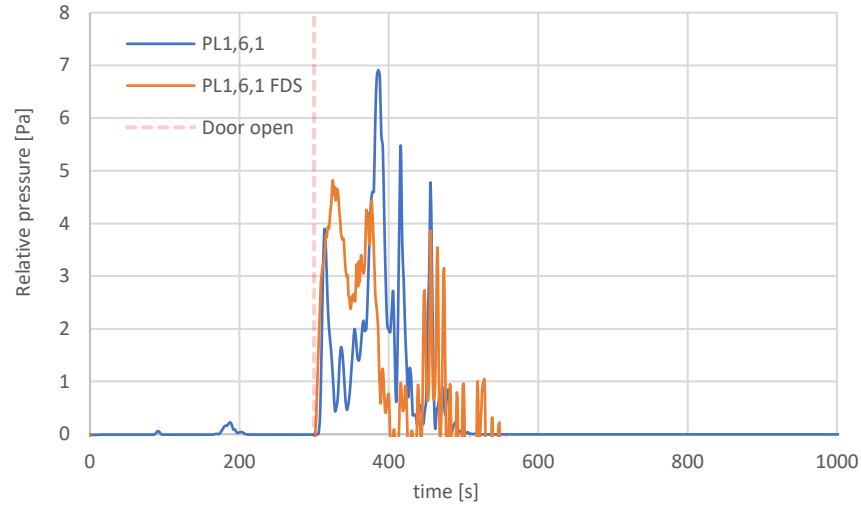
Temperatures in corridor (B6)



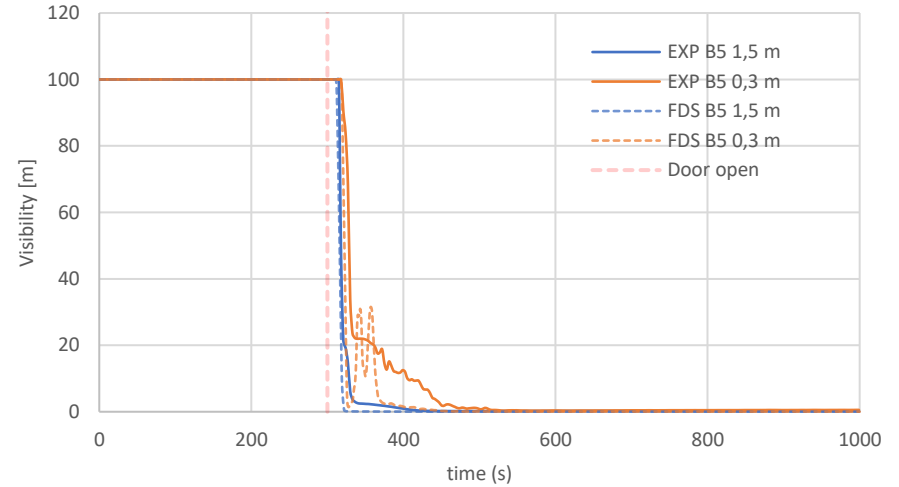
Pressure in corridor (B5)



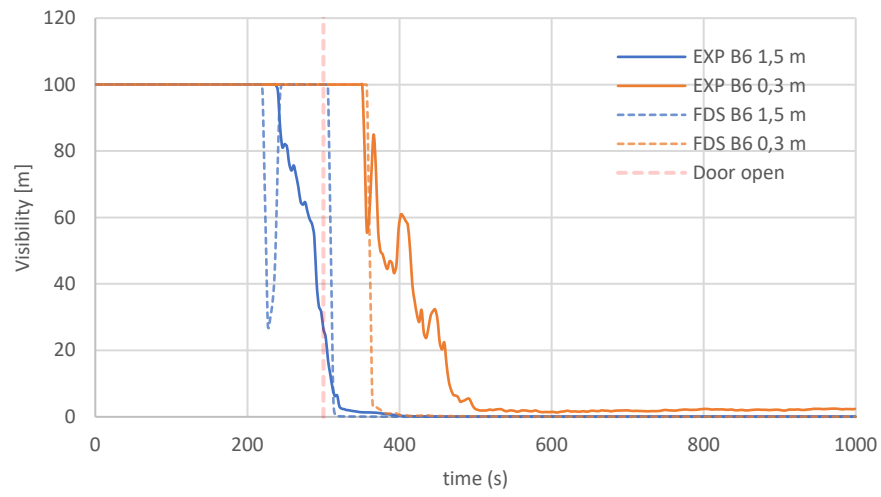
Pressure in corridor (B6)



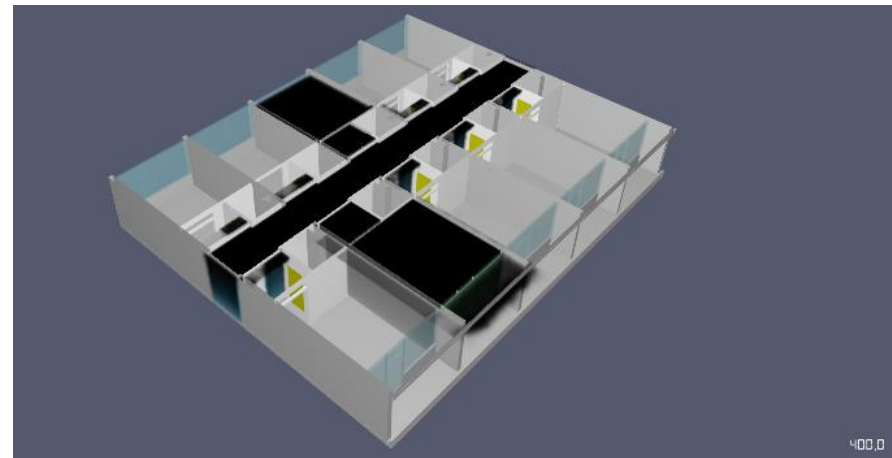
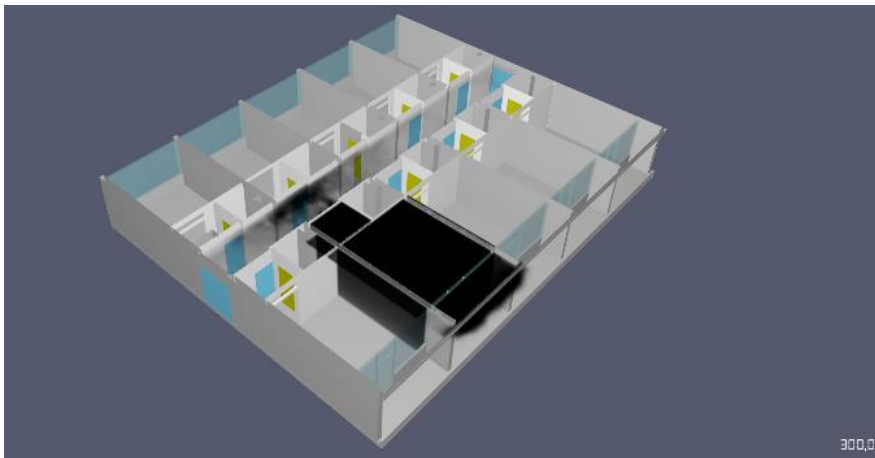
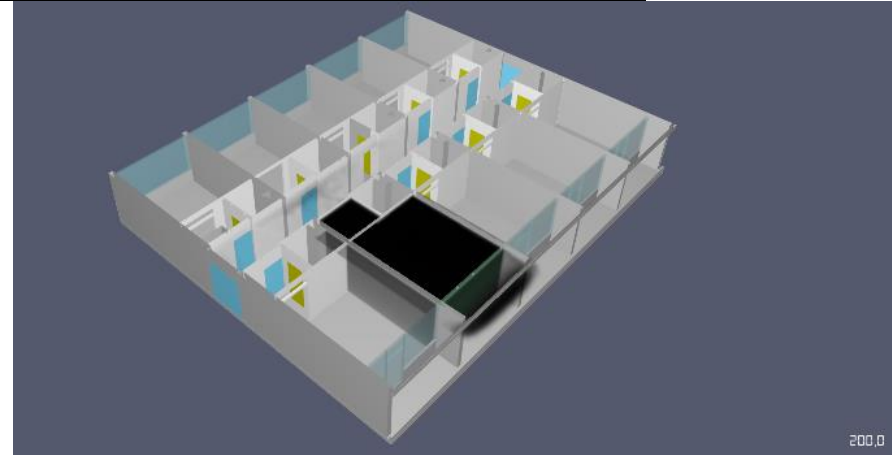
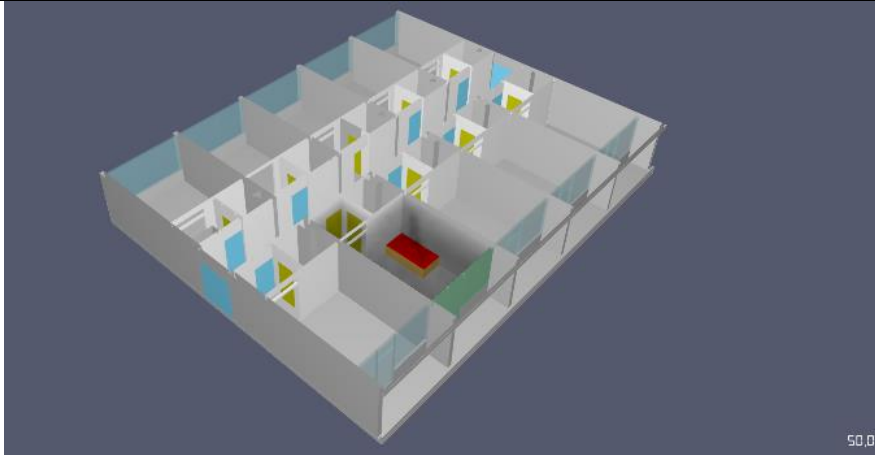
Visibility in corridor (B5)



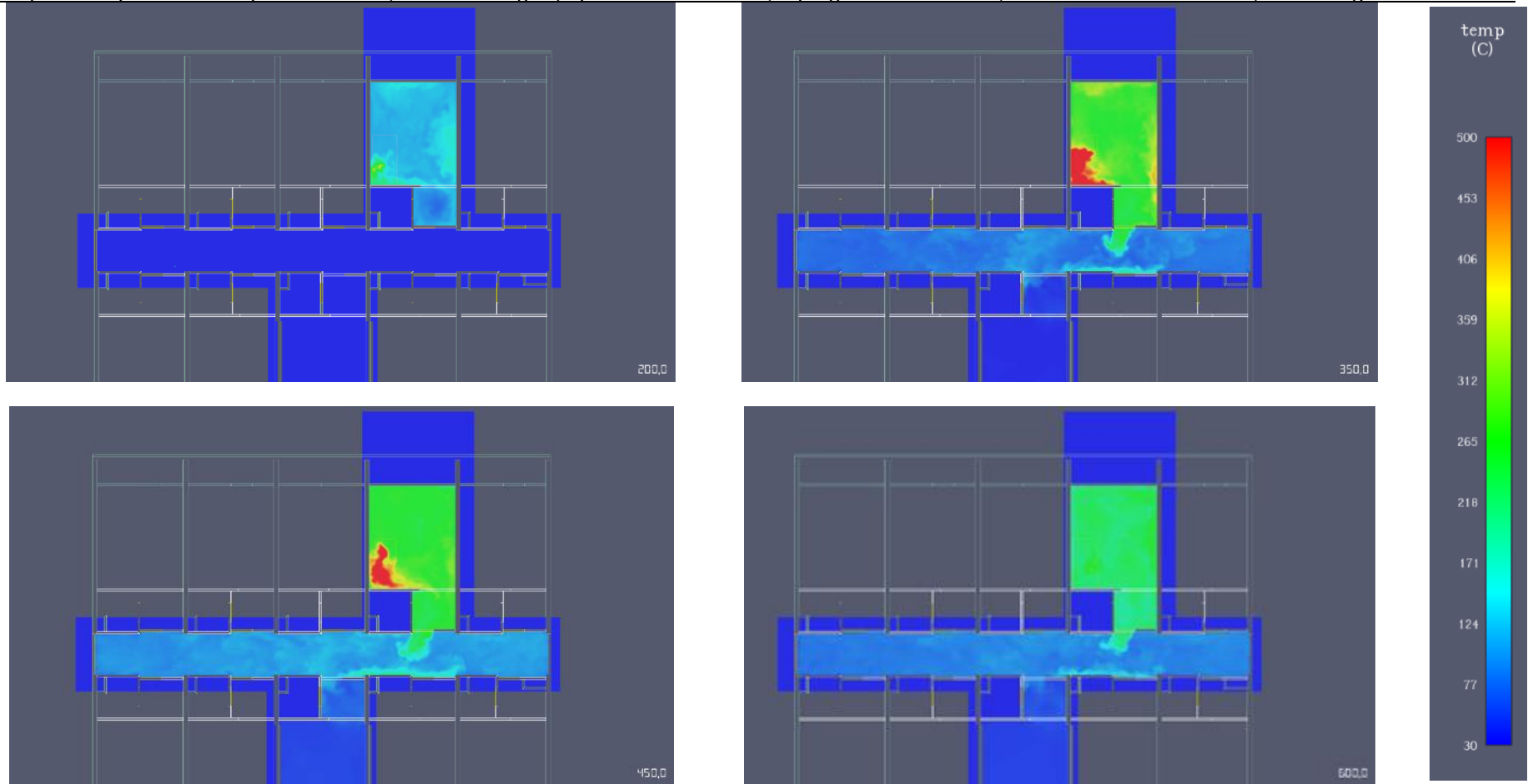
Visibility in corridor (B6)



Graphical depiction of smoke spread (top left: 50 seconds, top right: 200 seconds, bottom left: 300 seconds, bottom right 400 seconds)



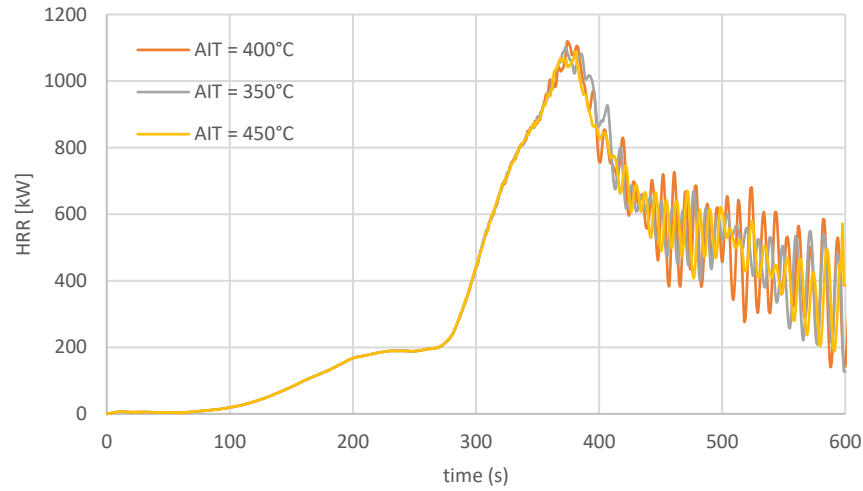
Graphical depiction of temperatures at 1,8 meters height (top left: 200 seconds, top right: 350 seconds, bottom left: 450 seconds, bottom right 600 seconds)



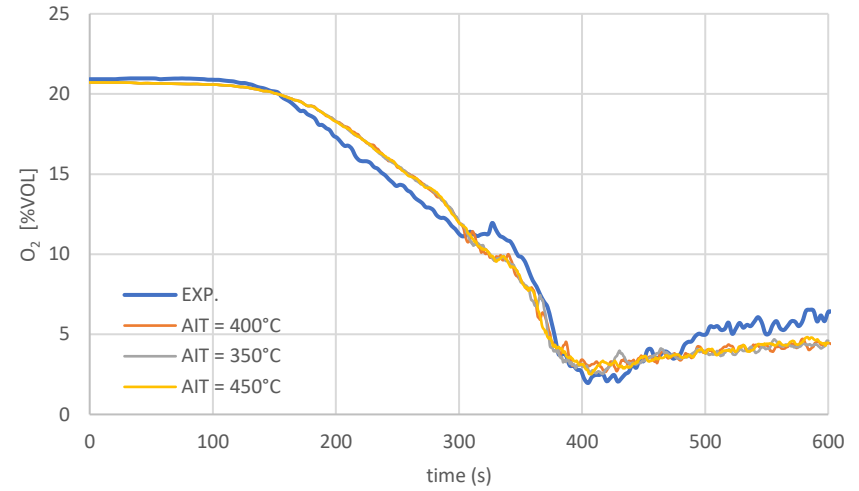
## Case study 2: sensitivity study

Auto-ignition temperature

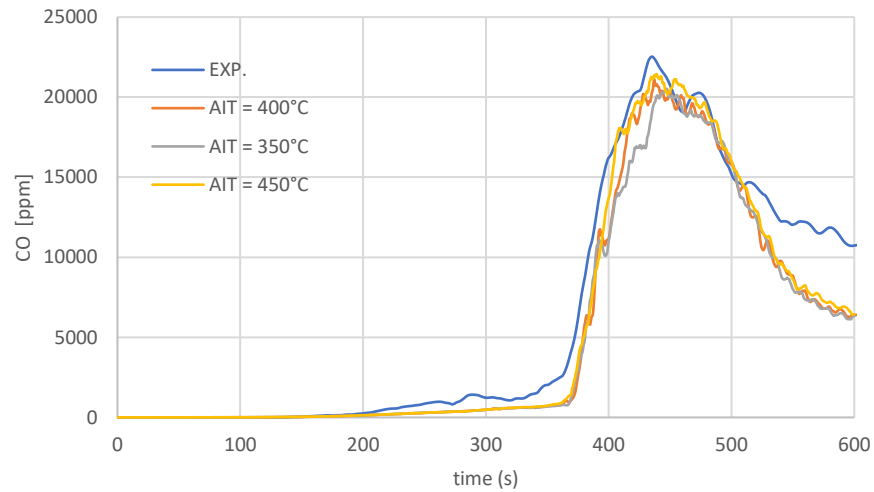
Heat Release Rate



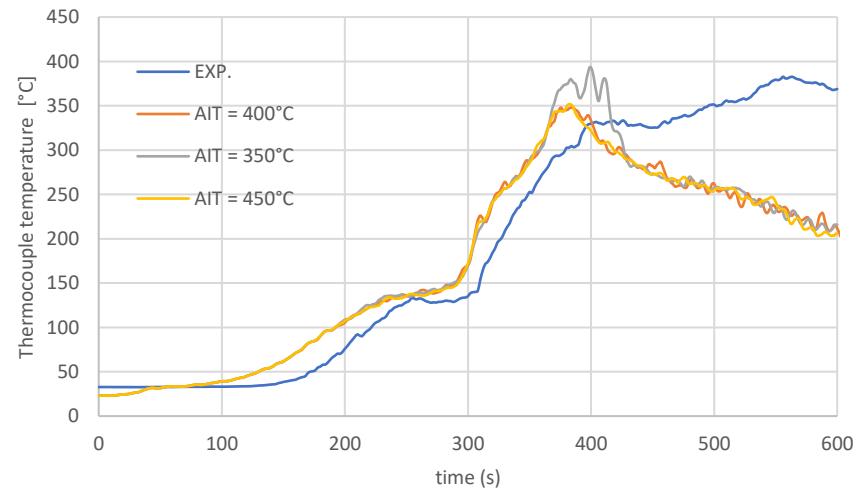
O<sub>2</sub> concentration in the apartment (1.5 meters)



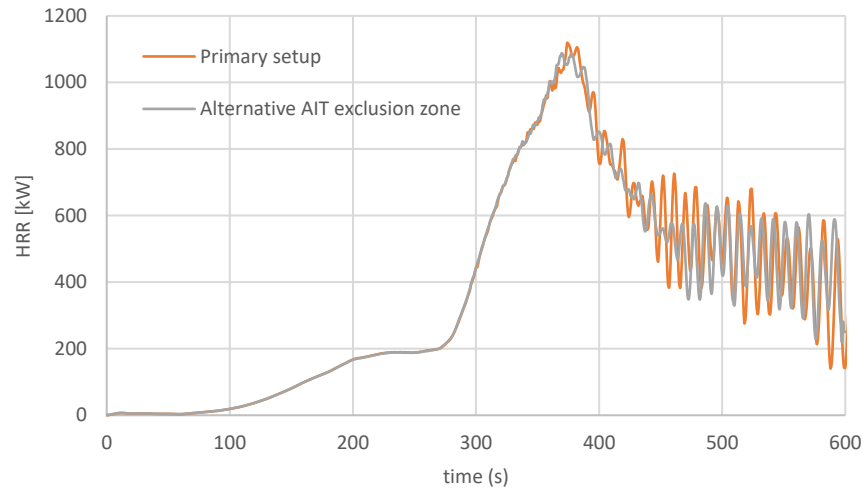
CO concentration in the apartment



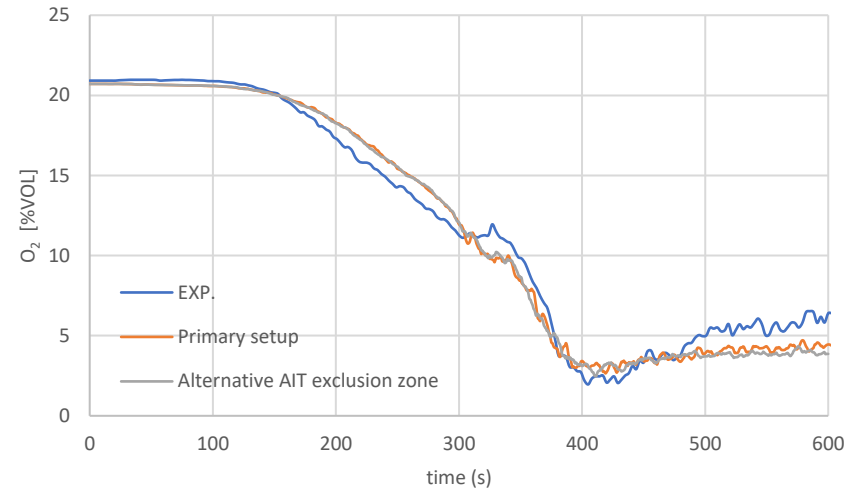
Temperature in the apartment (TK1.1.2)



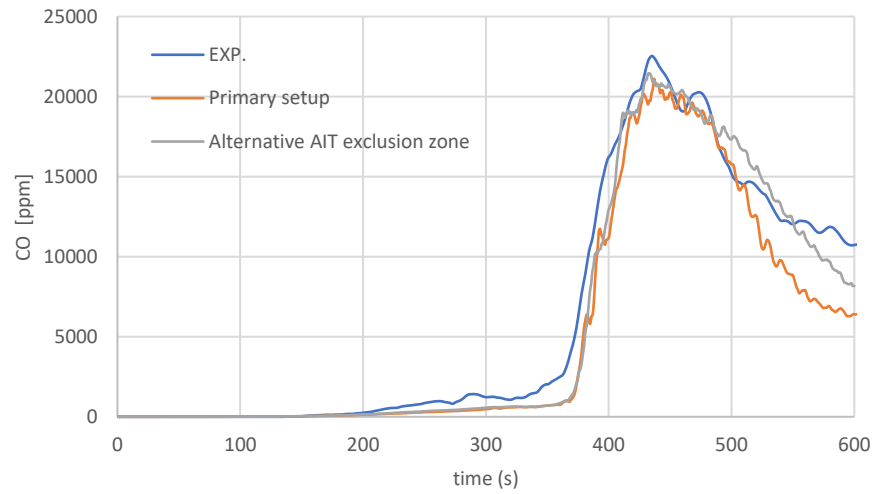
AIT exclusion zone  
Heat Release Rate



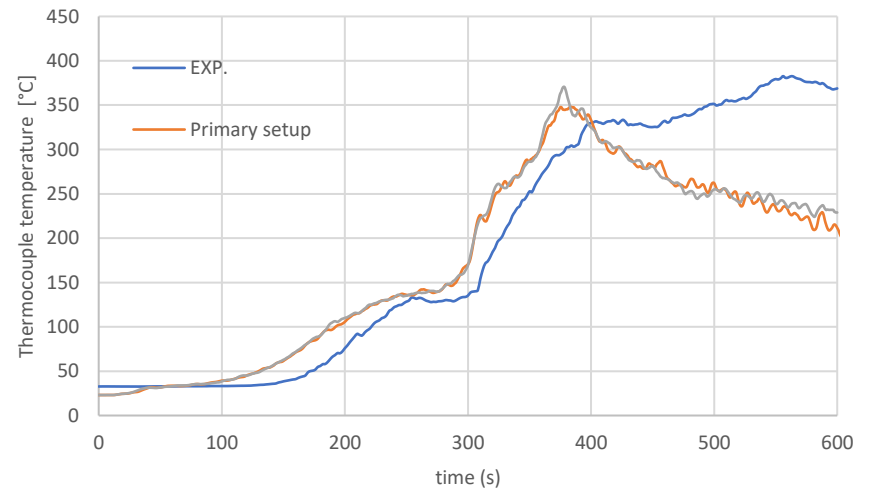
O<sub>2</sub> concentration in the apartment (1,5 meters)



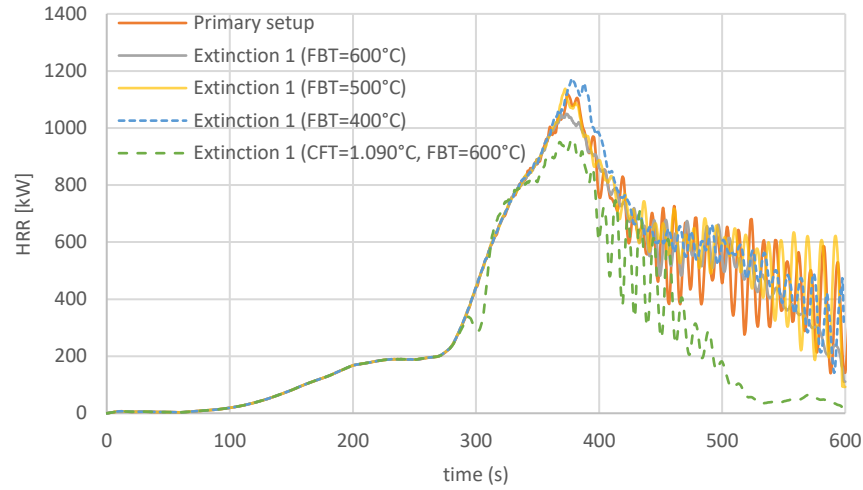
CO concentration in the apartment



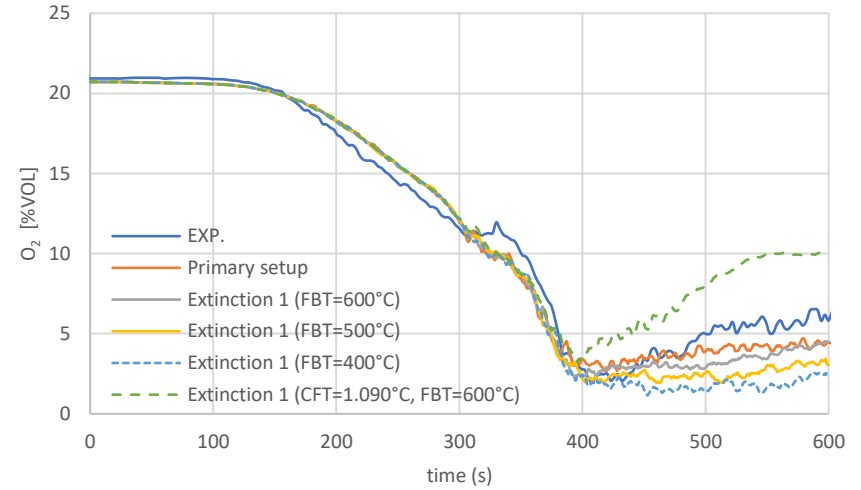
Temperature in the apartment (TK1.1.2)



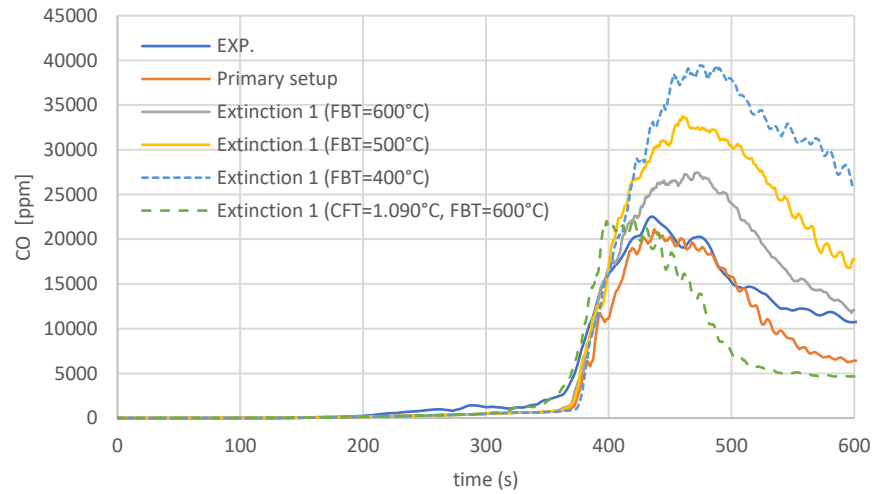
**Extinction model**  
**Heat Release Rate**



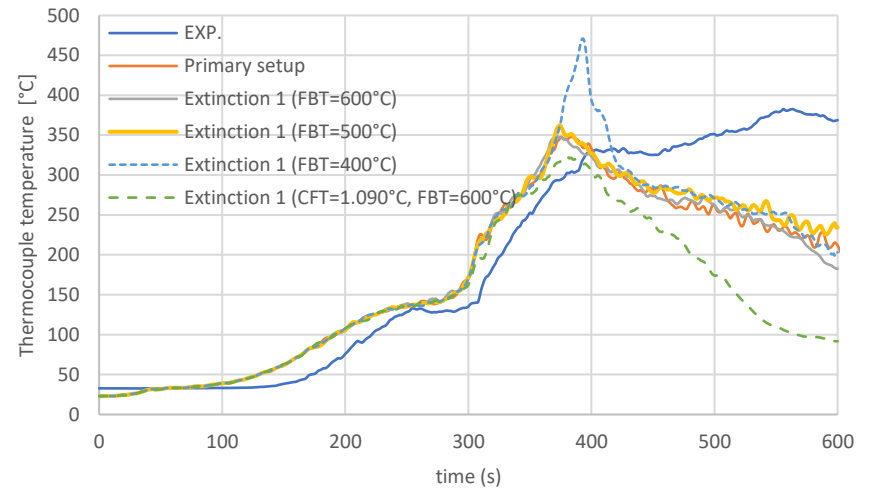
**O<sub>2</sub> concentration in the apartment (1,5 meters)**



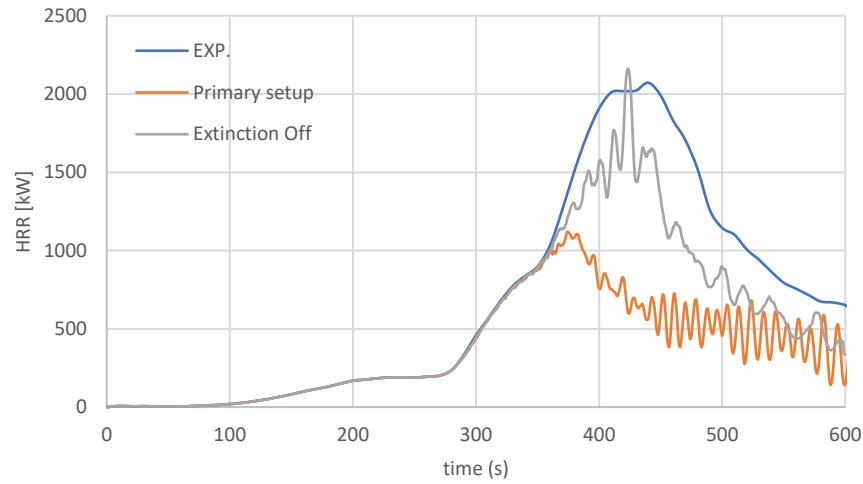
**CO concentration in the apartment**



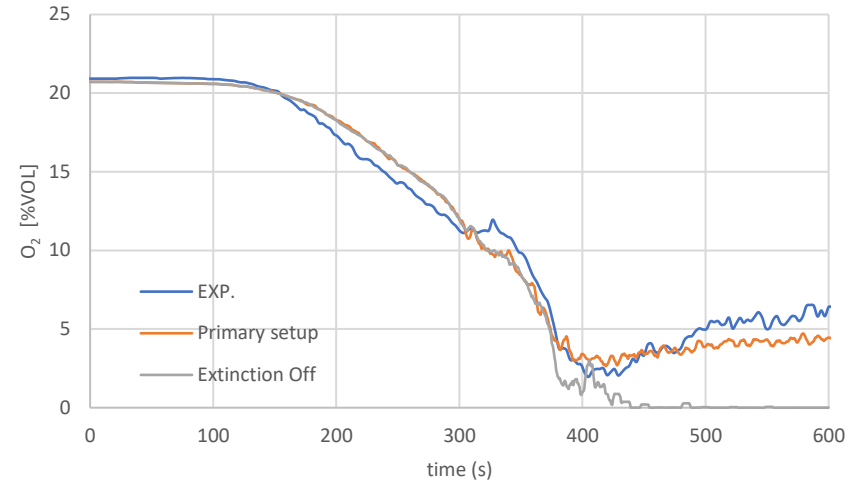
**Temperature in the apartment (TK1.1.2)**



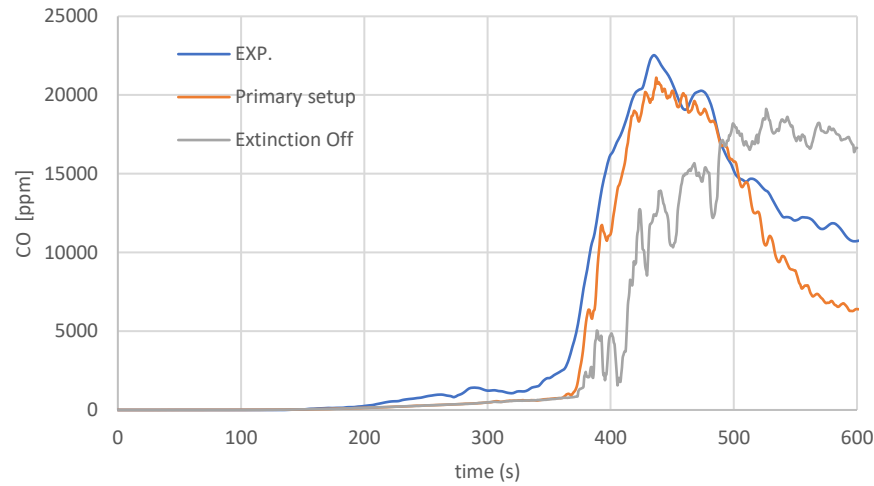
*No extinction model*  
Heat Release Rate



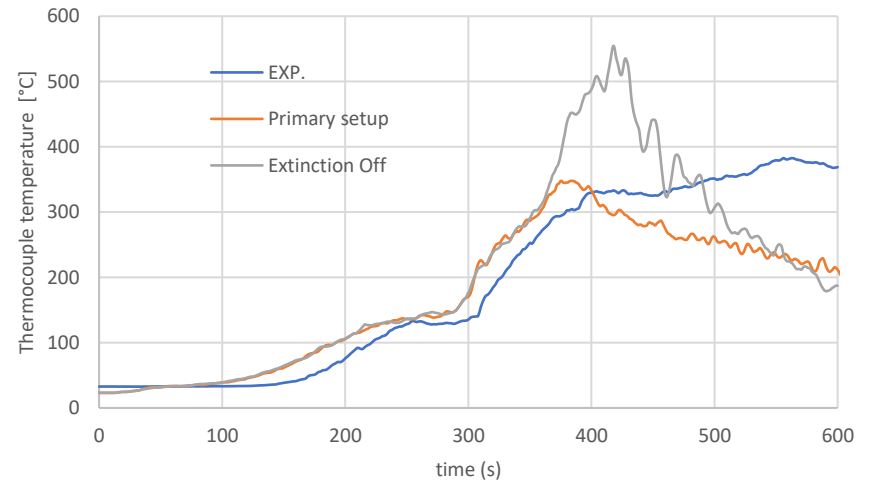
O<sub>2</sub> concentration in the apartment (1.5 meters)



CO concentration in the apartment

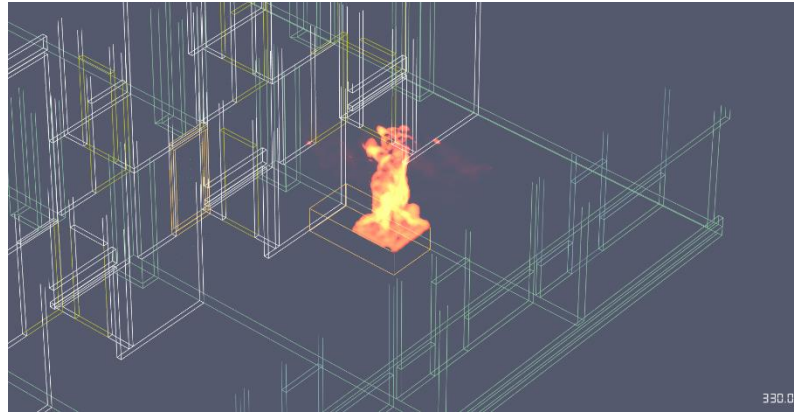


Temperature in the apartment (TK1.1.2)

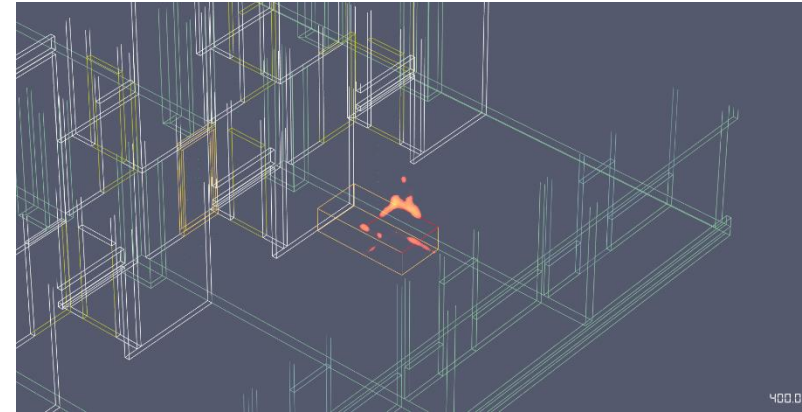


**Case study 3: door to corridor opened after 300 seconds and closed 30 seconds later**

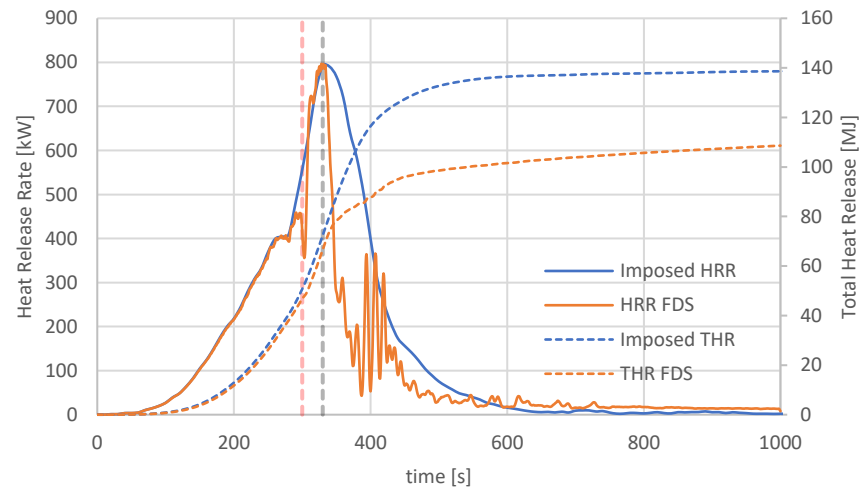
HRRPUV  
350 seconds



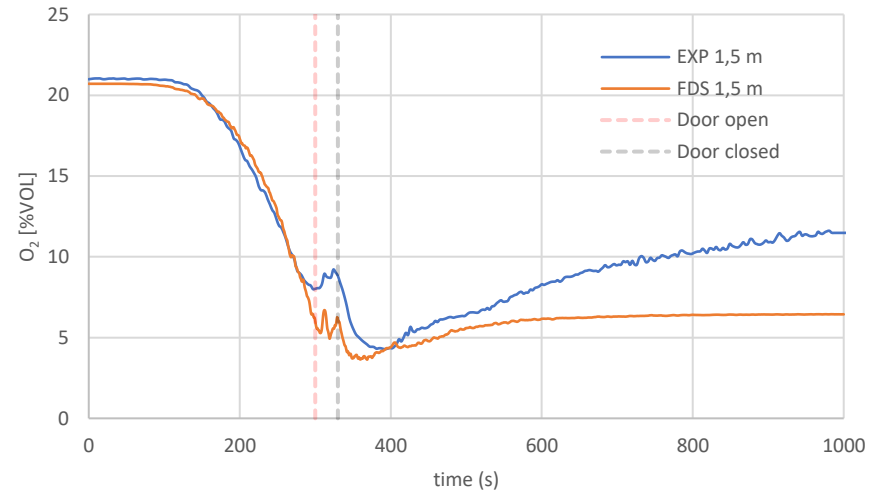
HRRPUV  
400 seconds



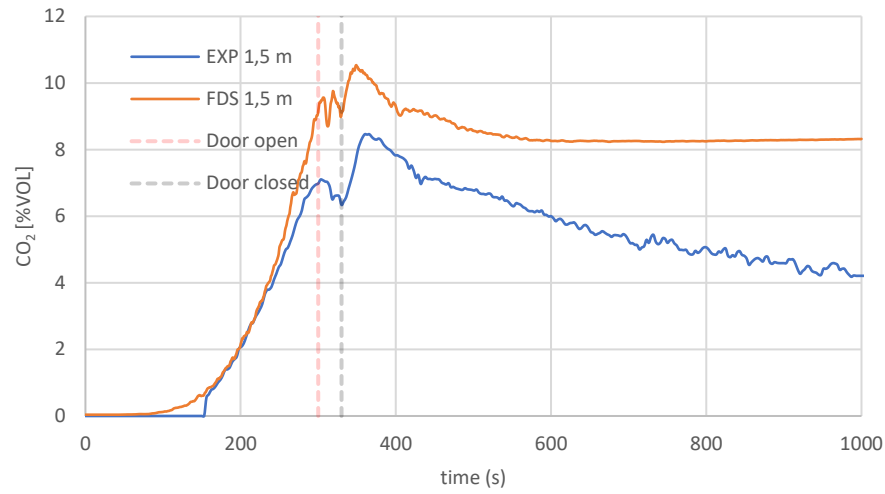
Heat Release Rate



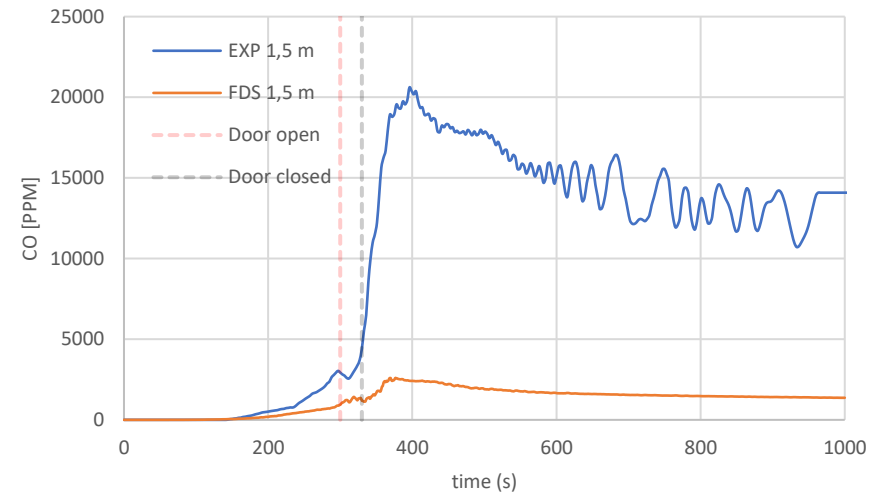
O<sub>2</sub> concentration in the apartment (1,5 meters)



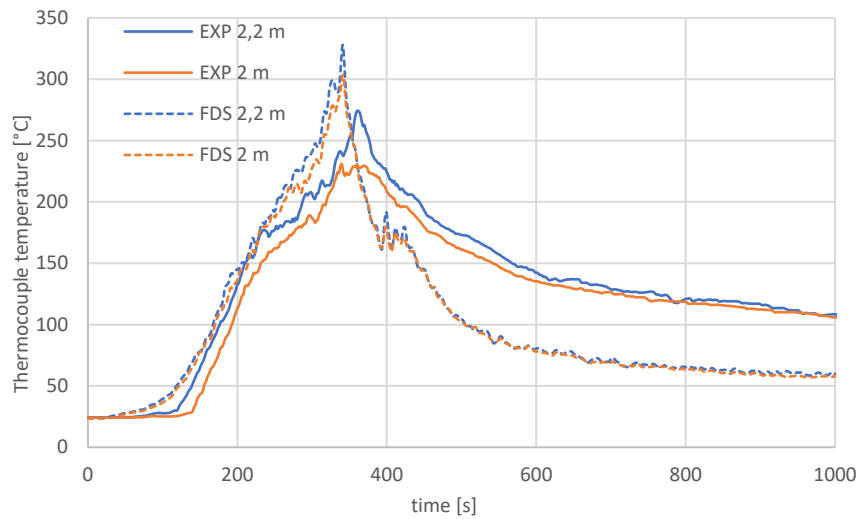
CO<sub>2</sub> concentration in the apartment



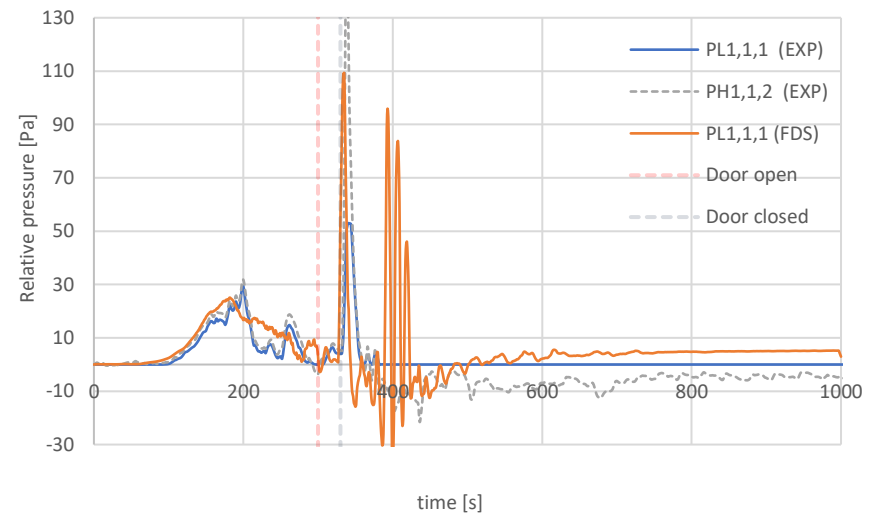
CO concentration in the apartment



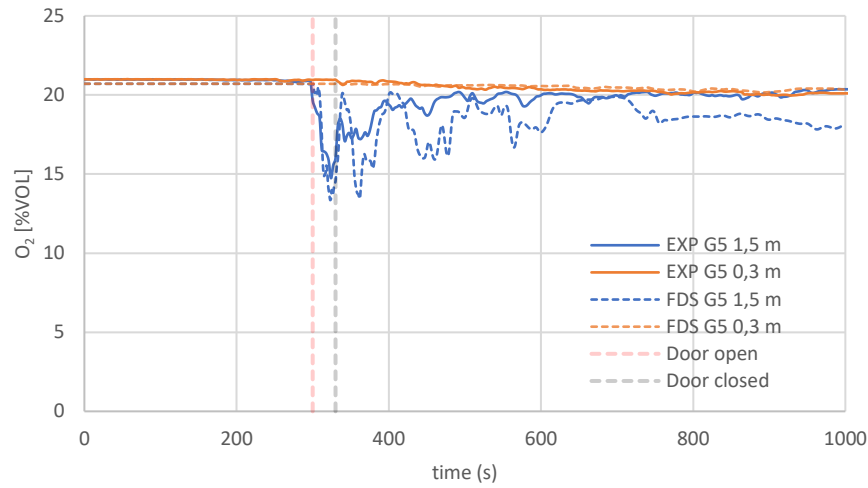
Temperatures in the apartment



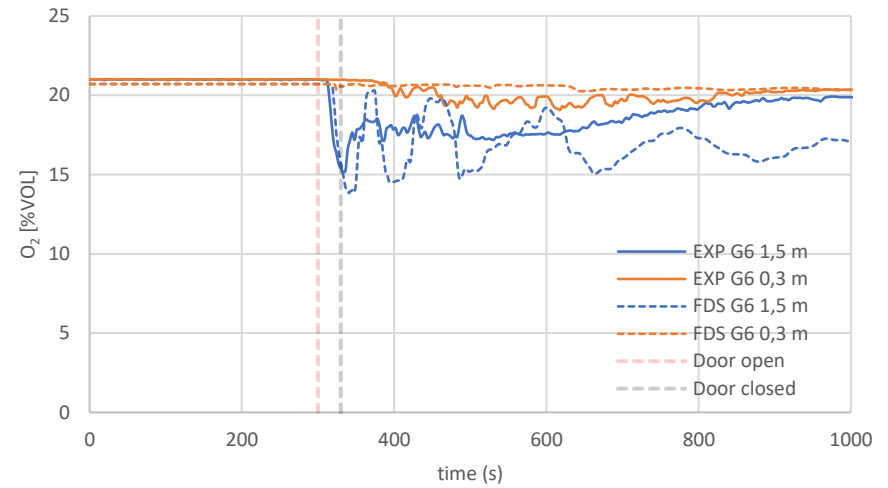
Pressure in the apartment (PL&PH equipment)



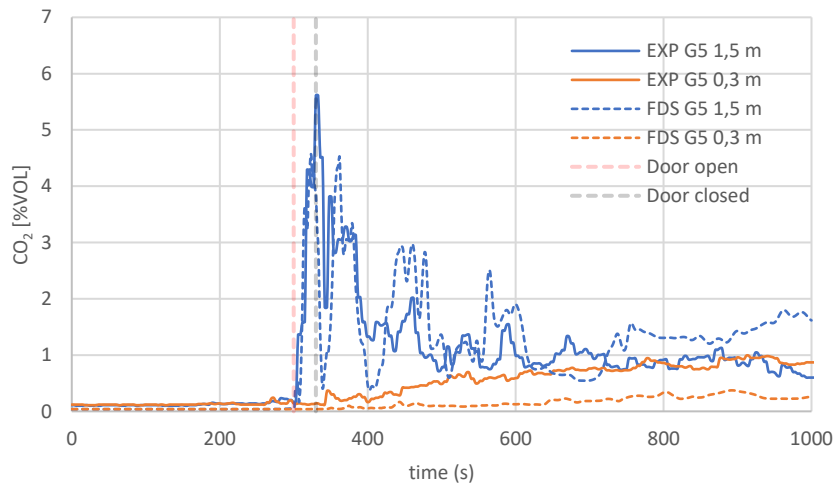
O<sub>2</sub> in corridor (G5)



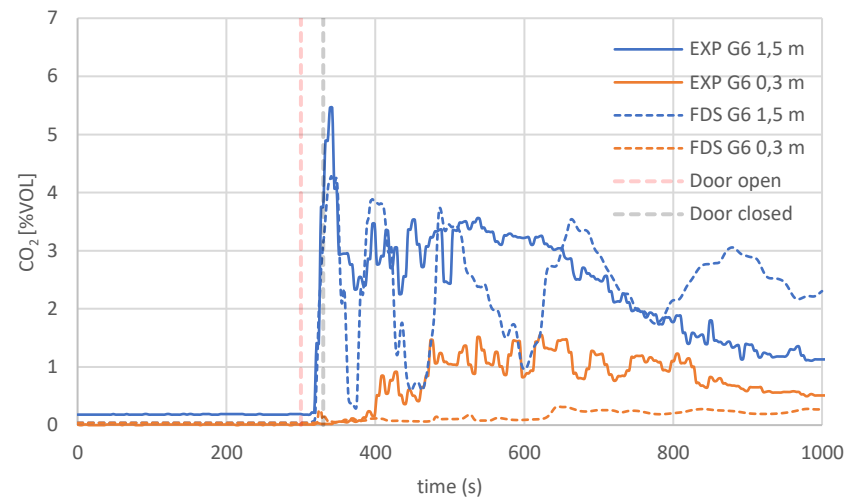
O<sub>2</sub> in corridor (G6)



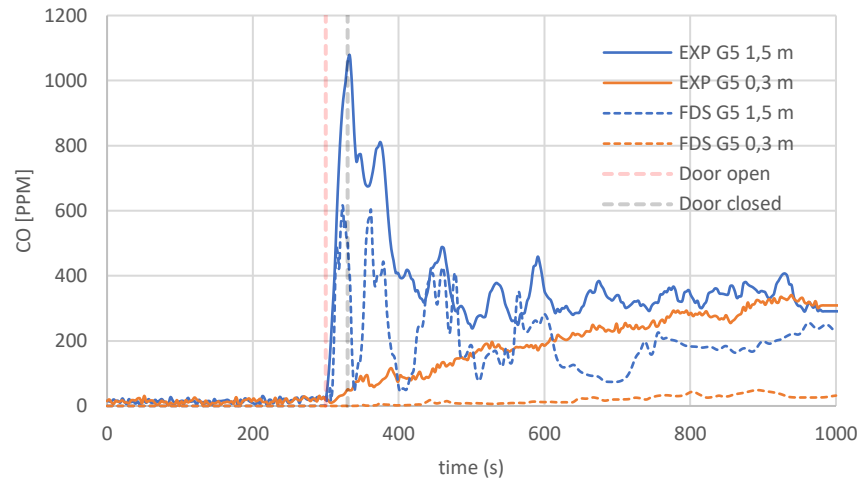
CO<sub>2</sub> in corridor (G5)



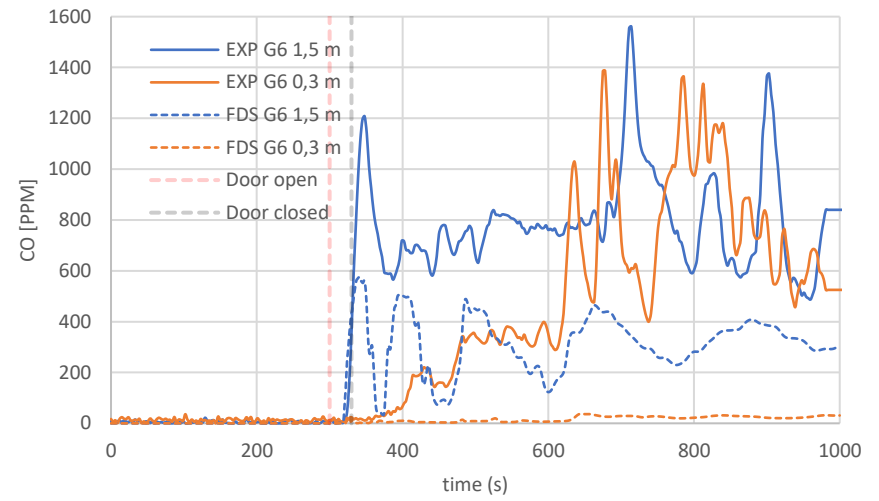
CO<sub>2</sub> in corridor (G6)



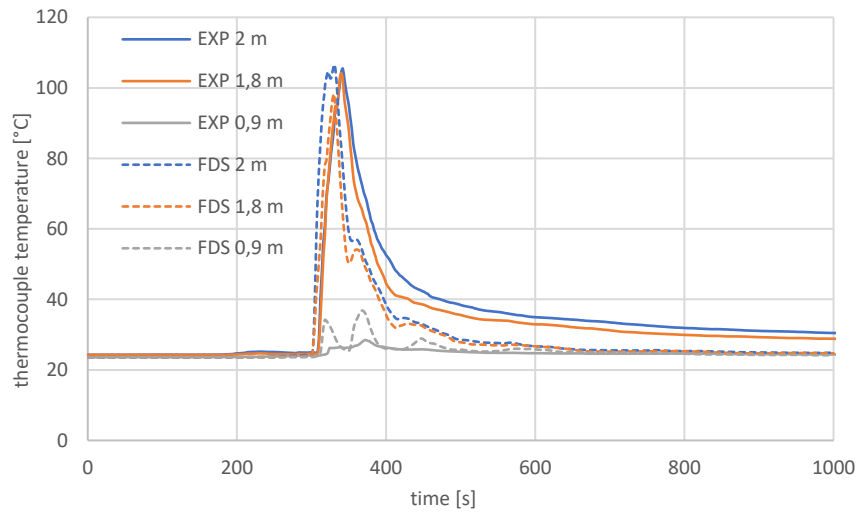
CO in corridor (G5)



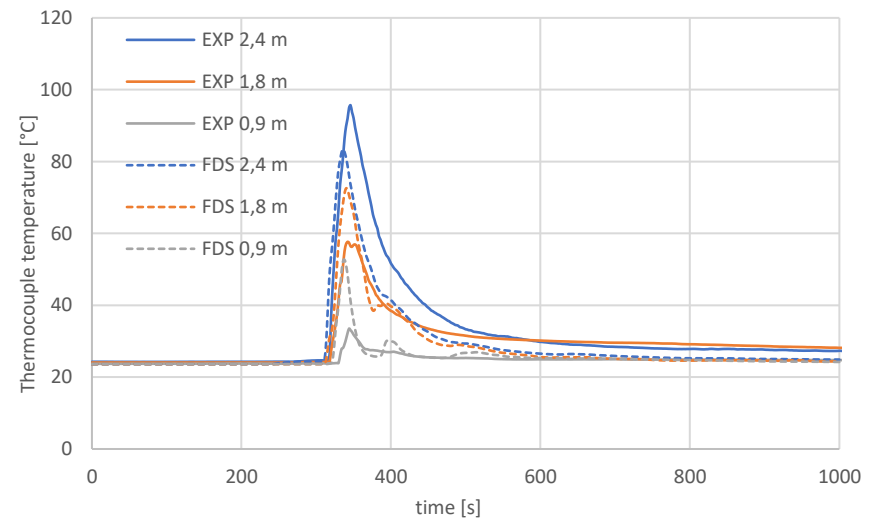
CO in corridor (G6)



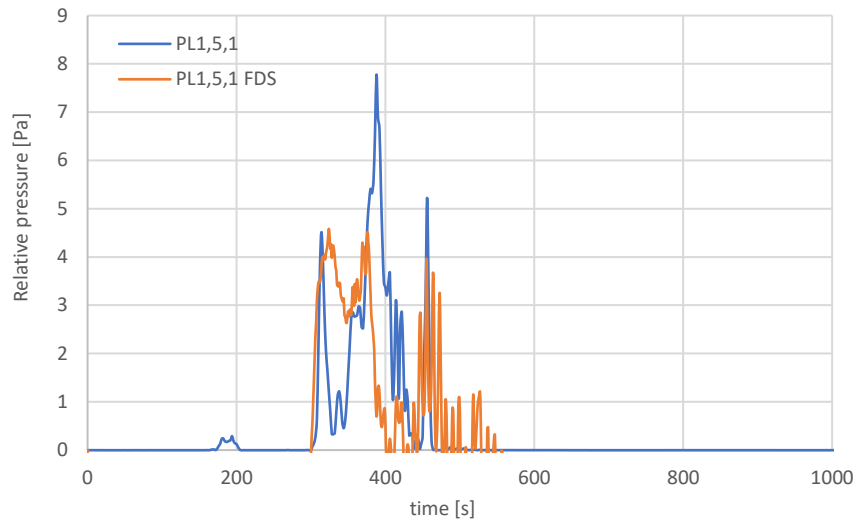
Temperatures in corridor (B5)



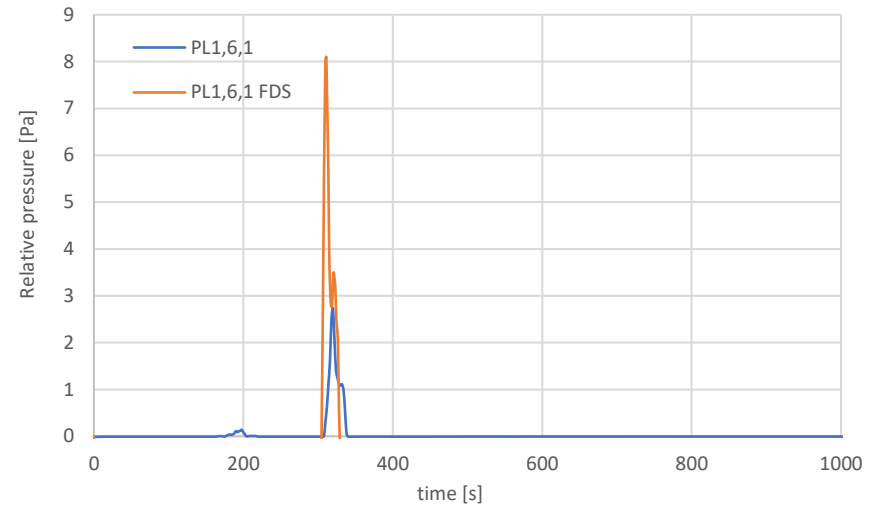
Temperatures in corridor (B6)



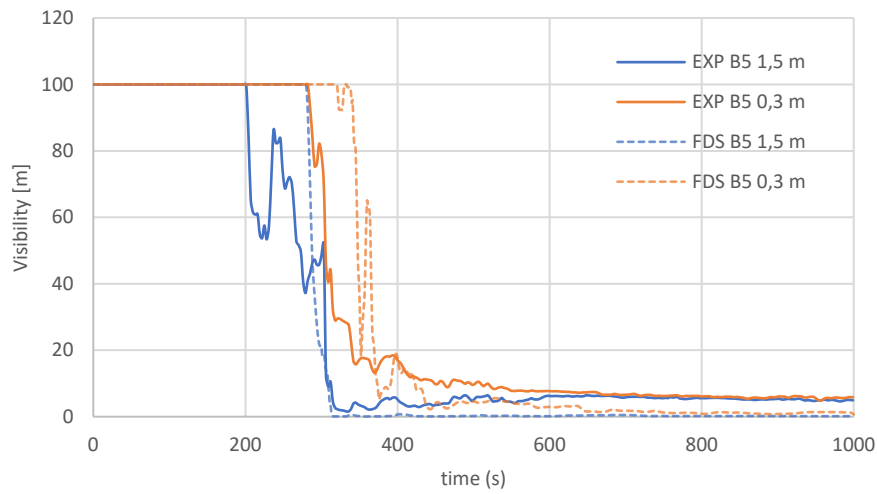
Pressure in the corridor (B5)



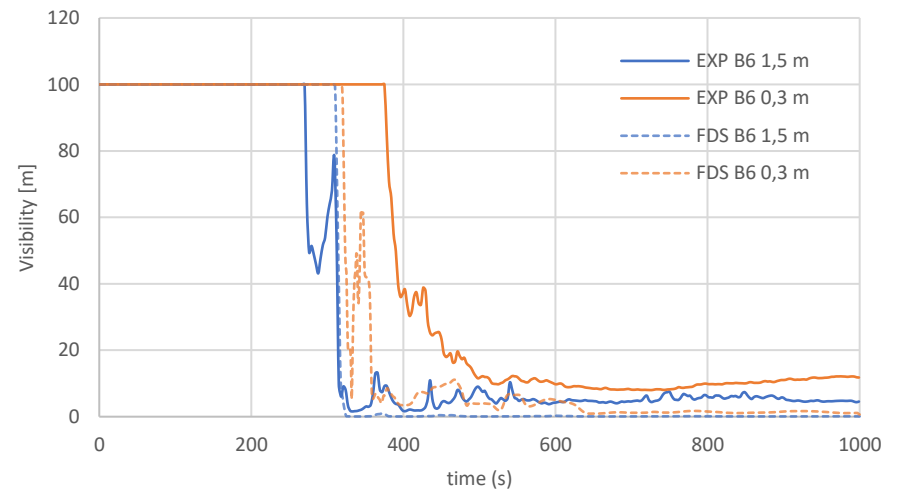
Pressure in the corridor (B5)



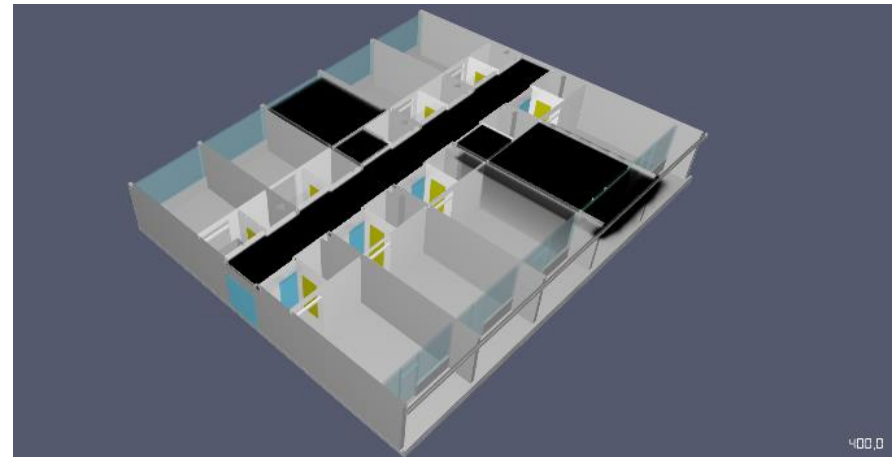
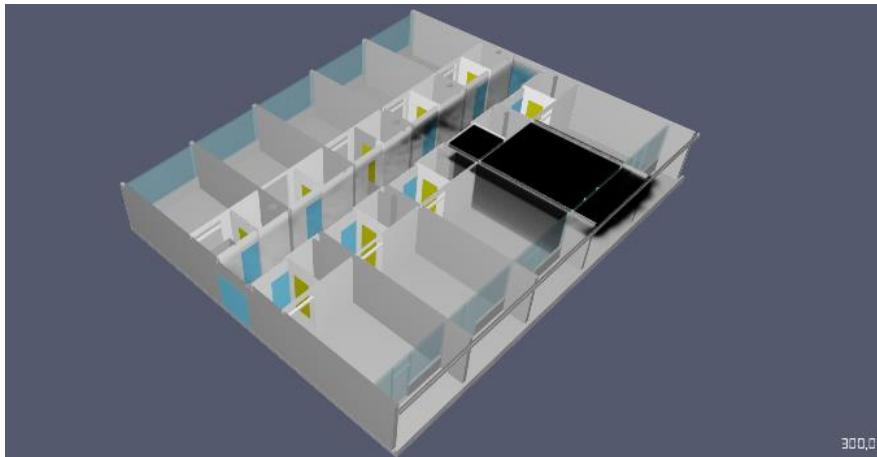
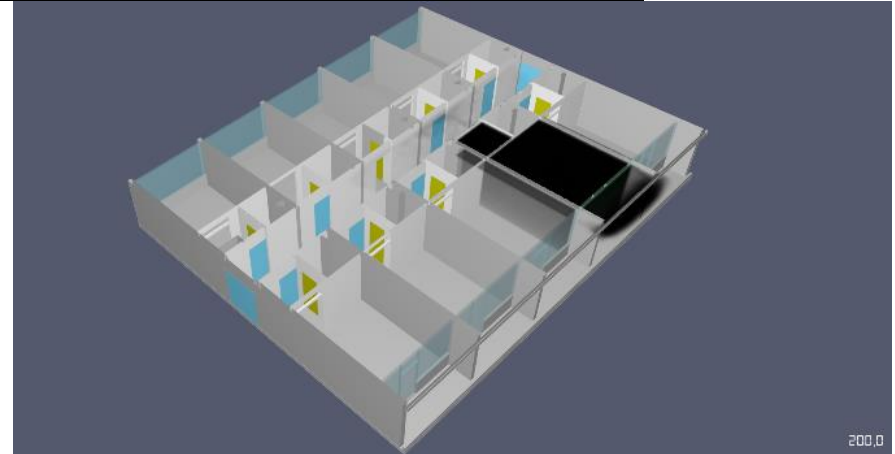
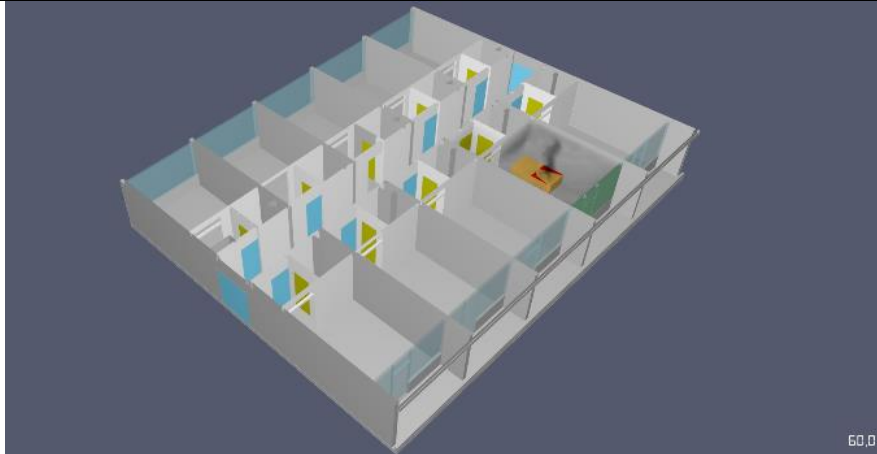
Visibility in corridor (B5)



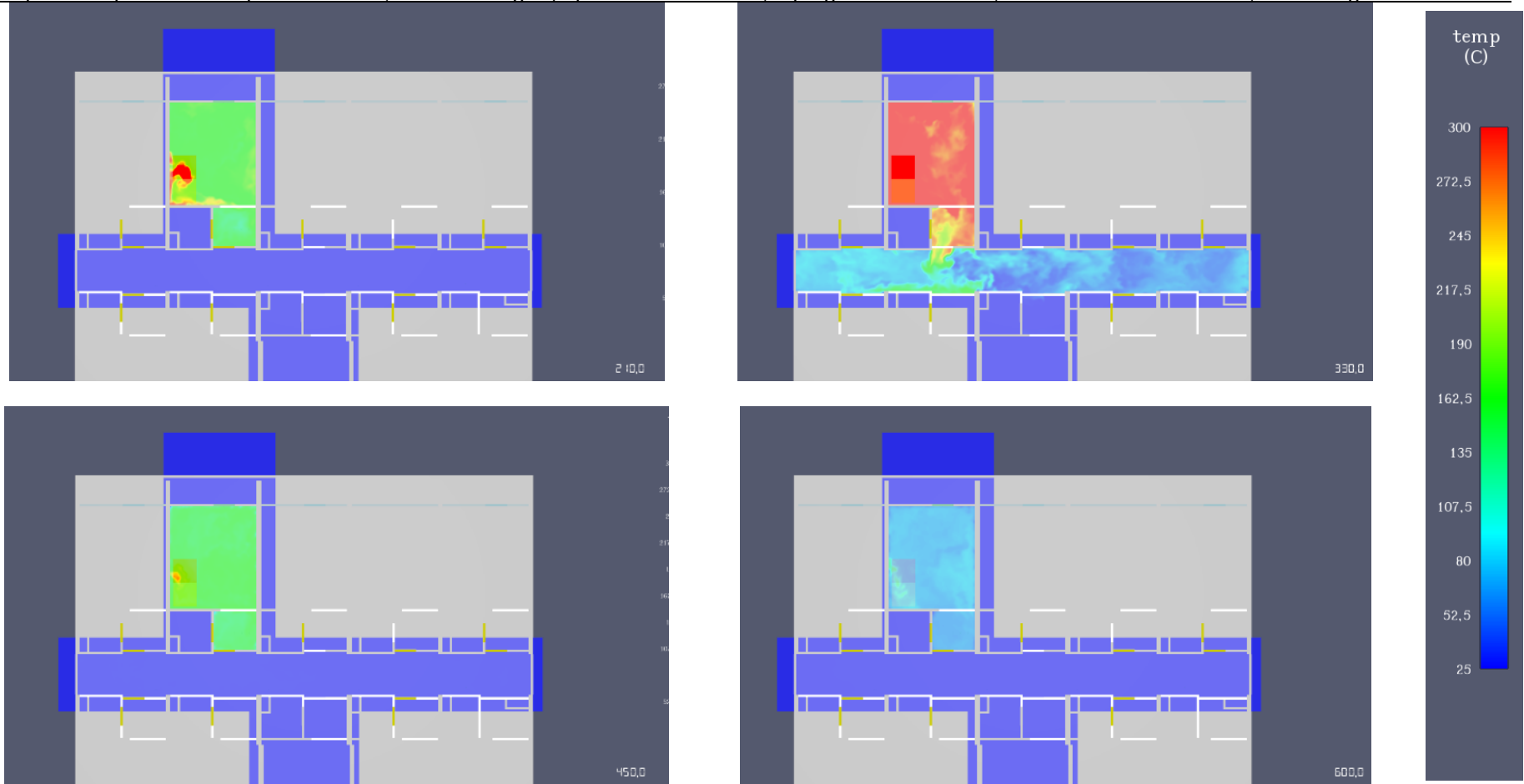
Visibility in corridor (B6)



Graphical depiction of smoke spread (top left: 60 seconds, top right: 200 seconds, bottom left: 300 seconds, bottom right 400 seconds)



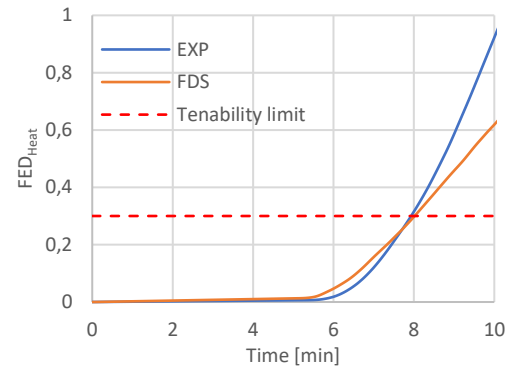
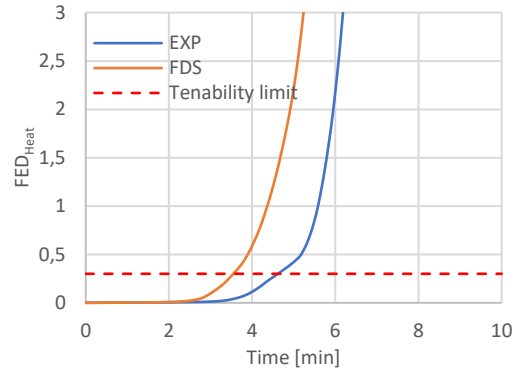
Graphical depiction of temperatures at 1,8 meters height (top left: 200 seconds, top right: 350 seconds, bottom left: 450 seconds, bottom right 600 seconds)



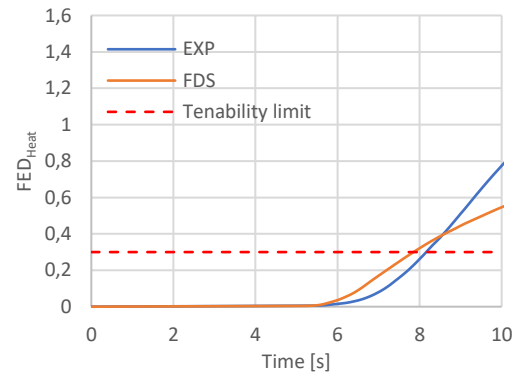
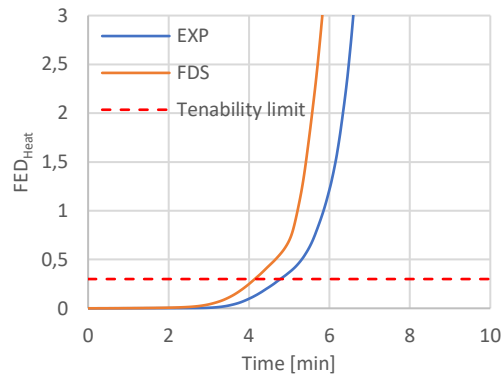
## Tenability

$FED_{heat}$

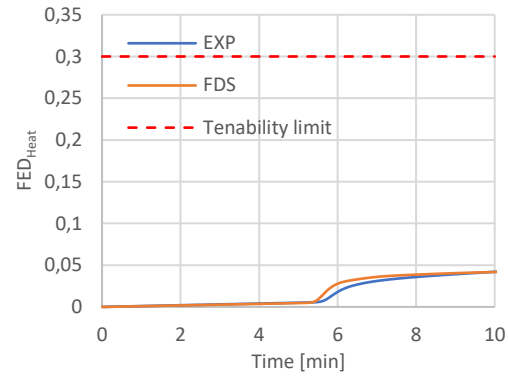
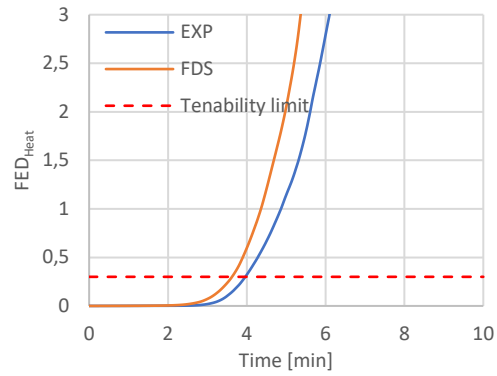
Case study 1:



Case study 2:

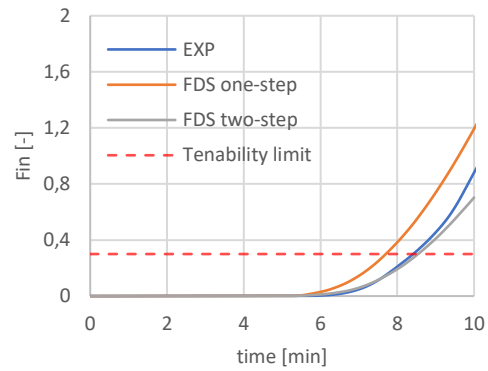
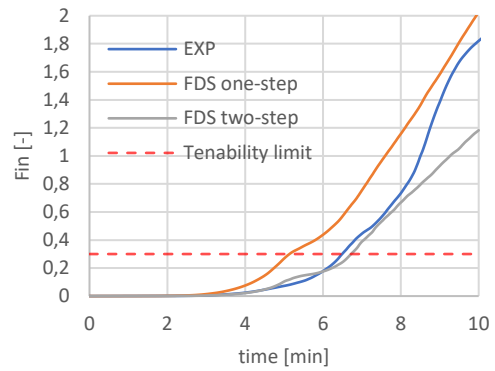


**Case study 3:**

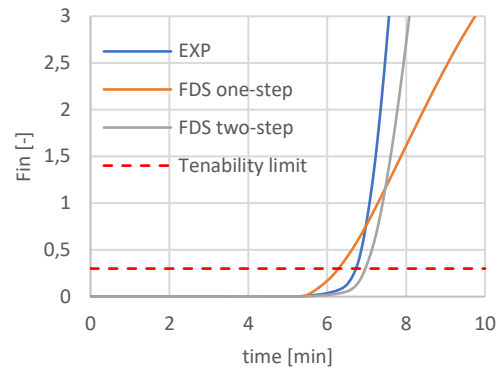
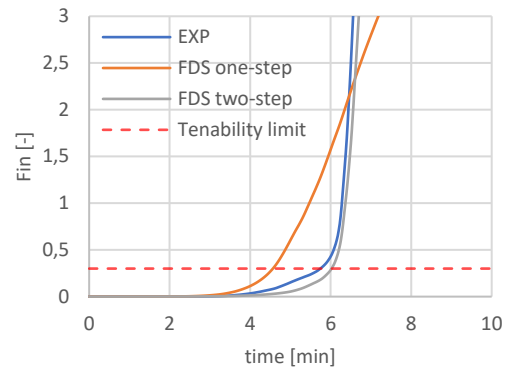


$F_{in}$

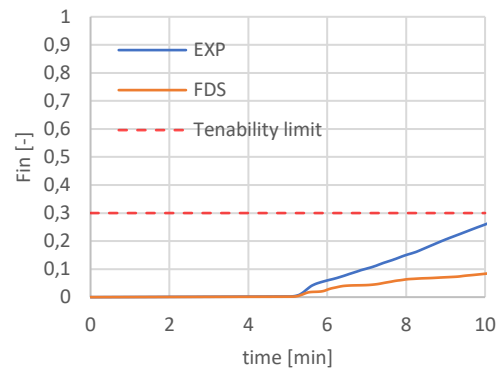
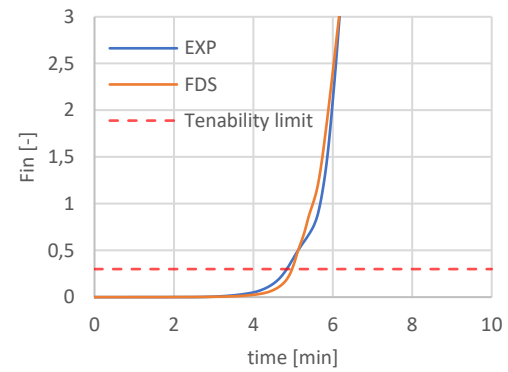
**Case study 1**



Case study 2:



Case study 3:



## APPENDIX 6: PARAMETRIC STUDIES

---

### Case study 2: Fire induced pressure in apartment

The airtightness of the apartment was measured prior to the experiments, giving insight in the leakage area of the enclosure. After the blowerdoor measurements but before experiment of this scenario however, alterations to the enclosure were made to make the of the apartment airtightness more representative, and to study the effects of fire safety measures (e.g. lower smoke permeability of the enclosure). While the fire safety measures were removed to the best extent possible, some effects on the airtightness are still expected. Therefore, the airtightness of the enclosure is prone to uncertainty. To limit this uncertainty, an a-priori parametric study is carried out to determine the most appropriate settings.

As using the  $\alpha t^n$  fire modelling method presented in paragraph 4.8 will result in slight over- or underestimates of the Heat Release Rate, which largely dictates pressure rise in the apartment, the parametric study uses the ramp methodology as discussed in paragraph 4.8. In this a-priori study, interest lies in the early stage of the fire, in which the fire is expected to be well-ventilated. Therefore, the well ventilated post-flame yields and critical flame temperature are used and only the first 300 seconds are shown.

The parameters most relevant for the pressure development in the enclosure are:

- The airtightness of the enclosure;
- The leak pressure exponent;
- The heat release rate (characterized here by the effective heat of combustion).

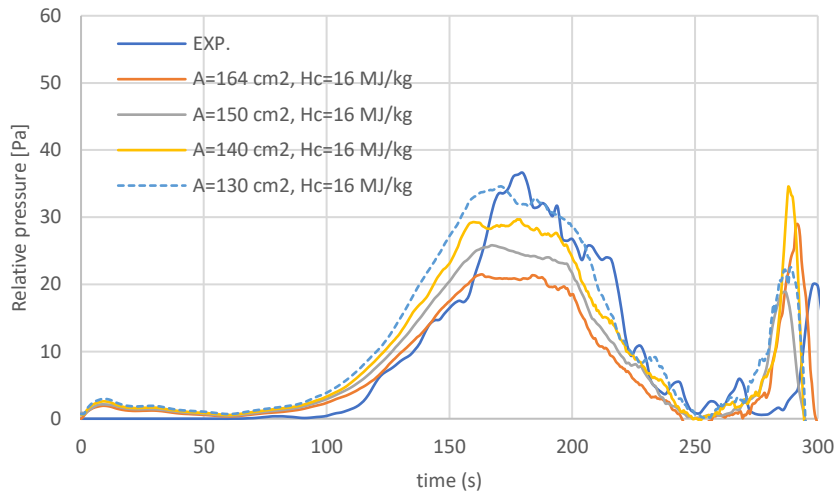
Furthermore, the effects of the leakage area of the door is examined through the measured visibility in the corridor. The parametric changes made are:

- Airtightness of the door;
- Location of leak;
- Leak enthalpy on or off.

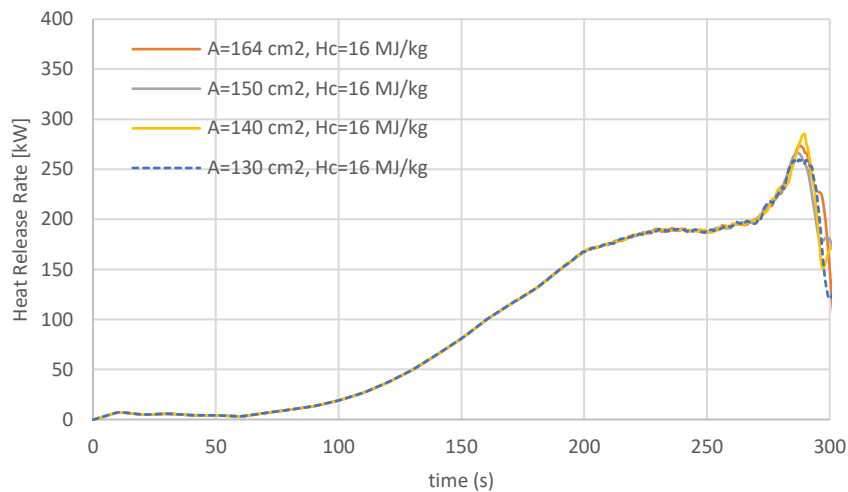
### Airtightness of the enclosure

Figure 47 shows the pressure development in the apartment for the first 300 seconds. Using the measured values ( $A = 164 \text{ cm}^2$ ), a under-estimate is observed at the initial peak around 170 seconds. The second peak is over-estimated. This is a result of the fire becoming increasingly ventilation controlled. Around that time, the extinction model begins to dictate the Heat Release Rate, as seen in the following image. All scenarios use a leak pressure exponent of 0,56.

A better airtightness is expected due to the alterations made to the enclosure. A value of  $130 \text{ cm}^2$  gives the best approximation of the overall pressure development, both in the first and the second peak. Slight differences in the overall buildup-period (100-150 seconds) exist, which can mainly be attributed to the way the fire is modelled. The overall trends and maximum pressures correspond quite well with the measured values.



Pressure development in the apartment

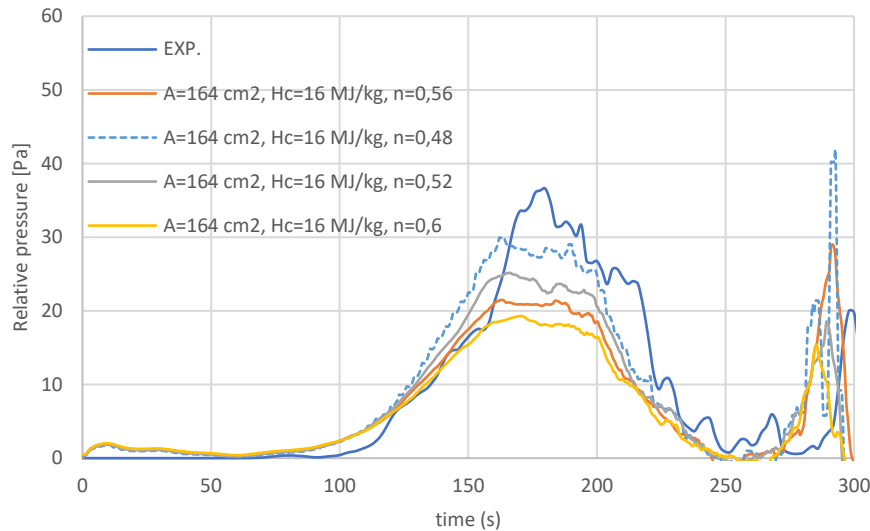


Heat Release Rate in the apartment

### Leak pressure exponent

The leak pressure exponent ( $n$ ) dictates the change in leakage area as the pressure rises. A higher exponent leads to a less steep pressure-rise. To study its effects, several simulations were run in which a different leakage exponent is used.

The measured value (0,56), shows an under-estimation of the initial pressure rise, while second pressure rise is somewhat over-estimated. Higher leakage exponents will, as expected, result in a lower pressure rise ( $n=0,6$ ), while lower leak exponents result in a higher pressure increase. The difference in pressure increase however, is not as explicit as it is for the increased airtightness of the apartment.

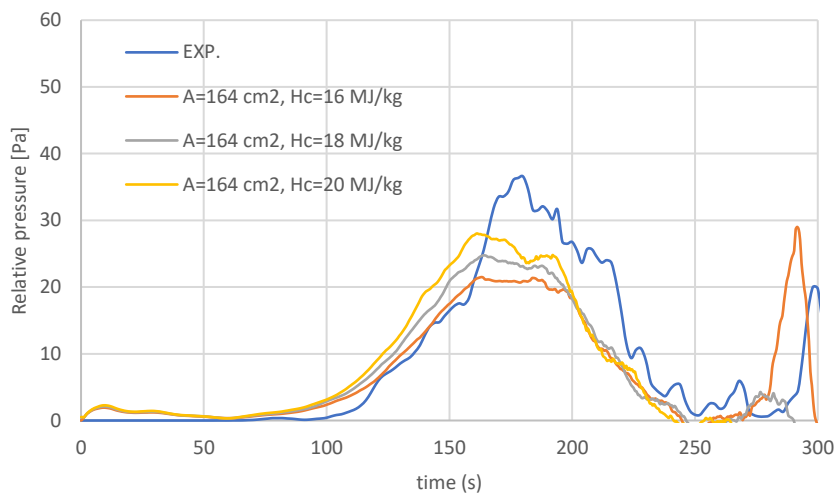


Pressure development in the apartment for different leak pressure exponents

### Heat Release Rate/effective heat of combustion

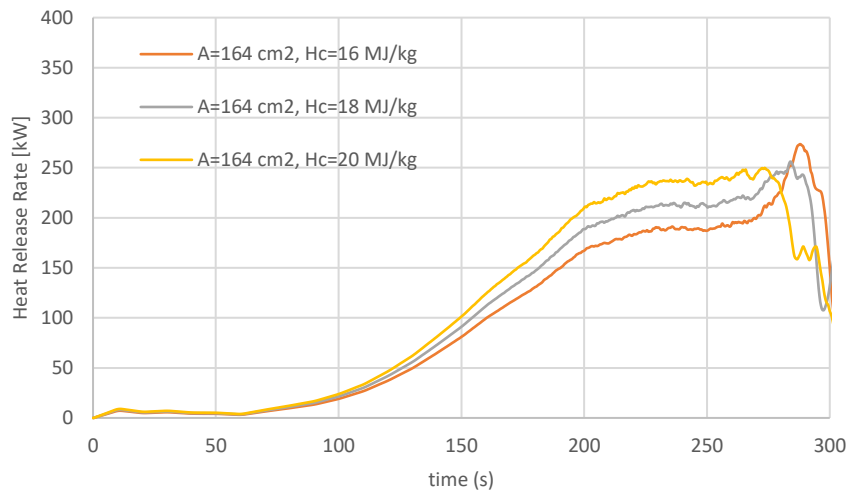
A higher heat release will result in higher gas temperatures in the enclosure. Gases are prone to expanding in volume at higher temperatures. Therefore, at a higher heat release, a higher pressure rise is expected. As the mass loss rate of the fuel is prescribed in the model, the effective heat of combustion is changed to study differences between different heat release rates.

Differences between different values for the heat of combustion are noticeable in the following figure. A higher heat release will lead to a higher over-pressure in the apartment as expected. Differences however, are not very pronounced. Using even higher values for the effective heat of combustion are unrealistic for the used fuel.



Pressure development in the apartment for values for the effective heat of combustion

The second peak in pressure increase does not occur for the simulations with a heightened effective heat of combustion. This is explainable through the fact that extinction is modelled to occur earlier in the fire development, even though the critical flame temperature for these reactions is changed accordingly with the higher heat release. This is observed in the following figure.



Heat Release Rate for the simulations with a higher effective heat of combustion.

### Chosen parameters for simulations

Using the measured airtightness values for the enclosure results in under-estimations for the fire-induced pressure in the apartment. This can most likely be attributed to changes made to the enclosure in between the moment the airtightness was measured and the actual experiments. The effects of a better airtightness is examined through a series of CFD-simulations. As explained, several parameters influence the pressure development in the apartment. Out of these parameters, the overall airtightness of the apartment is the most crucial for the pressure development, followed by the leak pressure exponent and the heat release of the fire.

Most likely, a combination of changes in these parameters will dictate the actual measured pressure-rise in the apartment. There is currently no indication of the leak pressure exponent actually being altered due to the changes to the enclosure. Furthermore, heightening the effective heat of combustion will likely result in over-estimates in temperatures elsewhere in the domain. Based on these observations and for the sake of simplicity, the following simulations are run with a better airtightness of the enclosure. An airtightness of 130 cm<sup>2</sup> best approximates the measured values and is therefore selected. The leak pressure exponent is kept at 0,56, while the effective heat of combustion is kept at 16 MJ/kg.

### Smoke leakage to the corridor

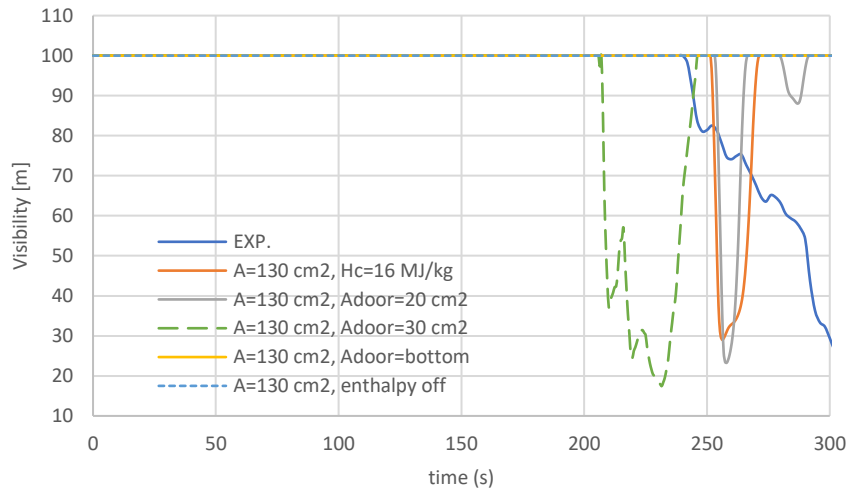
The experimental results show the visibility at measuring tree B6 (at a height of 1,5 meters) declining before the door was opened at around 240 seconds. The smoke leakage to the corridor depends on the pressure rise in the apartment, which was discussed in the earlier paragraphs. Furthermore, the exact leaks in the door between the apartment and the corridor influence the leakage. In this paragraph, different setups for the door configuration are compared:

- Leak area: the leak area of the door has a significant influence on the overall mass flow rate through the leak. In the initial simulations, a leak area of 10 cm<sup>2</sup> was used, based on an initial crude estimate. To check the sensitivity of the leakage on this value, another simulation is run with a door leakage of 20 cm<sup>2</sup> and 30 cm<sup>2</sup>. Distribution of the leaks is kept the same.
- Location of the leak: a typical door will have a higher leakage at the bottom than at the sides or top. Therefore, the initial simulations were run with 75% of the leakage located at the bottom and 25% distributed at the sides and top. To check the sensitivity of this assumption, a simulation was run with the entire leakage area located at the bottom of the door.
- Leak enthalpy: heat losses from the smoke to the area of the leak will result in the smoke being of a lower temperature when it exits the leak. FDS allows the heat losses to be (crudely) accounted for by adding the difference between the temperatures of the flow and the wall to the cell adjacent to the leak. In the initial simulations, the leak enthalpy option is enabled. To check this for sensitivity, a simulation is run with leak enthalpy disabled. If disabled, the temperature of the outflowing gases

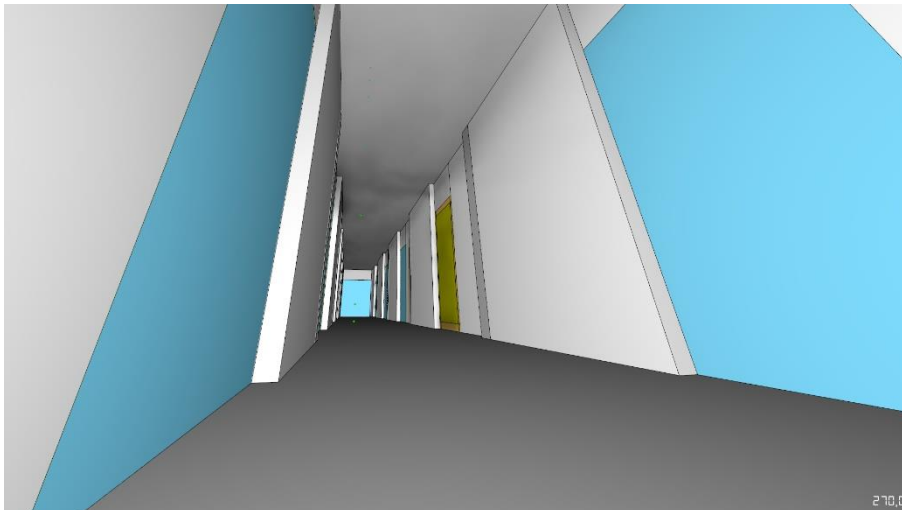
is assumed to be the same as the temperature of the surface of the wall where the gases exit the leak.

### Leakage area and location of the leak

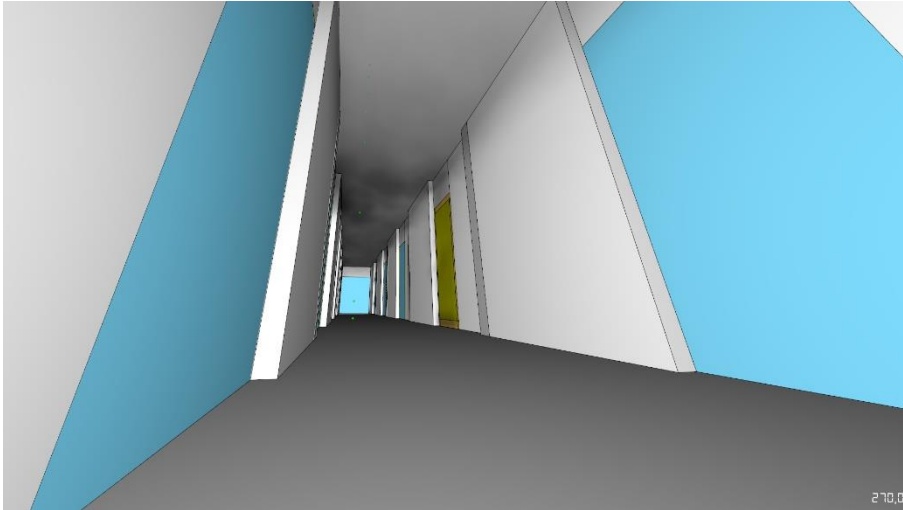
As seen in the following figure, none of the simulations show a direct correlation with the experimental results. Simulations with the entire leakage area located at the bottom and with the enthalpy turned off do not show a lowered visibility at all, while the initial simulations and the simulations with a higher leakage area show a decrease in visibility before being increased again. Results are shown graphically in the following figures. Results for a leak area of 20 cm<sup>2</sup> in the door show the best correlation with the experimental results.



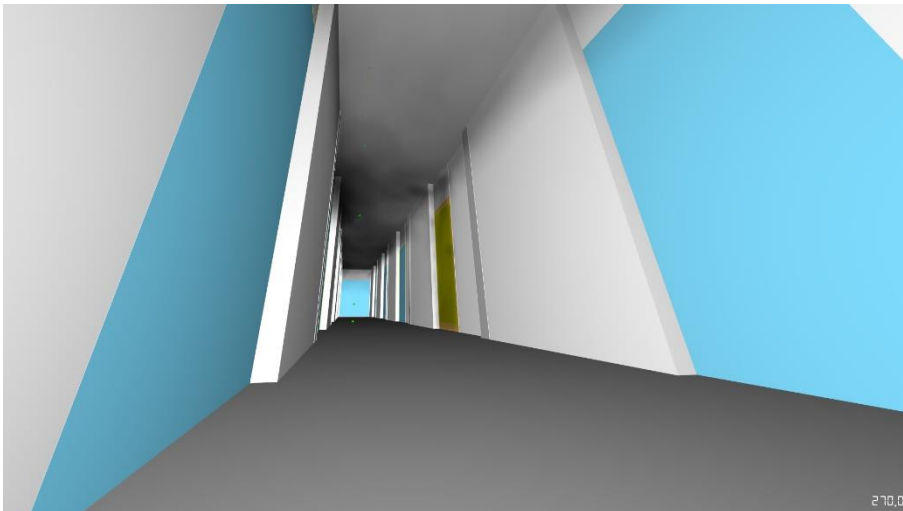
Visibility in the corridor at B6 at a height of 1,5 meters.



Soot density in the corridor for the simulation with a total leakage of 130 cm<sup>2</sup> and a door leakage of 10 cm<sup>2</sup> at 270 seconds



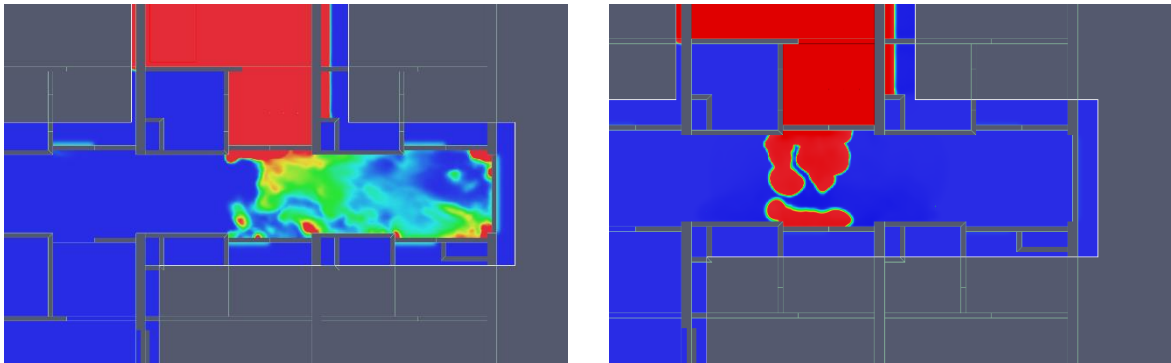
Soot density in the corridor for the simulation with a total leakage of 130 cm<sup>2</sup> and a door leakage of 20 cm<sup>2</sup> at 270 seconds.



Soot density in the corridor for the simulation with a total leakage of 130 cm<sup>2</sup> and a door leakage of 30 cm<sup>2</sup> at 270 seconds.

### *Enthalpy*

In the case of the scenario with enthalpy turned off, gases are assumed to have the same temperature as the surface they exit from. This results in a situation where the leaking gases only have limited (to none) temperature difference with the ambient compared with the simulations where enthalpy is turned on. As such, smoke movement is stagnant and limited to the area directly in front of the apartment door in the simulations with enthalpy off. In the case of the simulations with the enthalpy turned on, heat losses are (somewhat) more realistically taken into account. This results in the escaping gases being more buoyant with entrainment of ambient air and smoke propagation as a result. The following images show the soot concentration in the area in front of the apartment door. Differences are significant.



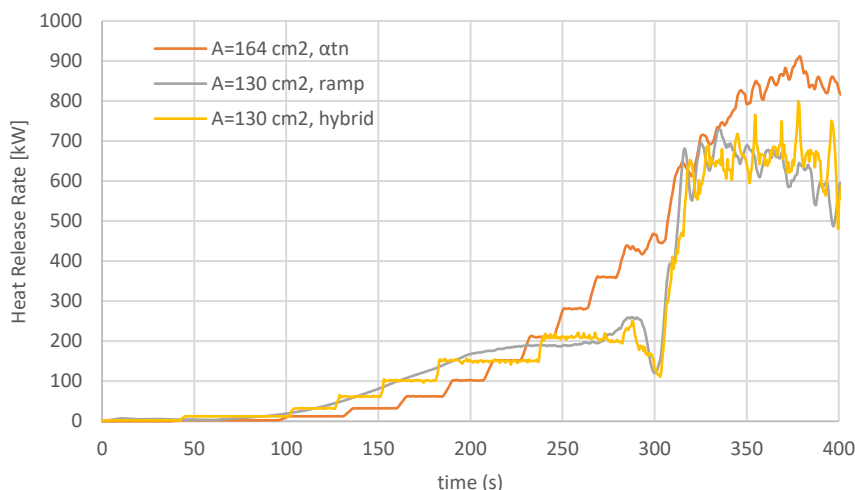
soot concentration at a height of 1,5 meters,  $t = 270$  seconds, enthalpy on (left) and off (right).  
Red =  $9,5 \cdot 10^{-6}$  kg/kg, blue = 0 kg/kg.

While the methodology for heat transfer from the gases to the inside of the leak implemented in FDS is to a certain extent rudimentary, it is clear to have a significant effect on the smoke movement in the corridor, prior to opening the apartment door. Therefore, enthalpy is left on for the remainder of the simulations.

### Case study 2: effects of method of fire modelling on pressure evolution

The main downside of the ramp method in FDS is the fact that the overall fire size is overestimated during the growing phase of the fire. This results in errors regarding flame length and momentum of the fire and smoke plume and affects the stratification in the apartment. The downside of using a radially growing fire based on a  $\alpha t^n$  curve is the fact that the heat release rate is not prescribed accurately. In this case, using the  $\alpha t^n$  approach results in significant errors in the pressure development in the enclosure.

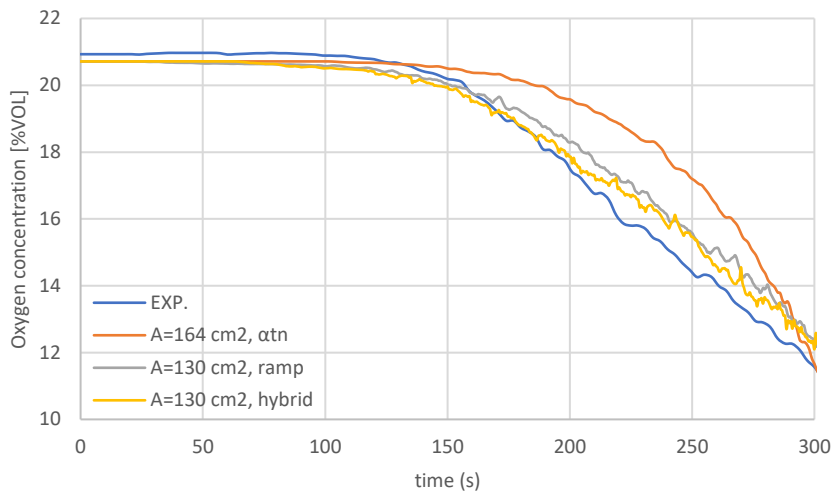
A solution might lie in combining the ramp and radial fire spread methodologies. In this methodology, the fire is modelled according to the actual measured mass loss rate instead of a fitted  $\alpha t^n$  curve. The modelled burning area is equal to the ratio of the measured mass loss rate and the mass loss rate per unit area (which is equal to the maximum mass loss rate measured divided by the area of the sofa). The resulting heat release rate curves are shown in the following figure.



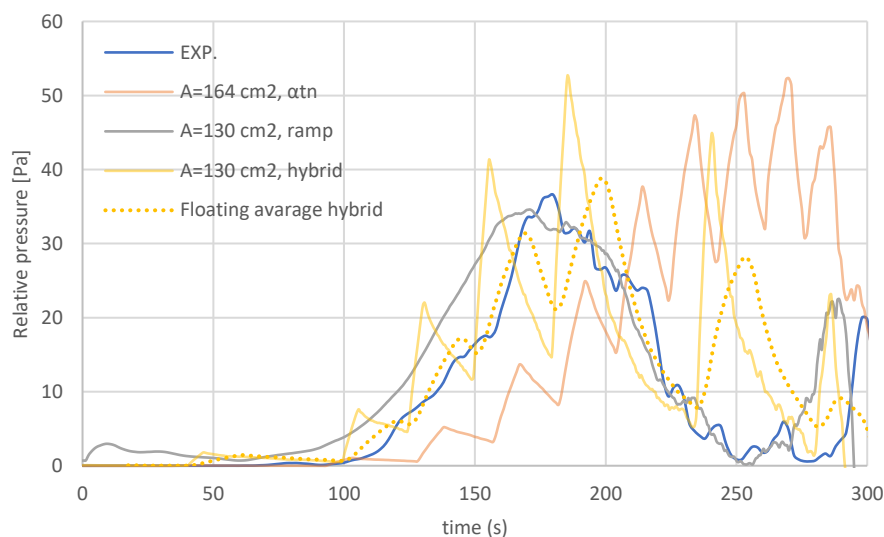
Heat release rates for different fire modelling methodologies

In all scenarios, flame extinction due to oxygen dilution is predicted to occur at more or less the same time (around 290 seconds), with small differences being contributed to the overall slightly higher total heat release of the ramp-function in the growing phase of the fire and the oxygen consumption being underpredicted in the  $\alpha t^n$ -model for the initial stages of the fire. This is shown in the following figure,

which showcases a good correlation for both the ramp and hybrid model, while the  $\alpha^n$ -model overestimates the oxygen concentration.



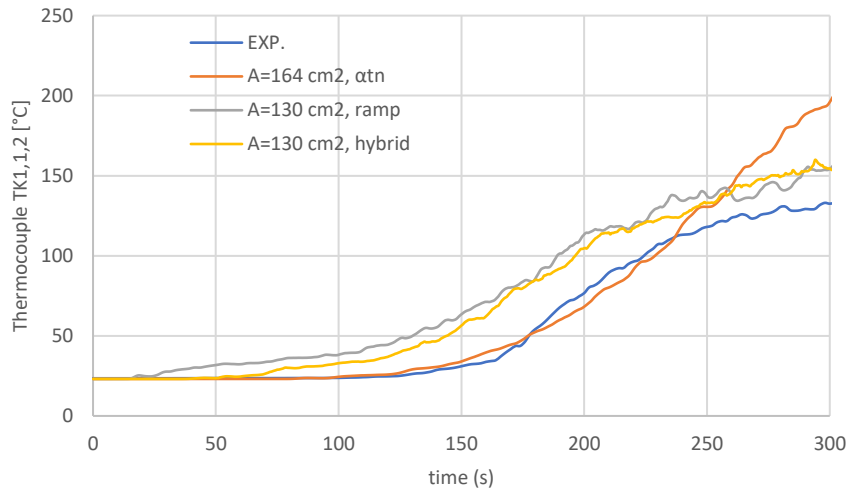
Oxygen concentration in the apartment for different scenarios.



Pressure buildup for different methods of fire modelling.

The methodology of instantaneously increasing the mass loss rate results in pressure development that looks more fabricated. The floating average for the hybrid model however, shows an overall good correlation with the initial growing phase of the fire. The peak at 250 seconds, which does not occur in the experimental results, can be attributed to the fact that at this time, the fire and its heat release rate are modelled to grow, while in reality the heat release rate is expected to be constant.

Using the mixed method does not result in significant changes for oxygen consumption or flame extinction in relation to the ramp method. Results regarding temperatures do show some differences as shown in the following figure.



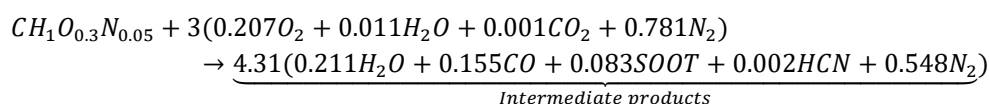
Temperature development for different methods of fire modelling.

### Case study 2: multiple fast reactions and (mis)using the extinction model

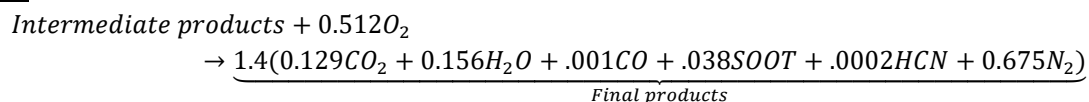
To take into account CO- and soot-generation inside the flame envelope as a result of oxygen starvation into account, a multiple step reaction scheme is employed. Several methods of setting a multiple step fast reaction scheme are possible in FDS. Most favorably, to take into account CO generation, a finite rate reaction can be used. Finite rate reaction schemes depend heavily on local quantities and might necessitate excessive grid resolution or a DNS methodology. This is not desirable. Therefore, a simple two step combustion scheme is used in which two infinitely fast reactions are executed in series.

In the reaction scheme below, the well ventilated post-flame yields for CO and soot are used, so that FDS models CO and soot to be formed even though sufficient oxygen is available in the initial stages of the fire development. In the reaction scheme, the carbon molecules in the fuel are modelled to react with oxygen (and hydrogen as soot is assumed to be hydrogenated) to form CO and soot. The default values for CO and soot-generation are used (2/3 of the carbon molecules react to form CO and 1/3 is used to form soot). While HCN generation is also taken into account, it is not further discussed here. This results in the following reaction scheme, in which polyurethane GM21 reacts with air:

#### Step 1:



#### Step 2:



Step 2 is only invoked should sufficient oxygen be available. Therefore, in the simulations, should the oxygen be diluted, the reaction stops at step 1, resulting in a heightened CO- and soot-generation. In reality, these reaction kinetics are significantly more complex. Moreover, no temperature dependence is in place, allowing the second reaction to occur independent of the cell temperature. In reality, higher temperatures typically lead to more efficient kinetics. Overall, the validation of this model for the far-field is limited and can be typically viewed as rudimentary.

#### Note on the effective heat of combustion

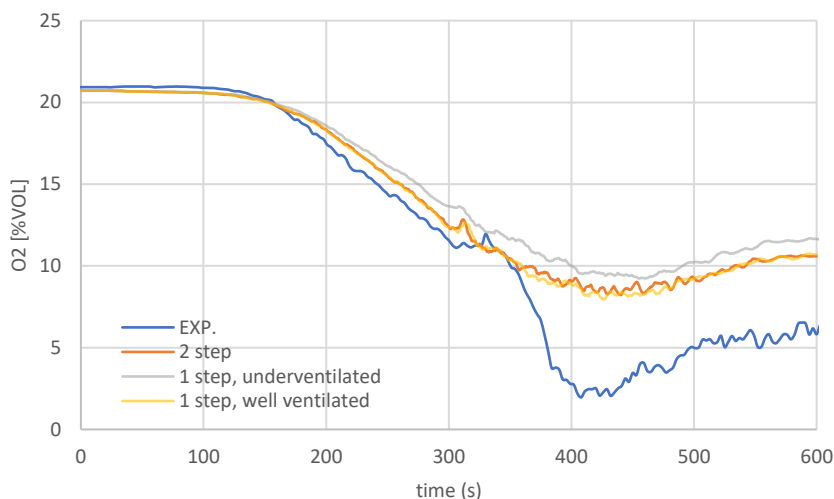
By default, the two step combustion model calculates the effective heat of combustion based on the species' enthalpy of formation/reaction. This essentially allows the effective heat of combustion be transient over the duration of the simulation: should step 2 not be allowed to occur, the energy released

by that reaction is not accounted for. Using this methodology will result in a higher initial effective heat of combustion than used in earlier simulations. The calculation of the effective heat of combustion is therefore initially overruled. A value of 16 MJ/kg is used instead in the following results. At a later stage, the effects of a dynamic heat of combustion are studied.

### Initial results

The initial results are shown in the following images. The oxygen-concentrations are shown to follow the experimental data in the early stages of the fire closely, with small deviations being explainable through small differences between the fuel-to-air ratio between the modelled and real chemical reactions in the flame sheet. Moreover, the used mass loss rate curve is a time-averaged from the experimental data. Around the time the door opens, the mass loss rate is measured to be more heavily affected by the effects of oxygen dilution in the flame sheet.

At around 350 seconds, FDS models flame extinction as a result of oxygen dilution to be taking place. This directly affects the oxygen concentrations in the apartment. After 350 seconds, the experiments show the oxygen concentration dropping to values as low as 2 %vol. This is an indication that the extinction model of FDS is not designed to predict these low values when used properly. A forced solution lies in using unrealistic values for the critical flame temperature and lower oxygen level.

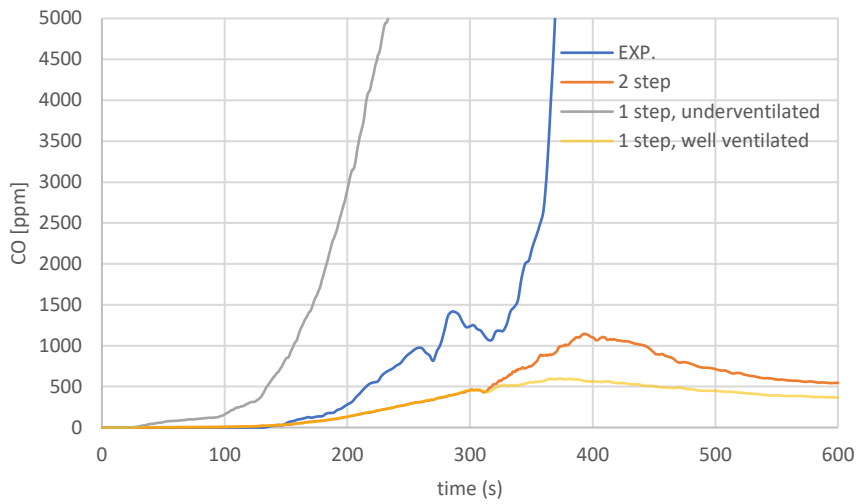


Oxygen concentrations using both the one-step and two-step combustion models

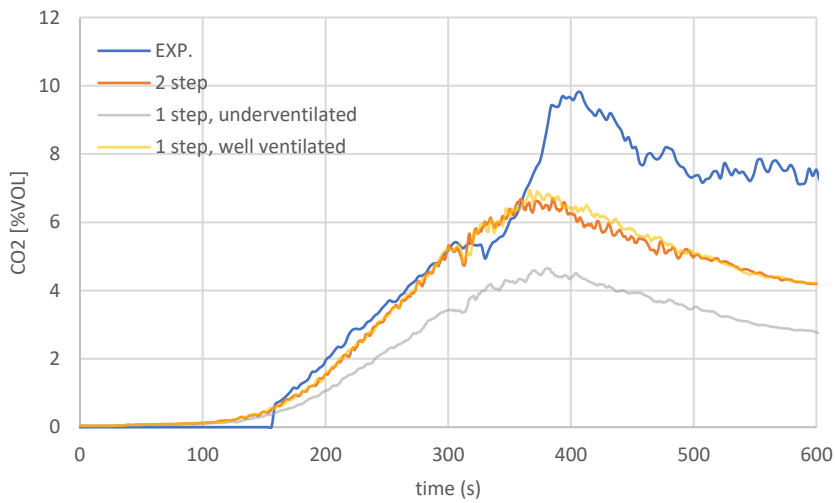
As the fire grows more under-ventilated, the two-step combustion model is expected to model an increase in CO-concentration in the apartment. While the increased concentration is clearly visible between the one- and two step combustion model, the results are nowhere near the measured concentrations. Given the nature of the two-step combustion model, the CO-concentrations are expected to increase exponentially at lower oxygen-concentrations. Modelling flame extinction to occur at lower oxygen concentrations is expected to lead to an exponential increase in CO in the apartment.

The CO<sub>2</sub>-concentrations in the apartment show the same trend as the oxygen concentrations, with the concentrations in the initial 350 seconds of the fire correlating well with the experimental data. Afterwards, the CO<sub>2</sub>-concentrations are underestimated. The CO<sub>2</sub>-concentrations in the apartment are expected to show an inverse trend of the exponential increase in CO in the apartment when using the two-step simple combustion model. As the oxygen-concentration in the apartment drops, CO and soot are prevented to oxidize to CO<sub>2</sub>.

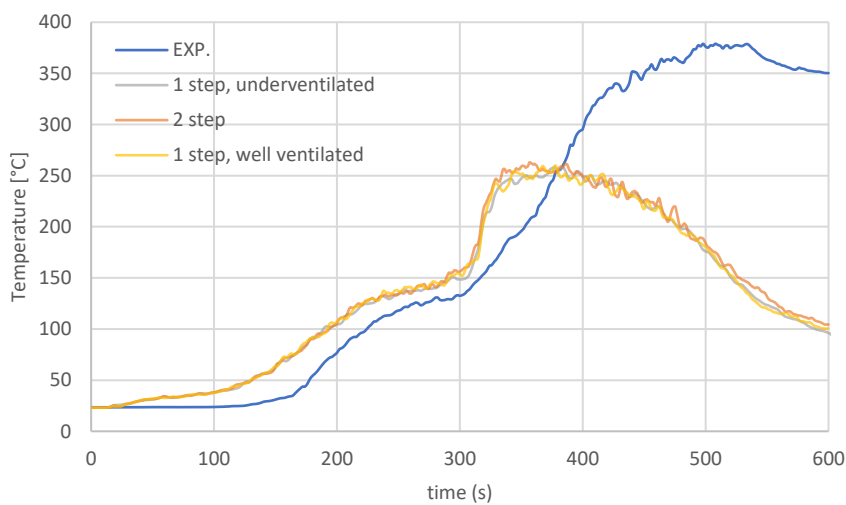
As a result of the FDS-simulations modelling flame extinction in an earlier stage than observed in the experiments, the temperatures in the enclosure are gravely underestimated.



CO concentrations in the apartment for different setups



CO<sub>2</sub> concentrations in the apartment



Temperatures at thermocouple TK1.1.2

### (mis)Using the extinction model

To effectively model CO-formation in the apartment as a result of oxygen dilution, extinction needs to be modelled in a way that more closely follows the oxygen concentration in the apartment. To that extent, a parametric study is carried out to study the effects of different parameters related to the extinction model. The default extinction model of FDS, extinction model 2, is used. The lower oxygen limit and critical flame temperature are changed incrementally until a reasonable fit with the experimental data is found. Note that the used values might not be realistic.

Figure 53 shows several simulation results for the oxygen concentrations at the measuring tree in the apartment compared with the experimental data. Both results for a lower oxygen limit of 0,08 and 0,07 show an overall good resemblance with the experimental data.

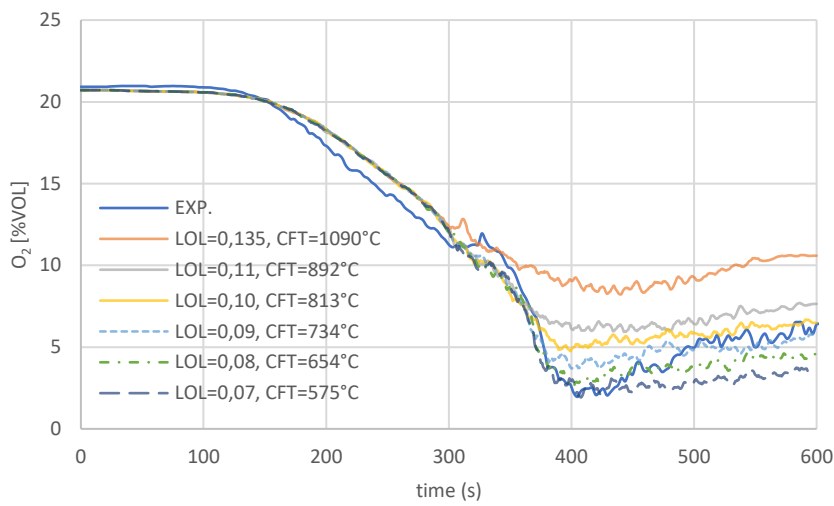
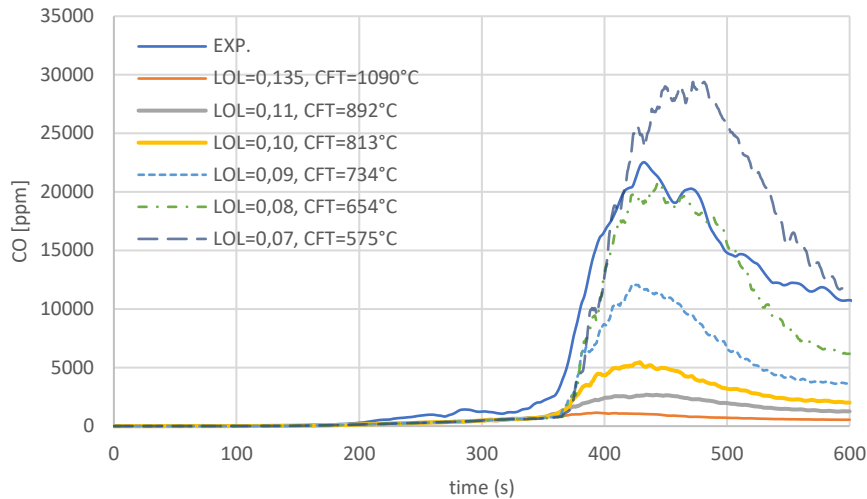


Figure 90: oxygen concentrations in the apartment for different values associated with the extinction model

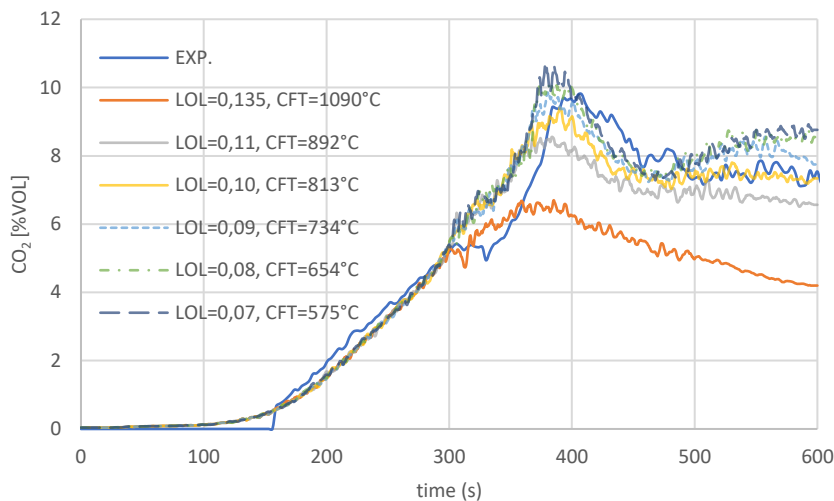
As discussed in the previous paragraph, the CO-concentrations are expected to increase exponentially at lower oxygen-concentrations in the apartment. This is observed in Figure 54. While some nuance differences are observable. The overall trends and maximum values for most notably the results using a lower oxygen limit of 0,08 and a critical flame temperature of 654°C show good comparison with the experimental data. At around 500 seconds, the oxygen-concentrations are simulated to be lower when compared with the experimental values while the CO-concentrations are found to be higher in the experiments. The inverse is true for the CO<sub>2</sub>-levels in the enclosure. This might be explainable through a more smoldering type of combustion, which was also observed in scenario 1 and is not further elaborated on.

The CO<sub>2</sub>- levels in the enclosure show an overall good correlation with the experimental data. Overall, the gas-concentrations in the enclosure are predicted to an acceptable level of accuracy when using values for the extinction model to fit the experimental data.

Given the fact that the fuel-to-air ratio is transient over the duration of the fire simulations, the critical flame temperature should also be of a dynamic nature to more accurately predict flame extinction. This however, is currently not implemented in FDS.



CO-concentrations in the apartment for different values associated with the extinction model



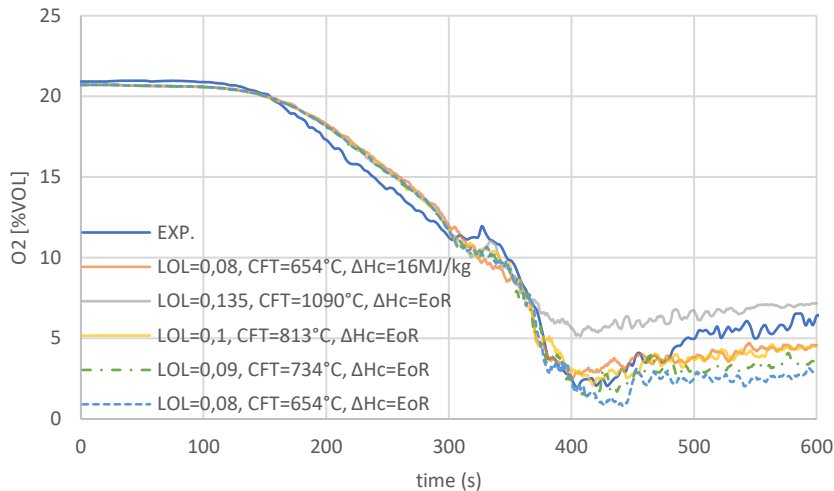
CO<sub>2</sub> concentrations in the apartment, using different values associated with the extinction model.

### Effective heat of combustion

In the previous simulation results, the effective heat of combustion was chosen based on the thermocouple measurements. The main issue however, is the fact that these measurements might not be a reliable representation of the actual gas-phase temperatures occurring near the measurements trees due to reasons outlined earlier in this document. While the calculated effective heat of combustion of 16 MJ/kg is based on the maximum temperatures measured and it was shown to yield adequate results in chapter 6, some simulations are carried out with the effective heat of combustion being calculated by FDS through the enthalpies of reaction/formation of the involved species. Calculating the overall effective heat of combustion through this methodology results in a value of approximately 21,1 MJ/kg, which more closely fits bench-scale measurement results [23]. Should there not be sufficient oxygen available for subsequent reaction to occur, the effective heat of combustion is lowered by the energy that would otherwise be generated by that reaction.

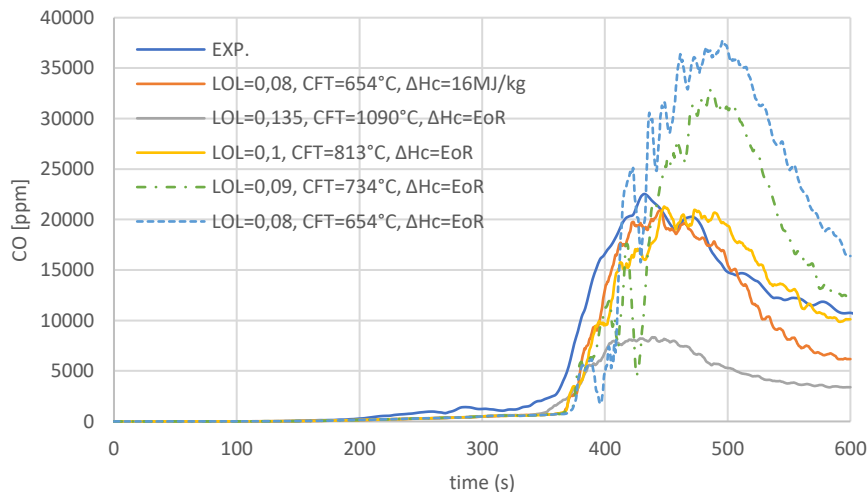
The effective heat of combustion affects the critical flame temperature. Therefore, the parameters associated with the extinction model are re-calibrated to fit the oxygen measurements in the apartment. To compare the simulation results with earlier results using a static effective heat of combustion of 16 MJ/kg, results for a lower oxygen limit of 0,08 are shown as well.

All simulations show to follow the oxygen concentrations in the apartment to an adequate level of accuracy in the initial 370 seconds. Afterwards, significant differences are observable. Overall, the scenario using a lower oxygen limit of 0,1, a critical flame temperature of 813°C and an effective heat of combustion based on the enthalpies of the involved species ('EoR' in the figures) fits the experimental data best. The oxygen concentrations are comparable with the simulation results from the previous paragraph using a static effective heat of combustion.



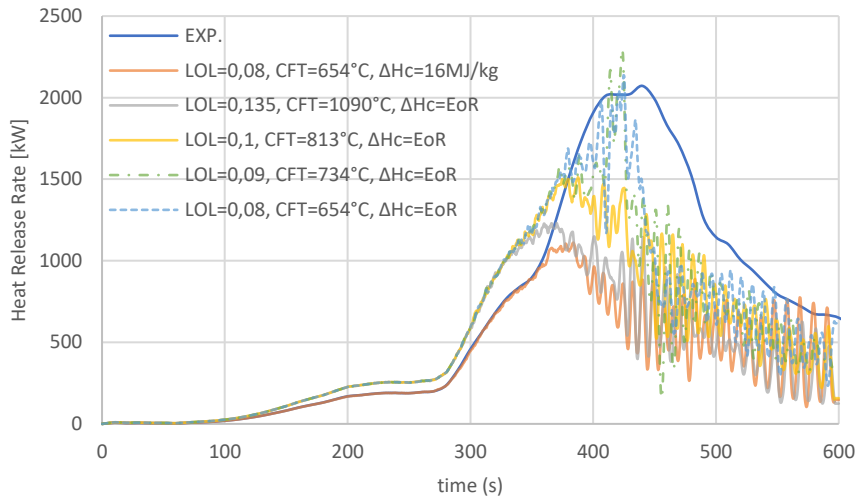
O<sub>2</sub> concentration using an enthalpy based effective heat of combustion for different parameters

The following figure shows the CO-concentrations in the apartment for the different numerical setups. Once more, the results of the simulations using a lower oxygen limit of 0,1 show the best correlation with both the experimental data and the results using a static heat of combustion. Nuance differences are explainable through small differences oxygen concentration enclosure which results in a difference in CO generation.



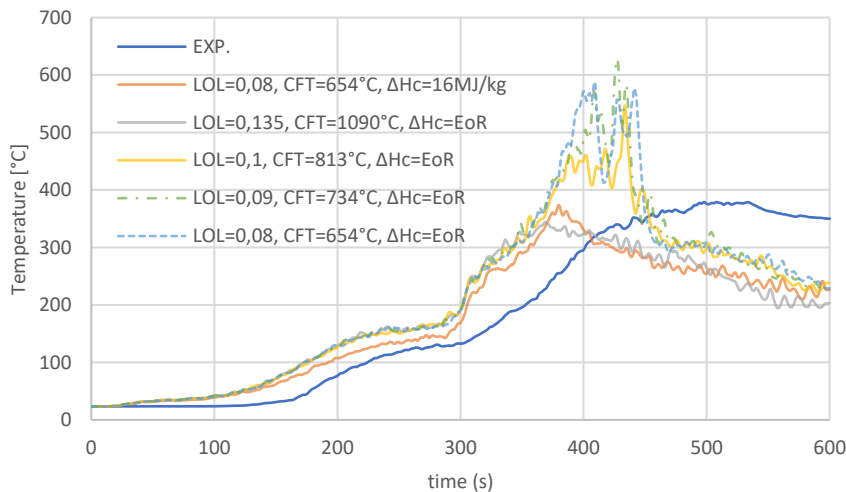
CO concentration using an enthalpy based effective heat of combustion for different parameters

The following figure shows both the experimental heat release rate based on a effective heat of combustion of 16 MJ/kg and the simulation results. In all scenarios, extinction is modelled to occur at approximately 370 seconds. The heat release rate for the simulations using a effective heat of combustion based on the enthalpies of the involved species however, is significantly higher when compared to the results when using a static effective heat of combustion.



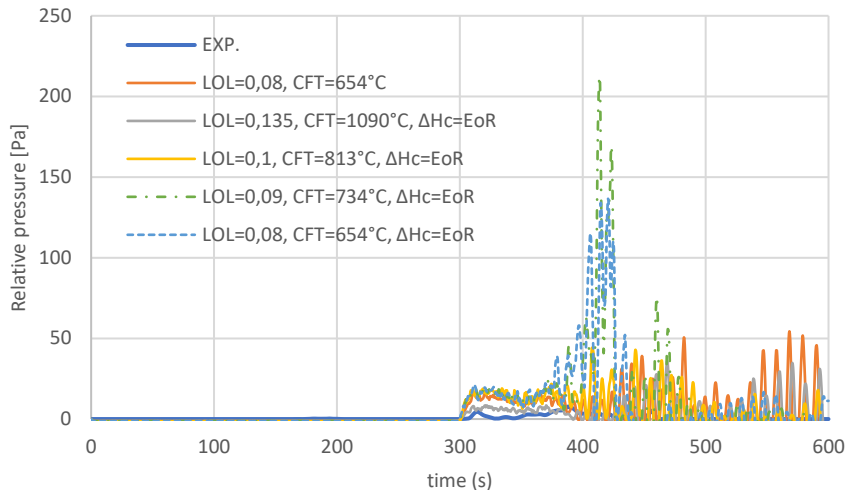
Heat Release Rate using an enthalpy based effective heat of combustion for different parameters

The higher heat release rate results in significantly higher temperatures in the domain, especially between 370 and 460 seconds. While the measured temperatures might not be a reliable representation of the actual gas phase temperatures, the trends and maximum temperatures are expected to correlate to some extent with the simulated temperatures. The following image shows the simulated temperatures compared to the experimental data. After approximately 450 seconds, all simulations show more or less the same temperatures. The simulation using a static effective heat of combustion showcases a maximum temperature that fits the experimental data quite well. In the experiments, the temperatures and thus the Heat Release Rate remain more or less the same.



Temperatures measured in thermocouple TK1,1,2 (at 2 meters height)

These higher gas phase temperatures should lead to significant increased relative pressures in both the apartment and the corridor. The following figure shows the relative pressure in the corridor. The experimental data shows only a limited increase in pressure after the door was opened, while the simulations using a effective heat of combustion based on the enthalpies of the involved species show a significant increase in pressure with peaks up to 100-150 Pa occurring. Note that the initial results using a static effective heat of combustion also show a higher pressure buildup compared to the experimental data. This indicates that the leakage area in the corridor might in reality be higher than initially assumed. This is discussed in the next paragraph.



Relative pressures measured in the corridor at measurement tree B5

While using an effective heat release rate based on the enthalpies of the involved species might theoretically be more correct, the simulation results show quite an over-estimation of most notably the temperatures and pressures in the enclosures. This indicates the Heat Release Rate is overestimated when using this method. The initially used value of 16 MJ/kg more closely fits the experimental results.

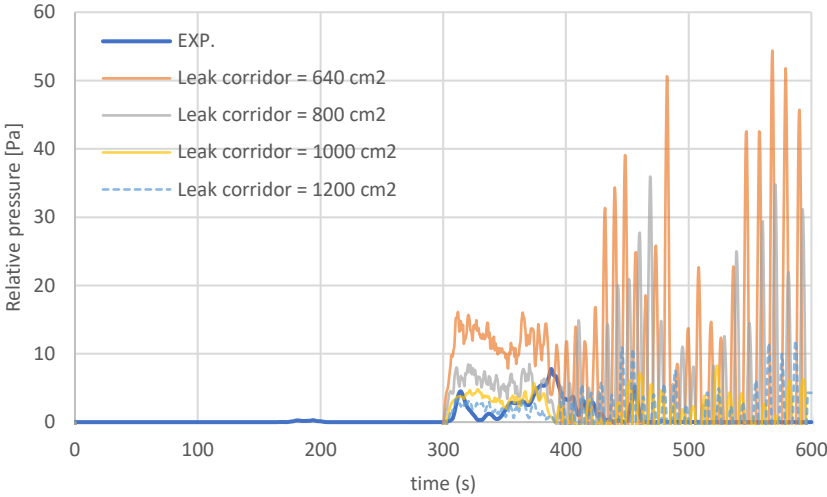
#### Airtightness of the corridor

Given the results shown in the previous paragraphs, the leakage area in the corridor is initially underestimated. Therefore, the pressures in the corridor are studied using different settings for the airtightness of the enclosure. The airtightness of the corridor is modelled using the bulk-leakage method. No information on the leak pressure exponent is known. Therefore, the default value of 0,5 is used (no increase in leakage area at higher pressures is assumed). Given the low measured pressures in the corridor, the exponent is expected to be of negligible influence on the overall pressure development. Simulations were run using:

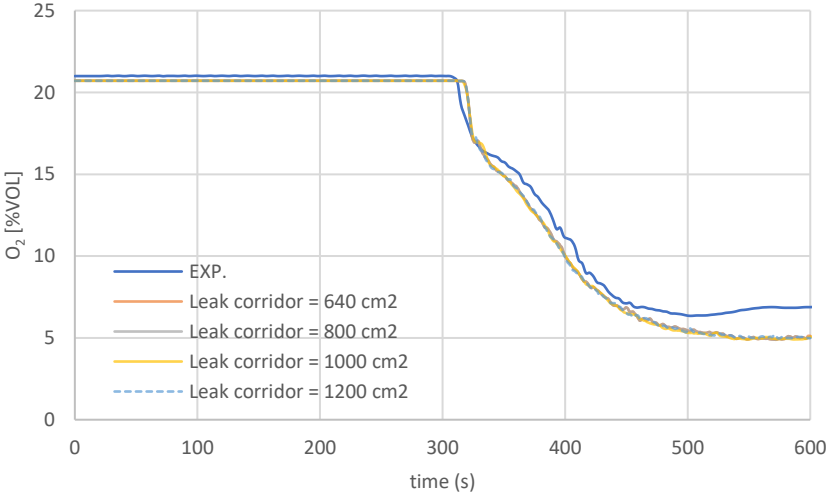
- A lower oxygen limit of 0,08 and a critical flame temperature of 654°C, as these result in the best fit regarding the gas-concentrations best;
- A leakage area in the apartment of 130 cm<sup>2</sup>, of which 20 cm<sup>2</sup> is associated with the door to the corridor;
- Multiple fast reactions in series using the two-step simple combustion model at default settings;
- A static effective heat of combustion of 16 MJ/kg.
- Heat Release Rate modelled using a ramp.

The following image shows the pressure evolution at measurement tree B5 for different leakage areas in the corridor. Using a leakage area of 640 m<sup>2</sup> results in a significant overestimate of the fire-induced pressure in the corridor. Increasing the leakage area logically leads to lower pressures. Note that the pressures at 400 seconds onwards start to oscillate due to the way the bulk leakage method works. Furthermore, the results from around 370 seconds onwards are dictated by the extinction model. Therefore, the validity of the results is limited.

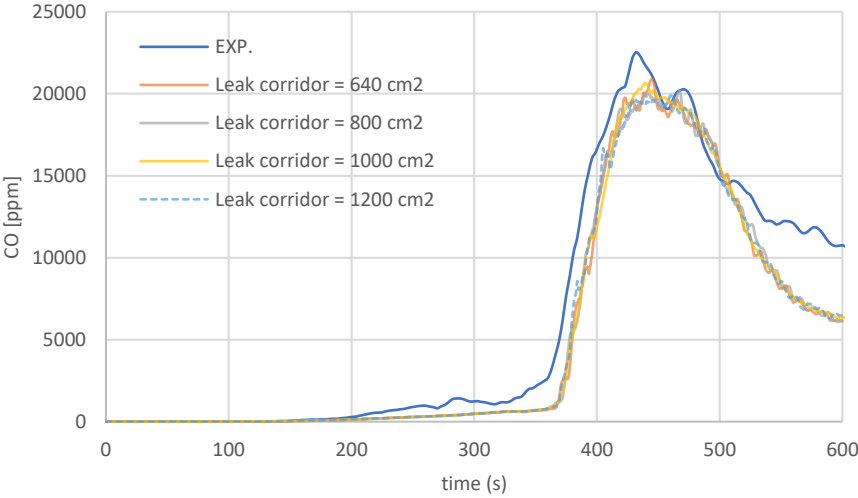
Other than the fire-induced pressure in the corridor, the effects of the leakage area in the corridor is of secondary importance. No significant differences are observed in both the O<sub>2</sub> and CO concentrations at 1,5 meters at measurement tree B5. A leakage area of 1.000 cm<sup>2</sup> is shown to fit the experimental data best.



pressure evolution in the corridor at measurement tree B5



O<sub>2</sub> concentration at measurement tree B5



CO concentration at measurement tree B5

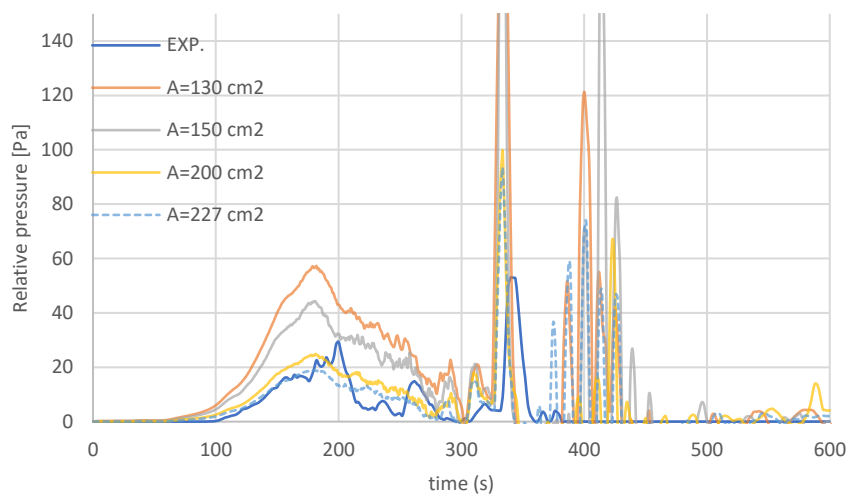
### Case study 3: a-priori parametric study fire-induced pressure

The measured airtightness of apartment 1.21 is somewhat higher than the airtightness of apartment 1.19. As was the case with case study 2, alterations to the enclosure were made to make the airtightness of both apartments more identical. The exact airtightness therefore is not known. Given the carried out adjustments to the enclosure, the airtightness of apartment 1.21 is expected to be more or less identical with apartment 1.19. Therefore, the same value as the one used for case study (leakage area of 130 cm<sup>2</sup> with a leak pressure exponent of 0,56) is used as a starting point.

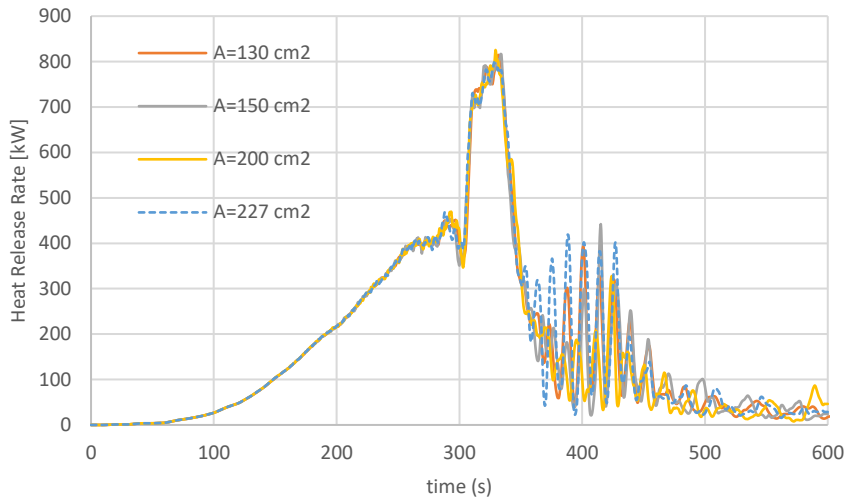
#### Apartment

The measured value (227 cm<sup>2</sup>) for apartment 1.21 prior to the experiments might not be representative as adjustments to the enclosure were made to make the airtightness comparable with apartment 1.19. Therefore the initial setting for leakage area in the apartment was set at 130 cm<sup>2</sup>, which was found to give appropriate results for apartment 1.19. The actual leakage area is assumed to lie anywhere in between these two values. Therefore, the effects of the leakage are once again studied before a numerical setting for the final simulations is chosen. In the following images, the results for a total leakage area of 130, 150, 200 and 227 cm<sup>2</sup> are shown. Leakage is modelled using the bulk leakage method, with the exception of the door between the apartment and the corridor, for which the localized leakage method was used. The leakage area over the door is set at 20 cm<sup>2</sup>. 75% of the leakage area is attributed to the bottom of the door. The remaining 25% is distributed evenly over top and two sides. All simulations use a leak pressure exponent of 0,56, which was measured (but might have changed).

Notice that the upper-limit for the measurements made with the more accurate 'PL' equipment is 50 Pa. The results from that equipment are shown below, while substantially higher peaks were found using the 'PH' equipment.



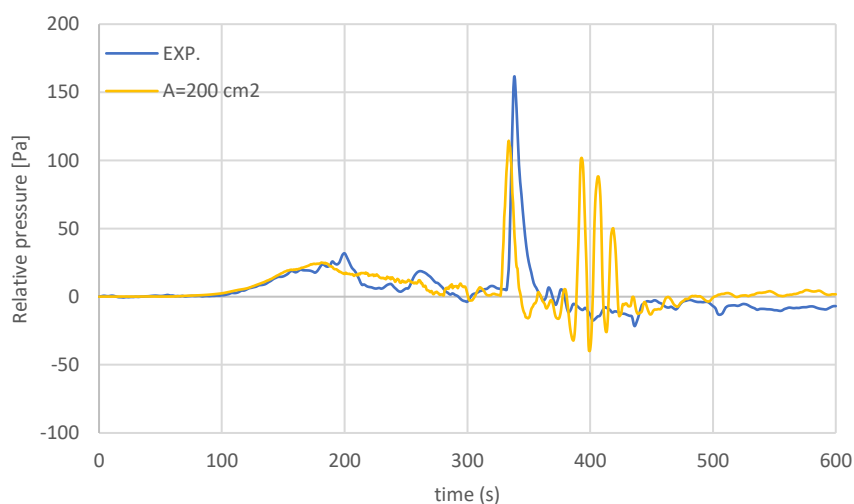
Pressure evolution in the apartment for different leakage areas



Heat Release Rate for different simulations

Using a leakage area of 130 cm<sup>2</sup> and 150 cm<sup>2</sup> clearly over-estimate the initial pressure-rise in the apartment while both a leakage area of 200 and 227 cm<sup>2</sup> show an appropriate correlation. The peak at around 350 seconds is significantly over-estimated by FDS in all studied simulations and starts somewhat earlier. This coincides with the first time in the simulation in which flame extinction is modelled, as shown in the previous figure. Therefore, at this time the fire-induced pressure is heavily affected by the extinction model.

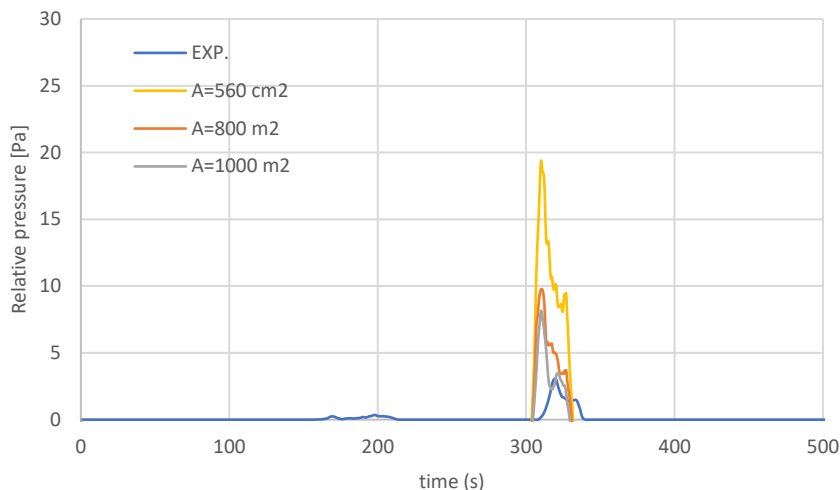
Peaks in the pressure from 400 seconds onwards are a result of oscillations due to the bulk leakage model. A comparison with the simulation data for a leakage area of 200 cm<sup>2</sup> with the experimental data for the equipment capable of measuring under-pressures is shown in the following image. If the limited accuracy and wide resolution of the used equipment and the limitations of the bulk-leakage model are taken into account, the simulation results correlate quite well with the experimental data, with the exception of the pressure oscillations around 400 seconds. The oscillations are a result of the bulk leakage model in combination with the extinction model used. Based on this, a leakage area of 200 cm<sup>2</sup> is chosen to carry out the remaining simulations.



Comparison of the experimental data for measuring under-pressures with simulation results.

### Fire-induced pressure in the corridor

After opening the door, the experimental data shows a small but pronounced peak in pressure. No measurements for under-pressure were done in the corridor. This comparison therefore only takes into account over-pressures. In the simulations carried out to study the airtightness of the apartment in the previous paragraph, a leakage area of 560 cm<sup>2</sup> for the corridor was used. In case study 2, this value was found to give over-estimates for the pressure. Other units of interest (gas concentrations and temperatures) were found not to be affected by the leakage area in the corridor and are therefore not studied in this case study. The following figure gives the pressure evolution in the corridor at measuring tree B5 for a leakage area of 560, 800 and 1.000 cm<sup>2</sup>.

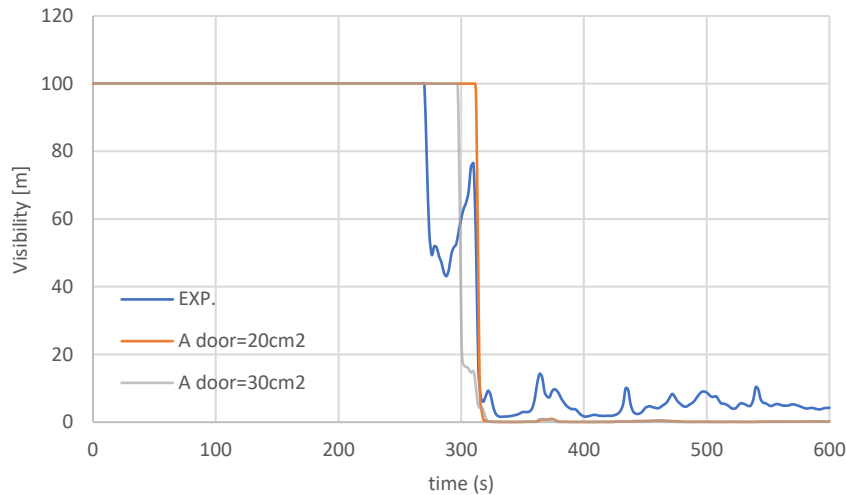


Fire-induced pressure in the corridor at measuring tree B5

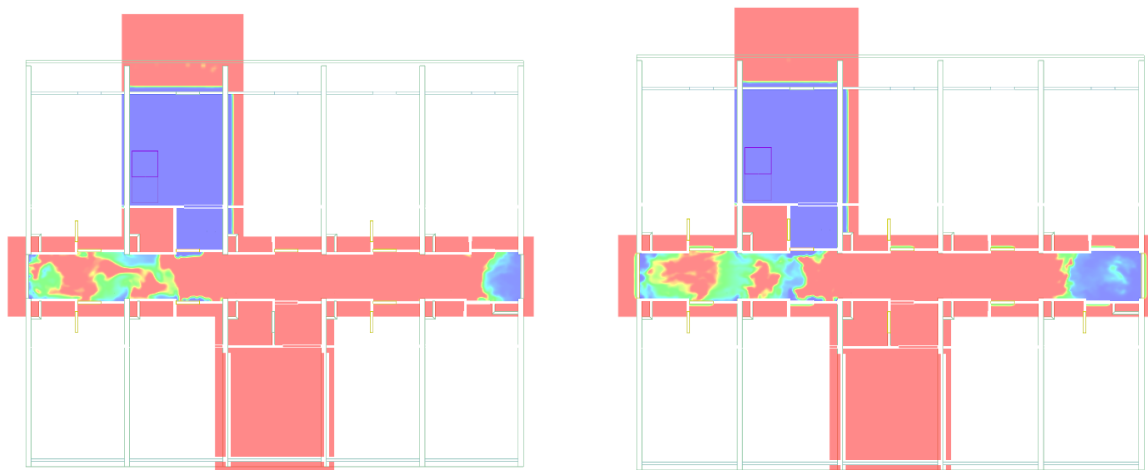
Prior to opening of the door at 300 seconds, no significant pressure buildup is observed. Directly after opening the door, pressure rises in both the experimental and simulation data. The experimental values develop somewhat slower. The pressure peak however, is in the order of a couple of Pascal, which makes the results sensitive to both measurement uncertainties and external influences such as wind. The results for a leakage area of 1.000 cm<sup>2</sup> shows the best correlation with the experimental data and is therefore used to carry out the remaining simulations.

### Airtightness of the door

The leakage area attributed to the door will affect the mass flow from the apartment towards the corridor prior to opening the door. The main affected attribute is the visibility in the corridor. The experimental data shows visibility dropping prior to opening the door at a height of 1,5 meters at measuring tree B6. Simulations ran with an airtightness of 20 cm<sup>2</sup> and 30 cm<sup>2</sup>. The used distribution is the same (bottom 75%, rest 25 %) as in the other casestudies. Both simulations do not capture the drop in visibility as measured in the experiments. As was the case in case study 2, this can most likely be attributed to the manner heat losses over the leakage paths are accounted for in FDS and over- or underestimates in the pressure evolution in the apartment prior to the door being opened.



Visibility at measurement tree B6 and a height of 1,5 meters

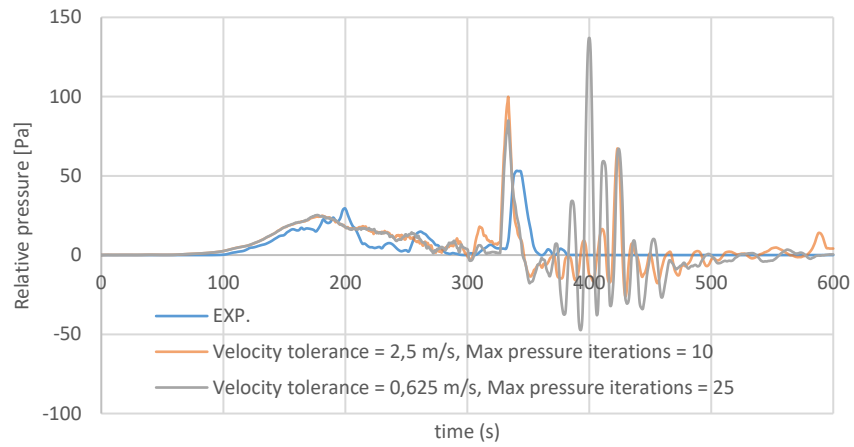


Visibility at a height of 1,5 meters in the enclosure at  $t=300$  seconds. Door leakage area left:  $20\text{cm}^2$ , right:  $30\text{cm}^2$ . Red=100 meters, blue=0 meters

### Maximum pressure iterations

In multiple mesh FDS runs the simplified form of the Poisson equation otherwise used in single mesh-runs cannot be used to calculate the global pressure solution. In these cases, the simplified Poisson solver is used per mesh in parallel. The pressure field on each mesh boundary is forced to match the adjacent one by an iterative approach. This results in a slight error in velocity at the mesh boundary. To limit the error, several iterations are run to reach the velocity tolerance which by default is half the cell width ( $\delta x/2$  or  $2,5\text{ m/s}$ ). The maximum number of iterations is set at 10 by default to limit excessive computational work.

Given the fact that this thesis uses multiple mesh FDS runs and the results for relative pressure show a oscillating behavior, one simulation is run with a smaller velocity tolerance ( $\delta x/8$  or  $0,625\text{ m/s}$ ) and a maximum of 25 pressure iterations. Results are shown in the following image. Indeed, the simulation using a lower velocity tolerance needs more iterations (16 for the normative mesh) than the initial setup (5 iterations for the normative mesh). Results in the early stage of the fire show no clear differences while the oscillations in the setup with the smaller velocity tolerance are more outspoken. Given the fact that the simulations with a lower velocity tolerance take approximately 25% longer to complete and the differences are somewhat limited, the default settings are used.



pressure evolution using different setups for the pressure solver

## APPENDIX 7: INPUT FILES (PRIMARY ONLY)

---

Input files for sensitivity studies are available on inquiry.

### Case study 1: balcony door open

v1\_8\_5\_cm.fds

Generated by PyroSim - Version 2021.4.1201

11-mrt-2022 10:55:56

```
&HEAD CHID='v1_8_5_cm', TITLE='simulation experiment fine mesh 05-07-2019 afternoon 1.19 [balcony door open door open after 5 min] PRES'
```

```
&TIME T_END=1000.0/
```

```
&DUMP DT_ISO=1.0, DT_PART=5.0, DT_SL3D=0.25/
```

```
&MISC TMPA=31.8, MAXIMUM_VISIBILITY=100.0/
```

```
&MESH ID='MESH00', IJK=46,14,32, XB=6.6,11.2,8.4,9.8,2.6,5.8, MPI_PROCESS =0/
&MESH ID='MESH01', IJK=23,23,16, XB=6.6,11.2,3.8,8.4,2.6,5.8, MPI_PROCESS =1/
&MESH ID='MESH02', IJK=40,31,64, XB=-1.4,0.6,9.8,11.35,2.6,5.8, MPI_PROCESS =2/
&MESH ID='MESH03', IJK=40,31,64, XB=0.6,2.6,9.8,11.35,2.6,5.8, MPI_PROCESS =3/
&MESH ID='MESH04', IJK=40,31,64, XB=2.6,4.6,9.8,11.35,2.6,5.8, MPI_PROCESS =4/
&MESH ID='MESH05', IJK=40,31,64, XB=4.6,6.6,9.8,11.35,2.6,5.8, MPI_PROCESS =5/
&MESH ID='MESH06', IJK=40,31,64, XB=6.6,8.6,9.8,11.35,2.6,5.8, MPI_PROCESS =6/
&MESH ID='MESH07', IJK=40,31,64, XB=8.6,10.6,9.8,11.35,2.6,5.8, MPI_PROCESS =7/
&MESH ID='MESH08', IJK=40,31,64, XB=10.6,12.6,9.8,11.35,2.6,5.8, MPI_PROCESS =8/
&MESH ID='MESH09', IJK=40,31,64, XB=12.6,14.6,9.8,11.35,2.6,5.8, MPI_PROCESS =9/
&MESH ID='MESH10', IJK=40,31,64, XB=14.6,16.6,9.8,11.35,2.6,5.8, MPI_PROCESS =10/
&MESH ID='MESH11', IJK=46,31,64, XB=16.6,18.9,9.8,11.35,2.6,5.8, MPI_PROCESS =11/
&MESH ID='MESH12', IJK=40,31,64, XB=-1.4,0.6,11.35,12.9,2.6,5.8, MPI_PROCESS =12/
&MESH ID='MESH13', IJK=40,31,64, XB=0.6,2.6,11.35,12.9,2.6,5.8, MPI_PROCESS =13/
&MESH ID='MESH14', IJK=40,31,64, XB=2.6,4.6,11.35,12.9,2.6,5.8, MPI_PROCESS =14/
&MESH ID='MESH15', IJK=40,31,64, XB=4.6,6.6,11.35,12.9,2.6,5.8, MPI_PROCESS =15/
&MESH ID='MESH16', IJK=40,31,64, XB=6.6,8.6,11.35,12.9,2.6,5.8, MPI_PROCESS =16/
&MESH ID='MESH17', IJK=40,31,64, XB=8.6,10.6,11.35,12.9,2.6,5.8, MPI_PROCESS =17/
&MESH ID='MESH18', IJK=40,31,64, XB=10.6,12.6,11.35,12.9,2.6,5.8, MPI_PROCESS =18/
&MESH ID='MESH19', IJK=40,31,64, XB=12.6,14.6,11.35,12.9,2.6,5.8, MPI_PROCESS =19/
&MESH ID='MESH20', IJK=40,31,64, XB=14.6,16.6,11.35,12.9,2.6,5.8, MPI_PROCESS =20/
&MESH ID='MESH21', IJK=46,31,64, XB=16.6,18.9,11.35,12.9,2.6,5.8, MPI_PROCESS =21/
&MESH ID='MESH22', IJK=46,30,64, XB=10.6,12.9,12.9,14.4,2.6,5.8, MPI_PROCESS =22/
&MESH ID='MESH23', IJK=46,30,64, XB=10.6,12.9,14.4,15.9,2.6,5.8, MPI_PROCESS =23/
&MESH ID='MESH24', IJK=46,30,64, XB=10.6,12.9,15.9,17.4,2.6,5.8, MPI_PROCESS =24/
&MESH ID='MESH25', IJK=46,30,64, XB=10.6,12.9,17.4,18.9,2.6,5.8, MPI_PROCESS =25/
&MESH ID='MESH26', IJK=48,30,64, XB=12.9,15.3,12.9,14.4,2.6,5.8, MPI_PROCESS =26/
&MESH ID='MESH27', IJK=48,30,64, XB=12.9,15.3,14.4,15.9,2.6,5.8, MPI_PROCESS =27/
&MESH ID='MESH28', IJK=48,30,64, XB=12.9,15.3,15.9,17.4,2.6,5.8, MPI_PROCESS =28/
&MESH ID='MESH29', IJK=48,30,64, XB=12.9,15.3,17.4,18.9,2.6,5.8, MPI_PROCESS =29/
&MESH ID='MESH30', IJK=47,26,32, XB=10.6,15.3,18.9,21.5,2.6,5.8, MPI_PROCESS =30/
```

```
&ZONE ID='Hallway leakage 1.19', XB=-0.6,18.4,10.4,12.3,2.8,5.2, LEAK_AREA=0.056/
```

```
&SPEC ID='Polyurethane GM21', FORMULA='C1H1.8O0.3N0.05'/
```

```
&PART ID='Flow tracer',
```

```
  FYI='Flow tracer',
```

```
  MASSLESS=.TRUE.,
```

```
  MONODISPERSE=.TRUE.,
```

```
  RGB=255,102,102,
```

```
  AGE=60.0/
```

```
&REAC ID='Polyurethane (well ventilated)',
```

```
  FYI='Polyurethane',
```

```
  FUEL='Polyurethane GM21',
```

```
  C=1.0,
```

```
  H=1.8,
```

O=0.3,  
 N=0.05,  
 CRITICAL\_FLAME\_TEMPERATURE=1140.0,  
 AUTO\_IGNITION\_TEMPERATURE=400.0,  
 CO\_YIELD=0.042846,  
 SOOT\_YIELD=0.139233,  
 HCN\_YIELD=0.02,  
 EPUMO2=9295.303237,  
 AIT\_EXCLUSION\_ZONE(1:6,1)=11,12,14.2,16.2,2.8,5.8/

EPUMO2 calculated from chemical equilibrium as 'HEAT\_OF\_COMBUSTION' did not work. Value results in an effective heat of combustion of 16 MJ/kg

//

&PROP ID='TK1.1.0 props', DIAMETER=0.00075/  
 &PROP ID='TK1.1.1 props', DIAMETER=0.00075/  
 &PROP ID='TK1.1.2 props', DIAMETER=0.00075/  
 &PROP ID='TK1.1.3 props', DIAMETER=0.00075/  
 &PROP ID='TK1.1.4 props', DIAMETER=0.00075/  
 &PROP ID='TK1.1.5 props', DIAMETER=0.00075/  
 &PROP ID='TK1.1.6 props', DIAMETER=0.00075/  
 &PROP ID='TK1.1.1alt props', DIAMETER=0.00075/  
 &PROP ID='TK1.1.2alt props', DIAMETER=0.00075/  
 &PROP ID='TK1.1.3alt props', DIAMETER=0.00075/  
 &PROP ID='TK1.1.4alt props', DIAMETER=0.00075/  
 &PROP ID='TK1.1.5alt props', DIAMETER=0.00075/  
 &PROP ID='TK1.1.6alt props', DIAMETER=0.00075/  
 &PROP ID='TK1.1.7alt props', DIAMETER=0.00075/  
 &PROP ID='TK1.1.6alt01 props', DIAMETER=0.00075/  
 &PROP ID='TK1.1.1alt01 props', DIAMETER=0.00075/  
 &PROP ID='TK1.1.2alt01 props', DIAMETER=0.00075/  
 &PROP ID='TK1.1.3alt01 props', DIAMETER=0.00075/  
 &PROP ID='TK1.1.4alt01 props', DIAMETER=0.00075/  
 &PROP ID='TK1.1.5alt01 props', DIAMETER=0.00075/  
 &PROP ID='TK1.1.7alt01 props', DIAMETER=0.00075/  
 &DEVC ID='CO(7)', QUANTITY='VOLUME FRACTION', SPEC\_ID='CARBON MONOXIDE', XYZ=14.2,13.1,4.3/  
 &DEVC ID='CO2(7)', QUANTITY='VOLUME FRACTION', SPEC\_ID='CARBON DIOXIDE', XYZ=14.2,13.1,4.3/  
 &DEVC ID='O2(7)', QUANTITY='VOLUME FRACTION', SPEC\_ID='OXYGEN', XYZ=14.2,13.1,4.3/  
 &DEVC ID='PP1,1,1', QUANTITY='PRESSURE', XYZ=14.2,13.1,3.0/  
 &DEVC ID='SP1,1,1', QUANTITY='RADIATIVE HEAT FLUX GAS', XYZ=14.2,13.1,4.3/  
 &DEVC ID='SP1,1,2', QUANTITY='RADIATIVE HEAT FLUX GAS', XYZ=14.2,13.1,3.1/  
 &DEVC ID='TK1.1.0', PROP\_ID='TK1.1.0 props', QUANTITY='THERMOCOUPLE', XYZ=14.2,13.1,5.2/  
 &DEVC ID='TK1.1.1', PROP\_ID='TK1.1.1 props', QUANTITY='THERMOCOUPLE', XYZ=14.2,13.1,5.0/  
 &DEVC ID='TK1.1.2', PROP\_ID='TK1.1.2 props', QUANTITY='THERMOCOUPLE', XYZ=14.2,13.1,4.8/  
 &DEVC ID='TK1.1.3', PROP\_ID='TK1.1.3 props', QUANTITY='THERMOCOUPLE', XYZ=14.2,13.1,4.6/  
 &DEVC ID='TK1.1.4', PROP\_ID='TK1.1.4 props', QUANTITY='THERMOCOUPLE', XYZ=14.2,13.1,4.3/  
 &DEVC ID='TK1.1.5', PROP\_ID='TK1.1.5 props', QUANTITY='THERMOCOUPLE', XYZ=14.2,13.1,3.7/  
 &DEVC ID='TK1.1.6', PROP\_ID='TK1.1.6 props', QUANTITY='THERMOCOUPLE', XYZ=14.2,13.1,3.1/  
 &DEVC ID='CO(11)', QUANTITY='VOLUME FRACTION', SPEC\_ID='CARBON MONOXIDE', XYZ=2.7,10.7,3.1/  
 &DEVC ID='CO(15)', QUANTITY='VOLUME FRACTION', SPEC\_ID='CARBON MONOXIDE', XYZ=2.7,10.7,4.3/  
 &DEVC ID='CO2(11)', QUANTITY='VOLUME FRACTION', SPEC\_ID='CARBON DIOXIDE', XYZ=2.7,10.7,3.1/  
 &DEVC ID='CO2(15)', QUANTITY='VOLUME FRACTION', SPEC\_ID='CARBON DIOXIDE', XYZ=2.7,10.7,4.3/  
 &DEVC ID='O2(11)', QUANTITY='VOLUME FRACTION', SPEC\_ID='OXYGEN', XYZ=2.7,10.7,3.1/  
 &DEVC ID='O2(15)', QUANTITY='VOLUME FRACTION', SPEC\_ID='OXYGEN', XYZ=2.7,10.7,4.3/  
 &DEVC ID='PP1,5,1', QUANTITY='PRESSURE', XYZ=2.7,10.7,3.0/  
 &DEVC ID='SB1,5,2', QUANTITY='RADIATIVE HEAT FLUX GAS', XYZ=2.7,10.7,3.1/  
 &DEVC ID='SP1,5,1', QUANTITY='RADIATIVE HEAT FLUX GAS', XYZ=2.7,10.7,4.3/  
 &DEVC ID='TK1,5,0', QUANTITY='THERMOCOUPLE', XYZ=2.7,10.7,5.15/  
 &DEVC ID='TK1,5,1', QUANTITY='THERMOCOUPLE', XYZ=2.7,10.7,5.0/  
 &DEVC ID='TK1,5,2', QUANTITY='THERMOCOUPLE', XYZ=2.7,10.7,4.8/  
 &DEVC ID='TK1,5,3', QUANTITY='THERMOCOUPLE', XYZ=2.7,10.7,4.6/  
 &DEVC ID='TK1,5,4', QUANTITY='THERMOCOUPLE', XYZ=2.7,10.7,4.3/  
 &DEVC ID='TK1,5,5', QUANTITY='THERMOCOUPLE', XYZ=2.7,10.7,3.7/  
 &DEVC ID='TK1,5,6', QUANTITY='THERMOCOUPLE', XYZ=2.7,10.7,3.1/  
 &DEVC ID='ZL1,5,1', QUANTITY='VISIBILITY', XYZ=2.7,10.7,4.3/

```

&DEVC ID='ZL1,5,2', QUANTITY='VISIBILITY', XYZ=2.7,10.7,3.1/
&DEVC ID='CO(21)', QUANTITY='VOLUME FRACTION', SPEC_ID='CARBON MONOXIDE', XYZ=15.7,10.8,3.1/
&DEVC ID='CO(23)', QUANTITY='VOLUME FRACTION', SPEC_ID='CARBON MONOXIDE', XYZ=15.7,10.8,4.3/
&DEVC ID='CO2(21)', QUANTITY='VOLUME FRACTION', SPEC_ID='CARBON DIOXIDE', XYZ=15.7,10.8,3.1/
&DEVC ID='CO2(23)', QUANTITY='VOLUME FRACTION', SPEC_ID='CARBON DIOXIDE', XYZ=15.7,10.8,4.3/
&DEVC ID='O2(21)', QUANTITY='VOLUME FRACTION', SPEC_ID='OXYGEN', XYZ=15.7,10.8,3.1/
&DEVC ID='O2(23)', QUANTITY='VOLUME FRACTION', SPEC_ID='OXYGEN', XYZ=15.7,10.8,4.3/
&DEVC ID='PP1,6,1', QUANTITY='PRESSURE', XYZ=15.7,10.8,3.0/
&DEVC ID='SB1,6,2', QUANTITY='RADIATIVE HEAT FLUX GAS', XYZ=15.7,10.8,3.1/
&DEVC ID='SP1,6,1', QUANTITY='RADIATIVE HEAT FLUX GAS', XYZ=15.7,10.8,4.3/
&DEVC ID='TK1,6,0', QUANTITY='THERMOCOUPLE', XYZ=15.7,10.8,5.15/
&DEVC ID='TK1,6,1', QUANTITY='THERMOCOUPLE', XYZ=15.7,10.8,5.0/
&DEVC ID='TK1,6,2', QUANTITY='THERMOCOUPLE', XYZ=15.7,10.8,4.8/
&DEVC ID='TK1,6,3', QUANTITY='THERMOCOUPLE', XYZ=15.7,10.8,4.6/
&DEVC ID='TK1,6,4', QUANTITY='THERMOCOUPLE', XYZ=15.7,10.8,4.3/
&DEVC ID='TK1,6,5', QUANTITY='THERMOCOUPLE', XYZ=15.7,10.8,3.7/
&DEVC ID='TK1,6,6', QUANTITY='THERMOCOUPLE', XYZ=15.7,10.8,3.1/
&DEVC ID='ZL1,6,1', QUANTITY='VISIBILITY', XYZ=15.7,10.8,4.3/
&DEVC ID='ZL1,6,2', QUANTITY='VISIBILITY', XYZ=15.7,10.8,3.1/
&DEVC ID='TEMP_FIRE_0,2', QUANTITY='TEMPERATURE', XYZ=11.5,15.2,3.6/
&DEVC ID='TEMP_FIRE_0,4', QUANTITY='TEMPERATURE', XYZ=11.5,15.2,3.8/
&DEVC ID='TEMP_FIRE_0,6', QUANTITY='TEMPERATURE', XYZ=11.5,15.2,4.0/
&DEVC ID='TEMP_FIRE_0,8', QUANTITY='TEMPERATURE', XYZ=11.5,15.2,4.2/
&DEVC ID='TEMP_FIRE_1,0', QUANTITY='TEMPERATURE', XYZ=11.5,15.2,4.4/
&DEVC ID='TEMP_FIRE_1,2', QUANTITY='TEMPERATURE', XYZ=11.5,15.2,4.6/
&DEVC ID='TEMP_FIRE_1,4', QUANTITY='TEMPERATURE', XYZ=11.5,15.2,4.8/
&DEVC ID='TEMP_FIRE_1,6', QUANTITY='TEMPERATURE', XYZ=11.5,15.2,5.0/
&DEVC ID='Positive hallway', QUANTITY='MASS FLOW +', XB=12.7,13.6,12.3,12.3,2.8,4.8/
&DEVC ID='Negative hallway', QUANTITY='MASS FLOW -', XB=12.7,13.6,12.3,12.3,2.8,4.8/
&DEVC ID='Positive balcony', QUANTITY='MASS FLOW +', XB=12.7,13.6,18.4,18.4,2.8,4.8/
&DEVC ID='Negative balcony', QUANTITY='MASS FLOW -', XB=12.7,13.6,18.4,18.4,2.8,4.8/
&DEVC ID='RH4', QUANTITY='LAYER HEIGHT', XB=7.4,7.4,10.7,10.7,2.8,5.4/
&DEVC ID='RH5', QUANTITY='LAYER HEIGHT', XB=11.2,11.2,10.7,10.7,2.8,5.4/
&DEVC ID='Oxygen_FIRE_0,2', QUANTITY='VOLUME FRACTION', SPEC_ID='OXYGEN', XYZ=11.5,15.2,3.6/
&DEVC ID='Oxygen_FIRE_0,4', QUANTITY='VOLUME FRACTION', SPEC_ID='OXYGEN', XYZ=11.5,15.2,3.8/
&DEVC ID='Oxygen_FIRE_0,6', QUANTITY='VOLUME FRACTION', SPEC_ID='OXYGEN', XYZ=11.5,15.2,4.0/
&DEVC ID='Oxygen_FIRE_0,8', QUANTITY='VOLUME FRACTION', SPEC_ID='OXYGEN', XYZ=11.5,15.2,4.2/
&DEVC ID='Oxygen_FIRE_1,0', QUANTITY='VOLUME FRACTION', SPEC_ID='OXYGEN', XYZ=11.5,15.2,4.4/
&DEVC ID='Oxygen_FIRE_1,2', QUANTITY='VOLUME FRACTION', SPEC_ID='OXYGEN', XYZ=11.5,15.2,4.6/
&DEVC ID='Oxygen_FIRE_1,4', QUANTITY='VOLUME FRACTION', SPEC_ID='OXYGEN', XYZ=11.5,15.2,4.8/
&DEVC ID='Oxygen_FIRE_1,6', QUANTITY='VOLUME FRACTION', SPEC_ID='OXYGEN', XYZ=11.5,15.2,5.0/
&DEVC ID='TK1.1.1alt', PROP_ID='TK1.1.1alt props', QUANTITY='THERMOCOUPLE', XYZ=13.9,13.1,5.2/
&DEVC ID='TK1.1.2alt', PROP_ID='TK1.1.2alt props', QUANTITY='THERMOCOUPLE', XYZ=13.9,13.1,5.0/
&DEVC ID='TK1.1.3alt', PROP_ID='TK1.1.3alt props', QUANTITY='THERMOCOUPLE', XYZ=13.9,13.1,4.8/
&DEVC ID='TK1.1.4alt', PROP_ID='TK1.1.4alt props', QUANTITY='THERMOCOUPLE', XYZ=13.9,13.1,4.6/
&DEVC ID='TK1.1.5alt', PROP_ID='TK1.1.5alt props', QUANTITY='THERMOCOUPLE', XYZ=13.9,13.1,4.3/
&DEVC ID='TK1.1.6alt', PROP_ID='TK1.1.6alt props', QUANTITY='THERMOCOUPLE', XYZ=13.9,13.1,3.7/
&DEVC ID='TK1.1.7alt', PROP_ID='TK1.1.7alt props', QUANTITY='THERMOCOUPLE', XYZ=13.9,13.1,3.1/
&DEVC ID='TK1.1.6alt01', PROP_ID='TK1.1.6alt01 props', QUANTITY='THERMOCOUPLE', XYZ=13.6,13.1,3.7/
&DEVC ID='TK1.1.1alt01', PROP_ID='TK1.1.1alt01 props', QUANTITY='THERMOCOUPLE', XYZ=13.6,13.1,5.2/
&DEVC ID='TK1.1.2alt01', PROP_ID='TK1.1.2alt01 props', QUANTITY='THERMOCOUPLE', XYZ=13.6,13.1,5.0/
&DEVC ID='TK1.1.3alt01', PROP_ID='TK1.1.3alt01 props', QUANTITY='THERMOCOUPLE', XYZ=13.6,13.1,4.8/
&DEVC ID='TK1.1.4alt01', PROP_ID='TK1.1.4alt01 props', QUANTITY='THERMOCOUPLE', XYZ=13.6,13.1,4.6/
&DEVC ID='TK1.1.5alt01', PROP_ID='TK1.1.5alt01 props', QUANTITY='THERMOCOUPLE', XYZ=13.6,13.1,4.3/
&DEVC ID='TK1.1.7alt01', PROP_ID='TK1.1.7alt01 props', QUANTITY='THERMOCOUPLE', XYZ=13.6,13.1,3.1/
&DEVC ID='TIMER->OUT', QUANTITY='TIME', XYZ=6.6,8.4,2.6, SETPOINT=300.0, INITIAL_STATE=.TRUE./
&DEVC ID='TIMER->OUT-2', QUANTITY='TIME', XYZ=6.6,8.4,2.6, SETPOINT=21.0/
&DEVC ID='TIMER->OUT-3', QUANTITY='TIME', XYZ=6.6,8.4,2.6, SETPOINT=56.0/
&DEVC ID='TIMER->OUT-4', QUANTITY='TIME', XYZ=6.6,8.4,2.6, SETPOINT=84.0/
&DEVC ID='TIMER->OUT-5', QUANTITY='TIME', XYZ=6.6,8.4,2.6, SETPOINT=110.0/
&DEVC ID='TIMER->OUT-6', QUANTITY='TIME', XYZ=6.6,8.4,2.6, SETPOINT=133.0/
&DEVC ID='TIMER->OUT-7', QUANTITY='TIME', XYZ=6.6,8.4,2.6, SETPOINT=154.0/
&DEVC ID='TIMER->OUT-8', QUANTITY='TIME', XYZ=6.6,8.4,2.6, SETPOINT=193.0/
&DEVC ID='TIMER->OUT-9', QUANTITY='TIME', XYZ=6.6,8.4,2.6, SETPOINT=211.0/
&DEVC ID='TIMER->OUT-10', QUANTITY='TIME', XYZ=6.6,8.4,2.6, SETPOINT=228.0/
&DEVC ID='TIMER->OUT-11', QUANTITY='TIME', XYZ=6.6,8.4,2.6, SETPOINT=244.0/

```

```
&DEVC ID='TIMER->OUT-12', QUANTITY='TIME', XYZ=6.6,8.4,2.6, SETPOINT=260.0/
&DEVC ID='TIMER->OUT-13', QUANTITY='TIME', XYZ=6.6,8.4,2.6, SETPOINT=274.0/
&DEVC ID='TIMER->OUT-14', QUANTITY='TIME', XYZ=6.6,8.4,2.6, SETPOINT=286.0/
&DEVC ID='TIMER->OUT-15', QUANTITY='TIME', XYZ=6.6,8.4,2.6, SETPOINT=298.0/
&DEVC ID='TIMER->OUT-16', QUANTITY='TIME', XYZ=6.6,8.4,2.6, SETPOINT=309.0/
&DEVC ID='TIMER->OUT-17', QUANTITY='TIME', XYZ=6.6,8.4,2.6, SETPOINT=319.0/
&DEVC ID='TIMER->OUT-18', QUANTITY='TIME', XYZ=6.6,8.4,2.6, SETPOINT=328.0/
&DEVC ID='TIMER->OUT-19', QUANTITY='TIME', XYZ=6.6,8.4,2.6, SETPOINT=337.0/
&DEVC ID='TIMER->OUT-20', QUANTITY='TIME', XYZ=6.6,8.4,2.6, SETPOINT=346.0/
&DEVC ID='TIMER->OUT-21', QUANTITY='TIME', XYZ=6.6,8.4,2.6, SETPOINT=354.0/
&DEVC ID='TIMER->OUT-22', QUANTITY='TIME', XYZ=6.6,8.4,2.6, SETPOINT=361.0/
&DEVC ID='TIMER->OUT-23', QUANTITY='TIME', XYZ=6.6,8.4,2.6, SETPOINT=367.0/
&DEVC ID='TIMER->OUT-24', QUANTITY='TIME', XYZ=6.6,8.4,2.6, SETPOINT=372.0/
&DEVC ID='TIMER->OUT-25', QUANTITY='TIME', XYZ=6.6,8.4,2.6, SETPOINT=376.0/
&DEVC ID='TIMER->OUT-26', QUANTITY='TIME', XYZ=6.6,8.4,2.6, SETPOINT=380.0/
&DEVC ID='TIMER->OUT-27', QUANTITY='TIME', XYZ=6.6,8.4,2.6, SETPOINT=383.0/
&DEVC ID='TIMER->OUT-28', QUANTITY='TIME', XYZ=6.6,8.4,2.6, SETPOINT=385.0/
&DEVC ID='TIMER->OUT-29', QUANTITY='TIME', XYZ=6.6,8.4,2.6, SETPOINT=387.0/
&DEVC ID='TIMER->OUT-30', QUANTITY='TIME', XYZ=6.6,8.4,2.6, SETPOINT=388.0/
&DEVC ID='TIMER->OUT-31', QUANTITY='TIME', XYZ=6.6,8.4,2.6, SETPOINT=394.0/
```

```
&MATL ID='GYPSUM PLASTER',
```

```
  FYI='Quintiere, Fire Behavior - NIST NRC Validation',
  SPECIFIC_HEAT=0.84,
  CONDUCTIVITY=0.48,
  DENSITY=1440.0/
```

```
&MATL ID='CONCRETE',
```

```
  FYI='NBSIR 88-3752 - ATF NIST Multi-Floor Validation',
  SPECIFIC_HEAT=1.04,
  CONDUCTIVITY=1.8,
  DENSITY=2280.0/
```

```
&MATL ID='Calcium stone',
```

```
  SPECIFIC_HEAT=0.84,
  CONDUCTIVITY=0.75,
  DENSITY=1900.0/
```

```
&MATL ID='YELLOW PINE',
```

```
  FYI='Quintiere, Fire Behavior - NIST NRC Validation',
  SPECIFIC_HEAT=2.85,
  CONDUCTIVITY=0.14,
  DENSITY=640.0/
```

```
&MATL ID='CALCIUM SILICATE',
```

```
  FYI='NBSIR 88-3752 - NBS Multi-Room Validation',
  SPECIFIC_HEAT_RAMP='CALCIUM SILICATE_SPECIFIC_HEAT_RAMP',
  CONDUCTIVITY=0.12,
  DENSITY=720.0,
  EMISSIVITY=0.83/
```

```
&RAMP ID='CALCIUM SILICATE_SPECIFIC_HEAT_RAMP', T=20.0, F=1.25/
```

```
&RAMP ID='CALCIUM SILICATE_SPECIFIC_HEAT_RAMP', T=200.0, F=1.25/
```

```
&RAMP ID='CALCIUM SILICATE_SPECIFIC_HEAT_RAMP', T=300.0, F=1.33/
```

```
&RAMP ID='CALCIUM SILICATE_SPECIFIC_HEAT_RAMP', T=600.0, F=1.55/
```

```
&MATL ID='DOUBLE GLAZING',
```

```
  SPECIFIC_HEAT=0.72,
  CONDUCTIVITY=5.68E-3,
  DENSITY=2500.0/
```

```
&SURF ID='CONCRETE_FLOORS',
```

```
  RGB=146,202,166,
  BACKING='VOID',
  MATL_ID(1,1)='GYPSUM PLASTER',
  MATL_ID(2,1)='CONCRETE',
  MATL_MASS_FRACTION(1,1)=1.0,
  MATL_MASS_FRACTION(2,1)=1.0,
  THICKNESS(1:2)=1.0E-3,0.2/
```

```
&SURF ID='CONCRETE_WALLS',
```

```
  RGB=146,202,166,
  BACKING='VOID',
```

```

MATL_ID(1,1)=CONCRETE',
MATL_MASS_FRACTION(1,1)=1.0,
THICKNESS(1)=0.2/
&SURF ID='CALCIUM SILICATE WALLS',
COLOR='WHITE',
BACKING='VOID',
MATL_ID(1,1)='Calcium stone',
MATL_MASS_FRACTION(1,1)=1.0,
THICKNESS(1)=0.1/
&SURF ID='DOOR',
RGB=204,204,0,
BACKING='VOID',
MATL_ID(1,1)='YELLOW PINE',
MATL_MASS_FRACTION(1,1)=1.0,
THICKNESS(1)=0.05/
&SURF ID='Windows fire room',
RGB=146,202,166,
BACKING='VOID',
MATL_ID(1,1)='CALCIUM SILICATE',
MATL_MASS_FRACTION(1,1)=1.0,
THICKNESS(1)=0.012/
&SURF ID='DOUBLE GLAZING',
RGB=146,193,202,
TRANSPARENCY=0.396078,
BACKING='VOID',
MATL_ID(1,1)='DOUBLE GLAZING',
MATL_MASS_FRACTION(1,1)=1.0,
THICKNESS(1)=0.012/
&SURF ID='Hallway-apartments',
RGB=127,221,255,
LEAK_PATH=1,0/
&SURF ID='Double door',
RGB=127,221,255,
LEAK_PATH=1,0/
&SURF ID='CEILING HALLWAY',
RGB=146,202,166,
BACKING='VOID',
MATL_ID(1,1)='CALCIUM SILICATE',
MATL_MASS_FRACTION(1,1)=1.0,
THICKNESS(1)=0.03/
&SURF ID='SofaFIRE01',
COLOR='RED',
MLRPUA=0.061887,
RAMP_Q='SofaFIRE01_RAMP_Q',
TMP_FRONT=300.0,
PART_ID='Flow tracer',
DT_INSERT=1.0/

```

VENTS AND RAMPS ASSOCIATED WITH FIRE DELETED FROM FILE AS THIS LEADS TO EXCESSIVE FILE LENGTH.  
AVAILABLE UPON INQUIRY.

```

&OBST ID='Obstruction', XB=-0.7,18.5,19.6,19.7,2.8,3.0, COLOR='GRAY 80', SURF_ID='CONCRETE_WALLS'/
&OBST ID='Obstruction', XB=-0.7,18.5,19.6,19.7,2.4,2.6, COLOR='GRAY 80', SURF_ID='CONCRETE_WALLS'/
&OBST ID='Bulkhead', XB=12.7,13.6,12.3,12.4,4.8,5.4, SURF_ID='CALCIUM SILICATE WALLS'/
&OBST ID='Bulkhead2', XB=12.6,12.7,12.7,13.5,4.8,5.4, SURF_ID='CALCIUM SILICATE WALLS'/
&OBST ID='Door 1.19-Hallway', XB=12.7,13.6,12.3,12.4,2.8,4.8, SURF_ID='DOOR', DEVC_ID='TIMER->OUT'/
&OBST ID='Door barchroom', XB=12.6,12.7,12.7,13.5,2.8,4.8, SURF_ID='DOOR'/
&OBST ID='Innerwall 5', XB=13.6,14.5,12.3,12.4,2.8,5.4, SURF_ID='CALCIUM SILICATE WALLS'/
&OBST ID='Innerwall1', XB=10.7,10.9,12.2,19.5,2.8,5.4, COLOR='GRAY 80', SURF_ID='CONCRETE_WALLS'/
&OBST ID='Innerwall2', XB=14.5,14.7,12.2,19.5,2.8,5.4, COLOR='GRAY 80', SURF_ID='CONCRETE_WALLS'/
&OBST ID='Innerwall3', XB=10.9,14.5,14.0,14.1,2.8,5.4, SURF_ID='CALCIUM SILICATE WALLS'/
&OBST ID='Innerwall6', XB=12.6,12.7,13.5,14.0,2.8,5.4, SURF_ID='CALCIUM SILICATE WALLS'/
&OBST ID='Overhead2', XB=12.7,13.6,18.4,18.5,2.8,5.4, COLOR='INVISIBLE', SURF_ID='Windows fire room'/
&OBST ID='Parapet1', XB=10.9,12.7,18.4,18.5,2.8,3.5, COLOR='INVISIBLE', SURF_ID='CONCRETE_WALLS'/
&OBST ID='Parapet2', XB=13.6,14.5,18.4,18.5,2.8,3.5, COLOR='INVISIBLE', SURF_ID='CONCRETE_WALLS'/
&OBST ID='Window backside', XB=10.9,12.7,18.4,18.5,3.5,5.4, COLOR='INVISIBLE', SURF_ID='Windows fire room'/

```

&OBST ID='Window backside 2', XB=13.6,14.5,18.4,18.5,3.5,5.4, COLOR='INVISIBLE', SURF\_ID='Windows fire room'/  
 &OBST ID='Balcony door', XB=8.9,9.8,18.4,18.5,2.8,4.8, SURF\_ID='DOUBLE GLAZING'/  
 &OBST ID='Bulkhead', XB=8.9,9.8,12.3,12.4,4.8,5.4, SURF\_ID='CALCIUM SILICATE WALLS'/  
 &OBST ID='Bulkhead2', XB=8.8,8.9,12.7,13.5,4.8,5.4, SURF\_ID='CALCIUM SILICATE WALLS'/  
 &OBST ID='Door 1.20-Hallway', XB=8.9,9.8,12.3,12.4,2.8,4.8, SURF\_ID6='DOOR','DOOR','Hallway-apartments','Hallway-apartments','DOOR','DOOR'/  
 &OBST ID='Door barchroom', XB=8.8,8.9,12.7,13.5,2.8,4.8, SURF\_ID='DOOR'/  
 &OBST ID='Innerwall 5', XB=9.8,10.7,12.3,12.4,2.8,5.4, SURF\_ID='CALCIUM SILICATE WALLS'/  
 &OBST ID='Innerwall1', XB=6.9,7.1,12.2,19.5,2.8,5.4, COLOR='GRAY 80', SURF\_ID='CONCRETE\_WALLS'/  
 &OBST ID='Innerwall3', XB=7.1,10.7,14.0,14.1,2.8,5.4, SURF\_ID='CALCIUM SILICATE WALLS'/  
 &OBST ID='Innerwall6', XB=8.8,8.9,13.5,14.0,2.8,5.4, SURF\_ID='CALCIUM SILICATE WALLS'/  
 &OBST ID='Overhead2', XB=8.9,9.8,18.4,18.5,4.8,5.4, SURF\_ID='DOUBLE GLAZING'/  
 &OBST ID='Parapet1', XB=7.1,8.9,18.4,18.5,2.8,3.5, COLOR='GRAY 80', SURF\_ID='CONCRETE\_WALLS'/  
 &OBST ID='Parapet2', XB=9.8,10.7,18.4,18.5,2.8,3.5, COLOR='GRAY 80', SURF\_ID='CONCRETE\_WALLS'/  
 &OBST ID='Window backside', XB=7.1,8.9,18.4,18.5,3.5,5.4, SURF\_ID='DOUBLE GLAZING'/  
 &OBST ID='Window backside 2', XB=9.8,10.7,18.4,18.5,3.5,5.4, SURF\_ID='DOUBLE GLAZING'/  
 &OBST ID='Balcony door', XB=5.1,6.0,18.4,18.5,2.8,4.8, SURF\_ID='DOUBLE GLAZING'/  
 &OBST ID='Bulkhead', XB=5.1,6.0,12.3,12.4,4.8,5.4, SURF\_ID='CALCIUM SILICATE WALLS'/  
 &OBST ID='Door 1.21-Hallway', XB=5.1,6.0,12.3,12.4,2.8,4.8, SURF\_ID6='DOOR','DOOR','Hallway-apartments','Hallway-apartments','DOOR','DOOR'/  
 &OBST ID='Bulkhead2', XB=5.0,5.1,12.7,13.5,4.8,5.4, SURF\_ID='CALCIUM SILICATE WALLS'/  
 &OBST ID='Door barchroom', XB=5.0,5.1,12.7,13.5,2.8,4.8, SURF\_ID='DOOR'/  
 &OBST ID='Innerwall 5', XB=6.0,6.9,12.3,12.4,2.8,5.4, SURF\_ID='CALCIUM SILICATE WALLS'/  
 &OBST ID='Innerwall1', XB=3.1,3.3,12.2,19.5,2.8,5.4, COLOR='GRAY 80', SURF\_ID='CONCRETE\_WALLS'/  
 &OBST ID='Innerwall3', XB=3.3,6.9,14.0,14.1,2.8,5.4, SURF\_ID='CALCIUM SILICATE WALLS'/  
 &OBST ID='Innerwall6', XB=5.0,5.1,13.5,14.0,2.8,5.4, SURF\_ID='CALCIUM SILICATE WALLS'/  
 &OBST ID='Overhead2', XB=5.1,6.0,18.4,18.5,4.8,5.4, SURF\_ID='DOUBLE GLAZING'/  
 &OBST ID='Parapet1', XB=3.3,5.1,18.4,18.5,2.8,3.5, COLOR='GRAY 80', SURF\_ID='CONCRETE\_WALLS'/  
 &OBST ID='Parapet2', XB=6.0,6.9,18.4,18.5,2.8,3.5, COLOR='GRAY 80', SURF\_ID='CONCRETE\_WALLS'/  
 &OBST ID='Window backside', XB=3.3,5.1,18.4,18.5,3.5,5.4, SURF\_ID='DOUBLE GLAZING'/  
 &OBST ID='Window backside 2', XB=6.0,6.9,18.4,18.5,3.5,5.4, SURF\_ID='DOUBLE GLAZING'/  
 &OBST ID='Balcony door', XB=1.3,2.2,18.4,18.5,2.8,4.8, SURF\_ID='DOUBLE GLAZING'/  
 &OBST ID='Bulkhead', XB=1.3,2.2,12.3,12.4,4.8,5.4, SURF\_ID='CALCIUM SILICATE WALLS'/  
 &OBST ID='Bulkhead2', XB=1.2,1.3,12.7,13.5,4.8,5.4, SURF\_ID='CALCIUM SILICATE WALLS'/  
 &OBST ID='Door 1.21-Hallway', XB=1.3,2.2,12.3,12.4,2.8,4.8, SURF\_ID6='DOOR','DOOR','Hallway-apartments','Hallway-apartments','DOOR','DOOR'/  
 &OBST ID='Door barchroom', XB=1.2,1.3,12.7,13.5,2.8,4.8, SURF\_ID='DOOR'/  
 &OBST ID='Innerwall 5', XB=2.2,3.1,12.3,12.4,2.8,5.4, SURF\_ID='CALCIUM SILICATE WALLS'/  
 &OBST ID='Innerwall1', XB=-0.7,-0.5,12.2,19.5,2.8,5.4, COLOR='GRAY 80', SURF\_ID='CONCRETE\_WALLS'/  
 &OBST ID='Innerwall3', XB=-0.5,3.1,14.0,14.1,2.8,5.4, SURF\_ID='CALCIUM SILICATE WALLS'/  
 &OBST ID='Innerwall6', XB=1.2,1.3,13.5,14.0,2.8,5.4, SURF\_ID='CALCIUM SILICATE WALLS'/  
 &OBST ID='Overhead2', XB=1.3,2.2,18.4,18.5,4.8,5.4, SURF\_ID='DOUBLE GLAZING'/  
 &OBST ID='Parapet1', XB=-0.5,1.3,18.4,18.5,2.8,3.5, COLOR='GRAY 80', SURF\_ID='CONCRETE\_WALLS'/  
 &OBST ID='Parapet2', XB=2.2,3.1,18.4,18.5,2.8,3.5, COLOR='GRAY 80', SURF\_ID='CONCRETE\_WALLS'/  
 &OBST ID='Window backside', XB=-0.5,1.3,18.4,18.5,3.5,5.4, SURF\_ID='DOUBLE GLAZING'/  
 &OBST ID='Window backside 2', XB=2.2,3.1,18.4,18.5,3.5,5.4, SURF\_ID='DOUBLE GLAZING'/  
 &OBST ID='Balcony door', XB=16.5,17.4,18.4,18.5,2.8,4.8, SURF\_ID='DOUBLE GLAZING'/  
 &OBST ID='Bulkhead', XB=16.5,17.4,12.3,12.4,4.8,5.4, SURF\_ID='CALCIUM SILICATE WALLS'/  
 &OBST ID='Bulkhead2', XB=16.4,16.5,12.7,13.5,4.8,5.4, SURF\_ID='CALCIUM SILICATE WALLS'/  
 &OBST ID='Door 1.18-Hallway', XB=16.5,17.4,12.3,12.4,2.8,4.8, SURF\_ID6='DOOR','DOOR','Hallway-apartments','Hallway-apartments','DOOR','DOOR'/  
 &OBST ID='Door barchroom', XB=16.4,16.5,12.7,13.5,2.8,4.8, SURF\_ID='DOOR'/  
 &OBST ID='Innerwall 5', XB=17.4,18.3,12.3,12.4,2.8,5.4, SURF\_ID='CALCIUM SILICATE WALLS'/  
 &OBST ID='Innerwall1', XB=14.5,14.7,12.2,19.5,2.8,5.4, COLOR='GRAY 80', SURF\_ID='CONCRETE\_WALLS'/  
 &OBST ID='Innerwall2', XB=18.3,18.5,12.2,19.5,2.8,5.4, COLOR='GRAY 80', SURF\_ID='CONCRETE\_WALLS'/  
 &OBST ID='Innerwall3', XB=14.7,18.3,14.0,14.1,2.8,5.4, SURF\_ID='CALCIUM SILICATE WALLS'/  
 &OBST ID='Innerwall6', XB=16.4,16.5,13.5,14.0,2.8,5.4, SURF\_ID='CALCIUM SILICATE WALLS'/  
 &OBST ID='Overhead2', XB=16.5,17.4,18.4,18.5,4.8,5.4, SURF\_ID='DOUBLE GLAZING'/  
 &OBST ID='Parapet1', XB=14.7,16.5,18.4,18.5,2.8,3.5, COLOR='GRAY 80', SURF\_ID='CONCRETE\_WALLS'/  
 &OBST ID='Parapet2', XB=17.4,18.3,18.4,18.5,2.8,3.5, COLOR='GRAY 80', SURF\_ID='CONCRETE\_WALLS'/  
 &OBST ID='Window backside', XB=14.7,16.5,18.4,18.5,3.5,5.4, SURF\_ID='DOUBLE GLAZING'/  
 &OBST ID='Window backside 2', XB=17.4,18.3,18.4,18.5,3.5,5.4, SURF\_ID='DOUBLE GLAZING'/  
 &OBST ID='Bulkhead', XB=12.7,13.6,10.3,10.4,4.8,5.4, SURF\_ID='CALCIUM SILICATE WALLS'/  
 &OBST ID='Bulkhead2', XB=12.6,12.7,9.2,10.0,4.8,5.4, SURF\_ID='CALCIUM SILICATE WALLS'/  
 &OBST ID='Door 1.26-Hallway', XB=12.7,13.6,10.3,10.4,2.8,4.8, SURF\_ID6='DOOR','DOOR','Hallway-apartments','Hallway-apartments','DOOR','DOOR'/

&OBST ID='Door barchroom', XB=12.6,12.7,9.2,10.0,2.8,4.8, SURF\_ID='DOOR'/  
 &OBST ID='Innerwall 5', XB=13.6,14.5,10.3,10.4,2.8,5.4, SURF\_ID='CALCIUM SILICATE WALLS'/  
 &OBST ID='Innerwall1', XB=10.7,10.9,4.0,10.5,2.8,5.4, COLOR='GRAY 80', SURF\_ID='CONCRETE\_WALLS'/  
 &OBST ID='Innerwall2', XB=14.5,14.7,4.0,10.5,2.8,5.4, COLOR='GRAY 80', SURF\_ID='CONCRETE\_WALLS'/  
 &OBST ID='Innerwall3', XB=10.9,14.5,8.6,8.7,2.8,5.4, SURF\_ID='CALCIUM SILICATE WALLS'/  
 &OBST ID='Innerwall6', XB=12.6,12.7,8.7,9.2,2.8,5.4, SURF\_ID='CALCIUM SILICATE WALLS'/  
 &OBST ID='Parapet1', XB=10.9,14.5,4.2,4.3,2.8,3.5, COLOR='GRAY 80', SURF\_ID='CONCRETE\_WALLS'/  
 &OBST ID='Window backside', XB=10.9,14.5,4.2,4.3,3.5,5.4, SURF\_ID='DOUBLE GLAZING'/  
 &OBST ID='Bulkhead', XB=16.3,17.2,10.3,10.4,4.8,5.4, SURF\_ID='CALCIUM SILICATE WALLS'/  
 &OBST ID='Bulkhead2', XB=16.2,16.3,9.2,10.0,4.8,5.4, SURF\_ID='CALCIUM SILICATE WALLS'/  
 &OBST ID='Door 1.28-Hallway', XB=16.3,17.2,10.3,10.4,2.8,4.8, SURF\_ID6='DOOR','DOOR','Hallway-apartments','Hallway-apartments','DOOR','DOOR'/  
 &OBST ID='Door barchroom', XB=16.2,16.3,9.2,10.0,2.8,4.8, SURF\_ID='DOOR'/  
 &OBST ID='Innerwall 5', XB=17.2,18.3,10.3,10.4,2.8,5.4, SURF\_ID='CALCIUM SILICATE WALLS'/  
 &OBST ID='Innerwall1', XB=14.5,14.7,4.0,10.5,2.8,5.4, COLOR='GRAY 80', SURF\_ID='CONCRETE\_WALLS'/  
 &OBST ID='Innerwall2', XB=18.3,18.5,4.0,10.5,2.8,5.4, COLOR='GRAY 80', SURF\_ID='CONCRETE\_WALLS'/  
 &OBST ID='Innerwall3', XB=14.7,18.3,8.6,8.7,2.8,5.4, SURF\_ID='CALCIUM SILICATE WALLS'/  
 &OBST ID='Innerwall6', XB=16.2,16.3,8.7,9.2,2.8,5.4, SURF\_ID='CALCIUM SILICATE WALLS'/  
 &OBST ID='Parapet1', XB=14.7,18.3,4.2,4.3,2.8,3.5, COLOR='GRAY 80', SURF\_ID='CONCRETE\_WALLS'/  
 &OBST ID='Window backside', XB=14.7,18.3,4.2,4.3,3.5,5.4, SURF\_ID='DOUBLE GLAZING'/  
 &OBST ID='Bulkhead', XB=8.9,9.8,10.3,10.4,4.8,5.4, SURF\_ID='CALCIUM SILICATE WALLS'/  
 &OBST ID='Bulkhead2', XB=8.8,8.9,9.2,10.0,4.8,5.4, COLOR='GRAY 80', SURF\_ID='CONCRETE\_WALLS'/  
 &OBST ID='Innerwall 5', XB=9.8,10.7,10.3,10.4,2.8,5.4, SURF\_ID='CALCIUM SILICATE WALLS'/  
 &OBST ID='Innerwall1', XB=6.9,7.1,4.0,10.5,2.8,5.4, COLOR='GRAY 80', SURF\_ID='CONCRETE\_WALLS'/  
 &OBST ID='Innerwall3', XB=7.1,10.7,8.6,8.7,2.8,5.4, SURF\_ID='CALCIUM SILICATE WALLS'/  
 &OBST ID='Innerwall6', XB=8.8,8.9,8.7,9.2,2.8,5.4, COLOR='GRAY 80', SURF\_ID='CONCRETE\_WALLS'/  
 &OBST ID='Parapet1', XB=7.1,10.7,4.2,4.3,2.8,3.5, COLOR='GRAY 80', SURF\_ID='CONCRETE\_WALLS'/  
 &OBST ID='Window backside', XB=7.1,10.7,4.2,4.3,3.5,5.4, SURF\_ID='DOUBLE GLAZING'/  
 &OBST ID='Bulkhead', XB=5.1,6.0,10.3,10.4,4.8,5.4, SURF\_ID='CALCIUM SILICATE WALLS'/  
 &OBST ID='Bulkhead2', XB=5.0,5.1,9.2,10.0,4.8,5.4, SURF\_ID='CALCIUM SILICATE WALLS'/  
 &OBST ID='Door 1.24-Hallway', XB=5.1,6.0,10.3,10.4,2.8,4.8, SURF\_ID6='DOOR','DOOR','Hallway-apartments','Hallway-apartments','DOOR','DOOR'/  
 &OBST ID='Door barchroom', XB=5.0,5.1,9.2,10.0,2.8,4.8, SURF\_ID='DOOR'/  
 &OBST ID='Innerwall 5', XB=6.0,6.9,10.3,10.4,2.8,5.4, SURF\_ID='CALCIUM SILICATE WALLS'/  
 &OBST ID='Innerwall1', XB=3.1,3.3,4.0,10.5,2.8,5.4, COLOR='GRAY 80', SURF\_ID='CONCRETE\_WALLS'/  
 &OBST ID='Innerwall3', XB=3.3,6.9,8.6,8.7,2.8,5.4, SURF\_ID='CALCIUM SILICATE WALLS'/  
 &OBST ID='Innerwall6', XB=5.0,5.1,8.7,9.2,2.8,5.4, SURF\_ID='CALCIUM SILICATE WALLS'/  
 &OBST ID='Parapet1', XB=3.3,6.9,4.2,4.3,2.8,3.5, COLOR='GRAY 80', SURF\_ID='CONCRETE\_WALLS'/  
 &OBST ID='Window backside', XB=3.3,6.9,4.2,4.3,3.5,5.4, SURF\_ID='DOUBLE GLAZING'/  
 &OBST ID='Door barchroom', XB=8.8,8.9,9.2,10.0,2.8,4.8, SURF\_ID='DOOR'/  
 &OBST ID='Bulkhead', XB=1.3,2.2,10.3,10.4,4.8,5.4, SURF\_ID='CALCIUM SILICATE WALLS'/  
 &OBST ID='Bulkhead2', XB=1.2,1.3,9.2,10.0,4.8,5.4, SURF\_ID='CALCIUM SILICATE WALLS'/  
 &OBST ID='Door 1.23-Hallway', XB=1.3,2.2,10.3,10.4,2.8,4.8, SURF\_ID6='DOOR','DOOR','Hallway-apartments','Hallway-apartments','DOOR','DOOR'/  
 &OBST ID='Door barchroom', XB=1.2,1.3,9.2,10.0,2.8,4.8, SURF\_ID='DOOR'/  
 &OBST ID='Innerwall 5', XB=2.2,3.1,10.3,10.4,2.8,5.4, SURF\_ID='CALCIUM SILICATE WALLS'/  
 &OBST ID='Innerwall1', XB=-0.7,-0.5,4.0,10.5,2.8,5.4, COLOR='GRAY 80', SURF\_ID='CONCRETE\_WALLS'/  
 &OBST ID='Innerwall3', XB=-0.5,3.1,8.6,8.7,2.8,5.4, SURF\_ID='CALCIUM SILICATE WALLS'/  
 &OBST ID='Innerwall6', XB=1.2,1.3,8.7,9.2,2.8,5.4, SURF\_ID='CALCIUM SILICATE WALLS'/  
 &OBST ID='Parapet1', XB=-0.5,3.1,4.2,4.3,2.8,3.5, COLOR='GRAY 80', SURF\_ID='CONCRETE\_WALLS'/  
 &OBST ID='Window backside', XB=-0.5,3.1,4.2,4.3,3.5,5.4, SURF\_ID='DOUBLE GLAZING'/  
 &OBST ID='Hallway double door left', XB=-0.7,-0.6,10.5,12.2,2.8,4.8, SURF\_ID6='Double door','Double door','DOOR','DOOR','DOOR','DOOR'/  
 &OBST ID='Hallway bulkhead left', XB=-0.7,-0.6,10.5,12.2,4.8,5.4, SURF\_ID='CALCIUM SILICATE WALLS'/  
 &OBST ID='Hallway bulkhead right', XB=18.4,18.5,10.5,12.2,4.8,5.4, COLOR='GRAY 80', SURF\_ID='CONCRETE\_WALLS'/  
 &OBST ID='Hallway double door right', XB=18.4,18.5,10.5,12.2,2.8,4.8, SURF\_ID6='Double door','Double door','DOOR','DOOR','DOOR','DOOR'/  
 &OBST ID='Obstruction', XB=-0.7,18.5,19.6,19.7,5.6,5.8, COLOR='GRAY 80', SURF\_ID='CONCRETE\_WALLS'/  
 &OBST ID='Obstruction', XB=-0.7,18.5,19.6,19.7,5.2,5.4, COLOR='GRAY 80', SURF\_ID='CONCRETE\_WALLS'/  
 &OBST ID='Balcony door', XB=12.7,13.6,18.4,18.5,5.6,7.6, SURF\_ID='DOUBLE GLAZING'/  
 &OBST ID='Bulkhead', XB=12.7,13.6,12.3,12.4,7.6,8.2, COLOR='GRAY 80', SURF\_ID='CONCRETE\_WALLS'/  
 &OBST ID='Bulkhead2', XB=12.6,12.7,12.7,13.5,7.6,8.2, COLOR='GRAY 80', SURF\_ID='CONCRETE\_WALLS'/  
 &OBST ID='Door 2.19-Hallway', XB=12.7,13.6,12.3,12.4,5.6,7.6, SURF\_ID='DOOR'/  
 &OBST ID='Door barchroom', XB=12.6,12.7,12.7,13.5,5.6,7.6, SURF\_ID='DOOR'/  
 &OBST ID='Innerwall 5', XB=13.6,14.5,12.3,12.4,5.6,8.2, COLOR='GRAY 80', SURF\_ID='CONCRETE\_WALLS'/  
 &OBST ID='Innerwall1', XB=10.7,10.9,12.2,19.5,5.6,8.2, COLOR='GRAY 80', SURF\_ID='CONCRETE\_WALLS'/

&OBST ID='Innerwall2', XB=14.5,14.7,12.2,19.5,5.6,8.2, COLOR='GRAY 80', SURF\_ID='CONCRETE\_WALLS'/  
 &OBST ID='Innerwall3', XB=10.9,14.5,14.0,14.1,5.6,8.2, COLOR='GRAY 80', SURF\_ID='CONCRETE\_WALLS'/  
 &OBST ID='Innerwall6', XB=12.6,12.7,13.5,14.0,5.6,8.2, COLOR='GRAY 80', SURF\_ID='CONCRETE\_WALLS'/  
 &OBST ID='Overhead2', XB=12.7,13.6,18.4,18.5,7.6,8.2, SURF\_ID='DOUBLE GLAZING'/  
 &OBST ID='Parapet1', XB=10.9,12.7,18.4,18.5,5.6,6.3, COLOR='GRAY 80', SURF\_ID='CONCRETE\_WALLS'/  
 &OBST ID='Parapet2', XB=13.6,14.5,18.4,18.5,5.6,6.3, COLOR='GRAY 80', SURF\_ID='CONCRETE\_WALLS'/  
 &OBST ID='Window backside', XB=10.9,12.7,18.4,18.5,6.3,8.2, SURF\_ID='DOUBLE GLAZING'/  
 &OBST ID='Window backside 2', XB=13.6,14.5,18.4,18.5,6.3,8.2, SURF\_ID='DOUBLE GLAZING'/  
 &OBST ID='Balcony door', XB=8.9,9.8,18.4,18.5,5.6,7.6, SURF\_ID='DOUBLE GLAZING'/  
 &OBST ID='Bulkhead', XB=8.9,9.8,12.3,12.4,7.6,8.2, COLOR='GRAY 80', SURF\_ID='CONCRETE\_WALLS'/  
 &OBST ID='Bulkhead2', XB=8.8,8.9,12.7,13.5,7.6,8.2, COLOR='GRAY 80', SURF\_ID='CONCRETE\_WALLS'/  
 &OBST ID='Door 2.20-Hallway', XB=8.9,9.8,12.3,12.4,5.6,7.6, SURF\_ID='DOOR'/  
 &OBST ID='Door barchroom', XB=8.8,8.9,12.7,13.5,5.6,7.6, SURF\_ID='DOOR'/  
 &OBST ID='Innerwall 5', XB=9.8,10.7,12.3,12.4,5.6,8.2, COLOR='GRAY 80', SURF\_ID='CONCRETE\_WALLS'/  
 &OBST ID='Innerwall1', XB=6.9,7.1,12.2,19.5,5.6,8.2, COLOR='GRAY 80', SURF\_ID='CONCRETE\_WALLS'/  
 &OBST ID='Innerwall3', XB=7.1,10.7,14.0,14.1,5.6,8.2, COLOR='GRAY 80', SURF\_ID='CONCRETE\_WALLS'/  
 &OBST ID='Innerwall6', XB=8.8,8.9,13.5,14.0,5.6,8.2, COLOR='GRAY 80', SURF\_ID='CONCRETE\_WALLS'/  
 &OBST ID='Overhead2', XB=8.9,9.8,18.4,18.5,7.6,8.2, SURF\_ID='DOUBLE GLAZING'/  
 &OBST ID='Parapet1', XB=7.1,8.9,18.4,18.5,5.6,6.3, COLOR='GRAY 80', SURF\_ID='CONCRETE\_WALLS'/  
 &OBST ID='Parapet2', XB=9.8,10.7,18.4,18.5,5.6,6.3, COLOR='GRAY 80', SURF\_ID='CONCRETE\_WALLS'/  
 &OBST ID='Window backside', XB=7.1,8.9,18.4,18.5,6.3,8.2, SURF\_ID='DOUBLE GLAZING'/  
 &OBST ID='Window backside 2', XB=9.8,10.7,18.4,18.5,6.3,8.2, SURF\_ID='DOUBLE GLAZING'/  
 &OBST ID='Balcony door', XB=5.1,6.0,18.4,18.5,5.6,7.6, SURF\_ID='DOUBLE GLAZING'/  
 &OBST ID='Bulkhead', XB=5.1,6.0,12.3,12.4,7.6,8.2, COLOR='GRAY 80', SURF\_ID='CONCRETE\_WALLS'/  
 &OBST ID='Bulkhead2', XB=5.0,5.1,12.7,13.5,7.6,8.2, COLOR='GRAY 80', SURF\_ID='CONCRETE\_WALLS'/  
 &OBST ID='Door 2.21-Hallway', XB=5.1,6.0,12.3,12.4,5.6,7.6, SURF\_ID='DOOR'/  
 &OBST ID='Door barchroom', XB=5.0,5.1,12.7,13.5,5.6,7.6, SURF\_ID='DOOR'/  
 &OBST ID='Innerwall 5', XB=6.0,6.9,12.3,12.4,5.6,8.2, COLOR='GRAY 80', SURF\_ID='CONCRETE\_WALLS'/  
 &OBST ID='Innerwall1', XB=3.1,3.3,12.2,19.5,5.6,8.2, COLOR='GRAY 80', SURF\_ID='CONCRETE\_WALLS'/  
 &OBST ID='Innerwall3', XB=3.3,6.9,14.0,14.1,5.6,8.2, COLOR='GRAY 80', SURF\_ID='CONCRETE\_WALLS'/  
 &OBST ID='Innerwall6', XB=5.0,5.1,13.5,14.0,5.6,8.2, COLOR='GRAY 80', SURF\_ID='CONCRETE\_WALLS'/  
 &OBST ID='Overhead2', XB=5.1,6.0,18.4,18.5,7.6,8.2, SURF\_ID='DOUBLE GLAZING'/  
 &OBST ID='Parapet1', XB=3.3,5.1,18.4,18.5,5.6,6.3, COLOR='GRAY 80', SURF\_ID='CONCRETE\_WALLS'/  
 &OBST ID='Parapet2', XB=6.0,6.9,18.4,18.5,5.6,6.3, COLOR='GRAY 80', SURF\_ID='CONCRETE\_WALLS'/  
 &OBST ID='Window backside', XB=3.3,5.1,18.4,18.5,6.3,8.2, SURF\_ID='DOUBLE GLAZING'/  
 &OBST ID='Window backside 2', XB=6.0,6.9,18.4,18.5,6.3,8.2, SURF\_ID='DOUBLE GLAZING'/  
 &OBST ID='Balcony door', XB=1.3,2.2,18.4,18.5,5.6,7.6, SURF\_ID='DOUBLE GLAZING'/  
 &OBST ID='Bulkhead', XB=1.3,2.2,12.3,12.4,7.6,8.2, COLOR='GRAY 80', SURF\_ID='CONCRETE\_WALLS'/  
 &OBST ID='Bulkhead2', XB=1.2,1.3,12.7,13.5,7.6,8.2, COLOR='GRAY 80', SURF\_ID='CONCRETE\_WALLS'/  
 &OBST ID='Door 2.21-Hallway', XB=1.3,2.2,12.3,12.4,5.6,7.6, SURF\_ID='DOOR'/  
 &OBST ID='Door barchroom', XB=1.2,1.3,12.7,13.5,5.6,7.6, SURF\_ID='DOOR'/  
 &OBST ID='Innerwall 5', XB=2.2,3.1,12.3,12.4,5.6,8.2, COLOR='GRAY 80', SURF\_ID='CONCRETE\_WALLS'/  
 &OBST ID='Innerwall1', XB=-0.7,-0.5,12.2,19.5,5.6,8.2, COLOR='GRAY 80', SURF\_ID='CONCRETE\_WALLS'/  
 &OBST ID='Innerwall3', XB=-0.5,3.1,14.0,14.1,5.6,8.2, COLOR='GRAY 80', SURF\_ID='CONCRETE\_WALLS'/  
 &OBST ID='Innerwall6', XB=1.2,1.3,13.5,14.0,5.6,8.2, COLOR='GRAY 80', SURF\_ID='CONCRETE\_WALLS'/  
 &OBST ID='Overhead2', XB=1.3,2.2,18.4,18.5,7.6,8.2, SURF\_ID='DOUBLE GLAZING'/  
 &OBST ID='Parapet1', XB=-0.5,1.3,18.4,18.5,5.6,6.3, COLOR='GRAY 80', SURF\_ID='CONCRETE\_WALLS'/  
 &OBST ID='Parapet2', XB=2.2,3.1,18.4,18.5,5.6,6.3, COLOR='GRAY 80', SURF\_ID='CONCRETE\_WALLS'/  
 &OBST ID='Window backside', XB=-0.5,1.3,18.4,18.5,6.3,8.2, SURF\_ID='DOUBLE GLAZING'/  
 &OBST ID='Window backside 2', XB=2.2,3.1,18.4,18.5,6.3,8.2, SURF\_ID='DOUBLE GLAZING'/  
 &OBST ID='Balcony door', XB=16.5,17.4,18.4,18.5,5.6,7.6, SURF\_ID='DOUBLE GLAZING'/  
 &OBST ID='Bulkhead', XB=16.5,17.4,12.3,12.4,7.6,8.2, COLOR='GRAY 80', SURF\_ID='CONCRETE\_WALLS'/  
 &OBST ID='Bulkhead2', XB=16.4,16.5,12.7,13.5,7.6,8.2, COLOR='GRAY 80', SURF\_ID='CONCRETE\_WALLS'/  
 &OBST ID='Door 2.18-Hallway', XB=16.5,17.4,12.3,12.4,5.6,7.6, SURF\_ID='DOOR'/  
 &OBST ID='Door barchroom', XB=16.4,16.5,12.7,13.5,5.6,7.6, SURF\_ID='DOOR'/  
 &OBST ID='Innerwall 5', XB=17.4,18.3,12.3,12.4,5.6,8.2, COLOR='GRAY 80', SURF\_ID='CONCRETE\_WALLS'/  
 &OBST ID='Innerwall1', XB=14.5,14.7,12.2,19.5,5.6,8.2, COLOR='GRAY 80', SURF\_ID='CONCRETE\_WALLS'/  
 &OBST ID='Innerwall2', XB=18.3,18.5,12.2,19.5,5.6,8.2, COLOR='GRAY 80', SURF\_ID='CONCRETE\_WALLS'/  
 &OBST ID='Innerwall3', XB=14.7,18.3,14.0,14.1,5.6,8.2, COLOR='GRAY 80', SURF\_ID='CONCRETE\_WALLS'/  
 &OBST ID='Innerwall6', XB=16.4,16.5,13.5,14.0,5.6,8.2, COLOR='GRAY 80', SURF\_ID='CONCRETE\_WALLS'/  
 &OBST ID='Overhead2', XB=16.5,17.4,18.4,18.5,7.6,8.2, SURF\_ID='DOUBLE GLAZING'/  
 &OBST ID='Parapet1', XB=14.7,16.5,18.4,18.5,5.6,6.3, COLOR='GRAY 80', SURF\_ID='CONCRETE\_WALLS'/  
 &OBST ID='Parapet2', XB=17.4,18.3,18.4,18.5,5.6,6.3, COLOR='GRAY 80', SURF\_ID='CONCRETE\_WALLS'/  
 &OBST ID='Window backside', XB=14.7,16.5,18.4,18.5,6.3,8.2, SURF\_ID='DOUBLE GLAZING'/  
 &OBST ID='Window backside 2', XB=17.4,18.3,18.4,18.5,6.3,8.2, SURF\_ID='DOUBLE GLAZING'/  
 &OBST ID='Bulkhead', XB=12.7,13.6,10.3,10.4,7.6,8.2, COLOR='GRAY 80', SURF\_ID='CONCRETE\_WALLS'/

&OBST ID='Bulkhead2', XB=12.6,12.7,9.2,10.0,7.6,8.2, COLOR='GRAY 80', SURF\_ID='CONCRETE\_WALLS'/  
 &OBST ID='Door 2.26-Hallway', XB=12.7,13.6,10.3,10.4,5.6,7.6, SURF\_ID='DOOR'/  
 &OBST ID='Door barchroom', XB=12.6,12.7,9.2,10.0,5.6,7.6, SURF\_ID='DOOR'/  
 &OBST ID='Innerwall 5', XB=13.6,14.5,10.3,10.4,5.6,8.2, COLOR='GRAY 80', SURF\_ID='CONCRETE\_WALLS'/  
 &OBST ID='Innerwall1', XB=10.7,10.9,4.0,10.5,5.6,8.2, COLOR='GRAY 80', SURF\_ID='CONCRETE\_WALLS'/  
 &OBST ID='Innerwall2', XB=14.5,14.7,4.0,10.5,5.6,8.2, COLOR='GRAY 80', SURF\_ID='CONCRETE\_WALLS'/  
 &OBST ID='Innerwall3', XB=10.9,14.5,8.6,8.7,5.6,8.2, COLOR='GRAY 80', SURF\_ID='CONCRETE\_WALLS'/  
 &OBST ID='Innerwall6', XB=12.6,12.7,8.7,9.2,5.6,8.2, COLOR='GRAY 80', SURF\_ID='CONCRETE\_WALLS'/  
 &OBST ID='Parapet1', XB=10.9,14.5,4.2,4.3,5.6,6.3, COLOR='GRAY 80', SURF\_ID='CONCRETE\_WALLS'/  
 &OBST ID='Window backside', XB=10.9,14.5,4.2,4.3,6.3,8.2, SURF\_ID='DOUBLE GLAZING'/  
 &OBST ID='Bulkhead', XB=16.3,17.2,10.3,10.4,7.6,8.2, COLOR='GRAY 80', SURF\_ID='CONCRETE\_WALLS'/  
 &OBST ID='Bulkhead2', XB=16.2,16.3,9.2,10.0,7.6,8.2, COLOR='GRAY 80', SURF\_ID='CONCRETE\_WALLS'/  
 &OBST ID='Door 2.28-Hallway', XB=16.3,17.2,10.3,10.4,5.6,7.6, SURF\_ID='DOOR'/  
 &OBST ID='Door barchroom', XB=16.2,16.3,9.2,10.0,5.6,7.6, SURF\_ID='DOOR'/  
 &OBST ID='Innerwall 5', XB=17.2,18.3,10.3,10.4,5.6,8.2, COLOR='GRAY 80', SURF\_ID='CONCRETE\_WALLS'/  
 &OBST ID='Innerwall1', XB=14.5,14.7,4.0,10.5,5.6,8.2, COLOR='GRAY 80', SURF\_ID='CONCRETE\_WALLS'/  
 &OBST ID='Innerwall2', XB=18.3,18.5,4.0,10.5,5.6,8.2, COLOR='GRAY 80', SURF\_ID='CONCRETE\_WALLS'/  
 &OBST ID='Innerwall3', XB=14.7,18.3,8.6,8.7,5.6,8.2, COLOR='GRAY 80', SURF\_ID='CONCRETE\_WALLS'/  
 &OBST ID='Innerwall6', XB=16.2,16.3,8.7,9.2,5.6,8.2, COLOR='GRAY 80', SURF\_ID='CONCRETE\_WALLS'/  
 &OBST ID='Parapet1', XB=14.7,18.3,4.2,4.3,5.6,6.3, COLOR='GRAY 80', SURF\_ID='CONCRETE\_WALLS'/  
 &OBST ID='Window backside', XB=14.7,18.3,4.2,4.3,6.3,8.2, SURF\_ID='DOUBLE GLAZING'/  
 &OBST ID='Bulkhead', XB=8.9,9.8,10.3,10.4,7.6,8.2, COLOR='GRAY 80', SURF\_ID='CONCRETE\_WALLS'/  
 &OBST ID='Bulkhead2', XB=8.8,8.9,9.2,10.0,7.6,8.2, COLOR='GRAY 80', SURF\_ID='CONCRETE\_WALLS'/  
 &OBST ID='Door 2.25-Hallway', XB=8.9,9.8,10.3,10.4,5.6,7.6, SURF\_ID='DOOR'/  
 &OBST ID='Door barchroom', XB=8.8,8.9,9.2,10.0,5.6,7.6, SURF\_ID='DOOR'/  
 &OBST ID='Innerwall 5', XB=9.8,10.7,10.3,10.4,5.6,8.2, COLOR='GRAY 80', SURF\_ID='CONCRETE\_WALLS'/  
 &OBST ID='Innerwall1', XB=6.9,7.1,4.0,10.5,5.6,8.2, COLOR='GRAY 80', SURF\_ID='CONCRETE\_WALLS'/  
 &OBST ID='Innerwall3', XB=7.1,10.7,8.6,8.7,5.6,8.2, COLOR='GRAY 80', SURF\_ID='CONCRETE\_WALLS'/  
 &OBST ID='Innerwall6', XB=8.8,8.9,8.7,9.2,5.6,8.2, COLOR='GRAY 80', SURF\_ID='CONCRETE\_WALLS'/  
 &OBST ID='Parapet1', XB=7.1,10.7,4.2,4.3,5.6,6.3, COLOR='GRAY 80', SURF\_ID='CONCRETE\_WALLS'/  
 &OBST ID='Window backside', XB=7.1,10.7,4.2,4.3,6.3,8.2, SURF\_ID='DOUBLE GLAZING'/  
 &OBST ID='Bulkhead', XB=5.1,6.0,10.3,10.4,7.6,8.2, COLOR='GRAY 80', SURF\_ID='CONCRETE\_WALLS'/  
 &OBST ID='Bulkhead2', XB=5.0,5.1,9.2,10.0,7.6,8.2, COLOR='GRAY 80', SURF\_ID='CONCRETE\_WALLS'/  
 &OBST ID='Door 2.24-Hallway', XB=5.1,6.0,10.3,10.4,5.6,7.6, SURF\_ID='DOOR'/  
 &OBST ID='Door barchroom', XB=5.0,5.1,9.2,10.0,5.6,7.6, SURF\_ID='DOOR'/  
 &OBST ID='Innerwall 5', XB=6.0,6.9,10.3,10.4,5.6,8.2, COLOR='GRAY 80', SURF\_ID='CONCRETE\_WALLS'/  
 &OBST ID='Innerwall1', XB=3.1,3.3,4.0,10.5,5.6,8.2, COLOR='GRAY 80', SURF\_ID='CONCRETE\_WALLS'/  
 &OBST ID='Innerwall3', XB=3.3,6.9,8.6,8.7,5.6,8.2, COLOR='GRAY 80', SURF\_ID='CONCRETE\_WALLS'/  
 &OBST ID='Innerwall6', XB=5.0,5.1,8.7,9.2,5.6,8.2, COLOR='GRAY 80', SURF\_ID='CONCRETE\_WALLS'/  
 &OBST ID='Parapet1', XB=3.3,6.9,4.2,4.3,5.6,6.3, COLOR='GRAY 80', SURF\_ID='CONCRETE\_WALLS'/  
 &OBST ID='Window backside', XB=3.3,6.9,4.2,4.3,6.3,8.2, SURF\_ID='DOUBLE GLAZING'/  
 &OBST ID='Bulkhead', XB=1.3,2.2,10.3,10.4,7.6,8.2, COLOR='GRAY 80', SURF\_ID='CONCRETE\_WALLS'/  
 &OBST ID='Bulkhead2', XB=1.2,1.3,9.2,10.0,7.6,8.2, COLOR='GRAY 80', SURF\_ID='CONCRETE\_WALLS'/  
 &OBST ID='Door 2.23-Hallway', XB=1.3,2.2,10.3,10.4,5.6,7.6, SURF\_ID='DOOR'/  
 &OBST ID='Door barchroom', XB=1.2,1.3,9.2,10.0,5.6,7.6, SURF\_ID='DOOR'/  
 &OBST ID='Innerwall 5', XB=2.2,3.1,10.3,10.4,5.6,8.2, COLOR='GRAY 80', SURF\_ID='CONCRETE\_WALLS'/  
 &OBST ID='Innerwall1', XB=-0.7,-0.5,4.0,10.5,5.6,8.2, COLOR='GRAY 80', SURF\_ID='CONCRETE\_WALLS'/  
 &OBST ID='Innerwall3', XB=-0.5,3.1,8.6,8.7,5.6,8.2, COLOR='GRAY 80', SURF\_ID='CONCRETE\_WALLS'/  
 &OBST ID='Innerwall6', XB=1.2,1.3,8.7,9.2,5.6,8.2, COLOR='GRAY 80', SURF\_ID='CONCRETE\_WALLS'/  
 &OBST ID='Parapet1', XB=-0.5,3.1,4.2,4.3,5.6,6.3, COLOR='GRAY 80', SURF\_ID='CONCRETE\_WALLS'/  
 &OBST ID='Window backside', XB=-0.5,3.1,4.2,4.3,6.3,8.2, SURF\_ID='DOUBLE GLAZING'/  
 &OBST ID='Hallway double door left', XB=-0.7,-0.6,10.5,12.2,5.6,7.6, SURF\_ID6='Double door','Double door','DOOR','DOOR','DOOR','DOOR'/  
 &OBST ID='Hallway bulkhead left', XB=-0.7,-0.6,10.5,12.2,7.6,8.2, COLOR='GRAY 80', SURF\_ID='CONCRETE\_WALLS'/  
 &OBST ID='Hallway bulkhead right', XB=18.4,18.5,10.5,12.2,7.6,8.2, COLOR='GRAY 80', SURF\_ID='CONCRETE\_WALLS'/  
 &OBST ID='Hallway double door right', XB=18.4,18.5,10.5,12.2,5.6,7.6, SURF\_ID6='Double door','Double door','DOOR','DOOR','DOOR','DOOR'/  
 &OBST ID='SOFA', XB=11.0,12.0,14.2,16.2,2.9,3.4, SURF\_ID='INERT'/  
 &OBST ID='Floor slab 1st', XB=6.6,11.2,8.4,9.8,2.6,2.8, COLOR='GRAY 80', SURF\_ID='CONCRETE\_FLOORS'/  
 &OBST ID='Floor slab 1st', XB=6.6,11.2,4.0,8.4,2.6,2.8, COLOR='GRAY 80', SURF\_ID='CONCRETE\_FLOORS'/  
 &OBST ID='Floor slab 1st', XB=-0.7,0.6,9.8,11.35,2.6,2.8, COLOR='GRAY 80', SURF\_ID='CONCRETE\_FLOORS'/  
 &OBST ID='Floor slab 1st', XB=0.6,2.6,9.8,11.35,2.6,2.8, COLOR='GRAY 80', SURF\_ID='CONCRETE\_FLOORS'/  
 &OBST ID='Floor slab 1st', XB=2.6,4.6,9.8,11.35,2.6,2.8, COLOR='GRAY 80', SURF\_ID='CONCRETE\_FLOORS'/  
 &OBST ID='Floor slab 1st', XB=4.6,6.6,9.8,11.35,2.6,2.8, COLOR='GRAY 80', SURF\_ID='CONCRETE\_FLOORS'/  
 &OBST ID='Floor slab 1st', XB=6.6,8.6,9.8,11.35,2.6,2.8, COLOR='GRAY 80', SURF\_ID='CONCRETE\_FLOORS'/  
 &OBST ID='Floor slab 1st', XB=8.6,10.6,9.8,11.35,2.6,2.8, COLOR='GRAY 80', SURF\_ID='CONCRETE\_FLOORS'/







&OBST ID='Floor slab 2nd', XB=12.6,14.6,11.35,12.9,5.4,5.6, COLOR='GRAY 80', SURF\_ID='CONCRETE\_FLOORS'/  
 &OBST ID='Floor slab 2nd', XB=14.6,16.6,11.35,12.9,5.4,5.6, COLOR='GRAY 80', SURF\_ID='CONCRETE\_FLOORS'/  
 &OBST ID='Floor slab 2nd', XB=16.6,18.5,11.35,12.9,5.4,5.6, COLOR='GRAY 80', SURF\_ID='CONCRETE\_FLOORS'/  
 &OBST ID='Floor slab 2nd', XB=10.6,12.9,12.9,14.4,5.4,5.6, COLOR='GRAY 80', SURF\_ID='CONCRETE\_FLOORS'/  
 &OBST ID='Floor slab 2nd', XB=10.6,12.9,14.4,15.9,5.4,5.6, COLOR='GRAY 80', SURF\_ID='CONCRETE\_FLOORS'/  
 &OBST ID='Floor slab 2nd', XB=10.6,12.9,15.9,17.4,5.4,5.6, COLOR='GRAY 80', SURF\_ID='CONCRETE\_FLOORS'/  
 &OBST ID='Floor slab 2nd', XB=10.6,12.9,17.4,18.9,5.4,5.6, COLOR='GRAY 80', SURF\_ID='CONCRETE\_FLOORS'/  
 &OBST ID='Floor slab 2nd', XB=12.9,15.3,12.9,14.4,5.4,5.6, COLOR='GRAY 80', SURF\_ID='CONCRETE\_FLOORS'/  
 &OBST ID='Floor slab 2nd', XB=12.9,15.3,14.4,15.9,5.4,5.6, COLOR='GRAY 80', SURF\_ID='CONCRETE\_FLOORS'/  
 &OBST ID='Floor slab 2nd', XB=12.9,15.3,15.9,17.4,5.4,5.6, COLOR='GRAY 80', SURF\_ID='CONCRETE\_FLOORS'/  
 &OBST ID='Floor slab 2nd', XB=12.9,15.3,17.4,18.9,5.4,5.6, COLOR='GRAY 80', SURF\_ID='CONCRETE\_FLOORS'/  
 &OBST ID='Floor slab 2nd', XB=10.6,15.3,18.9,19.7,5.4,5.6, COLOR='GRAY 80', SURF\_ID='CONCRETE\_FLOORS'/

&HOLE ID='Hole', XB=12.7,13.6,18.3,18.645028,2.8,4.8/  
 &HOLE ID='DOOR LIVING-KITCHEN', XB=13.0,14.5,13.9,14.2,2.8,4.8/  
 &HOLE ID='DOOR LIVING-KITCHEN', XB=9.2,10.7,13.9,14.2,2.8,4.8/  
 &HOLE ID='Overhead', XB=9.2,10.7,13.9,14.2,4.9,5.2/  
 &HOLE ID='DOOR LIVING-KITCHEN', XB=5.4,6.9,13.9,14.2,2.8,4.8/  
 &HOLE ID='Overhead', XB=5.4,6.9,13.9,14.2,4.9,5.2/  
 &HOLE ID='DOOR LIVING-KITCHEN', XB=1.6,3.1,13.9,14.2,2.8,4.8/  
 &HOLE ID='Overhead', XB=1.6,3.1,13.9,14.2,4.9,5.2/  
 &HOLE ID='DOOR LIVING-KITCHEN', XB=16.8,18.3,13.9,14.2,2.8,4.8/  
 &HOLE ID='Overhead', XB=16.8,18.3,13.9,14.2,4.9,5.2/  
 &HOLE ID='Overhead', XB=13.0,14.5,13.9,14.2,4.9,5.3/  
 &HOLE ID='DOOR LIVING-KITCHEN', XB=13.0,14.5,8.5,8.8,2.8,4.8/  
 &HOLE ID='Overhead', XB=13.0,14.5,8.5,8.8,4.8,5.3/  
 &HOLE ID='DOOR LIVING-KITCHEN', XB=16.8,18.3,8.5,8.8,2.8,4.8/  
 &HOLE ID='Overhead', XB=16.8,18.3,8.5,8.8,4.9,5.2/  
 &HOLE ID='DOOR LIVING-KITCHEN', XB=9.2,10.7,8.5,8.8,2.8,4.8/  
 &HOLE ID='Overhead', XB=9.2,10.7,8.5,8.8,4.9,5.2/  
 &HOLE ID='DOOR LIVING-KITCHEN', XB=5.4,6.9,8.5,8.8,2.8,4.8/  
 &HOLE ID='Overhead', XB=5.4,6.9,8.5,8.8,4.9,5.2/  
 &HOLE ID='DOOR LIVING-KITCHEN', XB=1.6,3.1,8.5,8.8,2.8,4.8/  
 &HOLE ID='Overhead', XB=1.6,3.1,8.5,8.8,4.9,5.2/  
 &HOLE ID='DOOR LIVING-KITCHEN', XB=13.0,14.5,13.9,14.2,5.6,7.6/  
 &HOLE ID='Overhead', XB=13.0,14.5,13.9,14.2,7.7,8.0/  
 &HOLE ID='DOOR LIVING-KITCHEN', XB=9.2,10.7,13.9,14.2,5.6,7.6/  
 &HOLE ID='Overhead', XB=9.2,10.7,13.9,14.2,7.7,8.0/  
 &HOLE ID='DOOR LIVING-KITCHEN', XB=5.4,6.9,13.9,14.2,5.6,7.6/  
 &HOLE ID='Overhead', XB=5.4,6.9,13.9,14.2,7.7,8.0/  
 &HOLE ID='DOOR LIVING-KITCHEN', XB=1.6,3.1,13.9,14.2,5.6,7.6/  
 &HOLE ID='Overhead', XB=1.6,3.1,13.9,14.2,7.7,8.0/  
 &HOLE ID='DOOR LIVING-KITCHEN', XB=16.8,18.3,13.9,14.2,5.6,7.6/  
 &HOLE ID='Overhead', XB=16.8,18.3,13.9,14.2,7.7,8.0/  
 &HOLE ID='DOOR LIVING-KITCHEN', XB=13.0,14.5,8.5,8.8,5.6,7.6/  
 &HOLE ID='Overhead', XB=13.0,14.5,8.5,8.8,7.7,8.0/  
 &HOLE ID='DOOR LIVING-KITCHEN', XB=16.8,18.3,8.5,8.8,5.6,7.6/  
 &HOLE ID='Overhead', XB=16.8,18.3,8.5,8.8,7.7,8.0/  
 &HOLE ID='DOOR LIVING-KITCHEN', XB=9.2,10.7,8.5,8.8,5.6,7.6/  
 &HOLE ID='Overhead', XB=9.2,10.7,8.5,8.8,7.7,8.0/  
 &HOLE ID='DOOR LIVING-KITCHEN', XB=5.4,6.9,8.5,8.8,5.6,7.6/  
 &HOLE ID='Overhead', XB=5.4,6.9,8.5,8.8,7.7,8.0/  
 &HOLE ID='DOOR LIVING-KITCHEN', XB=1.6,3.1,8.5,8.8,5.6,7.6/  
 &HOLE ID='Overhead', XB=1.6,3.1,8.5,8.8,7.7,8.0/

&VENT ID='Mesh Vent: MESH02 [XMAX]', SURF\_ID='OPEN', XB=11.2,11.2,3.8,8.4,2.6,5.8, COLOR='INVISIBLE'/  
 &VENT ID='Mesh Vent: MESH02 [XMIN]', SURF\_ID='OPEN', XB=6.6,6.6,3.8,8.4,2.6,5.8, COLOR='INVISIBLE'/  
 &VENT ID='Mesh Vent: MESH02 [YMIN]', SURF\_ID='OPEN', XB=6.6,11.2,3.8,3.8,2.6,5.8, COLOR='INVISIBLE'/  
 &VENT ID='Mesh Vent: MESH02 [ZMAX]', SURF\_ID='OPEN', XB=6.6,11.2,3.8,8.4,5.8,5.8, COLOR='INVISIBLE'/  
 &VENT ID='Mesh Vent: MESH02 [ZMIN]', SURF\_ID='OPEN', XB=6.6,11.2,3.8,8.4,2.6,2.6, COLOR='INVISIBLE'/  
 &VENT ID='Mesh Vent: MESH-c-e [XMAX]', SURF\_ID='OPEN', XB=15.3,15.3,18.9,21.5,2.6,5.8, COLOR='INVISIBLE'/  
 &VENT ID='Mesh Vent: MESH-c-e [XMIN]', SURF\_ID='OPEN', XB=10.6,10.6,18.9,21.5,2.6,5.8, COLOR='INVISIBLE'/  
 &VENT ID='Mesh Vent: MESH-c-e [YMAX]', SURF\_ID='OPEN', XB=10.6,15.3,21.5,21.5,2.6,5.8, COLOR='INVISIBLE'/  
 &VENT ID='Mesh Vent: MESH-c-e [ZMAX]', SURF\_ID='OPEN', XB=10.6,15.3,18.9,21.5,5.8,5.8, COLOR='INVISIBLE'/  
 &VENT ID='Mesh Vent: MESH-c-e [ZMIN]', SURF\_ID='OPEN', XB=10.6,15.3,18.9,21.5,2.6,2.6, COLOR='INVISIBLE'/  
 &VENT ID='Mesh Vent: MESH01 [XMAX]', SURF\_ID='OPEN', XB=11.2,11.2,8.4,9.8,2.6,5.8, COLOR='INVISIBLE'/



```
&VENT ID='Mesh Vent: MESH03-b-b-i [ZMIN]', SURF_ID='OPEN', XB=16.6,18.9,11.35,12.9,2.6,2.6, COLOR='INVISIBLE'/
&VENT ID='Inner wall 01', SURF_ID='INERT', XB=10.905654,10.905654,14.1,18.4,2.8,5.380981, COLOR='INVISIBLE'/
&VENT ID='Inner wall 02', SURF_ID='INERT', XB=14.5,14.5,12.4,18.4,2.8,5.380981/
&VENT ID='Inner wall 03', SURF_ID='INERT', XB=10.9,12.7,18.4,18.4,2.8,5.380981, COLOR='INVISIBLE'/
&VENT ID='Door 1 low', SURF_ID='INERT', XB=12.7,13.6,12.3,12.3,2.8,2.9/
&VENT ID='Door 2 low', SURF_ID='INERT', XB=12.7,13.6,12.4,12.4,2.8,2.9/
&VENT ID='Door 3 high', SURF_ID='INERT', XB=12.7,13.6,12.4,12.4,4.7,4.8/
&VENT ID='Door 4 high', SURF_ID='INERT', XB=12.7,13.6,12.3,12.3,4.7,4.8/
&VENT ID='Door 5 left', SURF_ID='INERT', XB=12.7,12.75,12.3,12.3,2.9,4.7/
&VENT ID='Door 6 left', SURF_ID='INERT', XB=12.7,12.75,12.4,12.4,2.9,4.7/
&VENT ID='Door 7 right', SURF_ID='INERT', XB=13.55,13.6,12.4,12.4,2.9,4.7/
&VENT ID='Door 8 right', SURF_ID='INERT', XB=13.55,13.6,12.3,12.3,2.9,4.7/
```

```
&HVAC ID='LEAK Apartment Interior', TYPE_ID='LEAK', VENT_ID='Inner wall 01', VENT2_ID='AMBIENT', AREA=7.7E-3,
LEAK_ENTHALPY=.TRUE./
&HVAC ID='LEAK Apartment interior 2', TYPE_ID='LEAK', VENT_ID='Inner wall 02', VENT2_ID='AMBIENT', AREA=7.7E-3,
LEAK_ENTHALPY=.TRUE./
&HVAC ID='Leak_apartment door right', TYPE_ID='LEAK', VENT_ID='Door 7 right', VENT2_ID='Door 8 right', AREA=8.3333E-5,
LEAK_ENTHALPY=.TRUE./
&HVAC ID='Leak_apartment door left', TYPE_ID='LEAK', VENT_ID='Door 5 left', VENT2_ID='Door 6 left', AREA=8.3333E-5,
LEAK_ENTHALPY=.TRUE./
&HVAC ID='Leak_apartment door_high', TYPE_ID='LEAK', VENT_ID='Door 3 high', VENT2_ID='Door 4 high', AREA=8.3333E-
5, LEAK_ENTHALPY=.TRUE./
&HVAC ID='Leak_apartment door_low', TYPE_ID='LEAK', VENT_ID='Door 1 low', VENT2_ID='Door 2 low', AREA=7.5E-4,
LEAK_ENTHALPY=.TRUE./
```

```
&ISOQ QUANTITY='TEMPERATURE', VALUE=50.0,100.0,200.0,400.0,500.0/
```

```
&SLCF QUANTITY='TEMPERATURE', PBX=13.2/
&SLCF QUANTITY='VISIBILITY', PBX=13.2/
&SLCF QUANTITY='TEMPERATURE', PBY=11.3/
&SLCF QUANTITY='VISIBILITY', PBY=11.3/
&SLCF QUANTITY='TEMPERATURE', PBX=14.2/
&SLCF QUANTITY='PRESSURE', PBX=13.2/
&SLCF QUANTITY='VOLUME FRACTION', SPEC_ID='OXYGEN', PBX=11.5/
&SLCF QUANTITY='VOLUME FRACTION', SPEC_ID='OXYGEN', PBY=11.3/
&SLCF QUANTITY='PRESSURE', PBY=11.3/
&SLCF QUANTITY='VELOCITY', VECTOR=.TRUE., PBX=13.2/
&SLCF QUANTITY='VELOCITY', VECTOR=.TRUE., PBY=11.3/
&SLCF QUANTITY='VOLUME FRACTION', SPEC_ID='HYDROGEN CYANIDE', PBY=11.3/
&SLCF QUANTITY='VOLUME FRACTION', SPEC_ID='Polyurethane GM21', PBY=11.3/
&SLCF QUANTITY='VOLUME FRACTION', SPEC_ID='Polyurethane GM21', PBX=11.5/
&SLCF QUANTITY='VOLUME FRACTION', SPEC_ID='OXYGEN', PBX=14.2/
&SLCF QUANTITY='TEMPERATURE', PBX=11.5/
&SLCF QUANTITY='VELOCITY', VECTOR=.TRUE., PBZ=5.2/
&SLCF QUANTITY='VELOCITY', VECTOR=.TRUE., PBZ=5.0/
&SLCF QUANTITY='VELOCITY', VECTOR=.TRUE., PBZ=4.8/
&SLCF QUANTITY='VELOCITY', VECTOR=.TRUE., PBZ=4.6/
&SLCF QUANTITY='VELOCITY', VECTOR=.TRUE., PBZ=4.3/
&SLCF QUANTITY='VELOCITY', VECTOR=.TRUE., PBZ=3.7/
&SLCF QUANTITY='VELOCITY', VECTOR=.TRUE., PBZ=3.1/
&SLCF QUANTITY='TEMPERATURE', VECTOR=.TRUE., PBZ=5.2/
&SLCF QUANTITY='TEMPERATURE', VECTOR=.TRUE., PBZ=5.0/
&SLCF QUANTITY='TEMPERATURE', VECTOR=.TRUE., PBZ=4.8/
&SLCF QUANTITY='TEMPERATURE', VECTOR=.TRUE., PBZ=4.6/
&SLCF QUANTITY='TEMPERATURE', VECTOR=.TRUE., PBZ=4.3/
&SLCF QUANTITY='TEMPERATURE', VECTOR=.TRUE., PBZ=3.7/
&SLCF QUANTITY='TEMPERATURE', VECTOR=.TRUE., PBZ=3.1/
&SLCF QUANTITY='VOLUME FRACTION', SPEC_ID='CARBON MONOXIDE', PBZ=3.1/
&SLCF QUANTITY='VOLUME FRACTION', SPEC_ID='CARBON MONOXIDE', PBZ=4.3/
&SLCF QUANTITY='MASS FRACTION', SPEC_ID='SOOT', PBZ=3.1/
&SLCF QUANTITY='MASS FRACTION', SPEC_ID='SOOT', PBZ=4.3/
&SLCF QUANTITY='VISIBILITY', PBY=10.7/
&SLCF QUANTITY='MASS FRACTION', SPEC_ID='SOOT', PBY=10.7/
&SLCF QUANTITY='VOLUME FRACTION', SPEC_ID='CARBON DIOXIDE', PBY=10.7/
&SLCF QUANTITY='VOLUME FRACTION', SPEC_ID='CARBON DIOXIDE', PBZ=3.1/
```

&SLCF QUANTITY='VOLUME FRACTION', SPEC\_ID='CARBON DIOXIDE', PBZ=4.3/

&TAIL /

## Case study 2: door opened after 300 seconds

v2\_33.fds

Generated by PyroSim - Version 2021.4.1201

20-feb-2022 13:45:23

&HEAD CHID='v2\_33', TITLE='simulation experiment fine mesh 04-07-2019 afternoon 1.19 [door open after 5 min] /

&TIME T\_END=1000.0/

&DUMP DT\_ISOF=10.0, DT\_SL3D=0.25/

&MISC TMPA=23.1, MAXIMUM\_VISIBILITY=100.0/

&COMB N\_SIMPLE\_CHEMISTRY\_REACTIONS=2/

&MESH ID='MESH00', IJK=46,14,32, XB=6.6,11.2,8.4,9.8,2.6,5.8, MPI\_PROCESS =0/  
 &MESH ID='MESH01', IJK=23,23,16, XB=6.6,11.2,3.8,8.4,2.6,5.8, MPI\_PROCESS =1/  
 &MESH ID='MESH02', IJK=40,31,64, XB=-1.4,0.6,9.8,11.35,2.6,5.8, MPI\_PROCESS =2/  
 &MESH ID='MESH03', IJK=40,31,64, XB=0.6,2.6,9.8,11.35,2.6,5.8, MPI\_PROCESS =3/  
 &MESH ID='MESH04', IJK=40,31,64, XB=2.6,4.6,9.8,11.35,2.6,5.8, MPI\_PROCESS =4/  
 &MESH ID='MESH05', IJK=40,31,64, XB=4.6,6.6,9.8,11.35,2.6,5.8, MPI\_PROCESS =5/  
 &MESH ID='MESH06', IJK=40,31,64, XB=6.6,8.6,9.8,11.35,2.6,5.8, MPI\_PROCESS =6/  
 &MESH ID='MESH07', IJK=40,31,64, XB=8.6,10.6,9.8,11.35,2.6,5.8, MPI\_PROCESS =7/  
 &MESH ID='MESH08', IJK=40,31,64, XB=10.6,12.6,9.8,11.35,2.6,5.8, MPI\_PROCESS =8/  
 &MESH ID='MESH09', IJK=40,31,64, XB=12.6,14.6,9.8,11.35,2.6,5.8, MPI\_PROCESS =9/  
 &MESH ID='MESH10', IJK=40,31,64, XB=14.6,16.6,9.8,11.35,2.6,5.8, MPI\_PROCESS =10/  
 &MESH ID='MESH11', IJK=46,31,64, XB=16.6,18.9,9.8,11.35,2.6,5.8, MPI\_PROCESS =11/  
 &MESH ID='MESH12', IJK=40,31,64, XB=-1.4,0.6,11.35,12.9,2.6,5.8, MPI\_PROCESS =12/  
 &MESH ID='MESH13', IJK=40,31,64, XB=0.6,2.6,11.35,12.9,2.6,5.8, MPI\_PROCESS =13/  
 &MESH ID='MESH14', IJK=40,31,64, XB=2.6,4.6,11.35,12.9,2.6,5.8, MPI\_PROCESS =14/  
 &MESH ID='MESH15', IJK=40,31,64, XB=4.6,6.6,11.35,12.9,2.6,5.8, MPI\_PROCESS =15/  
 &MESH ID='MESH16', IJK=40,31,64, XB=6.6,8.6,11.35,12.9,2.6,5.8, MPI\_PROCESS =16/  
 &MESH ID='MESH17', IJK=40,31,64, XB=8.6,10.6,11.35,12.9,2.6,5.8, MPI\_PROCESS =17/  
 &MESH ID='MESH18', IJK=40,31,64, XB=10.6,12.6,11.35,12.9,2.6,5.8, MPI\_PROCESS =18/  
 &MESH ID='MESH19', IJK=40,31,64, XB=12.6,14.6,11.35,12.9,2.6,5.8, MPI\_PROCESS =19/  
 &MESH ID='MESH20', IJK=40,31,64, XB=14.6,16.6,11.35,12.9,2.6,5.8, MPI\_PROCESS =20/  
 &MESH ID='MESH21', IJK=46,31,64, XB=16.6,18.9,11.35,12.9,2.6,5.8, MPI\_PROCESS =21/  
 &MESH ID='MESH22', IJK=46,30,64, XB=10.6,12.9,12.9,14.4,2.6,5.8, MPI\_PROCESS =22/  
 &MESH ID='MESH23', IJK=46,30,64, XB=10.6,12.9,14.4,15.9,2.6,5.8, MPI\_PROCESS =23/  
 &MESH ID='MESH24', IJK=46,30,64, XB=10.6,12.9,15.9,17.4,2.6,5.8, MPI\_PROCESS =24/  
 &MESH ID='MESH25', IJK=46,30,64, XB=10.6,12.9,17.4,18.9,2.6,5.8, MPI\_PROCESS =25/  
 &MESH ID='MESH26', IJK=48,30,64, XB=12.9,15.3,12.9,14.4,2.6,5.8, MPI\_PROCESS =26/  
 &MESH ID='MESH27', IJK=48,30,64, XB=12.9,15.3,14.4,15.9,2.6,5.8, MPI\_PROCESS =27/  
 &MESH ID='MESH28', IJK=48,30,64, XB=12.9,15.3,15.9,17.4,2.6,5.8, MPI\_PROCESS =28/  
 &MESH ID='MESH29', IJK=48,30,64, XB=12.9,15.3,17.4,18.9,2.6,5.8, MPI\_PROCESS =29/  
 &MESH ID='MESH30', IJK=47,26,32, XB=10.6,15.3,18.9,21.5,2.6,5.8, MPI\_PROCESS =30/

&ZONE ID='Apartment 1,19', XB=12.7,14.5,12.4,18.4,2.8,5.4, LEAK\_AREA=0.011, LEAK\_PRESSURE\_EXPONENT=0.56/

&ZONE ID='Hallway leakage 1.19', XB=-0.6,18.4,10.4,12.3,2.8,5.2, LEAK\_AREA=0.1/

&SPEC ID='Polyurethane GM21', FORMULA='C1H1.8O0.3N0.05'/

&REAC ID='Polyurethane (well ventilated)',

FYI='Polyurethane',

FUEL='Polyurethane GM21',

C=1.0,

H=1.8,

O=0.3,

N=0.05,

CRITICAL\_FLAME\_TEMPERATURE=654.0,

AUTO\_IGNITION\_TEMPERATURE=400.0,

CO\_YIELD=0.01,

SOOT\_YIELD=0.131,

HCN\_YIELD=2.0E-3,

EPUMO2=8950.0,  
 AIT\_EXCLUSION\_ZONE(1:6,1)=11,12,14.2,16.2,2.8,5.8,  
 HOC\_COMPLETE=16000,  
 LOWER\_OXYGEN\_LIMIT=0.08/

EPUMO2 calculated from chemical equilibrium as 'HEAT\_OF\_COMBUSTION' did not work. Value results in an effective heat of combustion of 16 MJ/kg. Overruled by HOC\_COMPLETE.

&PROP ID='TK1.1.0 props', DIAMETER=0.00075/  
 &PROP ID='TK1.1.1 props', DIAMETER=0.00075/  
 &PROP ID='TK1.1.2 props', DIAMETER=0.00075/  
 &PROP ID='TK1.1.3 props', DIAMETER=0.00075/  
 &PROP ID='TK1.1.4 props', DIAMETER=0.00075/  
 &PROP ID='TK1.1.5 props', DIAMETER=0.00075/  
 &PROP ID='TK1.1.6 props', DIAMETER=0.00075/  
 &PROP ID='TK1.1.1alt props', DIAMETER=0.00075/  
 &PROP ID='TK1.1.2alt props', DIAMETER=0.00075/  
 &PROP ID='TK1.1.3alt props', DIAMETER=0.00075/  
 &PROP ID='TK1.1.4alt props', DIAMETER=0.00075/  
 &PROP ID='TK1.1.5alt props', DIAMETER=0.00075/  
 &PROP ID='TK1.1.6alt props', DIAMETER=0.00075/  
 &PROP ID='TK1.1.7alt props', DIAMETER=0.00075/  
 &PROP ID='TK1.1.6alt01 props', DIAMETER=0.00075/  
 &PROP ID='TK1.1.1alt01 props', DIAMETER=0.00075/  
 &PROP ID='TK1.1.2alt01 props', DIAMETER=0.00075/  
 &PROP ID='TK1.1.3alt01 props', DIAMETER=0.00075/  
 &PROP ID='TK1.1.4alt01 props', DIAMETER=0.00075/  
 &PROP ID='TK1.1.5alt01 props', DIAMETER=0.00075/  
 &PROP ID='TK1.1.7alt01 props', DIAMETER=0.00075/  
 &DEVC ID='CO(7)', QUANTITY='VOLUME FRACTION', SPEC\_ID='CARBON MONOXIDE', XYZ=14.2,13.1,4.3/  
 &DEVC ID='CO2(7)', QUANTITY='VOLUME FRACTION', SPEC\_ID='CARBON DIOXIDE', XYZ=14.2,13.1,4.3/  
 &DEVC ID='O2(7)', QUANTITY='VOLUME FRACTION', SPEC\_ID='OXYGEN', XYZ=14.2,13.1,4.3/  
 &DEVC ID='PP1,1,1', QUANTITY='PRESSURE', XYZ=14.2,13.1,3.0/  
 &DEVC ID='SP1,1,1', QUANTITY='RADIATIVE HEAT FLUX GAS', XYZ=14.2,13.1,4.3/  
 &DEVC ID='SP1,1,2', QUANTITY='RADIATIVE HEAT FLUX GAS', XYZ=14.2,13.1,3.1/  
 &DEVC ID='TK1.1.0', PROP\_ID='TK1.1.0 props', QUANTITY='THERMOCOUPLE', XYZ=14.2,13.1,5.2/  
 &DEVC ID='TK1.1.1', PROP\_ID='TK1.1.1 props', QUANTITY='THERMOCOUPLE', XYZ=14.2,13.1,5.0/  
 &DEVC ID='TK1.1.2', PROP\_ID='TK1.1.2 props', QUANTITY='THERMOCOUPLE', XYZ=14.2,13.1,4.8/  
 &DEVC ID='TK1.1.3', PROP\_ID='TK1.1.3 props', QUANTITY='THERMOCOUPLE', XYZ=14.2,13.1,4.6/  
 &DEVC ID='TK1.1.4', PROP\_ID='TK1.1.4 props', QUANTITY='THERMOCOUPLE', XYZ=14.2,13.1,4.3/  
 &DEVC ID='TK1.1.5', PROP\_ID='TK1.1.5 props', QUANTITY='THERMOCOUPLE', XYZ=14.2,13.1,3.7/  
 &DEVC ID='TK1.1.6', PROP\_ID='TK1.1.6 props', QUANTITY='THERMOCOUPLE', XYZ=14.2,13.1,3.1/  
 &DEVC ID='CO(11)', QUANTITY='VOLUME FRACTION', SPEC\_ID='CARBON MONOXIDE', XYZ=2.7,10.7,3.1/  
 &DEVC ID='CO(15)', QUANTITY='VOLUME FRACTION', SPEC\_ID='CARBON MONOXIDE', XYZ=2.7,10.7,4.3/  
 &DEVC ID='CO2(11)', QUANTITY='VOLUME FRACTION', SPEC\_ID='CARBON DIOXIDE', XYZ=2.7,10.7,3.1/  
 &DEVC ID='CO2(15)', QUANTITY='VOLUME FRACTION', SPEC\_ID='CARBON DIOXIDE', XYZ=2.7,10.7,4.3/  
 &DEVC ID='O2(11)', QUANTITY='VOLUME FRACTION', SPEC\_ID='OXYGEN', XYZ=2.7,10.7,3.1/  
 &DEVC ID='O2(15)', QUANTITY='VOLUME FRACTION', SPEC\_ID='OXYGEN', XYZ=2.7,10.7,4.3/  
 &DEVC ID='PP1,5,1', QUANTITY='PRESSURE', XYZ=2.7,10.7,3.0/  
 &DEVC ID='SB1,5,2', QUANTITY='RADIATIVE HEAT FLUX GAS', XYZ=2.7,10.7,3.1/  
 &DEVC ID='SP1,5,1', QUANTITY='RADIATIVE HEAT FLUX GAS', XYZ=2.7,10.7,4.3/  
 &DEVC ID='TK1,5,0', QUANTITY='THERMOCOUPLE', XYZ=2.7,10.7,5.15/  
 &DEVC ID='TK1,5,1', QUANTITY='THERMOCOUPLE', XYZ=2.7,10.7,5.0/  
 &DEVC ID='TK1,5,2', QUANTITY='THERMOCOUPLE', XYZ=2.7,10.7,4.8/  
 &DEVC ID='TK1,5,3', QUANTITY='THERMOCOUPLE', XYZ=2.7,10.7,4.6/  
 &DEVC ID='TK1,5,4', QUANTITY='THERMOCOUPLE', XYZ=2.7,10.7,4.3/  
 &DEVC ID='TK1,5,5', QUANTITY='THERMOCOUPLE', XYZ=2.7,10.7,3.7/  
 &DEVC ID='TK1,5,6', QUANTITY='THERMOCOUPLE', XYZ=2.7,10.7,3.1/  
 &DEVC ID='ZL1,5,1', QUANTITY='VISIBILITY', XYZ=2.7,10.7,4.3/  
 &DEVC ID='ZL1,5,2', QUANTITY='VISIBILITY', XYZ=2.7,10.7,3.1/  
 &DEVC ID='CO(21)', QUANTITY='VOLUME FRACTION', SPEC\_ID='CARBON MONOXIDE', XYZ=15.7,10.8,3.1/  
 &DEVC ID='CO(23)', QUANTITY='VOLUME FRACTION', SPEC\_ID='CARBON MONOXIDE', XYZ=15.7,10.8,4.3/  
 &DEVC ID='CO2(21)', QUANTITY='VOLUME FRACTION', SPEC\_ID='CARBON DIOXIDE', XYZ=15.7,10.8,3.1/  
 &DEVC ID='CO2(23)', QUANTITY='VOLUME FRACTION', SPEC\_ID='CARBON DIOXIDE', XYZ=15.7,10.8,4.3/  
 &DEVC ID='O2(21)', QUANTITY='VOLUME FRACTION', SPEC\_ID='OXYGEN', XYZ=15.7,10.8,3.1/  
 &DEVC ID='O2(23)', QUANTITY='VOLUME FRACTION', SPEC\_ID='OXYGEN', XYZ=15.7,10.8,4.3/

```

&DEVC ID='PP1,6,1', QUANTITY='PRESSURE', XYZ=15.7,10.8,3.0/
&DEVC ID='SB1,6,2', QUANTITY='RADIATIVE HEAT FLUX GAS', XYZ=15.7,10.8,3.1/
&DEVC ID='SP1,6,1', QUANTITY='RADIATIVE HEAT FLUX GAS', XYZ=15.7,10.8,4.3/
&DEVC ID='TK1,6,0', QUANTITY='THERMOCOUPLE', XYZ=15.7,10.8,5.15/
&DEVC ID='TK1,6,1', QUANTITY='THERMOCOUPLE', XYZ=15.7,10.8,5.0/
&DEVC ID='TK1,6,2', QUANTITY='THERMOCOUPLE', XYZ=15.7,10.8,4.8/
&DEVC ID='TK1,6,3', QUANTITY='THERMOCOUPLE', XYZ=15.7,10.8,4.6/
&DEVC ID='TK1,6,4', QUANTITY='THERMOCOUPLE', XYZ=15.7,10.8,4.3/
&DEVC ID='TK1,6,5', QUANTITY='THERMOCOUPLE', XYZ=15.7,10.8,3.7/
&DEVC ID='TK1,6,6', QUANTITY='THERMOCOUPLE', XYZ=15.7,10.8,3.1/
&DEVC ID='ZL1,6,1', QUANTITY='VISIBILITY', XYZ=15.7,10.8,4.3/
&DEVC ID='ZL1,6,2', QUANTITY='VISIBILITY', XYZ=15.7,10.8,3.1/
&DEVC ID='TEMP_FIRE_0,2', QUANTITY='TEMPERATURE', XYZ=11.5,15.2,3.6/
&DEVC ID='TEMP_FIRE_0,4', QUANTITY='TEMPERATURE', XYZ=11.5,15.2,3.8/
&DEVC ID='TEMP_FIRE_0,6', QUANTITY='TEMPERATURE', XYZ=11.5,15.2,4.0/
&DEVC ID='TEMP_FIRE_0,8', QUANTITY='TEMPERATURE', XYZ=11.5,15.2,4.2/
&DEVC ID='TEMP_FIRE_1,0', QUANTITY='TEMPERATURE', XYZ=11.5,15.2,4.4/
&DEVC ID='TEMP_FIRE_1,2', QUANTITY='TEMPERATURE', XYZ=11.5,15.2,4.6/
&DEVC ID='TEMP_FIRE_1,4', QUANTITY='TEMPERATURE', XYZ=11.5,15.2,4.8/
&DEVC ID='TEMP_FIRE_1,6', QUANTITY='TEMPERATURE', XYZ=11.5,15.2,5.0/
&DEVC ID='Positive hallway', QUANTITY='MASS FLOW +', XB=12.7,13.6,12.3,12.3,2.8,4.8/
&DEVC ID='Negative hallway', QUANTITY='MASS FLOW -', XB=12.7,13.6,12.3,12.3,2.8,4.8/
&DEVC ID='Positive balcony', QUANTITY='MASS FLOW +', XB=12.7,13.6,18.4,18.4,2.8,4.8/
&DEVC ID='Negative balcony', QUANTITY='MASS FLOW -', XB=12.7,13.6,18.4,18.4,2.8,4.8/
&DEVC ID='RH4', QUANTITY='LAYER HEIGHT', XB=7.4,7.4,10.7,10.7,2.8,5.4/
&DEVC ID='RH5', QUANTITY='LAYER HEIGHT', XB=11.2,11.2,10.7,10.7,2.8,5.4/
&DEVC ID='Oxygen_FIRE_0,2', QUANTITY='VOLUME FRACTION', SPEC_ID='OXYGEN', XYZ=11.5,15.2,3.6/
&DEVC ID='Oxygen_FIRE_0,4', QUANTITY='VOLUME FRACTION', SPEC_ID='OXYGEN', XYZ=11.5,15.2,3.8/
&DEVC ID='Oxygen_FIRE_0,6', QUANTITY='VOLUME FRACTION', SPEC_ID='OXYGEN', XYZ=11.5,15.2,4.0/
&DEVC ID='Oxygen_FIRE_0,8', QUANTITY='VOLUME FRACTION', SPEC_ID='OXYGEN', XYZ=11.5,15.2,4.2/
&DEVC ID='Oxygen_FIRE_1,0', QUANTITY='VOLUME FRACTION', SPEC_ID='OXYGEN', XYZ=11.5,15.2,4.4/
&DEVC ID='Oxygen_FIRE_1,2', QUANTITY='VOLUME FRACTION', SPEC_ID='OXYGEN', XYZ=11.5,15.2,4.6/
&DEVC ID='Oxygen_FIRE_1,4', QUANTITY='VOLUME FRACTION', SPEC_ID='OXYGEN', XYZ=11.5,15.2,4.8/
&DEVC ID='Oxygen_FIRE_1,6', QUANTITY='VOLUME FRACTION', SPEC_ID='OXYGEN', XYZ=11.5,15.2,5.0/
&DEVC ID='TK1.1.1alt', PROP_ID='TK1.1.1alt props', QUANTITY='THERMOCOUPLE', XYZ=13.9,13.1,5.2/
&DEVC ID='TK1.1.2alt', PROP_ID='TK1.1.2alt props', QUANTITY='THERMOCOUPLE', XYZ=13.9,13.1,5.0/
&DEVC ID='TK1.1.3alt', PROP_ID='TK1.1.3alt props', QUANTITY='THERMOCOUPLE', XYZ=13.9,13.1,4.8/
&DEVC ID='TK1.1.4alt', PROP_ID='TK1.1.4alt props', QUANTITY='THERMOCOUPLE', XYZ=13.9,13.1,4.6/
&DEVC ID='TK1.1.5alt', PROP_ID='TK1.1.5alt props', QUANTITY='THERMOCOUPLE', XYZ=13.9,13.1,4.3/
&DEVC ID='TK1.1.6alt', PROP_ID='TK1.1.6alt props', QUANTITY='THERMOCOUPLE', XYZ=13.9,13.1,3.7/
&DEVC ID='TK1.1.7alt', PROP_ID='TK1.1.7alt props', QUANTITY='THERMOCOUPLE', XYZ=13.9,13.1,3.1/
&DEVC ID='TK1.1.6alt01', PROP_ID='TK1.1.6alt01 props', QUANTITY='THERMOCOUPLE', XYZ=13.6,13.1,3.7/
&DEVC ID='TK1.1.1alt01', PROP_ID='TK1.1.1alt01 props', QUANTITY='THERMOCOUPLE', XYZ=13.6,13.1,5.2/
&DEVC ID='TK1.1.2alt01', PROP_ID='TK1.1.2alt01 props', QUANTITY='THERMOCOUPLE', XYZ=13.6,13.1,5.0/
&DEVC ID='TK1.1.3alt01', PROP_ID='TK1.1.3alt01 props', QUANTITY='THERMOCOUPLE', XYZ=13.6,13.1,4.8/
&DEVC ID='TK1.1.4alt01', PROP_ID='TK1.1.4alt01 props', QUANTITY='THERMOCOUPLE', XYZ=13.6,13.1,4.6/
&DEVC ID='TK1.1.5alt01', PROP_ID='TK1.1.5alt01 props', QUANTITY='THERMOCOUPLE', XYZ=13.6,13.1,4.3/
&DEVC ID='TK1.1.7alt01', PROP_ID='TK1.1.7alt01 props', QUANTITY='THERMOCOUPLE', XYZ=13.6,13.1,3.1/
&DEVC ID='TIMER->OUT', QUANTITY='TIME', XYZ=6.6,8.4,2.6, SETPOINT=300.0, INITIAL_STATE=.TRUE./

&MATL ID='GYPSUM PLASTER',
  FYI='Quintiere, Fire Behavior - NIST NRC Validation',
  SPECIFIC_HEAT=0.84,
  CONDUCTIVITY=0.48,
  DENSITY=1440.0/
&MATL ID='CONCRETE',
  FYI='NBSIR 88-3752 - ATF NIST Multi-Floor Validation',
  SPECIFIC_HEAT=1.04,
  CONDUCTIVITY=1.8,
  DENSITY=2280.0/
&MATL ID='Calcium stone',
  SPECIFIC_HEAT=0.84,
  CONDUCTIVITY=0.75,
  DENSITY=1900.0/
&MATL ID='YELLOW PINE',
  FYI='Quintiere, Fire Behavior - NIST NRC Validation',

```

```

SPECIFIC_HEAT=2.85,
CONDUCTIVITY=0.14,
DENSITY=640.0/
&MATL ID='CALCIUM SILICATE',
FYI='NBSIR 88-3752 - NBS Multi-Room Validation',
SPECIFIC_HEAT_RAMP='CALCIUM SILICATE_SPECIFIC_HEAT_RAMP',
CONDUCTIVITY=0.12,
DENSITY=720.0,
EMISSIVITY=0.83/
&RAMP ID='CALCIUM SILICATE_SPECIFIC_HEAT_RAMP', T=20.0, F=1.25/
&RAMP ID='CALCIUM SILICATE_SPECIFIC_HEAT_RAMP', T=200.0, F=1.25/
&RAMP ID='CALCIUM SILICATE_SPECIFIC_HEAT_RAMP', T=300.0, F=1.33/
&RAMP ID='CALCIUM SILICATE_SPECIFIC_HEAT_RAMP', T=600.0, F=1.55/
&MATL ID='DOUBLE GLAZING',
SPECIFIC_HEAT=0.72,
CONDUCTIVITY=5.68E-3,
DENSITY=2500.0/

&SURF ID='CONCRETE_FLOORS',
RGB=146,202,166,
BACKING='VOID',
MATL_ID(1,1)='GYPSUM PLASTER',
MATL_ID(2,1)='CONCRETE',
MATL_MASS_FRACTION(1,1)=1.0,
MATL_MASS_FRACTION(2,1)=1.0,
THICKNESS(1:2)=1.0E-3,0.2/
&SURF ID='CONCRETE_WALLS',
RGB=146,202,166,
BACKING='VOID',
MATL_ID(1,1)='CONCRETE',
MATL_MASS_FRACTION(1,1)=1.0,
THICKNESS(1)=0.2/
&SURF ID='CALCIUM SILICATE WALLS',
COLOR='WHITE',
BACKING='VOID',
MATL_ID(1,1)='Calcium stone',
MATL_MASS_FRACTION(1,1)=1.0,
THICKNESS(1)=0.1/
&SURF ID='DOOR',
RGB=204,204,0,
BACKING='VOID',
MATL_ID(1,1)='YELLOW PINE',
MATL_MASS_FRACTION(1,1)=1.0,
THICKNESS(1)=0.05/
&SURF ID='Windows fire room',
RGB=146,202,166,
BACKING='VOID',
MATL_ID(1,1)='CALCIUM SILICATE',
MATL_MASS_FRACTION(1,1)=1.0,
THICKNESS(1)=0.012/
&SURF ID='DOUBLE GLAZING',
RGB=146,193,202,
TRANSPARENCY=0.396078,
BACKING='VOID',
MATL_ID(1,1)='DOUBLE GLAZING',
MATL_MASS_FRACTION(1,1)=1.0,
THICKNESS(1)=0.012/
&SURF ID='Hallway-apartments',
RGB=127,221,255,
LEAK_PATH=2,0/
&SURF ID='Double door',
RGB=127,221,255,
LEAK_PATH=2,0/
&SURF ID='CEILING HALLWAY',
RGB=146,202,166,
BACKING='VOID',

```

```

MATL_ID(1,1)=CALCIUM SILICATE',
MATL_MASS_FRACTION(1,1)=1.0,
THICKNESS(1)=0.03/
&SURF ID='Apartment1.19-Zone0',
  LEAK_PATH=1,0/
&SURF ID='SofaFIRE01',
  COLOR='RED',
  MLRPUA=0.064754,
  RAMP_Q='SofaFIRE01_RAMP_Q',
  TMP_FRONT=300.0/
&RAMP ID='SofaFIRE01_RAMP_Q', T=0.0, F=0.0/
&RAMP ID='SofaFIRE01_RAMP_Q', T=10.0, F=3.615991E-3/
&RAMP ID='SofaFIRE01_RAMP_Q', T=20.0, F=2.316719E-3/
&RAMP ID='SofaFIRE01_RAMP_Q', T=30.0, F=2.776608E-3/
&RAMP ID='SofaFIRE01_RAMP_Q', T=40.0, F=2.05341E-3/
&RAMP ID='SofaFIRE01_RAMP_Q', T=50.0, F=1.989901E-3/
&RAMP ID='SofaFIRE01_RAMP_Q', T=60.0, F=1.461971E-3/
&RAMP ID='SofaFIRE01_RAMP_Q', T=70.0, F=3.179356E-3/
&RAMP ID='SofaFIRE01_RAMP_Q', T=80.0, F=4.773311E-3/
&RAMP ID='SofaFIRE01_RAMP_Q', T=90.0, F=6.496977E-3/
&RAMP ID='SofaFIRE01_RAMP_Q', T=100.0, F=9.28022E-3/
&RAMP ID='SofaFIRE01_RAMP_Q', T=110.0, F=0.012991/
&RAMP ID='SofaFIRE01_RAMP_Q', T=120.0, F=0.018093/
&RAMP ID='SofaFIRE01_RAMP_Q', T=130.0, F=0.024128/
&RAMP ID='SofaFIRE01_RAMP_Q', T=140.0, F=0.031551/
&RAMP ID='SofaFIRE01_RAMP_Q', T=150.0, F=0.039305/
&RAMP ID='SofaFIRE01_RAMP_Q', T=160.0, F=0.048318/
&RAMP ID='SofaFIRE01_RAMP_Q', T=170.0, F=0.055947/
&RAMP ID='SofaFIRE01_RAMP_Q', T=180.0, F=0.063181/
&RAMP ID='SofaFIRE01_RAMP_Q', T=190.0, F=0.072664/
&RAMP ID='SofaFIRE01_RAMP_Q', T=200.0, F=0.081615/
&RAMP ID='SofaFIRE01_RAMP_Q', T=210.0, F=0.084786/
&RAMP ID='SofaFIRE01_RAMP_Q', T=220.0, F=0.088879/
&RAMP ID='SofaFIRE01_RAMP_Q', T=230.0, F=0.091448/
&RAMP ID='SofaFIRE01_RAMP_Q', T=240.0, F=0.091474/
&RAMP ID='SofaFIRE01_RAMP_Q', T=250.0, F=0.09073/
&RAMP ID='SofaFIRE01_RAMP_Q', T=260.0, F=0.093939/
&RAMP ID='SofaFIRE01_RAMP_Q', T=270.0, F=0.096387/
&RAMP ID='SofaFIRE01_RAMP_Q', T=280.0, F=0.113142/
&RAMP ID='SofaFIRE01_RAMP_Q', T=290.0, F=0.16052/
&RAMP ID='SofaFIRE01_RAMP_Q', T=300.0, F=0.220935/
&RAMP ID='SofaFIRE01_RAMP_Q', T=310.0, F=0.274118/
&RAMP ID='SofaFIRE01_RAMP_Q', T=320.0, F=0.327618/
&RAMP ID='SofaFIRE01_RAMP_Q', T=330.0, F=0.37369/
&RAMP ID='SofaFIRE01_RAMP_Q', T=340.0, F=0.404707/
&RAMP ID='SofaFIRE01_RAMP_Q', T=350.0, F=0.432965/
&RAMP ID='SofaFIRE01_RAMP_Q', T=360.0, F=0.497003/
&RAMP ID='SofaFIRE01_RAMP_Q', T=370.0, F=0.606822/
&RAMP ID='SofaFIRE01_RAMP_Q', T=380.0, F=0.728359/
&RAMP ID='SofaFIRE01_RAMP_Q', T=390.0, F=0.835963/
&RAMP ID='SofaFIRE01_RAMP_Q', T=400.0, F=0.920467/
&RAMP ID='SofaFIRE01_RAMP_Q', T=410.0, F=0.970393/
&RAMP ID='SofaFIRE01_RAMP_Q', T=420.0, F=0.974047/
&RAMP ID='SofaFIRE01_RAMP_Q', T=430.0, F=0.975763/
&RAMP ID='SofaFIRE01_RAMP_Q', T=440.0, F=1.0/
&RAMP ID='SofaFIRE01_RAMP_Q', T=450.0, F=0.961015/
&RAMP ID='SofaFIRE01_RAMP_Q', T=460.0, F=0.884364/
&RAMP ID='SofaFIRE01_RAMP_Q', T=470.0, F=0.823928/
&RAMP ID='SofaFIRE01_RAMP_Q', T=480.0, F=0.734048/
&RAMP ID='SofaFIRE01_RAMP_Q', T=490.0, F=0.607586/
&RAMP ID='SofaFIRE01_RAMP_Q', T=500.0, F=0.552532/
&RAMP ID='SofaFIRE01_RAMP_Q', T=510.0, F=0.531232/
&RAMP ID='SofaFIRE01_RAMP_Q', T=520.0, F=0.485788/
&RAMP ID='SofaFIRE01_RAMP_Q', T=530.0, F=0.45388/
&RAMP ID='SofaFIRE01_RAMP_Q', T=540.0, F=0.416993/
&RAMP ID='SofaFIRE01_RAMP_Q', T=550.0, F=0.383496/

```

&RAMP ID='SofaFIRE01\_RAMP\_Q', T=560.0, F=0.364994/  
 &RAMP ID='SofaFIRE01\_RAMP\_Q', T=570.0, F=0.345678/  
 &RAMP ID='SofaFIRE01\_RAMP\_Q', T=580.0, F=0.325437/  
 &RAMP ID='SofaFIRE01\_RAMP\_Q', T=590.0, F=0.32252/  
 &RAMP ID='SofaFIRE01\_RAMP\_Q', T=600.0, F=0.313969/  
 &RAMP ID='SofaFIRE01\_RAMP\_Q', T=610.0, F=0.290003/  
 &RAMP ID='SofaFIRE01\_RAMP\_Q', T=620.0, F=0.267305/  
 &RAMP ID='SofaFIRE01\_RAMP\_Q', T=630.0, F=0.241179/  
 &RAMP ID='SofaFIRE01\_RAMP\_Q', T=640.0, F=0.207914/  
 &RAMP ID='SofaFIRE01\_RAMP\_Q', T=650.0, F=0.176181/  
 &RAMP ID='SofaFIRE01\_RAMP\_Q', T=660.0, F=0.150651/  
 &RAMP ID='SofaFIRE01\_RAMP\_Q', T=670.0, F=0.126317/  
 &RAMP ID='SofaFIRE01\_RAMP\_Q', T=680.0, F=0.104604/  
 &RAMP ID='SofaFIRE01\_RAMP\_Q', T=690.0, F=0.086489/  
 &RAMP ID='SofaFIRE01\_RAMP\_Q', T=700.0, F=0.072235/  
 &RAMP ID='SofaFIRE01\_RAMP\_Q', T=710.0, F=0.061039/  
 &RAMP ID='SofaFIRE01\_RAMP\_Q', T=720.0, F=0.050822/  
 &RAMP ID='SofaFIRE01\_RAMP\_Q', T=730.0, F=0.043279/  
 &RAMP ID='SofaFIRE01\_RAMP\_Q', T=740.0, F=0.037215/  
 &RAMP ID='SofaFIRE01\_RAMP\_Q', T=750.0, F=0.032471/  
 &RAMP ID='SofaFIRE01\_RAMP\_Q', T=760.0, F=0.026159/  
 &RAMP ID='SofaFIRE01\_RAMP\_Q', T=770.0, F=0.025273/  
 &RAMP ID='SofaFIRE01\_RAMP\_Q', T=780.0, F=0.022149/  
 &RAMP ID='SofaFIRE01\_RAMP\_Q', T=790.0, F=0.020366/  
 &RAMP ID='SofaFIRE01\_RAMP\_Q', T=800.0, F=0.017848/  
 &RAMP ID='SofaFIRE01\_RAMP\_Q', T=810.0, F=0.016504/  
 &RAMP ID='SofaFIRE01\_RAMP\_Q', T=820.0, F=0.013858/  
 &RAMP ID='SofaFIRE01\_RAMP\_Q', T=830.0, F=0.012334/  
 &RAMP ID='SofaFIRE01\_RAMP\_Q', T=840.0, F=0.01113/  
 &RAMP ID='SofaFIRE01\_RAMP\_Q', T=850.0, F=0.011161/  
 &RAMP ID='SofaFIRE01\_RAMP\_Q', T=860.0, F=0.011223/  
 &RAMP ID='SofaFIRE01\_RAMP\_Q', T=870.0, F=0.012087/  
 &RAMP ID='SofaFIRE01\_RAMP\_Q', T=880.0, F=0.012453/  
 &RAMP ID='SofaFIRE01\_RAMP\_Q', T=890.0, F=0.011001/  
 &RAMP ID='SofaFIRE01\_RAMP\_Q', T=900.0, F=0.010847/  
 &RAMP ID='SofaFIRE01\_RAMP\_Q', T=910.0, F=0.011473/  
 &RAMP ID='SofaFIRE01\_RAMP\_Q', T=920.0, F=9.102926E-3/  
 &RAMP ID='SofaFIRE01\_RAMP\_Q', T=930.0, F=9.02187E-3/  
 &RAMP ID='SofaFIRE01\_RAMP\_Q', T=940.0, F=8.111176E-3/  
 &RAMP ID='SofaFIRE01\_RAMP\_Q', T=950.0, F=8.258756E-3/  
 &RAMP ID='SofaFIRE01\_RAMP\_Q', T=960.0, F=5.845823E-3/  
 &RAMP ID='SofaFIRE01\_RAMP\_Q', T=970.0, F=7.039403E-3/  
 &RAMP ID='SofaFIRE01\_RAMP\_Q', T=980.0, F=4.84236E-3/  
 &RAMP ID='SofaFIRE01\_RAMP\_Q', T=990.0, F=4.860915E-3/  
 &RAMP ID='SofaFIRE01\_RAMP\_Q', T=1000.0, F=3.567774E-3/

&OBST ID='Obstruction', XB=-0.7,18.5,19.6,19.7,2.8,3.0, COLOR='GRAY 80', SURF\_ID='CONCRETE\_WALLS'/  
 &OBST ID='Obstruction', XB=-0.7,18.5,19.6,19.7,2.4,2.6, COLOR='GRAY 80', SURF\_ID='CONCRETE\_WALLS'/  
 &OBST ID='Bulkhead', XB=12.7,13.6,12.3,12.4,4.8,5.4, SURF\_ID='CALCIUM SILICATE WALLS'/  
 &OBST ID='Bulkhead2', XB=12.6,12.7,12.7,13.5,4.8,5.4, SURF\_ID='CALCIUM SILICATE WALLS'/  
 &OBST ID='Door 1.19-Hallway', XB=12.7,13.6,12.3,12.4,2.8,4.8, SURF\_ID='DOOR', DEVC\_ID='TIMER->OUT'/  
 &OBST ID='Door barchroom', XB=12.6,12.7,12.7,13.5,2.8,4.8, SURF\_ID='DOOR'/  
 &OBST ID='Innerwall 5', XB=13.6,14.5,12.3,12.4,2.8,5.4, SURF\_ID='CALCIUM SILICATE WALLS'/  
 &OBST ID='Innerwall1', XB=10.7,10.9,12.2,19.5,2.8,5.4, COLOR='GRAY 80', SURF\_ID='CONCRETE\_WALLS'/  
 &OBST ID='Innerwall2', XB=14.5,14.7,12.2,19.5,2.8,5.4, COLOR='GRAY 80', SURF\_ID='CONCRETE\_WALLS'/  
 &OBST ID='Innerwall3', XB=10.9,14.5,14.0,14.1,2.8,5.4, SURF\_ID='CALCIUM SILICATE WALLS'/  
 &OBST ID='Innerwall6', XB=12.6,12.7,13.5,14.0,2.8,5.4, SURF\_ID='CALCIUM SILICATE WALLS'/  
 &OBST ID='Overhead2', XB=12.7,13.6,18.4,18.5,2.8,5.4, SURF\_ID='Windows fire room'/  
 &OBST ID='Parapet1', XB=10.9,12.7,18.4,18.5,2.8,3.5, COLOR='GRAY 80', SURF\_ID='CONCRETE\_WALLS'/  
 &OBST ID='Parapet2', XB=13.6,14.5,18.4,18.5,2.8,3.5, COLOR='GRAY 80', SURF\_ID='CONCRETE\_WALLS'/  
 &OBST ID='Window backside', XB=10.9,12.7,18.4,18.5,3.5,5.4, SURF\_ID='Windows fire room'/  
 &OBST ID='Window backside 2', XB=13.6,14.5,18.4,18.5,3.5,5.4, SURF\_ID='Windows fire room'/  
 &OBST ID='Balcony door', XB=8.9,9.8,18.4,18.5,2.8,4.8, SURF\_ID='DOUBLE GLAZING'/  
 &OBST ID='Bulkhead', XB=8.9,9.8,12.3,12.4,4.8,5.4, SURF\_ID='CALCIUM SILICATE WALLS'/  
 &OBST ID='Bulkhead2', XB=8.8,8.9,12.7,13.5,4.8,5.4, SURF\_ID='CALCIUM SILICATE WALLS'/

&OBST ID='Door 1.20-Hallway', XB=8.9,9.8,12.3,12.4,2.8,4.8, SURF\_ID6='DOOR','DOOR','Hallway-apartments','Hallway-apartments','DOOR','DOOR'/  
 &OBST ID='Door barchroom', XB=8.8,8.9,12.7,13.5,2.8,4.8, SURF\_ID='DOOR'/  
 &OBST ID='Innerwall 5', XB=9.8,10.7,12.3,12.4,2.8,5.4, SURF\_ID='CALCIUM SILICATE WALLS'/  
 &OBST ID='Innerwall1', XB=6.9,7.1,12.2,19.5,2.8,5.4, COLOR='GRAY 80', SURF\_ID='CONCRETE\_WALLS'/  
 &OBST ID='Innerwall3', XB=7.1,10.7,14.0,14.1,2.8,5.4, SURF\_ID='CALCIUM SILICATE WALLS'/  
 &OBST ID='Innerwall6', XB=8.8,8.9,13.5,14.0,2.8,5.4, SURF\_ID='CALCIUM SILICATE WALLS'/  
 &OBST ID='Overhead2', XB=8.9,9.8,18.4,18.5,4.8,5.4, SURF\_ID='DOUBLE GLAZING'/  
 &OBST ID='Parapet1', XB=7.1,8.9,18.4,18.5,2.8,3.5, COLOR='GRAY 80', SURF\_ID='CONCRETE\_WALLS'/  
 &OBST ID='Parapet2', XB=9.8,10.7,18.4,18.5,2.8,3.5, COLOR='GRAY 80', SURF\_ID='CONCRETE\_WALLS'/  
 &OBST ID='Window backside', XB=7.1,8.9,18.4,18.5,3.5,5.4, SURF\_ID='DOUBLE GLAZING'/  
 &OBST ID='Window backside 2', XB=9.8,10.7,18.4,18.5,3.5,5.4, SURF\_ID='DOUBLE GLAZING'/  
 &OBST ID='Balcony door', XB=5.1,6.0,18.4,18.5,2.8,4.8, SURF\_ID='DOUBLE GLAZING'/  
 &OBST ID='Bulkhead', XB=5.1,6.0,12.3,12.4,4.8,5.4, SURF\_ID='CALCIUM SILICATE WALLS'/  
 &OBST ID='Door 1.21-Hallway', XB=5.1,6.0,12.3,12.4,2.8,4.8, SURF\_ID6='DOOR','DOOR','Hallway-apartments','Hallway-apartments','DOOR','DOOR'/  
 &OBST ID='Bulkhead2', XB=5.0,5.1,12.7,13.5,4.8,5.4, SURF\_ID='CALCIUM SILICATE WALLS'/  
 &OBST ID='Door barchroom', XB=5.0,5.1,12.7,13.5,2.8,4.8, SURF\_ID='DOOR'/  
 &OBST ID='Innerwall 5', XB=6.0,6.9,12.3,12.4,2.8,5.4, SURF\_ID='CALCIUM SILICATE WALLS'/  
 &OBST ID='Innerwall1', XB=3.1,3.3,12.2,19.5,2.8,5.4, COLOR='GRAY 80', SURF\_ID='CONCRETE\_WALLS'/  
 &OBST ID='Innerwall3', XB=3.3,6.9,14.0,14.1,2.8,5.4, SURF\_ID='CALCIUM SILICATE WALLS'/  
 &OBST ID='Innerwall6', XB=5.0,5.1,13.5,14.0,2.8,5.4, SURF\_ID='CALCIUM SILICATE WALLS'/  
 &OBST ID='Overhead2', XB=5.1,6.0,18.4,18.5,4.8,5.4, SURF\_ID='DOUBLE GLAZING'/  
 &OBST ID='Parapet1', XB=3.3,5.1,18.4,18.5,2.8,3.5, COLOR='GRAY 80', SURF\_ID='CONCRETE\_WALLS'/  
 &OBST ID='Parapet2', XB=6.0,6.9,18.4,18.5,2.8,3.5, COLOR='GRAY 80', SURF\_ID='CONCRETE\_WALLS'/  
 &OBST ID='Window backside', XB=3.3,5.1,18.4,18.5,3.5,5.4, SURF\_ID='DOUBLE GLAZING'/  
 &OBST ID='Window backside 2', XB=6.0,6.9,18.4,18.5,3.5,5.4, SURF\_ID='DOUBLE GLAZING'/  
 &OBST ID='Balcony door', XB=1.3,2.2,18.4,18.5,2.8,4.8, SURF\_ID='DOUBLE GLAZING'/  
 &OBST ID='Bulkhead', XB=1.3,2.2,12.3,12.4,4.8,5.4, SURF\_ID='CALCIUM SILICATE WALLS'/  
 &OBST ID='Bulkhead2', XB=1.2,1.3,12.7,13.5,4.8,5.4, SURF\_ID='CALCIUM SILICATE WALLS'/  
 &OBST ID='Door 1.21-Hallway', XB=1.3,2.2,12.3,12.4,2.8,4.8, SURF\_ID6='DOOR','DOOR','Hallway-apartments','Hallway-apartments','DOOR','DOOR'/  
 &OBST ID='Door barchroom', XB=1.2,1.3,12.7,13.5,2.8,4.8, SURF\_ID='DOOR'/  
 &OBST ID='Innerwall 5', XB=2.2,3.1,12.3,12.4,2.8,5.4, SURF\_ID='CALCIUM SILICATE WALLS'/  
 &OBST ID='Innerwall1', XB=-0.7,-0.5,12.2,19.5,2.8,5.4, COLOR='GRAY 80', SURF\_ID='CONCRETE\_WALLS'/  
 &OBST ID='Innerwall3', XB=-0.5,3.1,14.0,14.1,2.8,5.4, SURF\_ID='CALCIUM SILICATE WALLS'/  
 &OBST ID='Innerwall6', XB=1.2,1.3,13.5,14.0,2.8,5.4, SURF\_ID='CALCIUM SILICATE WALLS'/  
 &OBST ID='Overhead2', XB=1.3,2.2,18.4,18.5,4.8,5.4, SURF\_ID='DOUBLE GLAZING'/  
 &OBST ID='Parapet1', XB=-0.5,1.3,18.4,18.5,2.8,3.5, COLOR='GRAY 80', SURF\_ID='CONCRETE\_WALLS'/  
 &OBST ID='Parapet2', XB=2.2,3.1,18.4,18.5,2.8,3.5, COLOR='GRAY 80', SURF\_ID='CONCRETE\_WALLS'/  
 &OBST ID='Window backside', XB=-0.5,1.3,18.4,18.5,3.5,5.4, SURF\_ID='DOUBLE GLAZING'/  
 &OBST ID='Window backside 2', XB=2.2,3.1,18.4,18.5,3.5,5.4, SURF\_ID='DOUBLE GLAZING'/  
 &OBST ID='Balcony door', XB=16.5,17.4,18.4,18.5,2.8,4.8, SURF\_ID='DOUBLE GLAZING'/  
 &OBST ID='Bulkhead', XB=16.5,17.4,12.3,12.4,4.8,5.4, SURF\_ID='CALCIUM SILICATE WALLS'/  
 &OBST ID='Bulkhead2', XB=16.4,16.5,12.7,13.5,4.8,5.4, SURF\_ID='CALCIUM SILICATE WALLS'/  
 &OBST ID='Door 1.18-Hallway', XB=16.5,17.4,12.3,12.4,2.8,4.8, SURF\_ID6='DOOR','DOOR','Hallway-apartments','Hallway-apartments','DOOR','DOOR'/  
 &OBST ID='Door barchroom', XB=16.4,16.5,12.7,13.5,2.8,4.8, SURF\_ID='DOOR'/  
 &OBST ID='Innerwall 5', XB=17.4,18.3,12.3,12.4,2.8,5.4, SURF\_ID='CALCIUM SILICATE WALLS'/  
 &OBST ID='Innerwall1', XB=14.5,14.7,12.2,19.5,2.8,5.4, COLOR='GRAY 80', SURF\_ID='CONCRETE\_WALLS'/  
 &OBST ID='Innerwall2', XB=18.3,18.5,12.2,19.5,2.8,5.4, COLOR='GRAY 80', SURF\_ID='CONCRETE\_WALLS'/  
 &OBST ID='Innerwall3', XB=14.7,18.3,14.0,14.1,2.8,5.4, SURF\_ID='CALCIUM SILICATE WALLS'/  
 &OBST ID='Innerwall6', XB=16.4,16.5,13.5,14.0,2.8,5.4, SURF\_ID='CALCIUM SILICATE WALLS'/  
 &OBST ID='Overhead2', XB=16.5,17.4,18.4,18.5,4.8,5.4, SURF\_ID='DOUBLE GLAZING'/  
 &OBST ID='Parapet1', XB=14.7,16.5,18.4,18.5,2.8,3.5, COLOR='GRAY 80', SURF\_ID='CONCRETE\_WALLS'/  
 &OBST ID='Parapet2', XB=17.4,18.3,18.4,18.5,2.8,3.5, COLOR='GRAY 80', SURF\_ID='CONCRETE\_WALLS'/  
 &OBST ID='Window backside', XB=14.7,16.5,18.4,18.5,3.5,5.4, SURF\_ID='DOUBLE GLAZING'/  
 &OBST ID='Window backside 2', XB=17.4,18.3,18.4,18.5,3.5,5.4, SURF\_ID='DOUBLE GLAZING'/  
 &OBST ID='Bulkhead', XB=12.7,13.6,10.3,10.4,4.8,5.4, SURF\_ID='CALCIUM SILICATE WALLS'/  
 &OBST ID='Bulkhead2', XB=12.6,12.7,9.2,10.0,4.8,5.4, SURF\_ID='CALCIUM SILICATE WALLS'/  
 &OBST ID='Door 1.26-Hallway', XB=12.7,13.6,10.3,10.4,2.8,4.8, SURF\_ID6='DOOR','DOOR','Hallway-apartments','Hallway-apartments','DOOR','DOOR'/  
 &OBST ID='Door barchroom', XB=12.6,12.7,9.2,10.0,2.8,4.8, SURF\_ID='DOOR'/  
 &OBST ID='Innerwall 5', XB=13.6,14.5,10.3,10.4,2.8,5.4, SURF\_ID='CALCIUM SILICATE WALLS'/  
 &OBST ID='Innerwall1', XB=10.7,10.9,4.0,10.5,2.8,5.4, COLOR='GRAY 80', SURF\_ID='CONCRETE\_WALLS'/  
 &OBST ID='Innerwall2', XB=14.5,14.7,4.0,10.5,2.8,5.4, COLOR='GRAY 80', SURF\_ID='CONCRETE\_WALLS'/

&OBST ID='Innerwall3', XB=10.9,14.5,8.6,8.7,2.8,5.4, SURF\_ID='CALCIUM SILICATE WALLS'/  
 &OBST ID='Innerwall6', XB=12.6,12.7,8.7,9.2,2.8,5.4, SURF\_ID='CALCIUM SILICATE WALLS'/  
 &OBST ID='Parapet1', XB=10.9,14.5,4.2,4.3,2.8,3.5, COLOR='GRAY 80', SURF\_ID='CONCRETE\_WALLS'/  
 &OBST ID='Window backside', XB=10.9,14.5,4.2,4.3,3.5,5.4, SURF\_ID='DOUBLE GLAZING'/  
 &OBST ID='Bulkhead', XB=16.3,17.2,10.3,10.4,4.8,5.4, SURF\_ID='CALCIUM SILICATE WALLS'/  
 &OBST ID='Bulkhead2', XB=16.2,16.3,9.2,10.0,4.8,5.4, SURF\_ID='CALCIUM SILICATE WALLS'/  
 &OBST ID='Door 1.28-Hallway', XB=16.3,17.2,10.3,10.4,2.8,4.8, SURF\_ID6='DOOR','DOOR','Hallway-apartments','Hallway-apartments','DOOR','DOOR'/  
 &OBST ID='Door barchroom', XB=16.2,16.3,9.2,10.0,2.8,4.8, SURF\_ID='DOOR'/  
 &OBST ID='Innerwall 5', XB=17.2,18.3,10.3,10.4,2.8,5.4, SURF\_ID='CALCIUM SILICATE WALLS'/  
 &OBST ID='Innerwall1', XB=14.5,14.7,4.0,10.5,2.8,5.4, COLOR='GRAY 80', SURF\_ID='CONCRETE\_WALLS'/  
 &OBST ID='Innerwall2', XB=18.3,18.5,4.0,10.5,2.8,5.4, COLOR='GRAY 80', SURF\_ID='CONCRETE\_WALLS'/  
 &OBST ID='Innerwall3', XB=14.7,18.3,8.6,8.7,2.8,5.4, SURF\_ID='CALCIUM SILICATE WALLS'/  
 &OBST ID='Innerwall6', XB=16.2,16.3,8.7,9.2,2.8,5.4, SURF\_ID='CALCIUM SILICATE WALLS'/  
 &OBST ID='Parapet1', XB=14.7,18.3,4.2,4.3,2.8,3.5, COLOR='GRAY 80', SURF\_ID='CONCRETE\_WALLS'/  
 &OBST ID='Window backside', XB=14.7,18.3,4.2,4.3,3.5,5.4, SURF\_ID='DOUBLE GLAZING'/  
 &OBST ID='Bulkhead', XB=8.9,9.8,10.3,10.4,4.8,5.4, SURF\_ID='CALCIUM SILICATE WALLS'/  
 &OBST ID='Bulkhead2', XB=8.8,8.9,9.2,10.0,4.8,5.4, COLOR='GRAY 80', SURF\_ID='CONCRETE\_WALLS'/  
 &OBST ID='Innerwall 5', XB=9.8,10.7,10.3,10.4,2.8,5.4, SURF\_ID='CALCIUM SILICATE WALLS'/  
 &OBST ID='Innerwall1', XB=6.9,7.1,4.0,10.5,2.8,5.4, COLOR='GRAY 80', SURF\_ID='CONCRETE\_WALLS'/  
 &OBST ID='Innerwall3', XB=7.1,10.7,8.6,8.7,2.8,5.4, SURF\_ID='CALCIUM SILICATE WALLS'/  
 &OBST ID='Innerwall6', XB=8.8,8.9,8.7,9.2,2.8,5.4, COLOR='GRAY 80', SURF\_ID='CONCRETE\_WALLS'/  
 &OBST ID='Parapet1', XB=7.1,10.7,4.2,4.3,2.8,3.5, COLOR='GRAY 80', SURF\_ID='CONCRETE\_WALLS'/  
 &OBST ID='Window backside', XB=7.1,10.7,4.2,4.3,3.5,5.4, SURF\_ID='DOUBLE GLAZING'/  
 &OBST ID='Bulkhead', XB=5.1,6.0,10.3,10.4,4.8,5.4, SURF\_ID='CALCIUM SILICATE WALLS'/  
 &OBST ID='Bulkhead2', XB=5.0,5.1,9.2,10.0,4.8,5.4, SURF\_ID='CALCIUM SILICATE WALLS'/  
 &OBST ID='Door 1.24-Hallway', XB=5.1,6.0,10.3,10.4,2.8,4.8, SURF\_ID6='DOOR','DOOR','Hallway-apartments','Hallway-apartments','DOOR','DOOR'/  
 &OBST ID='Door barchroom', XB=5.0,5.1,9.2,10.0,2.8,4.8, SURF\_ID='DOOR'/  
 &OBST ID='Innerwall 5', XB=6.0,6.9,10.3,10.4,2.8,5.4, SURF\_ID='CALCIUM SILICATE WALLS'/  
 &OBST ID='Innerwall1', XB=3.1,3.3,4.0,10.5,2.8,5.4, COLOR='GRAY 80', SURF\_ID='CONCRETE\_WALLS'/  
 &OBST ID='Innerwall3', XB=3.3,6.9,8.6,8.7,2.8,5.4, SURF\_ID='CALCIUM SILICATE WALLS'/  
 &OBST ID='Innerwall6', XB=5.0,5.1,8.7,9.2,2.8,5.4, SURF\_ID='CALCIUM SILICATE WALLS'/  
 &OBST ID='Parapet1', XB=3.3,6.9,4.2,4.3,2.8,3.5, COLOR='GRAY 80', SURF\_ID='CONCRETE\_WALLS'/  
 &OBST ID='Window backside', XB=3.3,6.9,4.2,4.3,3.5,5.4, SURF\_ID='DOUBLE GLAZING'/  
 &OBST ID='Door barchroom', XB=8.8,8.9,9.2,10.0,2.8,4.8, SURF\_ID='DOOR'/  
 &OBST ID='Bulkhead', XB=1.3,2.2,10.3,10.4,4.8,5.4, SURF\_ID='CALCIUM SILICATE WALLS'/  
 &OBST ID='Bulkhead2', XB=1.2,1.3,9.2,10.0,4.8,5.4, SURF\_ID='CALCIUM SILICATE WALLS'/  
 &OBST ID='Door 1.23-Hallway', XB=1.3,2.2,10.3,10.4,2.8,4.8, SURF\_ID6='DOOR','DOOR','Hallway-apartments','Hallway-apartments','DOOR','DOOR'/  
 &OBST ID='Door barchroom', XB=1.2,1.3,9.2,10.0,2.8,4.8, SURF\_ID='DOOR'/  
 &OBST ID='Innerwall 5', XB=2.2,3.1,10.3,10.4,2.8,5.4, SURF\_ID='CALCIUM SILICATE WALLS'/  
 &OBST ID='Innerwall1', XB=-0.7,-0.5,4.0,10.5,2.8,5.4, COLOR='GRAY 80', SURF\_ID='CONCRETE\_WALLS'/  
 &OBST ID='Innerwall3', XB=-0.5,3.1,8.6,8.7,2.8,5.4, SURF\_ID='CALCIUM SILICATE WALLS'/  
 &OBST ID='Innerwall6', XB=1.2,1.3,8.7,9.2,2.8,5.4, SURF\_ID='CALCIUM SILICATE WALLS'/  
 &OBST ID='Parapet1', XB=-0.5,3.1,4.2,4.3,2.8,3.5, COLOR='GRAY 80', SURF\_ID='CONCRETE\_WALLS'/  
 &OBST ID='Window backside', XB=-0.5,3.1,4.2,4.3,3.5,5.4, SURF\_ID='DOUBLE GLAZING'/  
 &OBST ID='Hallway double door left', XB=-0.7,-0.6,10.5,12.2,2.8,4.8, SURF\_ID6='Double door','Double door','DOOR','DOOR','DOOR','DOOR'/  
 &OBST ID='Hallway bulkhead left', XB=-0.7,-0.6,10.5,12.2,4.8,5.4, COLOR='GRAY 80', SURF\_ID='CONCRETE\_WALLS'/  
 &OBST ID='Hallway bulkhead right', XB=18.4,18.5,10.5,12.2,4.8,5.4, COLOR='GRAY 80', SURF\_ID='CONCRETE\_WALLS'/  
 &OBST ID='Hallway double door right', XB=18.4,18.5,10.5,12.2,2.8,4.8, SURF\_ID6='Double door','Double door','DOOR','DOOR','DOOR','DOOR'/  
 &OBST ID='Obstruction', XB=-0.7,18.5,19.6,19.7,5.6,5.8, COLOR='GRAY 80', SURF\_ID='CONCRETE\_WALLS'/  
 &OBST ID='Obstruction', XB=-0.7,18.5,19.6,19.7,5.2,5.4, COLOR='GRAY 80', SURF\_ID='CONCRETE\_WALLS'/  
 &OBST ID='Balcony door', XB=12.7,13.6,18.4,18.5,5.6,7.6, SURF\_ID='DOUBLE GLAZING'/  
 &OBST ID='Bulkhead', XB=12.7,13.6,12.3,12.4,7.6,8.2, COLOR='GRAY 80', SURF\_ID='CONCRETE\_WALLS'/  
 &OBST ID='Bulkhead2', XB=12.6,12.7,12.7,13.5,7.6,8.2, COLOR='GRAY 80', SURF\_ID='CONCRETE\_WALLS'/  
 &OBST ID='Door 2.19-Hallway', XB=12.7,13.6,12.3,12.4,5.6,7.6, SURF\_ID='DOOR'/  
 &OBST ID='Door barchroom', XB=12.6,12.7,12.7,13.5,5.6,7.6, SURF\_ID='DOOR'/  
 &OBST ID='Innerwall 5', XB=13.6,14.5,12.3,12.4,5.6,8.2, COLOR='GRAY 80', SURF\_ID='CONCRETE\_WALLS'/  
 &OBST ID='Innerwall1', XB=10.7,10.9,12.2,19.5,5.6,8.2, COLOR='GRAY 80', SURF\_ID='CONCRETE\_WALLS'/  
 &OBST ID='Innerwall2', XB=14.5,14.7,12.2,19.5,5.6,8.2, COLOR='GRAY 80', SURF\_ID='CONCRETE\_WALLS'/  
 &OBST ID='Innerwall3', XB=10.9,14.5,14.0,14.1,5.6,8.2, COLOR='GRAY 80', SURF\_ID='CONCRETE\_WALLS'/  
 &OBST ID='Innerwall6', XB=12.6,12.7,13.5,14.0,5.6,8.2, COLOR='GRAY 80', SURF\_ID='CONCRETE\_WALLS'/  
 &OBST ID='Overhead2', XB=12.7,13.6,18.4,18.5,7.6,8.2, SURF\_ID='DOUBLE GLAZING'/

&OBST ID='Parapet1', XB=10.9,12.7,18.4,18.5,5.6,6.3, COLOR='GRAY 80', SURF\_ID='CONCRETE\_WALLS'/  
 &OBST ID='Parapet2', XB=13.6,14.5,18.4,18.5,5.6,6.3, COLOR='GRAY 80', SURF\_ID='CONCRETE\_WALLS'/  
 &OBST ID='Window backside', XB=10.9,12.7,18.4,18.5,6.3,8.2, SURF\_ID='DOUBLE GLAZING'/  
 &OBST ID='Window backside 2', XB=13.6,14.5,18.4,18.5,6.3,8.2, SURF\_ID='DOUBLE GLAZING'/  
 &OBST ID='Balcony door', XB=8.9,9.8,18.4,18.5,5.6,7.6, SURF\_ID='DOUBLE GLAZING'/  
 &OBST ID='Bulkhead', XB=8.9,9.8,12.3,12.4,7.6,8.2, COLOR='GRAY 80', SURF\_ID='CONCRETE\_WALLS'/  
 &OBST ID='Bulkhead2', XB=8.8,8.9,12.7,13.5,7.6,8.2, COLOR='GRAY 80', SURF\_ID='CONCRETE\_WALLS'/  
 &OBST ID='Door 2.20-Hallway', XB=8.9,9.8,12.3,12.4,5.6,7.6, SURF\_ID='DOOR'/  
 &OBST ID='Door barchroom', XB=8.8,8.9,12.7,13.5,5.6,7.6, SURF\_ID='DOOR'/  
 &OBST ID='Innerwall 5', XB=9.8,10.7,12.3,12.4,5.6,8.2, COLOR='GRAY 80', SURF\_ID='CONCRETE\_WALLS'/  
 &OBST ID='Innerwall1', XB=6.9,7.1,12.2,19.5,5.6,8.2, COLOR='GRAY 80', SURF\_ID='CONCRETE\_WALLS'/  
 &OBST ID='Innerwall3', XB=7.1,10.7,14.0,14.1,5.6,8.2, COLOR='GRAY 80', SURF\_ID='CONCRETE\_WALLS'/  
 &OBST ID='Innerwall6', XB=8.8,8.9,13.5,14.0,5.6,8.2, COLOR='GRAY 80', SURF\_ID='CONCRETE\_WALLS'/  
 &OBST ID='Overhead2', XB=8.9,9.8,18.4,18.5,7.6,8.2, SURF\_ID='DOUBLE GLAZING'/  
 &OBST ID='Parapet1', XB=7.1,8.9,18.4,18.5,5.6,6.3, COLOR='GRAY 80', SURF\_ID='CONCRETE\_WALLS'/  
 &OBST ID='Parapet2', XB=9.8,10.7,18.4,18.5,5.6,6.3, COLOR='GRAY 80', SURF\_ID='CONCRETE\_WALLS'/  
 &OBST ID='Window backside', XB=7.1,8.9,18.4,18.5,6.3,8.2, SURF\_ID='DOUBLE GLAZING'/  
 &OBST ID='Window backside 2', XB=9.8,10.7,18.4,18.5,6.3,8.2, SURF\_ID='DOUBLE GLAZING'/  
 &OBST ID='Balcony door', XB=5.1,6.0,18.4,18.5,5.6,7.6, SURF\_ID='DOUBLE GLAZING'/  
 &OBST ID='Bulkhead', XB=5.1,6.0,12.3,12.4,7.6,8.2, COLOR='GRAY 80', SURF\_ID='CONCRETE\_WALLS'/  
 &OBST ID='Bulkhead2', XB=5.0,5.1,12.7,13.5,7.6,8.2, COLOR='GRAY 80', SURF\_ID='CONCRETE\_WALLS'/  
 &OBST ID='Door 2.21-Hallway', XB=5.1,6.0,12.3,12.4,5.6,7.6, SURF\_ID='DOOR'/  
 &OBST ID='Door barchroom', XB=5.0,5.1,12.7,13.5,5.6,7.6, SURF\_ID='DOOR'/  
 &OBST ID='Innerwall 5', XB=6.0,6.9,12.3,12.4,5.6,8.2, COLOR='GRAY 80', SURF\_ID='CONCRETE\_WALLS'/  
 &OBST ID='Innerwall1', XB=3.1,3.3,12.2,19.5,5.6,8.2, COLOR='GRAY 80', SURF\_ID='CONCRETE\_WALLS'/  
 &OBST ID='Innerwall3', XB=3.3,6.9,14.0,14.1,5.6,8.2, COLOR='GRAY 80', SURF\_ID='CONCRETE\_WALLS'/  
 &OBST ID='Innerwall6', XB=5.0,5.1,13.5,14.0,5.6,8.2, COLOR='GRAY 80', SURF\_ID='CONCRETE\_WALLS'/  
 &OBST ID='Overhead2', XB=5.1,6.0,18.4,18.5,7.6,8.2, SURF\_ID='DOUBLE GLAZING'/  
 &OBST ID='Parapet1', XB=3.3,5.1,18.4,18.5,5.6,6.3, COLOR='GRAY 80', SURF\_ID='CONCRETE\_WALLS'/  
 &OBST ID='Parapet2', XB=6.0,6.9,18.4,18.5,5.6,6.3, COLOR='GRAY 80', SURF\_ID='CONCRETE\_WALLS'/  
 &OBST ID='Window backside', XB=3.3,5.1,18.4,18.5,6.3,8.2, SURF\_ID='DOUBLE GLAZING'/  
 &OBST ID='Window backside 2', XB=6.0,6.9,18.4,18.5,6.3,8.2, SURF\_ID='DOUBLE GLAZING'/  
 &OBST ID='Balcony door', XB=1.3,2.2,18.4,18.5,5.6,7.6, SURF\_ID='DOUBLE GLAZING'/  
 &OBST ID='Bulkhead', XB=1.3,2.2,12.3,12.4,7.6,8.2, COLOR='GRAY 80', SURF\_ID='CONCRETE\_WALLS'/  
 &OBST ID='Bulkhead2', XB=1.2,1.3,12.7,13.5,7.6,8.2, COLOR='GRAY 80', SURF\_ID='CONCRETE\_WALLS'/  
 &OBST ID='Door 2.21-Hallway', XB=1.3,2.2,12.3,12.4,5.6,7.6, SURF\_ID='DOOR'/  
 &OBST ID='Door barchroom', XB=1.2,1.3,12.7,13.5,5.6,7.6, SURF\_ID='DOOR'/  
 &OBST ID='Innerwall 5', XB=2.2,3.1,12.3,12.4,5.6,8.2, COLOR='GRAY 80', SURF\_ID='CONCRETE\_WALLS'/  
 &OBST ID='Innerwall1', XB=-0.7,-0.5,12.2,19.5,5.6,8.2, COLOR='GRAY 80', SURF\_ID='CONCRETE\_WALLS'/  
 &OBST ID='Innerwall3', XB=-0.5,3.1,14.0,14.1,5.6,8.2, COLOR='GRAY 80', SURF\_ID='CONCRETE\_WALLS'/  
 &OBST ID='Innerwall6', XB=1.2,1.3,13.5,14.0,5.6,8.2, COLOR='GRAY 80', SURF\_ID='CONCRETE\_WALLS'/  
 &OBST ID='Overhead2', XB=1.3,2.2,18.4,18.5,7.6,8.2, SURF\_ID='DOUBLE GLAZING'/  
 &OBST ID='Parapet1', XB=-0.5,1.3,18.4,18.5,5.6,6.3, COLOR='GRAY 80', SURF\_ID='CONCRETE\_WALLS'/  
 &OBST ID='Parapet2', XB=2.2,3.1,18.4,18.5,5.6,6.3, COLOR='GRAY 80', SURF\_ID='CONCRETE\_WALLS'/  
 &OBST ID='Window backside', XB=-0.5,1.3,18.4,18.5,6.3,8.2, SURF\_ID='DOUBLE GLAZING'/  
 &OBST ID='Window backside 2', XB=2.2,3.1,18.4,18.5,6.3,8.2, SURF\_ID='DOUBLE GLAZING'/  
 &OBST ID='Balcony door', XB=16.5,17.4,18.4,18.5,5.6,7.6, SURF\_ID='DOUBLE GLAZING'/  
 &OBST ID='Bulkhead', XB=16.5,17.4,12.3,12.4,7.6,8.2, COLOR='GRAY 80', SURF\_ID='CONCRETE\_WALLS'/  
 &OBST ID='Bulkhead2', XB=16.4,16.5,12.7,13.5,7.6,8.2, COLOR='GRAY 80', SURF\_ID='CONCRETE\_WALLS'/  
 &OBST ID='Door 2.18-Hallway', XB=16.5,17.4,12.3,12.4,5.6,7.6, SURF\_ID='DOOR'/  
 &OBST ID='Door barchroom', XB=16.4,16.5,12.7,13.5,5.6,7.6, SURF\_ID='DOOR'/  
 &OBST ID='Innerwall 5', XB=17.4,18.3,12.3,12.4,5.6,8.2, COLOR='GRAY 80', SURF\_ID='CONCRETE\_WALLS'/  
 &OBST ID='Innerwall1', XB=14.5,14.7,12.2,19.5,5.6,8.2, COLOR='GRAY 80', SURF\_ID='CONCRETE\_WALLS'/  
 &OBST ID='Innerwall2', XB=18.3,18.5,12.2,19.5,5.6,8.2, COLOR='GRAY 80', SURF\_ID='CONCRETE\_WALLS'/  
 &OBST ID='Innerwall3', XB=14.7,18.3,14.0,14.1,5.6,8.2, COLOR='GRAY 80', SURF\_ID='CONCRETE\_WALLS'/  
 &OBST ID='Innerwall6', XB=16.4,16.5,13.5,14.0,5.6,8.2, COLOR='GRAY 80', SURF\_ID='CONCRETE\_WALLS'/  
 &OBST ID='Overhead2', XB=16.5,17.4,18.4,18.5,7.6,8.2, SURF\_ID='DOUBLE GLAZING'/  
 &OBST ID='Parapet1', XB=14.7,16.5,18.4,18.5,5.6,6.3, COLOR='GRAY 80', SURF\_ID='CONCRETE\_WALLS'/  
 &OBST ID='Parapet2', XB=17.4,18.3,18.4,18.5,5.6,6.3, COLOR='GRAY 80', SURF\_ID='CONCRETE\_WALLS'/  
 &OBST ID='Window backside', XB=14.7,16.5,18.4,18.5,6.3,8.2, SURF\_ID='DOUBLE GLAZING'/  
 &OBST ID='Window backside 2', XB=17.4,18.3,18.4,18.5,6.3,8.2, SURF\_ID='DOUBLE GLAZING'/  
 &OBST ID='Bulkhead', XB=12.7,13.6,10.3,10.4,7.6,8.2, COLOR='GRAY 80', SURF\_ID='CONCRETE\_WALLS'/  
 &OBST ID='Bulkhead2', XB=12.6,12.7,9.2,10.0,7.6,8.2, COLOR='GRAY 80', SURF\_ID='CONCRETE\_WALLS'/  
 &OBST ID='Door 2.26-Hallway', XB=12.7,13.6,10.3,10.4,5.6,7.6, SURF\_ID='DOOR'/  
 &OBST ID='Door barchroom', XB=12.6,12.7,9.2,10.0,5.6,7.6, SURF\_ID='DOOR'/  
 &OBST ID='Innerwall 5', XB=13.6,14.5,10.3,10.4,5.6,8.2, COLOR='GRAY 80', SURF\_ID='CONCRETE\_WALLS'/

&OBST ID='Innerwall1', XB=10.7,10.9,4.0,10.5,5.6,8.2, COLOR='GRAY 80', SURF\_ID='CONCRETE\_WALLS'/  
 &OBST ID='Innerwall2', XB=14.5,14.7,4.0,10.5,5.6,8.2, COLOR='GRAY 80', SURF\_ID='CONCRETE\_WALLS'/  
 &OBST ID='Innerwall3', XB=10.9,14.5,8.6,8.7,5.6,8.2, COLOR='GRAY 80', SURF\_ID='CONCRETE\_WALLS'/  
 &OBST ID='Innerwall6', XB=12.6,12.7,8.7,9.2,5.6,8.2, COLOR='GRAY 80', SURF\_ID='CONCRETE\_WALLS'/  
 &OBST ID='Parapet1', XB=10.9,14.5,4.2,4.3,5.6,6.3, COLOR='GRAY 80', SURF\_ID='CONCRETE\_WALLS'/  
 &OBST ID='Window backside', XB=10.9,14.5,4.2,4.3,6.3,8.2, SURF\_ID='DOUBLE GLAZING'/  
 &OBST ID='Bulkhead', XB=16.3,17.2,10.3,10.4,7.6,8.2, COLOR='GRAY 80', SURF\_ID='CONCRETE\_WALLS'/  
 &OBST ID='Bulkhead2', XB=16.2,16.3,9.2,10.0,7.6,8.2, COLOR='GRAY 80', SURF\_ID='CONCRETE\_WALLS'/  
 &OBST ID='Door 2.28-Hallway', XB=16.3,17.2,10.3,10.4,5.6,7.6, SURF\_ID='DOOR'/  
 &OBST ID='Door barchroom', XB=16.2,16.3,9.2,10.0,5.6,7.6, SURF\_ID='DOOR'/  
 &OBST ID='Innerwall 5', XB=17.2,18.3,10.3,10.4,5.6,8.2, COLOR='GRAY 80', SURF\_ID='CONCRETE\_WALLS'/  
 &OBST ID='Innerwall1', XB=14.5,14.7,4.0,10.5,5.6,8.2, COLOR='GRAY 80', SURF\_ID='CONCRETE\_WALLS'/  
 &OBST ID='Innerwall2', XB=18.3,18.5,4.0,10.5,5.6,8.2, COLOR='GRAY 80', SURF\_ID='CONCRETE\_WALLS'/  
 &OBST ID='Innerwall3', XB=14.7,18.3,8.6,8.7,5.6,8.2, COLOR='GRAY 80', SURF\_ID='CONCRETE\_WALLS'/  
 &OBST ID='Innerwall6', XB=16.2,16.3,8.7,9.2,5.6,8.2, COLOR='GRAY 80', SURF\_ID='CONCRETE\_WALLS'/  
 &OBST ID='Parapet1', XB=14.7,18.3,4.2,4.3,5.6,6.3, COLOR='GRAY 80', SURF\_ID='CONCRETE\_WALLS'/  
 &OBST ID='Window backside', XB=14.7,18.3,4.2,4.3,6.3,8.2, SURF\_ID='DOUBLE GLAZING'/  
 &OBST ID='Bulkhead', XB=8.9,9.8,10.3,10.4,7.6,8.2, COLOR='GRAY 80', SURF\_ID='CONCRETE\_WALLS'/  
 &OBST ID='Bulkhead2', XB=8.8,8.9,9.2,10.0,7.6,8.2, COLOR='GRAY 80', SURF\_ID='CONCRETE\_WALLS'/  
 &OBST ID='Door 2.25-Hallway', XB=8.9,9.8,10.3,10.4,5.6,7.6, SURF\_ID='DOOR'/  
 &OBST ID='Door barchroom', XB=8.8,8.9,9.2,10.0,5.6,7.6, SURF\_ID='DOOR'/  
 &OBST ID='Innerwall 5', XB=9.8,10.7,10.3,10.4,5.6,8.2, COLOR='GRAY 80', SURF\_ID='CONCRETE\_WALLS'/  
 &OBST ID='Innerwall1', XB=6.9,7.1,4.0,10.5,5.6,8.2, COLOR='GRAY 80', SURF\_ID='CONCRETE\_WALLS'/  
 &OBST ID='Innerwall3', XB=7.1,10.7,8.6,8.7,5.6,8.2, COLOR='GRAY 80', SURF\_ID='CONCRETE\_WALLS'/  
 &OBST ID='Innerwall6', XB=8.8,8.9,8.7,9.2,5.6,8.2, COLOR='GRAY 80', SURF\_ID='CONCRETE\_WALLS'/  
 &OBST ID='Parapet1', XB=7.1,10.7,4.2,4.3,5.6,6.3, COLOR='GRAY 80', SURF\_ID='CONCRETE\_WALLS'/  
 &OBST ID='Window backside', XB=7.1,10.7,4.2,4.3,6.3,8.2, SURF\_ID='DOUBLE GLAZING'/  
 &OBST ID='Bulkhead', XB=5.1,6.0,10.3,10.4,7.6,8.2, COLOR='GRAY 80', SURF\_ID='CONCRETE\_WALLS'/  
 &OBST ID='Bulkhead2', XB=5.0,5.1,9.2,10.0,7.6,8.2, COLOR='GRAY 80', SURF\_ID='CONCRETE\_WALLS'/  
 &OBST ID='Door 2.24-Hallway', XB=5.1,6.0,10.3,10.4,5.6,7.6, SURF\_ID='DOOR'/  
 &OBST ID='Door barchroom', XB=5.0,5.1,9.2,10.0,5.6,7.6, SURF\_ID='DOOR'/  
 &OBST ID='Innerwall 5', XB=6.0,6.9,10.3,10.4,5.6,8.2, COLOR='GRAY 80', SURF\_ID='CONCRETE\_WALLS'/  
 &OBST ID='Innerwall1', XB=3.1,3.3,4.0,10.5,5.6,8.2, COLOR='GRAY 80', SURF\_ID='CONCRETE\_WALLS'/  
 &OBST ID='Innerwall3', XB=3.3,6.9,8.6,8.7,5.6,8.2, COLOR='GRAY 80', SURF\_ID='CONCRETE\_WALLS'/  
 &OBST ID='Innerwall6', XB=5.0,5.1,8.7,9.2,5.6,8.2, COLOR='GRAY 80', SURF\_ID='CONCRETE\_WALLS'/  
 &OBST ID='Parapet1', XB=3.3,6.9,4.2,4.3,5.6,6.3, COLOR='GRAY 80', SURF\_ID='CONCRETE\_WALLS'/  
 &OBST ID='Window backside', XB=3.3,6.9,4.2,4.3,6.3,8.2, SURF\_ID='DOUBLE GLAZING'/  
 &OBST ID='Bulkhead', XB=1.3,2.2,10.3,10.4,7.6,8.2, COLOR='GRAY 80', SURF\_ID='CONCRETE\_WALLS'/  
 &OBST ID='Bulkhead2', XB=1.2,1.3,9.2,10.0,7.6,8.2, COLOR='GRAY 80', SURF\_ID='CONCRETE\_WALLS'/  
 &OBST ID='Door 2.23-Hallway', XB=1.3,2.2,10.3,10.4,5.6,7.6, SURF\_ID='DOOR'/  
 &OBST ID='Door barchroom', XB=1.2,1.3,9.2,10.0,5.6,7.6, SURF\_ID='DOOR'/  
 &OBST ID='Innerwall 5', XB=2.2,3.1,10.3,10.4,5.6,8.2, COLOR='GRAY 80', SURF\_ID='CONCRETE\_WALLS'/  
 &OBST ID='Innerwall1', XB=-0.7,-0.5,4.0,10.5,5.6,8.2, COLOR='GRAY 80', SURF\_ID='CONCRETE\_WALLS'/  
 &OBST ID='Innerwall3', XB=-0.5,3.1,8.6,8.7,5.6,8.2, COLOR='GRAY 80', SURF\_ID='CONCRETE\_WALLS'/  
 &OBST ID='Innerwall6', XB=1.2,1.3,8.7,9.2,5.6,8.2, COLOR='GRAY 80', SURF\_ID='CONCRETE\_WALLS'/  
 &OBST ID='Parapet1', XB=-0.5,3.1,4.2,4.3,5.6,6.3, COLOR='GRAY 80', SURF\_ID='CONCRETE\_WALLS'/  
 &OBST ID='Window backside', XB=-0.5,3.1,4.2,4.3,6.3,8.2, SURF\_ID='DOUBLE GLAZING'/  
 &OBST ID='Hallway double door left', XB=-0.7,-0.6,10.5,12.2,5.6,7.6, SURF\_ID6='Double door','Double door','DOOR','DOOR','DOOR','DOOR'/  
 &OBST ID='Hallway bulkhead left', XB=-0.7,-0.6,10.5,12.2,7.6,8.2, COLOR='GRAY 80', SURF\_ID='CONCRETE\_WALLS'/  
 &OBST ID='Hallway bulkhead right', XB=18.4,18.5,10.5,12.2,7.6,8.2, COLOR='GRAY 80', SURF\_ID='CONCRETE\_WALLS'/  
 &OBST ID='Hallway double door right', XB=18.4,18.5,10.5,12.2,5.6,7.6, SURF\_ID6='Double door','Double door','DOOR','DOOR','DOOR','DOOR'/  
 &OBST ID='SOFA', XB=11.0,12.0,14.2,16.2,2.9,3.4, SURF\_ID='INERT'/  
 &OBST ID='Floor slab 1st', XB=6.6,11.2,8.4,9.8,2.6,2.8, COLOR='GRAY 80', SURF\_ID='CONCRETE\_FLOORS'/  
 &OBST ID='Floor slab 1st', XB=6.6,11.2,4.0,8.4,2.6,2.8, COLOR='GRAY 80', SURF\_ID='CONCRETE\_FLOORS'/  
 &OBST ID='Floor slab 1st', XB=-0.7,0.6,9.8,11.35,2.6,2.8, COLOR='GRAY 80', SURF\_ID='CONCRETE\_FLOORS'/  
 &OBST ID='Floor slab 1st', XB=0.6,2.6,9.8,11.35,2.6,2.8, COLOR='GRAY 80', SURF\_ID='CONCRETE\_FLOORS'/  
 &OBST ID='Floor slab 1st', XB=2.6,4.6,9.8,11.35,2.6,2.8, COLOR='GRAY 80', SURF\_ID='CONCRETE\_FLOORS'/  
 &OBST ID='Floor slab 1st', XB=4.6,6.6,9.8,11.35,2.6,2.8, COLOR='GRAY 80', SURF\_ID='CONCRETE\_FLOORS'/  
 &OBST ID='Floor slab 1st', XB=6.6,8.6,9.8,11.35,2.6,2.8, COLOR='GRAY 80', SURF\_ID='CONCRETE\_FLOORS'/  
 &OBST ID='Floor slab 1st', XB=8.6,10.6,9.8,11.35,2.6,2.8, COLOR='GRAY 80', SURF\_ID='CONCRETE\_FLOORS'/  
 &OBST ID='Floor slab 1st', XB=10.6,12.6,9.8,11.35,2.6,2.8, COLOR='GRAY 80', SURF\_ID='CONCRETE\_FLOORS'/  
 &OBST ID='Floor slab 1st', XB=12.6,14.6,9.8,11.35,2.6,2.8, COLOR='GRAY 80', SURF\_ID='CONCRETE\_FLOORS'/  
 &OBST ID='Floor slab 1st', XB=14.6,16.6,9.8,11.35,2.6,2.8, COLOR='GRAY 80', SURF\_ID='CONCRETE\_FLOORS'/  
 &OBST ID='Floor slab 1st', XB=16.6,18.5,9.8,11.35,2.6,2.8, COLOR='GRAY 80', SURF\_ID='CONCRETE\_FLOORS'/







&OBST ID='Floor slab 2nd', XB=10.6,12.9,14.4,15.9,5.4,5.6, COLOR='GRAY 80', SURF\_ID='CONCRETE\_FLOORS'/  
 &OBST ID='Floor slab 2nd', XB=10.6,12.9,15.9,17.4,5.4,5.6, COLOR='GRAY 80', SURF\_ID='CONCRETE\_FLOORS'/  
 &OBST ID='Floor slab 2nd', XB=10.6,12.9,17.4,18.9,5.4,5.6, COLOR='GRAY 80', SURF\_ID='CONCRETE\_FLOORS'/  
 &OBST ID='Floor slab 2nd', XB=12.9,15.3,12.9,14.4,5.4,5.6, COLOR='GRAY 80', SURF\_ID='CONCRETE\_FLOORS'/  
 &OBST ID='Floor slab 2nd', XB=12.9,15.3,14.4,15.9,5.4,5.6, COLOR='GRAY 80', SURF\_ID='CONCRETE\_FLOORS'/  
 &OBST ID='Floor slab 2nd', XB=12.9,15.3,15.9,17.4,5.4,5.6, COLOR='GRAY 80', SURF\_ID='CONCRETE\_FLOORS'/  
 &OBST ID='Floor slab 2nd', XB=12.9,15.3,17.4,18.9,5.4,5.6, COLOR='GRAY 80', SURF\_ID='CONCRETE\_FLOORS'/  
 &OBST ID='Floor slab 2nd', XB=10.6,15.3,18.9,19.7,5.4,5.6, COLOR='GRAY 80', SURF\_ID='CONCRETE\_FLOORS'/

&HOLE ID='DOOR LIVING-KITCHEN', XB=13.0,14.5,13.9,14.2,2.8,4.8/  
 &HOLE ID='DOOR LIVING-KITCHEN', XB=9.2,10.7,13.9,14.2,2.8,4.8/  
 &HOLE ID='Overhead', XB=9.2,10.7,13.9,14.2,4.9,5.2/  
 &HOLE ID='DOOR LIVING-KITCHEN', XB=5.4,6.9,13.9,14.2,2.8,4.8/  
 &HOLE ID='Overhead', XB=5.4,6.9,13.9,14.2,4.9,5.2/  
 &HOLE ID='DOOR LIVING-KITCHEN', XB=1.6,3.1,13.9,14.2,2.8,4.8/  
 &HOLE ID='Overhead', XB=1.6,3.1,13.9,14.2,4.9,5.2/  
 &HOLE ID='DOOR LIVING-KITCHEN', XB=16.8,18.3,13.9,14.2,2.8,4.8/  
 &HOLE ID='Overhead', XB=16.8,18.3,13.9,14.2,4.9,5.2/  
 &HOLE ID='Overhead', XB=13.0,14.5,13.9,14.2,4.9,5.3/  
 &HOLE ID='DOOR LIVING-KITCHEN', XB=13.0,14.5,8.5,8.8,2.8,4.8/  
 &HOLE ID='Overhead', XB=13.0,14.5,8.5,8.8,4.8,5.3/  
 &HOLE ID='DOOR LIVING-KITCHEN', XB=16.8,18.3,8.5,8.8,2.8,4.8/  
 &HOLE ID='Overhead', XB=16.8,18.3,8.5,8.8,4.9,5.2/  
 &HOLE ID='DOOR LIVING-KITCHEN', XB=9.2,10.7,8.5,8.8,2.8,4.8/  
 &HOLE ID='Overhead', XB=9.2,10.7,8.5,8.8,4.9,5.2/  
 &HOLE ID='DOOR LIVING-KITCHEN', XB=5.4,6.9,8.5,8.8,2.8,4.8/  
 &HOLE ID='Overhead', XB=5.4,6.9,8.5,8.8,4.9,5.2/  
 &HOLE ID='DOOR LIVING-KITCHEN', XB=1.6,3.1,8.5,8.8,2.8,4.8/  
 &HOLE ID='Overhead', XB=1.6,3.1,8.5,8.8,4.9,5.2/  
 &HOLE ID='DOOR LIVING-KITCHEN', XB=13.0,14.5,13.9,14.2,5.6,7.6/  
 &HOLE ID='Overhead', XB=13.0,14.5,13.9,14.2,7.7,8.0/  
 &HOLE ID='DOOR LIVING-KITCHEN', XB=9.2,10.7,13.9,14.2,5.6,7.6/  
 &HOLE ID='Overhead', XB=9.2,10.7,13.9,14.2,7.7,8.0/  
 &HOLE ID='DOOR LIVING-KITCHEN', XB=5.4,6.9,13.9,14.2,5.6,7.6/  
 &HOLE ID='Overhead', XB=5.4,6.9,13.9,14.2,7.7,8.0/  
 &HOLE ID='DOOR LIVING-KITCHEN', XB=1.6,3.1,13.9,14.2,5.6,7.6/  
 &HOLE ID='Overhead', XB=1.6,3.1,13.9,14.2,7.7,8.0/  
 &HOLE ID='DOOR LIVING-KITCHEN', XB=16.8,18.3,13.9,14.2,5.6,7.6/  
 &HOLE ID='Overhead', XB=16.8,18.3,13.9,14.2,7.7,8.0/  
 &HOLE ID='DOOR LIVING-KITCHEN', XB=13.0,14.5,8.5,8.8,5.6,7.6/  
 &HOLE ID='Overhead', XB=13.0,14.5,8.5,8.8,7.7,8.0/  
 &HOLE ID='DOOR LIVING-KITCHEN', XB=16.8,18.3,8.5,8.8,5.6,7.6/  
 &HOLE ID='Overhead', XB=16.8,18.3,8.5,8.8,7.7,8.0/  
 &HOLE ID='DOOR LIVING-KITCHEN', XB=9.2,10.7,8.5,8.8,5.6,7.6/  
 &HOLE ID='Overhead', XB=9.2,10.7,8.5,8.8,7.7,8.0/  
 &HOLE ID='DOOR LIVING-KITCHEN', XB=5.4,6.9,8.5,8.8,5.6,7.6/  
 &HOLE ID='Overhead', XB=5.4,6.9,8.5,8.8,7.7,8.0/  
 &HOLE ID='DOOR LIVING-KITCHEN', XB=1.6,3.1,8.5,8.8,5.6,7.6/  
 &HOLE ID='Overhead', XB=1.6,3.1,8.5,8.8,7.7,8.0/

&VENT ID='Mesh Vent: MESH02 [XMAX]', SURF\_ID='OPEN', XB=11.2,11.2,3.8,8.4,2.6,5.8, COLOR='INVISIBLE'/  
 &VENT ID='Mesh Vent: MESH02 [XMIN]', SURF\_ID='OPEN', XB=6.6,6.6,3.8,8.4,2.6,5.8, COLOR='INVISIBLE'/  
 &VENT ID='Mesh Vent: MESH02 [YMIN]', SURF\_ID='OPEN', XB=6.6,11.2,3.8,3.8,2.6,5.8, COLOR='INVISIBLE'/  
 &VENT ID='Mesh Vent: MESH02 [ZMAX]', SURF\_ID='OPEN', XB=6.6,11.2,3.8,8.4,5.8,5.8, COLOR='INVISIBLE'/  
 &VENT ID='Mesh Vent: MESH02 [ZMIN]', SURF\_ID='OPEN', XB=6.6,11.2,3.8,8.4,2.6,2.6, COLOR='INVISIBLE'/  
 &VENT ID='Mesh Vent: MESH-c-e [XMAX]', SURF\_ID='OPEN', XB=15.3,15.3,18.9,21.5,2.6,5.8, COLOR='INVISIBLE'/  
 &VENT ID='Mesh Vent: MESH-c-e [XMIN]', SURF\_ID='OPEN', XB=10.6,10.6,18.9,21.5,2.6,5.8, COLOR='INVISIBLE'/  
 &VENT ID='Mesh Vent: MESH-c-e [YMAX]', SURF\_ID='OPEN', XB=10.6,15.3,21.5,21.5,2.6,5.8, COLOR='INVISIBLE'/  
 &VENT ID='Mesh Vent: MESH-c-e [ZMAX]', SURF\_ID='OPEN', XB=10.6,15.3,18.9,21.5,5.8,5.8, COLOR='INVISIBLE'/  
 &VENT ID='Mesh Vent: MESH-c-e [ZMIN]', SURF\_ID='OPEN', XB=10.6,15.3,18.9,21.5,2.6,2.6, COLOR='INVISIBLE'/  
 &VENT ID='Mesh Vent: MESH01 [XMAX]', SURF\_ID='OPEN', XB=11.2,11.2,8.4,9.8,2.6,5.8, COLOR='INVISIBLE'/  
 &VENT ID='Mesh Vent: MESH01 [XMIN]', SURF\_ID='OPEN', XB=6.6,6.6,8.4,9.8,2.6,5.8, COLOR='INVISIBLE'/  
 &VENT ID='Mesh Vent: MESH01 [ZMAX]', SURF\_ID='OPEN', XB=6.6,11.2,8.4,9.8,5.8,5.8, COLOR='INVISIBLE'/  
 &VENT ID='Mesh Vent: MESH01 [ZMIN]', SURF\_ID='OPEN', XB=6.6,11.2,8.4,9.8,2.6,2.6, COLOR='INVISIBLE'/  
 &VENT ID='Mesh Vent: MESH [XMAX]', SURF\_ID='OPEN', XB=15.3,15.3,12.9,18.9,2.6,5.8, COLOR='INVISIBLE'/  
 &VENT ID='Mesh Vent: MESH [XMIN]', SURF\_ID='OPEN', XB=10.6,10.6,12.9,18.9,2.6,5.8, COLOR='INVISIBLE'/



&VENT ID='Inner wall 01', SURF\_ID='Apartment1.19-Zone0', XB=10.905654,10.905654,14.1,18.4,2.8,5.380981, COLOR='INVISIBLE'/  
 &VENT ID='Door 4 high', SURF\_ID='INERT', XB=12.7,13.6,12.3,12.3,4.7,4.8/  
 &VENT ID='Inner wall 02', SURF\_ID='Apartment1.19-Zone0', XB=14.5,14.5,12.4,18.4,2.8,5.380981, COLOR='INVISIBLE'/  
 &VENT ID='Inner wall 03', SURF\_ID='Apartment1.19-Zone0', XB=10.9,14.5,18.4,18.4,2.8,5.380981, COLOR='INVISIBLE'/  
 &VENT ID='Inner wall 04', SURF\_ID='Apartment1.19-Zone0', XB=10.9,14.5,18.5,18.5,2.8,5.380981, COLOR='INVISIBLE'/  
 &VENT ID='Inner wall 05', SURF\_ID='Apartment1.19-Zone0', XB=14.7,14.7,12.4,18.4,2.8,5.380981, COLOR='INVISIBLE'/  
 &VENT ID='Inner wall 06', SURF\_ID='Apartment1.19-Zone0', XB=10.7,10.7,14.1,18.4,2.8,5.380981, COLOR='INVISIBLE'/  
 &VENT ID='Inner wall 07', SURF\_ID='Apartment1.19-Zone0', XB=12.7,12.7,12.4,14.0,2.8,5.380981, COLOR='INVISIBLE'/  
 &VENT ID='Inner wall 08', SURF\_ID='Apartment1.19-Zone0', XB=12.6,12.6,12.4,14.0,2.8,5.380981, COLOR='INVISIBLE'/  
 &VENT ID='Door 5 left', SURF\_ID='INERT', XB=12.7,12.75,12.3,12.3,2.8,4.8/  
 &VENT ID='Door 6 left', SURF\_ID='INERT', XB=12.7,12.75,12.4,12.4,2.8,4.8/  
 &VENT ID='Door 7 right', SURF\_ID='INERT', XB=13.55,13.6,12.4,12.4,2.8,4.8/  
 &VENT ID='Door 8 right', SURF\_ID='INERT', XB=13.55,13.6,12.3,12.3,2.8,4.8/  
 &VENT ID='Vent', SURF\_ID='SofaFIRE01', XB=11.0,12.0,14.2,16.2,3.4,3.4/

&HVAC ID='Leak\_apartment door\_low', TYPE\_ID='LEAK', VENT\_ID='Door 1 low', VENT2\_ID='Door 2 low', AREA=1.5E-3, LEAK\_ENTHALPY=.TRUE./  
 &HVAC ID='Leak\_apartment door\_high', TYPE\_ID='LEAK', VENT\_ID='Door 3 high', VENT2\_ID='Door 4 high', AREA=1.66666E-4, LEAK\_ENTHALPY=.TRUE./  
 &HVAC ID='Leak\_apartment door left', TYPE\_ID='LEAK', VENT\_ID='Door 5 left', VENT2\_ID='Door 6 left', AREA=1.66666E-4, LEAK\_ENTHALPY=.TRUE./  
 &HVAC ID='Leak\_apartment door right', TYPE\_ID='LEAK', VENT\_ID='Door 7 right', VENT2\_ID='Door 8 right', AREA=1.66666E-4, LEAK\_ENTHALPY=.TRUE./

&BNDF QUANTITY='RADIATIVE HEAT FLUX/'

&ISOF QUANTITY='TEMPERATURE', VALUE=50.0,100.0,200.0,300.0,400.0/

&SLCF QUANTITY='TEMPERATURE', PBX=13.2/  
 &SLCF QUANTITY='VISIBILITY', PBX=13.2/  
 &SLCF QUANTITY='TEMPERATURE', PBY=11.3/  
 &SLCF QUANTITY='VISIBILITY', PBY=11.3/  
 &SLCF QUANTITY='TEMPERATURE', PBX=14.2/  
 &SLCF QUANTITY='PRESSURE', PBX=13.2/  
 &SLCF QUANTITY='VOLUME FRACTION', SPEC\_ID='OXYGEN', PBX=11.5/  
 &SLCF QUANTITY='VOLUME FRACTION', SPEC\_ID='OXYGEN', PBY=11.3/  
 &SLCF QUANTITY='PRESSURE', PBY=11.3/  
 &SLCF QUANTITY='VELOCITY', VECTOR=.TRUE., PBX=13.2/  
 &SLCF QUANTITY='VELOCITY', VECTOR=.TRUE., PBY=11.3/  
 &SLCF QUANTITY='VOLUME FRACTION', SPEC\_ID='HYDROGEN CYANIDE', PBY=11.3/  
 &SLCF QUANTITY='VOLUME FRACTION', SPEC\_ID='Polyurethane GM21', PBY=11.3/  
 &SLCF QUANTITY='VOLUME FRACTION', SPEC\_ID='Polyurethane GM21', PBX=11.5/  
 &SLCF QUANTITY='VOLUME FRACTION', SPEC\_ID='OXYGEN', PBX=14.2/  
 &SLCF QUANTITY='TEMPERATURE', PBX=11.5/  
 &SLCF QUANTITY='VELOCITY', VECTOR=.TRUE., PBZ=5.2/  
 &SLCF QUANTITY='VELOCITY', VECTOR=.TRUE., PBZ=5.0/  
 &SLCF QUANTITY='VELOCITY', VECTOR=.TRUE., PBZ=4.8/  
 &SLCF QUANTITY='VELOCITY', VECTOR=.TRUE., PBZ=4.6/  
 &SLCF QUANTITY='VELOCITY', VECTOR=.TRUE., PBZ=4.3/  
 &SLCF QUANTITY='VELOCITY', VECTOR=.TRUE., PBZ=3.7/  
 &SLCF QUANTITY='VELOCITY', VECTOR=.TRUE., PBZ=3.1/  
 &SLCF QUANTITY='TEMPERATURE', VECTOR=.TRUE., PBZ=5.2/  
 &SLCF QUANTITY='TEMPERATURE', VECTOR=.TRUE., PBZ=5.0/  
 &SLCF QUANTITY='TEMPERATURE', VECTOR=.TRUE., PBZ=4.8/  
 &SLCF QUANTITY='TEMPERATURE', VECTOR=.TRUE., PBZ=4.6/  
 &SLCF QUANTITY='TEMPERATURE', VECTOR=.TRUE., PBZ=4.3/  
 &SLCF QUANTITY='TEMPERATURE', VECTOR=.TRUE., PBZ=3.7/  
 &SLCF QUANTITY='TEMPERATURE', VECTOR=.TRUE., PBZ=3.1/  
 &SLCF QUANTITY='VOLUME FRACTION', SPEC\_ID='CARBON MONOXIDE', PBZ=3.1/  
 &SLCF QUANTITY='VOLUME FRACTION', SPEC\_ID='CARBON MONOXIDE', PBZ=4.3/  
 &SLCF QUANTITY='MASS FRACTION', SPEC\_ID='SOOT', PBZ=3.1/  
 &SLCF QUANTITY='MASS FRACTION', SPEC\_ID='SOOT', PBZ=4.3/  
 &SLCF QUANTITY='VOLUME FRACTION', SPEC\_ID='OXYGEN', PBZ=3.1/  
 &SLCF QUANTITY='VOLUME FRACTION', SPEC\_ID='OXYGEN', PBZ=4.3/  
 &SLCF QUANTITY='VISIBILITY', PBZ=3.1/

```
&SLCF QUANTITY='VISIBILITY', PBZ=4.3/
&SLCF QUANTITY='VOLUME FRACTION', SPEC_ID='CARBON DIOXIDE', PBZ=3.1/
&SLCF QUANTITY='VOLUME FRACTION', SPEC_ID='CARBON DIOXIDE', PBZ=4.3/
&SLCF QUANTITY='TEMPERATURE', PBY=10.7/
&SLCF QUANTITY='VOLUME FRACTION', SPEC_ID='OXYGEN', PBY=10.7/
&SLCF QUANTITY='VOLUME FRACTION', SPEC_ID='HYDROGEN CYANIDE', PBY=10.7/
&SLCF QUANTITY='VOLUME FRACTION', SPEC_ID='Polyurethane GM21', PBY=10.7/
&SLCF QUANTITY='VOLUME FRACTION', SPEC_ID='CARBON MONOXIDE', PBY=10.7/
&SLCF QUANTITY='VOLUME FRACTION', SPEC_ID='CARBON DIOXIDE', PBY=10.7/
&SLCF QUANTITY='VISIBILITY', PBY=10.7/
```

```
&TAIL /
```

### Case study 3: door opened after 300 seconds and closed 30 seconds later

v3\_12.fds

Generated by PyroSim - Version 2021.4.1201

18-mrt-2022 15:12:56

```
&HEAD CHID='v3_12', TITLE='simulation experiment fine mesh 04-07-2019 morning 1.21 [door closed after 5.5 min] '/
&TIME T_END=1000.0/
&DUMP DT_ISO=10.0, DT_SL3D=10.0/
&MISC TMPA=23.6, MAXIMUM_VISIBILITY=100.0/
&COMB N_SIMPLE_CHEMISTRY_REACTIONS=2/
```

```
&MESH ID='MESH00', IJK=46,14,32, XB=6.6,11.2,8.4,9.8,2.6,5.8/
&MESH ID='MESH01', IJK=23,23,16, XB=6.6,11.2,3.8,8.4,2.6,5.8/
&MESH ID='MESH02', IJK=40,31,64, XB=-1.4,0.6,9.8,11.35,2.6,5.8/
&MESH ID='MESH03', IJK=40,31,64, XB=0.6,2.6,9.8,11.35,2.6,5.8/
&MESH ID='MESH04', IJK=40,31,64, XB=2.6,4.6,9.8,11.35,2.6,5.8/
&MESH ID='MESH05', IJK=40,31,64, XB=4.6,6.6,9.8,11.35,2.6,5.8/
&MESH ID='MESH06', IJK=40,31,64, XB=6.6,8.6,9.8,11.35,2.6,5.8/
&MESH ID='MESH07', IJK=40,31,64, XB=8.6,10.6,9.8,11.35,2.6,5.8/
&MESH ID='MESH08', IJK=40,31,64, XB=10.6,12.6,9.8,11.35,2.6,5.8/
&MESH ID='MESH09', IJK=40,31,64, XB=12.6,14.6,9.8,11.35,2.6,5.8/
&MESH ID='MESH10', IJK=40,31,64, XB=14.6,16.6,9.8,11.35,2.6,5.8/
&MESH ID='MESH11', IJK=46,31,64, XB=16.6,18.9,9.8,11.35,2.6,5.8/
&MESH ID='MESH12', IJK=40,31,64, XB=-1.4,0.6,11.35,12.9,2.6,5.8/
&MESH ID='MESH13', IJK=40,31,64, XB=0.6,2.6,11.35,12.9,2.6,5.8/
&MESH ID='MESH14', IJK=40,31,64, XB=2.6,4.6,11.35,12.9,2.6,5.8/
&MESH ID='MESH15', IJK=40,31,64, XB=4.6,6.6,11.35,12.9,2.6,5.8/
&MESH ID='MESH16', IJK=40,31,64, XB=6.6,8.6,11.35,12.9,2.6,5.8/
&MESH ID='MESH17', IJK=40,31,64, XB=8.6,10.6,11.35,12.9,2.6,5.8/
&MESH ID='MESH18', IJK=40,31,64, XB=10.6,12.6,11.35,12.9,2.6,5.8/
&MESH ID='MESH19', IJK=40,31,64, XB=12.6,14.6,11.35,12.9,2.6,5.8/
&MESH ID='MESH20', IJK=40,31,64, XB=14.6,16.6,11.35,12.9,2.6,5.8/
&MESH ID='MESH21', IJK=46,31,64, XB=16.6,18.9,11.35,12.9,2.6,5.8/
&MESH ID='MESH22', IJK=46,30,64, XB=3.0,5.3,12.9,14.4,2.6,5.8/
&MESH ID='MESH23', IJK=46,30,64, XB=3.0,5.3,14.4,15.9,2.6,5.8/
&MESH ID='MESH24', IJK=46,30,64, XB=3.0,5.3,15.9,17.4,2.6,5.8/
&MESH ID='MESH25', IJK=46,30,64, XB=3.0,5.3,17.4,18.9,2.6,5.8/
&MESH ID='MESH26', IJK=48,30,64, XB=5.3,7.7,12.9,14.4,2.6,5.8/
&MESH ID='MESH27', IJK=48,30,64, XB=5.3,7.7,14.4,15.9,2.6,5.8/
&MESH ID='MESH28', IJK=48,30,64, XB=5.3,7.7,15.9,17.4,2.6,5.8/
&MESH ID='MESH29', IJK=48,30,64, XB=5.3,7.7,17.4,18.9,2.6,5.8/
&MESH ID='MESH30', IJK=47,26,32, XB=3.0,7.7,18.9,21.5,2.6,5.8/
```

```
&ZONE ID='Apartment 1,21', XB=5.1,6.9,12.4,18.4,2.8,5.4, LEAK_AREA=0.018, LEAK_PRESSURE_EXPONENT=0.56/
&ZONE ID='Hallway leakage 1.21', XB=-0.6,18.4,10.4,12.3,2.8,5.2, LEAK_AREA=0.1/
```

```
&SPEC ID='Polyurethane GM21', FORMULA='C1H1.8O0.3N0.05'/
```

```
&REAC ID='Polyurethane (well ventilated)',
FYI='Polyurethane',
FUEL='Polyurethane GM21',
```

C=1.0,  
 H=1.8,  
 O=0.3,  
 N=0.05,  
 CRITICAL\_FLAME\_TEMPERATURE=654.0,  
 AUTO\_IGNITION\_TEMPERATURE=400.0,  
 CO\_YIELD=0.01,  
 SOOT\_YIELD=0.131,  
 HCN\_YIELD=2.0E-3,  
 EPUMO2=8950.0,  
 AIT\_EXCLUSION\_ZONE(1:6,1)=3.4,4.4,15.2,16.2,2.8,5.8,  
 HOC\_COMPLETE=16000,  
 LOWER\_OXYGEN\_LIMIT=0.08/

EPUMO2 calculated from chemical equilibrium as 'HEAT\_OF\_COMBUSTION' did not work. Value results in an effective heat of combustion of 16 MJ/kg. Overruled by HOC\_COMPLETE.

&RAMP ID='DOORCONTROL3\_RAMP', T=-0.25, F=-1.0/  
 &RAMP ID='DOORCONTROL3\_RAMP', T=0.25, F=1.0/  
 &RAMP ID='DOORCONTROL3\_RAMP', T=299.75, F=1.0/  
 &RAMP ID='DOORCONTROL3\_RAMP', T=300.25, F=-1.0/  
 &RAMP ID='DOORCONTROL3\_RAMP', T=329.75, F=-1.0/  
 &RAMP ID='DOORCONTROL3\_RAMP', T=330.25, F=1.0/  
 &PROP ID='TK1.1.0 props', DIAMETER=0.00075/  
 &PROP ID='TK1.1.1 props', DIAMETER=0.00075/  
 &PROP ID='TK1.1.2 props', DIAMETER=0.00075/  
 &PROP ID='TK1.1.3 props', DIAMETER=0.00075/  
 &PROP ID='TK1.1.4 props', DIAMETER=0.00075/  
 &PROP ID='TK1.1.5 props', DIAMETER=0.00075/  
 &PROP ID='TK1.1.6 props', DIAMETER=0.00075/  
 &PROP ID='TK1.1.1alt props', DIAMETER=0.00075/  
 &PROP ID='TK1.1.2alt props', DIAMETER=0.00075/  
 &PROP ID='TK1.1.3alt props', DIAMETER=0.00075/  
 &PROP ID='TK1.1.4alt props', DIAMETER=0.00075/  
 &PROP ID='TK1.1.5alt props', DIAMETER=0.00075/  
 &PROP ID='TK1.1.6alt props', DIAMETER=0.00075/  
 &PROP ID='TK1.1.7alt props', DIAMETER=0.00075/  
 &PROP ID='TK1.1.6alt01 props', DIAMETER=0.00075/  
 &PROP ID='TK1.1.1alt01 props', DIAMETER=0.00075/  
 &PROP ID='TK1.1.2alt01 props', DIAMETER=0.00075/  
 &PROP ID='TK1.1.3alt01 props', DIAMETER=0.00075/  
 &PROP ID='TK1.1.4alt01 props', DIAMETER=0.00075/  
 &PROP ID='TK1.1.5alt01 props', DIAMETER=0.00075/  
 &PROP ID='TK1.1.7alt01 props', DIAMETER=0.00075/  
 &CTRL ID='DOORCONTROL3', FUNCTION\_TYPE='CUSTOM', RAMP\_ID='DOORCONTROL3\_RAMP', LATCH=.FALSE.,  
 INPUT\_ID='TIME'/  
 &DEVC ID='CO(7)', QUANTITY='VOLUME FRACTION', SPEC\_ID='CARBON MONOXIDE', XYZ=6.6,13.1,4.3/  
 &DEVC ID='CO2(7)', QUANTITY='VOLUME FRACTION', SPEC\_ID='CARBON DIOXIDE', XYZ=6.6,13.1,4.3/  
 &DEVC ID='O2(7)', QUANTITY='VOLUME FRACTION', SPEC\_ID='OXYGEN', XYZ=6.6,13.1,4.3/  
 &DEVC ID='PP1,1,1', QUANTITY='PRESSURE', XYZ=6.6,13.1,3.0/  
 &DEVC ID='SP1,1,1', QUANTITY='RADIATIVE HEAT FLUX GAS', XYZ=6.6,13.1,4.3/  
 &DEVC ID='SP1,1,2', QUANTITY='RADIATIVE HEAT FLUX GAS', XYZ=6.6,13.1,3.1/  
 &DEVC ID='TK1.1.0', PROP\_ID='TK1.1.0 props', QUANTITY='THERMOCOUPLE', XYZ=6.6,13.1,5.2/  
 &DEVC ID='TK1.1.1', PROP\_ID='TK1.1.1 props', QUANTITY='THERMOCOUPLE', XYZ=6.6,13.1,5.0/  
 &DEVC ID='TK1.1.2', PROP\_ID='TK1.1.2 props', QUANTITY='THERMOCOUPLE', XYZ=6.6,13.1,4.8/  
 &DEVC ID='TK1.1.3', PROP\_ID='TK1.1.3 props', QUANTITY='THERMOCOUPLE', XYZ=6.6,13.1,4.6/  
 &DEVC ID='TK1.1.4', PROP\_ID='TK1.1.4 props', QUANTITY='THERMOCOUPLE', XYZ=6.6,13.1,4.3/  
 &DEVC ID='TK1.1.5', PROP\_ID='TK1.1.5 props', QUANTITY='THERMOCOUPLE', XYZ=6.6,13.1,3.7/  
 &DEVC ID='TK1.1.6', PROP\_ID='TK1.1.6 props', QUANTITY='THERMOCOUPLE', XYZ=6.6,13.1,3.1/  
 &DEVC ID='CO(11)', QUANTITY='VOLUME FRACTION', SPEC\_ID='CARBON MONOXIDE', XYZ=2.7,10.7,3.1/  
 &DEVC ID='CO(15)', QUANTITY='VOLUME FRACTION', SPEC\_ID='CARBON MONOXIDE', XYZ=2.7,10.7,4.3/  
 &DEVC ID='CO2(11)', QUANTITY='VOLUME FRACTION', SPEC\_ID='CARBON DIOXIDE', XYZ=2.7,10.7,3.1/  
 &DEVC ID='CO2(15)', QUANTITY='VOLUME FRACTION', SPEC\_ID='CARBON DIOXIDE', XYZ=2.7,10.7,4.3/  
 &DEVC ID='O2(11)', QUANTITY='VOLUME FRACTION', SPEC\_ID='OXYGEN', XYZ=2.7,10.7,3.1/  
 &DEVC ID='O2(15)', QUANTITY='VOLUME FRACTION', SPEC\_ID='OXYGEN', XYZ=2.7,10.7,4.3/  
 &DEVC ID='PP1,5,1', QUANTITY='PRESSURE', XYZ=2.7,10.7,3.0/

&DEVC ID='SB1,5,2', QUANTITY='RADIATIVE HEAT FLUX GAS', XYZ=2.7,10.7,3.1/  
 &DEVC ID='SP1,5,1', QUANTITY='RADIATIVE HEAT FLUX GAS', XYZ=2.7,10.7,4.3/  
 &DEVC ID='TK1,5,0', QUANTITY='THERMOCOUPLE', XYZ=2.7,10.7,5.15/  
 &DEVC ID='TK1,5,1', QUANTITY='THERMOCOUPLE', XYZ=2.7,10.7,5.0/  
 &DEVC ID='TK1,5,2', QUANTITY='THERMOCOUPLE', XYZ=2.7,10.7,4.8/  
 &DEVC ID='TK1,5,3', QUANTITY='THERMOCOUPLE', XYZ=2.7,10.7,4.6/  
 &DEVC ID='TK1,5,4', QUANTITY='THERMOCOUPLE', XYZ=2.7,10.7,4.3/  
 &DEVC ID='TK1,5,5', QUANTITY='THERMOCOUPLE', XYZ=2.7,10.7,3.7/  
 &DEVC ID='TK1,5,6', QUANTITY='THERMOCOUPLE', XYZ=2.7,10.7,3.1/  
 &DEVC ID='ZL1,5,1', QUANTITY='VISIBILITY', XYZ=2.7,10.7,4.3/  
 &DEVC ID='ZL1,5,2', QUANTITY='VISIBILITY', XYZ=2.7,10.7,3.1/  
 &DEVC ID='CO(21)', QUANTITY='VOLUME FRACTION', SPEC\_ID='CARBON MONOXIDE', XYZ=15.7,10.8,3.1/  
 &DEVC ID='CO(23)', QUANTITY='VOLUME FRACTION', SPEC\_ID='CARBON MONOXIDE', XYZ=15.7,10.8,4.3/  
 &DEVC ID='CO2(21)', QUANTITY='VOLUME FRACTION', SPEC\_ID='CARBON DIOXIDE', XYZ=15.7,10.8,3.1/  
 &DEVC ID='CO2(23)', QUANTITY='VOLUME FRACTION', SPEC\_ID='CARBON DIOXIDE', XYZ=15.7,10.8,4.3/  
 &DEVC ID='O2(21)', QUANTITY='VOLUME FRACTION', SPEC\_ID='OXYGEN', XYZ=15.7,10.8,3.1/  
 &DEVC ID='O2(23)', QUANTITY='VOLUME FRACTION', SPEC\_ID='OXYGEN', XYZ=15.7,10.8,4.3/  
 &DEVC ID='PP1,6,1', QUANTITY='PRESSURE', XYZ=15.7,10.8,3.0/  
 &DEVC ID='SB1,6,2', QUANTITY='RADIATIVE HEAT FLUX GAS', XYZ=15.7,10.8,3.1/  
 &DEVC ID='SP1,6,1', QUANTITY='RADIATIVE HEAT FLUX GAS', XYZ=15.7,10.8,4.3/  
 &DEVC ID='TK1,6,0', QUANTITY='THERMOCOUPLE', XYZ=15.7,10.8,5.15/  
 &DEVC ID='TK1,6,1', QUANTITY='THERMOCOUPLE', XYZ=15.7,10.8,5.0/  
 &DEVC ID='TK1,6,2', QUANTITY='THERMOCOUPLE', XYZ=15.7,10.8,4.8/  
 &DEVC ID='TK1,6,3', QUANTITY='THERMOCOUPLE', XYZ=15.7,10.8,4.6/  
 &DEVC ID='TK1,6,4', QUANTITY='THERMOCOUPLE', XYZ=15.7,10.8,4.3/  
 &DEVC ID='TK1,6,5', QUANTITY='THERMOCOUPLE', XYZ=15.7,10.8,3.7/  
 &DEVC ID='TK1,6,6', QUANTITY='THERMOCOUPLE', XYZ=15.7,10.8,3.1/  
 &DEVC ID='ZL1,6,1', QUANTITY='VISIBILITY', XYZ=15.7,10.8,4.3/  
 &DEVC ID='ZL1,6,2', QUANTITY='VISIBILITY', XYZ=15.7,10.8,3.1/  
 &DEVC ID='TEMP\_FIRE\_0,2', QUANTITY='TEMPERATURE', XYZ=3.9,15.2,3.6/  
 &DEVC ID='TEMP\_FIRE\_0,4', QUANTITY='TEMPERATURE', XYZ=3.9,15.2,3.8/  
 &DEVC ID='TEMP\_FIRE\_0,6', QUANTITY='TEMPERATURE', XYZ=3.9,15.2,4.0/  
 &DEVC ID='TEMP\_FIRE\_0,8', QUANTITY='TEMPERATURE', XYZ=3.9,15.2,4.2/  
 &DEVC ID='TEMP\_FIRE\_1,0', QUANTITY='TEMPERATURE', XYZ=3.9,15.2,4.4/  
 &DEVC ID='TEMP\_FIRE\_1,2', QUANTITY='TEMPERATURE', XYZ=3.9,15.2,4.6/  
 &DEVC ID='TEMP\_FIRE\_1,4', QUANTITY='TEMPERATURE', XYZ=3.9,15.2,4.8/  
 &DEVC ID='TEMP\_FIRE\_1,6', QUANTITY='TEMPERATURE', XYZ=3.9,15.2,5.0/  
 &DEVC ID='Positive hallway', QUANTITY='MASS FLOW +', XB=5.1,6.0,12.3,12.3,2.8,4.8/  
 &DEVC ID='Negative hallway', QUANTITY='MASS FLOW -', XB=5.1,6.0,12.3,12.3,2.8,4.8/  
 &DEVC ID='Positive balcony', QUANTITY='MASS FLOW +', XB=5.1,6.0,18.4,18.4,2.8,4.8/  
 &DEVC ID='Negative balcony', QUANTITY='MASS FLOW -', XB=5.1,6.0,18.4,18.4,2.8,4.8/  
 &DEVC ID='RH4', QUANTITY='LAYER HEIGHT', XB=7.4,7.4,10.7,10.7,2.8,5.4/  
 &DEVC ID='RH5', QUANTITY='LAYER HEIGHT', XB=11.2,11.2,10.7,10.7,2.8,5.4/  
 &DEVC ID='Oxygen\_FIRE\_0,2', QUANTITY='VOLUME FRACTION', SPEC\_ID='OXYGEN', XYZ=3.9,15.2,3.6/  
 &DEVC ID='Oxygen\_FIRE\_0,4', QUANTITY='VOLUME FRACTION', SPEC\_ID='OXYGEN', XYZ=3.9,15.2,3.8/  
 &DEVC ID='Oxygen\_FIRE\_0,6', QUANTITY='VOLUME FRACTION', SPEC\_ID='OXYGEN', XYZ=3.9,15.2,4.0/  
 &DEVC ID='Oxygen\_FIRE\_0,8', QUANTITY='VOLUME FRACTION', SPEC\_ID='OXYGEN', XYZ=3.9,15.2,4.2/  
 &DEVC ID='Oxygen\_FIRE\_1,0', QUANTITY='VOLUME FRACTION', SPEC\_ID='OXYGEN', XYZ=3.9,15.2,4.4/  
 &DEVC ID='Oxygen\_FIRE\_1,2', QUANTITY='VOLUME FRACTION', SPEC\_ID='OXYGEN', XYZ=3.9,15.2,4.6/  
 &DEVC ID='Oxygen\_FIRE\_1,4', QUANTITY='VOLUME FRACTION', SPEC\_ID='OXYGEN', XYZ=3.9,15.2,4.8/  
 &DEVC ID='Oxygen\_FIRE\_1,6', QUANTITY='VOLUME FRACTION', SPEC\_ID='OXYGEN', XYZ=3.9,15.2,5.0/  
 &DEVC ID='TK1.1.1alt', PROP\_ID='TK1.1.1alt props', QUANTITY='THERMOCOUPLE', XYZ=6.3,13.1,5.2/  
 &DEVC ID='TK1.1.2alt', PROP\_ID='TK1.1.2alt props', QUANTITY='THERMOCOUPLE', XYZ=6.3,13.1,5.0/  
 &DEVC ID='TK1.1.3alt', PROP\_ID='TK1.1.3alt props', QUANTITY='THERMOCOUPLE', XYZ=6.3,13.1,4.8/  
 &DEVC ID='TK1.1.4alt', PROP\_ID='TK1.1.4alt props', QUANTITY='THERMOCOUPLE', XYZ=6.3,13.1,4.6/  
 &DEVC ID='TK1.1.5alt', PROP\_ID='TK1.1.5alt props', QUANTITY='THERMOCOUPLE', XYZ=6.3,13.1,4.3/  
 &DEVC ID='TK1.1.6alt', PROP\_ID='TK1.1.6alt props', QUANTITY='THERMOCOUPLE', XYZ=6.3,13.1,3.7/  
 &DEVC ID='TK1.1.7alt', PROP\_ID='TK1.1.7alt props', QUANTITY='THERMOCOUPLE', XYZ=6.3,13.1,3.1/  
 &DEVC ID='TK1.1.6alt01', PROP\_ID='TK1.1.6alt01 props', QUANTITY='THERMOCOUPLE', XYZ=6.0,13.1,3.7/  
 &DEVC ID='TK1.1.1alt01', PROP\_ID='TK1.1.1alt01 props', QUANTITY='THERMOCOUPLE', XYZ=6.0,13.1,5.2/  
 &DEVC ID='TK1.1.2alt01', PROP\_ID='TK1.1.2alt01 props', QUANTITY='THERMOCOUPLE', XYZ=6.0,13.1,5.0/  
 &DEVC ID='TK1.1.3alt01', PROP\_ID='TK1.1.3alt01 props', QUANTITY='THERMOCOUPLE', XYZ=6.0,13.1,4.8/  
 &DEVC ID='TK1.1.4alt01', PROP\_ID='TK1.1.4alt01 props', QUANTITY='THERMOCOUPLE', XYZ=6.0,13.1,4.6/  
 &DEVC ID='TK1.1.5alt01', PROP\_ID='TK1.1.5alt01 props', QUANTITY='THERMOCOUPLE', XYZ=6.0,13.1,4.3/  
 &DEVC ID='TK1.1.7alt01', PROP\_ID='TK1.1.7alt01 props', QUANTITY='THERMOCOUPLE', XYZ=6.0,13.1,3.1/  
 &DEVC ID='TIME', QUANTITY='TIME', XYZ=6.6,8.4,2.6/

```

&MATL ID='GYPSUM PLASTER',
  FYI='Quintiere, Fire Behavior - NIST NRC Validation',
  SPECIFIC_HEAT=0.84,
  CONDUCTIVITY=0.48,
  DENSITY=1440.0/
&MATL ID='CONCRETE',
  FYI='NBSIR 88-3752 - ATF NIST Multi-Floor Validation',
  SPECIFIC_HEAT=1.04,
  CONDUCTIVITY=1.8,
  DENSITY=2280.0/
&MATL ID='Calcium stone',
  SPECIFIC_HEAT=0.84,
  CONDUCTIVITY=0.75,
  DENSITY=1900.0/
&MATL ID='YELLOW PINE',
  FYI='Quintiere, Fire Behavior - NIST NRC Validation',
  SPECIFIC_HEAT=2.85,
  CONDUCTIVITY=0.14,
  DENSITY=640.0/
&MATL ID='DOUBLE GLAZING',
  SPECIFIC_HEAT=0.72,
  CONDUCTIVITY=5.68E-3,
  DENSITY=2500.0/
&MATL ID='CALCIUM SILICATE',
  FYI='NBSIR 88-3752 - NBS Multi-Room Validation',
  SPECIFIC_HEAT_RAMP='CALCIUM SILICATE_SPECIFIC_HEAT_RAMP',
  CONDUCTIVITY=0.12,
  DENSITY=720.0,
  EMISSIVITY=0.83/
&RAMP ID='CALCIUM SILICATE_SPECIFIC_HEAT_RAMP', T=20.0, F=1.25/
&RAMP ID='CALCIUM SILICATE_SPECIFIC_HEAT_RAMP', T=200.0, F=1.25/
&RAMP ID='CALCIUM SILICATE_SPECIFIC_HEAT_RAMP', T=300.0, F=1.33/
&RAMP ID='CALCIUM SILICATE_SPECIFIC_HEAT_RAMP', T=600.0, F=1.55/

&SURF ID='CONCRETE_FLOORS',
  RGB=146,202,166,
  BACKING='VOID',
  MATL_ID(1,1)='GYPSUM PLASTER',
  MATL_ID(2,1)='CONCRETE',
  MATL_MASS_FRACTION(1,1)=1.0,
  MATL_MASS_FRACTION(2,1)=1.0,
  THICKNESS(1:2)=1.0E-3,0.2/
&SURF ID='CONCRETE_WALLS',
  RGB=146,202,166,
  BACKING='VOID',
  MATL_ID(1,1)='CONCRETE',
  MATL_MASS_FRACTION(1,1)=1.0,
  THICKNESS(1)=0.2/
&SURF ID='CALCIUM SILICATE WALLS',
  COLOR='WHITE',
  BACKING='VOID',
  MATL_ID(1,1)='Calcium stone',
  MATL_MASS_FRACTION(1,1)=1.0,
  THICKNESS(1)=0.1/
&SURF ID='Hallway-apartments',
  RGB=127,221,255,
  LEAK_PATH=2,0/
&SURF ID='DOOR',
  RGB=204,204,0,
  BACKING='VOID',
  MATL_ID(1,1)='YELLOW PINE',
  MATL_MASS_FRACTION(1,1)=1.0,
  THICKNESS(1)=0.05/
&SURF ID='DOUBLE GLAZING',
  RGB=146,193,202,
  TRANSPARENCY=0.396078,

```

```

BACKING='VOID',
MATL_ID(1,1)='DOUBLE GLAZING',
MATL_MASS_FRACTION(1,1)=1.0,
THICKNESS(1)=0.012/
&SURF ID='Windows fire room',
  RGB=146,202,166,
  BACKING='VOID',
  MATL_ID(1,1)='CALCIUM SILICATE',
  MATL_MASS_FRACTION(1,1)=1.0,
  THICKNESS(1)=0.012/
&SURF ID='Double door',
  RGB=127,221,255,
  LEAK_PATH=2,0/
&SURF ID='CEILING HALLWAY',
  RGB=146,202,166,
  BACKING='VOID',
  MATL_ID(1,1)='CALCIUM SILICATE',
  MATL_MASS_FRACTION(1,1)=1.0,
  THICKNESS(1)=0.03/
&SURF ID='Apartment1.19-Zone0',
  LEAK_PATH=1,0/
&SURF ID='SofaFIRE01',
  COLOR='RED',
  MLRPUA=0.04954,
  RAMP_Q='SofaFIRE01_RAMP_Q',
  TMP_FRONT=300.0/
&RAMP ID='SofaFIRE01_RAMP_Q', T=0.0, F=0.0/
&RAMP ID='SofaFIRE01_RAMP_Q', T=10.0, F=0.0/
&RAMP ID='SofaFIRE01_RAMP_Q', T=20.0, F=1.405365E-3/
&RAMP ID='SofaFIRE01_RAMP_Q', T=30.0, F=1.405365E-3/
&RAMP ID='SofaFIRE01_RAMP_Q', T=40.0, F=4.505261E-3/
&RAMP ID='SofaFIRE01_RAMP_Q', T=50.0, F=4.55764E-3/
&RAMP ID='SofaFIRE01_RAMP_Q', T=60.0, F=5.984509E-3/
&RAMP ID='SofaFIRE01_RAMP_Q', T=70.0, F=0.013231/
&RAMP ID='SofaFIRE01_RAMP_Q', T=80.0, F=0.018312/
&RAMP ID='SofaFIRE01_RAMP_Q', T=90.0, F=0.024916/
&RAMP ID='SofaFIRE01_RAMP_Q', T=100.0, F=0.033991/
&RAMP ID='SofaFIRE01_RAMP_Q', T=110.0, F=0.049102/
&RAMP ID='SofaFIRE01_RAMP_Q', T=120.0, F=0.060753/
&RAMP ID='SofaFIRE01_RAMP_Q', T=130.0, F=0.080462/
&RAMP ID='SofaFIRE01_RAMP_Q', T=140.0, F=0.103864/
&RAMP ID='SofaFIRE01_RAMP_Q', T=150.0, F=0.132197/
&RAMP ID='SofaFIRE01_RAMP_Q', T=160.0, F=0.15722/
&RAMP ID='SofaFIRE01_RAMP_Q', T=170.0, F=0.188069/
&RAMP ID='SofaFIRE01_RAMP_Q', T=180.0, F=0.22243/
&RAMP ID='SofaFIRE01_RAMP_Q', T=190.0, F=0.252579/
&RAMP ID='SofaFIRE01_RAMP_Q', T=200.0, F=0.275327/
&RAMP ID='SofaFIRE01_RAMP_Q', T=210.0, F=0.309052/
&RAMP ID='SofaFIRE01_RAMP_Q', T=220.0, F=0.35168/
&RAMP ID='SofaFIRE01_RAMP_Q', T=230.0, F=0.388635/
&RAMP ID='SofaFIRE01_RAMP_Q', T=240.0, F=0.418661/
&RAMP ID='SofaFIRE01_RAMP_Q', T=250.0, F=0.466062/
&RAMP ID='SofaFIRE01_RAMP_Q', T=260.0, F=0.502973/
&RAMP ID='SofaFIRE01_RAMP_Q', T=270.0, F=0.510006/
&RAMP ID='SofaFIRE01_RAMP_Q', T=280.0, F=0.51553/
&RAMP ID='SofaFIRE01_RAMP_Q', T=290.0, F=0.604412/
&RAMP ID='SofaFIRE01_RAMP_Q', T=300.0, F=0.701803/
&RAMP ID='SofaFIRE01_RAMP_Q', T=310.0, F=0.809317/
&RAMP ID='SofaFIRE01_RAMP_Q', T=320.0, F=0.928592/
&RAMP ID='SofaFIRE01_RAMP_Q', T=330.0, F=1.0/
&RAMP ID='SofaFIRE01_RAMP_Q', T=340.0, F=0.996972/
&RAMP ID='SofaFIRE01_RAMP_Q', T=350.0, F=0.9689/
&RAMP ID='SofaFIRE01_RAMP_Q', T=360.0, F=0.908997/
&RAMP ID='SofaFIRE01_RAMP_Q', T=370.0, F=0.80783/
&RAMP ID='SofaFIRE01_RAMP_Q', T=380.0, F=0.734766/
&RAMP ID='SofaFIRE01_RAMP_Q', T=390.0, F=0.631911/

```

&RAMP ID='SofaFIRE01\_RAMP\_Q', T=400.0, F=0.503801/  
 &RAMP ID='SofaFIRE01\_RAMP\_Q', T=410.0, F=0.386604/  
 &RAMP ID='SofaFIRE01\_RAMP\_Q', T=420.0, F=0.316443/  
 &RAMP ID='SofaFIRE01\_RAMP\_Q', T=430.0, F=0.260636/  
 &RAMP ID='SofaFIRE01\_RAMP\_Q', T=440.0, F=0.218507/  
 &RAMP ID='SofaFIRE01\_RAMP\_Q', T=450.0, F=0.197012/  
 &RAMP ID='SofaFIRE01\_RAMP\_Q', T=460.0, F=0.177996/  
 &RAMP ID='SofaFIRE01\_RAMP\_Q', T=470.0, F=0.15576/  
 &RAMP ID='SofaFIRE01\_RAMP\_Q', T=480.0, F=0.131075/  
 &RAMP ID='SofaFIRE01\_RAMP\_Q', T=490.0, F=0.112184/  
 &RAMP ID='SofaFIRE01\_RAMP\_Q', T=500.0, F=0.094982/  
 &RAMP ID='SofaFIRE01\_RAMP\_Q', T=510.0, F=0.082553/  
 &RAMP ID='SofaFIRE01\_RAMP\_Q', T=520.0, F=0.071604/  
 &RAMP ID='SofaFIRE01\_RAMP\_Q', T=530.0, F=0.061171/  
 &RAMP ID='SofaFIRE01\_RAMP\_Q', T=540.0, F=0.056182/  
 &RAMP ID='SofaFIRE01\_RAMP\_Q', T=550.0, F=0.049695/  
 &RAMP ID='SofaFIRE01\_RAMP\_Q', T=560.0, F=0.043307/  
 &RAMP ID='SofaFIRE01\_RAMP\_Q', T=570.0, F=0.034217/  
 &RAMP ID='SofaFIRE01\_RAMP\_Q', T=580.0, F=0.029976/  
 &RAMP ID='SofaFIRE01\_RAMP\_Q', T=590.0, F=0.024248/  
 &RAMP ID='SofaFIRE01\_RAMP\_Q', T=600.0, F=0.020264/  
 &RAMP ID='SofaFIRE01\_RAMP\_Q', T=610.0, F=0.017227/  
 &RAMP ID='SofaFIRE01\_RAMP\_Q', T=620.0, F=0.01368/  
 &RAMP ID='SofaFIRE01\_RAMP\_Q', T=630.0, F=0.010457/  
 &RAMP ID='SofaFIRE01\_RAMP\_Q', T=640.0, F=8.205984E-3/  
 &RAMP ID='SofaFIRE01\_RAMP\_Q', T=650.0, F=7.150864E-3/  
 &RAMP ID='SofaFIRE01\_RAMP\_Q', T=660.0, F=7.921884E-3/  
 &RAMP ID='SofaFIRE01\_RAMP\_Q', T=670.0, F=6.390911E-3/  
 &RAMP ID='SofaFIRE01\_RAMP\_Q', T=680.0, F=8.498561E-3/  
 &RAMP ID='SofaFIRE01\_RAMP\_Q', T=690.0, F=6.205489E-3/  
 &RAMP ID='SofaFIRE01\_RAMP\_Q', T=700.0, F=0.011488/  
 &RAMP ID='SofaFIRE01\_RAMP\_Q', T=710.0, F=0.012229/  
 &RAMP ID='SofaFIRE01\_RAMP\_Q', T=720.0, F=0.012229/  
 &RAMP ID='SofaFIRE01\_RAMP\_Q', T=730.0, F=8.998951E-3/  
 &RAMP ID='SofaFIRE01\_RAMP\_Q', T=740.0, F=0.010228/  
 &RAMP ID='SofaFIRE01\_RAMP\_Q', T=750.0, F=5.994083E-3/  
 &RAMP ID='SofaFIRE01\_RAMP\_Q', T=760.0, F=2.954789E-3/  
 &RAMP ID='SofaFIRE01\_RAMP\_Q', T=770.0, F=2.954789E-3/  
 &RAMP ID='SofaFIRE01\_RAMP\_Q', T=780.0, F=5.096689E-3/  
 &RAMP ID='SofaFIRE01\_RAMP\_Q', T=790.0, F=4.63804E-3/  
 &RAMP ID='SofaFIRE01\_RAMP\_Q', T=800.0, F=3.589832E-3/  
 &RAMP ID='SofaFIRE01\_RAMP\_Q', T=810.0, F=5.363408E-3/  
 &RAMP ID='SofaFIRE01\_RAMP\_Q', T=820.0, F=7.074998E-3/  
 &RAMP ID='SofaFIRE01\_RAMP\_Q', T=830.0, F=4.469765E-3/  
 &RAMP ID='SofaFIRE01\_RAMP\_Q', T=840.0, F=3.699053E-3/  
 &RAMP ID='SofaFIRE01\_RAMP\_Q', T=850.0, F=7.148055E-3/  
 &RAMP ID='SofaFIRE01\_RAMP\_Q', T=860.0, F=6.518173E-3/  
 &RAMP ID='SofaFIRE01\_RAMP\_Q', T=870.0, F=7.420258E-3/  
 &RAMP ID='SofaFIRE01\_RAMP\_Q', T=880.0, F=7.549245E-3/  
 &RAMP ID='SofaFIRE01\_RAMP\_Q', T=890.0, F=9.38745E-3/  
 &RAMP ID='SofaFIRE01\_RAMP\_Q', T=900.0, F=7.001247E-3/  
 &RAMP ID='SofaFIRE01\_RAMP\_Q', T=910.0, F=7.210983E-3/  
 &RAMP ID='SofaFIRE01\_RAMP\_Q', T=920.0, F=4.768786E-3/  
 &RAMP ID='SofaFIRE01\_RAMP\_Q', T=930.0, F=6.85545E-3/  
 &RAMP ID='SofaFIRE01\_RAMP\_Q', T=940.0, F=5.461447E-3/  
 &RAMP ID='SofaFIRE01\_RAMP\_Q', T=950.0, F=4.398648E-3/  
 &RAMP ID='SofaFIRE01\_RAMP\_Q', T=960.0, F=2.83133E-3/  
 &RAMP ID='SofaFIRE01\_RAMP\_Q', T=970.0, F=2.659853E-3/  
 &RAMP ID='SofaFIRE01\_RAMP\_Q', T=980.0, F=2.678436E-3/  
 &RAMP ID='SofaFIRE01\_RAMP\_Q', T=990.0, F=2.234234E-3/  
 &RAMP ID='SofaFIRE01\_RAMP\_Q', T=1000.0, F=2.510655E-3/

&OBST ID='Obstruction', XB=-0.7,18.5,19.6,19.7,2.8,3.0, COLOR='GRAY 80', SURF\_ID='CONCRETE\_WALLS'/  
 &OBST ID='Obstruction', XB=-0.7,18.5,19.6,19.7,2.4,2.6, COLOR='GRAY 80', SURF\_ID='CONCRETE\_WALLS'/  
 &OBST ID='Bulkhead', XB=12.7,13.6,12.3,12.4,4.8,5.4, SURF\_ID='CALCIUM SILICATE WALLS'/  
 &OBST ID='Bulkhead2', XB=12.6,12.7,12.7,13.5,4.8,5.4, SURF\_ID='CALCIUM SILICATE WALLS'/

&OBST ID='Door 1.19-Hallway', XB=12.7,13.6,12.3,12.406742,2.8,4.8, SURF\_ID6='DOOR','DOOR','Hallway-apartments','Hallway-apartments','DOOR','DOOR'/  
 &OBST ID='Door barchroom', XB=12.6,12.7,12.7,13.5,2.8,4.8, SURF\_ID='DOOR'/  
 &OBST ID='Innerwall 5', XB=13.6,14.5,12.3,12.4,2.8,5.4, SURF\_ID='CALCIUM SILICATE WALLS'/  
 &OBST ID='Innerwall1', XB=10.7,10.9,12.2,19.5,2.8,5.4, COLOR='GRAY 80', SURF\_ID='CONCRETE\_WALLS'/  
 &OBST ID='Innerwall2', XB=14.5,14.7,12.2,19.5,2.8,5.4, COLOR='GRAY 80', SURF\_ID='CONCRETE\_WALLS'/  
 &OBST ID='Innerwall3', XB=10.9,14.5,14.0,14.1,2.8,5.4, SURF\_ID='CALCIUM SILICATE WALLS'/  
 &OBST ID='Innerwall6', XB=12.6,12.7,13.5,14.0,2.8,5.4, SURF\_ID='CALCIUM SILICATE WALLS'/  
 &OBST ID='Overhead2', XB=12.7,13.6,18.4,18.5,2.8,5.4, SURF\_ID='DOUBLE GLAZING'/  
 &OBST ID='Parapet1', XB=10.9,12.7,18.4,18.5,2.8,3.5, COLOR='GRAY 80', SURF\_ID='CONCRETE\_WALLS'/  
 &OBST ID='Parapet2', XB=13.6,14.5,18.4,18.5,2.8,3.5, COLOR='GRAY 80', SURF\_ID='CONCRETE\_WALLS'/  
 &OBST ID='Window backside', XB=10.9,12.7,18.4,18.5,3.5,5.4, SURF\_ID='DOUBLE GLAZING'/  
 &OBST ID='Window backside 2', XB=13.6,14.5,18.4,18.5,3.5,5.4, SURF\_ID='DOUBLE GLAZING'/  
 &OBST ID='Balcony door', XB=8.9,9.8,18.4,18.5,2.8,4.8, SURF\_ID='DOUBLE GLAZING'/  
 &OBST ID='Bulkhead', XB=8.9,9.8,12.3,12.4,4.8,5.4, SURF\_ID='CALCIUM SILICATE WALLS'/  
 &OBST ID='Bulkhead2', XB=8.8,8.9,12.7,13.5,4.8,5.4, SURF\_ID='CALCIUM SILICATE WALLS'/  
 &OBST ID='Door 1.20-Hallway', XB=8.9,9.8,12.3,12.4,2.8,4.8, SURF\_ID6='DOOR','DOOR','Hallway-apartments','Hallway-apartments','DOOR','DOOR'/  
 &OBST ID='Door barchroom', XB=8.8,8.9,12.7,13.5,2.8,4.8, SURF\_ID='DOOR'/  
 &OBST ID='Innerwall 5', XB=9.8,10.7,12.3,12.4,2.8,5.4, SURF\_ID='CALCIUM SILICATE WALLS'/  
 &OBST ID='Innerwall1', XB=6.9,7.1,12.2,19.5,2.8,5.4, COLOR='GRAY 80', SURF\_ID='CONCRETE\_WALLS'/  
 &OBST ID='Innerwall3', XB=7.1,10.7,14.0,14.1,2.8,5.4, SURF\_ID='CALCIUM SILICATE WALLS'/  
 &OBST ID='Innerwall6', XB=8.8,8.9,13.5,14.0,2.8,5.4, SURF\_ID='CALCIUM SILICATE WALLS'/  
 &OBST ID='Overhead2', XB=8.9,9.8,18.4,18.5,4.8,5.4, SURF\_ID='DOUBLE GLAZING'/  
 &OBST ID='Parapet1', XB=7.1,8.9,18.4,18.5,2.8,3.5, COLOR='GRAY 80', SURF\_ID='CONCRETE\_WALLS'/  
 &OBST ID='Parapet2', XB=9.8,10.7,18.4,18.5,2.8,3.5, COLOR='GRAY 80', SURF\_ID='CONCRETE\_WALLS'/  
 &OBST ID='Window backside', XB=7.1,8.9,18.4,18.5,3.5,5.4, SURF\_ID='DOUBLE GLAZING'/  
 &OBST ID='Window backside 2', XB=9.8,10.7,18.4,18.5,3.5,5.4, SURF\_ID='DOUBLE GLAZING'/  
 &OBST ID='Balcony door', XB=5.1,6.0,18.4,18.5,2.8,4.8, SURF\_ID='Windows fire room'/  
 &OBST ID='Bulkhead', XB=5.1,6.0,12.3,12.4,4.8,5.4, SURF\_ID='CALCIUM SILICATE WALLS'/  
 &OBST ID='Door 1.21-Hallway', XB=5.1,6.0,12.3,12.4,2.8,4.8, SURF\_ID='DOOR', CTRL\_ID='DOORCONTROL3'/  
 &OBST ID='Bulkhead2', XB=5.0,5.1,12.7,13.5,4.8,5.4, SURF\_ID='CALCIUM SILICATE WALLS'/  
 &OBST ID='Door barchroom', XB=5.0,5.1,12.7,13.5,2.8,4.8, SURF\_ID='DOOR'/  
 &OBST ID='Innerwall 5', XB=6.0,6.9,12.3,12.4,2.8,5.4, SURF\_ID='CALCIUM SILICATE WALLS'/  
 &OBST ID='Innerwall1', XB=3.1,3.3,12.2,19.5,2.8,5.4, COLOR='GRAY 80', SURF\_ID='CONCRETE\_WALLS'/  
 &OBST ID='Innerwall3', XB=3.3,6.9,14.0,14.1,2.8,5.4, SURF\_ID='CALCIUM SILICATE WALLS'/  
 &OBST ID='Innerwall6', XB=5.0,5.1,13.5,14.0,2.8,5.4, SURF\_ID='CALCIUM SILICATE WALLS'/  
 &OBST ID='Overhead2', XB=5.1,6.0,18.4,18.5,4.8,5.4, SURF\_ID='Windows fire room'/  
 &OBST ID='Parapet1', XB=3.3,5.1,18.4,18.5,2.8,3.5, COLOR='GRAY 80', SURF\_ID='CONCRETE\_WALLS'/  
 &OBST ID='Parapet2', XB=6.0,6.9,18.4,18.5,2.8,3.5, COLOR='GRAY 80', SURF\_ID='CONCRETE\_WALLS'/  
 &OBST ID='Window backside', XB=3.3,5.1,18.4,18.5,3.5,5.4, SURF\_ID='Windows fire room'/  
 &OBST ID='Window backside 2', XB=6.0,6.9,18.4,18.5,3.5,5.4, SURF\_ID='Windows fire room'/  
 &OBST ID='Balcony door', XB=1.3,2.2,18.4,18.5,2.8,4.8, SURF\_ID='DOUBLE GLAZING'/  
 &OBST ID='Bulkhead', XB=1.3,2.2,12.3,12.4,4.8,5.4, SURF\_ID='CALCIUM SILICATE WALLS'/  
 &OBST ID='Bulkhead2', XB=1.2,1.3,12.7,13.5,4.8,5.4, SURF\_ID='CALCIUM SILICATE WALLS'/  
 &OBST ID='Door 1.21-Hallway', XB=1.3,2.2,12.3,12.4,2.8,4.8, SURF\_ID6='DOOR','DOOR','Hallway-apartments','Hallway-apartments','DOOR','DOOR'/  
 &OBST ID='Door barchroom', XB=1.2,1.3,12.7,13.5,2.8,4.8, SURF\_ID='DOOR'/  
 &OBST ID='Innerwall 5', XB=2.2,3.1,12.3,12.4,2.8,5.4, SURF\_ID='CALCIUM SILICATE WALLS'/  
 &OBST ID='Innerwall1', XB=-0.7,-0.5,12.2,19.5,2.8,5.4, COLOR='GRAY 80', SURF\_ID='CONCRETE\_WALLS'/  
 &OBST ID='Innerwall3', XB=-0.5,3.1,14.0,14.1,2.8,5.4, SURF\_ID='CALCIUM SILICATE WALLS'/  
 &OBST ID='Innerwall6', XB=1.2,1.3,13.5,14.0,2.8,5.4, SURF\_ID='CALCIUM SILICATE WALLS'/  
 &OBST ID='Overhead2', XB=1.3,2.2,18.4,18.5,4.8,5.4, SURF\_ID='DOUBLE GLAZING'/  
 &OBST ID='Parapet1', XB=-0.5,1.3,18.4,18.5,2.8,3.5, COLOR='GRAY 80', SURF\_ID='CONCRETE\_WALLS'/  
 &OBST ID='Parapet2', XB=2.2,3.1,18.4,18.5,2.8,3.5, COLOR='GRAY 80', SURF\_ID='CONCRETE\_WALLS'/  
 &OBST ID='Window backside', XB=-0.5,1.3,18.4,18.5,3.5,5.4, SURF\_ID='DOUBLE GLAZING'/  
 &OBST ID='Window backside 2', XB=2.2,3.1,18.4,18.5,3.5,5.4, SURF\_ID='DOUBLE GLAZING'/  
 &OBST ID='Balcony door', XB=16.5,17.4,18.4,18.5,2.8,4.8, SURF\_ID='DOUBLE GLAZING'/  
 &OBST ID='Bulkhead', XB=16.5,17.4,12.3,12.4,4.8,5.4, SURF\_ID='CALCIUM SILICATE WALLS'/  
 &OBST ID='Bulkhead2', XB=16.4,16.5,12.7,13.5,4.8,5.4, SURF\_ID='CALCIUM SILICATE WALLS'/  
 &OBST ID='Door 1.18-Hallway', XB=16.5,17.4,12.3,12.4,2.8,4.8, SURF\_ID6='DOOR','DOOR','Hallway-apartments','Hallway-apartments','DOOR','DOOR'/  
 &OBST ID='Door barchroom', XB=16.4,16.5,12.7,13.5,2.8,4.8, SURF\_ID='DOOR'/  
 &OBST ID='Innerwall 5', XB=17.4,18.3,12.3,12.4,2.8,5.4, SURF\_ID='CALCIUM SILICATE WALLS'/  
 &OBST ID='Innerwall1', XB=14.5,14.7,12.2,19.5,2.8,5.4, COLOR='GRAY 80', SURF\_ID='CONCRETE\_WALLS'/  
 &OBST ID='Innerwall2', XB=18.3,18.5,12.2,19.5,2.8,5.4, COLOR='GRAY 80', SURF\_ID='CONCRETE\_WALLS'/

&OBST ID='Innerwall3', XB=14.7,18.3,14.0,14.1,2.8,5.4, SURF\_ID='CALCIUM SILICATE WALLS'/  
 &OBST ID='Innerwall6', XB=16.4,16.5,13.5,14.0,2.8,5.4, SURF\_ID='CALCIUM SILICATE WALLS'/  
 &OBST ID='Overhead2', XB=16.5,17.4,18.4,18.5,4.8,5.4, SURF\_ID='DOUBLE GLAZING'/  
 &OBST ID='Parapet1', XB=14.7,16.5,18.4,18.5,2.8,3.5, COLOR='GRAY 80', SURF\_ID='CONCRETE\_WALLS'/  
 &OBST ID='Parapet2', XB=17.4,18.3,18.4,18.5,2.8,3.5, COLOR='GRAY 80', SURF\_ID='CONCRETE\_WALLS'/  
 &OBST ID='Window backside', XB=14.7,16.5,18.4,18.5,3.5,5.4, SURF\_ID='DOUBLE GLAZING'/  
 &OBST ID='Window backside 2', XB=17.4,18.3,18.4,18.5,3.5,5.4, SURF\_ID='DOUBLE GLAZING'/  
 &OBST ID='Bulkhead', XB=12.7,13.6,10.3,10.4,4.8,5.4, SURF\_ID='CALCIUM SILICATE WALLS'/  
 &OBST ID='Bulkhead2', XB=12.6,12.7,9.2,10.0,4.8,5.4, SURF\_ID='CALCIUM SILICATE WALLS'/  
 &OBST ID='Door 1.26-Hallway', XB=12.7,13.6,10.3,10.4,2.8,4.8, SURF\_ID6='DOOR','DOOR','Hallway-apartments','Hallway-apartments','DOOR','DOOR'/  
 &OBST ID='Door barchroom', XB=12.6,12.7,9.2,10.0,2.8,4.8, SURF\_ID='DOOR'/  
 &OBST ID='Innerwall 5', XB=13.6,14.5,10.3,10.4,2.8,5.4, SURF\_ID='CALCIUM SILICATE WALLS'/  
 &OBST ID='Innerwall1', XB=10.7,10.9,4.0,10.5,2.8,5.4, COLOR='GRAY 80', SURF\_ID='CONCRETE\_WALLS'/  
 &OBST ID='Innerwall2', XB=14.5,14.7,4.0,10.5,2.8,5.4, COLOR='GRAY 80', SURF\_ID='CONCRETE\_WALLS'/  
 &OBST ID='Innerwall3', XB=10.9,14.5,8.6,8.7,2.8,5.4, SURF\_ID='CALCIUM SILICATE WALLS'/  
 &OBST ID='Innerwall6', XB=12.6,12.7,8.7,9.2,2.8,5.4, SURF\_ID='CALCIUM SILICATE WALLS'/  
 &OBST ID='Parapet1', XB=10.9,14.5,4.2,4.3,2.8,3.5, COLOR='GRAY 80', SURF\_ID='CONCRETE\_WALLS'/  
 &OBST ID='Window backside', XB=10.9,14.5,4.2,4.3,3.5,5.4, SURF\_ID='DOUBLE GLAZING'/  
 &OBST ID='Bulkhead', XB=16.3,17.2,10.3,10.4,4.8,5.4, SURF\_ID='CALCIUM SILICATE WALLS'/  
 &OBST ID='Bulkhead2', XB=16.2,16.3,9.2,10.0,4.8,5.4, SURF\_ID='CALCIUM SILICATE WALLS'/  
 &OBST ID='Door 1.28-Hallway', XB=16.3,17.2,10.3,10.4,2.8,4.8, SURF\_ID6='DOOR','DOOR','Hallway-apartments','Hallway-apartments','DOOR','DOOR'/  
 &OBST ID='Door barchroom', XB=16.2,16.3,9.2,10.0,2.8,4.8, SURF\_ID='DOOR'/  
 &OBST ID='Innerwall 5', XB=17.2,18.3,10.3,10.4,2.8,5.4, SURF\_ID='CALCIUM SILICATE WALLS'/  
 &OBST ID='Innerwall1', XB=14.5,14.7,4.0,10.5,2.8,5.4, COLOR='GRAY 80', SURF\_ID='CONCRETE\_WALLS'/  
 &OBST ID='Innerwall2', XB=18.3,18.5,4.0,10.5,2.8,5.4, COLOR='GRAY 80', SURF\_ID='CONCRETE\_WALLS'/  
 &OBST ID='Innerwall3', XB=14.7,18.3,8.6,8.7,2.8,5.4, SURF\_ID='CALCIUM SILICATE WALLS'/  
 &OBST ID='Innerwall6', XB=16.2,16.3,8.7,9.2,2.8,5.4, SURF\_ID='CALCIUM SILICATE WALLS'/  
 &OBST ID='Parapet1', XB=14.7,18.3,4.2,4.3,2.8,3.5, COLOR='GRAY 80', SURF\_ID='CONCRETE\_WALLS'/  
 &OBST ID='Window backside', XB=14.7,18.3,4.2,4.3,3.5,5.4, SURF\_ID='DOUBLE GLAZING'/  
 &OBST ID='Bulkhead', XB=8.9,9.8,10.3,10.4,4.8,5.4, SURF\_ID='CALCIUM SILICATE WALLS'/  
 &OBST ID='Bulkhead2', XB=8.8,8.9,9.2,10.0,4.8,5.4, COLOR='GRAY 80', SURF\_ID='CONCRETE\_WALLS'/  
 &OBST ID='Innerwall 5', XB=9.8,10.7,10.3,10.4,2.8,5.4, SURF\_ID='CALCIUM SILICATE WALLS'/  
 &OBST ID='Innerwall1', XB=6.9,7.1,4.0,10.5,2.8,5.4, COLOR='GRAY 80', SURF\_ID='CONCRETE\_WALLS'/  
 &OBST ID='Innerwall3', XB=7.1,10.7,8.6,8.7,2.8,5.4, SURF\_ID='CALCIUM SILICATE WALLS'/  
 &OBST ID='Innerwall6', XB=8.8,8.9,8.7,9.2,2.8,5.4, COLOR='GRAY 80', SURF\_ID='CONCRETE\_WALLS'/  
 &OBST ID='Parapet1', XB=7.1,10.7,4.2,4.3,2.8,3.5, COLOR='GRAY 80', SURF\_ID='CONCRETE\_WALLS'/  
 &OBST ID='Window backside', XB=7.1,10.7,4.2,4.3,3.5,5.4, SURF\_ID='DOUBLE GLAZING'/  
 &OBST ID='Bulkhead', XB=5.1,6.0,10.3,10.4,4.8,5.4, SURF\_ID='CALCIUM SILICATE WALLS'/  
 &OBST ID='Bulkhead2', XB=5.0,5.1,9.2,10.0,4.8,5.4, SURF\_ID='CALCIUM SILICATE WALLS'/  
 &OBST ID='Door 1.24-Hallway', XB=5.1,6.0,10.3,10.4,2.8,4.8, SURF\_ID6='DOOR','DOOR','Hallway-apartments','Hallway-apartments','DOOR','DOOR'/  
 &OBST ID='Door barchroom', XB=5.0,5.1,9.2,10.0,2.8,4.8, SURF\_ID='DOOR'/  
 &OBST ID='Innerwall 5', XB=6.0,6.9,10.3,10.4,2.8,5.4, SURF\_ID='CALCIUM SILICATE WALLS'/  
 &OBST ID='Innerwall1', XB=3.1,3.3,4.0,10.5,2.8,5.4, COLOR='GRAY 80', SURF\_ID='CONCRETE\_WALLS'/  
 &OBST ID='Innerwall3', XB=3.3,6.9,8.6,8.7,2.8,5.4, SURF\_ID='CALCIUM SILICATE WALLS'/  
 &OBST ID='Innerwall6', XB=5.0,5.1,8.7,9.2,2.8,5.4, SURF\_ID='CALCIUM SILICATE WALLS'/  
 &OBST ID='Parapet1', XB=3.3,6.9,4.2,4.3,2.8,3.5, COLOR='GRAY 80', SURF\_ID='CONCRETE\_WALLS'/  
 &OBST ID='Window backside', XB=3.3,6.9,4.2,4.3,3.5,5.4, SURF\_ID='DOUBLE GLAZING'/  
 &OBST ID='Door barchroom', XB=8.8,8.9,9.2,10.0,2.8,4.8, SURF\_ID='DOOR'/  
 &OBST ID='Bulkhead', XB=1.3,2.2,10.3,10.4,4.8,5.4, SURF\_ID='CALCIUM SILICATE WALLS'/  
 &OBST ID='Bulkhead2', XB=1.2,1.3,9.2,10.0,4.8,5.4, SURF\_ID='CALCIUM SILICATE WALLS'/  
 &OBST ID='Door 1.23-Hallway', XB=1.3,2.2,10.3,10.4,2.8,4.8, SURF\_ID6='DOOR','DOOR','Hallway-apartments','Hallway-apartments','DOOR','DOOR'/  
 &OBST ID='Door barchroom', XB=1.2,1.3,9.2,10.0,2.8,4.8, SURF\_ID='DOOR'/  
 &OBST ID='Innerwall 5', XB=2.2,3.1,10.3,10.4,2.8,5.4, SURF\_ID='CALCIUM SILICATE WALLS'/  
 &OBST ID='Innerwall1', XB=-0.7,-0.5,4.0,10.5,2.8,5.4, COLOR='GRAY 80', SURF\_ID='CONCRETE\_WALLS'/  
 &OBST ID='Innerwall3', XB=-0.5,3.1,8.6,8.7,2.8,5.4, SURF\_ID='CALCIUM SILICATE WALLS'/  
 &OBST ID='Innerwall6', XB=1.2,1.3,8.7,9.2,2.8,5.4, SURF\_ID='CALCIUM SILICATE WALLS'/  
 &OBST ID='Parapet1', XB=-0.5,3.1,4.2,4.3,2.8,3.5, COLOR='GRAY 80', SURF\_ID='CONCRETE\_WALLS'/  
 &OBST ID='Window backside', XB=-0.5,3.1,4.2,4.3,3.5,5.4, SURF\_ID='DOUBLE GLAZING'/  
 &OBST ID='Hallway double door left', XB=-0.7,-0.6,10.5,12.2,2.8,4.8, SURF\_ID6='Double door','Double door','DOOR','DOOR','DOOR','DOOR'/  
 &OBST ID='Hallway bulkhead left', XB=-0.7,-0.6,10.5,12.2,4.8,5.4, COLOR='GRAY 80', SURF\_ID='CONCRETE\_WALLS'/  
 &OBST ID='Hallway bulkhead right', XB=18.4,18.5,10.5,12.2,4.8,5.4, COLOR='GRAY 80', SURF\_ID='CONCRETE\_WALLS'/

&OBST ID='Hallway double door right', XB=18.4,18.5,10.5,12.2,2.8,4.8, SURF\_ID6='Double door','Double door','DOOR','DOOR','DOOR','DOOR'/  
 &OBST ID='Obstruction', XB=-0.7,18.5,19.6,19.7,5.6,5.8, COLOR='GRAY 80', SURF\_ID='CONCRETE\_WALLS'/  
 &OBST ID='Obstruction', XB=-0.7,18.5,19.6,19.7,5.2,5.4, COLOR='GRAY 80', SURF\_ID='CONCRETE\_WALLS'/  
 &OBST ID='Balcony door', XB=12.7,13.6,18.4,18.5,5.6,7.6, SURF\_ID='DOUBLE GLAZING'/  
 &OBST ID='Bulkhead', XB=12.7,13.6,12.3,12.4,7.6,8.2, COLOR='GRAY 80', SURF\_ID='CONCRETE\_WALLS'/  
 &OBST ID='Bulkhead2', XB=12.6,12.7,12.7,13.5,7.6,8.2, COLOR='GRAY 80', SURF\_ID='CONCRETE\_WALLS'/  
 &OBST ID='Door 2.19-Hallway', XB=12.7,13.6,12.3,12.4,5.6,7.6, SURF\_ID='DOOR'/  
 &OBST ID='Door barchroom', XB=12.6,12.7,12.7,13.5,5.6,7.6, SURF\_ID='DOOR'/  
 &OBST ID='Innerwall 5', XB=13.6,14.5,12.3,12.4,5.6,8.2, COLOR='GRAY 80', SURF\_ID='CONCRETE\_WALLS'/  
 &OBST ID='Innerwall1', XB=10.7,10.9,12.2,19.5,5.6,8.2, COLOR='GRAY 80', SURF\_ID='CONCRETE\_WALLS'/  
 &OBST ID='Innerwall2', XB=14.5,14.7,12.2,19.5,5.6,8.2, COLOR='GRAY 80', SURF\_ID='CONCRETE\_WALLS'/  
 &OBST ID='Innerwall3', XB=10.9,14.5,14.0,14.1,5.6,8.2, COLOR='GRAY 80', SURF\_ID='CONCRETE\_WALLS'/  
 &OBST ID='Innerwall6', XB=12.6,12.7,13.5,14.0,5.6,8.2, COLOR='GRAY 80', SURF\_ID='CONCRETE\_WALLS'/  
 &OBST ID='Overhead2', XB=12.7,13.6,18.4,18.5,7.6,8.2, SURF\_ID='DOUBLE GLAZING'/  
 &OBST ID='Parapet1', XB=10.9,12.7,18.4,18.5,5.6,6.3, COLOR='GRAY 80', SURF\_ID='CONCRETE\_WALLS'/  
 &OBST ID='Parapet2', XB=13.6,14.5,18.4,18.5,5.6,6.3, COLOR='GRAY 80', SURF\_ID='CONCRETE\_WALLS'/  
 &OBST ID='Window backside', XB=10.9,12.7,18.4,18.5,6.3,8.2, SURF\_ID='DOUBLE GLAZING'/  
 &OBST ID='Window backside 2', XB=13.6,14.5,18.4,18.5,6.3,8.2, SURF\_ID='DOUBLE GLAZING'/  
 &OBST ID='Balcony door', XB=8.9,9.8,18.4,18.5,5.6,7.6, SURF\_ID='DOUBLE GLAZING'/  
 &OBST ID='Bulkhead', XB=8.9,9.8,12.3,12.4,7.6,8.2, COLOR='GRAY 80', SURF\_ID='CONCRETE\_WALLS'/  
 &OBST ID='Bulkhead2', XB=8.8,8.9,12.7,13.5,7.6,8.2, COLOR='GRAY 80', SURF\_ID='CONCRETE\_WALLS'/  
 &OBST ID='Door 2.20-Hallway', XB=8.9,9.8,12.3,12.4,5.6,7.6, SURF\_ID='DOOR'/  
 &OBST ID='Door barchroom', XB=8.8,8.9,12.7,13.5,5.6,7.6, SURF\_ID='DOOR'/  
 &OBST ID='Innerwall 5', XB=9.8,10.7,12.3,12.4,5.6,8.2, COLOR='GRAY 80', SURF\_ID='CONCRETE\_WALLS'/  
 &OBST ID='Innerwall1', XB=6.9,7.1,12.2,19.5,5.6,8.2, COLOR='GRAY 80', SURF\_ID='CONCRETE\_WALLS'/  
 &OBST ID='Innerwall3', XB=7.1,10.7,14.0,14.1,5.6,8.2, COLOR='GRAY 80', SURF\_ID='CONCRETE\_WALLS'/  
 &OBST ID='Innerwall6', XB=8.8,8.9,13.5,14.0,5.6,8.2, COLOR='GRAY 80', SURF\_ID='CONCRETE\_WALLS'/  
 &OBST ID='Overhead2', XB=8.9,9.8,18.4,18.5,7.6,8.2, SURF\_ID='DOUBLE GLAZING'/  
 &OBST ID='Parapet1', XB=7.1,8.9,18.4,18.5,5.6,6.3, COLOR='GRAY 80', SURF\_ID='CONCRETE\_WALLS'/  
 &OBST ID='Parapet2', XB=9.8,10.7,18.4,18.5,5.6,6.3, COLOR='GRAY 80', SURF\_ID='CONCRETE\_WALLS'/  
 &OBST ID='Window backside', XB=7.1,8.9,18.4,18.5,6.3,8.2, SURF\_ID='DOUBLE GLAZING'/  
 &OBST ID='Window backside 2', XB=9.8,10.7,18.4,18.5,6.3,8.2, SURF\_ID='DOUBLE GLAZING'/  
 &OBST ID='Balcony door', XB=5.1,6.0,18.4,18.5,5.6,7.6, SURF\_ID='DOUBLE GLAZING'/  
 &OBST ID='Bulkhead', XB=5.1,6.0,12.3,12.4,7.6,8.2, COLOR='GRAY 80', SURF\_ID='CONCRETE\_WALLS'/  
 &OBST ID='Bulkhead2', XB=5.0,5.1,12.7,13.5,7.6,8.2, COLOR='GRAY 80', SURF\_ID='CONCRETE\_WALLS'/  
 &OBST ID='Door 2.21-Hallway', XB=5.1,6.0,12.3,12.4,5.6,7.6, SURF\_ID='DOOR'/  
 &OBST ID='Door barchroom', XB=5.0,5.1,12.7,13.5,5.6,7.6, SURF\_ID='DOOR'/  
 &OBST ID='Innerwall 5', XB=6.0,6.9,12.3,12.4,5.6,8.2, COLOR='GRAY 80', SURF\_ID='CONCRETE\_WALLS'/  
 &OBST ID='Innerwall1', XB=3.1,3.3,12.2,19.5,5.6,8.2, COLOR='GRAY 80', SURF\_ID='CONCRETE\_WALLS'/  
 &OBST ID='Innerwall3', XB=3.3,6.9,14.0,14.1,5.6,8.2, COLOR='GRAY 80', SURF\_ID='CONCRETE\_WALLS'/  
 &OBST ID='Innerwall6', XB=5.0,5.1,13.5,14.0,5.6,8.2, COLOR='GRAY 80', SURF\_ID='CONCRETE\_WALLS'/  
 &OBST ID='Overhead2', XB=5.1,6.0,18.4,18.5,7.6,8.2, SURF\_ID='DOUBLE GLAZING'/  
 &OBST ID='Parapet1', XB=3.3,5.1,18.4,18.5,5.6,6.3, COLOR='GRAY 80', SURF\_ID='CONCRETE\_WALLS'/  
 &OBST ID='Parapet2', XB=6.0,6.9,18.4,18.5,5.6,6.3, COLOR='GRAY 80', SURF\_ID='CONCRETE\_WALLS'/  
 &OBST ID='Window backside', XB=3.3,5.1,18.4,18.5,6.3,8.2, SURF\_ID='DOUBLE GLAZING'/  
 &OBST ID='Window backside 2', XB=6.0,6.9,18.4,18.5,6.3,8.2, SURF\_ID='DOUBLE GLAZING'/  
 &OBST ID='Balcony door', XB=1.3,2.2,18.4,18.5,5.6,7.6, SURF\_ID='DOUBLE GLAZING'/  
 &OBST ID='Bulkhead', XB=1.3,2.2,12.3,12.4,7.6,8.2, COLOR='GRAY 80', SURF\_ID='CONCRETE\_WALLS'/  
 &OBST ID='Bulkhead2', XB=1.2,1.3,12.7,13.5,7.6,8.2, COLOR='GRAY 80', SURF\_ID='CONCRETE\_WALLS'/  
 &OBST ID='Door 2.21-Hallway', XB=1.3,2.2,12.3,12.4,5.6,7.6, SURF\_ID='DOOR'/  
 &OBST ID='Door barchroom', XB=1.2,1.3,12.7,13.5,5.6,7.6, SURF\_ID='DOOR'/  
 &OBST ID='Innerwall 5', XB=2.2,3.1,12.3,12.4,5.6,8.2, COLOR='GRAY 80', SURF\_ID='CONCRETE\_WALLS'/  
 &OBST ID='Innerwall1', XB=-0.7,-0.5,12.2,19.5,5.6,8.2, COLOR='GRAY 80', SURF\_ID='CONCRETE\_WALLS'/  
 &OBST ID='Innerwall3', XB=-0.5,3.1,14.0,14.1,5.6,8.2, COLOR='GRAY 80', SURF\_ID='CONCRETE\_WALLS'/  
 &OBST ID='Innerwall6', XB=1.2,1.3,13.5,14.0,5.6,8.2, COLOR='GRAY 80', SURF\_ID='CONCRETE\_WALLS'/  
 &OBST ID='Overhead2', XB=1.3,2.2,18.4,18.5,7.6,8.2, SURF\_ID='DOUBLE GLAZING'/  
 &OBST ID='Parapet1', XB=-0.5,1.3,18.4,18.5,5.6,6.3, COLOR='GRAY 80', SURF\_ID='CONCRETE\_WALLS'/  
 &OBST ID='Parapet2', XB=2.2,3.1,18.4,18.5,5.6,6.3, COLOR='GRAY 80', SURF\_ID='CONCRETE\_WALLS'/  
 &OBST ID='Window backside', XB=-0.5,1.3,18.4,18.5,6.3,8.2, SURF\_ID='DOUBLE GLAZING'/  
 &OBST ID='Window backside 2', XB=2.2,3.1,18.4,18.5,6.3,8.2, SURF\_ID='DOUBLE GLAZING'/  
 &OBST ID='Balcony door', XB=16.5,17.4,18.4,18.5,5.6,7.6, SURF\_ID='DOUBLE GLAZING'/  
 &OBST ID='Bulkhead', XB=16.5,17.4,12.3,12.4,7.6,8.2, COLOR='GRAY 80', SURF\_ID='CONCRETE\_WALLS'/  
 &OBST ID='Bulkhead2', XB=16.4,16.5,12.7,13.5,7.6,8.2, COLOR='GRAY 80', SURF\_ID='CONCRETE\_WALLS'/  
 &OBST ID='Door 2.18-Hallway', XB=16.5,17.4,12.3,12.4,5.6,7.6, SURF\_ID='DOOR'/  
 &OBST ID='Door barchroom', XB=16.4,16.5,12.7,13.5,5.6,7.6, SURF\_ID='DOOR'/

&OBST ID='Innerwall 5', XB=17.4,18.3,12.3,12.4,5.6,8.2, COLOR='GRAY 80', SURF\_ID='CONCRETE\_WALLS'/  
 &OBST ID='Innerwall1', XB=14.5,14.7,12.2,19.5,5.6,8.2, COLOR='GRAY 80', SURF\_ID='CONCRETE\_WALLS'/  
 &OBST ID='Innerwall2', XB=18.3,18.5,12.2,19.5,5.6,8.2, COLOR='GRAY 80', SURF\_ID='CONCRETE\_WALLS'/  
 &OBST ID='Innerwall3', XB=14.7,18.3,14.0,14.1,5.6,8.2, COLOR='GRAY 80', SURF\_ID='CONCRETE\_WALLS'/  
 &OBST ID='Innerwall6', XB=16.4,16.5,13.5,14.0,5.6,8.2, COLOR='GRAY 80', SURF\_ID='CONCRETE\_WALLS'/  
 &OBST ID='Overhead2', XB=16.5,17.4,18.4,18.5,7.6,8.2, SURF\_ID='DOUBLE GLAZING'/  
 &OBST ID='Parapet1', XB=14.7,16.5,18.4,18.5,5.6,6.3, COLOR='GRAY 80', SURF\_ID='CONCRETE\_WALLS'/  
 &OBST ID='Parapet2', XB=17.4,18.3,18.4,18.5,5.6,6.3, COLOR='GRAY 80', SURF\_ID='CONCRETE\_WALLS'/  
 &OBST ID='Window backside', XB=14.7,16.5,18.4,18.5,6.3,8.2, SURF\_ID='DOUBLE GLAZING'/  
 &OBST ID='Window backside 2', XB=17.4,18.3,18.4,18.5,6.3,8.2, SURF\_ID='DOUBLE GLAZING'/  
 &OBST ID='Bulkhead', XB=12.7,13.6,10.3,10.4,7.6,8.2, COLOR='GRAY 80', SURF\_ID='CONCRETE\_WALLS'/  
 &OBST ID='Bulkhead2', XB=12.6,12.7,9.2,10.0,7.6,8.2, COLOR='GRAY 80', SURF\_ID='CONCRETE\_WALLS'/  
 &OBST ID='Door 2.26-Hallway', XB=12.7,13.6,10.3,10.4,5.6,7.6, SURF\_ID='DOOR'/  
 &OBST ID='Door barchroom', XB=12.6,12.7,9.2,10.0,5.6,7.6, SURF\_ID='DOOR'/  
 &OBST ID='Innerwall 5', XB=13.6,14.5,10.3,10.4,5.6,8.2, COLOR='GRAY 80', SURF\_ID='CONCRETE\_WALLS'/  
 &OBST ID='Innerwall1', XB=10.7,10.9,4.0,10.5,5.6,8.2, COLOR='GRAY 80', SURF\_ID='CONCRETE\_WALLS'/  
 &OBST ID='Innerwall2', XB=14.5,14.7,4.0,10.5,5.6,8.2, COLOR='GRAY 80', SURF\_ID='CONCRETE\_WALLS'/  
 &OBST ID='Innerwall3', XB=10.9,14.5,8.6,8.7,5.6,8.2, COLOR='GRAY 80', SURF\_ID='CONCRETE\_WALLS'/  
 &OBST ID='Innerwall6', XB=12.6,12.7,8.7,9.2,5.6,8.2, COLOR='GRAY 80', SURF\_ID='CONCRETE\_WALLS'/  
 &OBST ID='Parapet1', XB=10.9,14.5,4.2,4.3,5.6,6.3, COLOR='GRAY 80', SURF\_ID='CONCRETE\_WALLS'/  
 &OBST ID='Window backside', XB=10.9,14.5,4.2,4.3,6.3,8.2, SURF\_ID='DOUBLE GLAZING'/  
 &OBST ID='Bulkhead', XB=16.3,17.2,10.3,10.4,7.6,8.2, COLOR='GRAY 80', SURF\_ID='CONCRETE\_WALLS'/  
 &OBST ID='Bulkhead2', XB=16.2,16.3,9.2,10.0,7.6,8.2, COLOR='GRAY 80', SURF\_ID='CONCRETE\_WALLS'/  
 &OBST ID='Door 2.28-Hallway', XB=16.3,17.2,10.3,10.4,5.6,7.6, SURF\_ID='DOOR'/  
 &OBST ID='Door barchroom', XB=16.2,16.3,9.2,10.0,5.6,7.6, SURF\_ID='DOOR'/  
 &OBST ID='Innerwall 5', XB=17.2,18.3,10.3,10.4,5.6,8.2, COLOR='GRAY 80', SURF\_ID='CONCRETE\_WALLS'/  
 &OBST ID='Innerwall1', XB=14.5,14.7,4.0,10.5,5.6,8.2, COLOR='GRAY 80', SURF\_ID='CONCRETE\_WALLS'/  
 &OBST ID='Innerwall2', XB=18.3,18.5,4.0,10.5,5.6,8.2, COLOR='GRAY 80', SURF\_ID='CONCRETE\_WALLS'/  
 &OBST ID='Innerwall3', XB=14.7,18.3,8.6,8.7,5.6,8.2, COLOR='GRAY 80', SURF\_ID='CONCRETE\_WALLS'/  
 &OBST ID='Innerwall6', XB=16.2,16.3,8.7,9.2,5.6,8.2, COLOR='GRAY 80', SURF\_ID='CONCRETE\_WALLS'/  
 &OBST ID='Parapet1', XB=14.7,18.3,4.2,4.3,5.6,6.3, COLOR='GRAY 80', SURF\_ID='CONCRETE\_WALLS'/  
 &OBST ID='Window backside', XB=14.7,18.3,4.2,4.3,6.3,8.2, SURF\_ID='DOUBLE GLAZING'/  
 &OBST ID='Bulkhead', XB=8.9,9.8,10.3,10.4,7.6,8.2, COLOR='GRAY 80', SURF\_ID='CONCRETE\_WALLS'/  
 &OBST ID='Bulkhead2', XB=8.8,8.9,9.2,10.0,7.6,8.2, COLOR='GRAY 80', SURF\_ID='CONCRETE\_WALLS'/  
 &OBST ID='Door 2.25-Hallway', XB=8.9,9.8,10.3,10.4,5.6,7.6, SURF\_ID='DOOR'/  
 &OBST ID='Door barchroom', XB=8.8,8.9,9.2,10.0,5.6,7.6, SURF\_ID='DOOR'/  
 &OBST ID='Innerwall 5', XB=9.8,10.7,10.3,10.4,5.6,8.2, COLOR='GRAY 80', SURF\_ID='CONCRETE\_WALLS'/  
 &OBST ID='Innerwall1', XB=6.9,7.1,4.0,10.5,5.6,8.2, COLOR='GRAY 80', SURF\_ID='CONCRETE\_WALLS'/  
 &OBST ID='Innerwall3', XB=7.1,10.7,8.6,8.7,5.6,8.2, COLOR='GRAY 80', SURF\_ID='CONCRETE\_WALLS'/  
 &OBST ID='Innerwall6', XB=8.8,8.9,8.7,9.2,5.6,8.2, COLOR='GRAY 80', SURF\_ID='CONCRETE\_WALLS'/  
 &OBST ID='Parapet1', XB=7.1,10.7,4.2,4.3,5.6,6.3, COLOR='GRAY 80', SURF\_ID='CONCRETE\_WALLS'/  
 &OBST ID='Window backside', XB=7.1,10.7,4.2,4.3,6.3,8.2, SURF\_ID='DOUBLE GLAZING'/  
 &OBST ID='Bulkhead', XB=5.1,6.0,10.3,10.4,7.6,8.2, COLOR='GRAY 80', SURF\_ID='CONCRETE\_WALLS'/  
 &OBST ID='Bulkhead2', XB=5.0,5.1,9.2,10.0,7.6,8.2, COLOR='GRAY 80', SURF\_ID='CONCRETE\_WALLS'/  
 &OBST ID='Door 2.24-Hallway', XB=5.1,6.0,10.3,10.4,5.6,7.6, SURF\_ID='DOOR'/  
 &OBST ID='Door barchroom', XB=5.0,5.1,9.2,10.0,5.6,7.6, SURF\_ID='DOOR'/  
 &OBST ID='Innerwall 5', XB=6.0,6.9,10.3,10.4,5.6,8.2, COLOR='GRAY 80', SURF\_ID='CONCRETE\_WALLS'/  
 &OBST ID='Innerwall1', XB=3.1,3.3,4.0,10.5,5.6,8.2, COLOR='GRAY 80', SURF\_ID='CONCRETE\_WALLS'/  
 &OBST ID='Innerwall3', XB=3.3,6.9,8.6,8.7,5.6,8.2, COLOR='GRAY 80', SURF\_ID='CONCRETE\_WALLS'/  
 &OBST ID='Innerwall6', XB=5.0,5.1,8.7,9.2,5.6,8.2, COLOR='GRAY 80', SURF\_ID='CONCRETE\_WALLS'/  
 &OBST ID='Parapet1', XB=3.3,6.9,4.2,4.3,5.6,6.3, COLOR='GRAY 80', SURF\_ID='CONCRETE\_WALLS'/  
 &OBST ID='Window backside', XB=3.3,6.9,4.2,4.3,6.3,8.2, SURF\_ID='DOUBLE GLAZING'/  
 &OBST ID='Bulkhead', XB=1.3,2.2,10.3,10.4,7.6,8.2, COLOR='GRAY 80', SURF\_ID='CONCRETE\_WALLS'/  
 &OBST ID='Bulkhead2', XB=1.2,1.3,9.2,10.0,7.6,8.2, COLOR='GRAY 80', SURF\_ID='CONCRETE\_WALLS'/  
 &OBST ID='Door 2.23-Hallway', XB=1.3,2.2,10.3,10.4,5.6,7.6, SURF\_ID='DOOR'/  
 &OBST ID='Door barchroom', XB=1.2,1.3,9.2,10.0,5.6,7.6, SURF\_ID='DOOR'/  
 &OBST ID='Innerwall 5', XB=2.2,3.1,10.3,10.4,5.6,8.2, COLOR='GRAY 80', SURF\_ID='CONCRETE\_WALLS'/  
 &OBST ID='Innerwall1', XB=-0.7,-0.5,4.0,10.5,5.6,8.2, COLOR='GRAY 80', SURF\_ID='CONCRETE\_WALLS'/  
 &OBST ID='Innerwall3', XB=-0.5,3.1,8.6,8.7,5.6,8.2, COLOR='GRAY 80', SURF\_ID='CONCRETE\_WALLS'/  
 &OBST ID='Innerwall6', XB=1.2,1.3,8.7,9.2,5.6,8.2, COLOR='GRAY 80', SURF\_ID='CONCRETE\_WALLS'/  
 &OBST ID='Parapet1', XB=-0.5,3.1,4.2,4.3,5.6,6.3, COLOR='GRAY 80', SURF\_ID='CONCRETE\_WALLS'/  
 &OBST ID='Window backside', XB=-0.5,3.1,4.2,4.3,6.3,8.2, SURF\_ID='DOUBLE GLAZING'/  
 &OBST ID='Hallway double door left', XB=-0.7,-0.6,10.5,12.2,5.6,7.6, SURF\_ID6='Double door','Double door','DOOR','DOOR','DOOR','DOOR'/  
 &OBST ID='Hallway bulkhead left', XB=-0.7,-0.6,10.5,12.2,7.6,8.2, COLOR='GRAY 80', SURF\_ID='CONCRETE\_WALLS'/  
 &OBST ID='Hallway bulkhead right', XB=18.4,18.5,10.5,12.2,7.6,8.2, COLOR='GRAY 80', SURF\_ID='CONCRETE\_WALLS'/







&OBST ID='Floor slab 2nd', XB=10.6,12.6,9.8,11.35,5.4,5.6, COLOR='GRAY 80', SURF\_ID='CONCRETE\_FLOORS'/  
 &OBST ID='Floor slab 2nd', XB=12.6,14.6,9.8,11.35,5.4,5.6, COLOR='GRAY 80', SURF\_ID='CONCRETE\_FLOORS'/  
 &OBST ID='Floor slab 2nd', XB=14.6,16.6,9.8,11.35,5.4,5.6, COLOR='GRAY 80', SURF\_ID='CONCRETE\_FLOORS'/  
 &OBST ID='Floor slab 2nd', XB=16.6,18.5,9.8,11.35,5.4,5.6, COLOR='GRAY 80', SURF\_ID='CONCRETE\_FLOORS'/  
 &OBST ID='Floor slab 2nd', XB=0.7,0.6,11.35,12.9,5.4,5.6, COLOR='GRAY 80', SURF\_ID='CONCRETE\_FLOORS'/  
 &OBST ID='Floor slab 2nd', XB=0.6,2.6,11.35,12.9,5.4,5.6, COLOR='GRAY 80', SURF\_ID='CONCRETE\_FLOORS'/  
 &OBST ID='Floor slab 2nd', XB=2.6,4.6,11.35,12.9,5.4,5.6, COLOR='GRAY 80', SURF\_ID='CONCRETE\_FLOORS'/  
 &OBST ID='Floor slab 2nd', XB=4.6,6.6,11.35,12.9,5.4,5.6, COLOR='GRAY 80', SURF\_ID='CONCRETE\_FLOORS'/  
 &OBST ID='Floor slab 2nd', XB=6.6,8.6,11.35,12.9,5.4,5.6, COLOR='GRAY 80', SURF\_ID='CONCRETE\_FLOORS'/  
 &OBST ID='Floor slab 2nd', XB=8.6,10.6,11.35,12.9,5.4,5.6, COLOR='GRAY 80', SURF\_ID='CONCRETE\_FLOORS'/  
 &OBST ID='Floor slab 2nd', XB=10.6,12.6,11.35,12.9,5.4,5.6, COLOR='GRAY 80', SURF\_ID='CONCRETE\_FLOORS'/  
 &OBST ID='Floor slab 2nd', XB=12.6,14.6,11.35,12.9,5.4,5.6, COLOR='GRAY 80', SURF\_ID='CONCRETE\_FLOORS'/  
 &OBST ID='Floor slab 2nd', XB=14.6,16.6,11.35,12.9,5.4,5.6, COLOR='GRAY 80', SURF\_ID='CONCRETE\_FLOORS'/  
 &OBST ID='Floor slab 2nd', XB=16.6,18.5,11.35,12.9,5.4,5.6, COLOR='GRAY 80', SURF\_ID='CONCRETE\_FLOORS'/  
 &OBST ID='Floor slab 2nd', XB=3.0,5.3,12.9,14.4,5.4,5.6, COLOR='GRAY 80', SURF\_ID='CONCRETE\_FLOORS'/  
 &OBST ID='Floor slab 2nd', XB=3.0,5.3,14.4,15.9,5.4,5.6, COLOR='GRAY 80', SURF\_ID='CONCRETE\_FLOORS'/  
 &OBST ID='Floor slab 2nd', XB=3.0,5.3,15.9,17.4,5.4,5.6, COLOR='GRAY 80', SURF\_ID='CONCRETE\_FLOORS'/  
 &OBST ID='Floor slab 2nd', XB=3.0,5.3,17.4,18.9,5.4,5.6, COLOR='GRAY 80', SURF\_ID='CONCRETE\_FLOORS'/  
 &OBST ID='Floor slab 2nd', XB=5.3,7.7,12.9,14.4,5.4,5.6, COLOR='GRAY 80', SURF\_ID='CONCRETE\_FLOORS'/  
 &OBST ID='Floor slab 2nd', XB=5.3,7.7,14.4,15.9,5.4,5.6, COLOR='GRAY 80', SURF\_ID='CONCRETE\_FLOORS'/  
 &OBST ID='Floor slab 2nd', XB=5.3,7.7,15.9,17.4,5.4,5.6, COLOR='GRAY 80', SURF\_ID='CONCRETE\_FLOORS'/  
 &OBST ID='Floor slab 2nd', XB=5.3,7.7,17.4,18.9,5.4,5.6, COLOR='GRAY 80', SURF\_ID='CONCRETE\_FLOORS'/  
 &OBST ID='Floor slab 2nd', XB=3.0,7.7,18.9,19.7,5.4,5.6, COLOR='GRAY 80', SURF\_ID='CONCRETE\_FLOORS'/

&HOLE ID='DOOR LIVING-KITCHEN', XB=13.0,14.5,13.9,14.2,2.8,4.8/  
 &HOLE ID='DOOR LIVING-KITCHEN', XB=9.2,10.7,13.9,14.2,2.8,4.8/  
 &HOLE ID='Overhead', XB=9.2,10.7,13.9,14.2,4.9,5.2/  
 &HOLE ID='DOOR LIVING-KITCHEN', XB=5.4,6.9,13.9,14.2,2.8,4.8/  
 &HOLE ID='Overhead', XB=5.4,6.9,13.9,14.2,4.9,5.2/  
 &HOLE ID='DOOR LIVING-KITCHEN', XB=1.6,3.1,13.9,14.2,2.8,4.8/  
 &HOLE ID='Overhead', XB=1.6,3.1,13.9,14.2,4.9,5.2/  
 &HOLE ID='DOOR LIVING-KITCHEN', XB=16.8,18.3,13.9,14.2,2.8,4.8/  
 &HOLE ID='Overhead', XB=16.8,18.3,13.9,14.2,4.9,5.2/  
 &HOLE ID='Overhead', XB=13.0,14.5,13.9,14.2,4.9,5.3/  
 &HOLE ID='DOOR LIVING-KITCHEN', XB=13.0,14.5,8.5,8.8,2.8,4.8/  
 &HOLE ID='Overhead', XB=13.0,14.5,8.5,8.8,4.8,5.3/  
 &HOLE ID='DOOR LIVING-KITCHEN', XB=16.8,18.3,8.5,8.8,2.8,4.8/  
 &HOLE ID='Overhead', XB=16.8,18.3,8.5,8.8,4.9,5.2/  
 &HOLE ID='DOOR LIVING-KITCHEN', XB=9.2,10.7,8.5,8.8,2.8,4.8/  
 &HOLE ID='Overhead', XB=9.2,10.7,8.5,8.8,4.9,5.2/  
 &HOLE ID='DOOR LIVING-KITCHEN', XB=5.4,6.9,8.5,8.8,2.8,4.8/  
 &HOLE ID='Overhead', XB=5.4,6.9,8.5,8.8,4.9,5.2/  
 &HOLE ID='DOOR LIVING-KITCHEN', XB=1.6,3.1,8.5,8.8,2.8,4.8/  
 &HOLE ID='Overhead', XB=1.6,3.1,8.5,8.8,4.9,5.2/  
 &HOLE ID='DOOR LIVING-KITCHEN', XB=13.0,14.5,13.9,14.2,5.6,7.6/  
 &HOLE ID='Overhead', XB=13.0,14.5,13.9,14.2,7.7,8.0/  
 &HOLE ID='DOOR LIVING-KITCHEN', XB=9.2,10.7,13.9,14.2,5.6,7.6/  
 &HOLE ID='Overhead', XB=9.2,10.7,13.9,14.2,7.7,8.0/  
 &HOLE ID='DOOR LIVING-KITCHEN', XB=5.4,6.9,13.9,14.2,5.6,7.6/  
 &HOLE ID='Overhead', XB=5.4,6.9,13.9,14.2,7.7,8.0/  
 &HOLE ID='DOOR LIVING-KITCHEN', XB=1.6,3.1,13.9,14.2,5.6,7.6/  
 &HOLE ID='Overhead', XB=1.6,3.1,13.9,14.2,7.7,8.0/  
 &HOLE ID='DOOR LIVING-KITCHEN', XB=16.8,18.3,13.9,14.2,5.6,7.6/  
 &HOLE ID='Overhead', XB=16.8,18.3,13.9,14.2,7.7,8.0/  
 &HOLE ID='DOOR LIVING-KITCHEN', XB=13.0,14.5,8.5,8.8,5.6,7.6/  
 &HOLE ID='Overhead', XB=13.0,14.5,8.5,8.8,7.7,8.0/  
 &HOLE ID='DOOR LIVING-KITCHEN', XB=16.8,18.3,8.5,8.8,5.6,7.6/  
 &HOLE ID='Overhead', XB=16.8,18.3,8.5,8.8,7.7,8.0/  
 &HOLE ID='DOOR LIVING-KITCHEN', XB=9.2,10.7,8.5,8.8,5.6,7.6/  
 &HOLE ID='Overhead', XB=9.2,10.7,8.5,8.8,7.7,8.0/  
 &HOLE ID='DOOR LIVING-KITCHEN', XB=5.4,6.9,8.5,8.8,5.6,7.6/  
 &HOLE ID='Overhead', XB=5.4,6.9,8.5,8.8,7.7,8.0/  
 &HOLE ID='DOOR LIVING-KITCHEN', XB=1.6,3.1,8.5,8.8,5.6,7.6/  
 &HOLE ID='Overhead', XB=1.6,3.1,8.5,8.8,7.7,8.0/

&VENT ID='Mesh Vent: MESH00 [XMAX]', SURF\_ID='OPEN', XB=11.2,11.2,8.4,9.8,2.6,5.8/

&VENT ID='Mesh Vent: MESH00 [XMIN]', SURF\_ID='OPEN', XB=6.6,6.6,8.4,9.8,2.6,5.8/  
 &VENT ID='Mesh Vent: MESH00 [ZMAX]', SURF\_ID='OPEN', XB=6.6,11.2,8.4,9.8,5.8,5.8/  
 &VENT ID='Mesh Vent: MESH00 [ZMIN]', SURF\_ID='OPEN', XB=6.6,11.2,8.4,9.8,2.6,2.6/  
 &VENT ID='Mesh Vent: MESH00 [XMAX]', SURF\_ID='OPEN', XB=11.2,11.2,3.8,8.4,2.6,5.8/  
 &VENT ID='Mesh Vent: MESH01 [XMIN]', SURF\_ID='OPEN', XB=6.6,6.6,3.8,8.4,2.6,5.8/  
 &VENT ID='Mesh Vent: MESH01 [YMIN]', SURF\_ID='OPEN', XB=6.6,11.2,3.8,3.8,2.6,5.8/  
 &VENT ID='Mesh Vent: MESH01 [ZMAX]', SURF\_ID='OPEN', XB=6.6,11.2,3.8,8.4,5.8,5.8/  
 &VENT ID='Mesh Vent: MESH01 [ZMIN]', SURF\_ID='OPEN', XB=6.6,11.2,3.8,8.4,2.6,2.6/  
 &VENT ID='Mesh Vent: MESH02 [XMIN]', SURF\_ID='OPEN', XB=-1.4,-1.4,9.8,11.35,2.6,5.8/  
 &VENT ID='Mesh Vent: MESH02 [YMIN]', SURF\_ID='OPEN', XB=-1.4,0.6,9.8,9.8,2.6,5.8/  
 &VENT ID='Mesh Vent: MESH02 [ZMAX]', SURF\_ID='OPEN', XB=-1.4,0.6,9.8,11.35,5.8,5.8/  
 &VENT ID='Mesh Vent: MESH02 [ZMIN]', SURF\_ID='OPEN', XB=-1.4,0.6,9.8,11.35,2.6,2.6/  
 &VENT ID='Mesh Vent: MESH03 [YMIN]', SURF\_ID='OPEN', XB=0.6,2.6,9.8,9.8,2.6,5.8/  
 &VENT ID='Mesh Vent: MESH03 [ZMAX]', SURF\_ID='OPEN', XB=0.6,2.6,9.8,11.35,5.8,5.8/  
 &VENT ID='Mesh Vent: MESH03 [ZMIN]', SURF\_ID='OPEN', XB=0.6,2.6,9.8,11.35,2.6,2.6/  
 &VENT ID='Mesh Vent: MESH04 [YMIN]', SURF\_ID='OPEN', XB=2.6,4.6,9.8,9.8,2.6,5.8/  
 &VENT ID='Mesh Vent: MESH04 [ZMAX]', SURF\_ID='OPEN', XB=2.6,4.6,9.8,11.35,5.8,5.8/  
 &VENT ID='Mesh Vent: MESH04 [ZMIN]', SURF\_ID='OPEN', XB=2.6,4.6,9.8,11.35,2.6,2.6/  
 &VENT ID='Mesh Vent: MESH05 [YMIN]', SURF\_ID='OPEN', XB=4.6,6.6,9.8,9.8,2.6,5.8/  
 &VENT ID='Mesh Vent: MESH05 [ZMAX]', SURF\_ID='OPEN', XB=4.6,6.6,9.8,11.35,5.8,5.8/  
 &VENT ID='Mesh Vent: MESH05 [ZMIN]', SURF\_ID='OPEN', XB=4.6,6.6,9.8,11.35,2.6,2.6/  
 &VENT ID='Mesh Vent: MESH06 [ZMAX]', SURF\_ID='OPEN', XB=6.6,8.6,9.8,11.35,5.8,5.8/  
 &VENT ID='Mesh Vent: MESH06 [ZMIN]', SURF\_ID='OPEN', XB=6.6,8.6,9.8,11.35,2.6,2.6/  
 &VENT ID='Mesh Vent: MESH07 [ZMAX]', SURF\_ID='OPEN', XB=8.6,10.6,9.8,11.35,5.8,5.8/  
 &VENT ID='Mesh Vent: MESH07 [ZMIN]', SURF\_ID='OPEN', XB=8.6,10.6,9.8,11.35,2.6,2.6/  
 &VENT ID='Mesh Vent: MESH08 [YMIN]', SURF\_ID='OPEN', XB=11.2,12.6,9.8,9.8,2.6,5.8/  
 &VENT ID='Mesh Vent: MESH08 [ZMAX]', SURF\_ID='OPEN', XB=10.6,12.6,9.8,11.35,5.8,5.8/  
 &VENT ID='Mesh Vent: MESH08 [ZMIN]', SURF\_ID='OPEN', XB=10.6,12.6,9.8,11.35,2.6,2.6/  
 &VENT ID='Mesh Vent: MESH09 [YMIN]', SURF\_ID='OPEN', XB=12.6,14.6,9.8,9.8,2.6,5.8/  
 &VENT ID='Mesh Vent: MESH09 [ZMAX]', SURF\_ID='OPEN', XB=12.6,14.6,9.8,11.35,5.8,5.8/  
 &VENT ID='Mesh Vent: MESH09 [ZMIN]', SURF\_ID='OPEN', XB=12.6,14.6,9.8,11.35,2.6,2.6/  
 &VENT ID='Mesh Vent: MESH10 [YMIN]', SURF\_ID='OPEN', XB=14.6,16.6,9.8,9.8,2.6,5.8/  
 &VENT ID='Mesh Vent: MESH10 [ZMAX]', SURF\_ID='OPEN', XB=14.6,16.6,9.8,11.35,5.8,5.8/  
 &VENT ID='Mesh Vent: MESH10 [ZMIN]', SURF\_ID='OPEN', XB=14.6,16.6,9.8,11.35,2.6,2.6/  
 &VENT ID='Mesh Vent: MESH11 [XMAX]', SURF\_ID='OPEN', XB=18.9,18.9,9.8,11.35,2.6,5.8/  
 &VENT ID='Mesh Vent: MESH11 [YMIN]', SURF\_ID='OPEN', XB=16.6,18.9,9.8,9.8,2.6,5.8/  
 &VENT ID='Mesh Vent: MESH11 [ZMAX]', SURF\_ID='OPEN', XB=16.6,18.9,9.8,11.35,5.8,5.8/  
 &VENT ID='Mesh Vent: MESH11 [ZMIN]', SURF\_ID='OPEN', XB=16.6,18.9,9.8,11.35,2.6,2.6/  
 &VENT ID='Mesh Vent: MESH12 [XMIN]', SURF\_ID='OPEN', XB=-1.4,-1.4,11.35,12.9,2.6,5.8/  
 &VENT ID='Mesh Vent: MESH12 [YMAX]', SURF\_ID='OPEN', XB=-1.4,0.6,12.9,12.9,2.6,5.8/  
 &VENT ID='Mesh Vent: MESH12 [ZMAX]', SURF\_ID='OPEN', XB=-1.4,0.6,11.35,12.9,5.8,5.8/  
 &VENT ID='Mesh Vent: MESH12 [ZMIN]', SURF\_ID='OPEN', XB=-1.4,0.6,11.35,12.9,2.6,2.6/  
 &VENT ID='Mesh Vent: MESH13 [YMAX]', SURF\_ID='OPEN', XB=0.6,2.6,12.9,12.9,2.6,5.8/  
 &VENT ID='Mesh Vent: MESH13 [ZMAX]', SURF\_ID='OPEN', XB=0.6,2.6,11.35,12.9,5.8,5.8/  
 &VENT ID='Mesh Vent: MESH13 [ZMIN]', SURF\_ID='OPEN', XB=0.6,2.6,11.35,12.9,2.6,2.6/  
 &VENT ID='Mesh Vent: MESH14 [YMAX]', SURF\_ID='OPEN', XB=2.6,3.0,12.9,12.9,2.6,5.8/  
 &VENT ID='Mesh Vent: MESH14 [ZMAX]', SURF\_ID='OPEN', XB=2.6,4.6,11.35,12.9,5.8,5.8/  
 &VENT ID='Mesh Vent: MESH14 [ZMIN]', SURF\_ID='OPEN', XB=2.6,4.6,11.35,12.9,2.6,2.6/  
 &VENT ID='Mesh Vent: MESH15 [ZMAX]', SURF\_ID='OPEN', XB=4.6,6.6,11.35,12.9,5.8,5.8/  
 &VENT ID='Mesh Vent: MESH15 [ZMIN]', SURF\_ID='OPEN', XB=4.6,6.6,11.35,12.9,2.6,2.6/  
 &VENT ID='Mesh Vent: MESH16 [YMAX]', SURF\_ID='OPEN', XB=7.7,8.6,12.9,12.9,2.6,5.8/  
 &VENT ID='Mesh Vent: MESH16 [ZMAX]', SURF\_ID='OPEN', XB=6.6,8.6,11.35,12.9,5.8,5.8/  
 &VENT ID='Mesh Vent: MESH16 [ZMIN]', SURF\_ID='OPEN', XB=6.6,8.6,11.35,12.9,2.6,2.6/  
 &VENT ID='Mesh Vent: MESH17 [YMAX]', SURF\_ID='OPEN', XB=8.6,10.6,12.9,12.9,2.6,5.8/  
 &VENT ID='Mesh Vent: MESH17 [ZMAX]', SURF\_ID='OPEN', XB=8.6,10.6,11.35,12.9,5.8,5.8/  
 &VENT ID='Mesh Vent: MESH17 [ZMIN]', SURF\_ID='OPEN', XB=8.6,10.6,11.35,12.9,2.6,2.6/  
 &VENT ID='Mesh Vent: MESH18 [YMAX]', SURF\_ID='OPEN', XB=10.6,12.6,12.9,12.9,2.6,5.8/  
 &VENT ID='Mesh Vent: MESH18 [ZMAX]', SURF\_ID='OPEN', XB=10.6,12.6,11.35,12.9,5.8,5.8/  
 &VENT ID='Mesh Vent: MESH18 [ZMIN]', SURF\_ID='OPEN', XB=10.6,12.6,11.35,12.9,2.6,2.6/  
 &VENT ID='Mesh Vent: MESH19 [YMAX]', SURF\_ID='OPEN', XB=12.6,14.6,12.9,12.9,2.6,5.8/  
 &VENT ID='Mesh Vent: MESH19 [ZMAX]', SURF\_ID='OPEN', XB=12.6,14.6,11.35,12.9,5.8,5.8/  
 &VENT ID='Mesh Vent: MESH19 [ZMIN]', SURF\_ID='OPEN', XB=12.6,14.6,11.35,12.9,2.6,2.6/  
 &VENT ID='Mesh Vent: MESH20 [YMAX]', SURF\_ID='OPEN', XB=14.6,16.6,12.9,12.9,2.6,5.8/  
 &VENT ID='Mesh Vent: MESH20 [ZMAX]', SURF\_ID='OPEN', XB=14.6,16.6,11.35,12.9,5.8,5.8/  
 &VENT ID='Mesh Vent: MESH20 [ZMIN]', SURF\_ID='OPEN', XB=14.6,16.6,11.35,12.9,2.6,2.6/  
 &VENT ID='Mesh Vent: MESH21 [XMAX]', SURF\_ID='OPEN', XB=18.9,18.9,11.35,12.9,2.6,5.8/

```

&VENT ID='Mesh Vent: MESH21 [YMAX]', SURF_ID='OPEN', XB=16.6,18.9,12.9,12.9,2.6,5.8/
&VENT ID='Mesh Vent: MESH21 [ZMAX]', SURF_ID='OPEN', XB=16.6,18.9,11.35,12.9,5.8,5.8/
&VENT ID='Mesh Vent: MESH21 [ZMIN]', SURF_ID='OPEN', XB=16.6,18.9,11.35,12.9,2.6,2.6/
&VENT ID='Mesh Vent: MESH22 [XMIN]', SURF_ID='OPEN', XB=3.0,3.0,12.9,14.4,2.6,5.8/
&VENT ID='Mesh Vent: MESH22 [ZMAX]', SURF_ID='OPEN', XB=3.0,5.3,12.9,14.4,5.8,5.8/
&VENT ID='Mesh Vent: MESH22 [ZMIN]', SURF_ID='OPEN', XB=3.0,5.3,12.9,14.4,2.6,2.6/
&VENT ID='Mesh Vent: MESH23 [XMIN]', SURF_ID='OPEN', XB=3.0,3.0,14.4,15.9,2.6,5.8/
&VENT ID='Mesh Vent: MESH23 [ZMAX]', SURF_ID='OPEN', XB=3.0,5.3,14.4,15.9,5.8,5.8/
&VENT ID='Mesh Vent: MESH23 [ZMIN]', SURF_ID='OPEN', XB=3.0,5.3,14.4,15.9,2.6,2.6/
&VENT ID='Mesh Vent: MESH24 [XMIN]', SURF_ID='OPEN', XB=3.0,3.0,15.9,17.4,2.6,5.8/
&VENT ID='Mesh Vent: MESH24 [ZMAX]', SURF_ID='OPEN', XB=3.0,5.3,15.9,17.4,5.8,5.8/
&VENT ID='Mesh Vent: MESH24 [ZMIN]', SURF_ID='OPEN', XB=3.0,5.3,15.9,17.4,2.6,2.6/
&VENT ID='Mesh Vent: MESH25 [XMIN]', SURF_ID='OPEN', XB=3.0,3.0,17.4,18.9,2.6,5.8/
&VENT ID='Mesh Vent: MESH25 [ZMAX]', SURF_ID='OPEN', XB=3.0,5.3,17.4,18.9,5.8,5.8/
&VENT ID='Mesh Vent: MESH25 [ZMIN]', SURF_ID='OPEN', XB=3.0,5.3,17.4,18.9,2.6,2.6/
&VENT ID='Mesh Vent: MESH26 [XMAX]', SURF_ID='OPEN', XB=7.7,7.7,12.9,14.4,2.6,5.8/
&VENT ID='Mesh Vent: MESH26 [ZMAX]', SURF_ID='OPEN', XB=5.3,7.7,12.9,14.4,5.8,5.8/
&VENT ID='Mesh Vent: MESH26 [ZMIN]', SURF_ID='OPEN', XB=5.3,7.7,12.9,14.4,2.6,2.6/
&VENT ID='Mesh Vent: MESH27 [XMAX]', SURF_ID='OPEN', XB=7.7,7.7,14.4,15.9,2.6,5.8/
&VENT ID='Mesh Vent: MESH27 [ZMAX]', SURF_ID='OPEN', XB=5.3,7.7,14.4,15.9,5.8,5.8/
&VENT ID='Mesh Vent: MESH27 [ZMIN]', SURF_ID='OPEN', XB=5.3,7.7,14.4,15.9,2.6,2.6/
&VENT ID='Mesh Vent: MESH28 [XMAX]', SURF_ID='OPEN', XB=7.7,7.7,15.9,17.4,2.6,5.8/
&VENT ID='Mesh Vent: MESH28 [ZMAX]', SURF_ID='OPEN', XB=5.3,7.7,15.9,17.4,5.8,5.8/
&VENT ID='Mesh Vent: MESH28 [ZMIN]', SURF_ID='OPEN', XB=5.3,7.7,15.9,17.4,2.6,2.6/
&VENT ID='Mesh Vent: MESH29 [XMAX]', SURF_ID='OPEN', XB=7.7,7.7,17.4,18.9,2.6,5.8/
&VENT ID='Mesh Vent: MESH29 [ZMAX]', SURF_ID='OPEN', XB=5.3,7.7,17.4,18.9,5.8,5.8/
&VENT ID='Mesh Vent: MESH29 [ZMIN]', SURF_ID='OPEN', XB=5.3,7.7,17.4,18.9,2.6,2.6/
&VENT ID='Mesh Vent: MESH30 [XMAX]', SURF_ID='OPEN', XB=7.7,7.7,18.9,21.5,2.6,5.8/
&VENT ID='Mesh Vent: MESH30 [XMIN]', SURF_ID='OPEN', XB=3.0,3.0,18.9,21.5,2.6,5.8/
&VENT ID='Mesh Vent: MESH30 [YMAX]', SURF_ID='OPEN', XB=3.0,7.7,21.5,21.5,2.6,5.8/
&VENT ID='Mesh Vent: MESH30 [ZMAX]', SURF_ID='OPEN', XB=3.0,7.7,18.9,21.5,5.8,5.8/
&VENT ID='Mesh Vent: MESH30 [ZMIN]', SURF_ID='OPEN', XB=3.0,7.7,18.9,21.5,2.6,2.6/
&VENT ID='Door 1 low', SURF_ID='INERT', XB=5.1,6.0,12.3,12.3,2.8,2.9/
&VENT ID='Door 2 low', SURF_ID='INERT', XB=5.1,6.0,12.4,12.4,2.8,2.9/
&VENT ID='Door 3 high', SURF_ID='INERT', XB=5.1,6.0,12.4,12.4,4.7,4.8/
&VENT ID='Inner wall 01', SURF_ID='Apartment1.19-Zone0', XB=3.305654,3.305654,14.1,18.4,2.8,5.380981,
COLOR='INVISIBLE'/
&VENT ID='Door 4 high', SURF_ID='INERT', XB=5.1,6.0,12.3,12.3,4.7,4.8/
&VENT ID='Inner wall 02', SURF_ID='Apartment1.19-Zone0', XB=6.9,6.9,12.4,18.4,2.8,5.380981, COLOR='INVISIBLE'/
&VENT ID='Inner wall 03', SURF_ID='Apartment1.19-Zone0', XB=3.3,6.9,18.4,18.4,2.8,5.380981, COLOR='INVISIBLE'/
&VENT ID='Inner wall 04', SURF_ID='Apartment1.19-Zone0', XB=3.3,6.9,18.5,18.5,2.8,5.380981, COLOR='INVISIBLE'/
&VENT ID='Inner wall 05', SURF_ID='Apartment1.19-Zone0', XB=7.1,7.1,12.4,18.4,2.8,5.380981, COLOR='INVISIBLE'/
&VENT ID='Inner wall 06', SURF_ID='Apartment1.19-Zone0', XB=3.1,3.1,14.1,18.4,2.8,5.380981, COLOR='INVISIBLE'/
&VENT ID='Inner wall 07', SURF_ID='Apartment1.19-Zone0', XB=5.1,5.1,12.4,14.0,2.8,5.380981, COLOR='INVISIBLE'/
&VENT ID='Inner wall 08', SURF_ID='Apartment1.19-Zone0', XB=5.0,5.0,12.4,14.0,2.8,5.380981, COLOR='INVISIBLE'/
&VENT ID='Door 5 left', SURF_ID='INERT', XB=5.1,5.15,12.3,12.3,2.9,4.7/
&VENT ID='Door 6 left', SURF_ID='INERT', XB=5.1,5.15,12.4,12.4,2.9,4.7/
&VENT ID='Door 7 right', SURF_ID='INERT', XB=5.95,6.0,12.4,12.4,2.9,4.7/
&VENT ID='Door 8 right', SURF_ID='INERT', XB=5.95,6.0,12.3,12.3,2.9,4.7/
&VENT ID='Vent', SURF_ID='SofaFIRE01', XB=3.4,4.4,15.2,16.2,3.4,3.4/

&HVAC ID='Leak_apartment door_low', TYPE_ID='LEAK', VENT_ID='Door 1 low', VENT2_ID='Door 2 low', AREA=1.5E-3,
LEAK_ENTHALPY=.TRUE./
&HVAC ID='Leak_apartment door_high', TYPE_ID='LEAK', VENT_ID='Door 3 high', VENT2_ID='Door 4 high', AREA=1.66666E-
4, LEAK_ENTHALPY=.TRUE./
&HVAC ID='Leak_apartment door left', TYPE_ID='LEAK', VENT_ID='Door 5 left', VENT2_ID='Door 6 left', AREA=1.66666E-4,
LEAK_ENTHALPY=.TRUE./
&HVAC ID='Leak_apartment door right', TYPE_ID='LEAK', VENT_ID='Door 7 right', VENT2_ID='Door 8 right', AREA=1.66666E-
4, LEAK_ENTHALPY=.TRUE./

&BNDF QUANTITY='RADIATIVE HEAT FLUX'/

&ISOF QUANTITY='TEMPERATURE', VALUE=50.0,100.0,200.0,300.0,400.0/

&SLCF QUANTITY='TEMPERATURE', PBX=5.6/
&SLCF QUANTITY='VISIBILITY', PBX=5.6/

```

```

&SLCF QUANTITY='TEMPERATURE', PBX=11.3/
&SLCF QUANTITY='VISIBILITY', PBX=11.3/
&SLCF QUANTITY='TEMPERATURE', PBX=6.6/
&SLCF QUANTITY='PRESSURE', PBX=5.6/
&SLCF QUANTITY='VOLUME FRACTION', SPEC_ID='OXYGEN', PBX=3.9/
&SLCF QUANTITY='VOLUME FRACTION', SPEC_ID='OXYGEN', PBX=11.3/
&SLCF QUANTITY='PRESSURE', PBX=11.3/
&SLCF QUANTITY='VELOCITY', VECTOR=.TRUE., PBX=5.6/
&SLCF QUANTITY='VELOCITY', VECTOR=.TRUE., PBX=11.3/
&SLCF QUANTITY='VOLUME FRACTION', SPEC_ID='HYDROGEN CYANIDE', PBX=11.3/
&SLCF QUANTITY='VOLUME FRACTION', SPEC_ID='Polyurethane GM21', PBX=11.3/
&SLCF QUANTITY='VOLUME FRACTION', SPEC_ID='Polyurethane GM21', PBX=3.9/
&SLCF QUANTITY='VOLUME FRACTION', SPEC_ID='OXYGEN', PBX=6.6/
&SLCF QUANTITY='TEMPERATURE', PBX=3.9/
&SLCF QUANTITY='VELOCITY', VECTOR=.TRUE., PBZ=5.2/
&SLCF QUANTITY='VELOCITY', VECTOR=.TRUE., PBZ=5.0/
&SLCF QUANTITY='VELOCITY', VECTOR=.TRUE., PBZ=4.8/
&SLCF QUANTITY='VELOCITY', VECTOR=.TRUE., PBZ=4.6/
&SLCF QUANTITY='VELOCITY', VECTOR=.TRUE., PBZ=4.3/
&SLCF QUANTITY='VELOCITY', VECTOR=.TRUE., PBZ=3.7/
&SLCF QUANTITY='VELOCITY', VECTOR=.TRUE., PBZ=3.1/
&SLCF QUANTITY='TEMPERATURE', VECTOR=.TRUE., PBZ=5.2/
&SLCF QUANTITY='TEMPERATURE', VECTOR=.TRUE., PBZ=5.0/
&SLCF QUANTITY='TEMPERATURE', VECTOR=.TRUE., PBZ=4.8/
&SLCF QUANTITY='TEMPERATURE', VECTOR=.TRUE., PBZ=4.6/
&SLCF QUANTITY='TEMPERATURE', VECTOR=.TRUE., PBZ=4.3/
&SLCF QUANTITY='TEMPERATURE', VECTOR=.TRUE., PBZ=3.7/
&SLCF QUANTITY='TEMPERATURE', VECTOR=.TRUE., PBZ=3.1/
&SLCF QUANTITY='VOLUME FRACTION', SPEC_ID='CARBON MONOXIDE', PBZ=3.1/
&SLCF QUANTITY='VOLUME FRACTION', SPEC_ID='CARBON MONOXIDE', PBZ=4.3/
&SLCF QUANTITY='MASS FRACTION', SPEC_ID='SOOT', PBZ=3.1/
&SLCF QUANTITY='MASS FRACTION', SPEC_ID='SOOT', PBZ=4.3/
&SLCF QUANTITY='VOLUME FRACTION', SPEC_ID='OXYGEN', PBZ=3.1/
&SLCF QUANTITY='VOLUME FRACTION', SPEC_ID='OXYGEN', PBZ=4.3/
&SLCF QUANTITY='VISIBILITY', PBZ=3.1/
&SLCF QUANTITY='VISIBILITY', PBZ=4.3/
&SLCF QUANTITY='VOLUME FRACTION', SPEC_ID='CARBON DIOXIDE', PBZ=3.1/
&SLCF QUANTITY='VOLUME FRACTION', SPEC_ID='CARBON DIOXIDE', PBZ=4.3/
&SLCF QUANTITY='TEMPERATURE', PBX=10.7/
&SLCF QUANTITY='VOLUME FRACTION', SPEC_ID='OXYGEN', PBX=10.7/
&SLCF QUANTITY='VOLUME FRACTION', SPEC_ID='HYDROGEN CYANIDE', PBX=10.7/
&SLCF QUANTITY='VOLUME FRACTION', SPEC_ID='Polyurethane GM21', PBX=10.7/
&SLCF QUANTITY='VOLUME FRACTION', SPEC_ID='CARBON MONOXIDE', PBX=10.7/
&SLCF QUANTITY='VOLUME FRACTION', SPEC_ID='CARBON DIOXIDE', PBX=10.7/
&SLCF QUANTITY='VISIBILITY', PBX=10.7/
&SLCF QUANTITY='VOLUME FRACTION', SPEC_ID='CARBON DIOXIDE', XB=-0.6,18.4,10.5,12.2,2.8,5.4, FYI=[Species:
CARBON DIOXIDE] Volume Fraction/
&SLCF QUANTITY='VOLUME FRACTION', SPEC_ID='CARBON MONOXIDE', XB=-0.6,18.4,10.5,10.5,2.8,5.4, FYI=[Species:
CARBON MONOXIDE] Volume Fraction/
&SLCF QUANTITY='VOLUME FRACTION', SPEC_ID='OXYGEN', XB=-0.6,18.4,10.5,12.2,2.8,5.4, FYI=[Species: OXYGEN]
Volume Fraction/

```

&TAIL /